MOUNTAIN-PLAINS CONSORTIUM

MPC 23-498 | H. Burns, E. Lawton, and P. Romero

FORENSIC EVALUATION OF GEOGRID-REINFORCED FLEXIBLE PAVEMENT SECTIONS ON SR-10 NEAR EMERY, UTAH

MOUNTAIN-PLAINS CONSORTIUM REGION 8

A University Transportation Center sponsored by the U.S. Department of Transportation serving the Mountain-Plains Region. Consortium members:

Colorado State University
North Dakota State University
South Dakota State University
University of Colorado Denver
University of Denver
University of Utah
Utah State University
University of Wyoming

Technical Report Documentation Page

1. Report No.	2. Government Accession No.	3. Recipient's Catalog No.
MPC-587		

4. Title and Subtitle	5. Report Date
Forensic Evaluation of Geogrid-reinforced Flexible Pavement Sections on SR-10 Near Emery, Utah	August 2023
	6. Performing Organization Code

7. Author(s)	8. Performing Organization Report No.
Henrik Burns, Graduate Student Evert Lawton, Professor Pedro Romero, Professor	MPC 23-498

9. Performing Organization Name and Address	10. Work Unit No. (TRAIS)
The University of Utah 201 President Circle Salt Lake City, UT 84112	11. Contract or Grant No.

12. Sponsoring Agency Name and Address	13. Type of Report and Period Covered
Mountain-Plains Consortium North Dakota State University PO Box 6050, Fargo, ND 58108	Final Report
	14. Sponsoring Agency Code

15. Supplementary Notes

Supported by a grant from the US DOT, University Transportation Centers Program

16. Abstract

The purpose of this research project was to investigate and determine the reasons for the premature deterioration of the geogrid-reinforced pavement system on the section of SR-10 between Muddy Creek and Emery, Utah. Statistical analyses and evaluations indicate that the structural design of the primary pavement system was adequate, as the stiffness measurements of the primary layers did not correlate with measured pavement distress. Even though the asphalt-concrete layer was subjected to significant deformations in the longitudinal and transverse directions, it displayed negligible cracking. Therefore, the geogrid likely provided the necessary tensile reinforcement to prevent tension cracking in the asphalt-concrete layer despite large movements within the embankment and subgrade.

The characteristics of the fill and subgrade likely dominated the performance of the pavement. The structural design of the pavement system did not take into account the vulnerability of the subgrade and embankment to loading-induced and wetting-induced volume changes.

Subgrade soil from cut sections was sampled and tested for collapse and swell potential. It was found to swell under low overburden pressures and collapse under medium to high overburden pressures. This soil, or similar native soil, was likely used as native embankment fill in some pavement sections. Sections with embankment fills under the negative direction of travel were vulnerable to loading-induced and wetting-induced volume changes.

Additional commentary and recommendations are provided in this report for suitable embankment fill material and pavement support materials, along with effective placement of geogrid and geotextile in a pavement section for future UDOT projects.

17. Key Word	18. Distribution Statement
field tests, geogrids, laboratory tests, pavement maintenance, properties of materials, service life	Public distribution

19. Security Classif. (of this report)	20. Security Classif. (of this page)	21. No. of Pages	22. Price
Unclassified	Unclassified	304	n/a

FORENSIC EVALUATION OF GEOGRID-REINFORCED FLEXIBLE PAVEMENT SECTIONS ON SR-10 NEAR EMERY, UTAH

Henrik Burns
Graduate Student

Evert Lawton
Professor

Pedro Romero
Professor

Department of Civil and Environmental Engineering
The University of Utah

August 2023

Acknowledgments

The authors sincerely appreciate and acknowledge the financial support for this research project provided by the Mountain Plains Consortium (MPC) under Contract No. MPC-587 and the Utah Department of Transportation (UDOT) under Contract No. 198002 (Research PIC No. UT18.102). The authors gratefully acknowledge the extensive help and guidance from the following individuals from UDOT who served on the Technical Advisory Committee:

Steven Anderson
Jeffery Sadler
Scott Andrus
Jason Simmons

Thanks are also due to David Eixenberger and David Stevens, who managed the project for the UDOT Research and Innovation Division. Sincere thanks are owed to Mike Christensen, the UDOT shed foreman in Emery, and his crew for providing traffic control and other assistance during the field tests. The authors would like to thank Daniel Seely and Jerry Flannery of Intermountain GeoEnvironmental Services Inc. for their help with carbonate testing of soils and the use of their plate-load testing equipment. The authors would also like to thank Faramarz Safazadeh and Bao Shuangli for their help and guidance with testing the asphalt-concrete samples. Finally, the authors would like to thank Larry Mattke of Mandli Communications, Michael Butler of WCEC Engineers, and Stan Burns of Integrated Inventory for their help in extracting the pavement distress data for SR-10.

Disclaimer

ABSTRACT

The purpose of this research project was to investigate and determine the reasons for premature deterioration of the geogrid-reinforced pavement system on the section of SR-10 between Muddy Creek and Emery, Utah.

The statistical analyses and evaluations indicate that the structural design of the primary pavement system was adequate as the stiffness measurements of the primary layers did not correlate with measured pavement distress. Even though the asphalt-concrete layer was subjected to significant deformations in the longitudinal and transverse directions, it displayed negligible cracking. Therefore, the upper layer of geogrid likely provided the necessary tensile reinforcement to prevent tension cracking in the asphalt-concrete layer despite large movements in the embankment and subgrade. The characteristics of the fill and subgrade likely dominated the performance of the pavement. The structural design of the pavement system did not consider the vulnerability of the subgrade and embankment to loading-induced and wetting-induced volume changes.

Statistical analyses showed that the presence of soil behavior types 3, 4, 8, and 9 in the fill plus subgrade layer were adequate predictors of IRI performance and good predictors of rutting performance. Subgrade soil from cut sections was sampled and tested for collapse and swell potential. It was found to swell under low overburden pressures and collapse under medium to high overburden pressures. This soil, or similar native soil, was likely used as native embankment fill in some pavement sections. Sections with embankment fills under the negative direction of travel were vulnerable to loading-induced and wetting-induced volume changes.

Additional commentary and recommendations are provided in this report for suitable embankment fill material and pavement support materials, along with effective placement of geogrid and geotextile in a pavement section for future UDOT projects.

TABLE OF CONTENTS

LIST OF TABLES

LIST OF FIGURES

UNIT CONVERSION FACTORS

SI* (MODERN METRIC) CONVERSION FACTORS

APPROXIMATE CONVERSIONS TO SI UNITS

Symbol	When You Know	Multiply By	To Find	Symbol
		LENGTH		
in	inches	25.4	millimeters	mm
ft	feet	0.305	meters	m
yd	yards	0.914	meters	m
mi	miles	1.61	kilometers	km
		AREA		
in^2	square inches	645.2	square millimeters	mm^2
ft^2	square feet	0.093	square meters	m^2
yd^2	square yard	0.836	square meters	m^2
ac	acres	0.405	hectares	ha
mi^2	square miles	2.59	square kilometers	km^2
		VOLUME		
fl oz	fluid ounces	29.57	milliliters	mL
gal	gallons	3.785	liters	L
ft^3	cubic feet	0.028	cubic meters	m^3
yd^3	cubic yards	0.765	cubic meters	m^3
		NOTE: volumes greater than 1000 L shall be shown in m^3		
		MASS		
oz	ounces	28.35	grams	g
lb	pounds	0.454	kilograms	kg
T	short tons (2000 lb)	0.907	megagrams (or "metric ton")	Mg (or "t")
		TEMPERATURE (exact degrees)		
°F	Fahrenheit	5 (F-32)/9 or (F-32)/1.8	Celsius	°C
		ILLUMINATION		
fc	foot-candles	10.76	lux	lx
fl	foot-Lamberts	3.426	$candela/m^2$	cd/m^2
		FORCE and PRESSURE or STRESS		
lbf	poundforce	4.45	newtons	N
lbf/in^2	poundforce per square inch	6.89	kilopascals	kPa

APPROXIMATE CONVERSIONS FROM SI UNITS

Symbol	When You Know	Multiply By	To Find	Symbol
		LENGTH		
mm	millimeters	0.039	inches	in
m	meters	3.28	feet	ft
m	meters	1.09	yards	yd
km	kilometers	0.621	miles	mi
		AREA		
mm^2	square millimeters	0.0016	square inches	in^2
m^2	square meters	10.764	square feet	ft^2
m^2	square meters	1.195	square yards	yd^2
ha	hectares	2.47	acres	ac
km^2	square kilometers	0.386	square miles	mi^2
		VOLUME		
mL	milliliters	0.034	fluid ounces	fl oz
L	liters	0.264	gallons	gal
m^3	cubic meters	35.314	cubic feet	ft^3
m^3	cubic meters	1.307	cubic yards	yd^3
		MASS		
g	grams	0.035	ounces	oz
kg	kilograms	2.202	pounds	lb
Mg (or "t")	megagrams (or "metric ton")	1.103	short tons (2000 lb)	T
		TEMPERATURE (exact degrees)		
°C	Celsius	1.8C+32	Fahrenheit	°F
		ILLUMINATION		
lx	lux	0.0929	foot-candles	fc
cd/m^2	$candela/m^2$	0.2919	foot-Lamberts	fl
		FORCE and PRESSURE or STRESS		
N	newtons	0.225	poundforce	lbf
kPa	kilopascals	0.145	poundforce per square inch	lbf/in^2

*SI is the symbol for the International System of Units. (Adapted from FHWA report template, Revised March 2003)

LIST OF ACRONYMS

AADT	Average Annual Daily Traffic
AASHTO	American Association of State Highway and Transportation Officials
AC	Asphalt-Concrete
ASTM	American Society for Testing and Materials
CBR	California Bearing Ratio
CPT	Cone Penetration Test
DCPT	Dynamic Cone Penetrometer Test
FHWA	Federal Highway Administration
FI	Flexibility Index
FWD	Falling Weight Deflectometer
GB	Granular Borrow
IFIT	Illinois Flexibility Index Test
IRI	International Roughness Index
LL	Liquid Limit
MP	Milepost
OWC	Optimum Water Content
PI	Plasticity Index
PL	Plastic Limit
RC	Relative Compaction
UDOT	Utah Department of Transportation
USCS	Unified Soil Classification System
UTBC	Untreated Base Course

EXECUTIVE SUMMARY

The purpose of this research project was to investigate and determine the reasons for premature pavement system deterioration on the geogrid-reinforced section of SR-10 between Muddy Creek and Emery, Utah. This section of SR-10 was reconstructed between November 2009 and October 2010. Field and laboratory testing was carried out as part of this investigation. In addition, the construction reports and testing results available from 2009 to 2010 were evaluated. Lastly, the pavement distress data collected by UDOT were analyzed. The results of these findings will be presented in this report.

The nature of this roadway and the type of data that were available allowed a unique opportunity to study the symptoms and causes of loading-induced versus wetting-induced stresses and deformations in a pavement system reinforced with geogrids.

The pavement system performed well with respect to cracking. The adequate performance of the asphalt-concrete layer was confirmed by analyzing pavement distress data, visual observation, and Illinois Flexibility Index Tests (I-FIT) performed on samples of asphalt-concrete.

The pavement system also performed well with respect to rutting. With the exception of 2018 for the northbound (positive) direction, pavement distress data showed that surface rutting was within acceptable thresholds for all years and both directions. Statistical analyses indicated that the parameters that best predicted location-specific rutting distress were moduli of subgrade reaction determined from static plate-load tests, percentage of soil behavior types 3 and 4 in the fill plus subgrade layer, and tip resistance from cone penetration tests (CPT). Rutting varied with wheel-path. For the positive direction of travel, the right wheel-path performed better than the left wheel-path with respect to rutting. This difference was likely because the right wheel-path overlapped with the old roadway alignment while the left wheel-path was underlain by fresh subgrade or embankment fill.

The pavement system performed adequately with respect to the International Roughness Index (IRI) for the positive direction with the exception of 2018. However, in 2012 after only two years of service, the southbound (negative) direction IRI was greater than the allowable thresholds, and ride quality became worse each year. Ride quality varied transversely across the width of the roadway. IRI was highest under the right wheel-path of the negative direction and lowest under the right wheel-path of the positive direction.

Construction drawings showed typical cross-sections with deep embankment fill under the negative direction travel lane. The CPT-derived soil behavior type of locations 1, 3, and 4 showed high percentages of clay and silt mixtures between 1.33 ft. and 10.0 ft. These areas performed poorly with respect to ride quality. Statistical analyses showed that the presence of soil behavior types 3, 4, 8, and 9 were good predictors of poor IRI performance. Subgrade soil from cut sections was sampled and tested for collapse and swell potential. It was found to swell under low overburden pressures and collapse under medium to high overburden pressures. This soil, or similar native soil, was likely used as native embankment fill in some pavement sections. Sections with embankment fills under the negative direction of travel were vulnerable to loading-induced and wetting-induced volume changes. The soil would swell when wetted and shrink when dried. Negative direction IRI was 62% higher for areas with culverts compared with areas without culverts. Statistical analyses of field-testing results from the cone penetration tests, dynamic cone penetrometer tests, static plate load tests, and falling weight deflectometer tests revealed that poor IRI performance was unrelated to the stiffness of the primary pavement system; this was likely the result of wetting-induced volume changes (swelling, shrinkage, and collapse) and loading-induced volume changes (compression) within the embankments and subgrades composed of cohesive materials.

The statistical analyses and evaluations indicate that the structural design of the primary pavement system was adequate as the stiffness measurements of the primary layers did not correlate with measured pavement distress. Even though the asphalt-concrete layer was subjected to significant deformations in the longitudinal and transverse directions, it displayed negligible cracking. Therefore, the upper layer of geogrid likely provided the necessary tensile reinforcement to prevent tension cracking in the asphalt-concrete layer despite large movements in the embankment and subgrade. The characteristics of the fill and subgrade likely dominated the performance of the pavement. The structural design of the pavement system did not consider the vulnerability of the subgrade and embankment to loading-induced and wetting-induced volume changes.

Additional commentary and recommendations are provided in this report for suitable embankment fill material and pavement support materials, along with effective placement of geogrid and geotextile in a pavement section for future UDOT projects.

1. INTRODUCTION

The purpose of this research project was to investigate and determine the reasons for premature pavement system deterioration on the geogrid-reinforced section of State Route 10 (SR-10) between Muddy Creek and Emery, Utah. Field and laboratory tests were carried out as part of the research investigation. In addition, construction reports and testing results available from 2009 to 2010 were evaluated. Lastly, pavement distress data collected by the Utah Department of Transportation (UDOT) during the service life of this section of the roadway were analyzed. The results from these findings will be presented in this report. Also in this study, and available from UDOT and the authors, a separate interim report containing the results of a thorough literature review on the value added to the pavement section by geogrids was prepared and provided to UDOT.

The nature of this roadway and the type of data that were available allowed a unique opportunity to study the symptoms and causes of loading-induced versus wetting-induced stresses and deformations in a pavement system reinforced with geogrids.

1.1 General Project Boundaries

The project covered the section of State Route 10 that was rebuilt and widened between 2009 and 2010 as part of UDOT Federal/State Project S-00010(40)13. The reconstructed section begins at the intersection of Main Street and 200 East in Emery (milepost 12.83 and station 105+50) and continues northeast to the bridge at Muddy Creek (milepost 15.86 and station 265+13) for a total length of 3.03 miles.

The reconstructed pavement system incorporated the use of geogrid. The use of geogrid allowed a thinner untreated base course (UTBC) and granular borrow (GB) to be used in the design. The typical pavement system was designed as follows: 1.5 inches stone matrix asphalt, 6.5 inches hot mix asphalt, 6 inches UTBC, geogrid type 1, 10 inches GB, and geogrid type 1. The pavement was designed for a service life of 20 years. The upper geogrid layer was extended 1.3 feet beyond the edge of the travel lane. The lower geogrid layer between the GB and the subgrade was extended 2 feet beyond the edge of the travel lane. Except for the first 1,200 feet of the project, Tensar Biaxial Geogrid (BX1100) was used for both geogrid layers for the entire length of the reconstructed section.

For an equivalent 20-year service life without geogrid, the pavement system was designed as follows: 1.5 inches stone matrix asphalt, 6.5 inches hot mix asphalt, 8 inches UTBC, and 18.5 inches GB. Comparing the designs with and without geogrid, the use of geogrid reduced the thicknesses of the UTBC and GB by 2 inches and 8.5 inches, respectively.

1.2 Locations of Geogrid Products within the Test Section

The first 1,200 feet of the reconstructed section was used as a test section to compare the performance of geogrids from four different manufacturers. A different geogrid product was placed every 240 feet. Tenax MX 220B geogrid was placed between station 105+50 and 107+90. Between station 107+90 and 110+30, Tensar BX 1100 was placed in the left (southbound) lane, while Tenax was placed in the right (northbound) lane. Tencate Mirafi BXG geogrid was placed between station 110+30 and 112+70. Naue Securgrid 30/30 was placed between station 112+70 and 115+10. Tensar BX 1100 geogrid was placed in the last 240 feet of the test section between station 115+10 and 117+50.

1.3 Visual Inspection of Pavement Conditions

A visual field inspection of the roadway was carried out on July 24, 2018. The length of the roadway was driven twice, first beginning at Muddy Creek and ending in Emery (Southbound). Initial observations were made from the vehicle. The entire length of the test section was walked. No wheel-path or other cracking was observed. Wheel-path rutting was visually observed but not physically measured. No patches or potholes were observed in the test section either.

After the visual inspection of the test section was complete, the section between the test section and Muddy Creek was driven again in the opposite (northbound) direction. Ten areas with patches were observed along the way, two of which appeared to be rotomills. The vehicle was stopped at 11 points along the route to walk the area and inspect the pavement condition. Five of the locations that were walked had patches. No visible wheel-path, fatigue, or environmental cracking was observed. Five of the 10 patches were only applied to the southbound (negative) lane.

Table 1.1 shows the location of visible patches and other treatments in the negative direction (southbound lane). Mandli Communication's Roadview Explorer was used to estimate the time of patch (or rotomill) treatment.

Table 1.1 Location and Time of Pavement Treatments Along SR-10

UDOT MP	Patch (year)	Both Lanes?
15.31	(May 2014)	No
15.17	(May 2014)	No
15.06	(May 2014)	No
14.95	(October 2015)	No
14.92	(May 2014)	Yes
14.81	(May 2014)	Yes
14.65	(October 2015)	No
13.73	Rotomill (August 2017)	Yes
13.67	Rotomill (October 2015)	No
13.58	Rotomill (August 2017)	Yes

In terms of the ride quality, the pavement system was in worse condition in the negative (southbound) direction compared with the positive (northbound) direction. The poor ride quality was observed during the first field visit, as well as a subsequent visit on July 5, 2019, to obtain samples of native soils that were likely used as fill material beneath the pavement system. Severe longitudinal surface deformations were noticeable when traveling in the negative direction at highway speeds. UDOT officials also highlighted the poor ride quality in the southbound lane. "Dips" of varying severity were present in the negative direction of travel. A longitudinal surface deformation is visible near the wheel-path closest to the shoulder on the left side of Figure 1.1, as indicated by the red arrow.

Figure 1.1 Photograph Showing a Visible "Dip" in the Negative Direction of Travel as Indicated by the Red Arrow (Courtesy of UDOT/Mandli Communications)

1.4 Traffic Data Between Emery and Muddy Creek

SR-10 receives significant traffic from trucks transporting coal from the Sufco mine to the PacifiCorp plant in Hunter. During the first field tests, a coal truck traveling northbound or southbound was observed every couple of minutes. Interestingly, the coal trucks are fully loaded when traveling in the positive (northbound) direction and empty in the negative (southbound) direction. Annual average daily traffic (AADT) values collected by UDOT with percent of single-axle and combo-axle trucks for 2010 through 2016 are shown in Table 1.2. AADT values in 2016 correspond to about 1.4 combo trucks per minute over a 24-hour period.

Table 1.2 AADT Data for SR-10 Between Emery and Muddy Creek, Utah

	AADT	SINGLE	COMBO
2016	3,900	9%	50%
2015	3,755	8%	50%
2014	5,510	8%	50%
2013	5,420	8%	50%
2012	5,245	8%	50%
2011	2,840	8%	50%
2010	2,850	8%	50%

1.5 Outline of the Report

The remainder of this report will be structured and ordered as follows.

- Overview of Field Testing and Field Sampling
- Evaluation of Pavement Distress Data
- Evaluation of Construction Documents
- Evaluation of Results from Laboratory Testing
- Evaluation of Field Testing Data
- Commentary on the Effect of Geogrid on the Pavement System
- Commentary on the Geogrid Design Guide
- Summary, Conclusions, and Recommendations

2. OVERVIEW OF FIELD TESTING AND SAMPLING

Locations to carry out testing were scouted and chosen the day before primary field testing on July 24, 2018. A map with primary testing locations marked with blue diamonds is shown in Figure 2.1. A secondary sampling of the subgrade embankment material was done on July 5, 2019. Secondary sampling locations are marked with green diamonds.

Location numbers increase in the negative (southbound) direction, beginning with Location 1 near Muddy Creek and ending with Location 14 in Emery. The station and milepost of each testing and sampling location are provided in Table 2.1. Mileposts for each location were determined using the latitude and longitude given by the cone penetrometer rig and UDOT's route linear referencing system. The rightmost column indicates if a patch or rotomill treatment was present at the testing location.

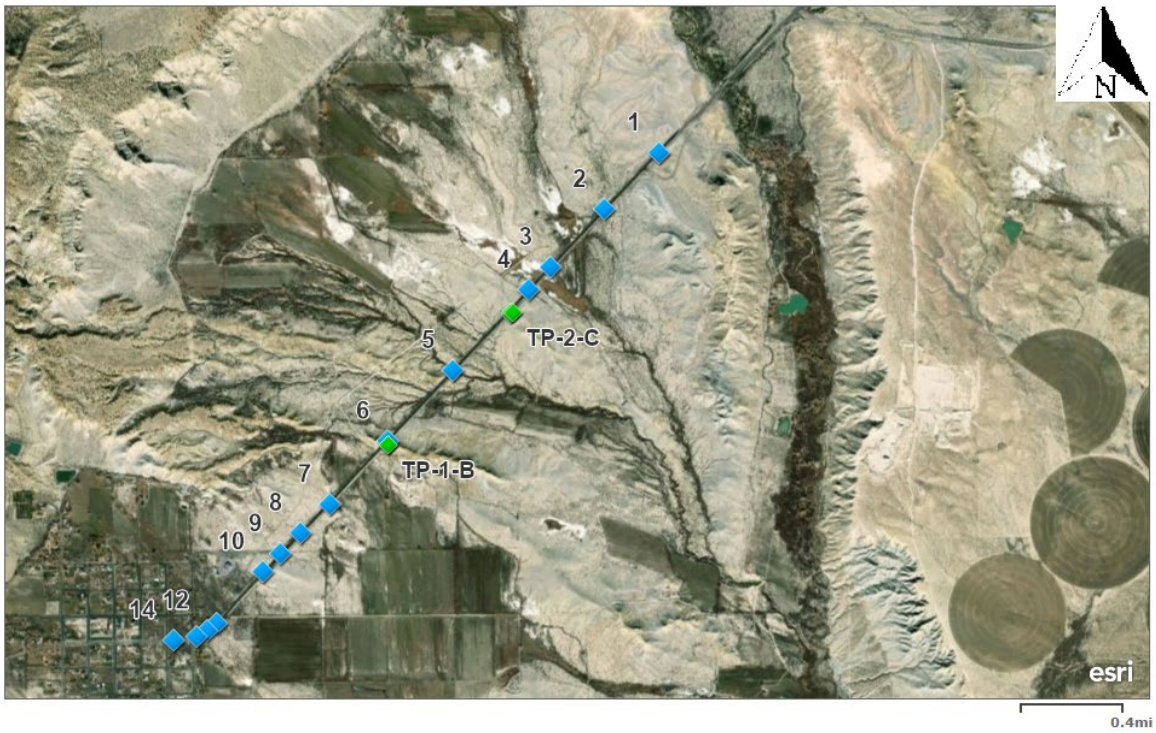

Figure 2.1 Map of Testing and Sampling Locations

Locations were chosen based on the presence of features indicating pavement degradation such as skin patches and features that may have contributed to pavement degradation, such as the presence of pipe culverts. Control locations without any sign of degradation were also chosen. Four of the 14 locations were placed within the test section. The locations within the test section were spaced such that there was at least one location for each geogrid product.

The tests conducted on the in-situ pavement system and the subgrade as part of the field investigation are shown in Table 2.2.

Table 2.1 List of Locations

Location	Station	MP	Patch
14	106+18	12.852	No (Test Section)
13	110+95	12.943	No (Test Section)
12	113+38	12.989	No (Test Section)
11	115+89	13.036	No (Test Section)
10	129+92	13.302	No
9	134+97	13.398	No (Shed Entrance)
8	140+83	13.509	No
7	149+06	13.665	Yes (Rotomill)
6	166+46	13.994	No (Crest of Hill)
5	185+76	14.360	No
4	208+13	14.783	Yes
3	214+46	14.903	Yes
2	230+44	15.206	No
1	246+25	15.505	No

Table 2.2 In-Situ Pavement Tests

Field Test:	ASTM Standard:
Dynamic Cone Penetrometer	D6951-18
Repetitive Static Plate Load Test	D1195-09 (2015)
Falling Weight Deflectometer	D4964
Cone Penetration Test	D5778-12

The repetitive static plate load test (RSPLT) and falling weight deflectometer (FWD) are non-destructive tests that can be conducted directly on the surface of the pavement system. The dynamic cone penetrometer test (DCPT) and cone penetration test (CPT) can only be pushed through untreated/non-cemented soil materials. A 5.9-inch (150 mm) diameter core of the 8-inch asphalt-concrete layer was removed at each location so that the DCPT and CPT could be conducted on the underlying soil layers. The RSPLT, FWD, and CPT were performed on the area in the middle of the travel lane between the wheel-paths. The DCPT was performed on the edge of the lane and the shoulder, for traffic safety purposes. Datasheets with results from the RSPLT, DCPT, and CPT are shown in the Appendix. Except for the RSPLT, all tests were performed at each location. The RSPLT was performed at Locations 1, 4, 6, 8, 11, and 12.

2.1 Repetitive Static Plate Load Test

The Repetitive Static Plate Load Test (RSPLT) is a non-destructive test typically used to assess the bearing capacity of a pavement system or compacted fill. The test is carried out by loading a set of stacked steel plates with a diameter of 24 to 30 inches and measuring the deflection with either digital or analog dials. A 24-inch plate was used in this investigation with a combination of digital and analog dial gauges. The load was generated by jacking against a dump truck provided by UDOT. Ottawa sand was placed beneath the plate to create a uniform bearing pressure on the pavement surface. A picture of the

test setup is shown in Figure 2.2. The modulus of subgrade reaction can be determined by plotting a stress-displacement curve, as shown in Figure 2.3.

Figure 2.2 Plate Load Test Setup

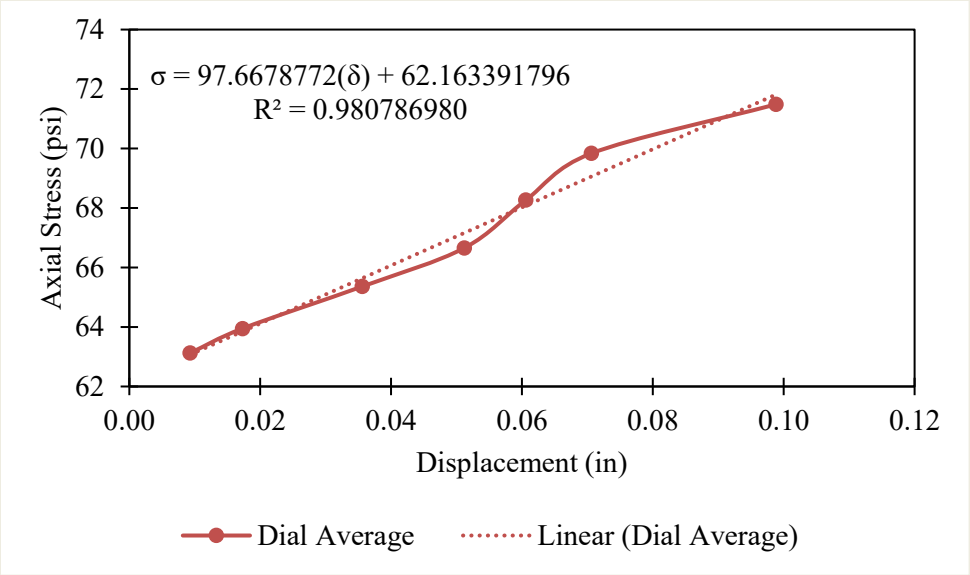

Figure 2.3 Derivation of Coefficient of Subgrade Reaction

The coefficient of subgrade reaction (k) is the slope of the relationship formed by plotting stress versus displacement. The modulus of subgrade reaction (K) is calculated by multiplying the coefficient of subgrade reaction by the diameter of the load plate.

2.2 Falling Weight Deflectometer

The falling weight deflectometer (FWD) is a non-destructive test used to determine the bearing capacity of the pavement system. The test is carried out by dropping a known weight from a given height and measuring the displacement generated at the locations of a set of geophones spaced at standard distances from the area of impact. The FWD test was carried out by UDOT. The geophone spacing configuration used by UDOT is shown in Table 2.3.

The displacement at each geophone is measured at a frequency of six times per second for approximately 150 seconds. A plot showing the displacement measured at each geophone as a function of time is shown in Figure 2.4.

Table 2.3 UDOT FWD Geophone Spacing

Geophone:	1	2	3	4	5	6	7	8	9
Distance (in.):	0	8	12	18	24	36	48	60	-9

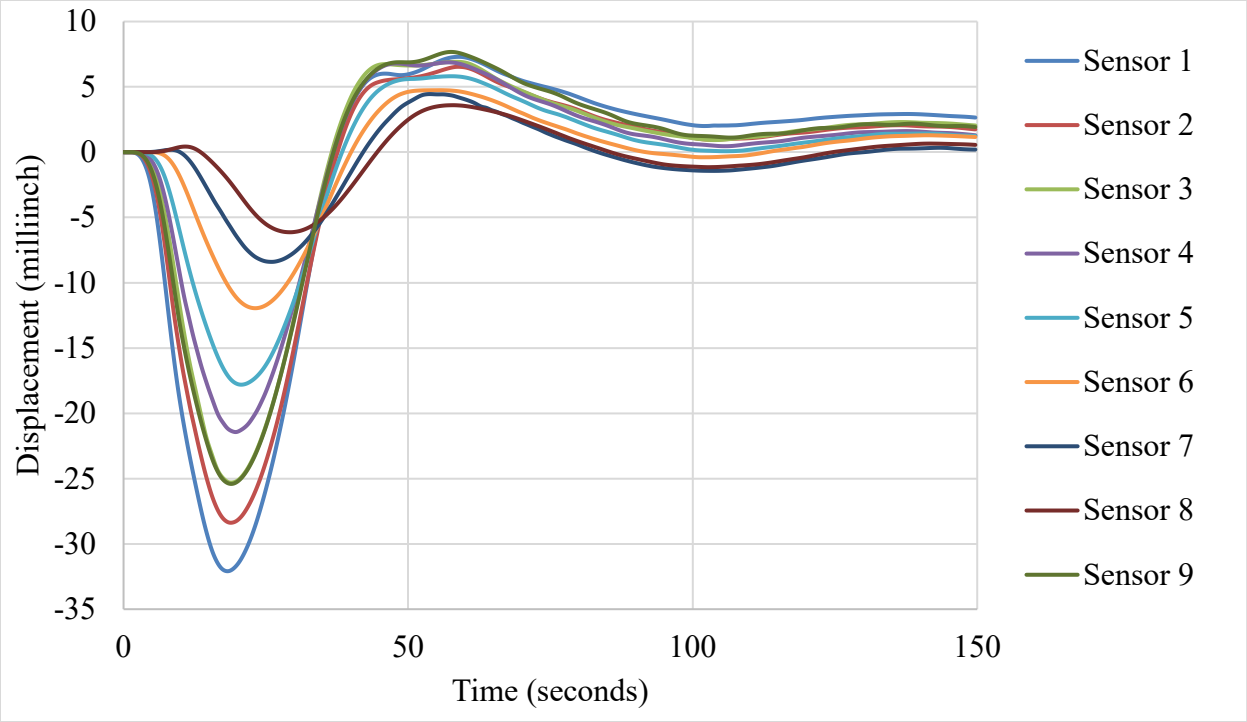

Figure 2.4 FWD Sensor Deflection as a Function of Time for Location 1 Drop 2

The geophone closest to the loading location reads maximum displacement first. The geophone farthest from the loading location takes the longest to read the maximum displacement at that location. The moduli of the pavement system layers can be estimated using the maximum displacement for each geophone. Estimating the pavement system moduli involves an iterative approach where a calculated deflection bowl is matched with the measured deflection bowl of the FWD test. A plot of the measured deflection bowl and two calculated bowls for Location 1 is shown in Figure 2.5.

The modulus of each layer is adjusted until the calculated bowl matches the measured bowl within an acceptable limit of variance. Commercial software programs are available to carry out the iterative back-calculation process.

The resilient modulus was estimated using the correction factors shown in Table 2.4. Datasheets for the FWD test are given in Appendix E.

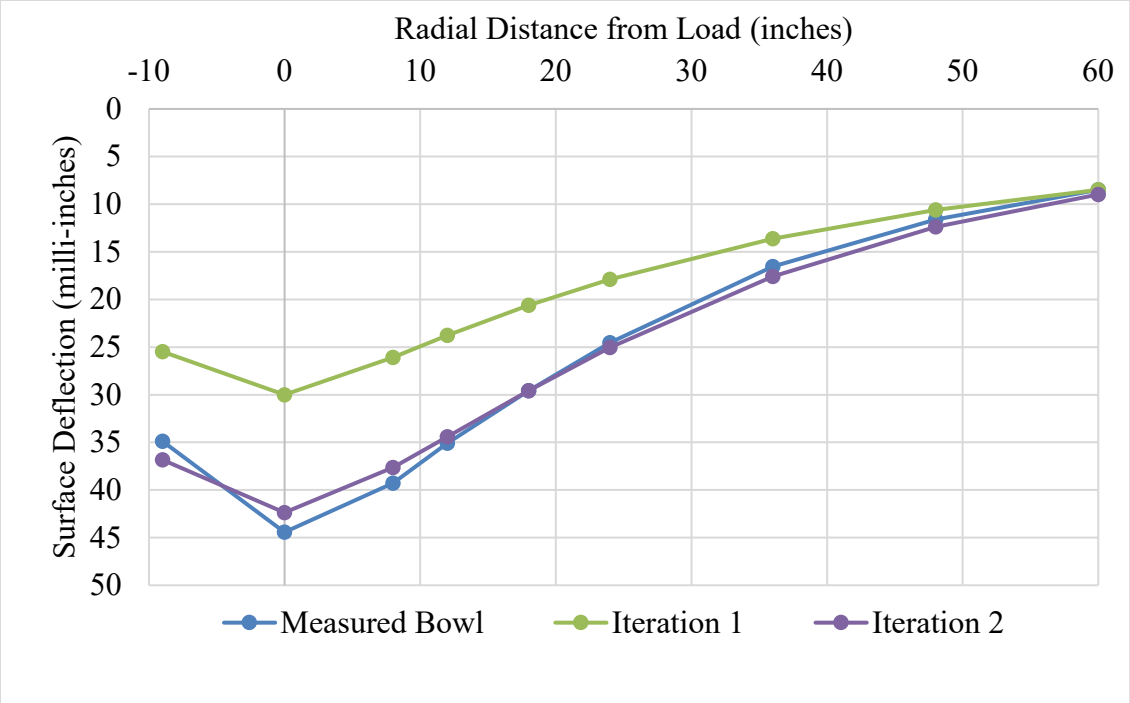

Figure 2.5 Measured vs. Calculated Deflection Bowls from FWD for Location 1

Table 2.4 FWD Resilient Modulus Correction Factors

Layer:	Correction Factor:
HMA	$0.1632e^{0.0267(Temperature)}$
UTBC/GB	0.67
SG	0.55

2.3 Cone Penetration Test

The cone penetration test is one of the most widely used and accepted methods of determining subsurface stratigraphy, soil behavior type, and estimated properties of soils. The test consists of pushing a penetrometer with a conical tip of standard build and geometry into the ground at a constant rate of 20 mm/s (ASTM D5778-12). The device measures the tip or cone resistance (q_t.), sleeve friction (f_s), and pore water pressure (u_2). Correlations between these measured parameters and most fundamental engineering properties of soils are available.

The CPT can only be pushed through un-cemented or untreated soil layers. The test was therefore conducted through the opening created in the asphalt-concrete layer by asphalt coring. Bedke Geotechnical Field Services carried out the CPTs. A plot of the CPT tip resistance for the untreated base course and granular borrow layers of Location 1 is shown in Figure 2.6. The zero-depth on the figure is set to the top of the UTBC layer. CPT logs for each location are given in Appendix D.

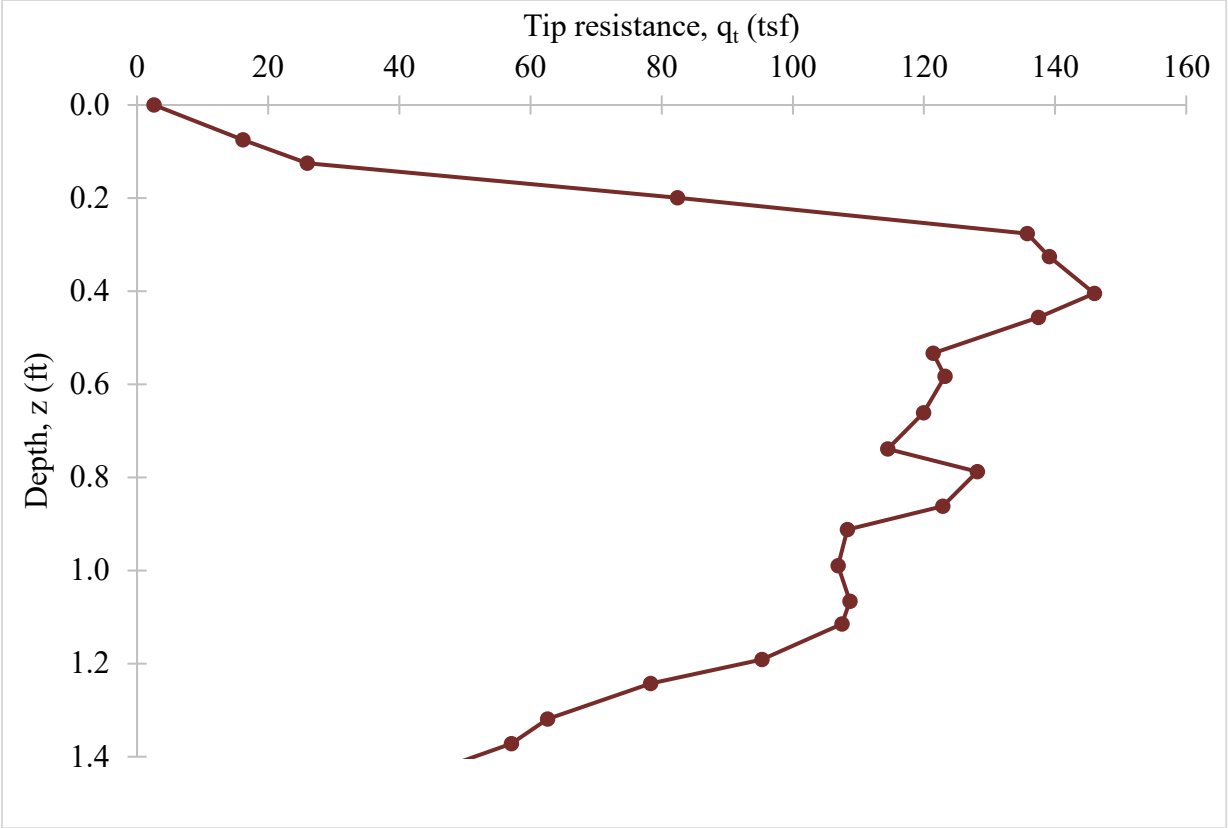

Figure 2.6 CPT Tip Resistance vs. Depth for UTBC and GB of Location 1

2.4 Dynamic Cone Penetrometer Test

The dynamic cone penetrometer test is a standard lightweight test for estimating the stiffness of surface layers (ASTM D6951-18). The test is performed by dropping an 8-kilogram (17.64-pound) weight onto an anvil that drives a steel cone of standard build into the ground. By measuring the number of blows required to drive the cone a given distance, the California Bearing Ratio (CBR) can be estimated from correlations. There exist correlations between CBR and other soil stiffness properties. CBR for all locations was estimated using the equation derived by the U.S. Army Corps of Engineers, Equation 2.1. Datasheets for each location are given in Appendix G.

$$\boldsymbol{BR = \frac{292}{(DCP * 25.4)^{1.12}}} \qquad \textbf{(Equation 2.1)}$$

Where:

$DCP = in/blow$

Sample calculation:

$DCP = 0.50\ in/blow$

$CBR = \frac{292}{(0.50*25.4)^{1.12}} = 16\%$

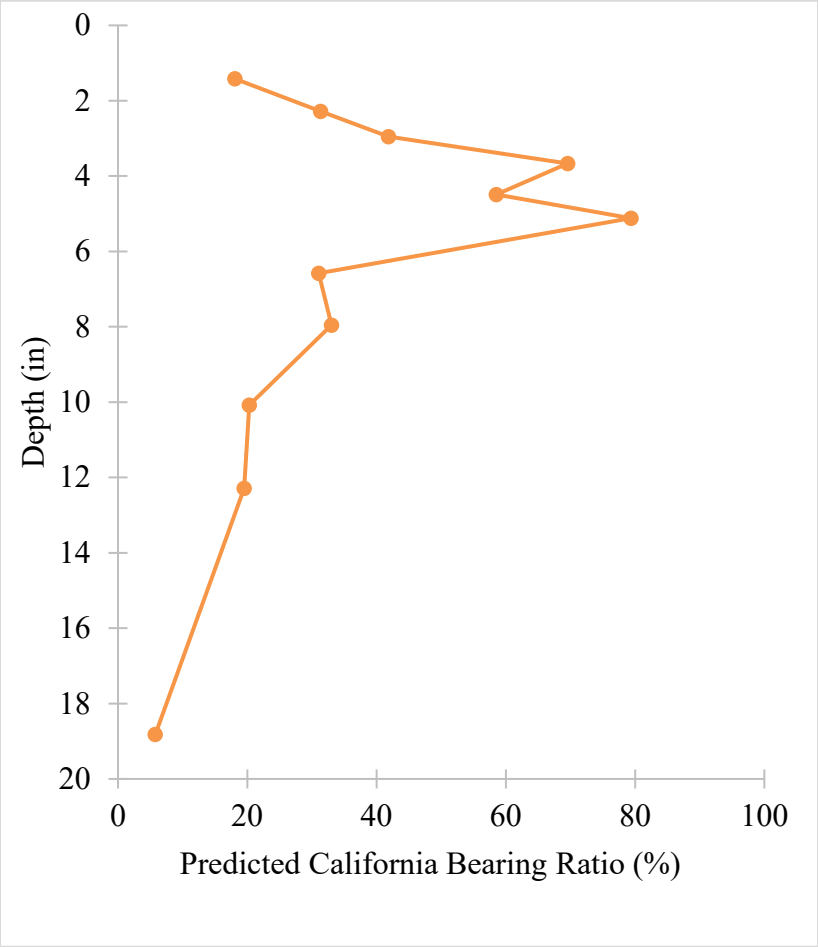

Figure 2.7 DCPT-Derived Predicted California Bearing Ratio for Location 1

2.5 Field Sampling

Field samples were collected at each location. Three asphalt-concrete cores were collected at each location: One at centerline (A), one at the center of the travel lane between the wheel-paths (B), and one at the edge of the lane and the shoulder (C). The sampling layout is shown in Figure 2.8. All cores and samples were taken in the southbound direction only.

Asphalt-concrete cores were marked with a location number and letter indicating the location with respect to the transverse direction of the roadway.

Figure 2.8 Sampling Layout for All Locations

Samples of untreated base course (UTBC) and granular borrow (GB) were collected at each location. With the exception of Location 1, which was collected at centerline (A), all subsequent soil sampling was done at the edge of the lane and shoulder (C). Samples were collected at the shoulder rather than centerline for safety reasons because the traffic in the northbound lane was coming too close to the centerline. Soil sampling was done by hand through the hole opened by asphalt-concrete coring.

The first 6 inches of soil retrieved was assumed to be UTBC, while subsequent soil was classed as GB. Sampling was typically done to a depth of 20 inches below the surface or the first 6 inches of the GB layer. Samples were collected in double-layered resealable plastic bags. An average of 3.8 kilograms and 4.0 kilograms of UTBC and GB samples were collected, respectively. The weights of the samples at each location are listed in Table 2.5. Additional field sampling was done on July 5, 2019. Native soil from cut sections was collected to characterize the soil that was used as embankment fill for the southbound lane of travel. Samples of native soil were collected at two primary locations. The number of each type of sample collected is listed in Table 2.6.

Table 2.5 Weights of UTBC and GB Samples Collected at Each Location

Location	UTBC Sample (g)	GB Sample (g)
1	2080	2570
2	3360	2740
3	3160	1550
4	4930	2410
5	5720	10700
6	4680	4280
7	3090	3310
8	3230	5510
9	2670	4510
10	3390	5090
11	3990	4360
12	5602	3690
13	3860	3440
14	4300	2430

Table 2.6 Number of Samples Collected

Sample Type	Number of Samples Collected
Asphalt-Concrete	42
Untreated Base Course	14
Granular Borrow	14
Native Soil	5

The type of test performed and sampling done at each location is summarized in Table 2.7. In addition, location-specific notes from soil sampling are also provided. During soil sampling, it was noted if and at what depth geogrid was located. In six of 14 sampling locations, no geogrid was found.

Table 2.7 Location Field Testing and Sampling Summary

Location	Test Type	Samples	Sampling Notes
1	RSPLT, DCPT, CPT, FWD	AC, UTBC, GB	Geogrid at 13''
2	DCPT, CPT, FWD	AC, UTBC, GB	Geogrid at 13'' and 19''
3	DCPT, CPT, FWD	AC, UTBC, GB	Geogrid at 13'' and 20.5''
4	RSPLT, DCPT, CPT, FWD	AC, UTBC, GB	No geogrid
5	DCPT, CPT, FWD	AC, UTBC, GB	No geogrid
6	RSPLT, DCPT, CPT, FWD	AC, UTBC, GB	No geogrid
7	DCPT, CPT, FWD	AC, UTBC, GB	No geogrid
8	RSPLT, DCPT, CPT, FWD	AC, UTBC, GB	No geogrid
9	DCPT, CPT, FWD	AC, UTBC, GB	Geogrid at 15''
10	DCPT, CPT, FWD	AC, UTBC, GB	No geogrid
11	RSPLT, DCPT, CPT, FWD	AC, UTBC, GB	Geogrid at 14''
12	RSPLT, DCPT, CPT, FWD	AC, UTBC, GB	Geogrid at 13.5''
13	DCPT, CPT, FWD	AC, UTBC, GB	Geogrid at 13.5''
14	DCPT, CPT, FWD	AC, UTBC, GB	Geogrid at 15''

3. EVALUATION OF PAVEMENT DISTRESS DATA

3.1 Evaluation of IRI, Rutting, and Cracking Distresses

The pavement distress metrics collected by UDOT include, among others, international roughness index (IRI), wheel-path rutting, longitudinal cracking, and transverse cracking. The primary metrics that were analyzed in this study were IRI, rutting, and cracking. IRI and rutting measurements are available for both the left and right wheel-paths. Cracking measurements are available in the transverse and longitudinal directions.

The pavement distress data are valuable because they allow a characterization of the type of failure or deterioration that has occurred. Consequently, if the type of failure is known, a better estimation of the cause(s) of failure can be made. Additionally, it can be used as a baseline metric to compare with the results from field testing on a location-by-location basis.

Pavement distress data were collected at intervals of 0.01 miles. For the given section of SR-10 from mileposts 12.83 to 15.86, there were 302 individual 0.01-mile segments with independent distress data available.

The most recent year for which pavement distress metrics were collected for both the negative and positive directions was 2017. In Figure 3.1, the 2017 values of IRI for the negative and positive directions are presented versus milepost. Each direction represents the average of the left and right wheel-path values.

The pavement in the negative direction has performed worse than the positive direction with respect to ride quality. The presence of IRI "spikes" is more common, and they are more extreme in the negative direction. Poor IRI performance in the negative direction may be initially unexpected given that coal trucks are fully loaded when traveling in the northbound (positive) direction and unloaded in the southbound (negative direction).

A comparison of the 2015 rutting for the negative and positive directions is shown in Figure 3.2. The values presented are an average of the values for the left and right wheel-paths.

The positive direction performed worse than the negative direction with respect to wheel-path rutting. It is reasonable that there is more rutting in the positive direction given that the coal trucks were fully loaded in that direction.

The cracking index is a composite of the various cracking distresses, including low, medium, and high-severity transverse cracking (T), non-wheel-path longitudinal cracking (L), and block cracking (B). Each cracking distress is classed as low, medium, and high severity. The equation used to determine the cracking index is given in Equation 3.1. Values of cracking index for both the negative and positive directions for 2017 are shown in Figure 3.3 by milepost.

The US Department of Transportation has published pavement distress thresholds for classifying pavement systems on a "good, fair, poor" basis. The thresholds for each classification are shown in Table 3.1. Each 0.01-mile measured segment was classed as good, fair, or poor with regard to ride quality, cracking, and rutting.

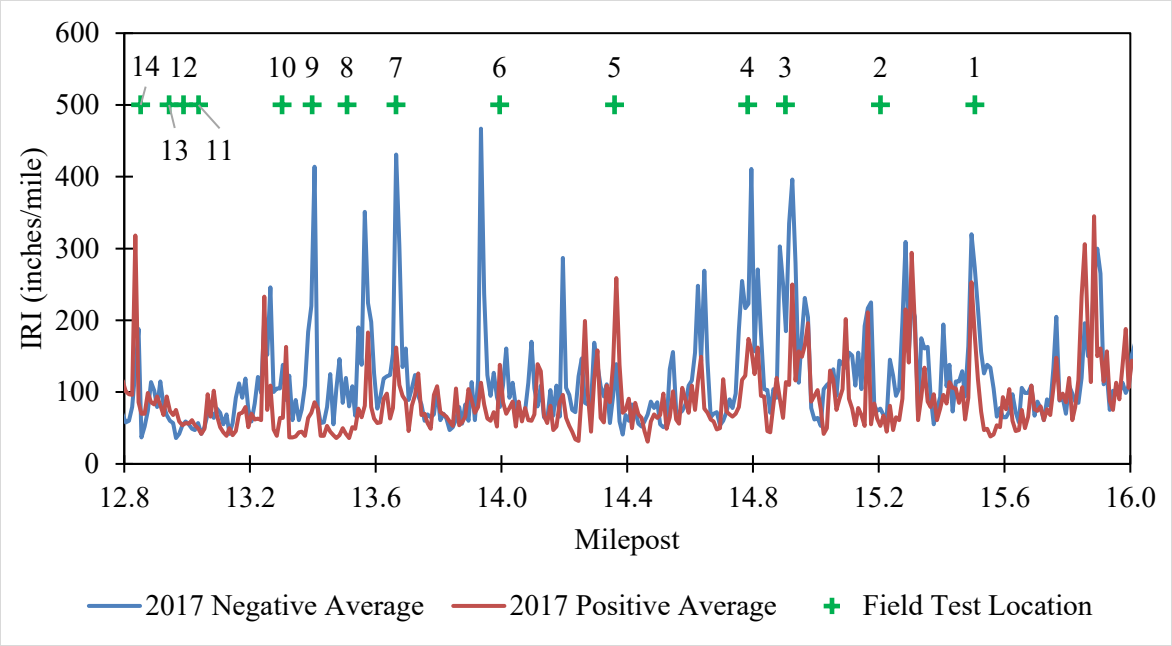

Figure 3.1 2017 International Roughness Index Between Emery and Muddy Creek, Utah

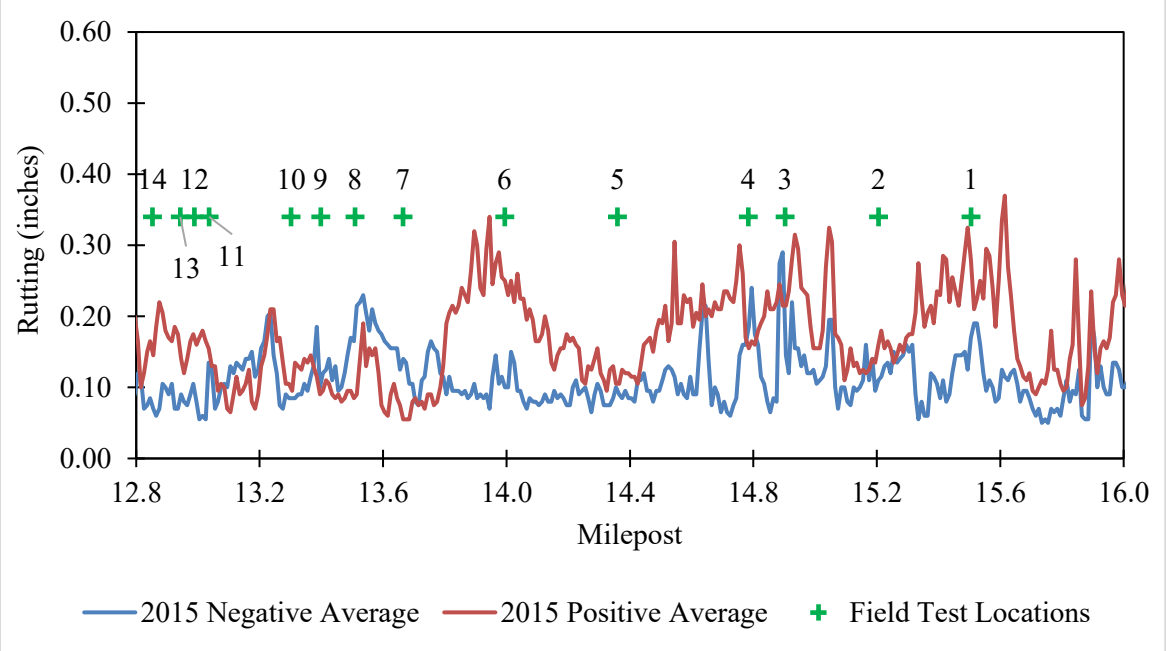

Figure 3.2 2015 Surface Rutting Between Emery and Muddy Creek, Utah

$$\boldsymbol{Cracking\ Index} = \mathbf{100} - \left[\left(\frac{\mathbf{50}}{\mathbf{52.8}}\right)(\boldsymbol{Low\ T}) + \left(\frac{\mathbf{50}}{\mathbf{39.6}}\right)(\boldsymbol{Med\ T}) + \left(\frac{\mathbf{50}}{\mathbf{26.4}}\right)(\boldsymbol{High\ T}) + \left(\frac{\mathbf{50}}{\mathbf{1584}}\right)(\boldsymbol{Low\ L}) + \left(\frac{\mathbf{50}}{\mathbf{1188}}\right)(\boldsymbol{Med\ L}) + \left(\frac{\mathbf{50}}{\mathbf{792}}\right)(\boldsymbol{High\ L}) + \left(\frac{\mathbf{50}}{\mathbf{6336}}\right)(\boldsymbol{Low\ B}) + \left(\frac{\mathbf{50}}{\mathbf{4752}}\right)(\boldsymbol{Med\ B}) + \left(\frac{\mathbf{50}}{\mathbf{3168}}\right)(\boldsymbol{High\ B})\right]$$ **Equation 3.1**

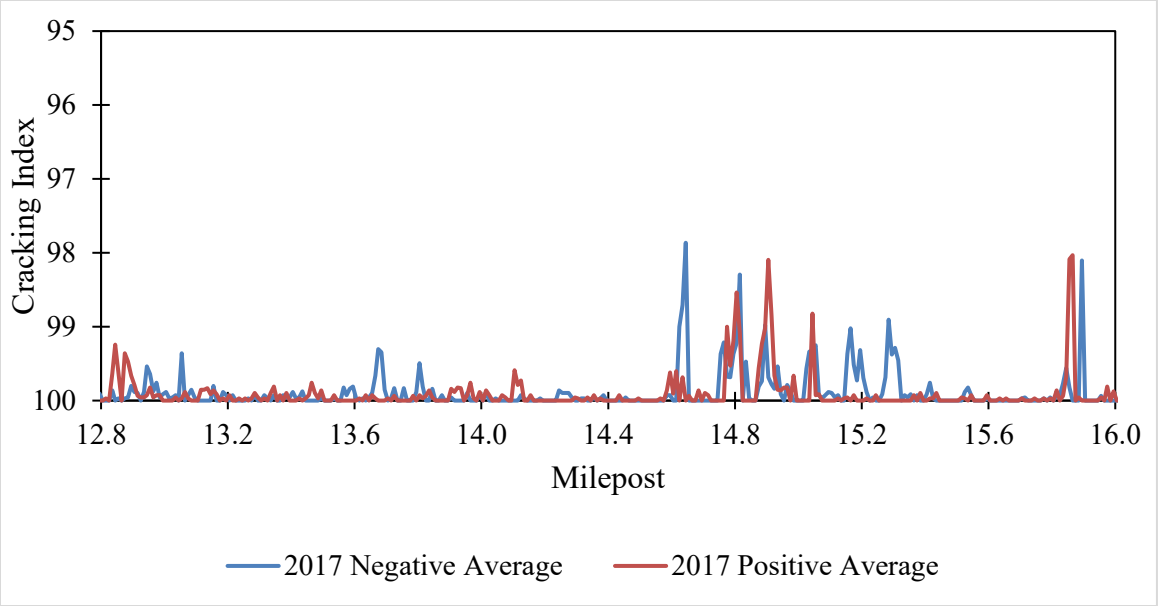

Figure 3.3 2017 Surface Cracking Between Emery and Muddy Creek, Utah

The performance of pavement for the northbound direction of travel with respect to IRI is shown in Figure 3.4. The performance of the pavement in the southbound direction of travel with respect to IRI is shown in Figure 3.5. The red and yellow dotted lines represent the acceptable percent of segments performing to a given condition. The percentage of segments performing poorly should not exceed 5%, while the percentage of segments performing fairly and poorly should not exceed 40%.

Table 3.1 Pavement Distress Metric Thresholds

Pavement Distress Metric Thresholds. Source: USDOT (2017)			
Metric	Good	Fair	Poor
IRI (inches per mile)	<95	95-170	>170
Cracking Index	>80	80-50	<50
Rutting (inches)	<0.20	0.20-0.40	>0.40

Clearly, the pavement in the negative direction has performed worse than in the positive direction. It is also clear that the pavement condition is deteriorating with age. It is noted that already in 2012, 6.6% of segments were performing poorly.

In Figure 3.6, the performance of the pavement in the positive direction of travel with respect to rutting is provided. The performance of the pavement in the negative direction of travel with respect to rutting is shown in Figure 3.7. The pavement in the negative direction is performing better than the positive direction with respect to rutting, which is expected because the coal trucks are fully loaded in the positive direction and unloaded in the negative direction.

From the results shown in Figures 3.6 and 3.7, it is clear that the pavement system is generally performing adequately with respect to rutting. The one exception is the positive direction for the year 2018, where the percentage of good segments fell below 60%.

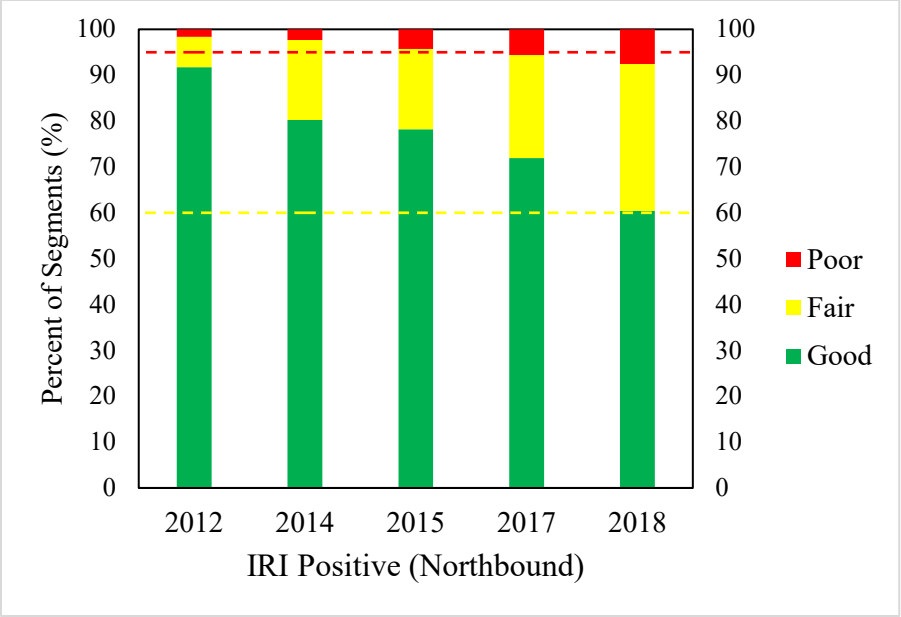

Figure 3.4 IRI in Positive Direction from 2012 to 2018

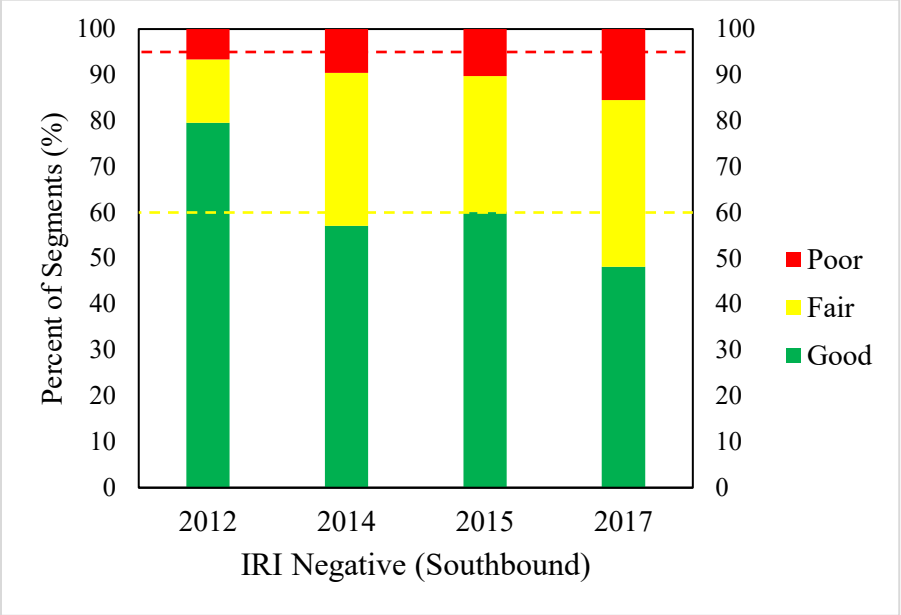

Figure 3.5 Negative Direction IRI from 2012 to 2017

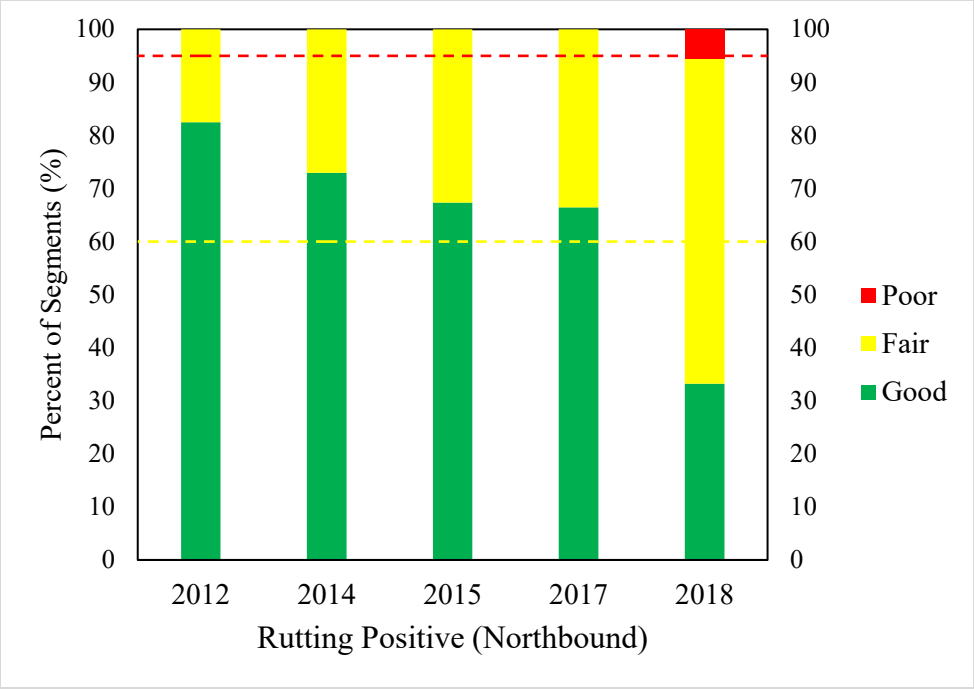

Figure 3.6 Positive Direction Rutting from 2012 to 2018

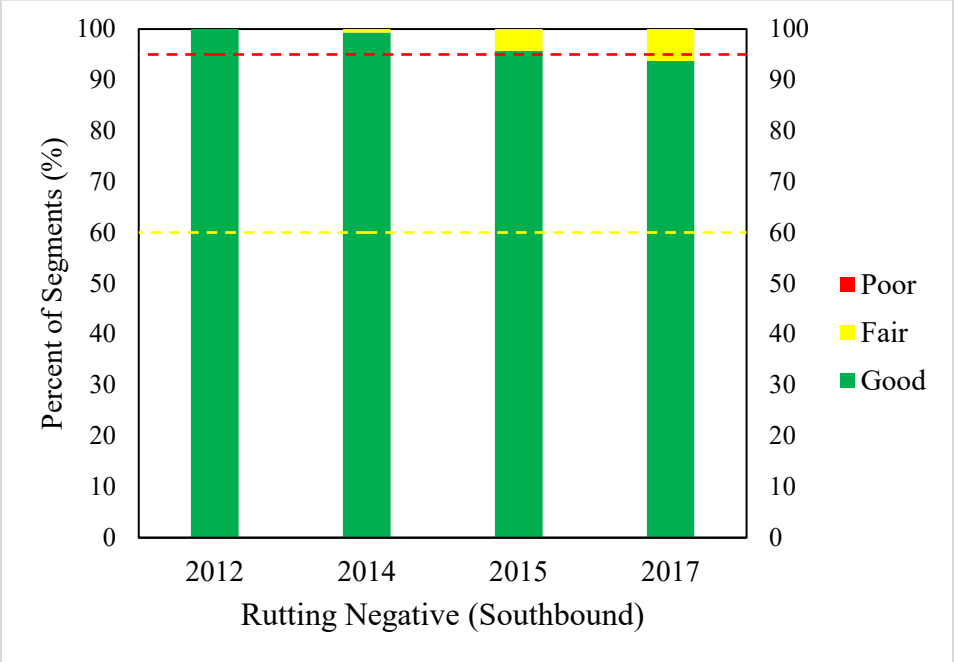

Figure 3.7 Negative Direction Rutting from 2012 to 2017

However, with respect to ride quality (IRI), the pavement is not performing adequately. For the negative direction of travel, the percentage of poor segments had already exceeded the acceptable amount in 2012. The percentage of poor plus fair segments exceeded the acceptable amount in 2014. The performance in the positive direction was better, barely exceeding the acceptable amount of poor segments in 2017 and exceeding the amount of poor plus fair segments in 2018.

All segments in both the positive and negative direction for all years classed as "good" with respect to cracking distress as shown in Table 3.2.

The pavement distress data alone allow a preliminary evaluation of pavement system successes and failures. The fact that there was very little transverse or longitudinal cracking in both the positive and negative directions seems to indicate that the asphalt-concrete layer is holding up well. Additionally, it is impressive that the asphalt is displaying so little cracking distress despite being subjected to large deformations in the longitudinal (IRI) and transverse (rutting) directions. The fact that ride quality is worse in the southbound direction despite receiving less direct loading from truck traffic indicates that the distresses are not loading-induced. The fact that the sections of the roadway were already performing poorly in 2012 with respect to IRI also indicates that the distresses are not loading-induced. It seems likely then that the cause of IRI and rutting distresses is due to the performance of materials beneath the asphalt-concrete.

Table 3.2 Cracking Index Ratings for Both Directions Between 2012 and 2017

Rating	2017	2017	2015	2015	2014	2014	2012	2012
	Positive	Negative	Positive	Negative	Positive	Negative	Positive	Negative
Good (%)	100	100	100	100	100	100	100	100
Fair (%)	0	0	0	0	0	0	0	0
Poor (%)	0	0	0	0	0	0	0	0
Average Cracking Index	99.91	99.88	99.98	99.93	99.87	99.87	99.94	99.95

Problems with bearing materials below that asphalt-concrete layer were also indicated by the variation in the right and left wheel-path rutting for the positive (northbound) direction. Typically, one would expect the rutting in the right wheel-path to be worse than the left wheel-path given that the pavement system is usually stiffest closest to the centerline where the confining stresses are higher. Stiffness decreases in the transverse direction outward toward the shoulder. As shown in Figure 3.8, rutting distress was significantly worse in the left compared with the right wheel-path for the positive (northbound) direction.

The roadway plans show that the new alignment and lane widening required building most of the road over native subgrade and embankment fill. The rightmost side of the positive lane of travel was partially built over the existing roadway, while the rest of the roadway was built over native subgrade. The fact that the rightmost side of the positive direction was built over the existing alignment likely explains why the right wheel-path had less rutting than the left wheel-path in the positive direction. A similar trend is apparent by comparing each IRI wheel-path distress. In Figure 3.9, the distresses are displayed in the order of the wheel-paths, as they would appear in the up-station (positive, northbound) direction.

It was possible to quantify the pavement system deterioration over time by averaging the pavement distresses for each year, plotting the results, and performing regression on the data, as shown in Figures 3.10 and 3.11.

Figure 3.8 Comparison of Right and Left Wheel-Path Rutting for the Positive Direction

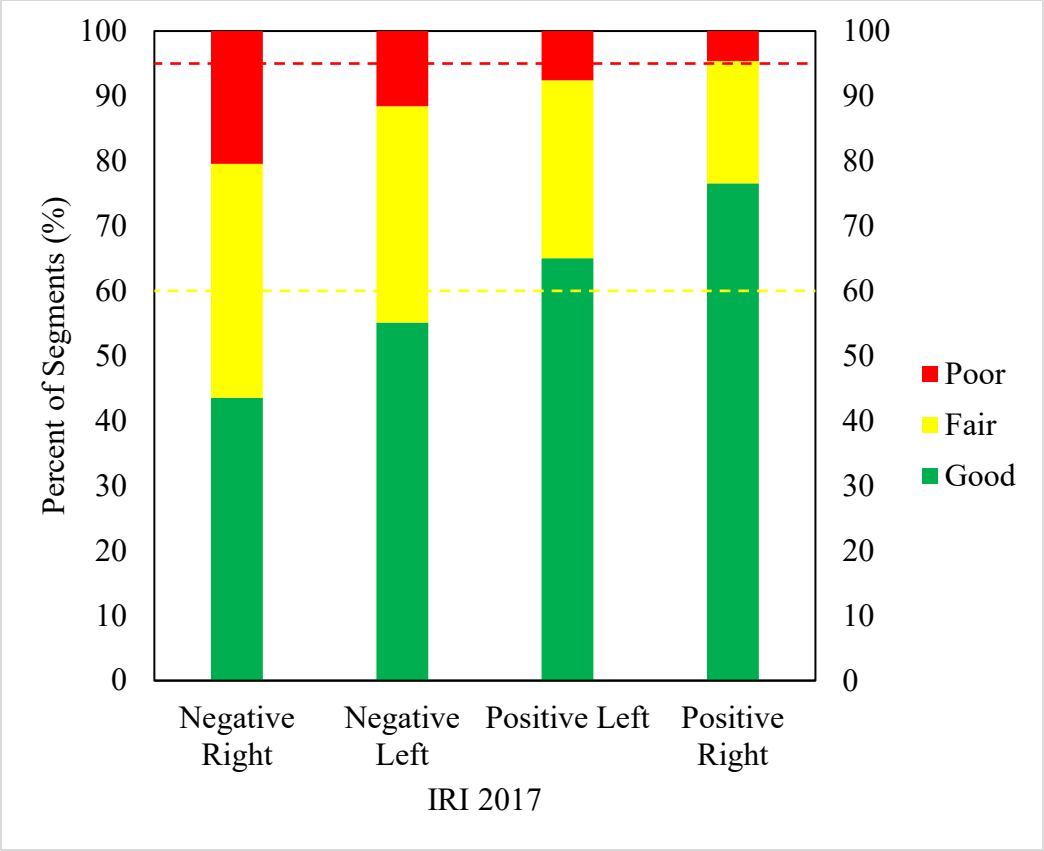

Figure 3.9 Comparison of Right and Left Wheel-Path IRI for Both Directions

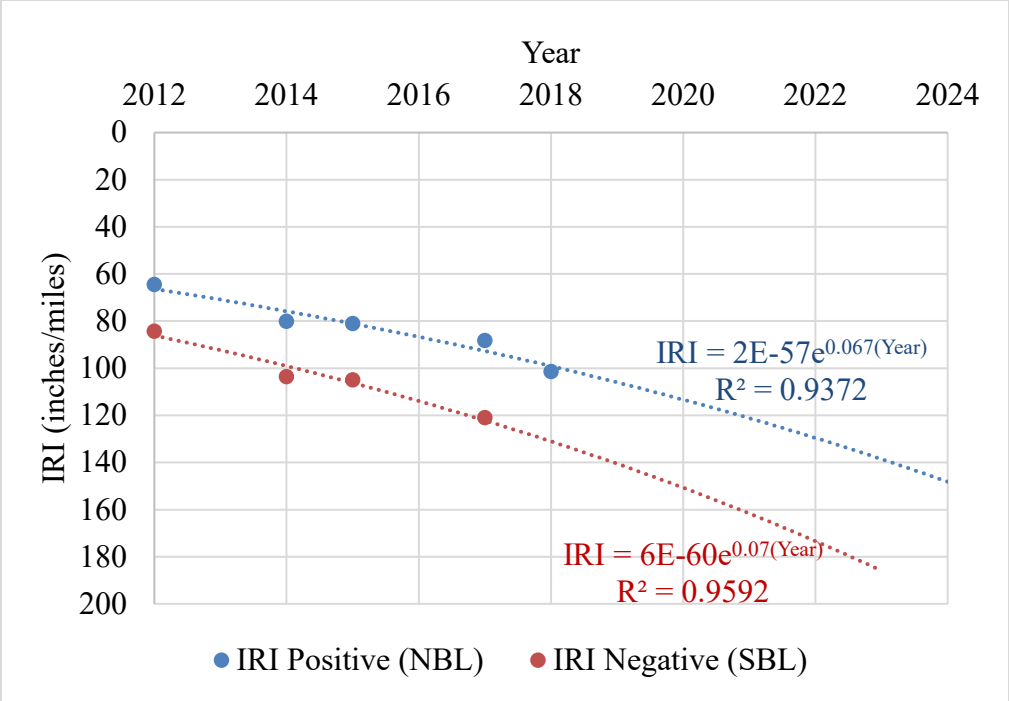

Figure 3.10 IRI as a Function of Time

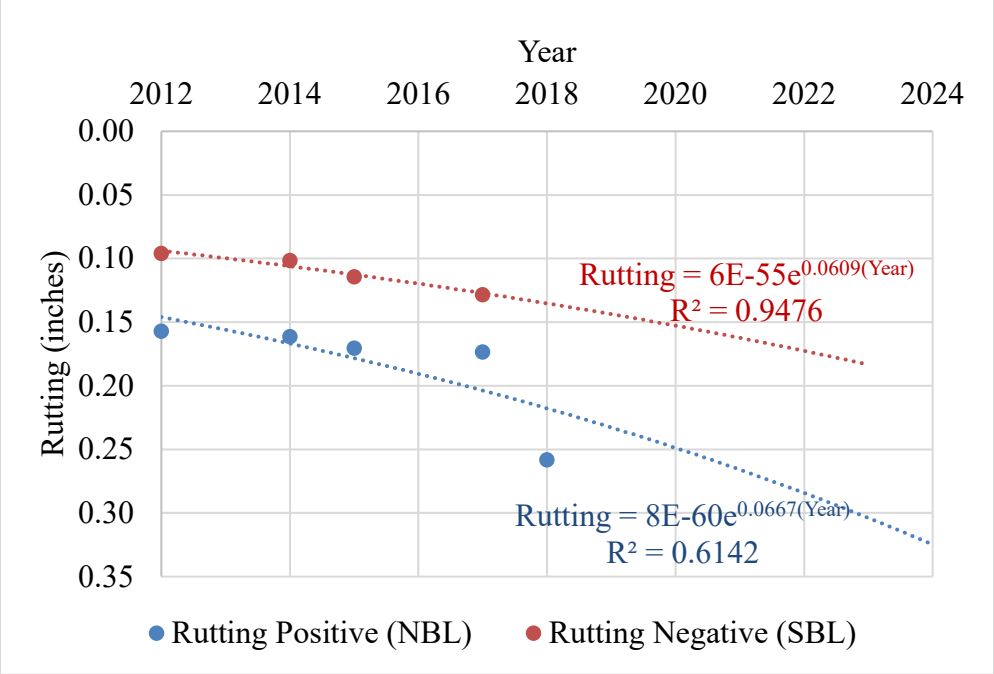

Figure 3.11 Rutting as a Function of Time

For both IRI and rutting, it is clear that the pavement condition is getting worse over time. It is also clear that the pavement in the negative direction is deteriorating faster with respect to IRI while the pavement in the positive direction of travel is deteriorating faster with respect to rutting.

3.2 Location-Specific Pavement Distress Data

The pavement distress data were used as a baseline metric with which to compare the results from field testing. Location-specific pavement distresses were determined by taking a weighted average over a 0.01-mile segment (52.8 ft) and a 0.02-mile segment (105.6 ft). All field testing was performed for the negative direction of travel. The milepost and equivalent station number for each field test location are provided in Table 3.3. The presence of patches at each location is also noted in the table.

Table 3.3 Station and Milepost Data for Each Location

Location	Station	MP	Patch
14	106.18	12.852	No (Test Section)
13	110.95	12.943	No (Test Section)
12	113.38	12.989	No (Test Section)
11	115.89	13.036	No (Test Section)
10	129.92	13.302	No
9	134.97	13.398	No (Shed Entrance)
8	140.83	13.509	No
7	149.06	13.665	Yes (Rotomill)
6	166.46	13.994	No (Crest of Hill)
5	185.76	14.360	No
4	208.13	14.783	Yes
3	214.46	14.903	Yes
2	230.44	15.206	No
1	246.25	15.505	No

Weighted averages of IRI and rutting distress in the negative direction for each location over both a 0.01-mile segment and a 0.02-mile segment are shown in Figures 3.12 and 3.13. There is generally relatively little variation in the values of IRI and rutting between the 0.01-mile and 0.02-mile weighted segments. The exception was Location 7, which recorded a higher IRI distress when weighted over a 0.01-mile segment than a 0.02-mile segment.

In Figures 3.14 and 3.15, a comparison of negative and positive direction IRI and rutting values by testing location is provided. Values shown are those for 0.02-mile segment weighted averages. In Figures 3.16 and 3.17, a comparison is provided between the right and left wheel-paths for the southbound negative direction for IRI and rutting distresses for each testing location.

The distresses at the testing locations mostly match the overall trends found earlier for the entire section. The positive direction performs better with respect to IRI, while the negative direction performs better with respect to rutting. In addition, the performance of the pavement for the right wheel-path is generally worse than the left wheel-path in the negative direction for both IRI and rutting distresses.

There are some limitations associated with using network-level data such as the pavement distresses with location-specific test data. Caution and engineering judgment should be used when comparing the two. Pavement distress data are collected at highway speeds and there may be some error in the collection. To limit variation, location-specific test data are compared with the 0.02-mile weighted average rather than the 0.01-mile weighted average.

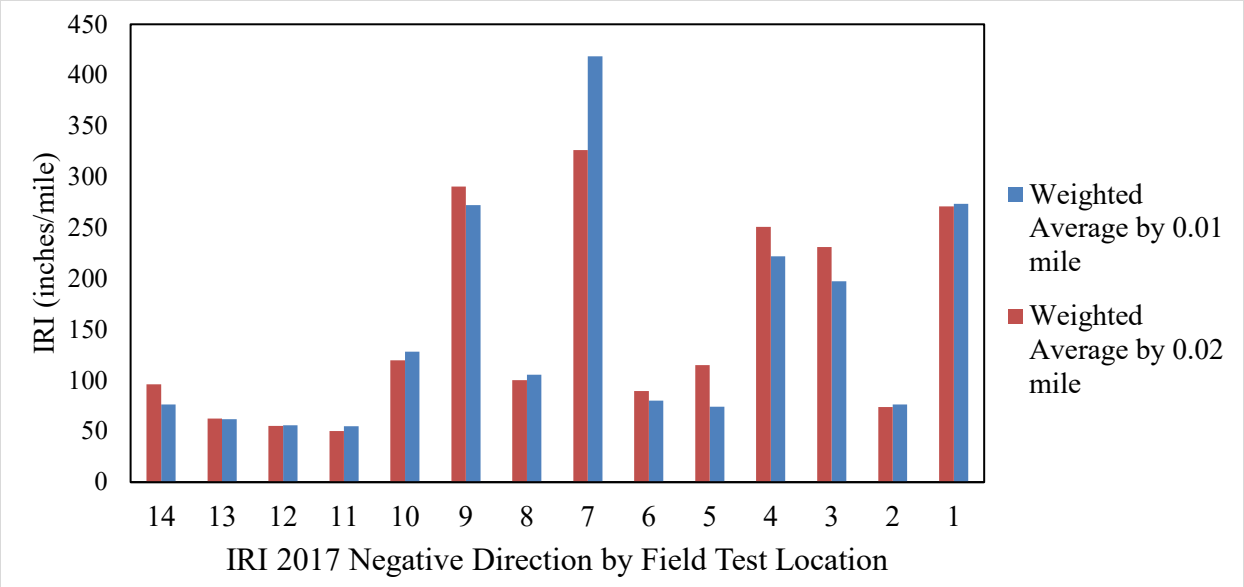

Figure 3.12 2017 Negative Direction IRI by Location

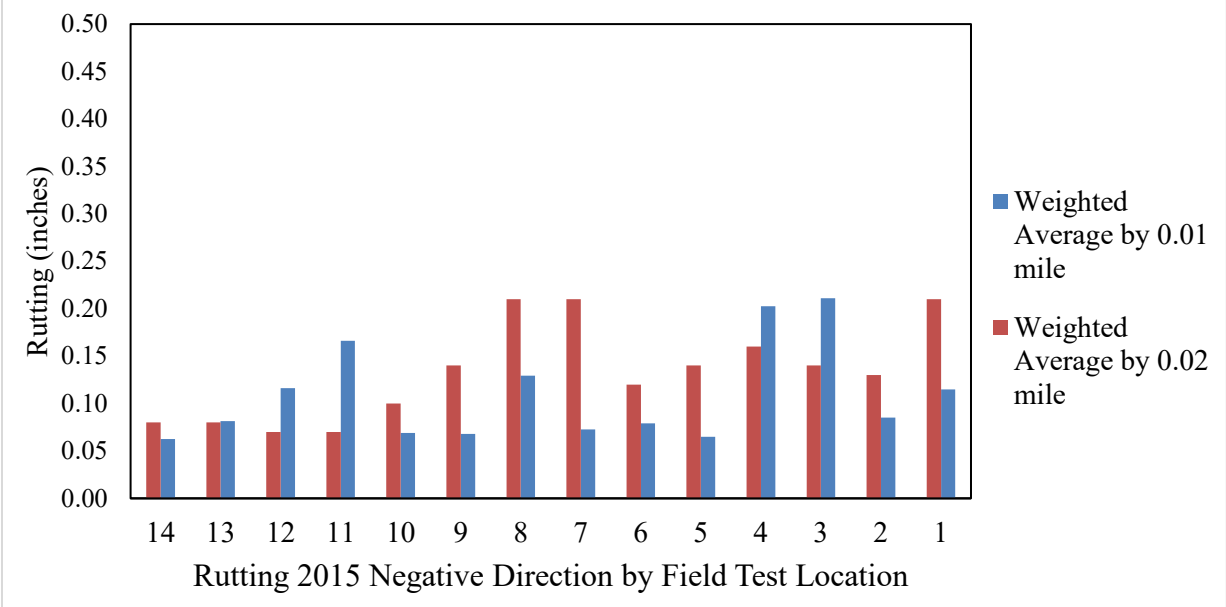

Figure 3.13 2015 Negative Direction Rutting by Location

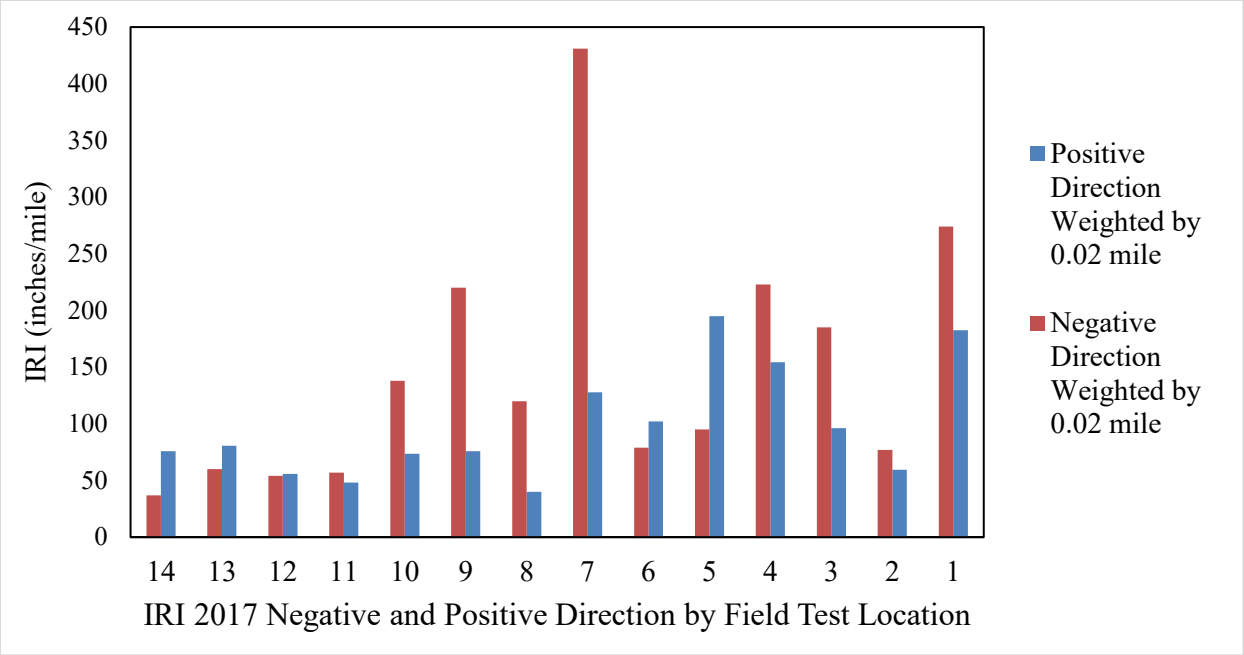

Figure 3.14 Comparison of Negative and Positive Direction 2017 IRI by Location

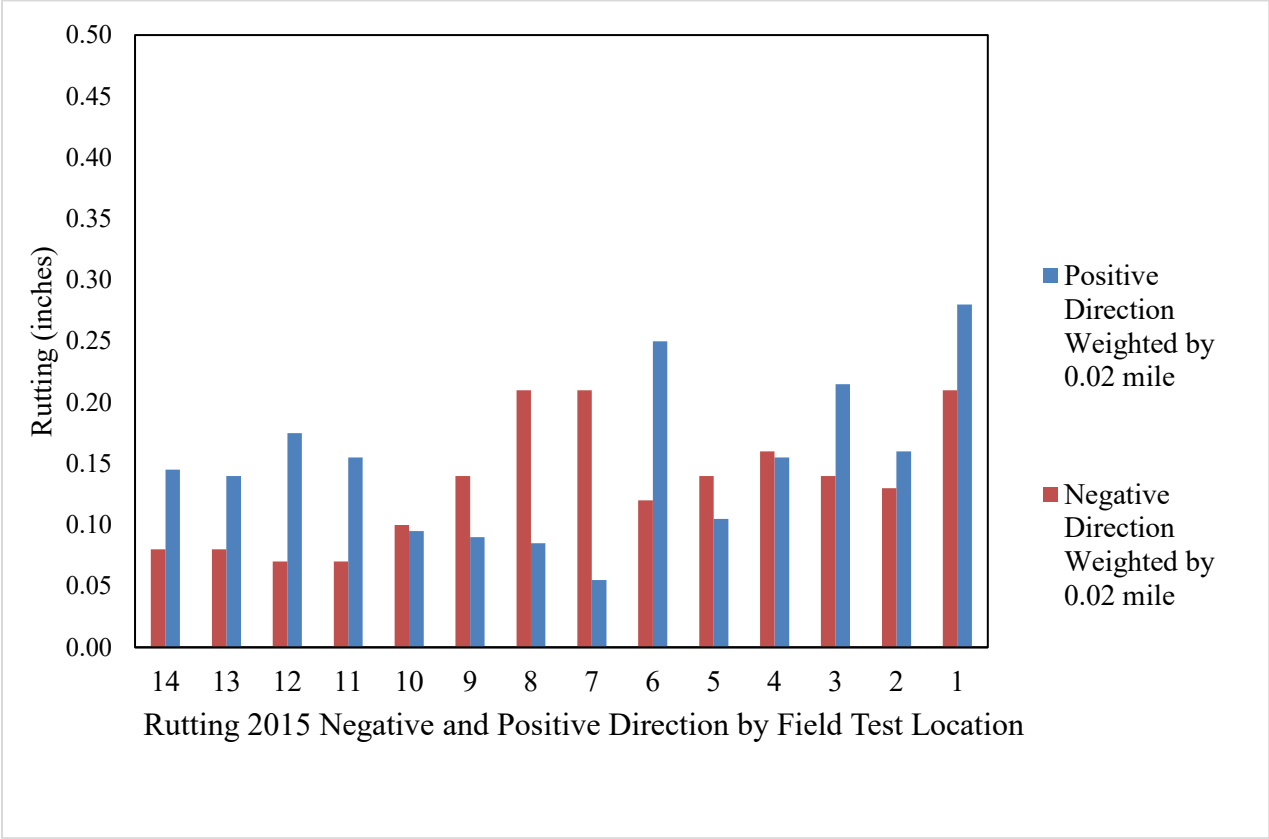

Figure 3.15 Comparison of Negative and Positive Direction 2015 Rutting by Location

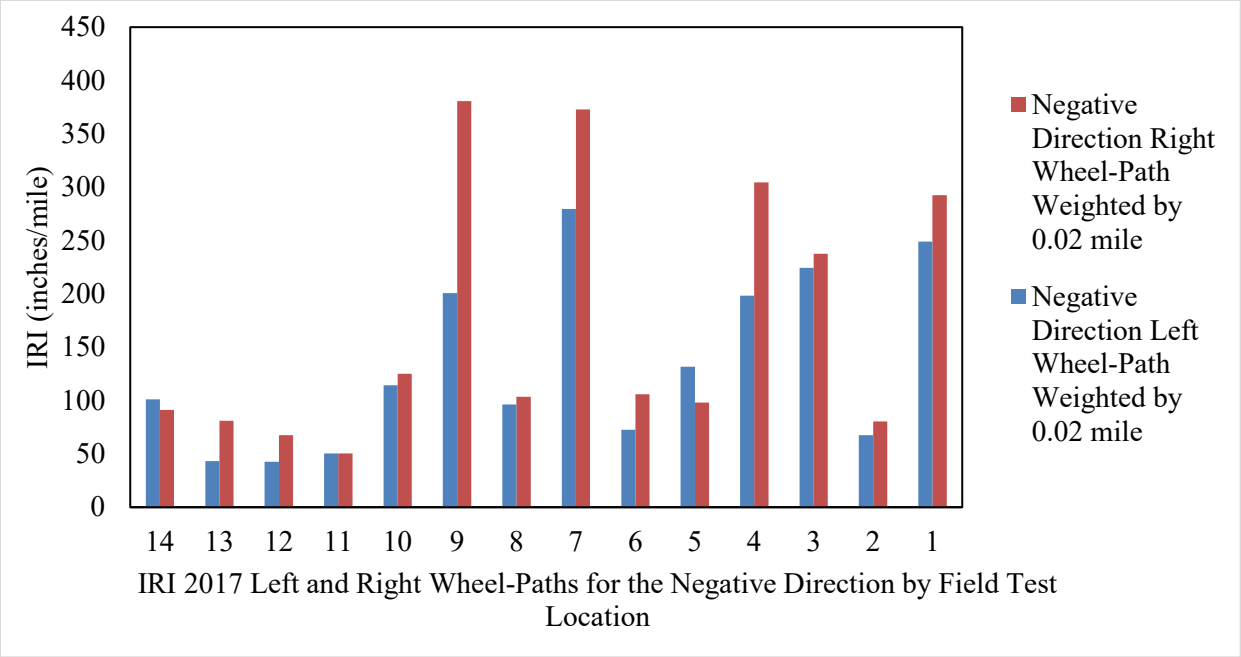

Figure 3.16 Comparison of Left and Right Wheel-Path 2017 Negative Direction IRI by Location

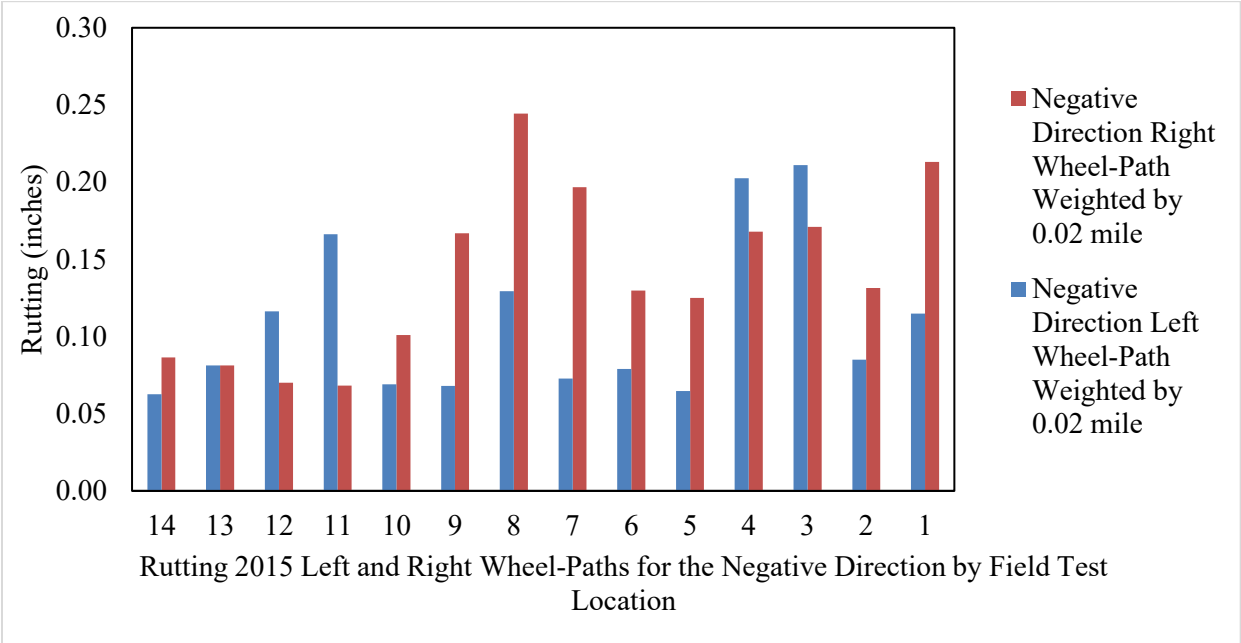

Figure 3.17 Comparison of Left and Right Wheel-Path 2015 Negative Direction Rutting by Location

3.3 Additional Field Condition Data

Although it is not immediately relevant to the problem statement, it is interesting to evaluate the frictional resistance of the wearing surface. UDOT collects skid data for state routes and interstates every year. Skid values are collected at approximately every milepost. The skid data for SR-10 between mileposts 11.02 and 17.02 are summarized in Table 3.4. According to UDOT guidelines, greater than 45 is acceptable, 35 to 45 is marginal, and less than 35 is unacceptable for non-interstate routes. Acceptable values are highlighted in green in Table 3.4; those that are marginal are highlighted in yellow, and those that are unacceptable are highlighted in red. From the skid data provided in Table 3.4, it is apparent that the section between Muddy Creek (MP 15.8) and Emery (12.8) is performing worse than the adjacent mileposts for all years from 2012 through 2018. UDOT Report No. UT-13.03 (Anderson, 2013) lists polishing aggregates and surface bleeding as the two primary causes for loss of skid resistance for asphalt-concrete pavements. A review of the pavement images from Roadview Explorer was unable to reveal significant areas with asphalt bleeding. Bleeding was not identified during the field visits.

Table 3.4 Skid Data for SR-10 Between Mileposts 11.02 and 17.02

Milepost	2012 Skid	2013 Skid	2014 Skid	2015 Skid	2016 Skid	2017 Skid	2018 Skid
11.02	55.4	59.4	55.7	55.8	68.9	65.3	60.0
12.02	51.1	55.0	53.0	52.8	59.4	50.4	57.3
13.02	27.8	36.4	27.5	26.8	40.1	39.2	30.5
14.02	30.4	44.1	33.6	31.8	39.9	37.8	38.0
15.02	31.5	41.9	37.0	34.0	47.0	40.6	37.4
16.02	50.2	51.9	41.8	41.1	48.7	60.6	65.8
17.02	42.1	48.6	44.2	46.4	47.7	61.0	65.5

4. EVALUATION OF CONSTRUCTION DOCUMENTS

The construction documents, including the construction plans, report, and laboratory testing results, were reviewed for possible sources of information regarding failures and successes of the different portions of the pavement system along the section of SR-10 being evaluated.

4.1 Roadway Alignment

The design plans show that as part of the reconstruction of SR-10 between Emery and Muddy Creek, a new alignment was chosen. In addition, the roadway was widened in several places to include passing and acceleration lanes. Additionally, the vertical curvature was changed, necessitating the use of cut and fill. These changes resulted in a large portion of the new roadway needing to be constructed on either native subgrade or fill. In Figure 4.1, the roadway alignment between stations 117+00 (MP 13.06) and 122+00 (MP 13.15) is shown.

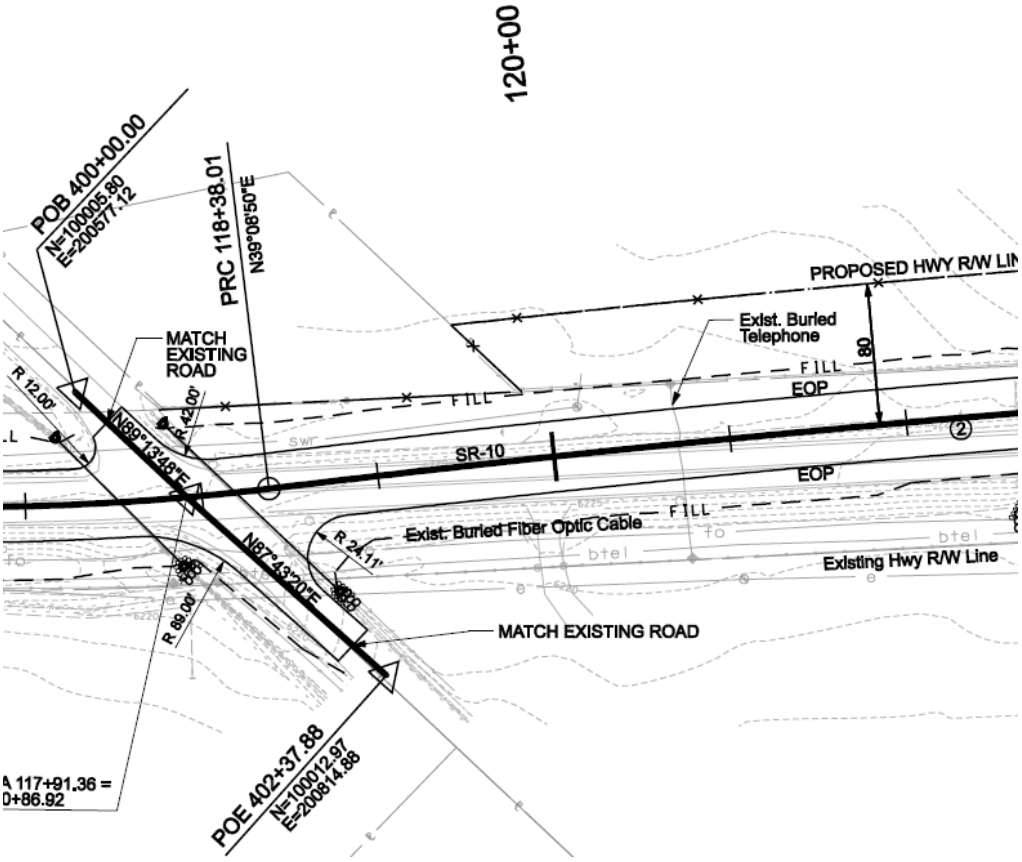

Figure 4.1 Roadway Plan Between Stations 117 and 122

Note how the new alignment begins to diverge from the existing alignment at approximately station 118+50. By station 122+00, only the rightmost half (looking up-station) of the new alignment is consistent with the existing alignment. The new alignment only partially overlaps with the old alignment for the rest of the 3.03-mile section. The new alignment does not rejoin the existing alignment until station 255+00 right before Muddy Creek, as shown in Figure 4.2.

The new alignment from station 217+00 to 222+00, which is shown in Figure 4.3, is a good representation of most of the 3.03-mile segment. Only a small portion of the positive lane of travel of the new alignment overlaps with the existing alignment. The rest of the new roadway was built on native subgrade soil or fill composed of native soils.

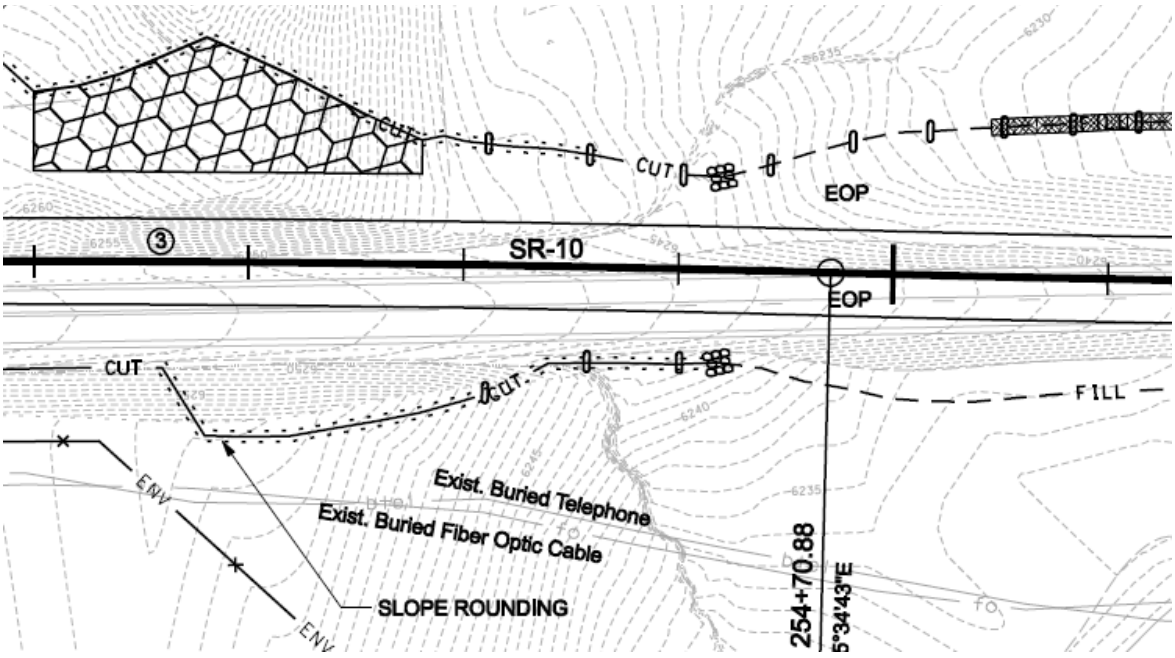

Figure 4.2 Roadway Plan Between Stations 251 and 256

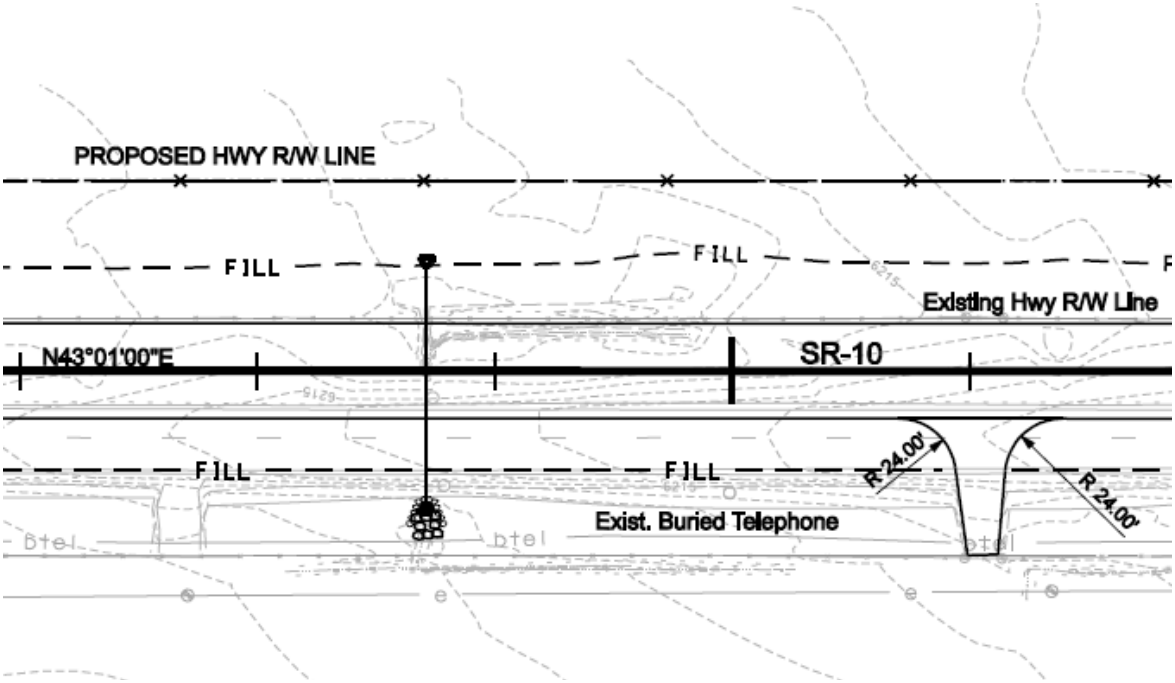

Figure 4.3 Roadway Plan Between Stations 217 and 222

The section of roadway that overlaps with the old alignment is approximately between mileposts 12.83 (Station 105) and 13.13 (Station 121) and between mileposts 15.63 (Station 253) and 15.86 (Station 265). In Figures 4.4 and 4.5, comparisons of distress ratings between the sections that overlap with the existing alignment and those that do not are provided.

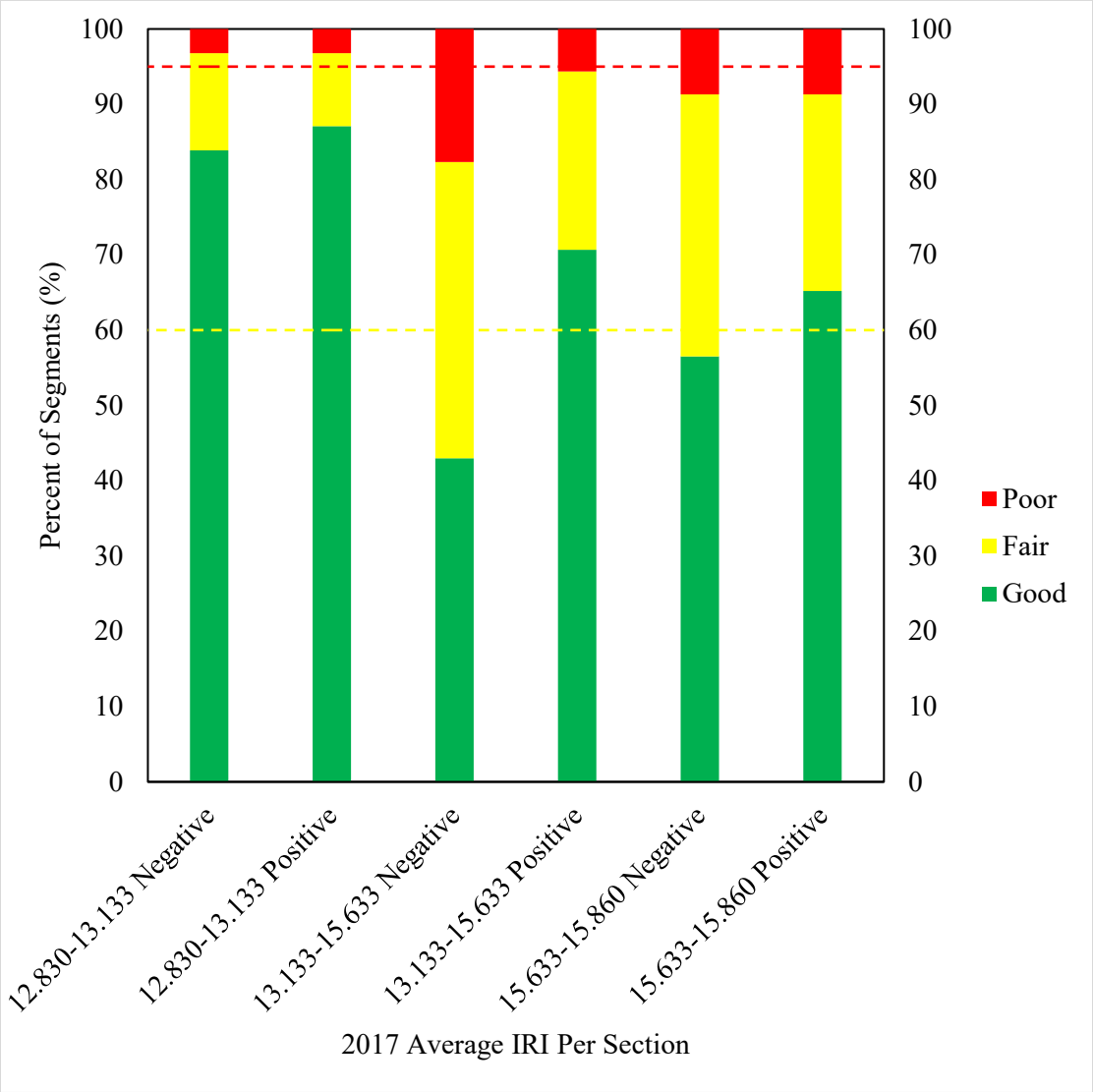

Figure 4.4 Comparison of 2017 Negative and Positive Direction IRI by Roadway Section

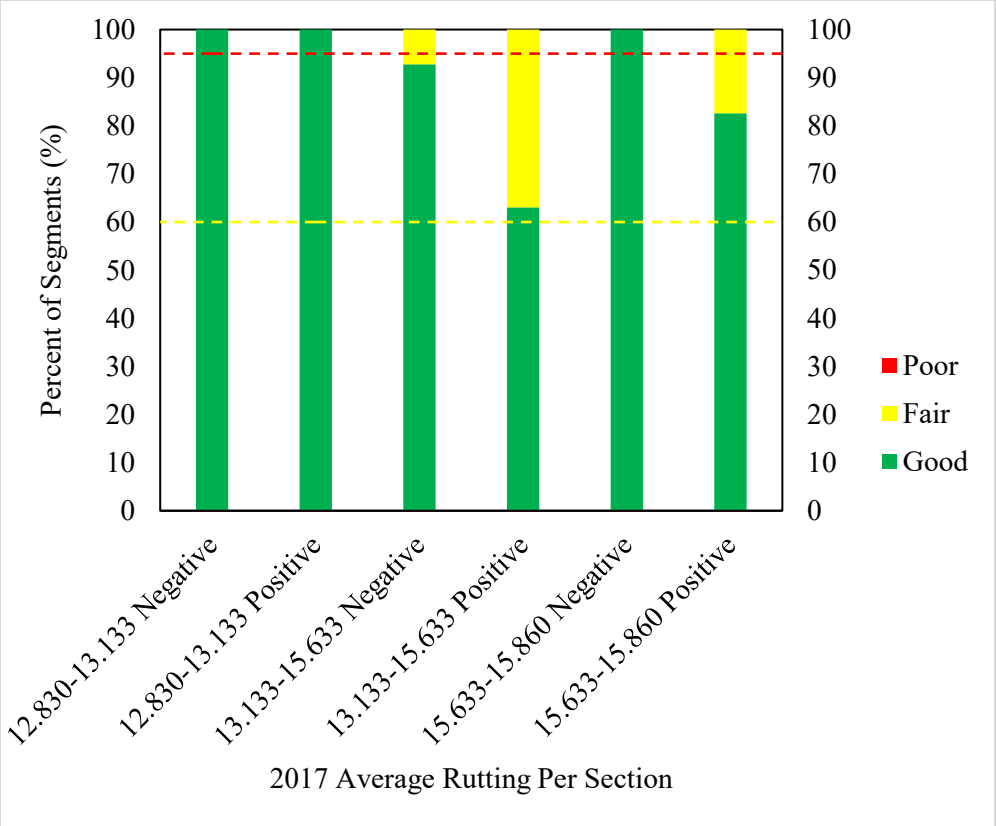

Figure 4.5 Comparison of 2017 Negative and Positive Direction Rutting by Roadway Section

The section between mileposts 12.830 and 13.133 has performed better than the section between mileposts 13.133 and 15.633. This difference is likely because the first section was built over the old alignment while the second section was built on native subgrade or fills of varying depth composed of native soils. The section between 15.633 and 15.860 also appears to have been built on the old alignment but is performing worse than the test section. This difference may be because this section is the approach to the bridge at Muddy Creek.

Note that test Locations 11, 12, 13, and 14 (stations 115.89, 113.38, 110.95, and 106.18, respectively) were all within the section of roadway that overlapped with the old alignment. The rest of the test locations were on sections of the roadway where only a small portion of the positive direction of travel overlapped with the existing alignment.

4.2 Embankment Fill

In addition to building much of the new alignment over native subgrade, embankment fill was needed to develop the vertical design grade and cross-slope. The construction documents include a super-elevation diagram with the centerline difference between the proposed and existing ground surface elevations at intervals of 50 feet (half-station). From these data, it was possible to determine the fill and cut heights at the centerline. Embankment depths are shown in Figure 4.6. Positive values denote fill, and negative values denote cut. The same data are plotted in Figure 4.7, with the 2017 IRI average of both directions superimposed on the same plot.

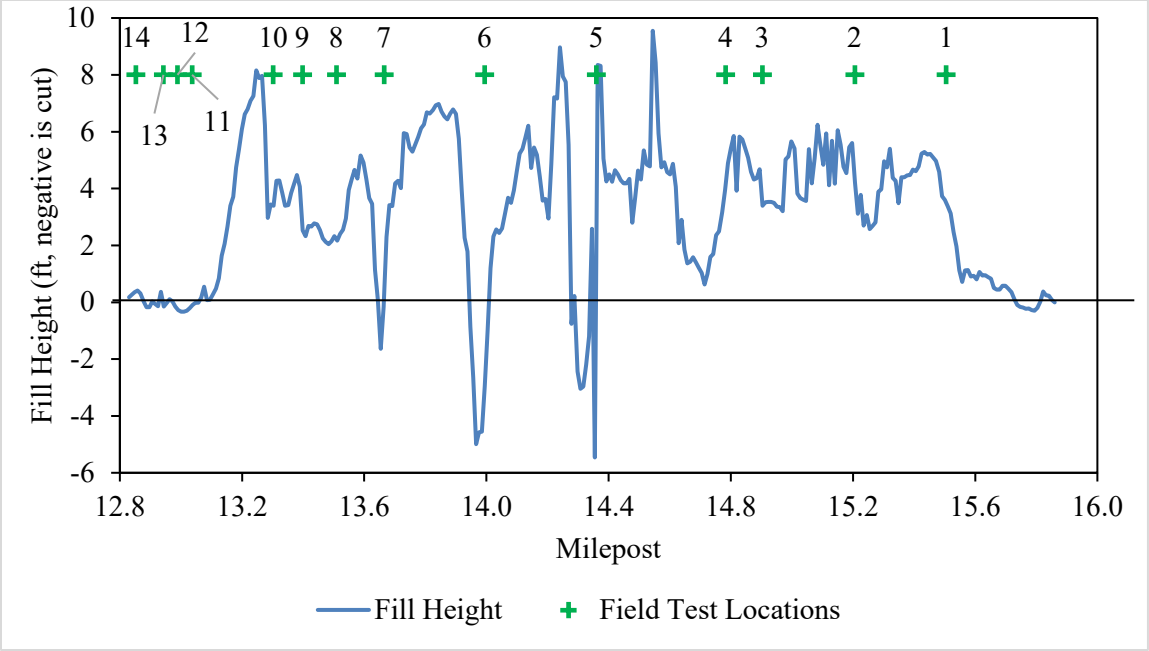

Figure 4.6 Centerline Cut and Fill Depths

The construction documents include typical cross-sections where embankment fill was needed to achieve the design cross-slope. A typical cross-section between stations 140+00 (MP 13.493) and 157+15 (MP 13.865) is shown in Figure 4.8.

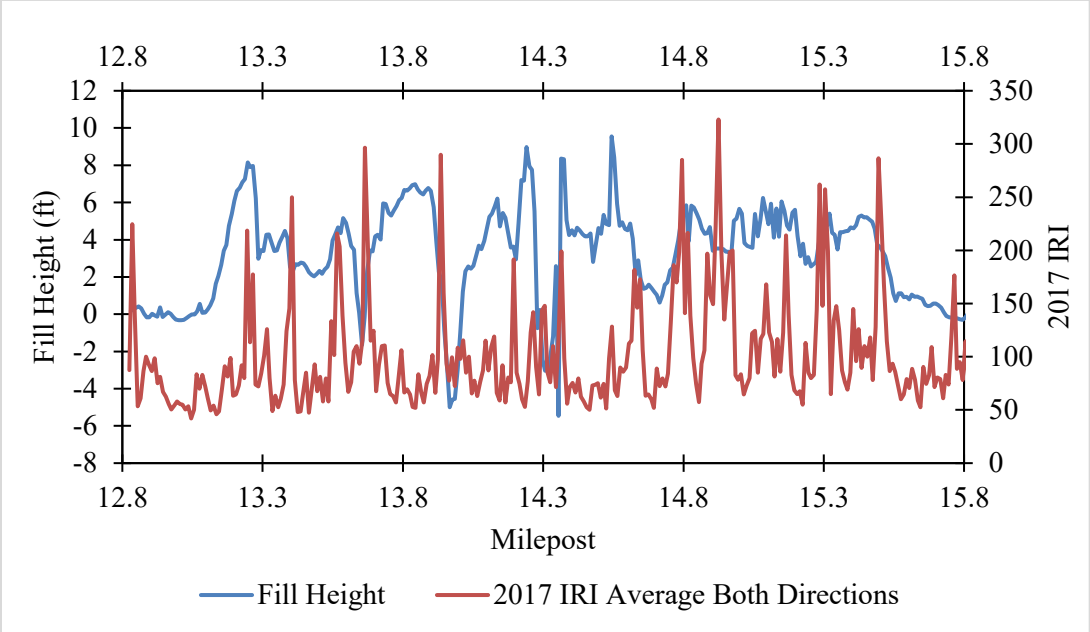

Figure 4.7 Comparison of 2017 IRI and Centerline Fill Height

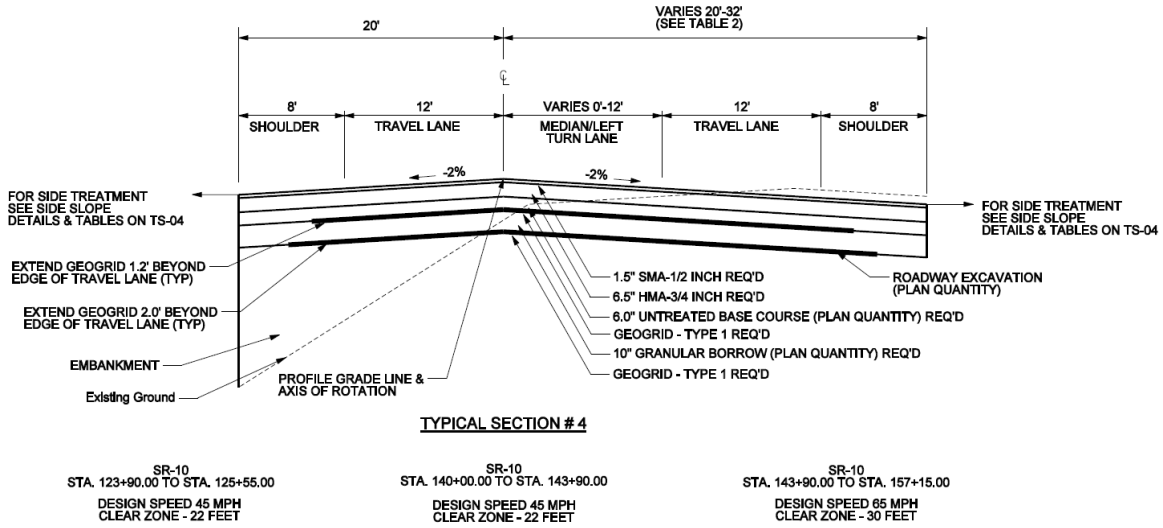

Figure 4.8 Typical Cross-Section Showing Deep Embankment Fill beneath the Negative Direction of Travel

A significant embankment fill was needed below the negative travel lane to produce the design cross-slope. From Figure 3.1, it is clear that several IRI spikes occur in the negative direction between mileposts 13.5 and 13.9, where the above cross-section is representative. It is likely that the characteristics of the embankment fill or native subgrade soil are negatively affecting the performance of the pavement.

Individual cross-sections for each station were acquired late in the project. A simple evaluation of the cross-sections revealed that the embankment fill was much deeper for the southbound lane, sometimes ranging in depths from 5 to 20 feet, as shown in Figure 4.9 (note that the scale varies for the x and y-axes).

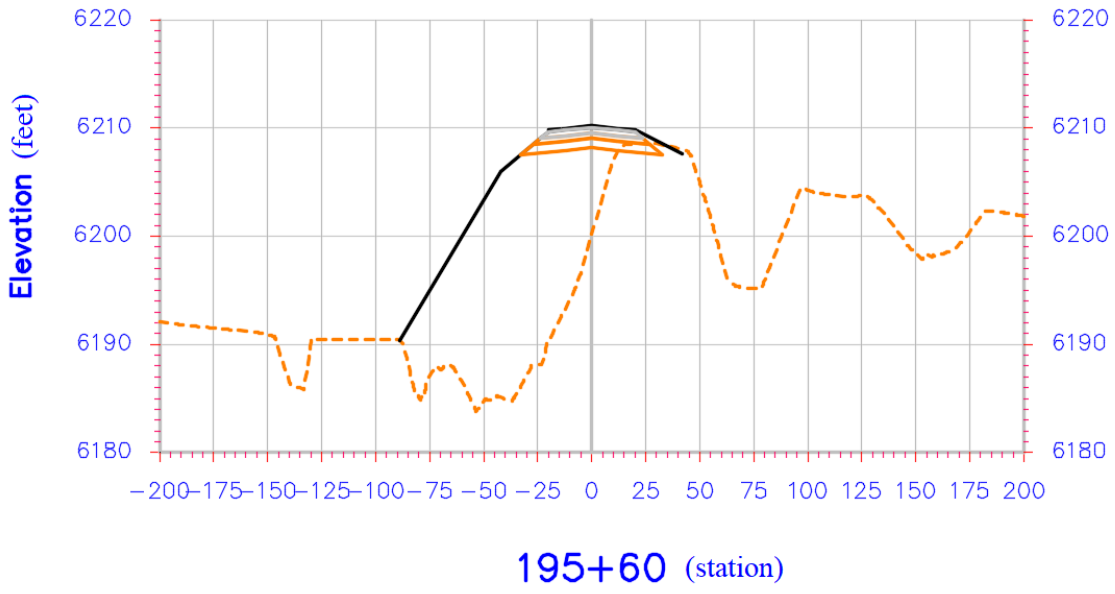

Figure 4.9 Cross-Section at Station 195+60 Showing Deep Embankment Fill

The amount of roadway excavation is specified in the summary of items in the construction plans. However, the amount of embankment fill is not specified, nor is the type of material that is to be used as embankment fill. UDOT Standard Specifications require that a "suitable granular material" be used as embankment fill. From the construction report, it is evident that native soils from roadway excavations were used as embankment fill at adjacent stations. The quotes below are from the construction report logs (UDOT, 2010).

> "Continued hauling material from cut section lt of sta-164+00 to sta-168+00 to fill area at sta-225- to- sta-228 lt." User ID: Imanzana Date: 2/11/2010
>
> "Embankment is being placed using 2 scrapers, a grader, sheepsfoot and a water truck. The material is coming from the cut @200-207." User ID: dmblack Date: 1/06/2010
>
> "The Scrapers are hauling material from the cut @ 170 to135 for embankment." User ID: dmblack Date: 1/25/2010
>
> "Nielson contractor scarified grade material from sta- 225+00 to sta-228+00 and rerolled before placing any more embankment in this area. Continued hauling material from cut section lt of sta-164+00 to sta-168+00 to fill area at sta-225- to- sta-228 lt." User ID: Imanzana Date: 2/11/2010"

The centerline fill height at each test location was determined by linearly interpolating between the two closest known mileposts. The fill heights for each location are shown in Figure 4.10. It should be noted that these are the centerline fill heights. The fill heights are generally greater for the negative direction of travel. Results from grain size distribution and Proctor tests performed on the roadway excavation/ embankment fill by UDOT personnel in 2009 and 2010 are shown in Figure 4.11.

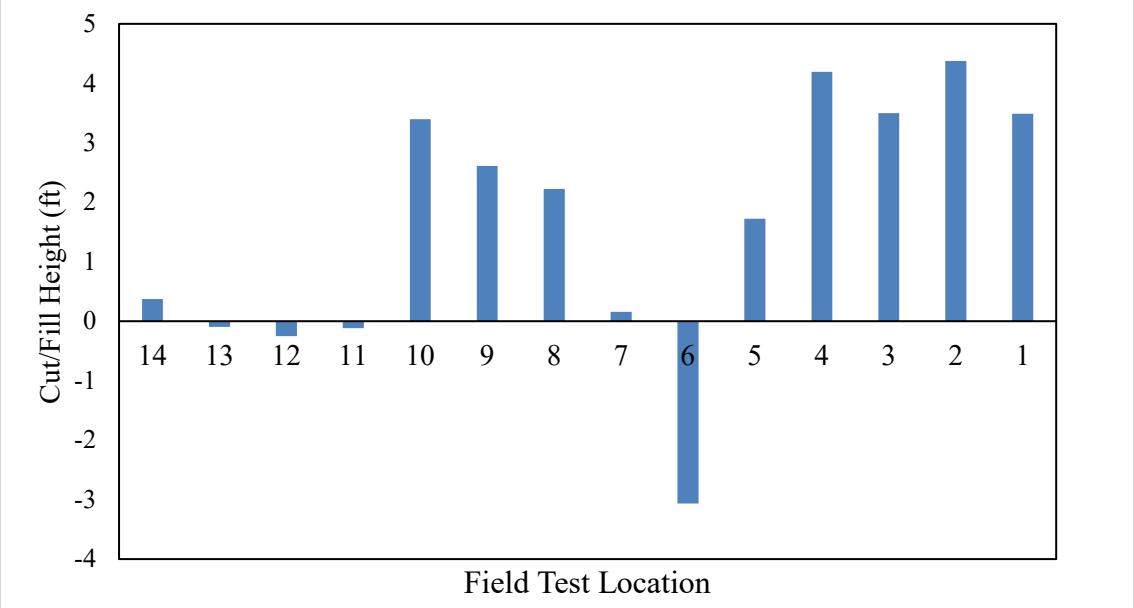

Figure 4.10 Centerline Fill Depth by Field Test Location

Project Name: US-10; Emery to Muddy Creek
Project Number: S-0010(40)13

Lab #	Description	3/4	#4	#10	#40	#200	LL	PI	Dry Den.	Opt. H2O	Soil Class	Date
5527	Roadway X Sta.223+25	100	97	96	95	85	33.65	16.33	106.5	15.5%	A-6(10)	11/23/2009
5526	Pipe Backfill (UTBC)	91	35	21	12	8	18.91	3.31	140.5	7.2%	A-1-a(0)	11/23/2009
5529	Roadway X Sta.223+25	68	68	68	66	59	39.21	24.78	116.4	19.4%	A-6(11)	12/3/2009
5530	Granular Borrow Vic Price Pit	98	48	36	30	15	NP	NP	138	7.0%	A-1-a(0)	12/11/2009
5528	Pipe Backfill -2" Granular Borrow	88	27	17	11	7	16.9	1.81	141.2	7.3%	A-1-a(0)	12/1/2009
5500	-2" Granular Borrow	86	24	14	8	5	18.65	1.76	142.9	5.2%	A-1-a(0)	1/12/2010
5501	Roadway X Sta.223+25	88	78	69	61	37			119.4	11.3%		1/19/2010

Figure 4.11 Construction Log for Soil Testing of Roadway Excavation and Granular Borrow

From the test results, it is clear that the roadway excavation was mainly composed of fine-grained material. The fines fraction ranged from 37% on the low end to 85% on the high end. These results were confirmed by subsequent field sampling done on two cut locations, as described in Section 5.2 on the testing of subgrade materials.

If the embankment fills were mainly a fine-grained soil, as seems probable from the available data, it is likely that the embankments are vulnerable to wetting-induced volume changes.

4.3 Culverts

Another element that should be investigated is the presence of culverts relative to areas showing poor pavement condition performance. A plot of IRI in the negative direction for 2017 is shown in Figure 4.12, with the locations of culverts superimposed on the same plot.

Without doing a hydrological analysis of the surrounding topography, the location of culverts can be used to indicate the presence of seasonal surface water flow. If culverts were not draining properly, it could lead to nearby embankment fill being saturated. The saturation of embankment fill could lead to wetting-induced volume changes, especially if the soil were fine-grained and cohesive. Additionally, it is possible that differential settlements would occur given that the granular backfill (UTBC) used around the culvert is less vulnerable to wetting-induced volume changes. Of particular importance are the spikes in IRI between mileposts 13.5 and 13.9, where cross-sections with deep embankment fill beneath the negative direction of travel were common. A photograph of a patch area with a visible IRI undulation in the negative direction of travel is provided in Figure 4.13. Note the presence of culvert markers next to the undulation.

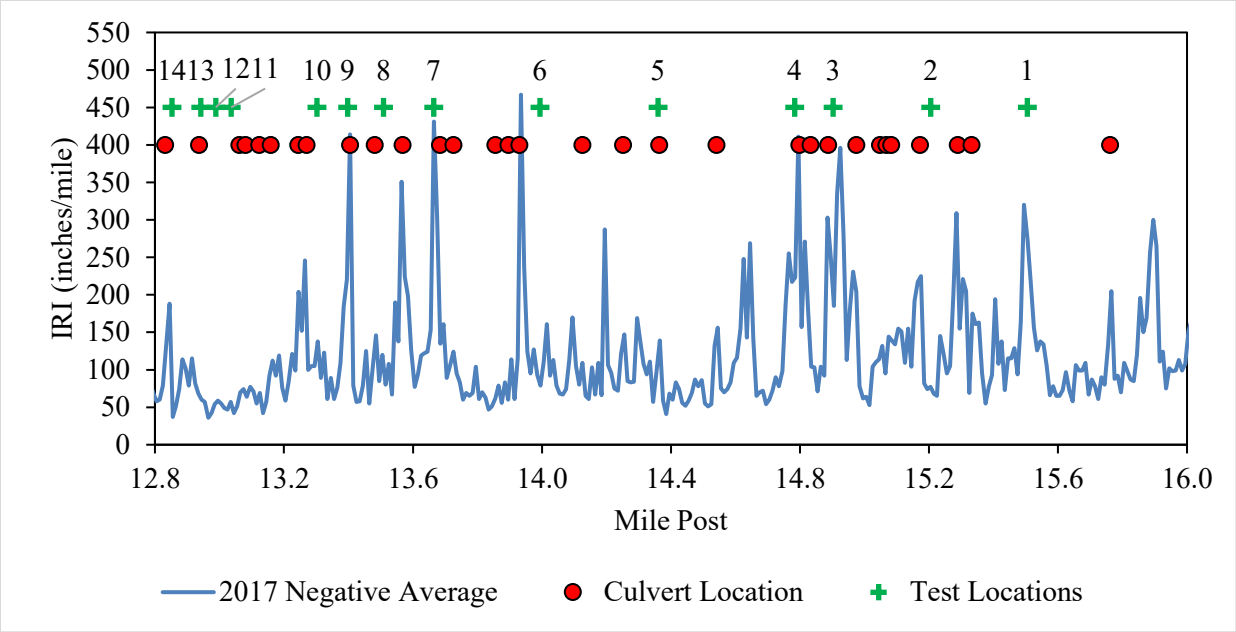

Figure 4.12 Comparison of Location of Culverts with 2017 Negative Direction IRI

Figure 4.13 Photograph Looking Northbound (Positive Direction) of Patch Area with IRI Undulation in the Negative Direction of Travel Indicated by Red Arrows. Culvert Markers are Indicated by Green Arrows. (Courtesy of UDOT/Mandli Communications)

The values of IRI in the negative direction for 2017 at the location of each culvert were determined and compared with the 3.03-mile section. The results are shown in Figure 4.14 and Table 4.1.

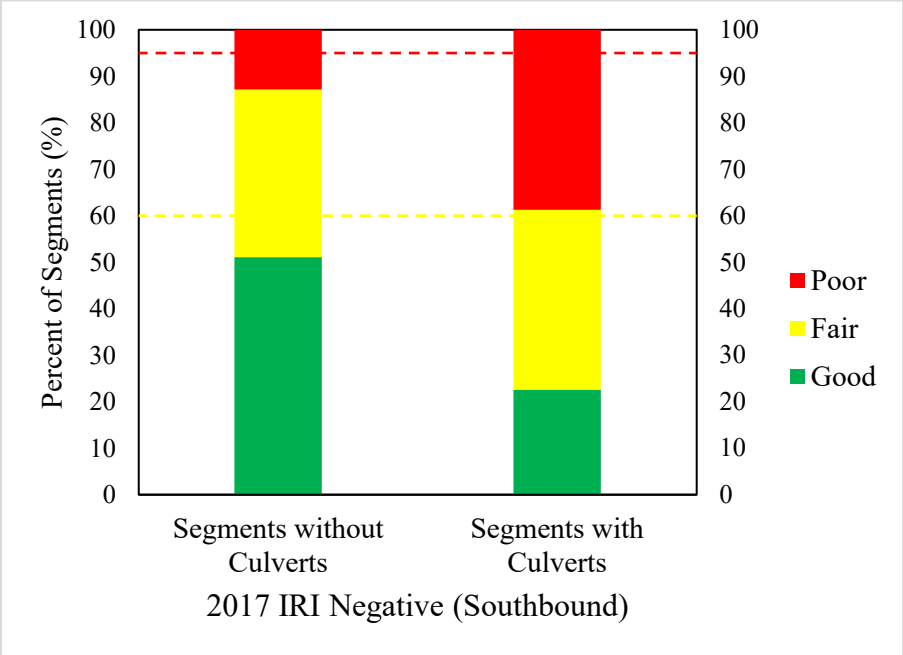

Figure 4.14 Comparison of 2017 Negative Direction IRI Between Segments with and without Culverts

Table 4.1 Comparison of 2017 Negative Direction IRI Between Segments with and without Culverts

	Segments without Culverts	Segments with Culverts
Good (%):	51.1	22.6
Fair (%):	36.0	38.7
Poor (%):	12.9	38.7
Average IRI:	110	179

More than twice as many 0.01-mile segments were in poor condition in areas with culverts compared with areas without culverts along the 3.03-mile section being analyzed. The IRI in the negative direction was, on average, 61.9% higher for segments with culverts. Therefore, it is clear that the pavement condition is worse in areas with culverts compared with areas without culverts.

4.4 Compaction at Low Temperatures

The temperature at which the compaction of the pavement system was carried out may have had a negative effect on the performance. The construction log indicated that a significant portion of compaction of the subgrade, GB, and UTBC layers was done between December and March, with temperatures typically ranging from the teens to mid-40s. The daily construction logs list the daily high and low temperatures. UDOT Standard Specifications do not have a minimum temperature at which compaction operations must cease. However, the standard does say that material cannot be placed on "frozen and snow-covered areas." Snow and frozen material must be removed from the area of placement before compaction. The construction logs indicate that UDOT field engineers asked the contractor to

remove frozen material from the embankment on multiple occasions (December 3, 2009; December 21, 2009; January 12, 2010).

The influence of temperature on the moisture-density relationships of sand with a trace of silt is shown in Figure 4.15. As the temperature of the soil decreases, the as-compacted dry density of the soil achieved using constant energy and a consistent method of compaction decreases considerably (Waidelich, 1990). At lower temperatures, more compactive effort is needed to achieve the same value of as-compacted dry density. As a consequence, it is difficult to obtain the required minimum value of relative compaction when temperatures are near or below freezing. Insufficient compaction could have caused differential settlement during the service life of the pavement. If cohesive soils are compacted at temperatures at or below freezing, the borrow material tends to contain hard clods that are stiff and brittle when frozen. These clods are difficult to compact and the resulting as-compacted soil typically contains either the original hard clods or broken pieces of clods with large void spaces between them. Later, when the compacted soil thaws, the clods become soft and will compress under the existing loads from the pavement system and embankment fill above it. The result is usually differential settlement of the entire pavement system that occurs relatively soon after the compacted soil thaws. From the available evidence, it seems likely that this type of phenomenon probably contributed to the poor performance of the pavement system for those sections that contained embankment fills.

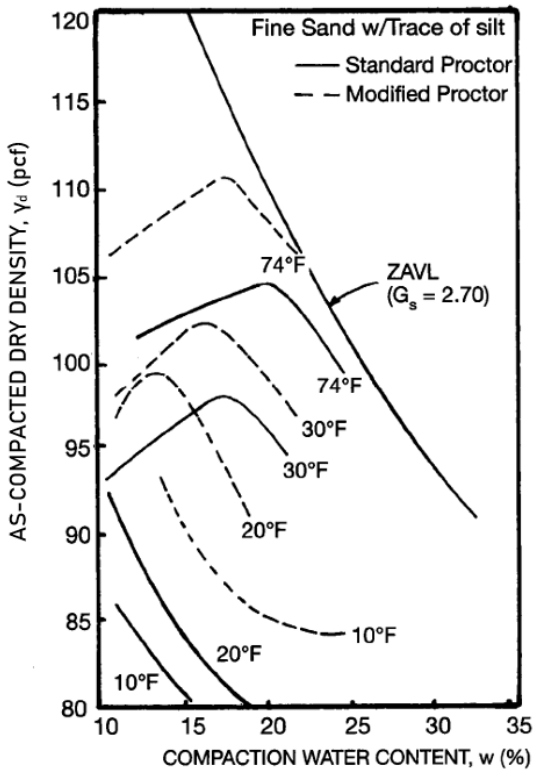

Figure 4.15 Influence of Temperature on Moisture-Density Relationships of Compacted Soil (from Waidelich, 1990, as cited in Lawton, 2001)

5. EVALUATION OF RESULTS FROM LABORATORY TESTING

Samples collected during field testing on July 25, 2018, were taken from Emery, Utah, to the University of Utah's Geotechnical Engineering and Materials Laboratories in Salt Lake City, Utah. Samples were taken from the pavement system, including asphalt cores and bag samples of the untreated base course and the granular borrow layers. Additional field sampling was carried out in July 2019. The purpose of the additional sampling was to gather native subgrade soil that may have been used as fill material (roadway excavation) when SR-10 was reconstructed in 2009-2010. The researchers were not permitted to get samples from directly beneath the pavement system, so samples were taken from several areas where fill material was excavated (the cut sections for the roadway realignment).

The purpose of the laboratory testing program was to determine the engineering properties and characteristics of the pavement system, namely the asphalt-concrete, untreated base course, granular borrow, and excavated fill/native subgrade layers. The broader goal of the laboratory testing can be broken down as follows:

- Determine if sampled materials met as-constructed specifications as set out by UDOT.
- Note material characteristics that could explain pavement system degradation and failure.
- Use results from laboratory testing to compare with field-testing and baseline pavement distress data.

Unless otherwise stated, the ASTM or other relevant standard was followed for all laboratory testing.

5.1 Evaluation of Results from Laboratory Testing of Untreated Base Course and Granular Borrow

The following tests were performed on the bagged untreated base course (UTBC) and granular borrow (GB) samples obtained during the first round of field testing:

- Particle-size analysis – ASTM D422
- Amount of material finer than 75-μm (No. 200) sieve – ASTM D1140
- Liquid limit, plastic limit, and plasticity index – ASTM D4318
- Soil classification – ASTM D2487
- Liquid limit, plastic limit, and plasticity index via fall cone method – ISO17892

The liquid limit and plasticity index used to determine the soil classification of materials were based on testing performed using the standard ASTM method with the Casagrande apparatus. Complete datasets for Atterberg limit tests for both the standard and fall cone method are shown in Appendix A. Plots showing the position of the fine-grained portion of the tested soil on a plasticity chart are also included.

Particle-size analysis was carried out with the following sieves: 1½ inch, ¾ inch, ⅜ inch, #4, #10, #40, #60, #100, #140, #200. Detailed datasets for the particle-size analysis, including percent passing each sieve, particle size for which 60%, 30%, and 10% of the soil passes (D_{60}, D_{30}, D_{10}, respectively), coefficient of curvature (C_c), and coefficient of uniformity (C_u), are included in Appendix A. Results of gradation, Atterberg limits, and classification according to the Unified Soil Classification System and the AASHTO Classification System are summarized in Table 5.1 for the UTBC samples and in Table 5.2 for the GB samples.

Table 5.1 Summary of Results from Laboratory Testing of UTBC

Location ID	Gravel (%)	Sand (%)	Fines (%)	Gradation	Liquid Limit	Plasticity Index	USCS (Full)	AASHTO
1-A	52	37	10	Poor	30	12	GP-GC	A-2-6(0)
			(Poorly graded gravel with clay and sand)					
2-C	51	37	12	Poor	21	6	GP-GC	A-2-4(0)
			(Poorly graded gravel with silty clay and sand)					
3-C	58	31	10	Poor	27	10	GP-GC	A-2-4(0)
			(Poorly graded gravel with clay and sand)					
4-C	56	33	11	Poor	22	8	GP-GC	A-2-4(0)
			(Poorly graded gravel with clay and sand)					
5-C	48	39	13	NA	21	6	GC	A-1-a(0)
			(Silty, clayey gravel with sand)					
6-C	57	32	12	Well	27	9	GW-GC	A-2-4(0)
			(Well-graded gravel with clay and sand)					
7-C	49	39	13	NA	21	5	GC-GM	A-1-a(0)
			(Silty, clayey gravel with sand)					
8-C	50	37	13	NA	19	4	GC-GM	A-1-a(0)
			(Silty, clayey gravel with sand)					
9-C	45	41	14	NA	23	7	GC-GM	A-2-4(0)
			(Silty, clayey gravel with sand)					
10-C	55	34	11	Well	26	8	GW-GC	A-2-4(0)
			(Well-graded gravel with clay and sand)					
11-C	52	38	10	Well	22	6	GW-GC	A-1-a(0)
			(Well-graded gravel with silty clay and sand)					
12-C	43	44	13	NA	22	6	SC-SM	A-1-a(0)
			(Silty, clayey sand with gravel)					
13-C	54	37	9	Well	22	8	GW-GC	A-2-4(0)
			(Well-graded gravel with clay and sand)					
14-C	38	45	17	NA	20	4	SM	A-1-a(0)
			(Silty sand with gravel)					

Note: The name in parentheses on the second line for each soil is the full USCS name.

Table 5.2 Summary of Results from Laboratory Testing of GB

Location ID	Gravel (%)	Sand (%)	Fines (%)	Gradation	Liquid Limit	Plasticity Index	USCS (Full)	AASHTO
1-A	52	33	15	NA	17	5	GC-GM	A-1-a(0)
				(Silty, clayey gravel with sand)				
2-C	41	44	15	NA	30	12	SC	A-2-6(0)
				(Clayey sand with gravel)				
3-C	41	36	23	NA	19	6	GC-GM	A-1-b(0)
				(Silty, clayey gravel with sand)				
4-C	49	37	14	NA	25	8	GC	A-2-4(0)
				(Clayey gravel with sand)				
5-C	44	41	15	NA	15	2	GM	A-1-a(0)
				(Silty gravel with sand)				
6-C	47	36	17	NA	25	9	GC	A-2-4(0)
				(Clayey gravel with sand)				
7-C	47	37	15	NA	21	7	GC-GM	A-2-4(0)
				(Silty, clayey gravel with sand)				
8-C	48	39	13	NA	27	11	GC	A-2-6(0)
				(Clayey gravel with sand)				
9-C	49	38	13	NA	24	8	GC	A-2-4(0)
				(Clayey gravel with sand)				
10-C	55	31	13	NA	16	3	GM	A-1-a(0)
				(Silty gravel with sand)				
11-C	47	41	12	Well	22	7	GW-GC	A-2-4(0)
				(Silty, clayey gravel with sand)				
12-C	51	39	10	Poor	29	11	GP-GC	A-2-6(0)
				(Well-graded silty, clayey gravel with sand)				
13-C	48	40	12	Poor	20	3	GP-GM	A-1-a(0)
				(Poorly graded clayey gravel with sand)				
14-C	36	50	14	NA	23	13	SC	A-2-6(0)
				(Clayey sand with gravel)				

Note: The name in parentheses on the second line for each soil is the full USCS name.

UDOT standard specifications for the gradation of the UTBC are shown in Table 5.3. UDOT specifications for the soil classification and plasticity of the UTBC and GB are shown in Table 5.4.

Results indicate that 93% of the UTBC fell within either the target band or tolerance for job mix gradation, 57% of UTBC samples fell outside the target band and within the tolerance for the amount of fines, and 14% of GB samples fell outside the limit of 15% fines. The average amount of fines in the UTBC and GB samples was 12% and 14%, respectively. Additionally, 50% of the UTBC and 33% of the GB classified as A-1-a, and 100% of the UTBC and GB samples contained plastic fines. The average value of the plasticity index (PI) of the sampled UTBC and GB was 7 and 8, respectively.

Table 5.3 UDOT Gradation Limits for UTBC

Sieve Size	Job Mix Gradation Target Band	Job Mix Gradation Tolerance
1½ inch	100	
1 inch	90 - 100	±9.0
¾ inch	70 - 85	±9.0
½ inch	65 - 80	±9.0
⅜ inch	55 - 75	±9.0
No. 4	40 - 65	±7.0
No. 16	25 - 40	±5.0
No. 200	11-7	±3.0

Table 5.4 UDOT Soil Classification and Plasticity Limits for UTBC and GB

Material	Classification (AASHTO)	Plasticity	Fines (%)	Gradation
UTBC	>A-1-a	Non-Plastic	7-11 (+/-3.0)	Well
GB	>A-1-a	Non-Plastic	<15	Well

The presence of clay in the samples was noticeable after samples were air-dried in preparation for processing, as shown in Figure 5.1. A hammer was needed to break down the sample due to extensive bonding between cohesive and granular particles. The presence of plastic fines in the pavement system may be attributed to one or more of the following factors:

- Plastic fines not screened out at the source (gravel pit).
- Plastic fines introduced into the pavement system during the construction phase by, for example, driving heavy equipment over inadequately compacted layers, thereby churning the GB into the subgrade.
- Inadequate control of the UTBC and GB stockpiles to prevent contamination with other soils, or mixing of the UTBC or GB with subgrade soils during placement
- Plastic fines migrated into the pavement system during the service life.

The Atterberg limits of the soil samples were determined using both the Casagrande and fall cone methods. The fall cone method is the standard procedure used to determine the Atterberg limits in Europe and Asia. The test itself is more objective, repeatable, and faster than the traditional Casagrande method. U.S. government agencies have at times considered its adoption, but the Casagrande method remains the industry standard. A comparison of the results obtained by both test methods are shown in Figure 5.2 and Figure 5.3.

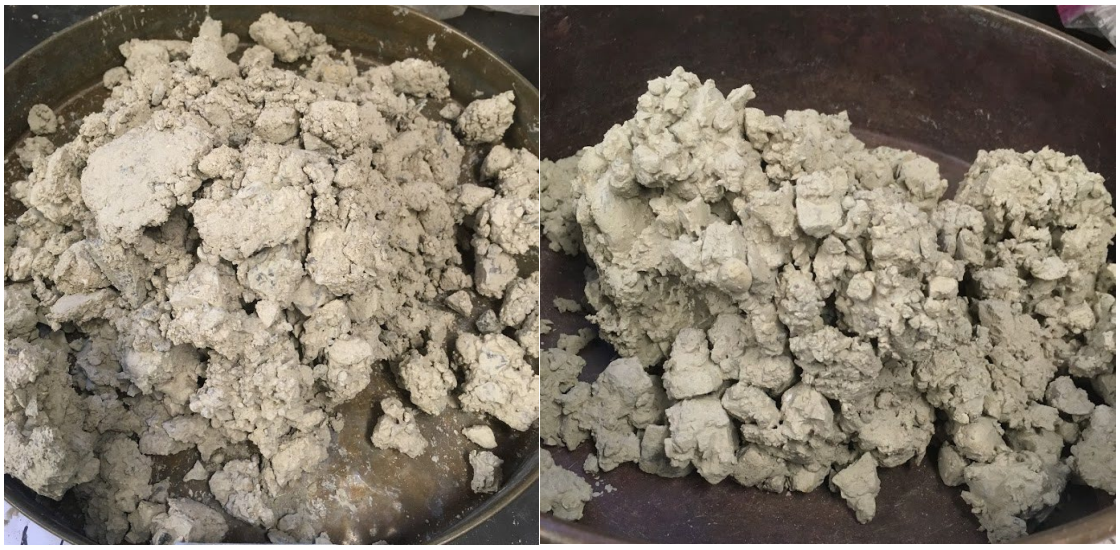

Figure 5.1 Air-Dried Samples of UTBC from Location 7 and GB from Location 8, Respectively.

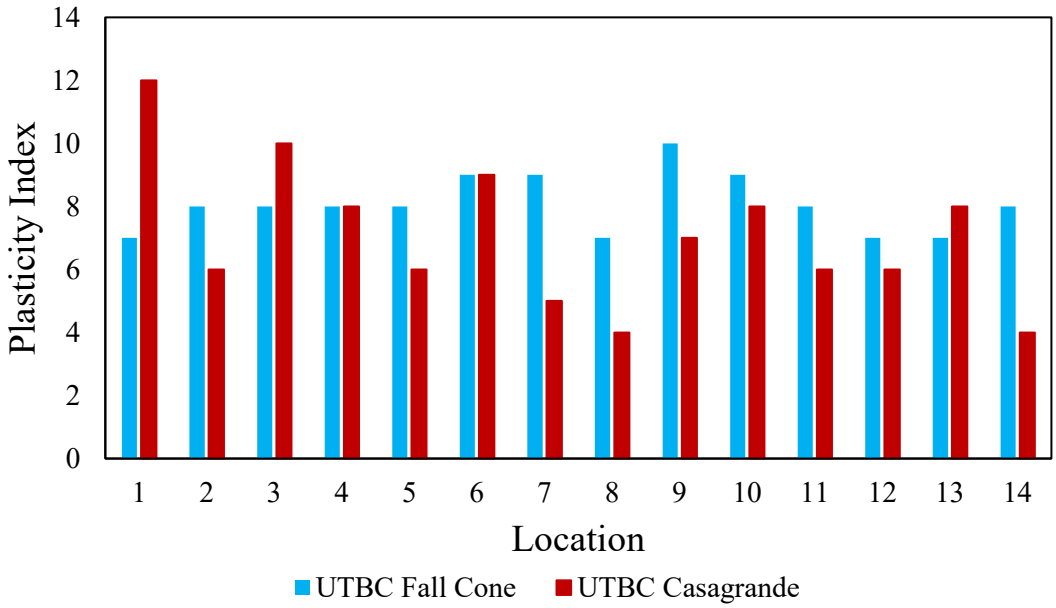

Figure 5.2 Comparison of Plasticity Index Derived from the Fall Cone Versus Casagrande Method for UTBC

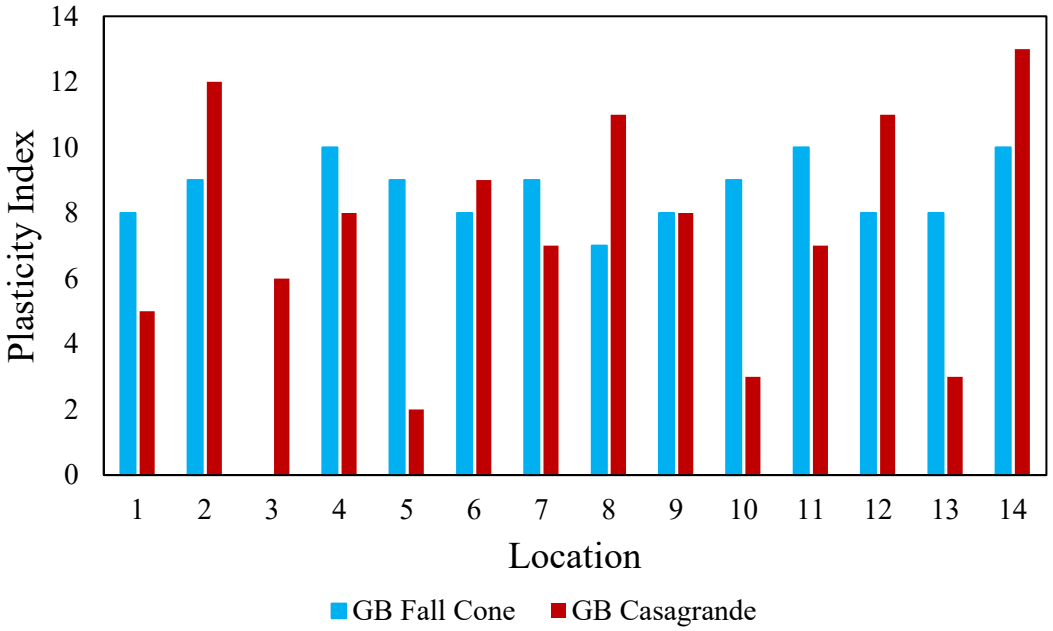

Figure 5.3 Comparison of Plasticity Index Derived from the Fall Cone Versus Casagrande Method for GB

5.2 Evaluation of Results from Laboratory Testing of Subgrade Samples

The following tests were performed on bagged subgrade samples obtained during the second round of field sampling:

- Particle-size analysis – ASTM D422
- Amount of material finer than 75-µm (No. 200) sieve – ASTM D1140
- Liquid limit, plastic limit, and plasticity index – ASTM D4318
- Soil classification – ASTM D2487
- Carbonate content – ASTM D4373
- Maximum dry density and optimum water content – ASTM D698/AASHTO T99
- Maximum dry density and optimum water content via Harvard miniature method – Wilson (1970)
- One-dimensional swell or collapse – ASTM D 4546

The Harvard miniature test method for determining the moisture-density relationships of compacted cohesive soils is less commonly known and used than the Proctor tests, so a brief description will be provided here. The test was developed to use a kneading method of compaction that better simulates the compaction of cohesive soils in the field, using sheepsfoot and tamping foot rollers, than the Proctor tests, which use an impact method of compaction. Recommended procedures for the test were published by ASTM (Wilson 1970) but an ASTM standard was never authorized for the test. Historically, the method has been used primarily to prepare specimens for triaxial testing. The main advantage of the test is that a better estimate of the line of optimums is obtained than from the Proctor tests, and accurate delineation of the line of optimums is critical to developing proper compaction specifications for cohesive soil. The main disadvantage of the test is the small size of the specimen (2 13/16 inches tall and 1 5/16 inches in diameter), but it works well for cohesive soils with less than 5% of the particles larger than the #4 sieve.

The procedure used in the Harvard miniature test consists of compacting a given number of soil layers with a given number of tamps. The kneading tamper is a 0.5-inch diameter steel rod with a flat bottom encased in a spring-loaded apparatus. Springs with different stiffnesses can be used to apply different values of kneading force to the soil. Each tamp consists of pushing the tamper into the soil until the spring begins to deflect, at which point a standardized force has been applied to the soil.

Figure 5.4 shows the moisture-density relationships for the standard Proctor, modified Proctor, and Harvard miniature test. The Harvard miniature tests were carried out at tamping forces of 13.3 and 40 lbs. Twenty-five tamps were applied per lift for a total of five lifts. In Figure 5.4, the line of optimums is drawn through the peak point of the dry density-water content curve for the Harvard miniature test for a tamping effort of 40 lb. From the figure, it is clear that kneading compaction results in a higher degree of optimum saturation than impact compaction. The degree of saturation for the Harvard miniature tests at 13.3 and 40 lbs. was 86.8% and 88.6%, respectively. The degree of saturation for the standard and modified Proctor curves was 71.8% and 74.3%, respectively.

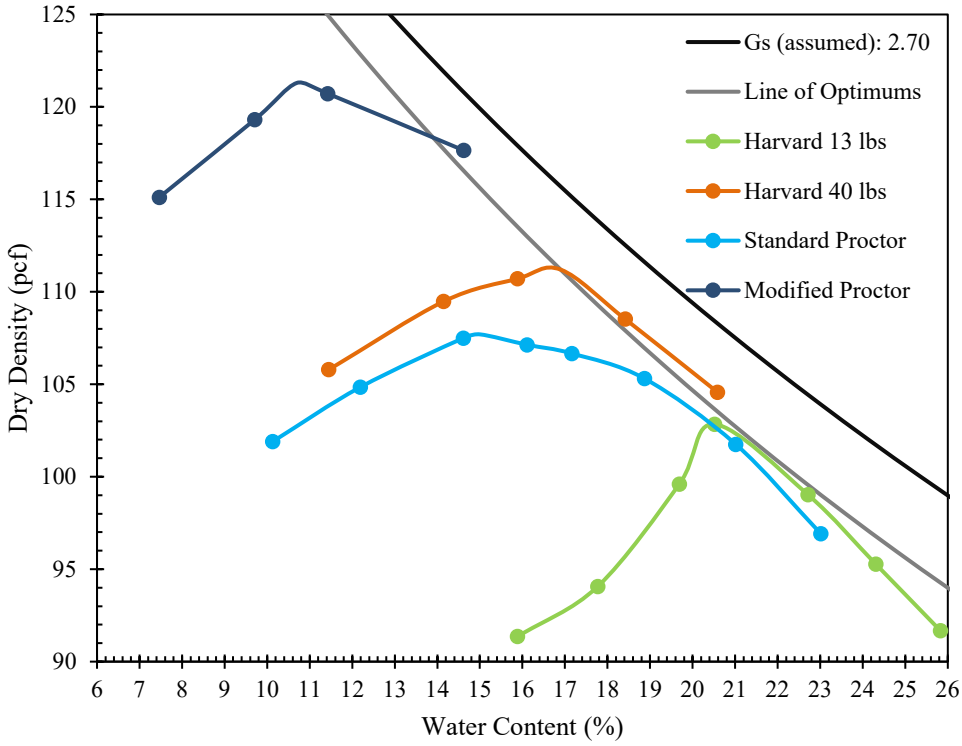

Figure 5.4 Determination of the Line of Optimums from Harvard Miniature and Standard Proctor-Derived Dry Density-Water Content Curves

Sampling was carried out at two primary locations. TP-1 was located at milepost 14.012. TP-2 was located at milepost 14.707. Both sampling locations were done in cut areas, as shown in Figure 5.5. The photograph in Figure 5.5 was taken at the sampling location of TP-1, which was close to field test Location 6. TP-2 was taken from a cut section adjacent to field test Locations 3 and 4, as shown in Figure 5.6.

Figure 5.5 Photograph of Sampling Location for TP-1

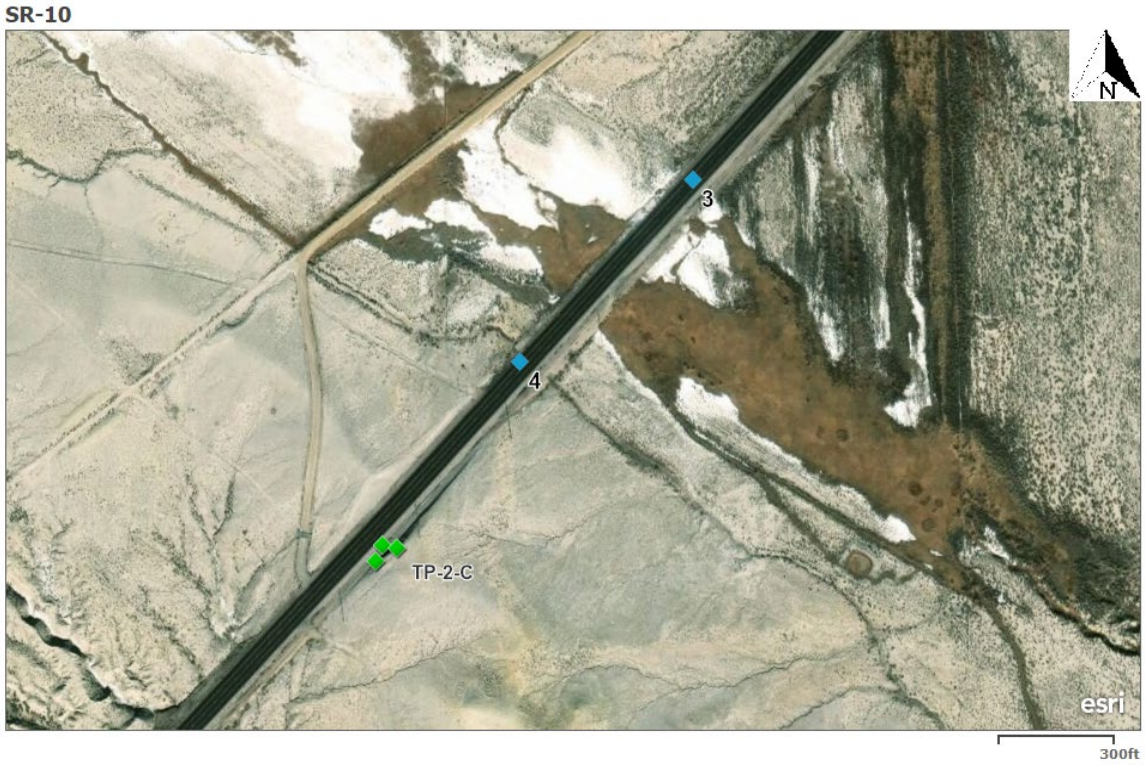

Figure 5.6 Sampling Location TP-2 Relative to Field Test Locations 3 and 4

To conserve undisturbed material for consolidation and collapse/swell testing, the sub-location samples were combined into two large samples on which moisture-density tests were performed. Results from the testing of the subgrade samples are summarized in Table 5.5. For the sampled locations, the subgrade soil consisted of a sandy lean clay to lean clay according to the Unified Soil Classification System (USCS) and an A-6 to A-7-6 soil according to the AASHTO rating. The fines' content of the sampled soils ranged from 66% to 98%. These soils are generally considered "fair to poor" as a subgrade according to AASHTO. UDOT Standard Specifications require that material to be used in excavated fill in the top layers of the embankment or roadbed should consist of "suitable granular materials." It does not take a large percentage of fines to change the engineering behavior of a granular material. The following quote is taken from "Introduction to Geotechnical Engineering" by Holtz, Kovacs, and Sheehan (2011).

"As the amount of clay increases, the behavior of the soil is increasingly governed by the properties of the clay. When the clay content is about 25% to 35%, the coarser grains are essentially floating in a clay matrix and have little effect on the soil's engineering behavior. Another characteristic of clay soils is that water markedly affects their behavior, but the grain size distribution has relatively little influence."

Classification of surficial soils along the roadway by percentage is provided in Table 5.6. The values are based on survey data from the U.S. Department of Agriculture (USDA, 2010). Soils with a high percentage of plastic fines may be vulnerable to wetting-induced swell or collapse. The swell or collapse potential of the soil may depend on one or a combination of the following variables.

- Method of compaction
- As-compacted dry density
- As-compacted water content
- The magnitude of design loads
- Depth of embankment

Additionally, testing revealed a relatively high percentage of carbonate content in the sampled soils. Soils with high carbonate content may also be vulnerable to wetting-induced volume changes.

Table 5.5 Summary of Results from Laboratory Testing on Subgrade Samples

Location:	TP-1	TP-1	TP-2	TP-2	TP-2
Sub-Location:	A	B	A	B	C
Depth (ft.):	0.5	1.0	1.0	1.0	1.5
Moisture Content (%):	2	11	13	14	14
Fines Content (%):	98	97	66	94	94
Liquid Limit:	40	37	48	43	46
Plasticity Index:	20	17	24	20	20
Carbonate Content, Calcite Equivalent (%):	20	20	22	22	20
Maximum Dry Density (pcf) – Standard/Modified Proctor:	109.9		107.7/121.3		
Optimum Water Content (%) – Standard/Modified Proctor:	15.8		15.0/10.7		
Optimum Degree of Saturation (%) – Standard/Modified Proctor	80.0		71.8/74.3		
Maximum Dry Density (pcf) - Harvard Miniature 13.3/40 lb:	104.5/113.7		102.8/111.2		
Optimum Water Content (%) - Harvard Miniature 13.3/40 lb:	19.4/15.0		20.5/16.9		
Optimum Degree of Saturation (%) – Harvard Miniature 13.3/40 lb:	85.6/84.2		86.8/88.6		
USCS Classification:	CL Lean Clay	CL Lean Clay	CL Sandy Lean Clay	CL Lean Clay	CL Lean Clay
AASHTO Classification:	A-6(21)	A-6(17)	A-7-6(15)	A-7-6(21)	A-7-6(21)

Results from additional testing on the swell and collapse potential of the soils are shown in Figure 5.7 and Figure 5.8. In these figures, plots of axial strain versus overburden pressure are plotted for four sets of specimens compacted at different water contents to dry densities. The double oedometer method was used to characterize the swell or collapse potential of the subgrade soil. The method involves preparing two identical sets of specimens at pre-determined dry densities and water contents. After an initial seating load has been applied to both specimens, one specimen is inundated with distilled water (soaked) and the other specimen is left at its as-compacted water content for the duration of the test. Both specimens are subjected to a pre-determined loading schedule. For these tests, a loading schedule of 0.01 (seating), 0.25, 0.50, 1, 2, 4, 8, and 0.01 tsf (unloading) was used. The axial strain after each load was applied and measured at time intervals of 0, 0.1, 0.25, 0.5, 1, 2, 4, 8, 15, 30, 60, 120, and 1,440 minutes. After the 24-hour reading was taken, the next load was applied. In Figure 5.7 and Figure 5.8, axial strain as a function of the overburden pressure is plotted for the set of soaked and as-compacted specimens. Positive strain indicates settlement and negative strain indicates heave. Specimens were tested at the following combinations of relative compaction (based on Standard Proctor) and water contents: RC = 106% and w = 14%, RC = 96% and w = 16%, RC = 96% and w = 14%, and RC = 96% and w = 12%. The combinations of relative compaction and water content were selected based on UDOT specifications. Embankment fill must be compacted to a relative compaction of 96% of Standard Proctor and a water content plus or minus 2% of optimum. The optimum water content for the sampled soil was approximately 14%.

Table 5.6 Surficial Soil by AASHTO Classification from USDA Data

AASHTO Classification	Area of Interest (%)
A-4	1.80
A-6	49.0
A-7-6	49.2

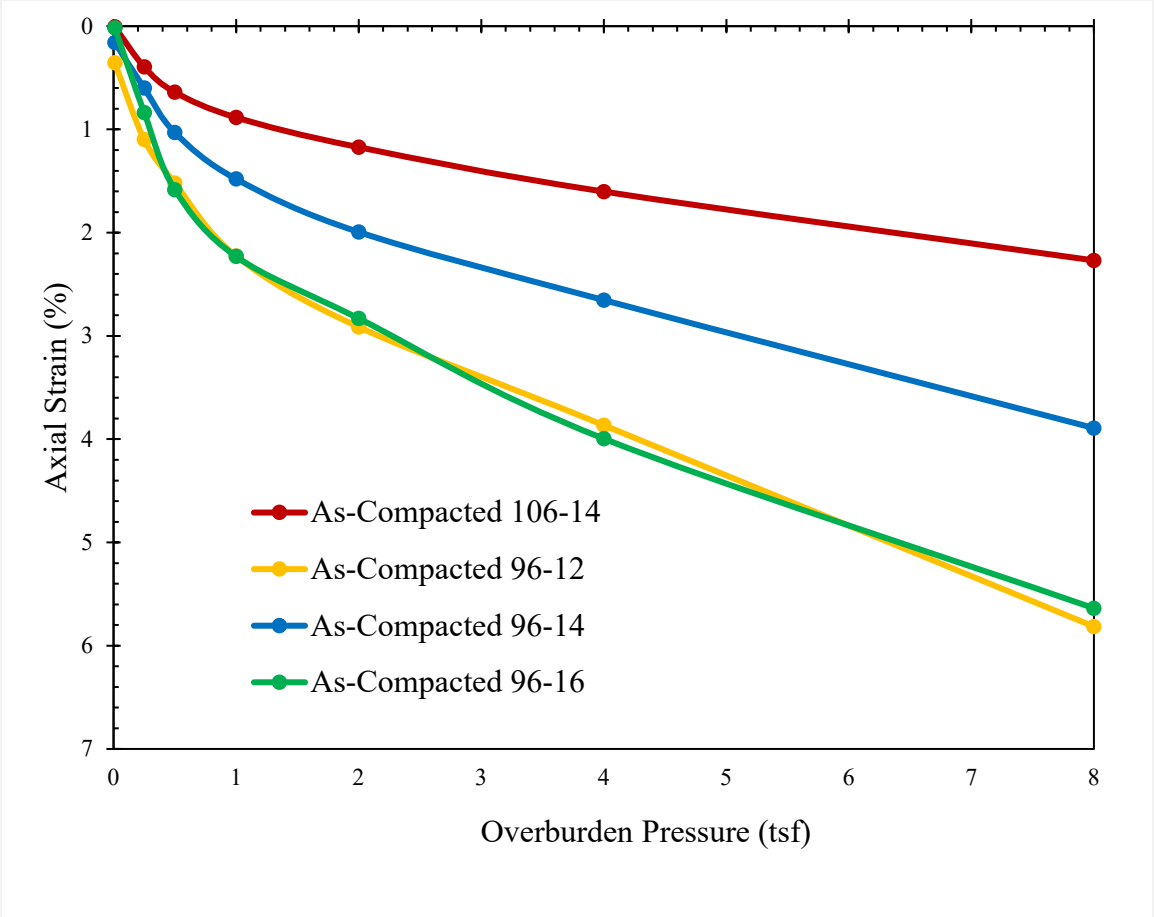

Figure 5.7 Measured Axial Strain as a Function of Overburden Pressure for As-Compacted Specimens

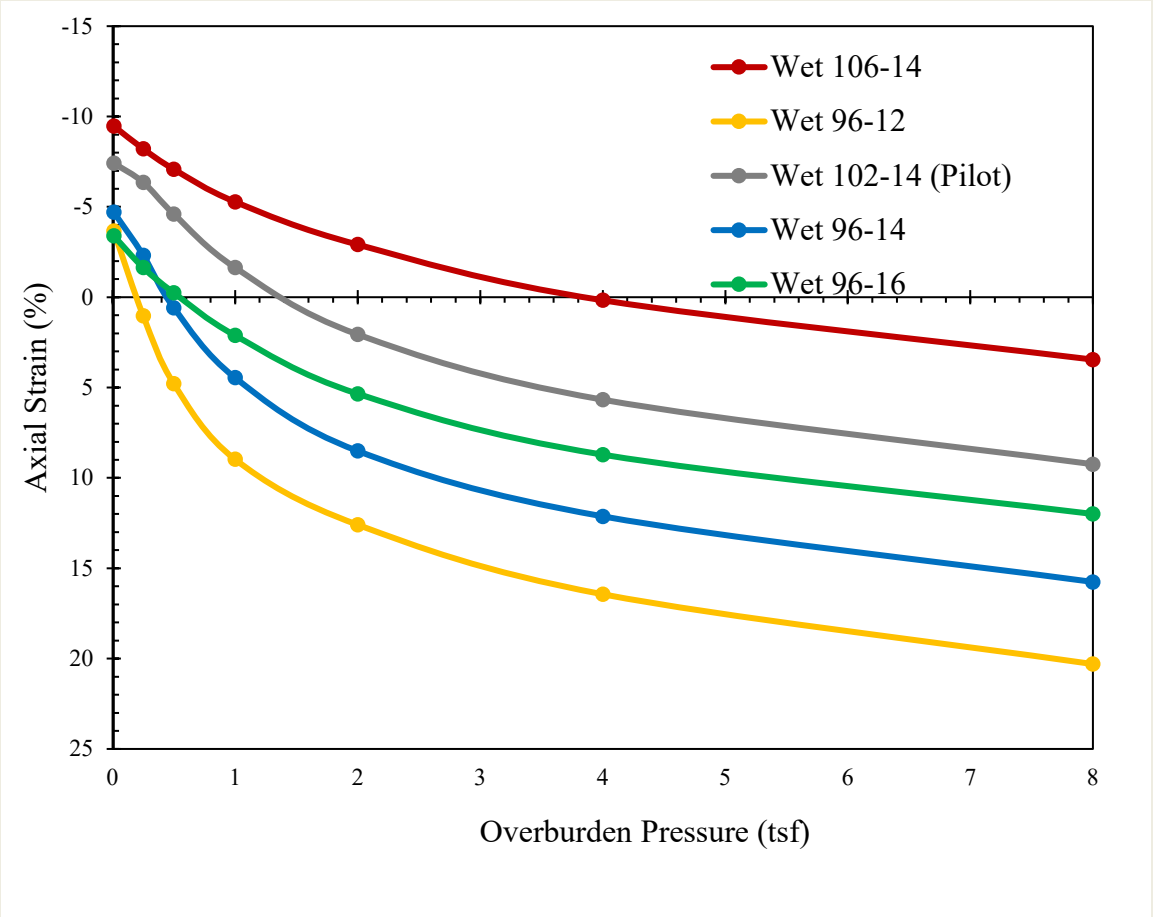

Figure 5.8 Measured Axial Strain of Wetted Specimens

The predicted wetting-induced volume change at each load increment can be predicted by subtracting the measured axial strain of the as-compacted specimen from the axial strain of the wetted specimen. The predicted wetting-induced swell and collapse of the subgrade soil is shown in Figure 5.9. Positive strain indicates collapse and negative strain indicates swell.

Swell and collapse testing showed that the subgrade soil obtained from the cut sections is vulnerable to significant wetting-induced volume changes. At the minimum required value of RC (96%), the soil swelled under low confining stresses between 0 and 1 tsf (2000 psf) and collapsed under medium to high confining stresses between 1 and 8 tsf (16000 psf). The swell or collapse potential of the soil varied as a function of the as-compacted water content and the as-compacted dry-density. The swell potential increased with increasing dry density and decreasing water content. The collapse potential increased with decreasing dry density and decreasing water content. Comparing the results for the two tests at which the specimens were compacted at w = 14%, it is obvious that compacting the soil to higher RC results in greater swell or less collapse potential at all values of overburden pressure. This relationship creates a dilemma when using expansive materials within embankments supporting structures of any type, including roadways. Higher values of RC are needed to obtain the desired strength and stiffness, but higher values of RC induced greater potential for wetting-induced swell. Swell potential is particularly problematic in the upper parts of the fill where the swell potential is greatest, which can be particularly problematic for fills supporting pavement systems because even short fills can contribute to pavement distress if the fills become wetted.

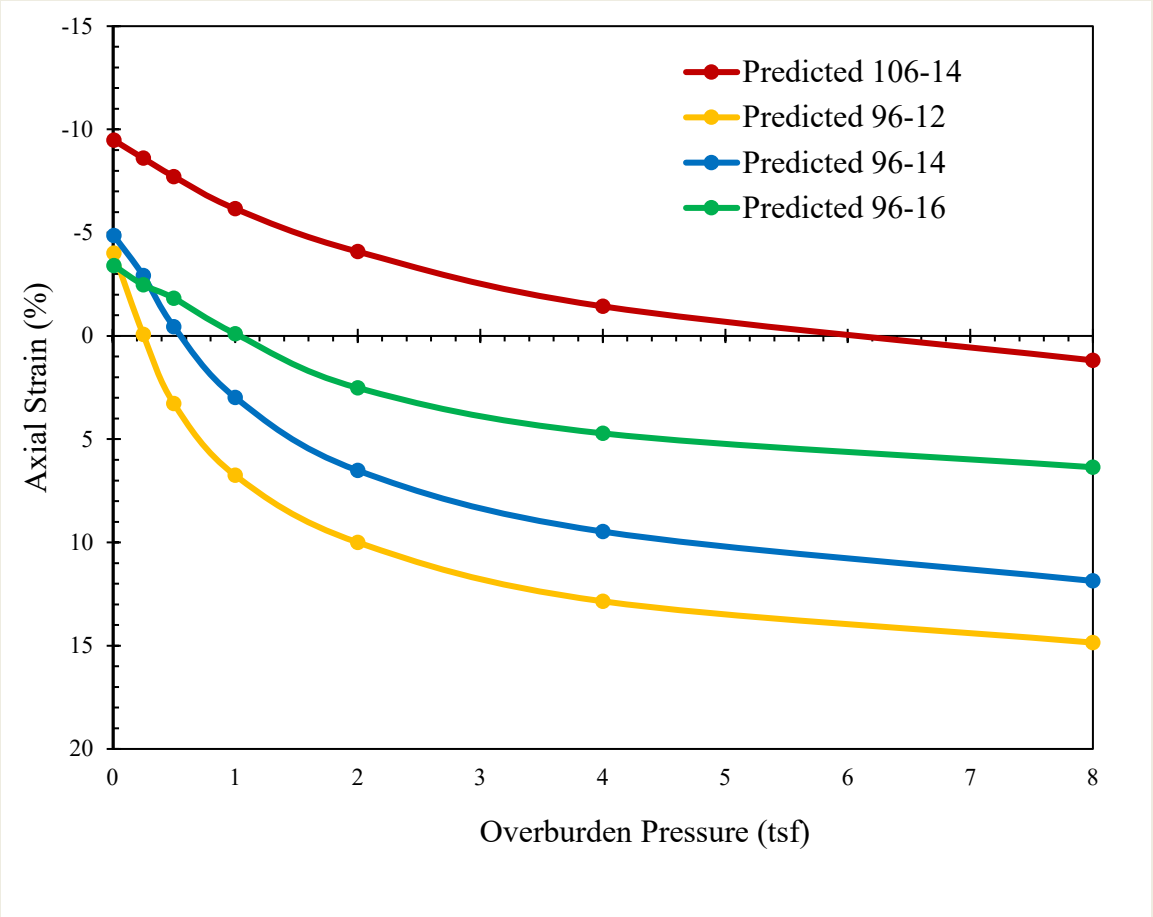

Figure 5.9 Predicted Wetting-Induced Volume Change from Double Oedometer Tests

There are several mechanisms by which a partially saturated embankment fill may become fully saturated at some point in time during its design life. They are summarized in Figure 5.10.

CPT data showed that the groundwater table was located 10 to 12 feet below the ground surface in locations where data for the equilibrium pore pressure was gathered. Given that the field testing was conducted in July, the water table was likely at a seasonal low elevation. During spring, the groundwater table would likely rise several feet due to infiltration from snowmelt and rainfall.

In a fine-grained material, the potential capillary zone, consisting of a saturated and continuous moisture zone, could be as high as several feet. Additionally, vapor movements from the saturated to unsaturated zone could increase the moisture content in the soil beneath the impermeable wearing surface.

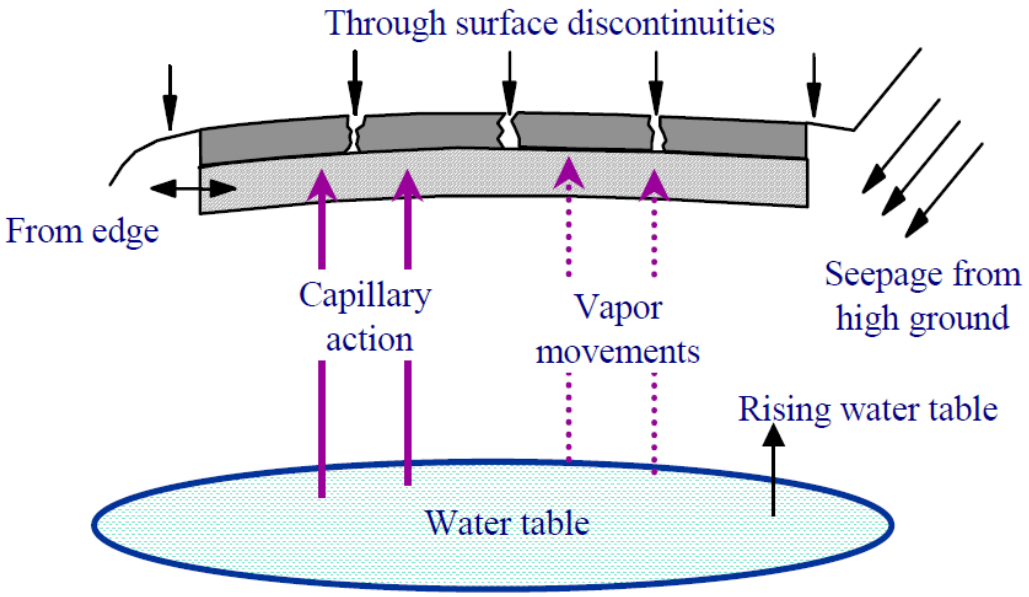

Figure 5.10 Mechanisms by Which a Pavement System May Become Saturated (from FHWA, 2006)

The natural topography for most of SR-10 is such that higher ground is adjacent to the negative direction of travel and the lower ground is adjacent to the positive direction of travel. The natural topography may make the negative direction more vulnerable to seepage from higher ground, especially if culverts are inadequate and spring runoff is pooling on the higher ground surface next to the roadway embankment. The embankment may then become saturated, and swell or collapse can occur. Due to these factors, it is likely that the embankment and primary pavement system would become fully saturated at some point in the service life of the roadway. Cycles of wetting and drying of cohesive soils, similar to the materials taken from the cut section and those identified from the CPTs, could lead to several types of differential settlement:

- In the transverse direction between the consolidated subgrade soil beneath the old alignment and the unconsolidated subgrade beneath the new alignment
- In the transverse direction between the consolidated subgrade soil beneath the old alignment and wetting-induced volume changes in deep embankment fill beneath sections of the new alignment
- In the longitudinal direction between wetting-induced volume changes in the fine-grained native embankment fill and the free-draining granular backfill around culverts
- In all directions due to variations in UTBC, GB, subgrade, and fill materials

5.3 Evaluation of Results from Laboratory Testing of Asphalt-Concrete

The asphalt-concrete samples were tested using the Illinois Flexibility Index Test (IFIT). IFIT testing was carried out according to Illinois Test Procedure 405, “Determining the Fracture Potential of Asphalt Mixtures Using the Illinois Flexibility Index Test” (Illinois Department of Transportation, 2016). Unlike the tests done on the UTBC and GB samples, the IFIT test is fairly new and therefore less well known and the significance and interpretation of the results less understood. The testing procedure will therefore be described in brief detail before a presentation of the results.

The IFIT test was developed by researchers at the University of Illinois (Urbana-Champaign) as a method of testing the fracture resistance of asphalt-concrete mix designs. The test has primarily been used to rate laboratory and contractor mix designs but has also been used to test samples taken from the field. The IFIT test is performed on 150-mm diameter asphalt-concrete samples made in the laboratory or taken from the field. Two 50-mm thick "pucks" are cut from the asphalt-concrete sample, as shown in Figure 5.11.

A specially equipped masonry saw was used to cut specimens from the asphalt-concrete sample. Care was taken to cut the sample such that the top 1.5 inches of stone-matrix asphalt was not included in any of the tested specimens. An effort was also made to cut the sample such that none of the 50-mm pucks included more than one lift.

Each 50-mm puck was cut exactly in half to produce two half-disc specimens each, for a total of four specimens to be tested per sample. A 15-mm (+/- 1 mm) notch was cut down the middle of each half-disc specimen. The geometry of each specimen was recorded by measuring the radius, thickness, and length of the notch. Each specimen was cured in an environmental chamber at the standard testing temperature of 25°C (77 °F) for 24 hours before testing, as shown in Figure 5.12.

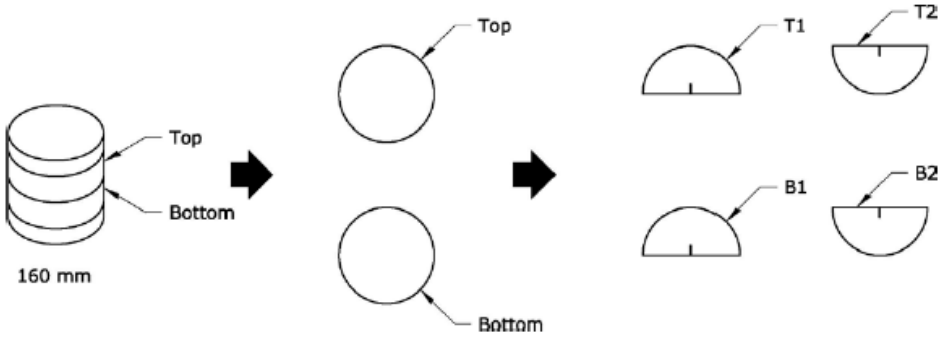

Figure 5.11 IFIT Specimen Preparation (figure taken from Illinois, 2016)

Figure 5.12 Half-Disc Specimens Curing in the Environmental Chamber

Half-disc specimens were tested on a Test-Quip load frame built specifically for the IFIT test. The same testing equipment was used in a study conducted for UDOT by Romero and VanFrank (2017), as documented in UDOT Report No. UT-17.21. Specimens are loaded at a rate of 50 mm/minute at a standard temperature of 25°C. Displacement and load measurements are recorded at a 40 Hz frequency. A load versus displacement curve is generated for each test, as shown in Figure 5.13. From this curve, it is possible to calculate the fracture energy (area under the curve) and post-peak slope. Using these parameters and a unit conversion constant, the flexibility index is calculated. Equation 5.1 is used to calculate the flexibility index number.

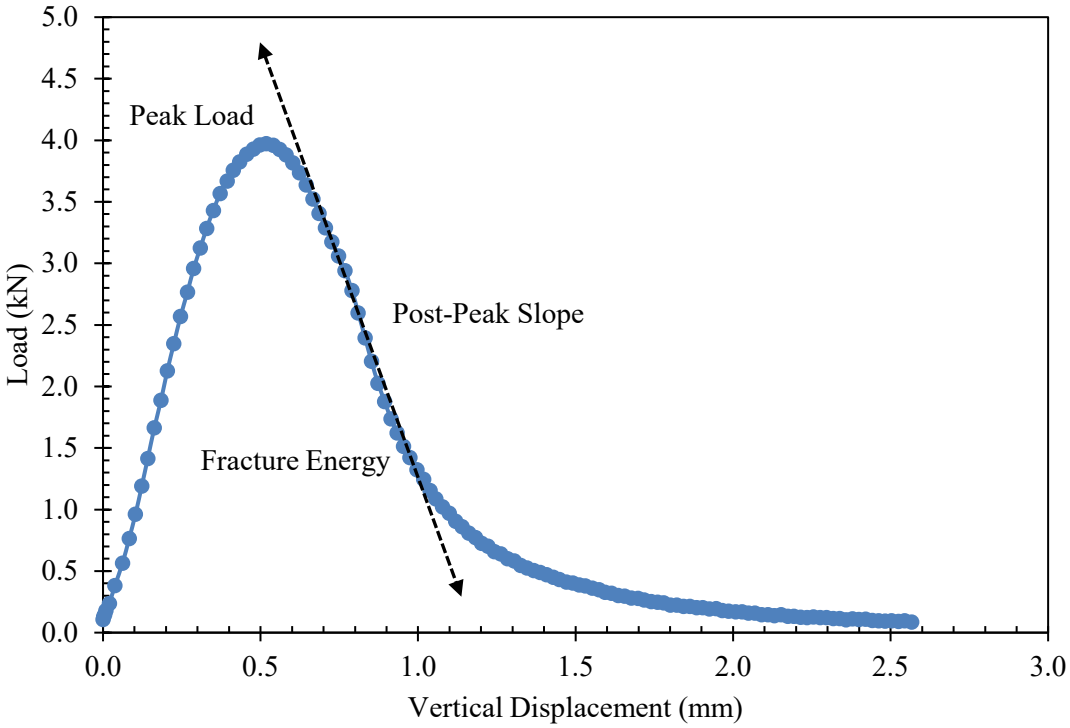

Figure 5.13 Load Versus Displacement Curve for Specimen 2-B-B1

$$\boldsymbol{FI = \frac{G_f}{|m|} * A} \qquad \textbf{(Equation 5.1)}$$

Where:

$m = post - peak\ slope\ (kN/mm)$

$G_f = fracture\ energy\ (Joules/m^2)$

$A = 0.01\ (unit\ conversion\ and\ scaling\ constant)$

From Equation 5.1, it is apparent that the steeper (more brittle) the post-peak slope, the smaller the flexibility index. The greater the area under the curve, the more work is required to generate permanent cracking; thus, the higher the flexibility index.

A comparison of the cracks in the two specimens in Figure 5.14 illustrates how crack propagation affects the flexibility index number and explains variability between specimens from the same sample. The crack on the right specimen formed through larger pieces of aggregate and a smaller amount of binder than the

specimen on the left. Consequently, the post-peak slope was steeper for the right specimen, generating a substantially lower flexibility number than the left specimen (3.0 versus 6.4, respectively). On laboratory-prepared samples, Romero and VanFrank found that the flexibility index increases monotonically with increased binder content.

The flexibility index test can be used to evaluate the resistance of the asphalt-concrete layer to long-term (fatigue) cracking. Each sample produces two discs, which in turn produce two half-discs, for a total of four specimens per sample. The mean value for each disc and the mean value for each field-testing location are provided in Table 5.7. The mean flexibility index is plotted in Figure 5.15 by field test location.

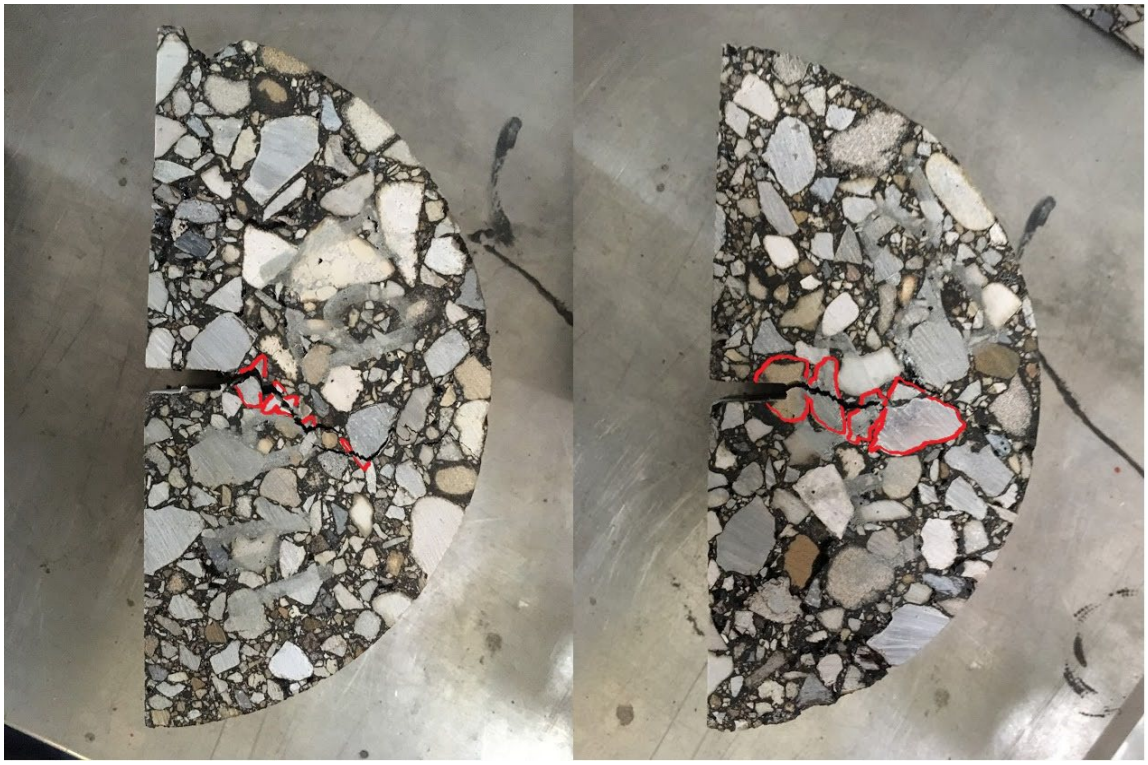

Figure 5.14 Comparison of Crack Propagation Between Specimen 14-B-B1 (Left, Slope = -1.43 kN/mm, FI = 6.4) and 14-B-B2 (Right, Slope = -2.82 kN/mm, FI = 3.0)

In the report by Al-Qadi et al. (2015), where the flexibility index testing parameter was developed, the researchers noted that for the field cores tested, flexibility index values greater than 10 were generally considered "good," values between 2.0 to 6.0 were considered "intermediate," and values less than 2.0 were considered "poor." According to the researchers, the calculated FI values correlated well with measured pavement distress indexes and values.

These researchers also noted that flexibility index values declined considerably with pavement age. For pavements built between 2013 and 2014 (1 to 2 years old), flexibility index values ranged from 6.0 to 25.1; between 2008 and 2009 (6 to 7 years old), from 2.3 to 5.0; and between 2003 to 2004 (11 to 12 years old), from 0.7 to 1.3 (Al-Qadi et al., 2015). It should be noted that the interpretation of these values might vary based on differences between Utah and Illinois in terms of climate, materials used in the AC, etc.

Table 5.7 Results from Illinois Flexibility Index Testing of Asphalt-Concrete Specimens

	Disc Mean		
Location	Top	Bottom	Location Mean
1	3.83	3.60	3.71
2	4.28	1.83	3.05
3	5.87	1.85	3.86
4	3.95	2.54	3.25
5	6.50	3.40	4.95
6	2.05	1.19	1.62
7	3.85	1.30	2.58
8	1.30	0.885	1.09
9	4.40	1.55	2.98
10	3.58	3.00	3.29
11	3.43	2.23	2.83
12	3.08	2.72	2.90
13	3.00	3.05	3.03
14	4.08	4.95	4.51

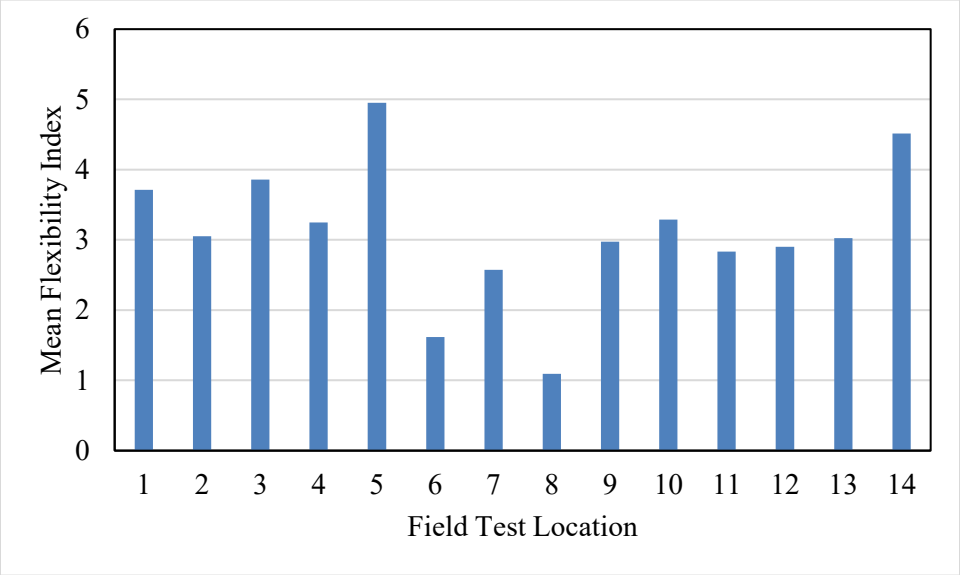

Figure 5.15 Mean Flexibility Index by Field Test Location

With the age of the asphalt-concrete field cores in mind, most of the mean values of flexibility index measured for this section of SR-10 appear to indicate that the flexibility of the asphalt-concrete was satisfactory. Locations 6, 7, and 8 had the lowest flexibility index values of the tested locations. Interestingly, Locations 6 and 8 performed well while Location 7 performed poorly according to the pavement distress metrics of rutting and ride quality. Locations 1, 3, 4, and 9 also performed poorly according to the pavement distress metrics despite the relatively high to intermediate values of flexibility index at these locations.

In Figure 5.16, flexibility index values are compared for the top and bottom specimen discs for each location. Clearly, there is considerable variation between the top and bottom discs. The average flexibility index of the top and bottom discs was 3.81 and 2.38, respectively. The flexibility index of the top disc was, on average, 59.8% greater than that of the bottom disc. The variation between the discs may be explained by the presence of higher quality binders in the top lifts of the asphalt-concrete layer, including the surface layer of stone matrix asphalt. Higher quality binders are more effective at the top of the pavement, as it is more critical that top-down cracking of the pavement surface is prevented. Cracking at the surface of the pavement allows the penetration of free water, which will further exacerbate the pavement deterioration cycle.

Location-specific distresses are plotted in Figure 5.17 and Figure 5.18 versus mean flexibility index for the location of each field test. There does not appear to be a clear relationship between the measured pavement distresses and the mean flexibility index. The flexibility index is primarily a predictor of resistance to cracking failure, so it is not surprising that there is no relationship with rutting and roughness.

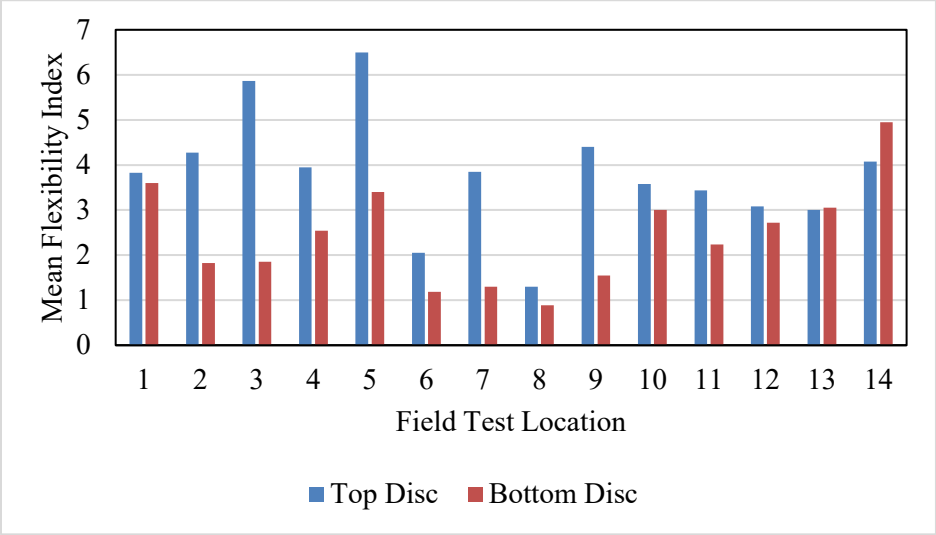

Figure 5.16 Comparison of Top and Bottom Disc Mean Flexibility Index by Location

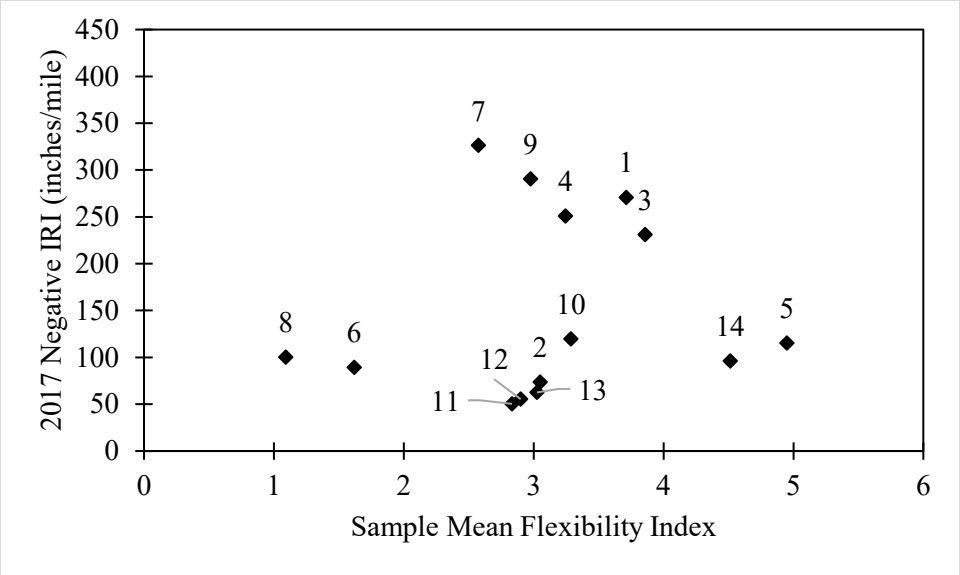

Figure 5.17 2017 Negative Direction IRI Versus Mean Flexibility Index

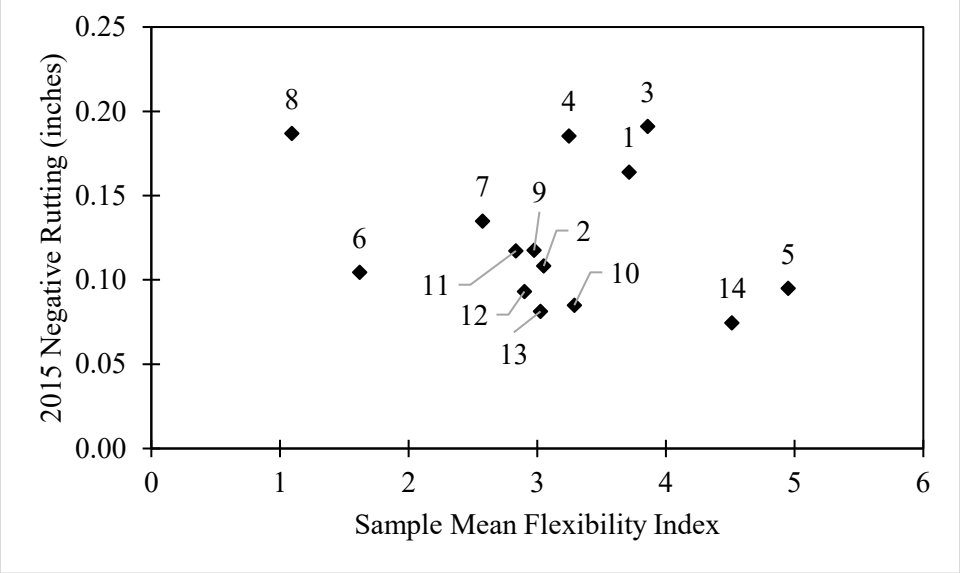

Figure 5.18 2015 Negative Direction Rutting Versus Mean Flexibility Index

6. EVALUATION OF DATA FROM FIELD TESTING

Results from the various field tests carried out in July 2018 were evaluated. Findings from the evaluation will be presented in the following order.

- Dynamic cone penetrometer test (DCPT)
- Falling weight deflectometer (FWD)
- Repetitive static plate load test (RSPLT)
- Cone penetration test (CPT)

6.1 Evaluation of Data from Dynamic Cone Penetrometer Test

The results from the DCPT for each location are summarized in Table 6.1. Values are based on a combined untreated base course and granular base course layer of approximately 16 inches. The standard ASTM/U.S. Army Corps of Engineers correlation (ASTM D6951-18) was used to derive the California bearing ratio (CBR) from the DCP stiffness index, as explained in Section 2.4. The table includes both an arithmetic and harmonic mean for the CBR value. It also includes the maximum and minimum values of CBR for the combined UTBC-GB layer.

Table 6.1 Results from Dynamic Cone Penetrometer Test

Dynamic Cone Penetrometer Test				
	Predicted California Bearing Ratio (%)			
Location	Harmonic Mean	Arithmetic Mean	Max	Min
1	22.4	37.1	79.4	5.8
2	164	260	635	24.9
3	72.8	153	517	11.2
4	69.7	160	517	8.3
5	52.6	139	815	11.2
6	64.9	144	517	16.7
7	84.6	174	517	16.0
8	36.6	45.5	79.4	15.4
9	48.0	53.7	79.4	25.3
10	22.3	27.8	52.0	10.1
11	46.7	54.4	79.4	18.6
12	90.3	151	517	20.6
13	69.7	84.7	238	29.8
14	134	209	815	29.8

The DCPT indicated the presence of a stiff layer (CBR > 100) at most locations (2, 3, 4, 5, 6, 7, 12, 13, and 14). The stiff layer was typically encountered in the upper third of the combined UTBC-GB layer. The stiff layer was likely at the interface of the biaxial geogrid interface between the UTBC and GB layers. The minimum CBR value was either at the interface between the GB layer and the subgrade or embankment fill, or at the top of the UTBC layer, where the horizontal confining stress was lowest. In Figure 6.1, the values of IRI in the negative direction in 2017 weighted by 0.02–mile increments for the

right wheel-path are plotted versus the harmonic mean of CBR predicted from DCPT. In Figure 6.2, rutting in the negative direction in 2015 weighted by 0.02–mile increments for the right wheel-path is plotted versus the harmonic mean of CBR predicted from DCPT.

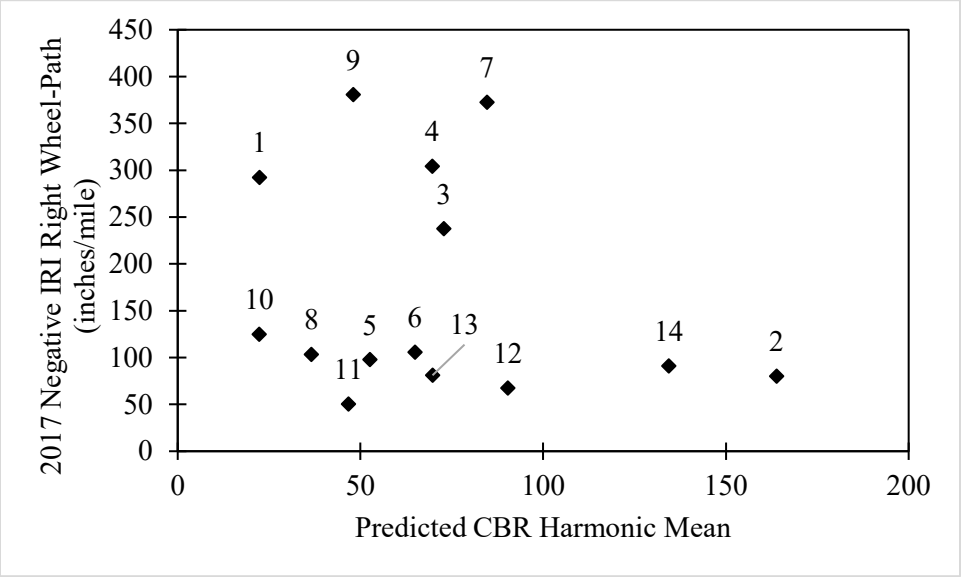

Figure 6.1 2017 Negative Direction Right Wheel-Path IRI Versus Harmonic Mean of CBR Predicted from DCPT

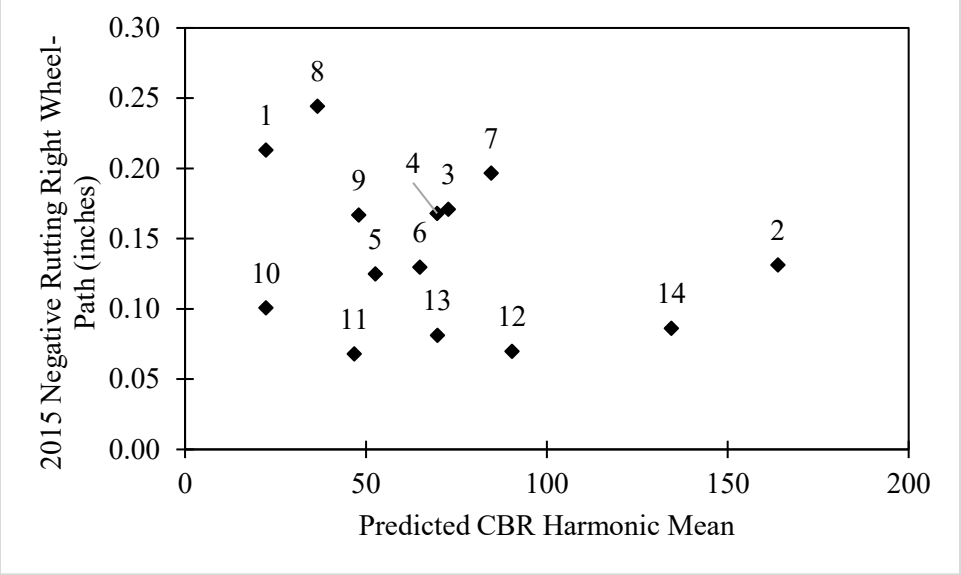

Figure 6.2 2015 Negative Direction Right Wheel-Path Rutting Versus Harmonic Mean of CBR Predicted from DCPT

It is clear from the results shown in Figures 6.1 and 6.2 that there is significant scatter in the data and not a clear relationship between the pavement distresses and the predicted harmonic mean of the CBR for the UTBC + GB layer.

DCPT profile for Locations 1, 13, and 14 are compared in Figure 6.3. All locations with the exception of 13 and 14 showed a decrease in predicted CBR for the last blows similar to Location 1. The decrease in predicted CBR indicates the end of the primary pavement system and the beginning of weaker native subgrade soils or embankment fills. In contrast, Locations 13 and 14 showed an increase in predicted CBR for the last blows. The increase in stiffness at the bottom of the pavement system is reasonable given that the new alignment overlapped with the old alignment between Locations 11 and 14. At a depth of 15 to 16 inches, the penetrometer was likely hitting the base course layer of the old roadway.

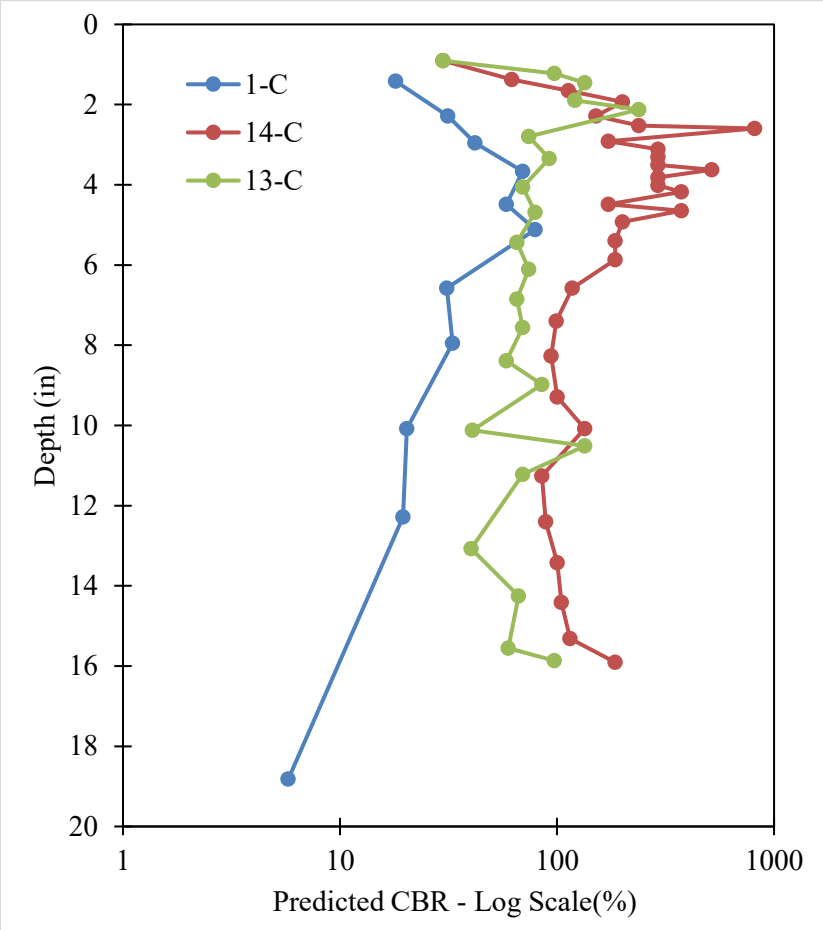

Figure 6.3 Predicted CBR from DCPT Versus Depth for Locations 1, 13, and 14

6.2 Evaluation of Data from Falling Weight Deflectometer

Falling weight deflectometer (FWD) tests were performed at each test location. For analysis, the three-layer system was composed of an 8-inch asphalt-concrete layer, 16-inch untreated base course plus granular borrow layer, and an infinite thickness subgrade layer. Values of Young's modulus and resilient modulus normalized for temperature and moisture changes were calculated for each layer using the techniques described in Section 2.2. The calculated values of each parameter for each layer are summarized in Table 6.2. Of note are the exceptionally low values of moduli for the subgrade and combined UTBC+GB layers for Location 1. Locations 2, 3, and 14 had the highest moduli for the combined UTBC+GB layer. Locations 6, 5, and 9 had the highest moduli for the subgrade.

In Figures 6.4 and 6.5, values of IRI and rutting distress are plotted versus the FWD-derived values of Young's modulus for the asphalt-concrete layer. There is significant scatter in the data and no clear relationship between the stiffness of the asphalt-concrete layer and the performance of the pavement. Therefore, an increase in the FWD-derived asphalt-concrete modulus does not correlate with a decrease in the pavement distresses for this section of roadway.

Table 6.2 Values of Young's Modulus and Resilient Modulus Back-calculated from Results of Falling Weight Deflectometer Tests

Location	Falling Weight Deflectometer					
	Young's Modulus (ksi)			Resilient Modulus (ksi)		
	Asphalt-Concrete	UTBC+GB	Subgrade	Asphalt-Concrete	UTBC+GB	Subgrade
1	354	3.26	7.91	413	2.18	4.35
2	337	112	20.1	430	74.7	11.1
3	494	71.0	17.9	592	47.6	9.85
4	575	54.2	16.1	680	36.3	8.84
5	368	16.6	29.5	437	11.1	16.2
6	482	14.1	65.5	627	9.45	36.0
7	452	27.9	12.6	606	18.7	6.93
8	378	36.5	21.3	495	24.5	11.7
9	611	51.5	29.2	767	34.5	16.1
10	459	13.1	13.2	623	8.79	7.26
11	453	31.7	22.1	620	21.2	12.1
12	524	33.6	21.1	744	22.5	11.6
13	463	29.0	24.3	663	19.4	13.4
14	382	103	22.7	558	68.7	12.5

In Figures 6.6 and 6.7, the pavement distresses are plotted versus the FWD-derived Young's modulus of the combined UTBC + GB layer. Like the asphalt-concrete, neither the rutting nor the ride quality is correlated to any significant extent with the Young's modulus of the combined UTBC + GB layer.

In Figures 6.8 and 6.9, the pavement distresses are plotted versus the FWD-derived Young's modulus for the subgrade layer. Again, there is significant scatter in the data. However, there appears to be a very weak correlation between increased stiffness of the subgrade and increased pavement condition performance.

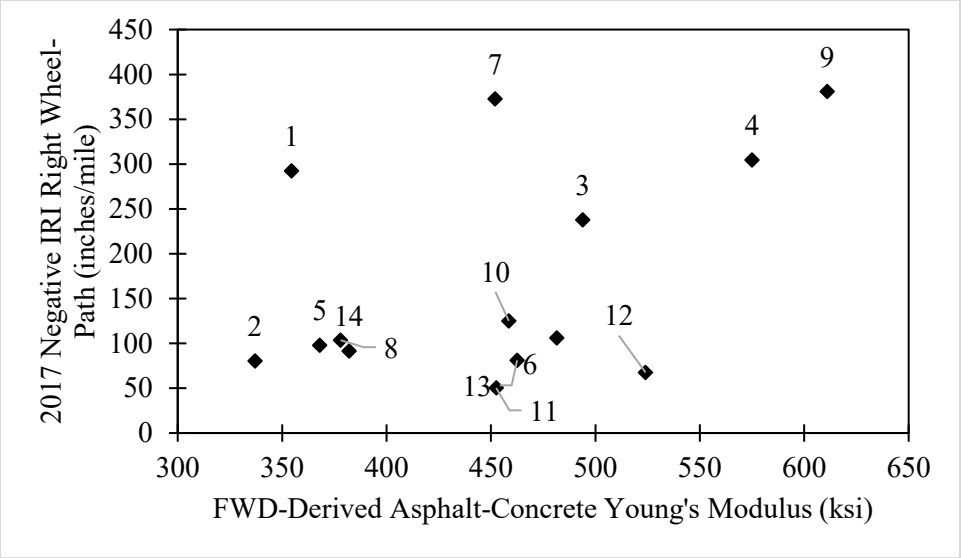

Figure 6.4 2017 Negative Direction Right Wheel-Path IRI Versus FWD-Derived Young's Modulus of the Asphalt-Concrete Layer

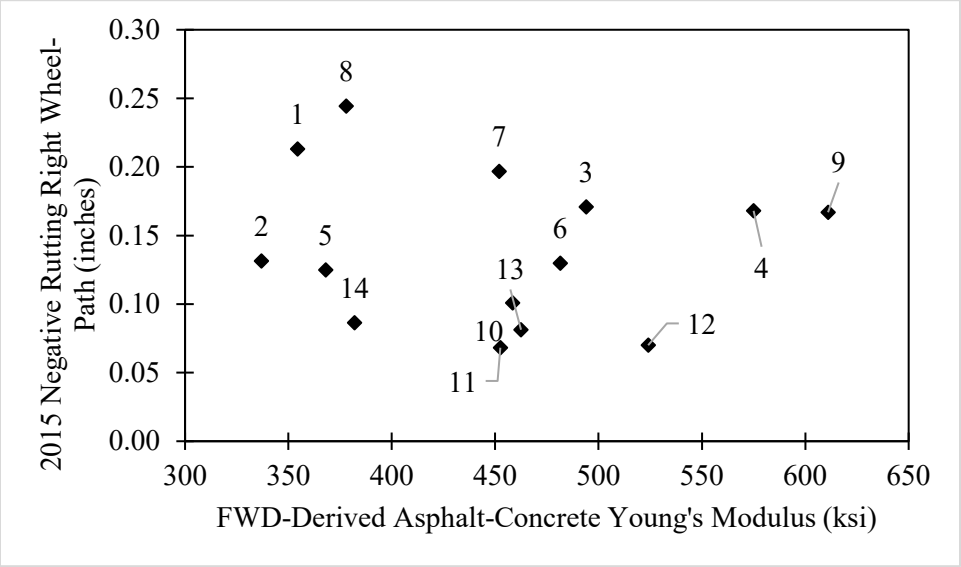

Figure 6.5 2015 Negative Direction Right Wheel-Path Rutting Versus FWD-Derived Young's Modulus of the Asphalt-Concrete Layer

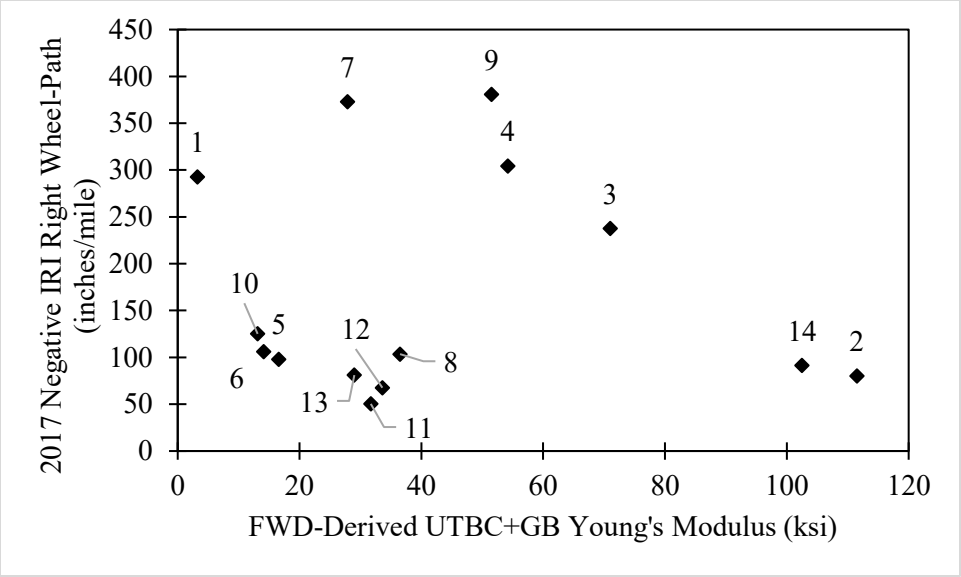

Figure 6.6 2017 Negative Direction Right Wheel-Path IRI Versus FWD-Derived Young's Modulus of the Combined UTBC + GB Layer

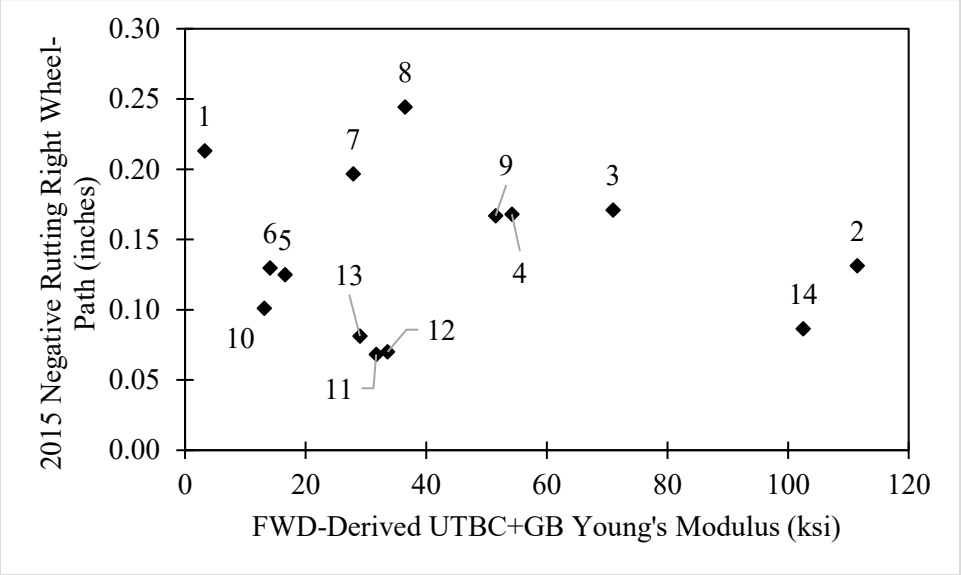

Figure 6.7 2015 Negative Direction Right Wheel-Path Rutting Versus FWD-Derived Young's Modulus of the Combined UTBC + GB Layer

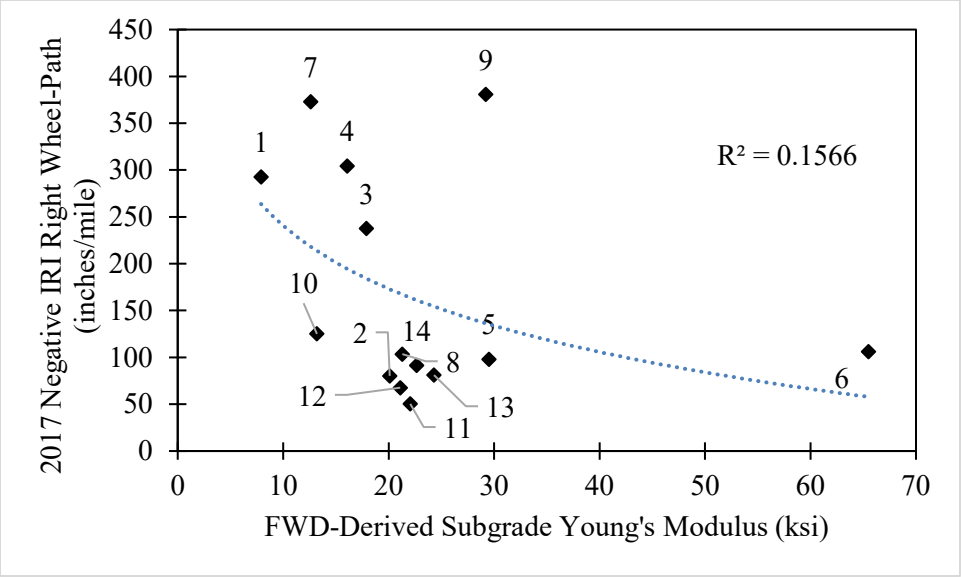

Figure 6.8 2017 Negative Direction Right Wheel-Path IRI Versus FWD-Derived Young's Modulus of the Subgrade Layer

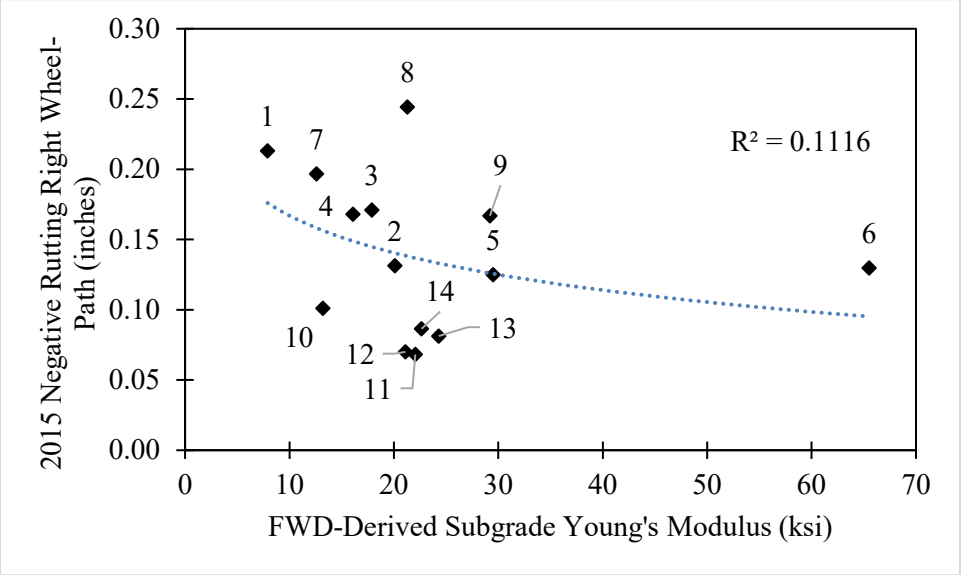

Figure 6.9 2015 Negative Direction Right Wheel-Path Rutting Versus FWD-Derived Young's Modulus of the Subgrade Layer

Similar to the DCPT-derived harmonic mean of the combined UTBC+GB layer, the stiffness of the primary pavement system appears to be, at best, a weak indicator of overall pavement performance. It is noted that at the time of testing (late July) the pavement system below the asphalt-concrete was likely at its stiffest. Local officials noted that it had not rained for months, so the water table was likely at a seasonal low. Consequently, the primary pavement system and some of the embankment fill would have been relatively dry with low degrees of saturation. Therefore, the soils supporting the asphalt-concrete would have had high values of effective stress due to the high values of matric suction, which would have increased the strength or stiffness of the soils. In particular, the cohesive soils within the UTBC+GB and the subgrade would have been extremely stiff and strong in comparison with the wetter conditions during other times of the year.

In addition to the data collected at the time of field-testing, FWD data were also collected between 2012 and 2018. Data were not collected at the same locations as those chosen in July of 2019, and the dates were generally different, so a direct comparison of those earlier results with those conducted during the field testing at the test locations was not possible. To obtain a general understanding of how the FWD results changed with time, temperature and moisture-normalized averages along the entire section were calculated and plotted, as shown in Figure 6.10.

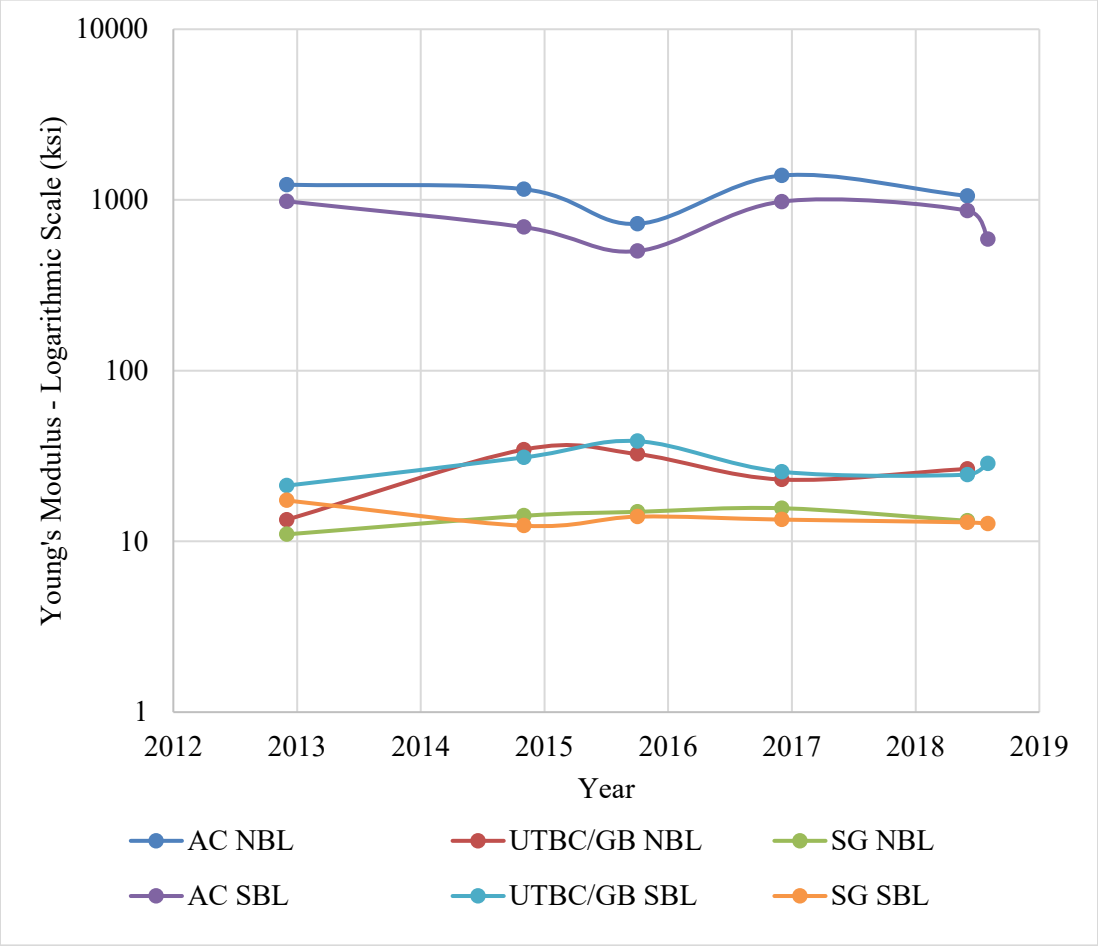

Figure 6.10 Variation of FWD Moduli with Time

There are no clear trends in the average values of Young's modulus with time. For the AC layer, Young's modulus is, on average, 28% lower for the southbound lane (SBL) than for the northbound lane (NBL) for the years 2012 to 2018. For the UTBC/GB and subgrade layers, there does not appear to be a significant difference between the values of Young's modulus for the northbound and southbound directions. That there are generally no discernible trends in the values over time is to be expected because the collection frequencies, dates of testing, and testing locations varied from year to year.

6.3 Evaluation of Data from Repetitive Static Plate Load Test

Repetitive static plate load (RSPL) tests were carried out at Locations 1, 4, 6, 8, 11, and 12. Values of the coefficient of subgrade reaction (k) and modulus of subgrade reaction (K) were calculated from the results of the RSPL tests using the techniques described in Section 2.1. The results are provided in Table 6.3.

Table 6.3 Results from Repetitive Static Plate Load Tests

Location	Coefficient of Subgrade Reaction, k (lb/in^3)			Modulus of Subgrade Reaction, K (ksi)
	Dial 1	Dial 2	Dial Average	Dial Average
1	103	93.8	98.1	2.35
4	466	509	487	11.7
6	424	578	489	11.7
8	466	352	403	9.67
11	1,110	901	997	23.9
12	1,240	791	980	23.5

The modulus of subgrade reaction is plotted versus IRI for the right wheel-path and values of rutting distress for the negative direction of travel in Figures 6.11 and 6.12. There is some scatter in the data, but the general trend is that the pavement distress decreases as the modulus of subgrade reaction increases. The correlation is better for rutting than IRI.

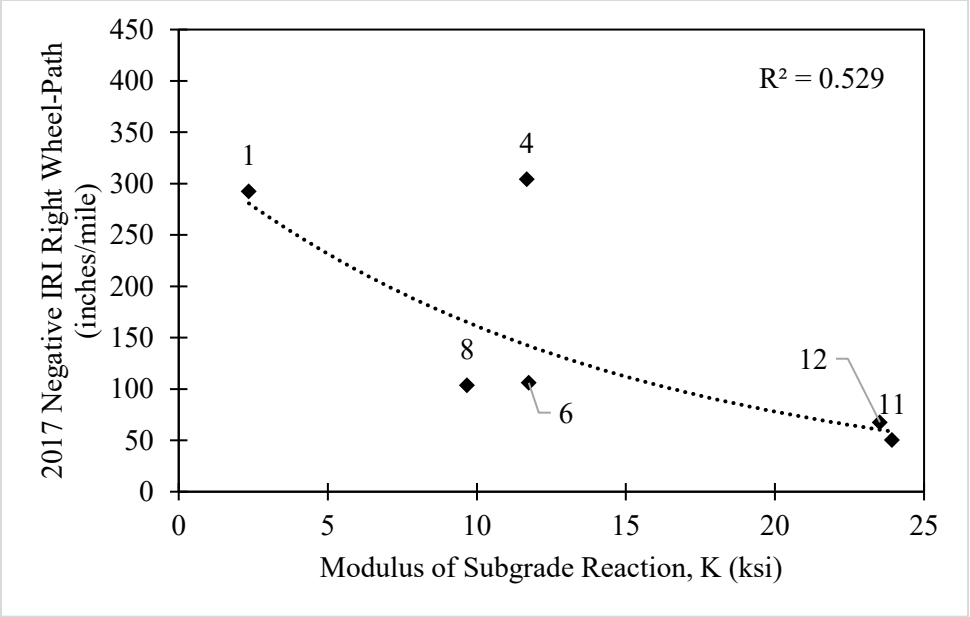

Figure 6.11 2017 Negative Direction Right Wheel-Path IRI Versus Modulus of Subgrade Reaction

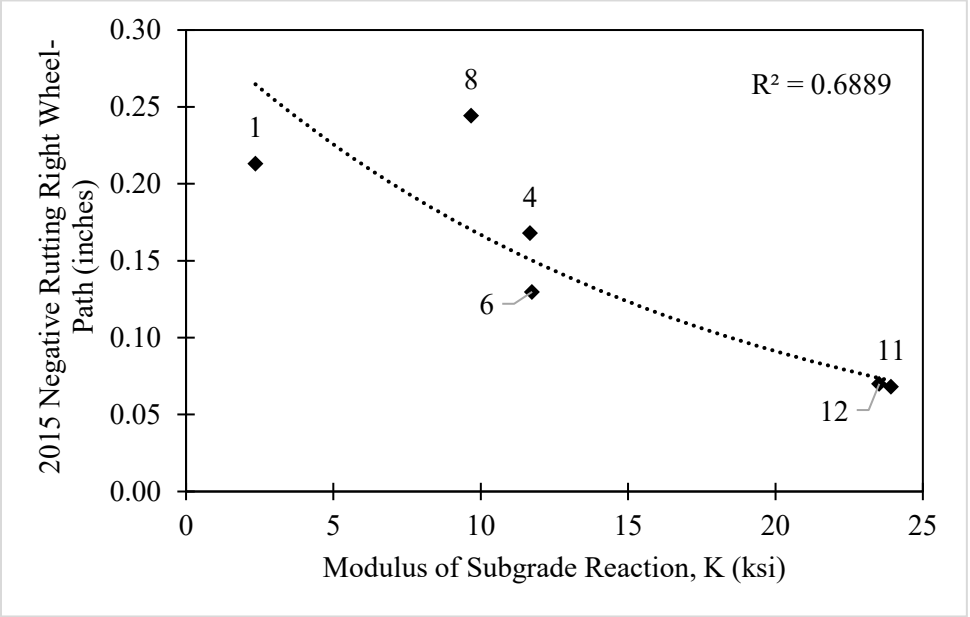

Figure 6.12 2015 Negative Direction Right Wheel-Path Rutting Versus Modulus of Subgrade Reaction

6.4 Evaluation of Data from the Cone Penetration Test

The cone penetration test (CPT) was performed at each field test location. The data from the CPT are valuable in multiple respects. The data help to:

- Characterize the stiffness of the untreated base course and granular borrow layers via the measurement of cone tip resistance
- Characterize the stiffness of the embankment fill or native subgrade soil beneath the primary pavement system
- Identify the soil behavior type via correlations with cone tip resistance, sleeve friction, and excess pore pressure

The CPT data may also be used to identify depths of embankment fill beneath the negative direction of travel for locations where it is presumed that embankment fill was used. All test locations, except those within the geogrid test section (11, 12, 13, and 14) and Location 6 (within a cut section), had a significant amount of embankment fill beneath the negative direction of travel. Location 7 is also presumed to have had embankment fill given that it was located in a section where cross-sections similar to that shown in Figure 4.8 were typical.

The fact that Locations 11, 12, 13, and 14 have extremely weak layers (cone tip resistance as low as 5.0 ksf, see Appendix D) between 5 and 20 feet below the ground surface and are still performing well indicates that the primary pavement system, plus the layers of the pavement system remaining from the original alignment, are adequate to support the new pavement system despite the underlying soft and weak subgrade.

The nominal depth of the combined UTBC+GB layer for the new pavement system was 16 inches. The depth was confirmed at each location by the DCPTs. Each test was advanced to a depth of approximately 16 inches. With the exception of Locations 13 and 14, the stiffness index decreased for the last blows, indicating the end of the primary pavement system and the beginning of native subgrade or embankment fill.

The CPT data can be used to quantify the presence of fine-grained soils similar to those tested in Section 5.2 that were vulnerable to wetting-induced volume changes. Figure 6.13 shows the percent of each soil behavior type (SBT) for the depth of soil beneath the primary pavement system that is either embankment fill or subgrade soil, or a combination of both. The depth was set to 1.33 to 10.0 feet below the ground surface for each field test location.

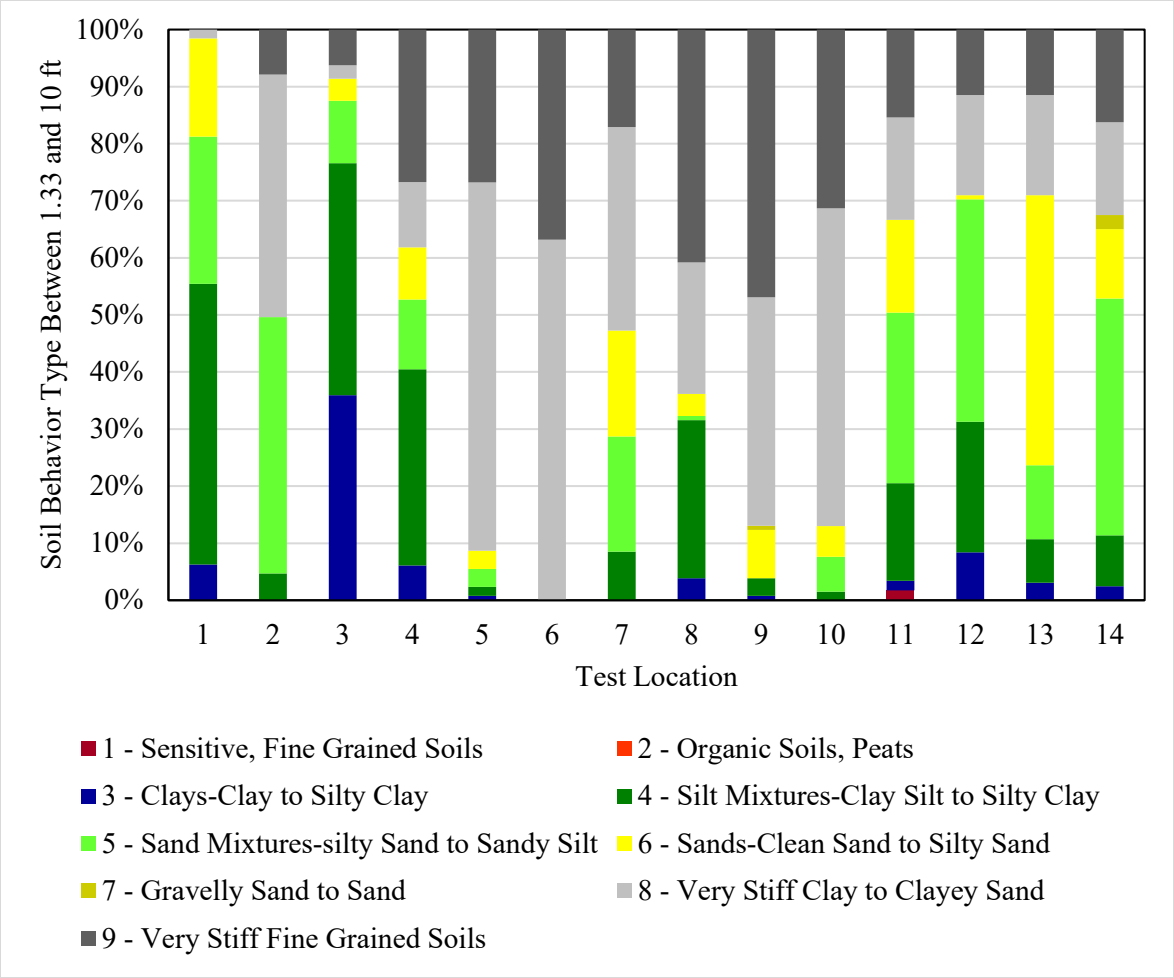

Figure 6.13 CPT-Derived Soil Behavior Type for Each Location Between 1.33 and 10 Feet Below the Ground Surface

SBT 3 (clays - clay to silty clay), SBT 4 (silt mixtures - clayey silt to silty), SBT 8 (very stiff clay to clayey sand), and SBT 9 (very stiff fine-grained soils) are more likely to be more vulnerable to wetting-induced volume changes, primarily swelling and shrinkage under low vertical stresses (shallower depths) and collapse under high vertical stresses (deeper depths). Locations 1, 3, 4, 8, and 12 had percentages of SBT 3 and 4 greater than 30% of the evaluated depth. Locations 1, 3, and 4 had percentages that were greater than 40%. These areas also performed poorly with respect to ride quality. Locations 7 and 9 performed poorly with respect to ride quality but do not have significant amounts of soil types 3 and 4. However, soil types 8 and 9, very stiff clay to clayey sand and very stiff fine-grained soils, respectively, may also be vulnerable to wetting-induced volume changes. Note that the soil behavior type, particularly for soil type 3 – clays and type 8 – very stiff clays, would vary based on the moisture content of the soil. A type 3 soil might classify as a type 8 soil if the water content is very low.

Figure 6.14 shows the CPT tip resistance profile for Location 3 where ride quality was poor. The tip resistance profile is shown for two maximum-value ranges: 0 to 1000 ksf and 0 to 200 ksf.

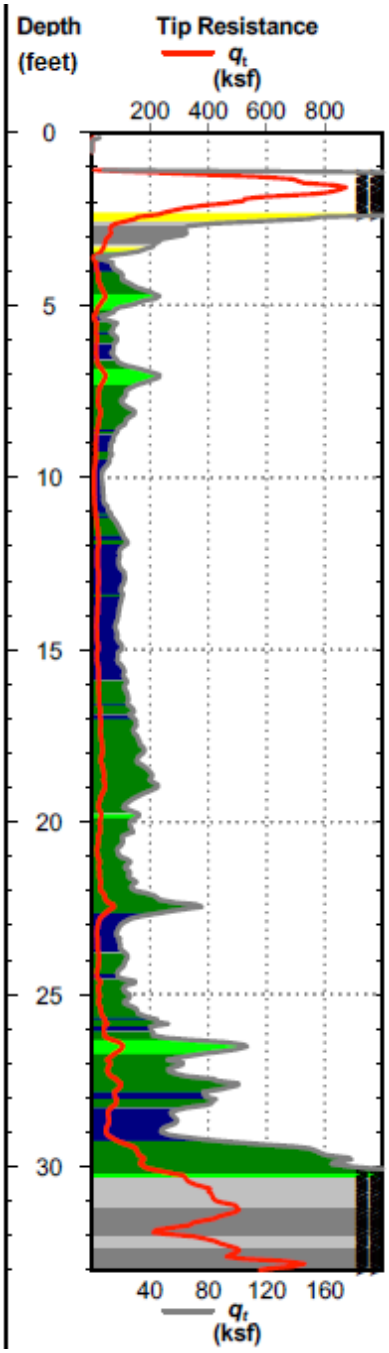

Figure 6.14 CPT Profile for Location 3

Note the presence of the combined UTBC + GB layer between depths 1 and 2.5 feet. Beneath the initial pavement system, the cone tip resistance decreases, and the soil type changes to a combination of soil types 3, 4, and 5. The slightly higher tip resistance between depths of 3 and 8 feet compared with depths between 8 and 15 feet may indicate the presence of a compacted embankment fill layer between 3 and 8 feet. Note that the tip resistance does not register as greater than zero until a depth of 1 foot, so the actual location of the ground surface on the CPT log is closer to a depth of 1 foot.

To quantify the effect of the different SBTs on the performance of the pavement system, pavement distresses at each location were plotted against the percent of SBTs in the fill plus subgrade layer. The fill plus subgrade layer is taken as the soil between 1.33 and 10.0 feet below the top of the UTBC layer. Figures 6.15 and 6.16 show IRI plotted against the percent of SBT 3 and 4, and percent of SBT 3, 4, 8, and 9, respectively. Location 6 is not included in Figure 6.16. Location 6 was located in an area with a deep cut, so the soil was likely either shale or highly over-consolidated fine-grained soil. The soil was so stiff that it was only possible to advance the cone penetrometer to a depth of 3.2 feet.

Figures 6.15 and 6.16 show a somewhat weak relationship between the variables. The relationship between the variables is improved for Figure 6.16 when Location 6 is excluded from the dataset. The percentage of SBTs 3, 4, 8, and 9 within the fill plus subgrade layer appears to be a somewhat good predictor of poor IRI performance.

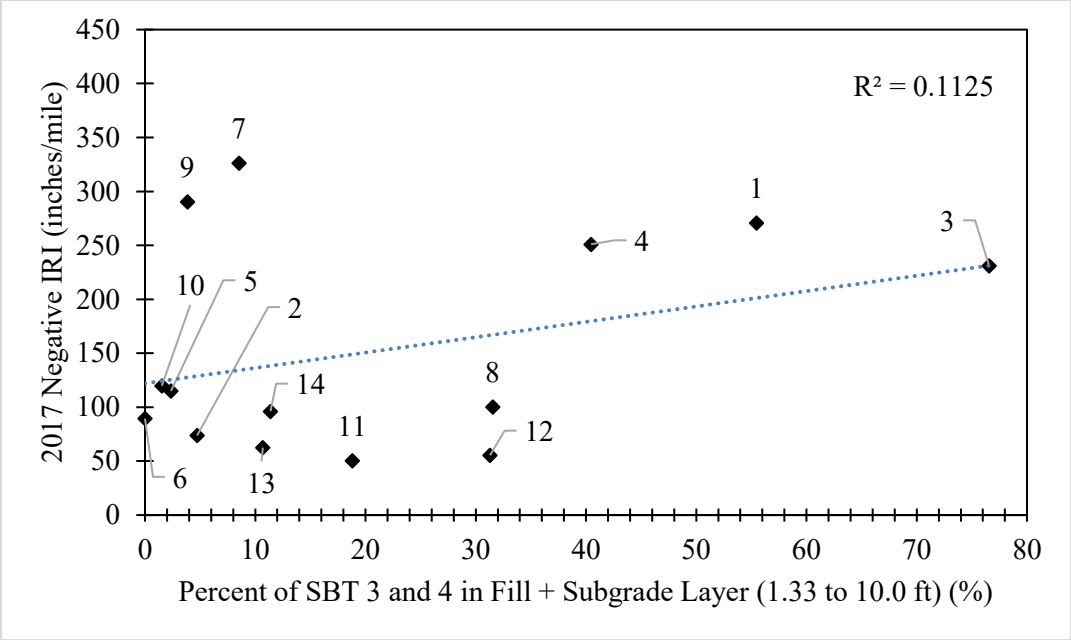

Figure 6.15 2017 Negative Direction IRI Versus Percent of SBT 3 and 4 in Fill + Subgrade Layer

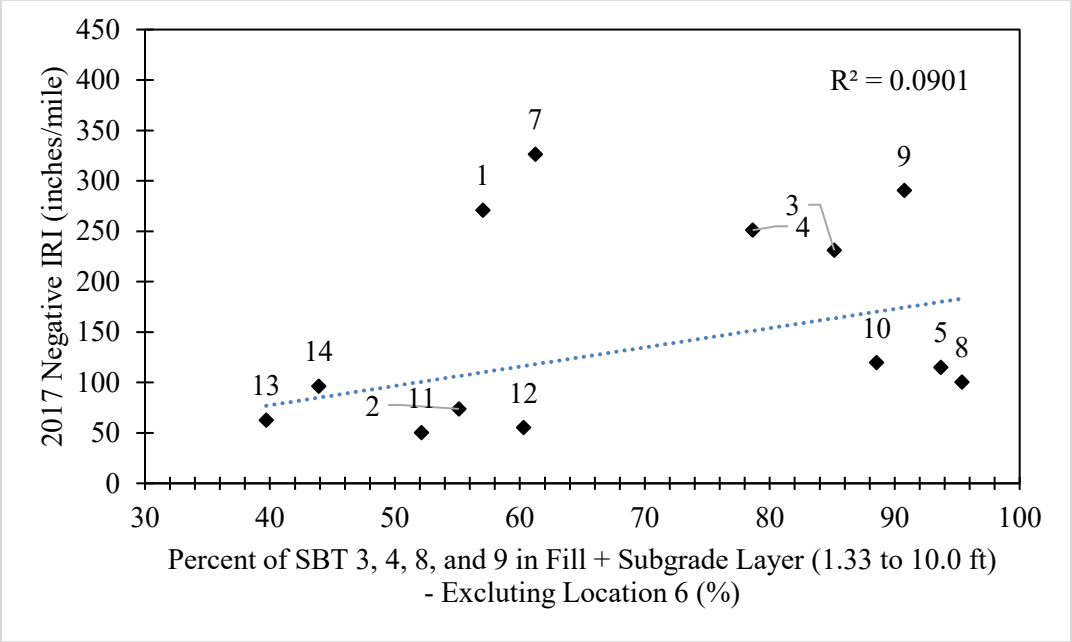

Figure 6.16 2017 Negative Direction IRI Versus Percent of SBT 3, 4, 8, and 9 in Fill + Subgrade Layer – Excluding Location 6

Figures 6.17 and 6.18 plot negative direction rutting versus the percentage of SBT 4 and SBTs 3 and 4, respectively. The percentage of SBTs 3 and 4 appear to be significantly better predictors of rutting performance than IRI performance. Figures 6.19 and 6.20 plot the same data while excluding Locations 11 through 14. Locations 11 through 14 were on sections of roadway that overlapped with the old alignment. The subgrade at these locations would therefore already be consolidated, and the rutting performance of the new roadway would be less dependent on the soil types of the subgrade compared with locations built on fresh subgrade.

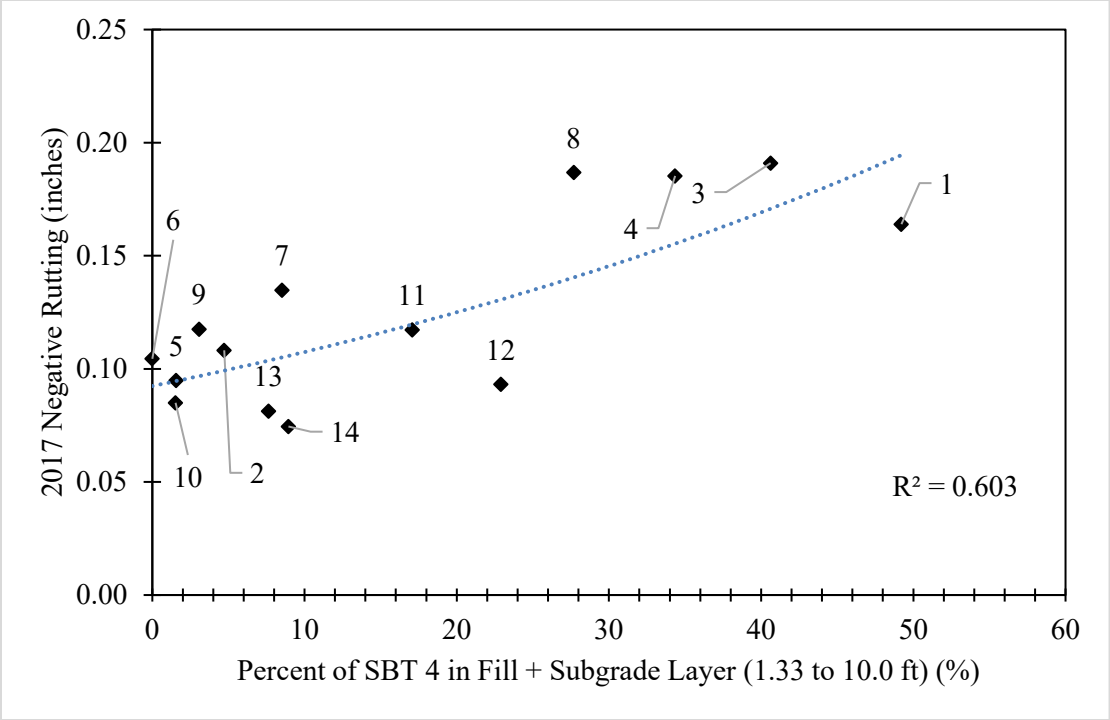

Figure 6.17 2017 Negative Direction Rutting Versus Percent of SBT 4 in Fill + Subgrade Layer

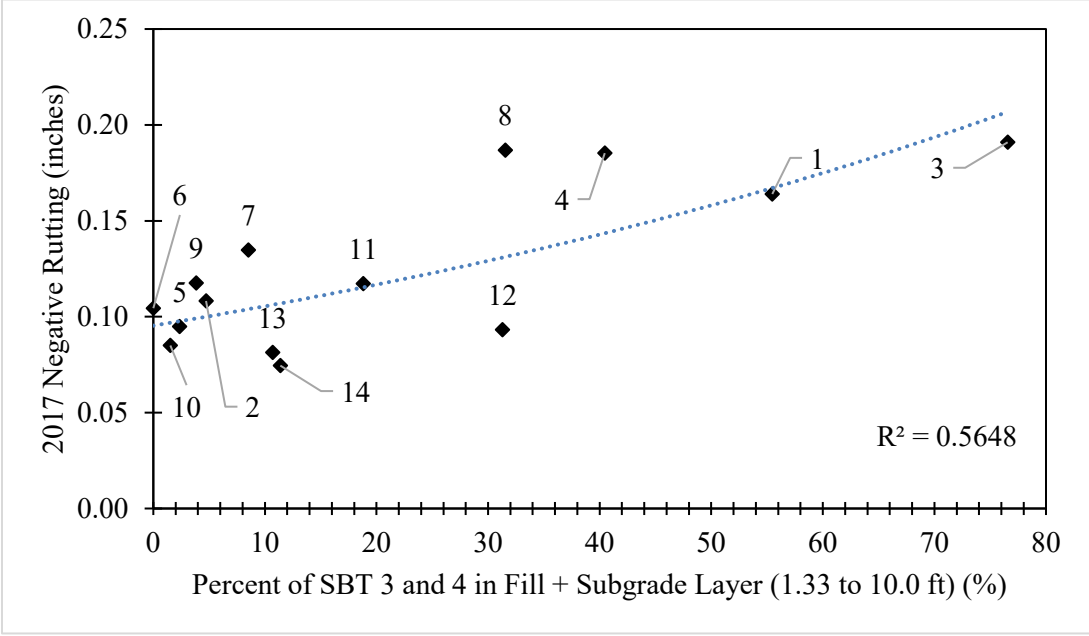

Figure 6.18 2017 Negative Direction Rutting Versus Percent of SBT 3 and 4 in Fill + Subgrade Layer

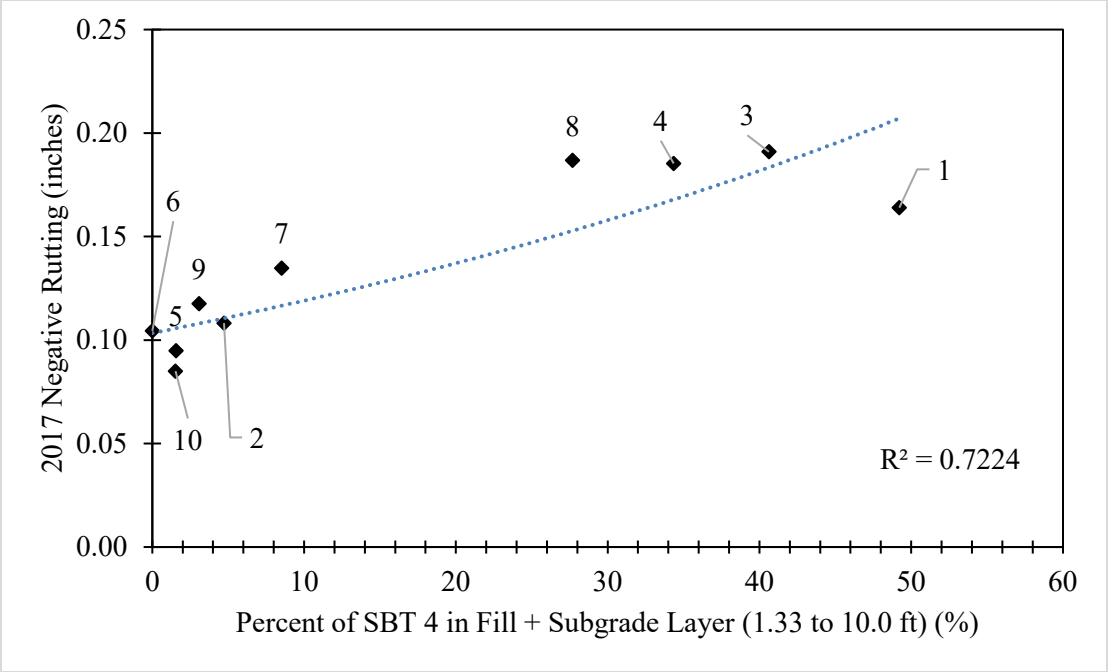

Figure 6.19 Negative Direction Rutting Versus Percent of SBT 4 in Fill + Subgrade Layer, Excluding Locations 11-14

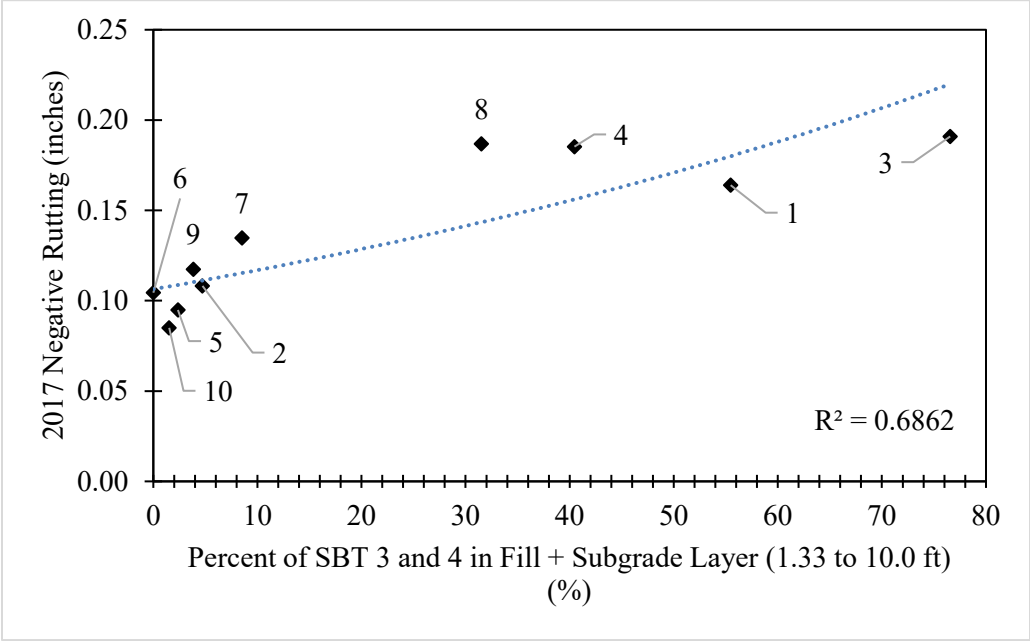

Figure 6.20 Negative Direction Rutting Versus Percent of SBT 3 and 4 in Fill + Subgrade Layer, Excluding Locations 11-14

Removing Locations 11 through 14 from the analysis improves the relation between the variables. The group of locations with high percentages of SBTs 3 and 4 are performing worse with respect to rutting compared with the group of locations with low percentages of SBTs 3 and 4. Wetting-induced volume

changes in SBTs 3 and 4 in the embankment and subgrade are likely contributing to poor rutting performance.

The stiffness of the soil layers can be quantified by the CPT. Figure 6.21 shows a comparison between the CPT cone tip resistance profiles for Locations 3 and 14 for the first 3 feet below the top of the UTBC layer. The zero-depth on the figure is set to the top of the UTBC layer.

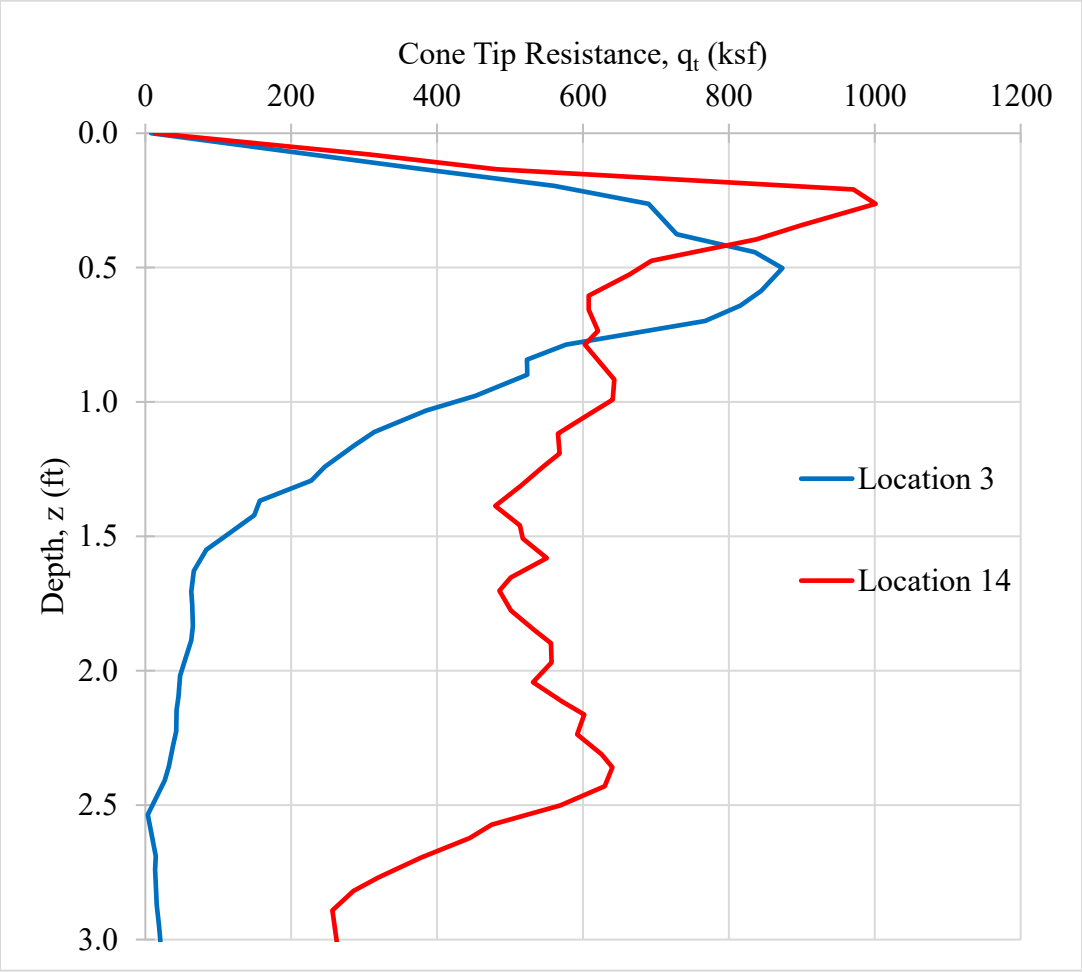

Figure 6.21 Cone Tip Resistance for the First 3 Feet Below the AC-UTBC Interface

The profiles and maximum cone tip resistance are similar for the first 1 ft. (near the bottom of the GB layer) but diverge after this. The cone tip resistance is significantly higher for Location 14 compared with Location 3 between depths 1.0 to 2.5 ft. This difference can be explained by the presence of higher quality and fully consolidated aggregate and soils under the old alignment. Location 14 was located in a section where the new alignment overlapped with the existing alignment, while Location 3 was built on native subgrade soil. The profiles for Locations 1-10 also displayed low tip resistance below 1.33 ft.

Table 6.4 shows the average and harmonic cone tip resistance for the depth of the combined UTBC + GB layer and an embankment fill + subgrade layer. For each location, the depth of the ground surface was set to the depth at which the cone tip resistance was greater than 1 ksf. The combined UTBC + GB layer was averaged over a depth of 0 to 1.33 feet. The embankment fill + subgrade layer was averaged over a depth of 1.33 to 10.0 feet.

Table 6.4 Mean Cone Tip Resistance for Each Location for the UTBC + GB Layer and Embankment Fill + Subgrade Layer

	UTBC + GB (0 to 1.33 ft) Average Cone Tip Resistance, q_t (ksf)		Embankment Fill + Subgrade (1.33 to 10.0 ft) Average Cone Tip Resistance, q_t (ksf)	
Location	Arithmetic	Harmonic	Arithmetic	Harmonic
1	198	64.4	65.5	28.3
2	989	193	137	117
3	511	118	26.9	15.9
4	447	79.1	78	60.5
5	460	72.6	252	170
6	390	71.5	446	123
7	436	250	129	72.5
8	231	72.5	101	65.4
9	412	57.8	247	129
10	163	33.1	257	117
11	315	70.6	69.2	28.7
12	298	47.9	62.3	43.8
13	444	79.7	169	73.1
14	620	185	133	24.5

Figures 6.22 and 6.23 plot the arithmetic and harmonic mean cone tip resistance for the UTBC + GB and fill + subgrade layers for each location.

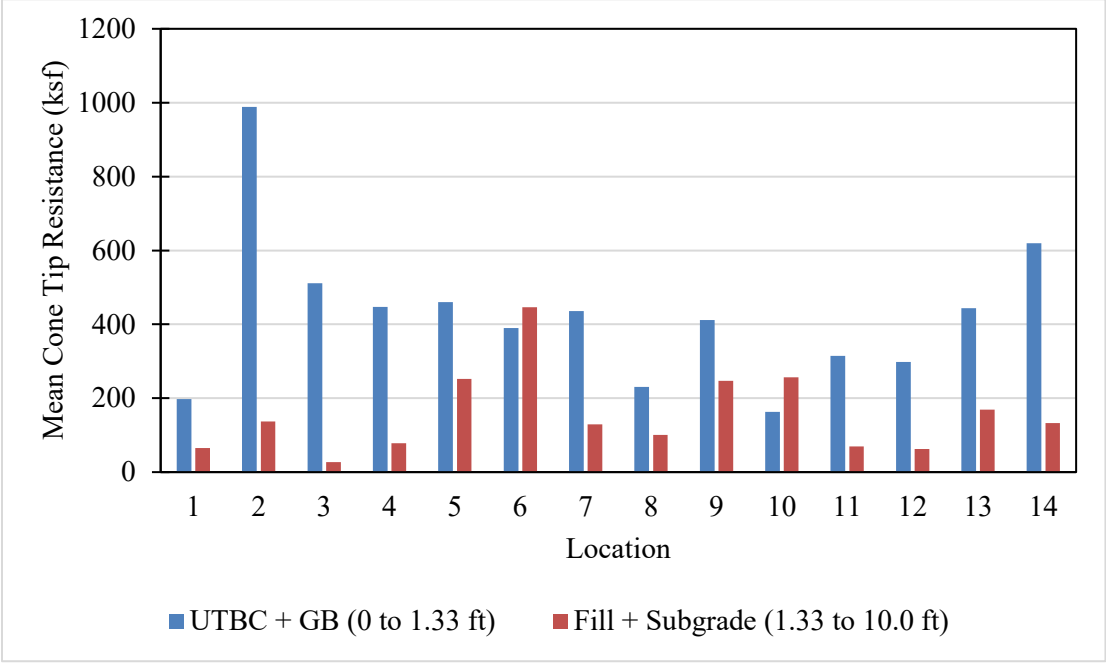

Figure 6.22 Mean Cone Tip Resistance by Location

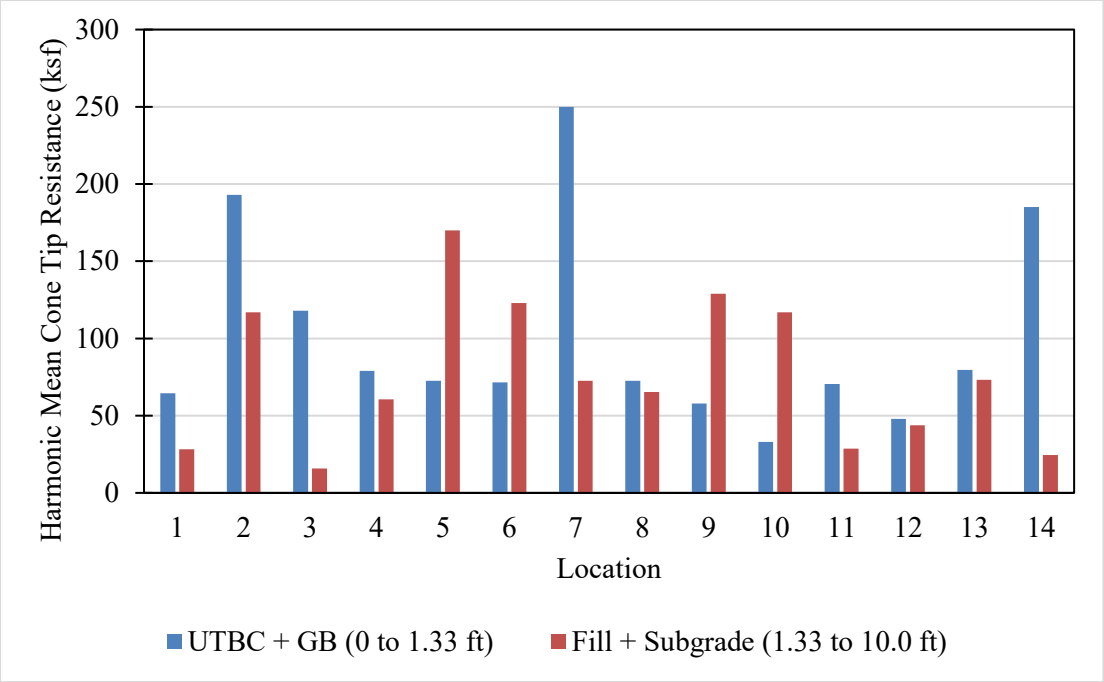

Figure 6.23 Harmonic Mean Cone Tip Resistance by Location

Figures 6.24 and 6.25 plot the location-specific pavement distresses as a function of the mean cone tip resistance for the UTBC + GB layer.

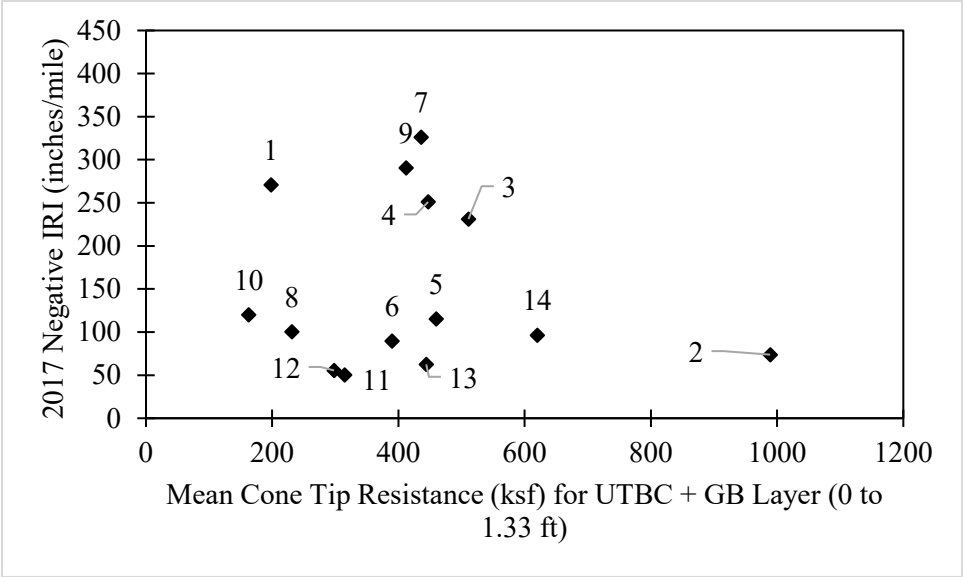

Figure 6.24 2017 Negative Direction IRI Versus Mean Cone Tip Resistance for the UTBC + GB Layer

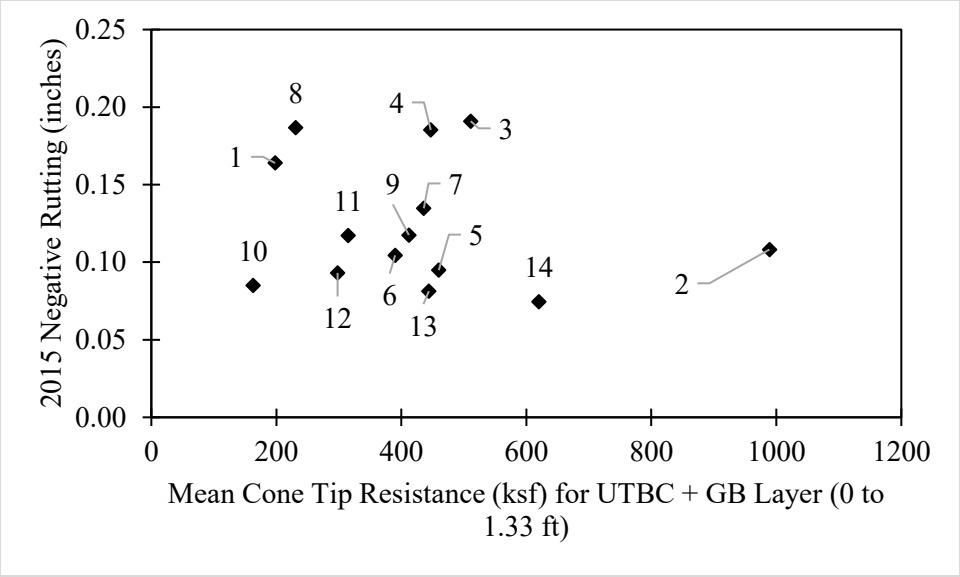

Figure 6.25 2015 Negative Direction Rutting Versus Mean Cone Tip Resistance for the UTBC + GB Layer

Similar to the DCPT-derived CBR and FWD-derived modulus, the mean cone tip resistance for the UTBC-GB layer does not appear to be a good predictor of pavement performance. It appears to show that the stiffness of the UTBC + GB layer is not related to the measured pavement distresses.

Figures 6.26 and 6.27 show the pavement distresses plotted versus the mean cone tip resistance for the fill + subgrade layer.

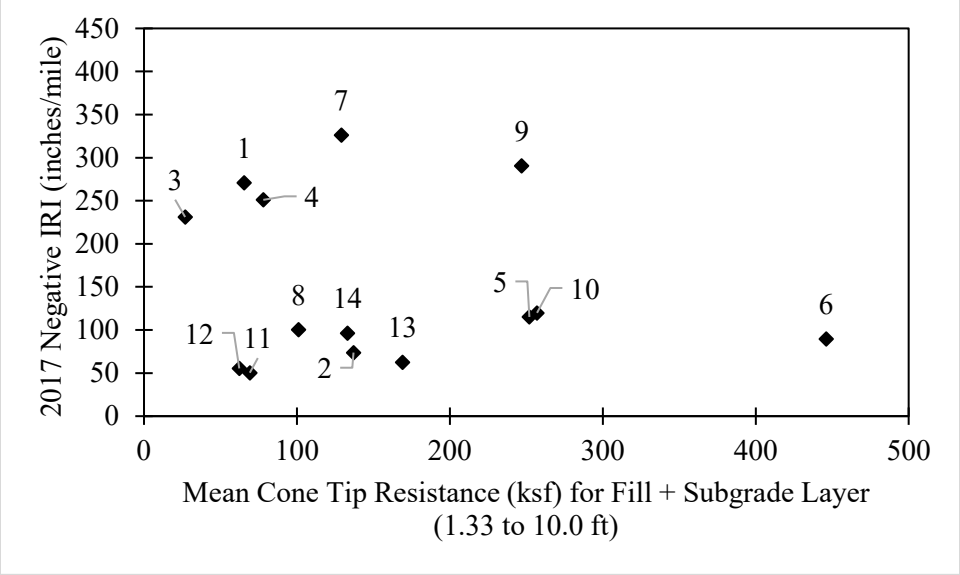

Figure 6.26 2017 Negative Direction IRI Versus Mean Cone Tip Resistance for the Fill + Subgrade Layer

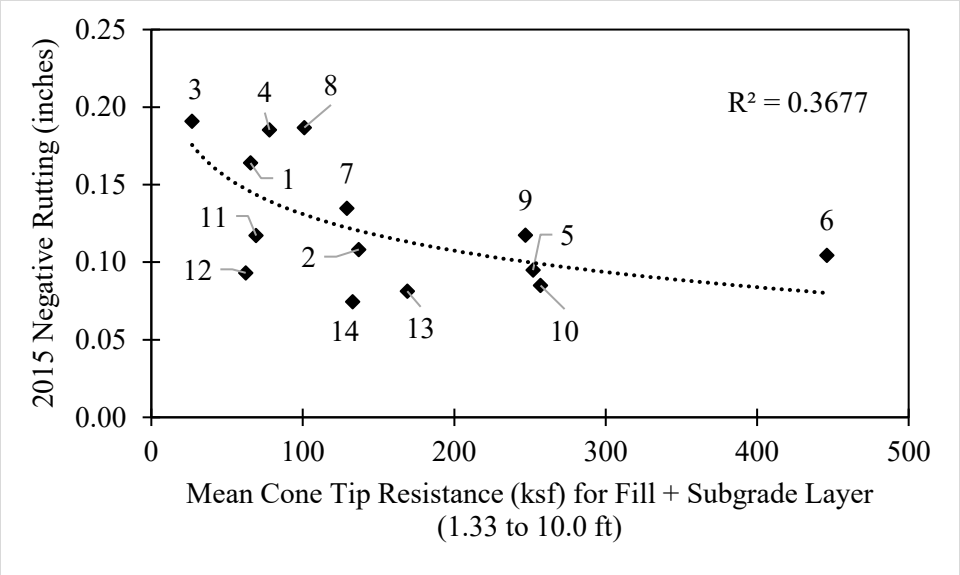

Figure 6.27 2015 Negative Direction Rutting Versus Mean Cone Tip Resistance for the Fill + Subgrade Layer

Unlike IRI, rutting performance does appear to be somewhat related to the mean cone tip resistance of the fill plus subgrade layer. The relation between rutting performance and cone tip resistance was consistent with the results comparing the pavement performance with the FWD-derived modulus of the subgrade layer. An increase in embankment fill and subgrade stiffness leads to a decrease in pavement surface rutting.

These results appear to be consistent with the analysis of the pavement distress data and construction documents presented earlier. The primary pavement system appears to be adequate as neither AC, UTBC, nor GB stiffness correlates with the measured pavement distresses. IRI distress is likely attributed to wetting-induced volume changes in the embankment fill, while rutting may be attributed to soft embankment fill and subgrade soil beneath the primary pavement system.

7. COMMENTARY ON EFFECT OF GEOGRIDS IN PAVEMENT SYSTEM

The 20-year pavement system design included two layers of biaxial geogrid at different depths. The uppermost geogrid (BX1100 or equivalent) was placed at the interface of the 6-inch UTBC layer and the 10-inch GB layer. The second geogrid (BX1100 or equivalent) was placed at the bottom of the GB layer, at the interface with the embankment fill or native subgrade soil.

One of the primary purposes of the geogrid is to add lateral confining stress (or increase the lateral earth pressure coefficient) to the pavement structure, thereby increasing the vertical stress distribution and increasing the strength and stiffness of the support system for the asphalt-concrete. For the geogrid to be effective, the soil at the soil-geogrid interface must be granular and angular enough to induce interlock with the geogrid. If the soil at the soil-geogrid interface is cohesive and highly plastic, it will primarily flow around the geogrid without producing significant interlock. Secondly, there must be enough vertical stress to provide sufficient frictional, adhesive, and passive (bearing) resistance as the geogrid moves relative to the soil and mobilizes tension within the geogrid.

CPT cone tip resistance at Locations 3 and 4 is plotted versus depth in Figure 7.1. Zero depth is set at the top of the hole left by the asphalt-coring (at the top of the UTBC layer). From the figure, it is clear that Locations 3 and 4 have similar profiles of tip resistance versus depth. Tip resistance peaks at about 900 ksf at a depth of about 0.5 ft, then stabilizes at about 50-100 ksf at depths from about 1.5 to 2.0 ft. This profile is similar to most of the profiles for Locations 1-10. This profile is also similar to the profiles of blow counts versus depth from the results of the DCPTs at Locations 3 and 4, as shown in Figure 7.2. The spike in tip resistance occurs at the approximate location of the UTBC-geogrid-GB interface (since the nominal thickness of the UTBC is 6 inches), which indicates that the uppermost geogrid is effective in increasing the resistance to applied load at that location. The effect is most pronounced at the location of the geogrid, but there appears to be a zone of influence that extends several inches in both directions from the interface.

In contrast, at a depth of 16 inches (1.33 ft), which corresponds to the nominal depth of the GB-geogrid-subgrade/fill interface, there is no noticeable change in the tip resistance. Therefore, it appears that the geogrid at the bottom of the GB layer is ineffective at increasing the resistance to applied load. The apparent ineffectiveness of the lower layer of geogrid is likely due to the embankment fill in Locations 1-10 being composed primarily of cohesive, moderately to highly plastic soils. Along interfaces between a strong and weak material, the weak material will control the engineering behavior. The second geogrid was likely floating in a matrix of cohesive embankment fill or native subgrade instead of interlocking with the GB layer. Thus, it appears that the second geogrid did not increase the resistance to applied load of the support system for the asphalt-concrete.

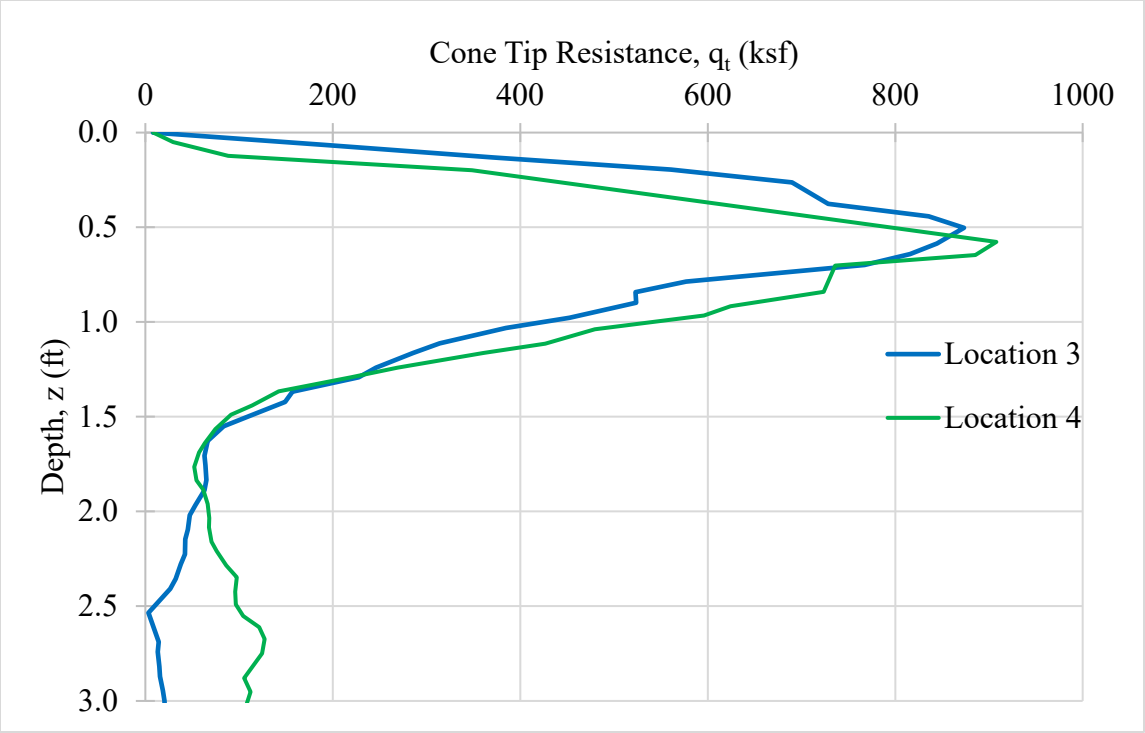

Figure 7.1 Cone Tip Resistance for First 3 Feet Below AC-UTBC Interface

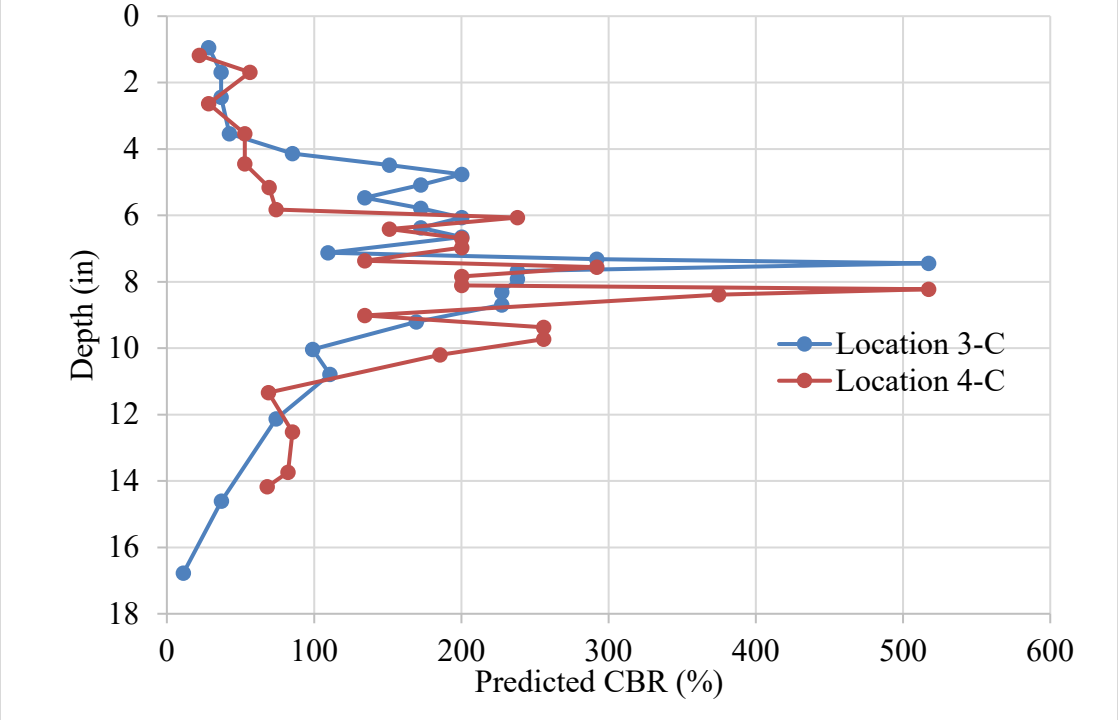

Figure 7.2 DCPT-Derived Predicted CBR for UTBC + Geogrid + GB Layer for Locations 3 and 4

8. COMMENTARY ON RESULTS FROM DATA EVALUATION WITH RESPECT TO UDOT GEOGRID DESIGN GUIDE

As part of this research project, the UDOT Materials Group requested that the University of Utah review the latest draft of the document *Guide for Geosynthetics for Subgrade Improvement* (Utah Department of Transportation, 2018) and provide them with our recommendations for changes or improvements, if any. It is our understanding that this document was developed by the Four Corners Task Force to assist with designing pavement sections reinforced with geogrid, and that this guide will become part of the updated UDOT *Pavement ME Design Manual of Instruction* as soon as a new version is published. In this chapter, the results from the forensic investigation described previously in this report will be analyzed with respect to the new guidelines. Suggested changes and improvements to the guidelines will then be provided.

According to the 2018 *Guide for Geosynthetics*, the recommended composite system for soft subgrade soil conditions (resilient modulus from 0.5 to 5 ksi) consists of an asphalt-concrete layer, a minimum of 6 inches of aggregate base course, a geosynthetic, a minimum of 6 inches of stabilizing material, and a final layer of geosynthetic between the stabilizing material and the subgrade. Figure 8.1 shows a figure of the idealized composite system.

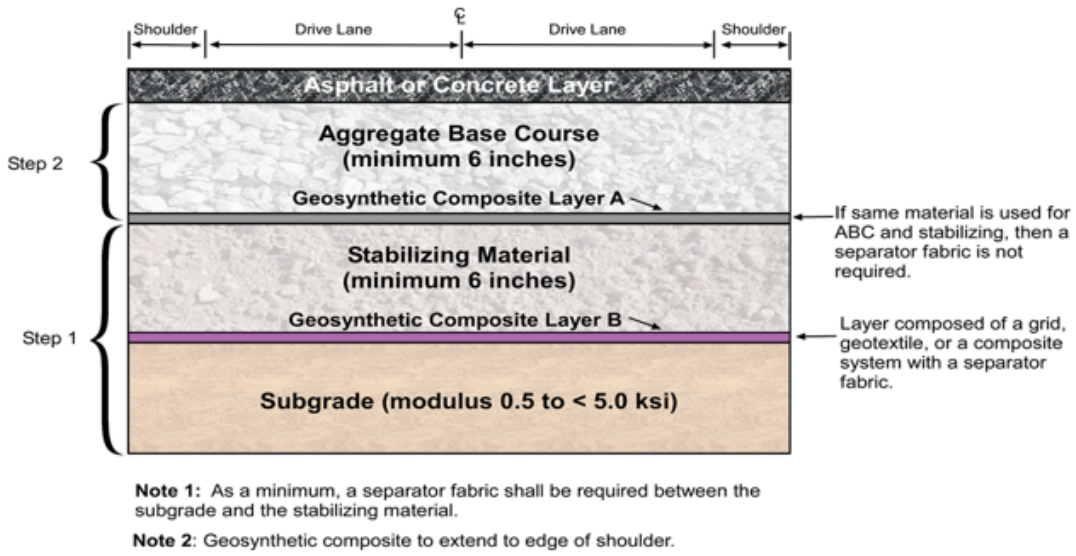

Figure 8.1 Idealized Geosynthetic-Reinforced Pavement System for Soft Subgrades

The geosynthetic-reinforced pavement system designed for SR-10 between Emery and Muddy Creek consisted of 8 inches of asphalt-concrete, 6 inches of untreated base course, a biaxial geogrid, 10 inches of granular borrow, and a biaxial geogrid at the interface of the granular borrow and the subgrade or embankment fill.

The guide specifies that the base course shall meet applicable DOT requirements. Laboratory testing of the untreated base course layer for SR-10 found that the plasticity index was higher than the allowable value for most samples, as discussed in Chapter 5.

The guide specifies that the gradation of the stabilizing material shall not be greater than the 3-inch sieve. Laboratory testing confirmed that the gradation of all granular borrow samples passed this requirement.

The guide further specifies that the material should have less than 12% passing the #200 sieve and a plasticity index less than 6. Most sampled granular borrow did not meet these requirements.

The design guide states that "expansive soils shall be mitigated prior to using the geosynthetic composite system." Soils with a swell greater than 2% are considered expansive. The sampled subgrade soil in one cut section compacted to a minimum requirement of 96% relative compaction based on maximum dry density from the standard Proctor test swelled as much as 5% under low overburden pressures. The swell potential of the subgrade soil likely contributed to the poor IRI performance of some sections of the roadway.

Evaluation of the pavement distress data in this report showed that the pavement system performed well in the "test section" area where the new alignment overlapped with the existing alignment. In addition to results from FWD, DCPT, and CPT testing of the combined UTBC + GB layer stiffness, it appears that the designed geosynthetic composite system is performing adequately in areas with shallow or no embankment fill.

Interestingly, DCPT and CPT data indicate the presence of a stiff layer in the upper third of the combined UTBC + GB layer. The stiff layer is likely at the interface between the biaxial geogrid that separates the UTBC and GB layers, which shows that the geogrid is providing additional resistance to applied load. However, the lower layer of geogrid, located at the bottom of the GB layer, does not appear to provide any additional resistance to applied load but may be providing some value as a separator, yet is certainly not as effective a separator as geotextile would have been.

Based on the results of our forensic investigation of SR-10 and a review of the literature on geosynthetic-reinforced pavement systems, we suggest that three changes be made to the guide. Each of these three suggested changes will be discussed below.

First, the use of triaxial geogrid should be allowed as an alternate to biaxial geogrid. Research shows that triaxial geogrid is more effective than biaxial geogrid in stabilizing a pavement system. Although only one company currently manufactures and sells triaxial geogrid, the increased efficiency of triaxial geogrids compared with biaxial geogrids will likely result in better-performing and longer-lasting pavement systems.

The second suggested change relates to the location of geogrid layers within the support system for the asphalt or concrete layer. In Luo et al. (2017), a report referenced in the guide, the following statement is made:

> According to the literature…geosynthetics were reported to be more effective in flexible pavements when placed at the base-subgrade interface of thin base sections (such as 6 inches) and near the midpoint of thicker base layers (such as 10 or more inches).

In support of this statement, the guide referenced six papers (Al-Qadi et al., 2011; Aran, 2006; Chan et al., 1989; Haas et al., 1988; Moghaddas-Nejad and Small, 1996; Perkins, 1999). However, after a thorough review of these six papers, it became apparent that the most efficient location of the geosynthetic reinforcement depends on several factors, including thicknesses and stiffnesses of the asphalt concrete, the base course, the subbase, and the subgrade, as well as the width of the loaded area (footprint of the tires). For most of the tests reported in these references, there was no subbase (stabilizing layer), and for one of the thin layers of base course, the reinforcement was more effective in the middle of the base course than at the interface of the base course and the subgrade (Moghaddas-Nejad and Small, 1996). Thus, it appears there has been insufficient research to determine the optimum location for the upper layer of geogrid for all component variations within pavement systems. Therefore, the following

recommendations are made for the location of the geogrid layer supporting the base course for flexible pavement systems:

> *Thickness of base course 6 inches or less:* Locate geogrid along interface with stabilizing layer.
>
> *Thickness of base course more than 6 inches but less than 10 inches:* Locate geogrid one-third the thickness of the base course upward from the interface with the stabilizing layer. For example, for a 9-inch thick base course, the geogrid would be located 3 inches above the top of the stabilizing layer.
>
> *Thickness of base course 10 inches or more:* Locate geogrid at the mid-height of the base course.

Third, if the stabilizing layer is thick, the use of a geocomposite composed of geogrid plus geotextile at the interface of the stabilizing layer and the subgrade will probably provide insignificant reinforcement, but the geotextile will certainly act as a separator and therefore provide an important function. Therefore, it is recommended that if the thickness of the stabilizing layer is 8 inches or more, either geotextile alone be used at the interface of the stabilizing layer and the subgrade for separation and perhaps some reinforcement, or geotextile alone be used at the interface of the stabilizing layer and the subgrade for separation, with geotextile located at the mid-height of the stabilizing layer for more efficient reinforcement.

9. SUMMARY, CONCLUSIONS, AND RECOMMENDATIONS

9.1 Summary

In this research project, a forensic evaluation of an existing roadway in central Utah was carried out. As part of the investigation, field testing and multiple sampling collections were performed on the roadway and roadway materials. Laboratory testing was conducted on the sampled materials, including the AC, UTBC, GB, and native subgrade soil. The pavement distress data, construction documents, field testing data, and laboratory testing data were evaluated for possible sources of premature pavement system deterioration.

9.2 Conclusions

Construction drawings showed typical cross-sections with deep embankment fill under most of the negative (southbound) travel lanes, but little or no embankment fill under most of the positive (northbound) travel lanes. Based on information found in the construction logs, it is highly likely that most or all of the embankment fill was constructed from native soils taken from the cut sections of the roadway. Samples of native soils obtained from cut sections of the roadway were tested in the laboratory and found to be fine-grained, cohesive soils that are vulnerable to large loading-induced and wetting-induced volume changes.

The pavement system performed well with respect to cracking. The pavement distress data, visual observation, and the IFIT testing of asphalt-concrete samples confirmed the adequate performance of the asphalt-concrete layer.

The pavement system also performed well with respect to rutting. With the exception of 2018 for the northbound positive direction, the pavement distress data showed that surface rutting was within the acceptable thresholds for all years and both directions. Statistical analyses indicated that the parameters that best predicted location-specific rutting distress were modulus of subgrade reaction determined from static plate-load tests, percentage of soil behavior types 3 and 4 (clay, silty clay, clayey silt) in the fill plus subgrade layer, and tip resistance from CPT. Rutting varied with wheel-path. For the positive direction of travel, the right wheel-path performed better than the left wheel-path with respect to rutting. The difference in rutting performance was likely due to the right wheel-path overlapping with the old roadway alignment while the left wheel-path was underlain by fresh subgrade or embankment fill.

The pavement system performed adequately with respect to IRI for the positive direction with the exception of 2018. However, already in 2012 the negative direction IRI was greater than the allowable thresholds. Ride quality varied transversely across the width of the roadway due to the negative direction being constructed on fresh subgrade. IRI was highest under the right wheel-path of the negative direction and lowest under the right wheel-path of the positive direction. An increase in the percentage of soil behavior types 3, 4, 8, and 9 (clay, silty clay, clayey silt, very stiff sand to clayey sand, and very stiff fine-grained soil) in the fill plus subgrade layer correlated slightly with an increase in IRI. The CPT-derived soil behavior type at Locations 1, 3, and 4 showed high percentages of clay and silt mixtures at depths between 1.33 and 10.0 ft. These areas performed poorly with respect to ride quality. From the statistical analyses of the field-testing results, it was determined that poor IRI performance was unrelated to the stiffness of the primary pavement system and was likely caused by the vulnerability of the embankment fill to loading-induced and wetting-induced volume changes, resulting in differential settlements throughout the roadway. Loading-induced volume changes resulted from the weight of the overburden (self-weight of the embankment material plus weight of the pavement system) and produced settlement of the pavement system. This loading-induced settlement likely occurred over a period of several months or

years because of the cohesiveness of the embankment material. Volume changes from wetting produced settlement from collapse within the deeper portions of the embankments and heave from swell within the upper portions. Drying produced settlement from shrinkage within the upper portions of the embankments.

The presence of culverts running underneath the roadway negatively affected the performance of the pavement system supporting the southbound lane. Negative direction IRI was 62% higher for areas with culverts compared with areas without culverts. This correlation provides further evidence that problems with roughness in the negative direction were at least partially attributable to wetting-induced volume changes.

The statistical analyses and evaluations mentioned above indicate that the structural design of the primary pavement system was adequate as the stiffness measurements of the primary layers did not correlate with the measured pavement distresses. Even though the asphalt-concrete layer was subjected to significant deformations in the longitudinal and transverse directions, there was negligible cracking. The upper layer geogrid likely provided the necessary tensile reinforcement to prevent tension cracking in the asphalt-concrete layer despite large movements in the embankment and subgrade. The characteristics of the fill and subgrade likely dominated the performance of the pavement. The structural design of the pavement system did not account for the vulnerability of the native soil to loading-induced and wetting-induced volume changes. The large differential movements in the subgrade and fill caused severe undulations in the surface of the pavement.

9.3 Additional Research

It is recommended that additional research be conducted to provide a better understanding of the causes of individual IRI spikes along the negative direction of travel. As noted at the beginning of the study, there was some uncertainty about the presence of both geogrid layers at some of the field-testing locations. Geogrid was not located in all sampling locations. Ground penetrating radar could be used to characterize the layering of subsurface materials and determine if geogrid was missing in some sections. Another option for additional research would be to trench some of the locations that had severe IRI spikes. By trenching, it would be possible to determine in which soil layers the deformation was occurring. Additionally, it would be possible to take soil samples of the actual subgrade or embankment fill beneath the problem areas to determine their engineering characteristics, particularly with respect to loading and wetting-induced volume changes. Furthermore, moisture sensors could be placed in problem areas at various depths to measure the seasonal variation in moisture within the UTBC, GB, subgrade, and embankment fill. To allow better utilization of the data collected from the FWD tests, FWD testing should be conducted at the same locations each year. Preferably, FWD tests should be performed every three months at the same locations so that seasonal variations in pavement stiffness can be measured and monitored over the service life of the roadway.

From a thorough review of the literature, it appears there has been insufficient research conducted to determine the optimum location for the upper layer of geogrid for all component variations within pavement systems. Therefore, it is recommended that research be conducted to determine the optimum location of all layers of geosynthetics used to reinforce pavement systems consisting of various components and thicknesses of those components. This research could consist of large-scale laboratory tests, numerical analyses, or instrumented field test sections. The most effective research would consist of a combination of these three types.

9.4 Recommendations

The primary issue facing the pavement system studied in this research project was the high IRI values and IRI spikes for the negative (southbound) direction of travel. To reduce the risk of surface longitudinal deformations on similar projects, the following actions should be considered:

- If possible, avoid unnecessary horizontal realignments. Build as much of the new roadway over the existing alignment as possible.
- If the new alignment is designed such that significant portions of the travel lanes overlap with native subgrade instead of the existing alignment, basic to intermediate-level testing should be performed on samples of the subgrade materials from the areas where the new alignment will cross. Testing should include basic soil classification, as well as consolidation and swell/collapse properties of the subgrade.
- Tighten specifications for using native excavated material as embankment fill. A new vertical and horizontal alignment may generate cross-sections with requirements for significant cut and fill. UDOT Standard Specifications allow on-site material excavated as part of the job to be used as embankment fill in fill sections. If fill volumes exceed cut volumes, material must be imported and the material must meet the requirements of borrow (A-1-a through A-4). On-site materials are currently only required to be of a "suitable granular material." In the case of this project, the tested excavated subgrade materials were mostly fine-grained. To reduce the risk of constructing fills that will be vulnerable to significant loading-induced and wetting-induced volume changes, which have the potential to cause significant and damaging surface deformations in the pavement system during its service life, specifications for using on-site material as embankment fill should be tightened. At a minimum, clear specifications should be provided as to what properties a "suitable granular material" should have. It is recommended that these requirements be the same as the current requirements for granular borrow. Alternately, it could be specified that cohesive materials be chemically stabilized to reduce or eliminate the potential for significant settlement or heave to occur. Lime, Portland cement, and fly ash are commonly used for these purposes. Detailed information on proper mix design and construction procedures for chemically stabilizing compacted soils supporting roadways can be found in many references (e.g., Lawton, 2001).
- When constructing a roadway on fresh subgrade that is vulnerable to swell, the subgrade should be chemically stabilized to a depth that will prevent significant deformation from occurring within the pavement system.
- A geotextile filter should be placed at the interface of the granular borrow and subgrade to reduce infiltration of plastic fines into the primary pavement system.
- As part of the three suggested changes to the *Guide for Geosynthetics* given in Chapter 8, the recommendations with regard to the placement of the geogrid reinforcement based on the thickness of the base course layer are repeated here:

  Thickness of base course 6 inches or less: Locate geogrid along interface with stabilizing layer.

  Thickness of base course more than 6 inches but less than 10 inches: Locate geogrid one-third the thickness of the base course upward from the interface with the stabilizing layer. For example, for a 9-inch thick base course, the geogrid would be located 3 inches above the top of the stabilizing layer.

Thickness of base course 10 inches or more: Locate geogrid at the mid-height of the base course.

- Compaction of pavement system materials in freezing weather should not be permitted. UDOT Standard Specifications allow borrow material to be placed during freezing and snowing conditions, but states that snow and frozen material must be removed from the subgrade or embankment surface before additional compaction can be performed. Additionally, the standard does not allow the delivery or use of frozen borrow. While the standard applies a minimum allowable temperature (50°F air temperature) for placing HMA and SMA, there is not a similar limit when placing or compacting borrow materials. It is recommended that placement and compaction of any borrow material not be permitted in air temperatures below 40°F.

10. REFERENCES

Al-Qadi, I. L, Dessouki, S., Tutumluer, E., and Kwon, J. (2011). "Geogrid Mechanism in Low-Volume Flexible Pavements: Accelerated Testing of Full Scale heavily Instrumented Pavement Sections." *International Journal of Pavement Engineering*, Vol. 12, No. 2, pp. 121-135.

Al-Qadi, I. L., Ozer, H., Lambros, J., El Khatib, A., Singhvi, P., Khan, T., and Doll, B. (2015). "Testing Protocols to Ensure Performance of High Asphalt Binder Replacement Mixes Using RAP and RAS." *Research Report No. FHWA-ICT-15-017.* Illinois Center for Transportation.

American Association of State Highway and Transportation Officials (2018). "Standard Method of Test for Moisture-Density Relations of Soils Using a 2.5-kg (5.5-lb) Rammer and a 305-mm (12-in.) Drop." *T 99-18*. AASHTO.

Anderson, D. I. (2013). "Skid Correction Program - User's Manual." *Report No. UT - 13.03*. Salt Lake City: Utah Department of Transportation.

Aran, S. (2006). "Base Reinforcement with Biaxial Geogrid." *Transportation Research Record: Journal of the Transportation Research Board*, No. 1975, pp. 115-123.

ASTM Standard (2007). "Standard Test Method for Particle-Size Analysis of Soils." *D 422 - 63*. ASTM International, West Conshohocken, PA.

ASTM Standard (2005). "Standard Test Methods for Liquid Limit, Plastic Limit, and Plasticity Index of Soils." *D 4318 - 05*. ASTM International, West Conshohocken, PA.

ASTM Standard (2014). "Standard Test Method for Rapid Determination of Carbonate Content of Soils." *D4373-14*. ASTM International, West Conshohocken, PA.

ASTM Standard (2015). "Standard Test Methods for Laboratory Compaction Characteristics of Soil Using Standard Effort (12,400 ft-lbf/ft3 (600 kN-m/m3)." *D698-12*. ASTM International, West Conshohocken, PA.

ASTM Standard (2017). "Standard Practice for Classification of Soils for Engineering Purposes (Unified Soil Classification System)." *D2487-17*. ASTM International, West Conshohocken, PA.

ASTM Standard (2018). "Standard Test Methods for One-Dimensional Swell or Collapse of Soils." *D4546 - 14*. ASTM International, West Conshohocken, PA.

ASTM Standard (2015). "Standard Test Method for Repetitive Static Plate Load Tests of Soils and Flexible Pavement Components, for Use in Evaluation and Design of Airport and Highway Pavements." *D1195/D1195M*. ASTM International, West Conshohocken, PA.

ASTM Standard. (2018). "Standard Test Method for use of the Dynamic Cone Penetrometer in Shallow Pavement Applications." *D6951/D6951M.* ASTM International, West Conshohocken, PA.

ASTM International (2018). "Standard Test Methods for One-Dimensional Swell or Collapse of Soils." *D4546*. ASTM. ASTM International, West Conshohocken, PA.

Chan, F., Barksdale, R., and Brown, S. (1989). “Aggregate Base Reinforcement of Surfaced Pavements.” *Geotextiles and Geomembranes*, Vol. 8, No. 3, pp. 165-189.

Doelling, H., and Kuehne, P. (2016). “Interim Geologic Map Of The East Half Of The Salina 30' X 60' Quadrangle, Emery, Sevier And Wayne Counties, Utah.” Utah Geological Survey, Salt Lake City, UT.

Federal Highway Administration. (2006). “Geotechnical Aspects of Pavements.” *Publication No. FHWA NHI-05-037*. U.S. Department of Transportation.

Haas, R., Walls, J., and Carroll, R.G. (1988). “Geogrid Reinforcement of Granular Bases in Flexible Pavements.” *Transportation Research Record: Journal of the Transportation Research Board*, No. 1188, pp. 19-27.

Holtz, R., Kovacs, W., and Sheahan, T. (2011). *An Introduction to Geotechnical Engineering.* Pearson Education.

Illinois Department of Transportation (2016). “Determining the Fracture Potential of Asphalt Mixtures Using the Illinois Flexibility Index Test (I-FIT).” *Illinois Test Procedure 405.*

International Organization for Standardization (2018). “Geotechnical investigation and testing - Laboratory testing of soil - Determination of liquid and plastic limits.” *ISO 17892-12*. ISO.

Lawton, E. C. (2001). “Soil Improvement and Stabilization: Non-Grouting Techniques.” Section 6A in *Practical Foundation Engineering Handbook*, 2nd edition, edited by R.W. Brown. New York: McGraw-Hill.

Moghaddas-Nejad, F., and Small, J.C. (1996). “Effect of Geogrid Reinforcement in Model Track Tests on Pavement.” *Journal of Transportation Engineering*, Vol. 122, No. 6, pp. 468-474.

National Cooperative Highway Research Council. (2007). “Cone Penetration Testing - A Synthesis of Highway Practice.” *NCHRP Synthesis 368.* Transportation Research Board of the National Academies, Atlanta, GA.

Perkins, S.W. (1999). “Mechanical Response of Geosynthetic-Reinforced Flexible Pavements.” *Geosynthetics International*, Volume 6, No. 5, pp. 347-381.

Romero, P., and VanFrank, K. (2017). “Balanced Asphalt Concrete Mix Performance; Phase II: Analysis of BBR and SCB-IFIT Tests.” *Report No. UT-17.21*. Utah Department of Transportation.

Utah Department of Transportation (2018). “Guide for Geosynthetics for Subgrade Improvement.” UDOT.

Utah Department of Transportation (2019). “Pavement Design Manual of Instruction.” UDOT.

Utah Department of Transportation (2017). “Standard Specifications for Road and Bridge Construction.” UDOT.

Wilson, S. D. (1970). “Suggested Method of Test for Moisture-Density Relations of Soils using Harvard Compaction Apparatus.” *STP 479*, ASTM International, West Conshohocken, PA, pp. 101-103.

11. APPENDIX A: LABORATORY TESTING OF UNTREATED BASE COURSE AND GRANULAR BORROW

Particle size analysis (ASTM D422) was carried out for all collected soil samples. In addition to a table and plot of the distribution, calculated values of coefficient of uniformity and coefficient of curvature are included. Results from Atterberg limits testing, from both the Casagrande and fall cone methods, are provided after the data from the particle size analysis. Soil classification was based on the values of liquid limit and plastic limit obtained from the Casagrande method.

Project:	SR-10		Date:	8/22/2018	Shaker:	Mechanical
Location:	1-A-UTBC		Personnel:	HB	Time:	10 min

Sieve Number	Sieve Opening (mm)	Cumulative Retained (g)	Cumulative Passing (g)	Percent Passing (%)	Shape, Uniformity, and Classification	
1 1/2	37.500	0.00	2080.78	100.00	Gravel (%)	52.23
3/4	19.000	227.85	1852.93	89.05	Sand (%)	37.37
3/8	9.500	789.66	1291.12	62.05	Fines (%)	10.40
4	4.750	1086.69	994.09	47.77	D_{60}	8.69
10	2.000	1398.57	682.21	32.79	D_{30}	1.45
40	0.425	1635.33	445.45	21.41	D_{10}	0.07
60	0.250	1733.26	347.52	16.70	C_u	120.53
100	0.150	1780.18	300.60	14.45	C_c	3.35
140	0.106	1861.84	218.94	10.52	Gradation	Poor
200	0.075	1863.22	216.31	10.40	USCS	GP-GC

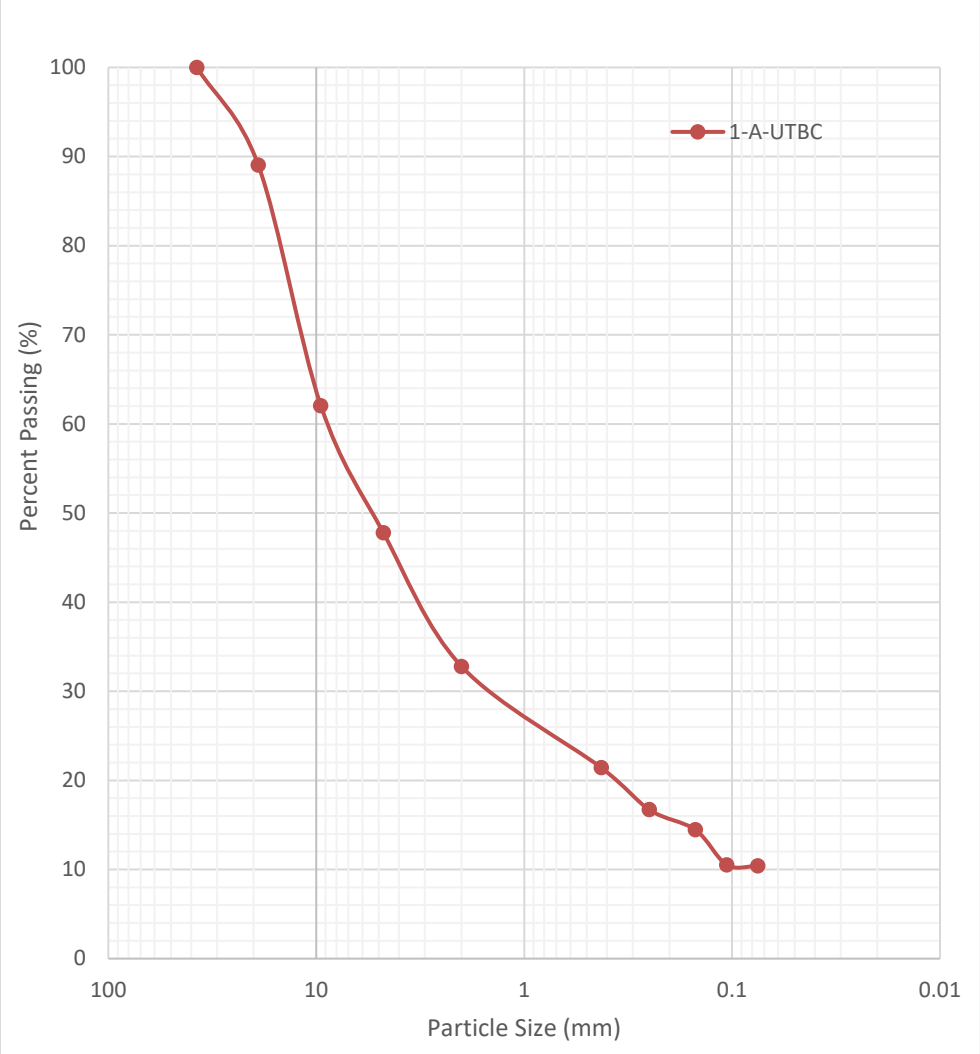

Project:	SR-10		Date:	8/23/2018	Shaker:	Mechanical
Location:	1-A-GB		Personnel:	HB	Time:	10 min
Sieve Number	Sieve Opening (mm)	Cumulative Retained (g)	Cumulative Passing (g)	Percent Passing (%)	Shape, Uniformity, and Classification	
1 1/2	37.500	73.63	2571.07	100.00	Gravel (%)	51.96
3/4	19.000	535.81	2035.26	79.16	Sand (%)	32.76
3/8	9.500	1032.02	1539.05	59.86	Fines (%)	15.28
4	4.750	1335.95	1235.12	48.04	D_{60}	9.56
10	2.000	1607.47	963.60	37.48	D_{30}	0.86
40	0.425	1931.31	639.76	24.88	D_{10}	0.05
60	0.250	2019.86	551.21	21.44	C_u	194.65
100	0.150	2090.66	480.41	18.69	C_c	1.58
140	0.106	2172.94	398.13	15.49	Gradation	NA
200	0.075	2174.24	392.10	15.28	USCS	GC-GM

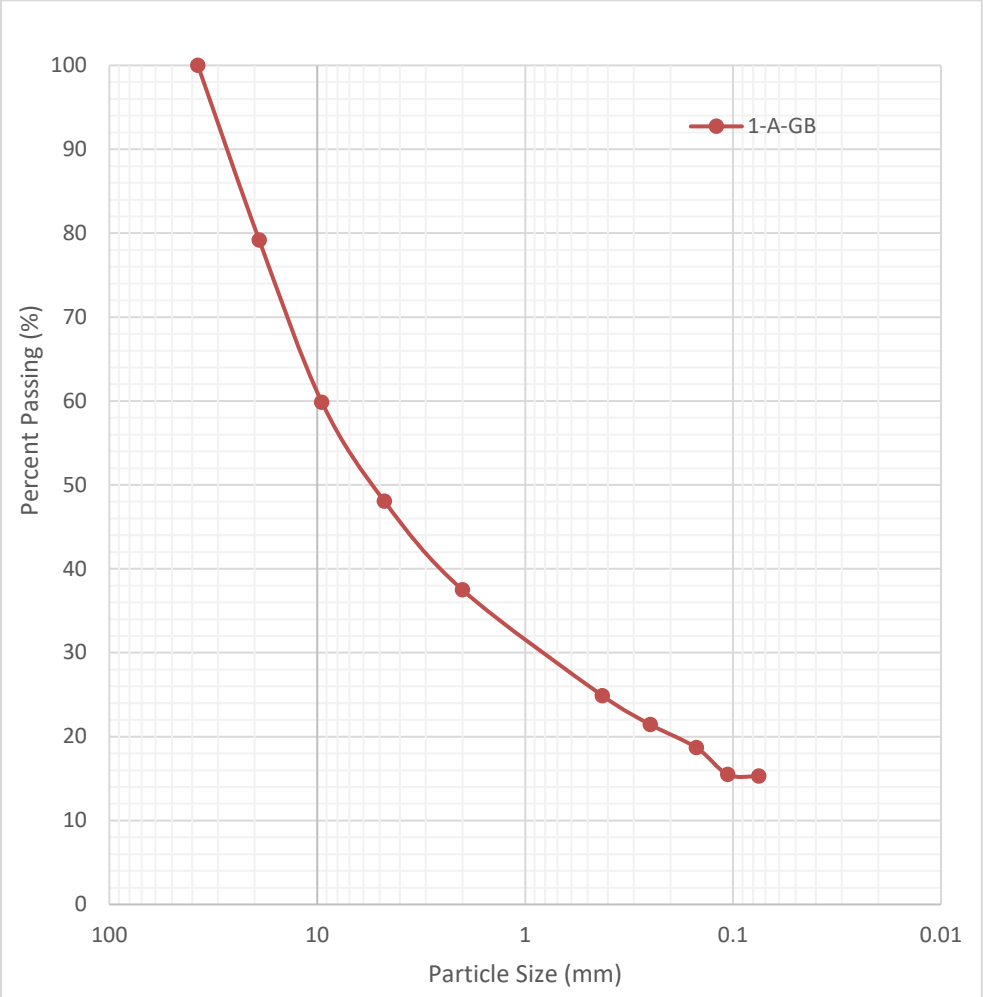

Project:	SR-10		Date:	8/27/2018	Shaker:	Mechanical
Location:	2-C-UTBC		Personnel:	HB	Time:	10 min

Sieve Number	Sieve Opening (mm)	Cumulative Retained (g)	Cumulative Passing (g)	Percent Passing (%)	Shape, Uniformity, and Classification	
1 1/2	37.500	0.00	3358.38	100.00	Gravel (%)	50.88
3/4	19.000	284.42	3073.96	91.53	Sand (%)	37.15
3/8	9.500	1198.68	2159.70	64.31	Fines (%)	11.98
4	4.750	1708.71	1649.67	49.12	D_{60}	7.95
10	2.000	2205.83	1152.55	34.32	D_{30}	1.23
40	0.425	2606.74	751.64	22.38	D_{10}	0.06
60	0.250	2710.13	648.25	19.30	C_u	126.91
100	0.150	2813.96	544.42	16.21	C_c	3.03
140	0.106	2945.23	413.15	12.30	Gradation	Poor
200	0.075	2949.10	401.22	11.98	USCS	GP-GC

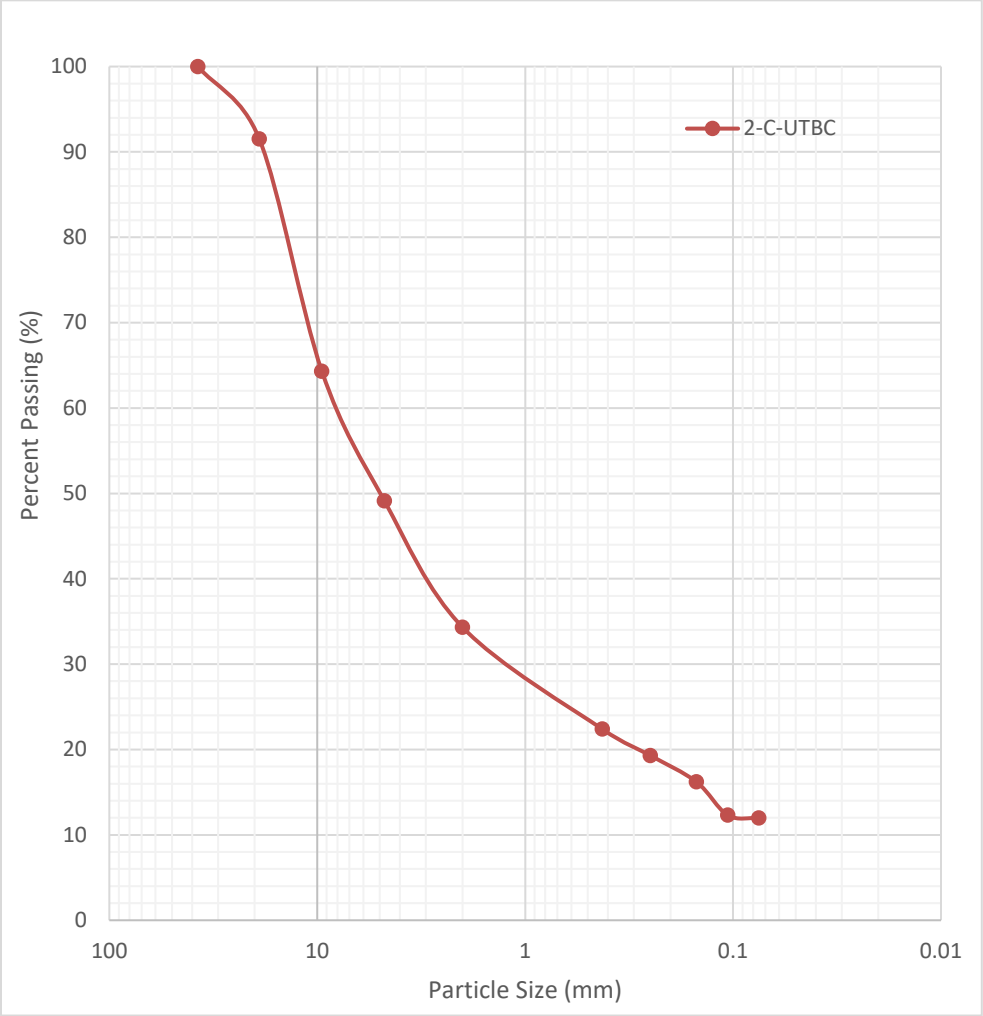

Project:	SR-10		Date:	8/27/2018	Shaker:	Mechanical
Location:	2-C-GB		Personnel:	HB	Time:	10 min
Sieve Number	Sieve Opening (mm)	Cumulative Retained (g)	Cumulative Passing (g)	Percent Passing (%)	Shape, Uniformity, and Classification	
1 1/2	37.500	0.00	2739.25	100.00	Gravel (%)	41.13
3/4	19.000	162.36	2576.89	94.07	Sand (%)	43.55
3/8	9.500	740.92	1998.33	72.95	Fines (%)	15.32
4	4.750	1126.79	1612.46	58.87	D_{60}	5.05
10	2.000	1477.57	1261.68	46.06	D_{30}	0.37
40	0.425	1877.17	862.08	31.47	D_{10}	0.05
60	0.250	2031.55	707.70	25.84	C_u	103.20
100	0.150	2150.95	588.30	21.48	C_c	0.56
140	0.106	2282.96	456.29	16.66	Gradation	NA
200	0.075	2291.42	414.55	15.32	USCS	SC

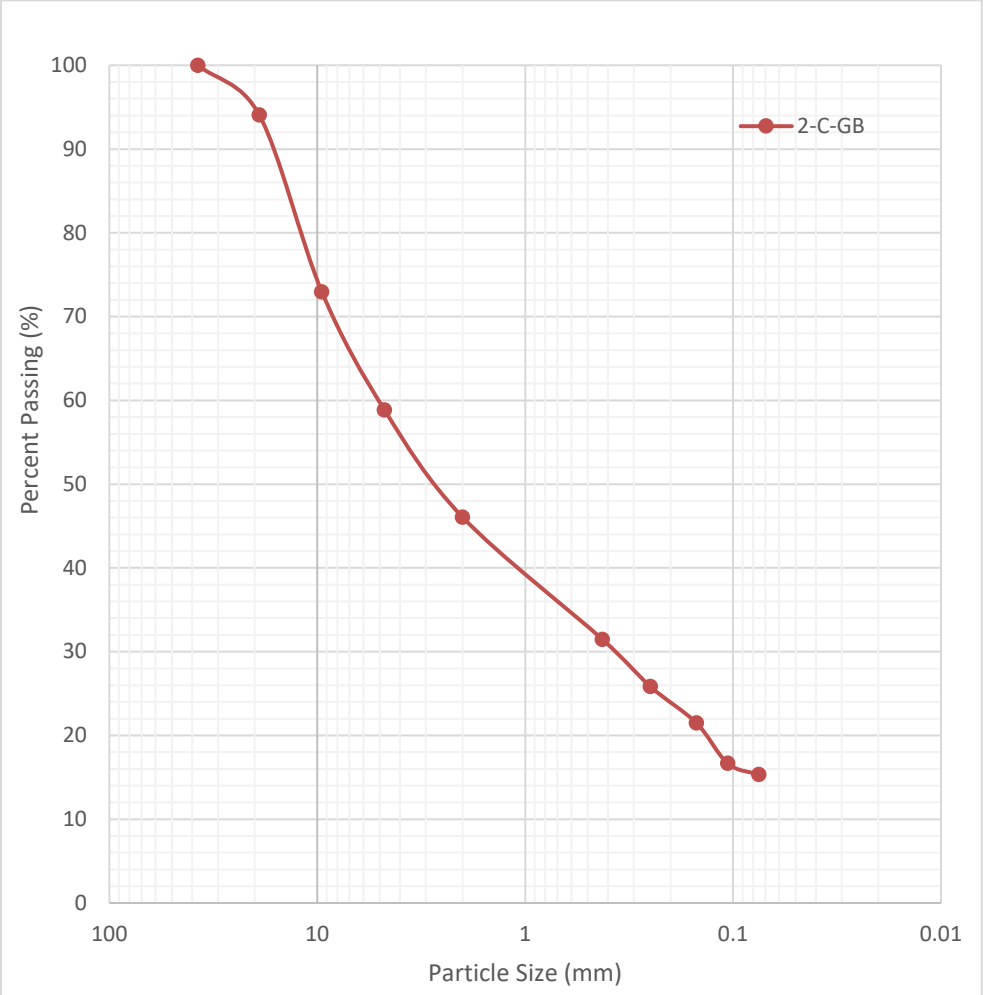

Project:	SR-10		Date:	8/23/2018	Shaker:	Mechanical
Location:	3-C-UTBC		Personnel:	HB	Time:	10 min
Sieve Number	Sieve Opening (mm)	Cumulative Retained (g)	Cumulative Passing (g)	Percent Passing (%)	Shape, Uniformity, and Classification	
1 1/2	37.500	0.00	3157.92	100.00	Gravel (%)	58.18
3/4	19.000	368.02	2789.90	88.35	Sand (%)	31.41
3/8	9.500	1437.92	1720.00	54.47	Fines (%)	10.40
4	4.750	1837.43	1320.49	41.82	D_{60}	10.91
10	2.000	2157.94	999.98	31.67	D_{30}	1.57
40	0.425	2449.18	708.74	22.44	D_{10}	0.07
60	0.250	2605.74	552.18	17.49	C_u	151.35
100	0.150	2701.16	456.76	14.46	C_c	3.13
140	0.106	2819.63	338.29	10.71	Gradation	Poor
200	0.075	2823.86	327.83	10.40	USCS	GP-GC

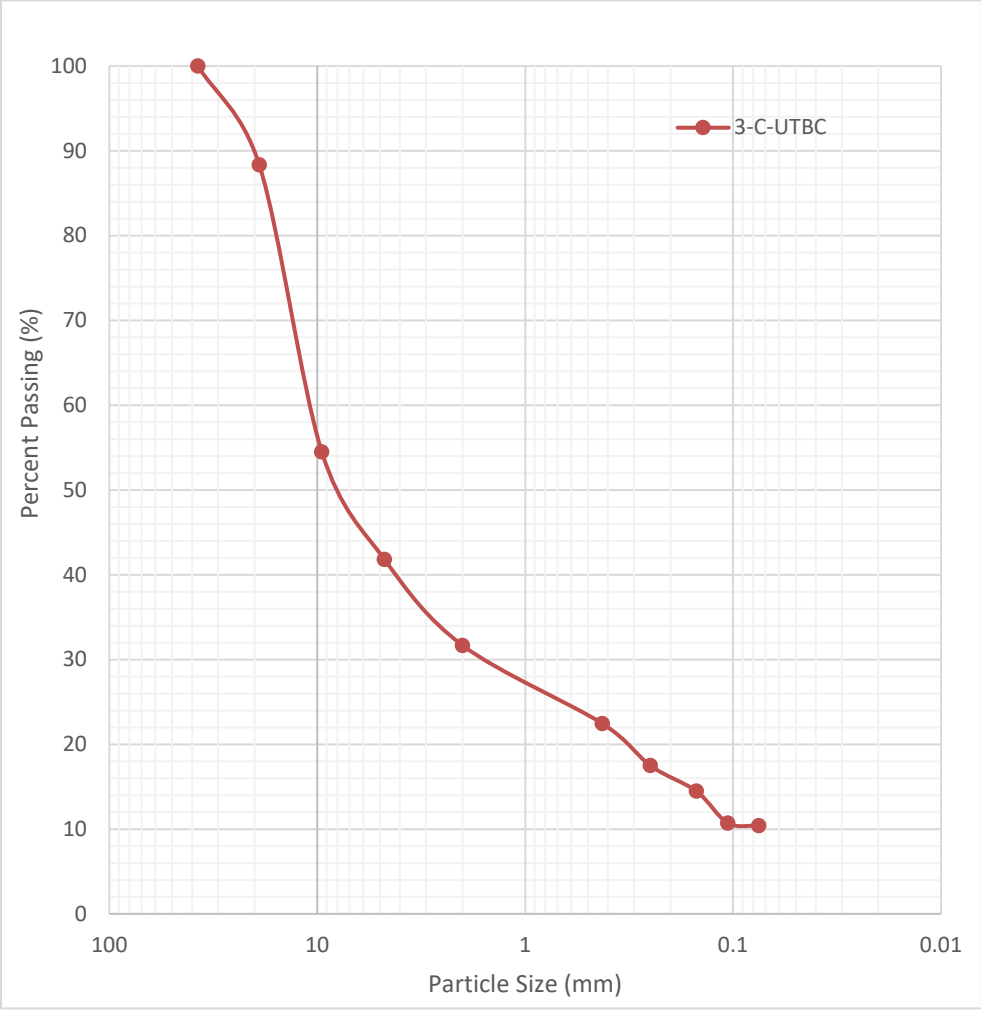

Project:	SR-10		Date:	8/23/2018	Shaker:	Mechanical
Location:	3-C-GB		Personnel:	HB	Time:	10 min
Sieve Number	Sieve Opening (mm)	Cumulative Retained (g)	Cumulative Passing (g)	Percent Passing (%)		Shape, Uniformity, and Classification
1 1/2	37.500	0.00	1545.07	100.00	Gravel (%)	40.61
3/4	19.000	113.04	1432.03	92.68	Sand (%)	36.41
3/8	9.500	442.71	1102.36	71.35	Fines (%)	22.98
4	4.750	627.50	917.57	59.39	D_{60}	4.94
10	2.000	825.08	719.99	46.60	D_{30}	0.45
40	0.425	1087.95	457.12	29.59	D_{10}	<0.07
60	0.250	1129.78	415.29	26.88	C_u	NA
100	0.150	1151.55	393.52	25.47	C_c	NA
140	0.106	1184.70	360.37	23.32	Gradation	NA
200	0.075	1185.82	353.76	22.98	USCS	GC-GM

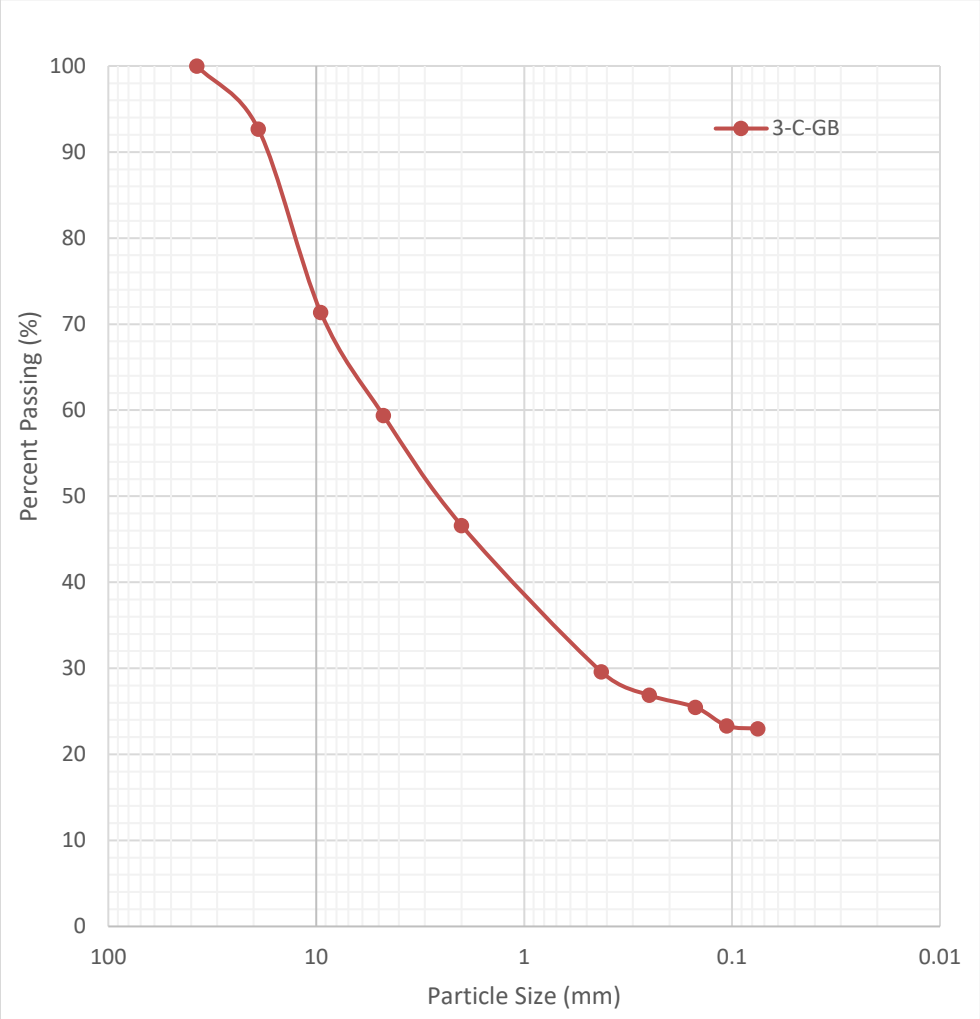

Project:	SR-10		Date:	9/10/2018	Shaker:	Mechanical
Location:	4-C-UTBC		Personnel:	HB	Time:	10 min
Sieve Number	Sieve Opening (mm)	Cumulative Retained (g)	Cumulative Passing (g)	Percent Passing (%)	Shape, Uniformity, and Classification	
1 1/2	37.500	0.00	4931.87	100.00	Gravel (%)	55.54
3/4	19.000	503.46	4428.41	89.79	Sand (%)	33.34
3/8	9.500	2042.80	2889.07	58.58	Fines (%)	11.13
4	4.750	2739.03	2192.84	44.46	D_{60}	9.88
10	2.000	3352.59	1579.28	32.02	D_{30}	1.55
40	0.425	3872.07	1059.80	21.49	D_{10}	0.07
60	0.250	3997.57	934.30	18.94	C_u	146.51
100	0.150	4148.50	783.37	15.88	C_c	3.62
140	0.106	4327.33	604.54	12.26	Gradation	Poor
200	0.075	4349.00	544.40	11.13	USCS	GP-GC

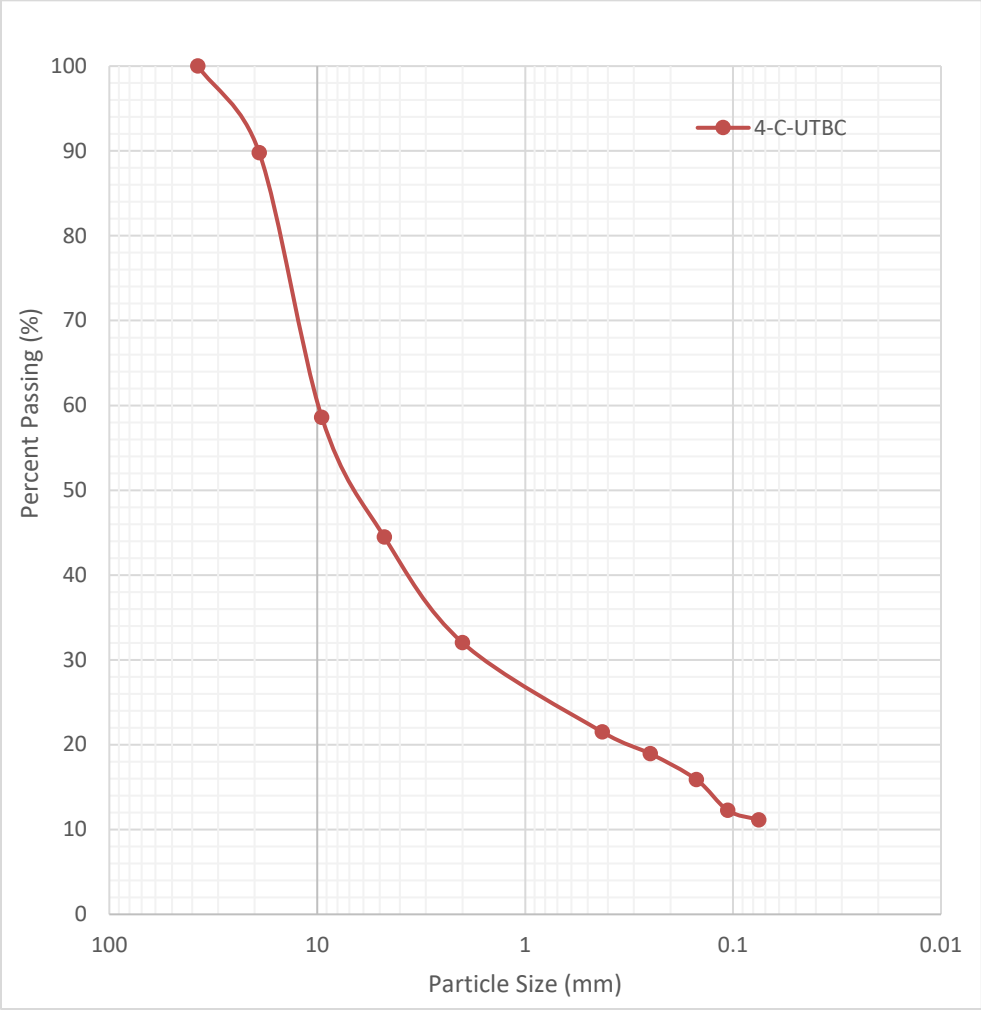

Project:	SR-10		Date:	9/10/2018	Shaker:	Mechanical
Location:	4-C-GB		Personnel:	HB	Time:	10 min
Sieve Number	Sieve Opening (mm)	Cumulative Retained (g)	Cumulative Passing (g)	Percent Passing (%)	Shape, Uniformity, and Classification	
1 1/2	37.500	0.00	2405.56	100.00	Gravel (%)	48.85
3/4	19.000	162.94	2242.62	93.23	Sand (%)	36.94
3/8	9.500	869.29	1536.27	63.86	Fines (%)	14.21
4	4.750	1175.08	1230.48	51.15	D_{60}	7.82
10	2.000	1493.24	912.32	37.93	D_{30}	1.07
40	0.425	1892.94	512.62	21.31	D_{10}	0.05
60	0.250	1955.50	450.06	18.71	C_u	148.14
100	0.150	2007.62	397.94	16.54	C_c	2.75
140	0.106	2056.91	348.65	14.49	Gradation	NA
200	0.075	2059.09	341.11	14.21	USCS	GC

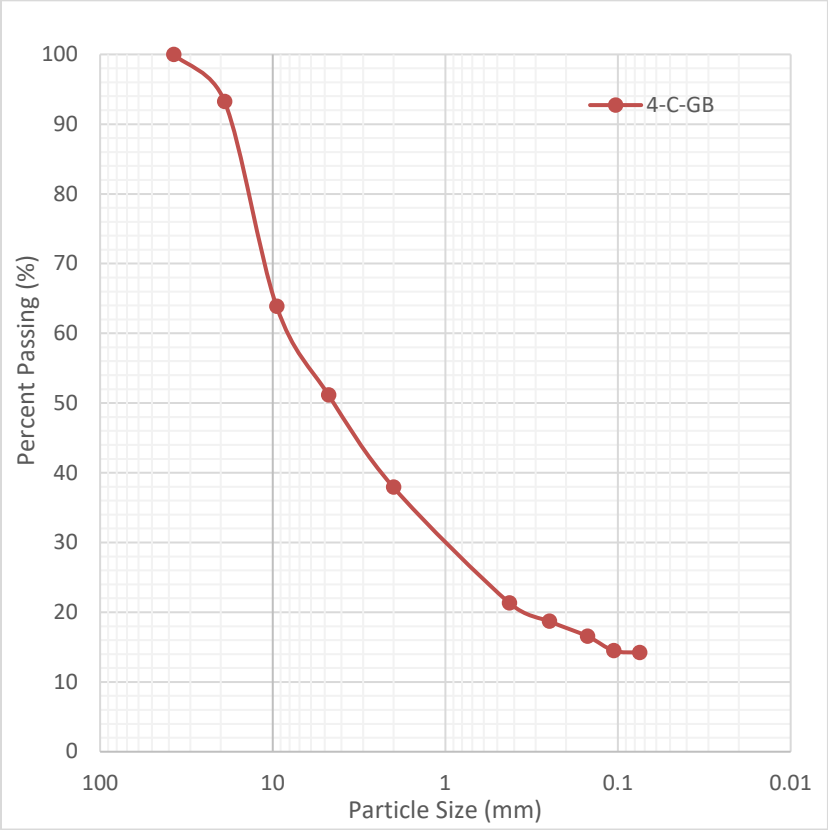

Project:	SR-10		Date:	9/7/2018	Shaker:	Mechanical
Location:	5-C-UTBC		Personnel:	HB	Time:	10 min

Sieve Number	Sieve Opening (mm)	Cumulative Retained (g)	Cumulative Passing (g)	Percent Passing (%)	Shape, Uniformity, and Classification	
1 1/2	37.500	0.00	5713.51	100.00	Gravel (%)	48.37
3/4	19.000	357.94	5355.57	93.74	Sand (%)	38.80
3/8	9.500	1902.62	3810.89	66.70	Fines (%)	12.84
4	4.750	2763.54	2949.97	51.63	D_{60}	7.13
10	2.000	3552.34	2161.17	37.83	D_{30}	0.83
40	0.425	4280.20	1433.31	25.09	D_{10}	0.06
60	0.250	4482.57	1230.94	21.54	C_u	122.09
100	0.150	4724.42	989.09	17.31	C_c	1.67
140	0.106	4944.94	768.57	13.45	Gradation	NA
200	0.075	4960.26	730.49	12.84	USCS	GC

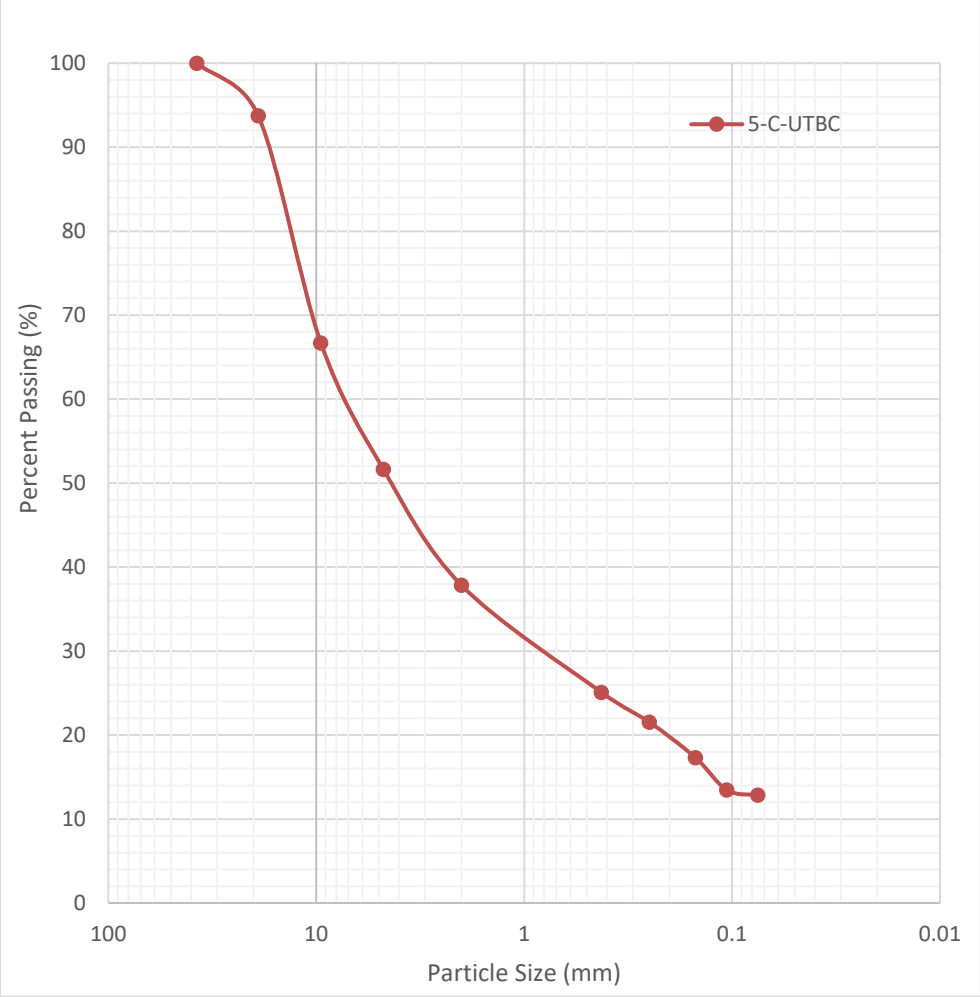

Project:	SR-10		Date:	9/7/2018	Shaker:	Mechanical
Location:	5-C-GB		Personnel:	HB	Time:	10 min
Sieve Number	Sieve Opening (mm)	Cumulative Retained (g)	Cumulative Passing (g)	Percent Passing (%)	Shape, Uniformity, and Classification	
1 1/2	37.500	98.12	10684.28	100.00	Gravel (%)	43.77
3/4	19.000	1240.94	9443.34	88.39	Sand (%)	40.82
3/8	9.500	3275.58	7408.70	69.34	Fines (%)	15.40
4	4.750	4676.88	6007.40	56.23	D_{60}	5.89
10	2.000	6097.42	4586.86	42.93	D_{30}	0.71
40	0.425	8009.52	2674.76	25.03	D_{10}	0.05
60	0.250	8506.18	2178.10	20.39	C_u	120.92
100	0.150	8724.06	1960.22	18.35	C_c	1.78
140	0.106	8937.81	1746.47	16.35	Gradation	NA
200	0.075	8967.33	1632.76	15.40	USCS	GM

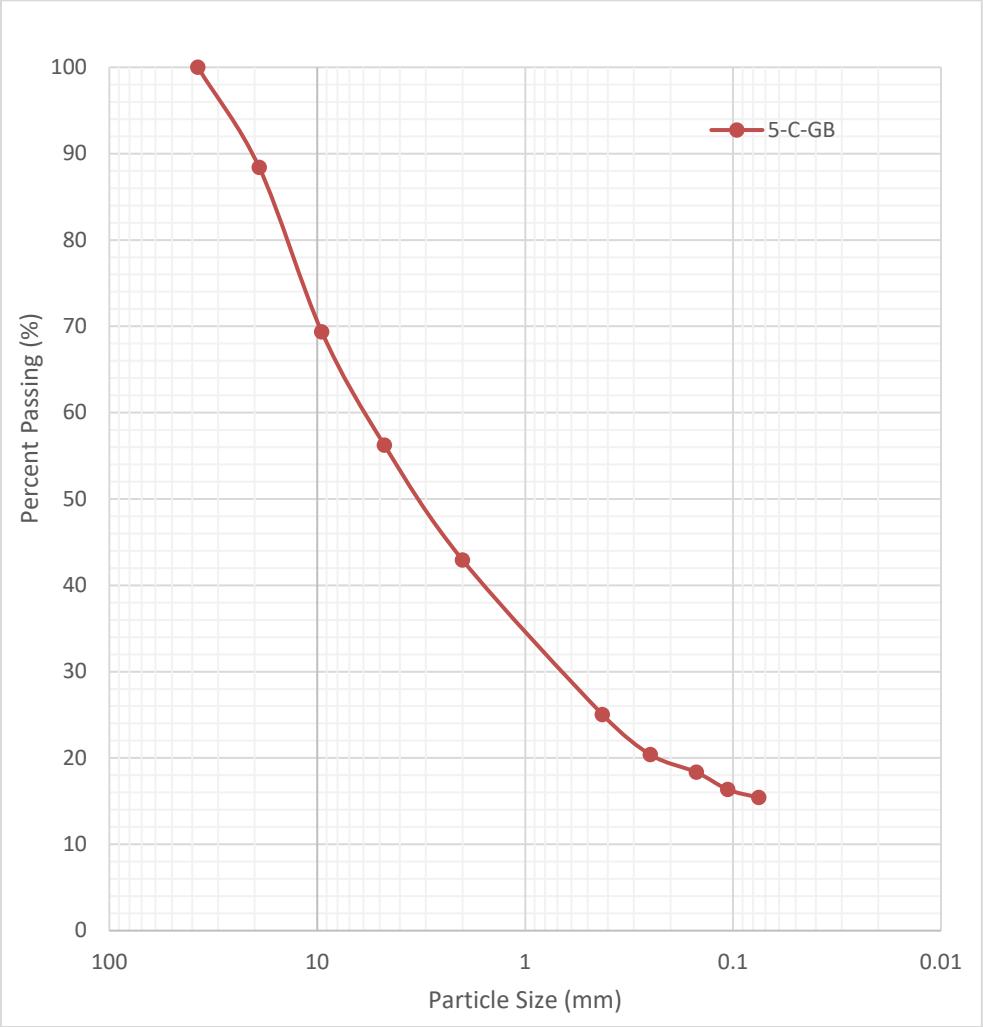

Project:	SR-10		Date:	9/23/2018	Shaker:	Mechanical
Location:	6-C-UTBC		Personnel:	HB	Time:	10 min
Sieve Number	Sieve Opening (mm)	Cumulative Retained (g)	Cumulative Passing (g)	Percent Passing (%)	Shape, Uniformity, and Classification	
1 1/2	37.500	0.00	4675.43	100.00	Gravel (%)	56.71
3/4	19.000	512.75	4162.68	89.03	Sand (%)	31.69
3/8	9.500	1933.75	2741.68	58.64	Fines (%)	11.60
4	4.750	2651.34	2024.09	43.29	D_{60}	9.87
10	2.000	3149.68	1525.75	32.63	D_{30}	1.37
40	0.425	3594.25	1081.18	23.12	D_{10}	0.06
60	0.250	3741.68	933.75	19.97	C_u	152.64
100	0.150	3911.46	763.97	16.34	C_c	2.94
140	0.106	4099.69	575.74	12.31	Gradation	Well
200	0.075	4120.38	540.71	11.60	USCS	GW-GC

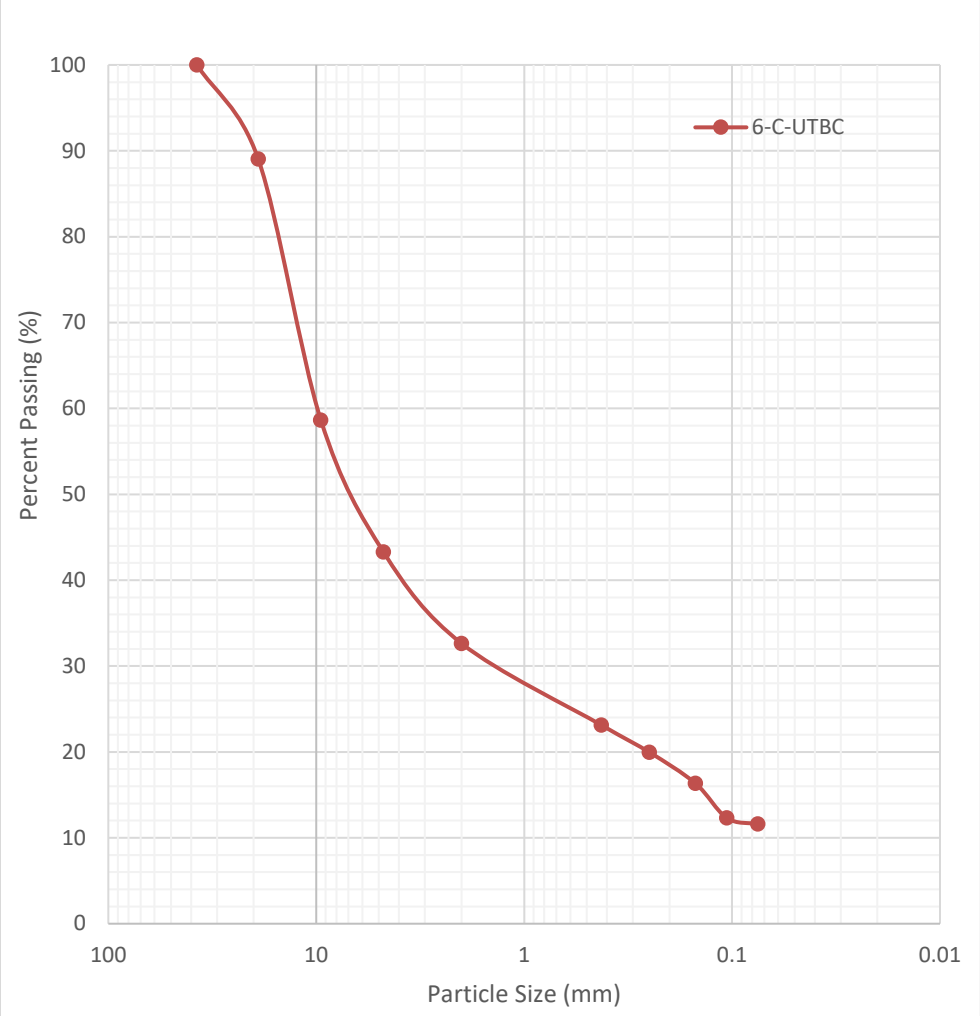

Project:	SR-10		Date:	9/28/2018	Shaker:	Mechanical
Location:	6-C-GB		Personnel:	HB	Time:	10 min
Sieve Number	Sieve Opening (mm)	Cumulative Retained (g)	Cumulative Passing (g)	Percent Passing (%)	Shape, Uniformity, and Classification	
1 1/2	37.500	0.00	4278.40	100.00	Gravel (%)	46.69
3/4	19.000	719.33	3559.07	83.19	Sand (%)	36.04
3/8	9.500	1436.32	2842.08	66.43	Fines (%)	17.27
4	4.750	1997.45	2280.95	53.31	D_{60}	6.89
10	2.000	2465.05	1813.35	42.38	D_{30}	0.39
40	0.425	2958.96	1319.44	30.84	D_{10}	0.04
60	0.250	3144.93	1133.47	26.49	C_u	158.72
100	0.150	3315.71	962.69	22.50	C_c	0.50
140	0.106	3505.56	772.84	18.06	Gradation	NA
200	0.075	3523.35	735.49	17.27	USCS	GC

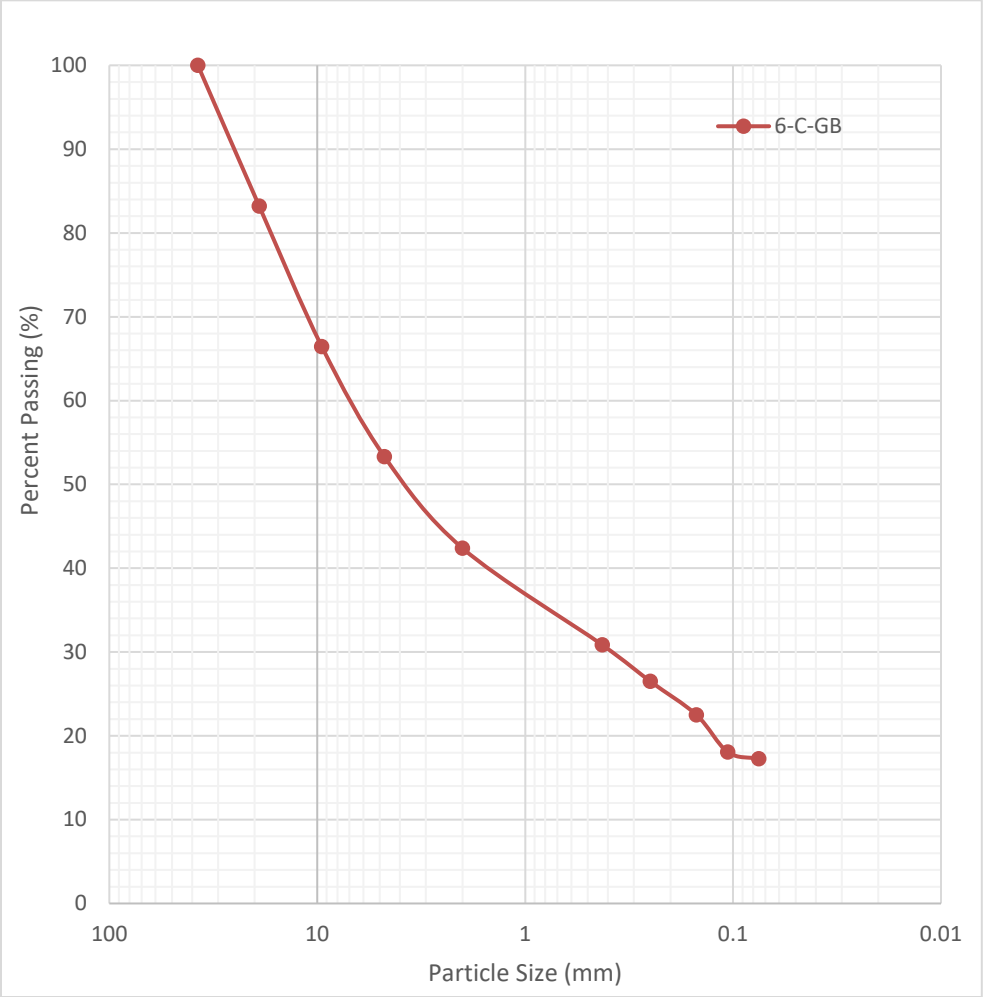

Project:	SR-10		Date:	9/28/2018	Shaker:	Mechanical
Location:	7-C-UTBC		Personnel:	HB	Time:	10 min

Sieve Number	Sieve Opening (mm)	Cumulative Retained (g)	Cumulative Passing (g)	Percent Passing (%)	Shape, Uniformity, and Classification	
1 1/2	37.500	0.00	3088.79	100.00	Gravel (%)	48.73
3/4	19.000	250.11	2838.68	91.90	Sand (%)	38.57
3/8	9.500	1085.72	2003.07	64.85	Fines (%)	12.69
4	4.750	1505.29	1583.50	51.27	D_{60}	7.55
10	2.000	1897.89	1190.90	38.56	D_{30}	0.67
40	0.425	2254.14	834.65	27.02	D_{10}	0.06
60	0.250	2421.20	667.59	21.61	C_u	127.83
100	0.150	2600.92	487.87	15.79	C_c	1.01
140	0.106	2683.70	405.09	13.11	Gradation	NA
200	0.075	2687.62	390.69	12.69	USCS	GC-GM

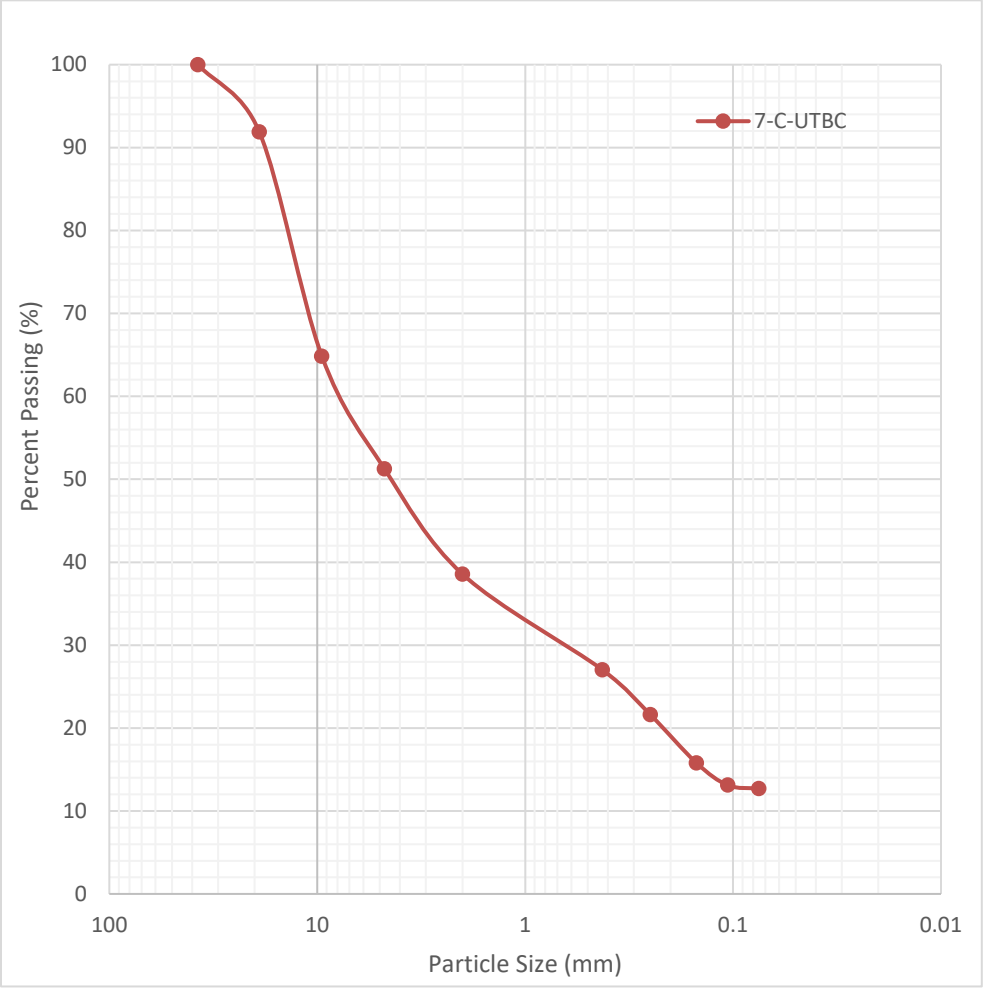

Project:	SR-10		Date:	10/5/2018	Shaker:	Mechanical
Location:	7-C-GB		Personnel:	HB	Time:	10 min
Sieve Number	Sieve Opening (mm)	Cumulative Retained (g)	Cumulative Passing (g)	Percent Passing (%)	Shape, Uniformity, and Classification	
1 1/2	37.500	0.00	3311.15	100.00	Gravel (%)	47.25
3/4	19.000	316.15	2995.00	90.45	Sand (%)	37.43
3/8	9.500	1081.50	2229.65	67.34	Fines (%)	15.33
4	4.750	1564.38	1746.77	52.75	D_{60}	6.85
10	2.000	2068.31	1242.84	37.54	D_{30}	0.81
40	0.425	2466.34	844.81	25.51	D_{10}	0.05
60	0.250	2595.19	715.96	21.62	C_u	139.88
100	0.150	2729.54	581.61	17.57	C_c	1.98
140	0.106	2795.60	515.55	15.57	Gradation	NA
200	0.075	2798.30	506.45	15.33	USCS	GC-GM

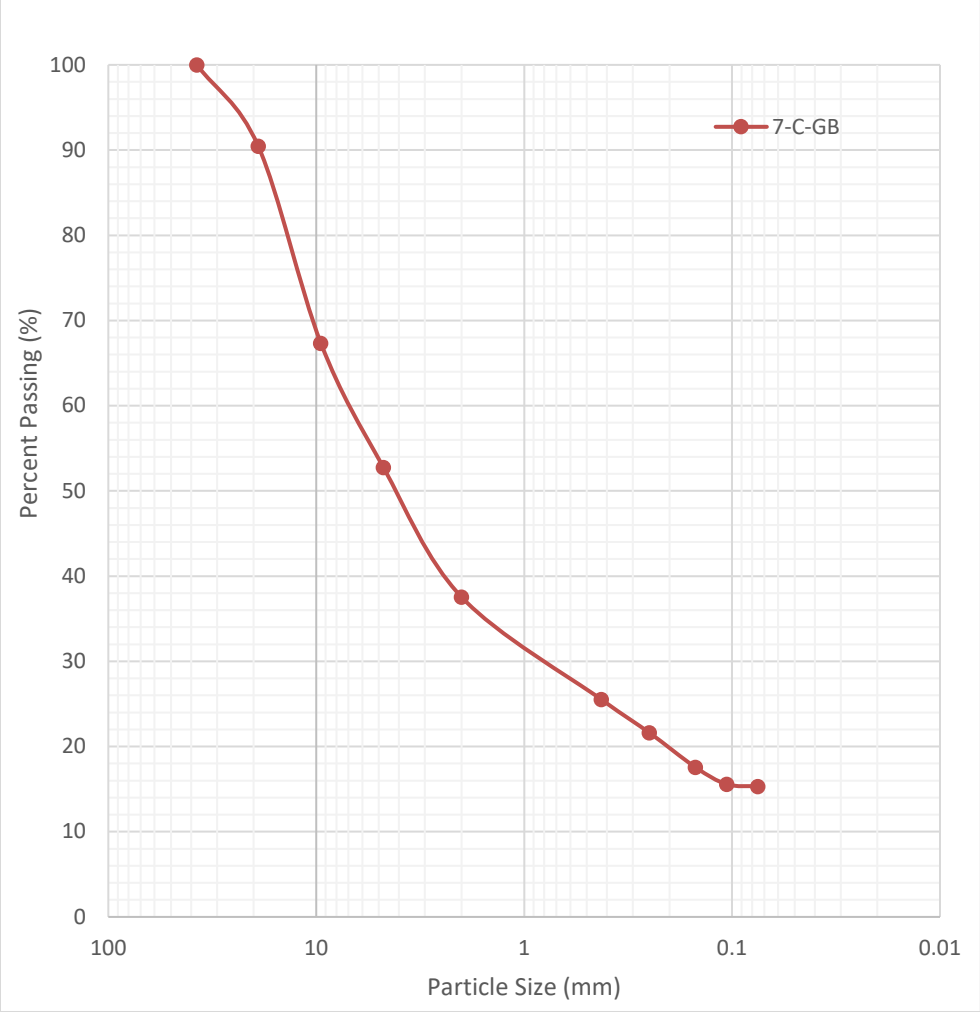

Project:	SR-10		Date:	10/1/2018	Shaker:	Mechanical
Location:	8-C-UTBC		Personnel:	HB	Time:	10 min
Sieve Number	Sieve Opening (mm)	Cumulative Retained (g)	Cumulative Passing (g)	Percent Passing (%)	Shape, Uniformity, and Classification	
1 1/2	37.500	0.00	3225.95	100.00	Gravel (%)	50.25
3/4	19.000	216.15	3009.80	93.30	Sand (%)	37.19
3/8	9.500	1169.64	2056.31	63.74	Fines (%)	12.56
4	4.750	1621.14	1604.81	49.75	D_{60}	8.02
10	2.000	1976.66	1249.29	38.73	D_{30}	0.60
40	0.425	2325.81	900.14	27.90	D_{10}	0.06
60	0.250	2547.80	678.15	21.02	C_u	134.31
100	0.150	2721.25	504.70	15.64	C_c	0.75
140	0.106	2810.51	415.44	12.88	Gradation	NA
200	0.075	2815.69	404.37	12.56	USCS	GC-GM

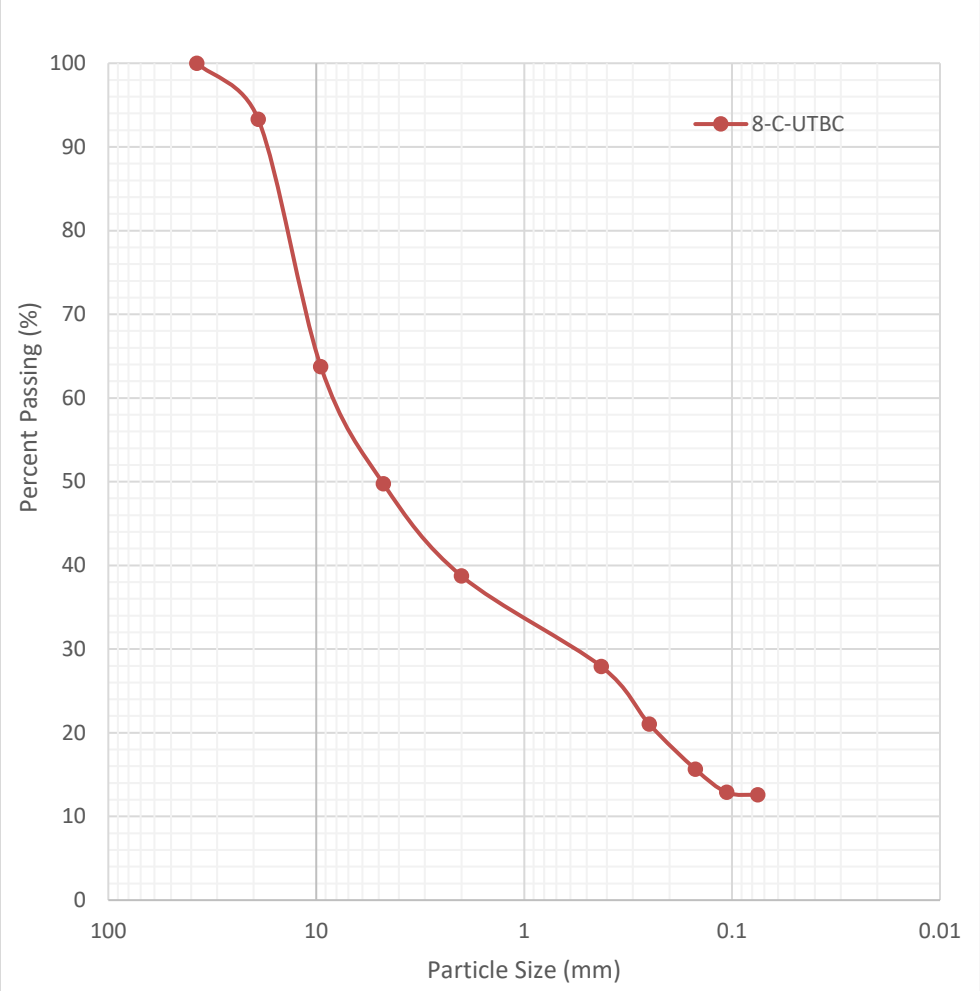

Project:	SR-10		Date:	10/1/2018	Shaker:	Mechanical
Location:	8-C-GB		Personnel:	HB	Time:	10 min
Sieve Number	Sieve Opening (mm)	Cumulative Retained (g)	Cumulative Passing (g)	Percent Passing (%)	Shape, Uniformity, and Classification	
1 1/2	37.500	0.00	5505.08	100.00	Gravel (%)	47.95
3/4	19.000	696.10	4808.98	87.36	Sand (%)	38.67
3/8	9.500	1934.65	3570.43	64.86	Fines (%)	13.38
4	4.750	2639.81	2865.27	52.05	D_{60}	7.43
10	2.000	3297.99	2207.09	40.09	D_{30}	0.61
40	0.425	3996.07	1509.01	27.41	D_{10}	0.06
60	0.250	4307.66	1197.42	21.75	C_u	132.64
100	0.150	4614.48	890.60	16.18	C_c	0.90
140	0.106	4755.72	749.36	13.61	Gradation	NA
200	0.075	4761.80	735.64	13.38	USCS	GC

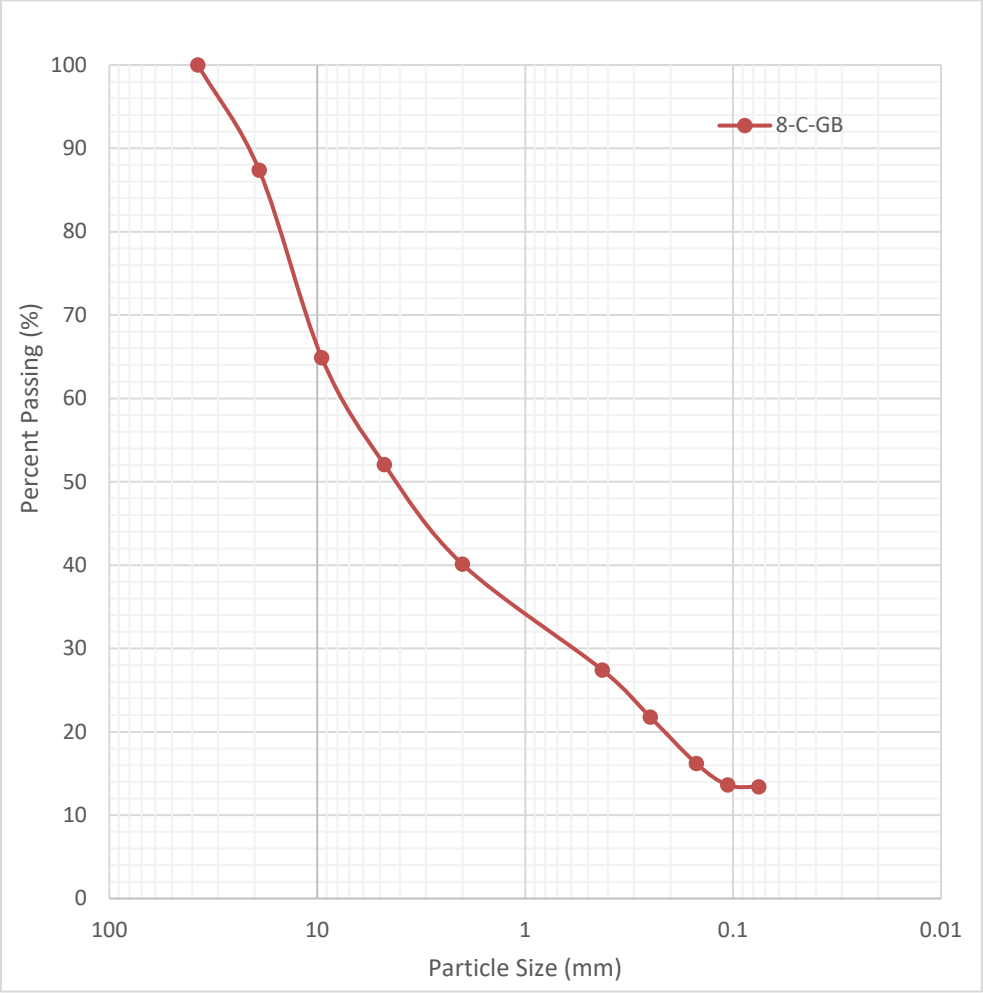

Project:	SR-10		Date:	10/11/2018	Shaker:	Mechanical
Location:	9-C-UTBC		Personnel:	HB	Time:	10 min

Sieve Number	Sieve Opening (mm)	Cumulative Retained (g)	Cumulative Passing (g)	Percent Passing (%)	Shape, Uniformity, and Classification	
1 1/2	37.500	0.00	2669.56	100.00	Gravel (%)	45.11
3/4	19.000	215.34	2454.22	91.93	Sand (%)	40.74
3/8	9.500	864.31	1805.25	67.62	Fines (%)	14.15
4	4.750	1204.33	1465.23	54.89	D_{60}	6.39
10	2.000	1573.41	1096.15	41.06	D_{30}	0.64
40	0.425	1952.48	717.08	26.86	D_{10}	0.05
60	0.250	2149.94	519.62	19.46	C_u	120.43
100	0.150	2264.31	405.25	15.18	C_c	1.20
140	0.106	2289.47	380.09	14.24	Gradation	NA
200	0.075	2289.93	377.29	14.15	USCS	GC-GM

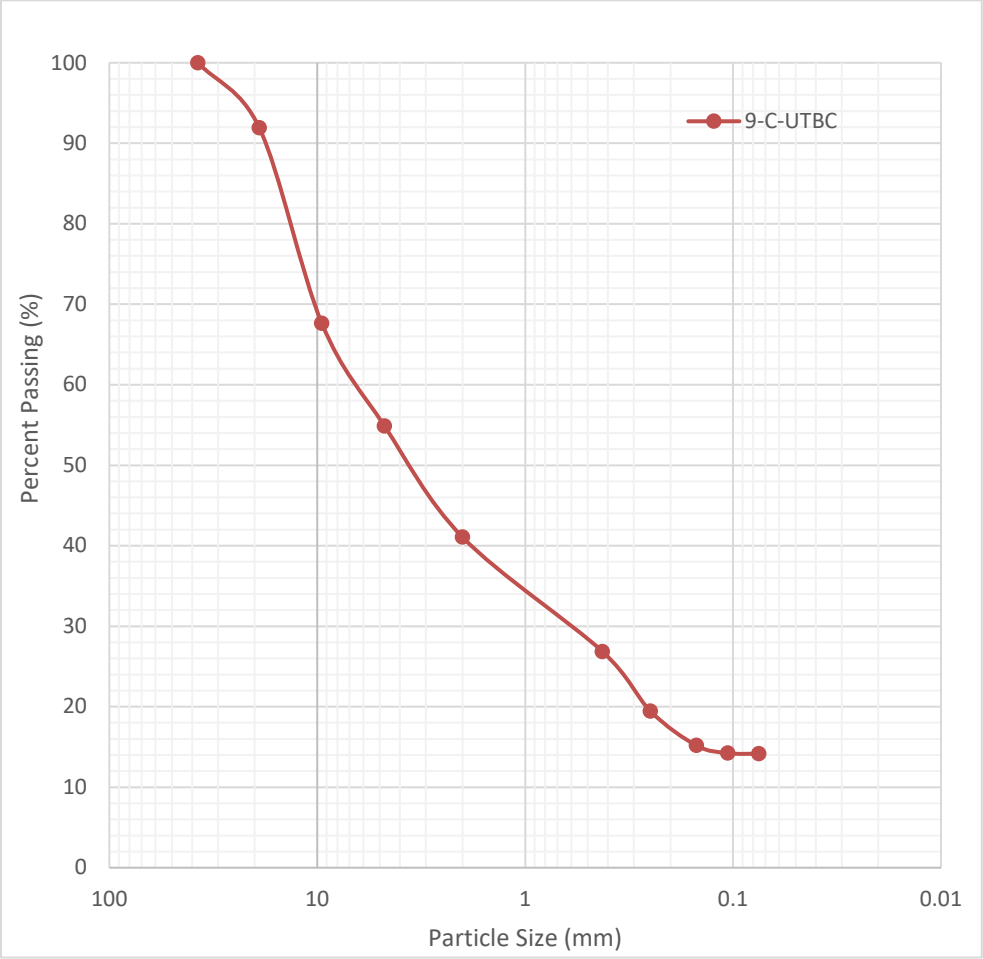

Project:	SR-10		Date:	10/9/2018	Shaker:	Mechanical
Location:	9-C-GB		Personnel:	HB	Time:	10 min
Sieve Number	Sieve Opening (mm)	Cumulative Retained (g)	Cumulative Passing (g)	Percent Passing (%)	Shape, Uniformity, and Classification	
1 1/2	37.500	0.00	4512.36	100.00	Gravel (%)	49.31
3/4	19.000	510.64	4001.72	88.68	Sand (%)	37.82
3/8	9.500	1653.19	2859.17	63.36	Fines (%)	12.87
4	4.750	2225.22	2287.14	50.69	D_{60}	8.02
10	2.000	2861.59	1650.77	36.58	D_{30}	1.13
40	0.425	3548.23	964.13	21.37	D_{10}	0.06
60	0.250	3678.12	834.24	18.49	C_u	137.60
100	0.150	3713.78	798.58	17.70	C_c	2.73
140	0.106	3918.64	593.72	13.16	Gradation	NA
200	0.075	3924.39	579.56	12.87	USCS	GC

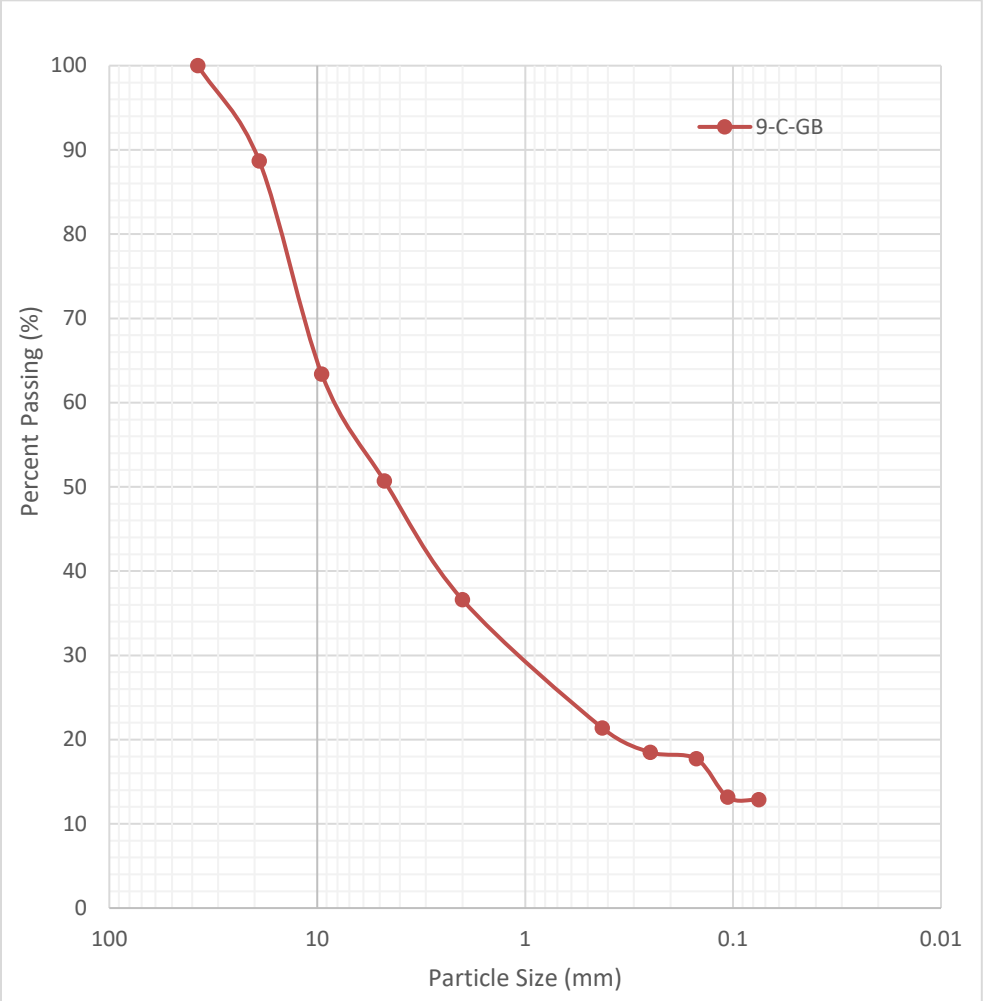

Project:	SR-10		Date:	10/15/2018	Shaker:	Mechanical
Location:	10-C-UTBC		Personnel:	HB	Time:	10 min

Sieve Number	Sieve Opening (mm)	Cumulative Retained (g)	Cumulative Passing (g)	Percent Passing (%)	Shape, Uniformity, and Classification	
1 1/2	37.500	0.00	3392.47	100.00	Gravel (%)	54.51
3/4	19.000	365.83	3026.64	89.22	Sand (%)	34.09
3/8	9.500	1366.09	2026.38	59.73	Fines (%)	11.40
4	4.750	1849.17	1543.30	45.49	D_{60}	9.57
10	2.000	2226.68	1165.79	34.36	D_{30}	1.02
40	0.425	2538.32	854.15	25.18	D_{10}	0.07
60	0.250	2668.40	724.07	21.34	C_u	145.54
100	0.150	2884.15	508.32	14.98	C_c	1.64
140	0.106	2984.32	408.15	12.03	Gradation	Well
200	0.075	2992.24	385.04	11.40	USCS	GW-GC

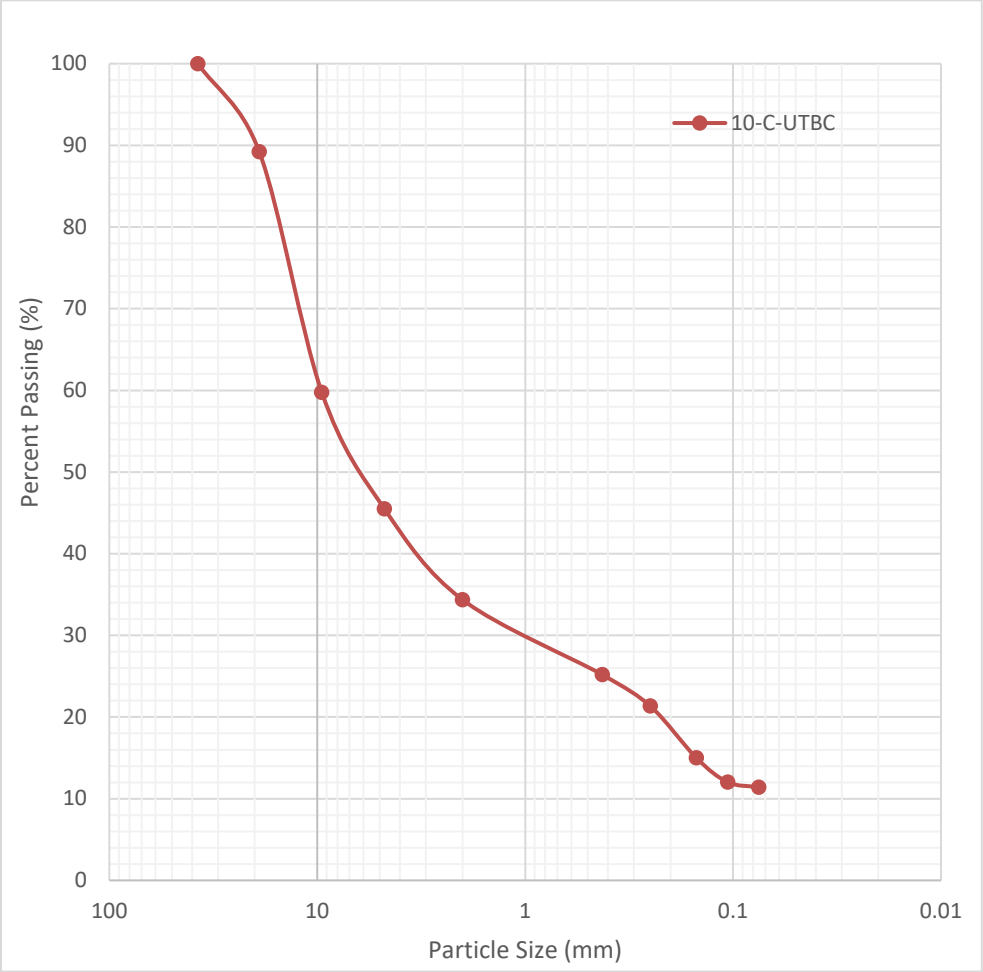

Project:	SR-10		Date:	10/15/2018	Shaker:	Mechanical
Location:	10-C-GB		Personnel:	HB	Time:	10 min
Sieve Number	Sieve Opening (mm)	Cumulative Retained (g)	Cumulative Passing (g)	Percent Passing (%)	Shape, Uniformity, and Classification	
1 1/2	37.500	0.00	5092.61	100.00	Gravel (%)	55.31
3/4	19.000	875.93	4216.68	82.80	Sand (%)	31.23
3/8	9.500	2199.09	2893.52	56.82	Fines (%)	13.46
4	4.750	2816.78	2275.83	44.69	D_{60}	10.50
10	2.000	3317.87	1774.74	34.85	D_{30}	0.98
40	0.425	3807.96	1284.65	25.23	D_{10}	0.06
60	0.250	4046.95	1045.66	20.53	C_u	188.51
100	0.150	4251.87	840.74	16.51	C_c	1.63
140	0.106	4371.59	721.02	14.16	Gradation	NA
200	0.075	4386.49	682.36	13.46	USCS	GM

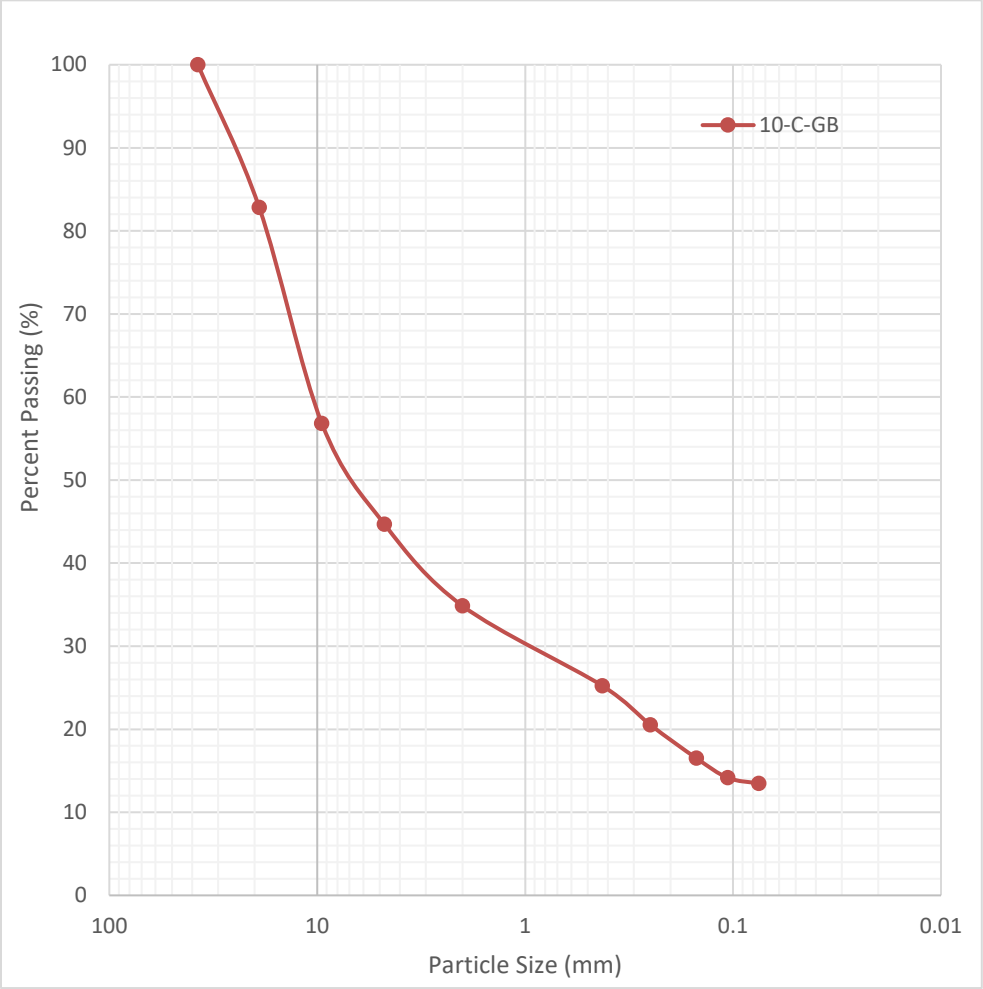

Project:	SR-10		Date:	10/15/2018	Shaker:	Mechanical
Location:	11-C-UTBC		Personnel:	HB	Time:	10 min

Sieve Number	Sieve Opening (mm)	Cumulative Retained (g)	Cumulative Passing (g)	Percent Passing (%)	Shape, Uniformity, and Classification	
1 1/2	37.500	0.00	3994.04	100.00	Gravel (%)	51.90
3/4	19.000	452.96	3541.08	88.66	Sand (%)	37.76
3/8	9.500	1487.07	2506.97	62.77	Fines (%)	10.33
4	4.750	2073.10	1920.94	48.10	D_{60}	8.45
10	2.000	2576.97	1417.07	35.48	D_{30}	1.01
40	0.425	3022.72	971.32	24.32	D_{10}	0.07
60	0.250	3271.38	722.66	18.09	C_u	116.39
100	0.150	3499.34	494.70	12.39	C_c	1.65
140	0.106	3571.66	422.38	10.58	Gradation	Well
200	0.075	3576.31	412.15	10.33	USCS	GW-GC

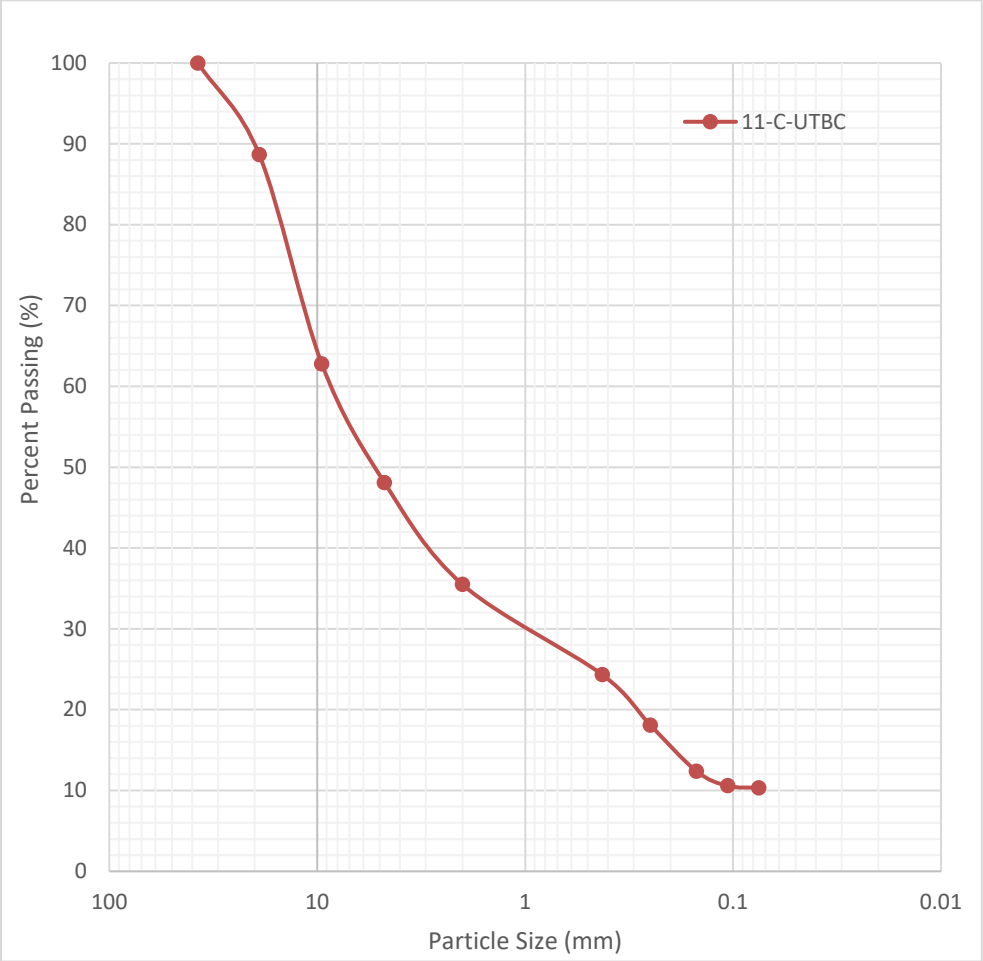

Project:	SR-10		Date:	10/11/2018	Shaker:	Mechanical
Location:	11-C-GB		Personnel:	HB	Time:	10 min
Sieve Number	Sieve Opening (mm)	Cumulative Retained (g)	Cumulative Passing (g)	Percent Passing (%)	Shape, Uniformity, and Classification	
1 1/2	37.500	0.00	4355.53	100.00	Gravel (%)	46.92
3/4	19.000	628.31	3727.22	85.57	Sand (%)	41.34
3/8	9.500	1472.47	2883.06	66.19	Fines (%)	11.75
4	4.750	2043.42	2312.11	53.08	D_{60}	6.98
10	2.000	2666.06	1689.47	38.79	D_{30}	1.01
40	0.425	3410.49	945.04	21.70	D_{10}	0.06
60	0.250	3622.98	732.55	16.82	C_u	109.29
100	0.150	3739.22	616.31	14.15	C_c	2.28
140	0.106	3835.17	520.36	11.95	Gradation	Well
200	0.075	3838.20	510.85	11.75	USCS	GW-GC

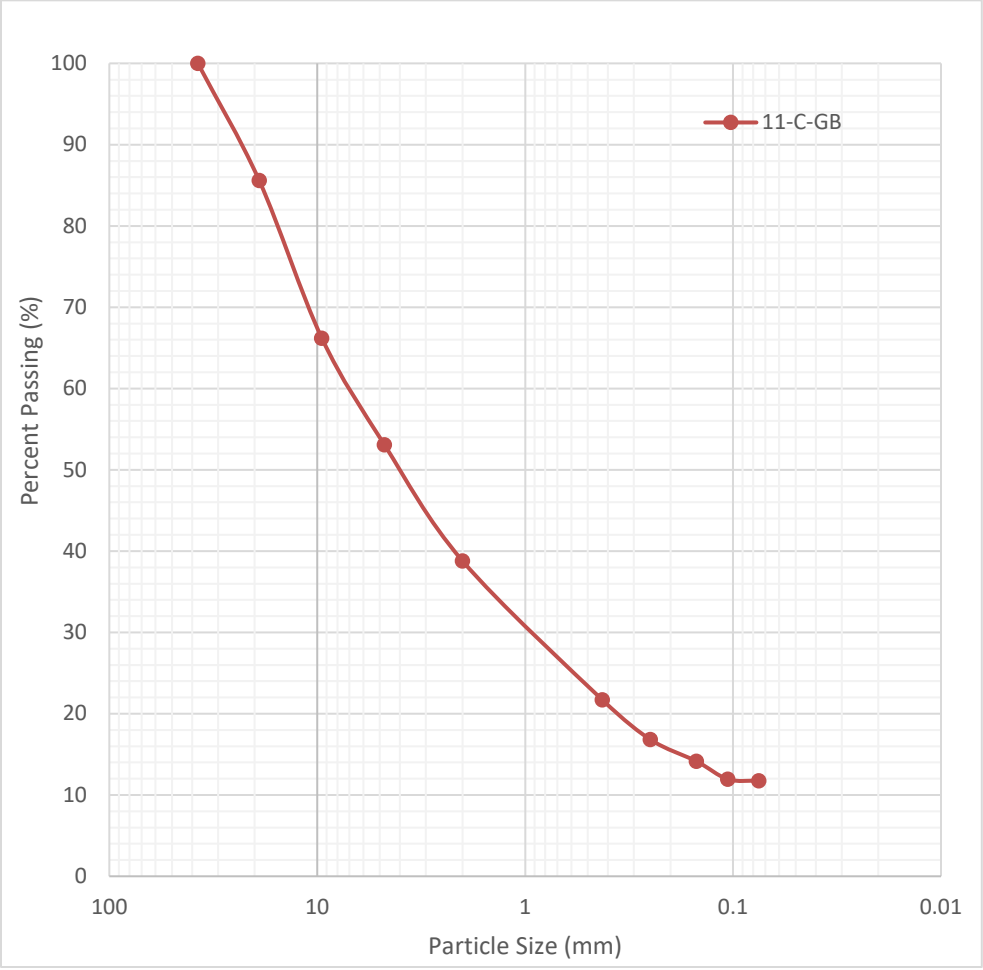

Project:	SR-10		Date:	10/5/2018	Shaker:	Mechanical
Location:	12-C-UTBC		Personnel:	HB	Time:	10 min

Sieve Number	Sieve Opening (mm)	Cumulative Retained (g)	Cumulative Passing (g)	Percent Passing (%)	Shape, Uniformity, and Classification	
1 1/2	37.500	0.00	5059.02	100.00	Gravel (%)	43.07
3/4	19.000	296.97	4762.05	94.13	Sand (%)	44.23
3/8	9.500	1305.31	3753.71	74.20	Fines (%)	12.70
4	4.750	2178.89	2880.13	56.93	D_{60}	5.45
10	2.000	3005.27	2053.75	40.60	D_{30}	0.76
40	0.425	3797.10	1261.92	24.94	D_{10}	0.06
60	0.250	4001.68	1057.34	20.90	C_u	92.29
100	0.150	4205.43	853.59	16.87	C_c	1.82
140	0.106	4391.02	668.00	13.20	Gradation	NA
200	0.075	4403.57	640.73	12.70	USCS	SC-SM

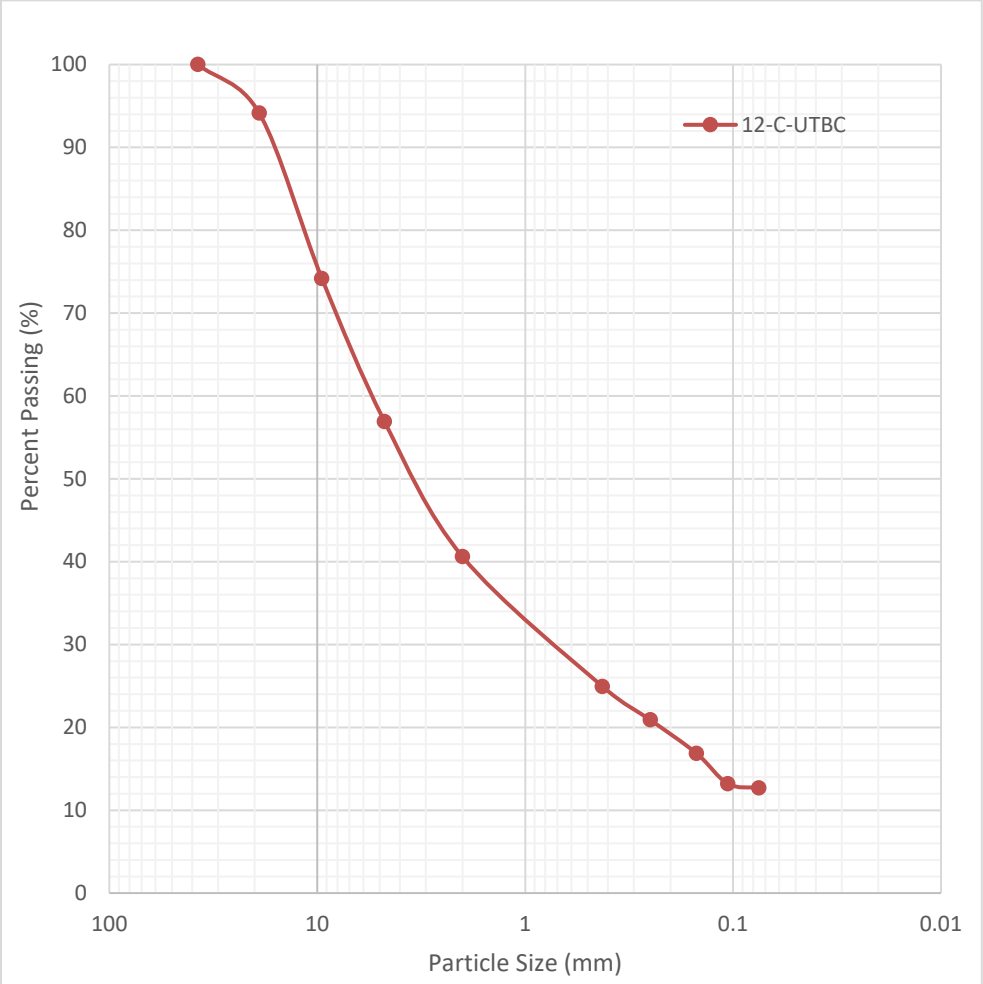

Project:	SR-10		Date:	10/9/2018	Shaker:	Mechanical
Location:	12-C-GB		Personnel:	HB	Time:	10 min
Sieve Number	Sieve Opening (mm)	Cumulative Retained (g)	Cumulative Passing (g)	Percent Passing (%)	Shape, Uniformity, and Classification	
1 1/2	37.500	0.00	3687.07	100.00	Gravel (%)	51.04
3/4	19.000	690.21	2996.86	81.28	Sand (%)	38.82
3/8	9.500	1439.03	2248.04	60.97	Fines (%)	10.14
4	4.750	1881.92	1805.15	48.96	D_{60}	9.03
10	2.000	2387.78	1299.29	35.24	D_{30}	1.43
40	0.425	3073.78	613.29	16.63	D_{10}	0.07
60	0.250	3189.27	497.80	13.50	C_u	122.13
100	0.150	3246.66	440.41	11.94	C_c	3.08
140	0.106	3301.81	385.26	10.45	Gradation	Poor
200	0.075	3304.73	373.05	10.14	USCS	GP-GC

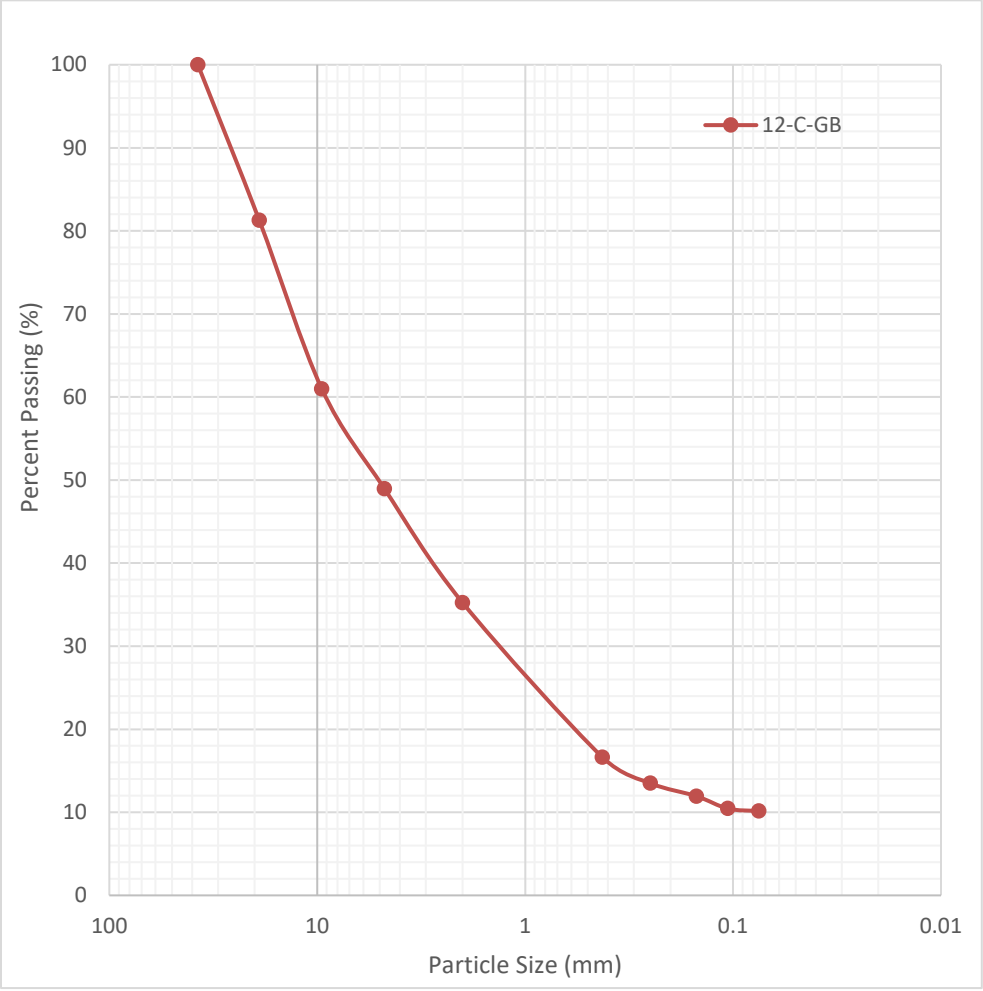

Project:	SR-10		Date:	10/5/2018	Shaker:	Mechanical
Location:	13-C-UTBC		Personnel:	HB	Time:	10 min

Sieve Number	Sieve Opening (mm)	Cumulative Retained (g)	Cumulative Passing (g)	Percent Passing (%)	Shape, Uniformity, and Classification	
1 1/2	37.500	0.00	3854.76	100.00	Gravel (%)	53.96
3/4	19.000	378.93	3475.83	90.17	Sand (%)	36.63
3/8	9.500	1562.38	2292.38	59.47	Fines (%)	9.41
4	4.750	2079.99	1774.77	46.04	D_{60}	9.64
10	2.000	2560.61	1294.15	33.57	D_{30}	1.32
40	0.425	3004.93	849.83	22.05	D_{10}	0.11
60	0.250	3183.29	671.47	17.42	C_u	89.20
100	0.150	3334.91	519.85	13.49	C_c	1.68
140	0.106	3476.09	378.67	9.82	Gradation	Well
200	0.075	3482.14	361.89	9.41	USCS	GW-GC

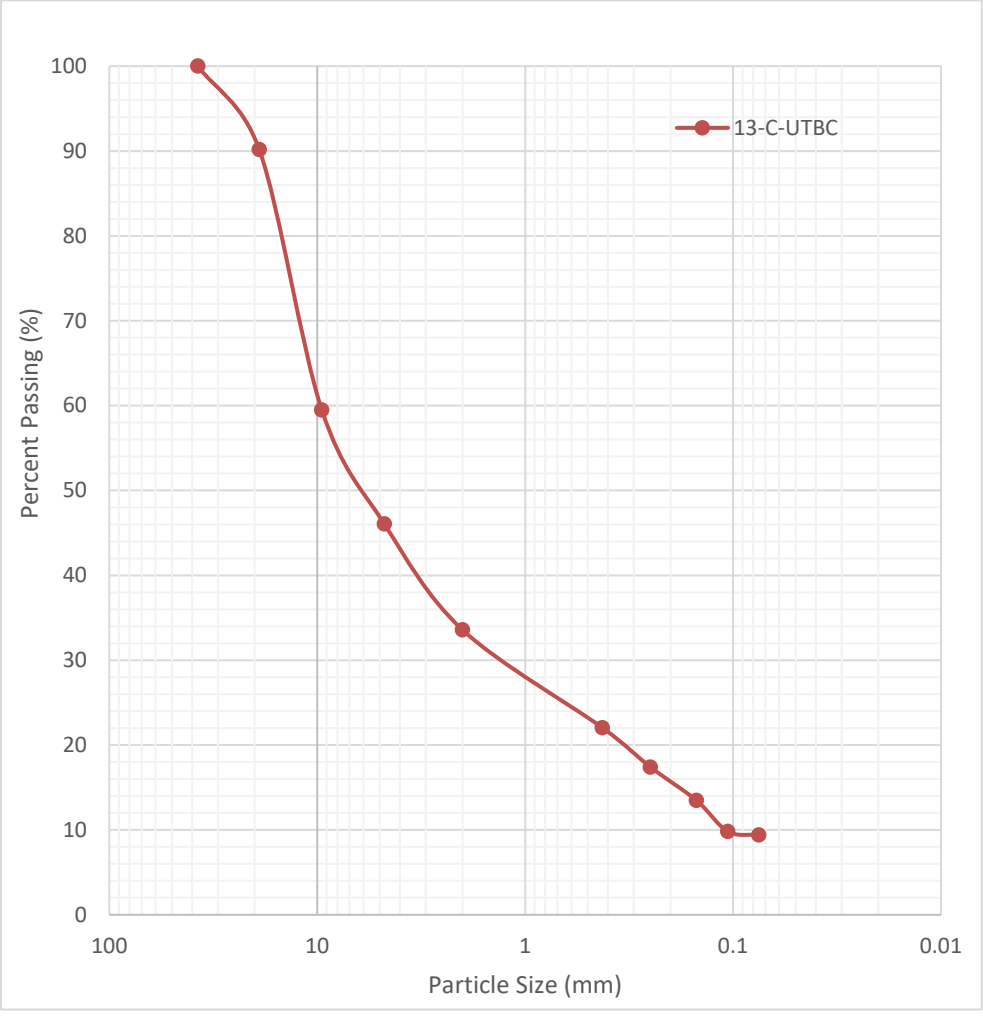

Project:	SR-10		Date:	10/1/2018	Shaker:	Mechanical
Location:	13-C-GB		Personnel:	HB	Time:	10 min
Sieve Number	Sieve Opening (mm)	Cumulative Retained (g)	Cumulative Passing (g)	Percent Passing (%)	Shape, Uniformity, and Classification	
1 1/2	37.500	0.00	3434.81	100.00	Gravel (%)	48.24
3/4	19.000	565.29	2869.52	83.54	Sand (%)	40.24
3/8	9.500	1214.77	2220.04	64.63	Fines (%)	11.52
4	4.750	1656.89	1777.92	51.76	D_{60}	7.53
10	2.000	2186.81	1248.00	36.33	D_{30}	1.27
40	0.425	2782.53	652.28	18.99	D_{10}	0.07
60	0.250	2880.43	554.38	16.14	C_u	115.71
100	0.150	2989.83	444.98	12.96	C_c	3.27
140	0.106	3034.33	400.48	11.66	Gradation	Poor
200	0.075	3026.64	394.15	11.52	USCS	GP-GM

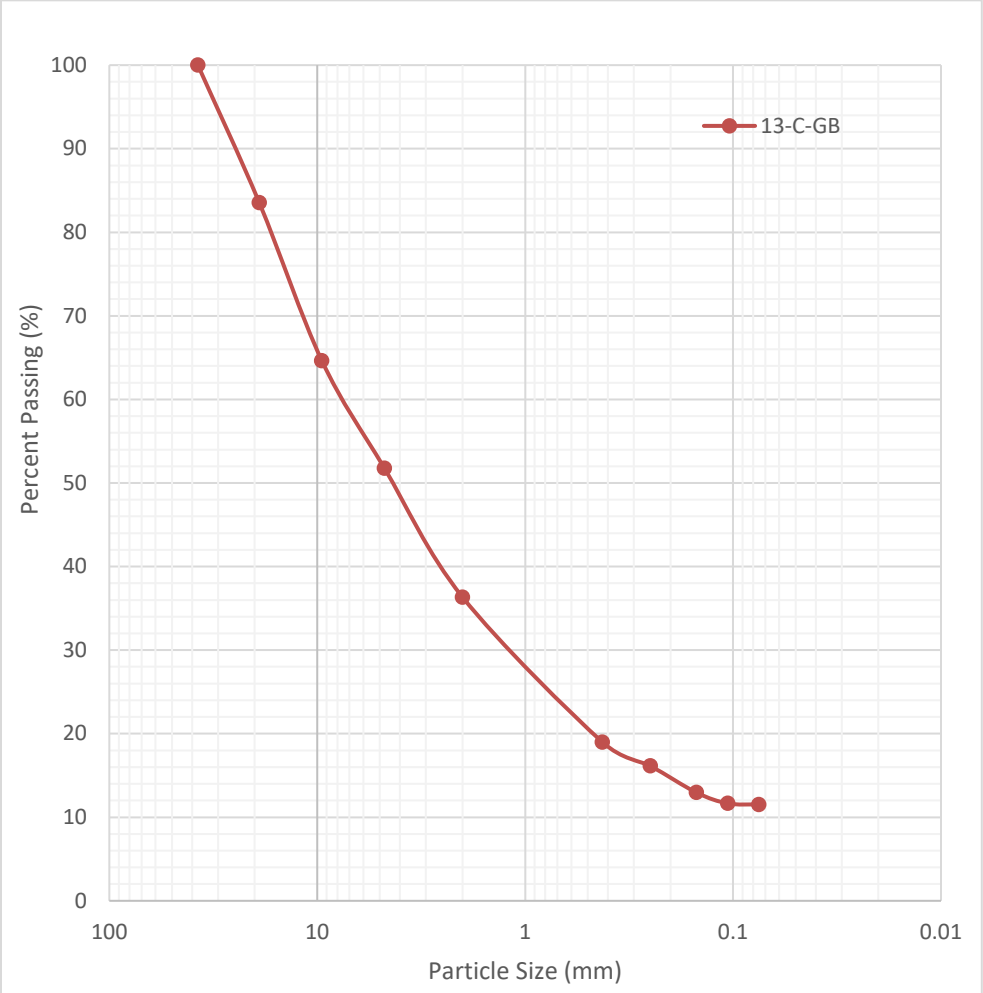

Project:	SR-10		Date:	10/11/2018	Shaker:	Mechanical
Location:	14-C-UTBC		Personnel:	HB	Time:	10 min
Sieve Number	Sieve Opening (mm)	Cumulative Retained (g)	Cumulative Passing (g)	Percent Passing (%)	Shape, Uniformity, and Classification	
1 1/2	37.500	0.00	4302.72	100.00	Gravel (%)	38.06
3/4	19.000	203.11	4099.61	95.28	Sand (%)	45.06
3/8	9.500	1070.79	3231.93	75.11	Fines (%)	16.88
4	4.750	1637.50	2665.22	61.94	D_{60}	4.34
10	2.000	2340.04	1962.68	45.61	D_{30}	0.45
40	0.425	3033.03	1269.69	29.51	D_{10}	0.04
60	0.250	3390.06	912.66	21.21	C_u	97.71
100	0.150	3502.01	800.71	18.61	C_c	1.05
140	0.106	3575.08	727.64	16.91	Gradation	NA
200	0.075	3575.37	726.22	16.88	USCS	SM

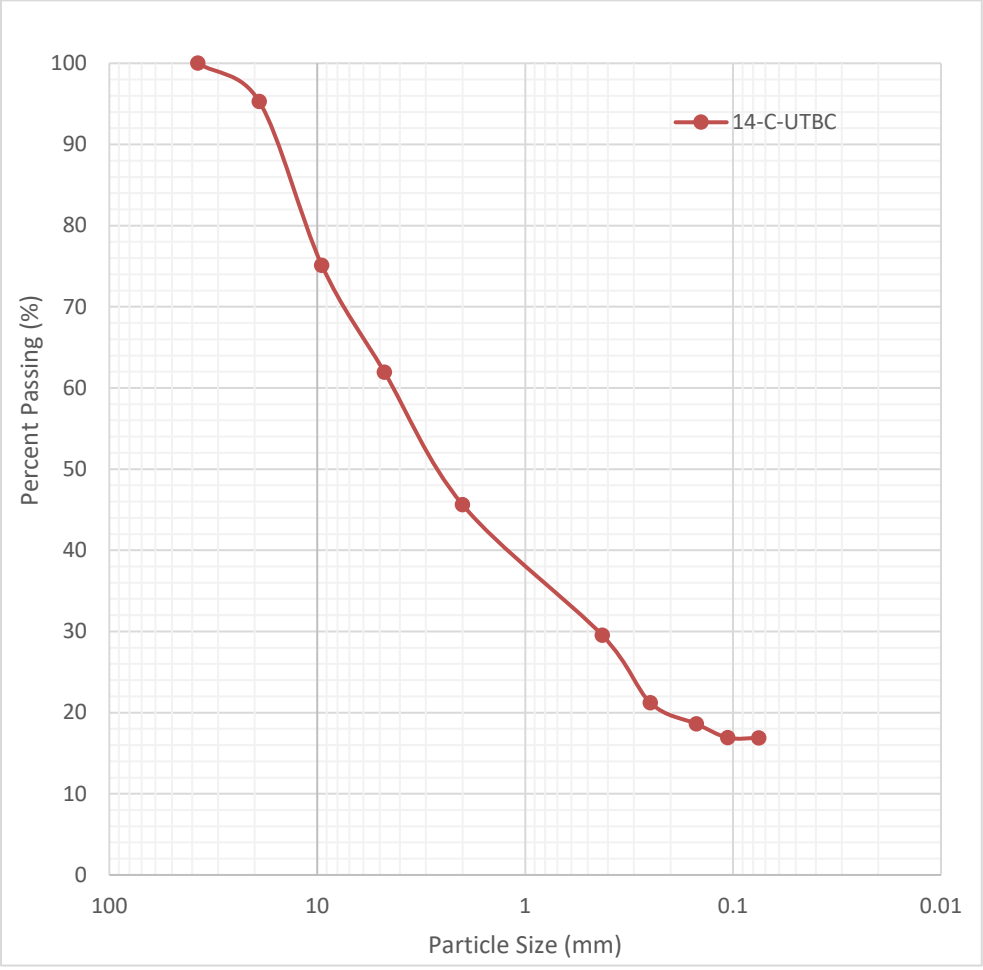

Project:	SR-10		Date:	10/11/2018	Shaker:	Mechanical
Location:	14-C-GB		Personnel:	HB	Time:	10 min
Sieve Number	Sieve Opening (mm)	Cumulative Retained (g)	Cumulative Passing (g)	Percent Passing (%)	Shape, Uniformity, and Classification	
1 1/2	37.500	0.00	2426.83	100.00	Gravel (%)	36.26
3/4	19.000	157.83	2269.00	93.50	Sand (%)	50.12
3/8	9.500	567.24	1859.59	76.63	Fines (%)	13.62
4	4.750	880.01	1546.82	63.74	D_{60}	3.95
10	2.000	1263.49	1163.34	47.94	D_{30}	0.46
40	0.425	1718.66	708.17	29.18	D_{10}	0.06
60	0.250	1864.39	562.44	23.18	C_u	71.81
100	0.150	1970.92	455.91	18.79	C_c	0.99
140	0.106	2036.13	390.70	16.10	Gradation	NA
200	0.075	2056.83	324.37	13.62	USCS	SC

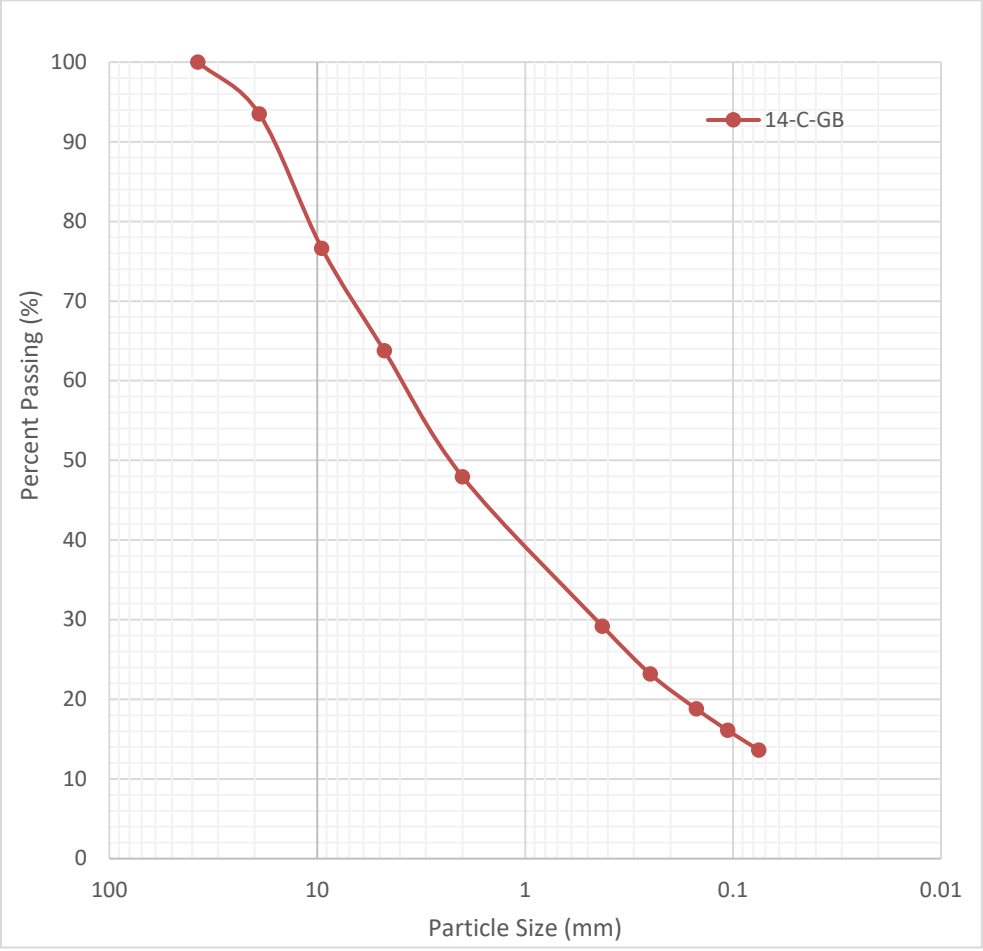

ASTM D4318 Standard Test Methods for Liquid Limit, Plastic Limit, and Plasticity Index of Soils					
Project:	SR-10		Date:	3/28/2019	
Location:	1-A-UTBC		Personnel:	HB	
	Liquid Limit Determination			Plastic Limit Determination	
Tare No.:	17	5	1	11	4
Tare wt. (g):	22.82	20.38	27.26	22.98	27.82
Wet + tare wt. (g):	35.89	30.46	38.47	29.14	34.06
Dry + tare wt. (g):	32.87	28.02	35.76	28.2	33.12
Water content (%):	30.05	31.94	31.88	18.01	17.74
Blows:	25	20	17		
Log Blows:	1.40	1.30	1.23		

Slope:	-11.45
Intercept:	46.29
Liquid Limit:	30
Plastic Limit:	18
Plasticity Index:	12

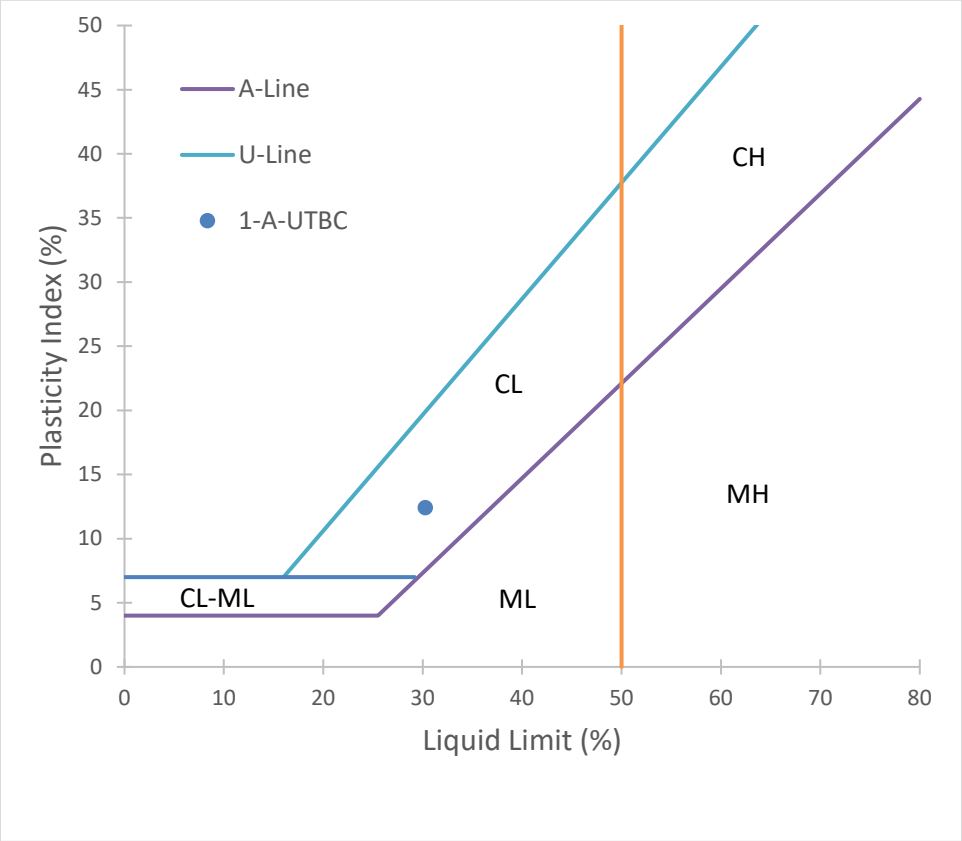

ASTM D4318 Standard Test Methods for Liquid Limit, Plastic Limit, and Plasticity Index of Soils					
Project:	SR-10		Date:	4/8/2019	
Location:	1-A-GB		Personnel:	HB	
	Liquid Limit Determination			Plastic Limit Determination	
Tare No.:	9	2	5	3	17
Tare wt. (g):	26.18	26.96	26.51	26.75	28.48
Wet + tare wt. (g):	39.14	41.63	43.22	33.14	35.05
Dry + tare wt. (g):	37.27	39.43	40.67	32.42	34.31
Water content (%):	16.86	17.64	18.01	12.70	12.69
Blows:	31	20	15		
Log Blows:	1.49	1.30	1.18		

Slope:	-3.67
Intercept:	22.37
Liquid Limit:	17
Plastic Limit:	13
Plasticity Index:	5

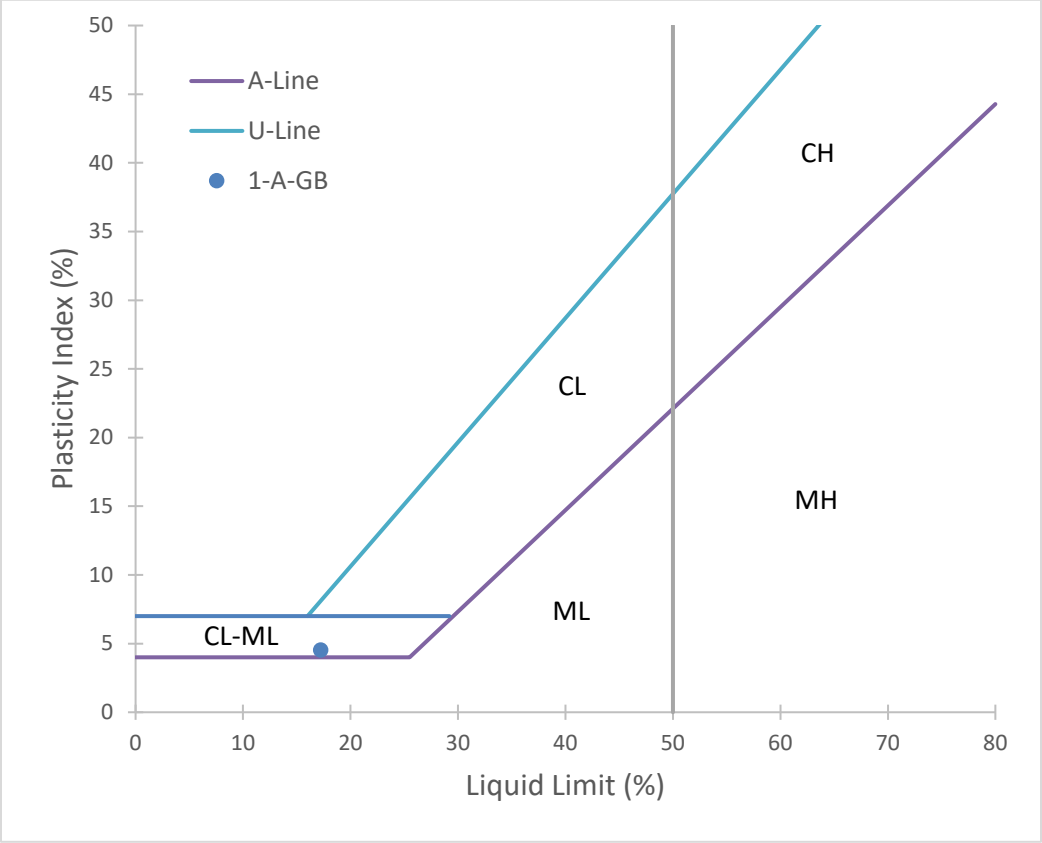

ASTM D4318 Standard Test Methods for Liquid Limit, Plastic Limit, and Plasticity Index of Soils					
Project:	SR-10		Date:	3/15/2019	
Location:	2-C-UTBC		Personnel:	HB	
	Liquid Limit Determination			Plastic Limit Determination	
Tare No.:	9	23	1	4	19
Tare wt. (g):	26.18	22.39	26.59	26.22	22.71
Wet + tare wt. (g):	44.85	42.84	50.36	35.53	29.19
Dry + tare wt. (g):	41.83	39.34	46.16	34.35	28.37
Water content (%):	19.30	20.65	21.46	14.51	14.49
Blows:	51	26	20		
Log Blows:	1.71	1.41	1.30		
Slope:	-5.18				
Intercept:	28.11				
Liquid Limit:	21				
Plastic Limit:	15				
Plasticity Index:	6				

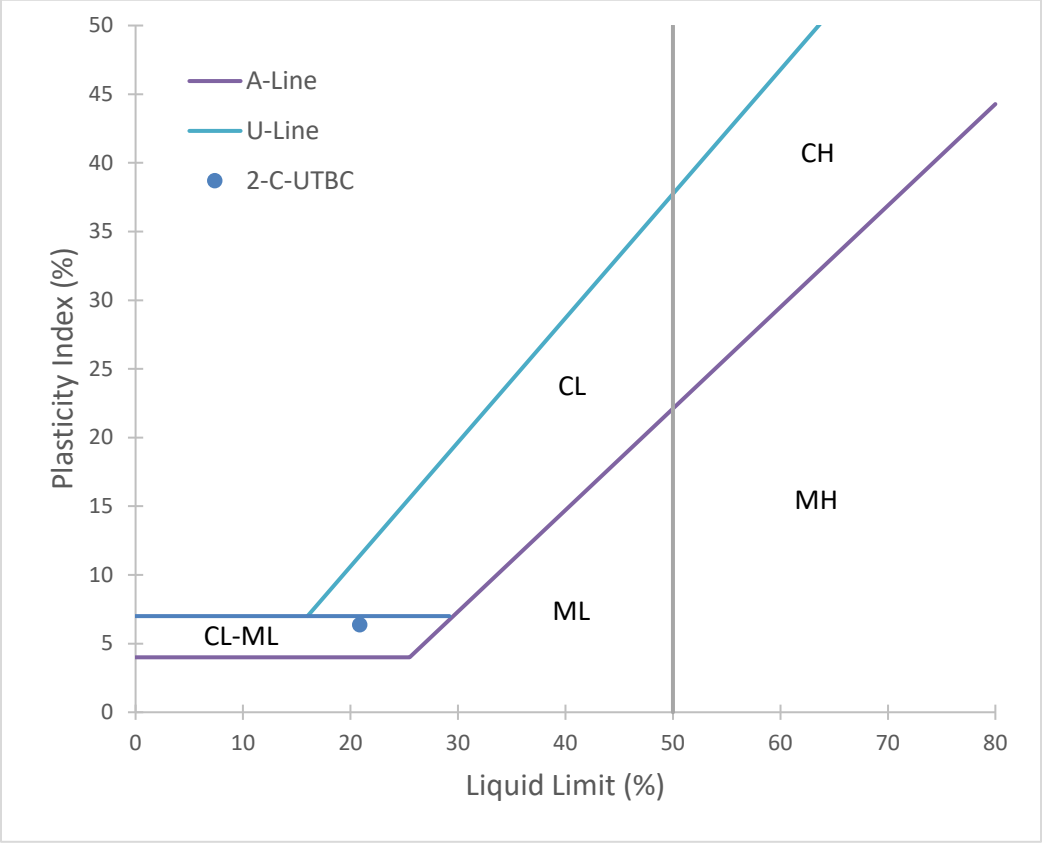

ASTM D4318 Standard Test Methods for Liquid Limit, Plastic Limit, and Plasticity Index of Soils					
Project:	SR-10		Date:	2/11/2019	
Location:	2-C-GB		Personnel:	HB	
	Liquid Limit Determination			Plastic Limit Determination	
Tare No.:	17	5	22	20	18
Tare wt. (g):	22.94	20.35	25.76	27.80	26.91
Wet + tare wt. (g):	48.49	42.36	45.72	33.10	31.29
Dry + tare wt. (g):	42.80	37.30	40.97	32.31	30.66
Water content (%):	28.65	29.85	31.23	17.52	16.80
Blows:	30	21	20		
Log Blows:	1.48	1.32	1.30		

Slope:	-12.07
Intercept:	46.41
Liquid Limit:	30
Plastic Limit:	17
Plasticity Index:	12

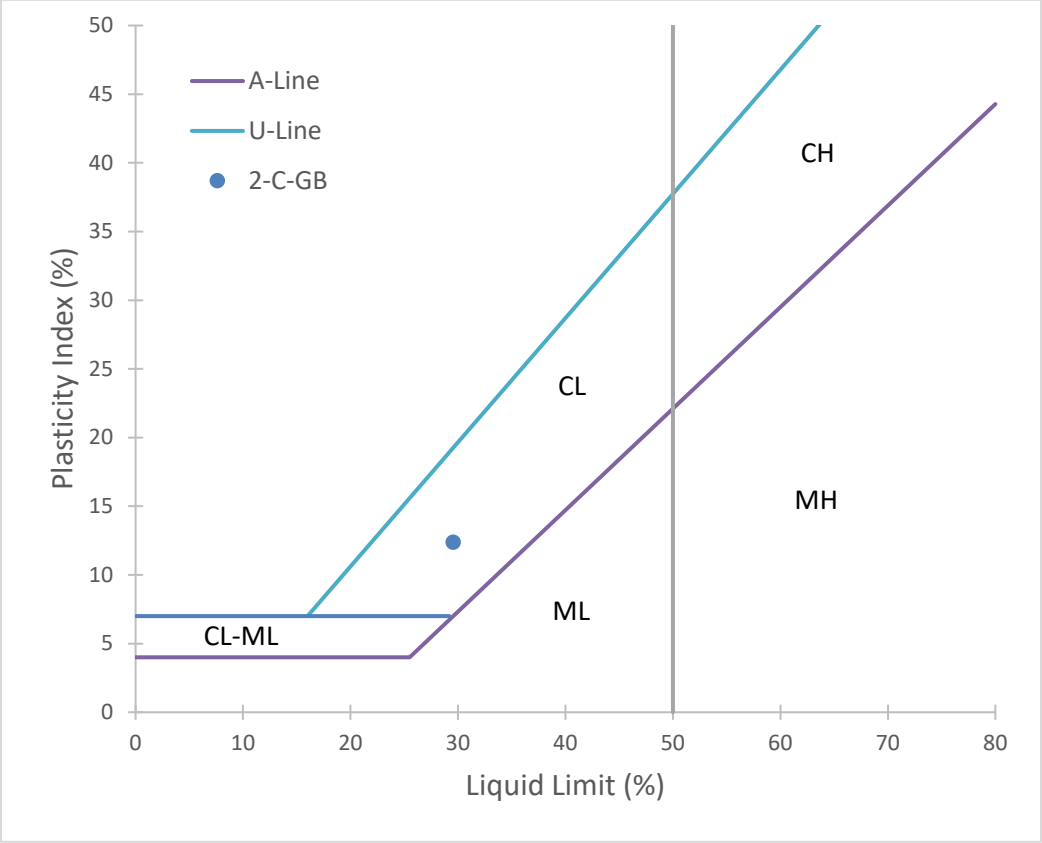

ASTM D4318 Standard Test Methods for Liquid Limit, Plastic Limit, and Plasticity Index of Soils					
Project:	SR-10		Date:	3/28/2019	
Location:	3-C-UTBC		Personnel:	HB	
	Liquid Limit Determination			Plastic Limit Determination	
Tare No.:	13	18	3	2	6
Tare wt. (g):	22.92	26.69	26.72	26.96	24.98
Wet + tare wt. (g):	33.27	39.53	39.83	33.68	31.38
Dry + tare wt. (g):	31.12	36.79	36.86	32.69	30.45
Water content (%):	26.22	27.13	29.29	17.28	17.00
Blows:	31	20	15		
Log Blows:	1.49	1.30	1.18		
Slope:	-9.33				
Intercept:	39.89				
Liquid Limit:	27				
Plastic Limit:	17				
Plasticity Index:	10				

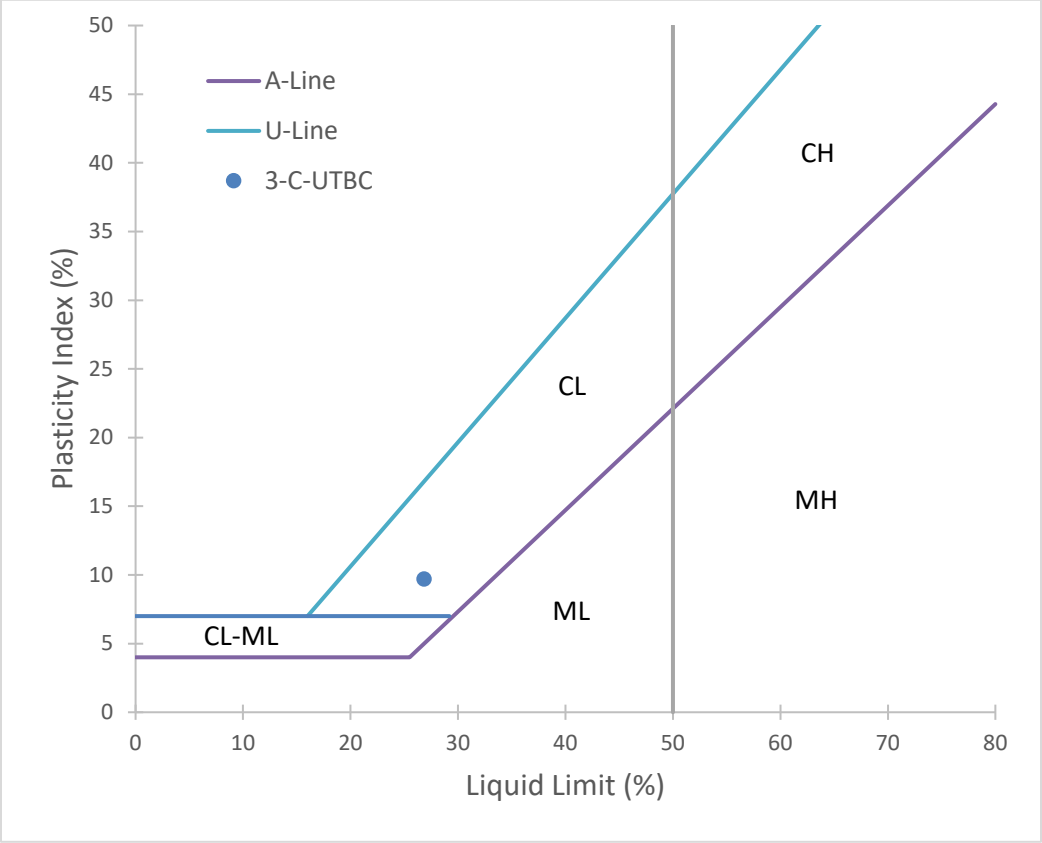

ASTM D4318 Standard Test Methods for Liquid Limit, Plastic Limit, and Plasticity Index of Soils						
Project:	SR-10		Date:	2/11/2019		
Location:	3-C-GB		Personnel:	HB		
	Liquid Limit Determination				Plastic Limit Determination	
Tare No.:	5	6	9	19	2	4
Tare wt. (g):	22.96	25.78	22.79	26.73	26.58	26.93
Wet + tare wt. (g):	35.72	42.00	38.58	44.87	33.42	33.71
Dry + tare wt. (g):	33.72	39.39	35.96	41.73	32.57	32.93
Water content (%):	18.59	19.18	19.89	20.93	14.19	13.00
Blows:	35	29	18	17		
Log Blows:	1.54	1.46	1.26	1.23		
Slope:	-6.10					
Intercept:	28.02					
Liquid Limit:	19					
Plastic Limit:	14					
Plasticity Index:	6					

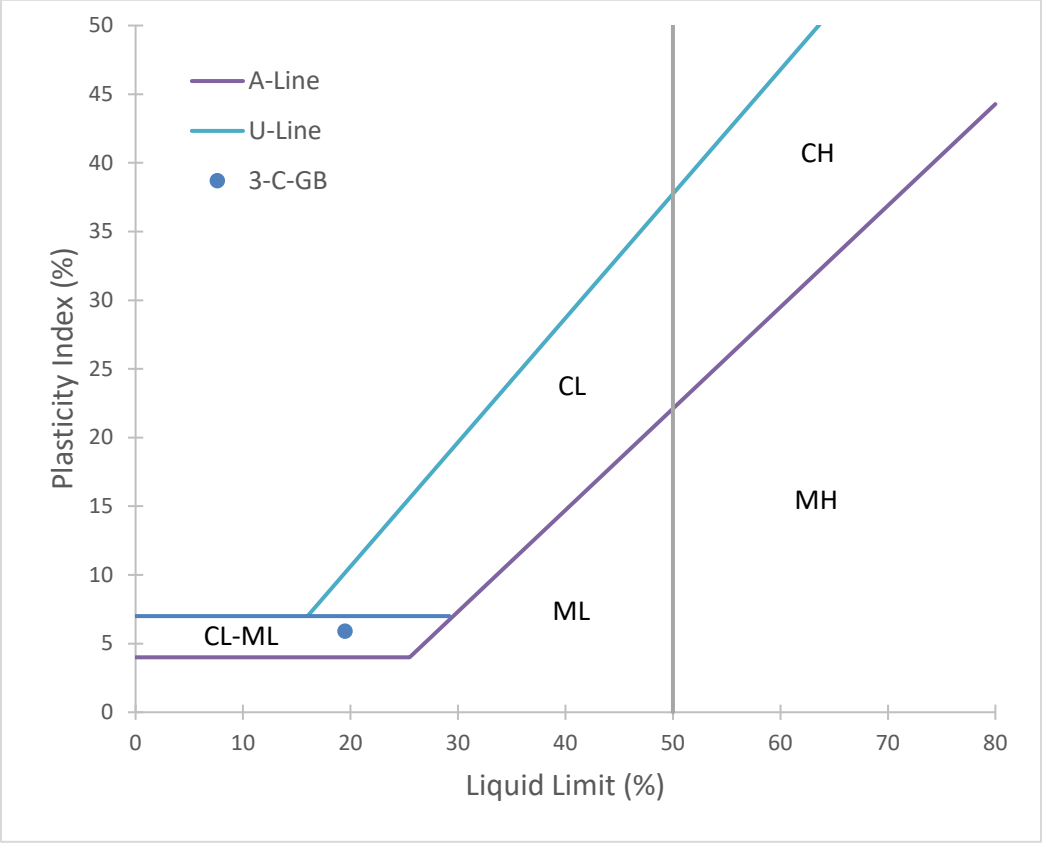

ASTM D4318 Standard Test Methods for Liquid Limit, Plastic Limit, and Plasticity Index of Soils					
Project:	SR-10		Date:	3/16/2019	
Location:	4-C-UTBC		Personnel:	HB	
	Liquid Limit Determination			Plastic Limit Determination	
Tare No.:	22	18	5	20	17
Tare wt. (g):	25.75	26.89	20.34	27.81	22.97
Wet + tare wt. (g):	38.99	43.39	48.39	34.03	29.34
Dry + tare wt. (g):	36.53	40.41	43.17	33.27	28.55
Water content (%):	22.82	22.04	22.86	13.92	14.16
Blows:	16	25	20		
Log Blows:	1.20	1.40	1.30		
Slope:	-4.02				
Intercept:	27.80				
Liquid Limit:	22				
Plastic Limit:	14				
Plasticity Index:	8				

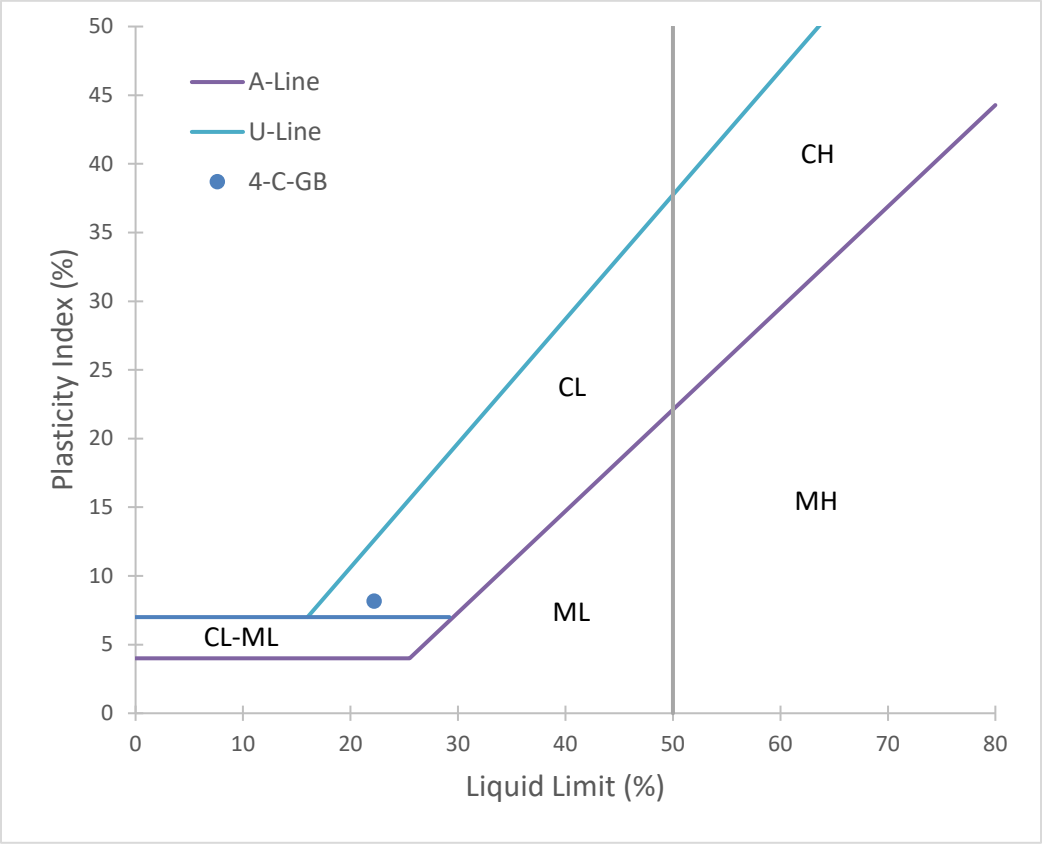

ASTM D4318 Standard Test Methods for Liquid Limit, Plastic Limit, and Plasticity Index of Soils						
Project:	SR-10		Date:	2/11/2019		
Location:	4-C-GB		Personnel:	HB		
	Liquid Limit Determination				Plastic Limit Determination	
Tare No.:	5	6	9	19	2	4
Tare wt. (g):	22.38	27.33	22.69	22.99	26.24	22.81
Wet + tare wt. (g):	37.75	44.68	40.17	42.72	33.51	26.70
Dry + tare wt. (g):	34.69	41.16	36.52	38.45	32.47	26.14
Water content (%):	24.86	25.45	26.39	27.62	16.69	16.82
Blows:	26.00	23.00	18.00	15.00		
Log Blows:	1.41	1.36	1.26	1.18		
Slope:	-11.17					
Intercept:	40.63					
Liquid Limit:	25					
Plastic Limit:	17					
Plasticity Index:	8					

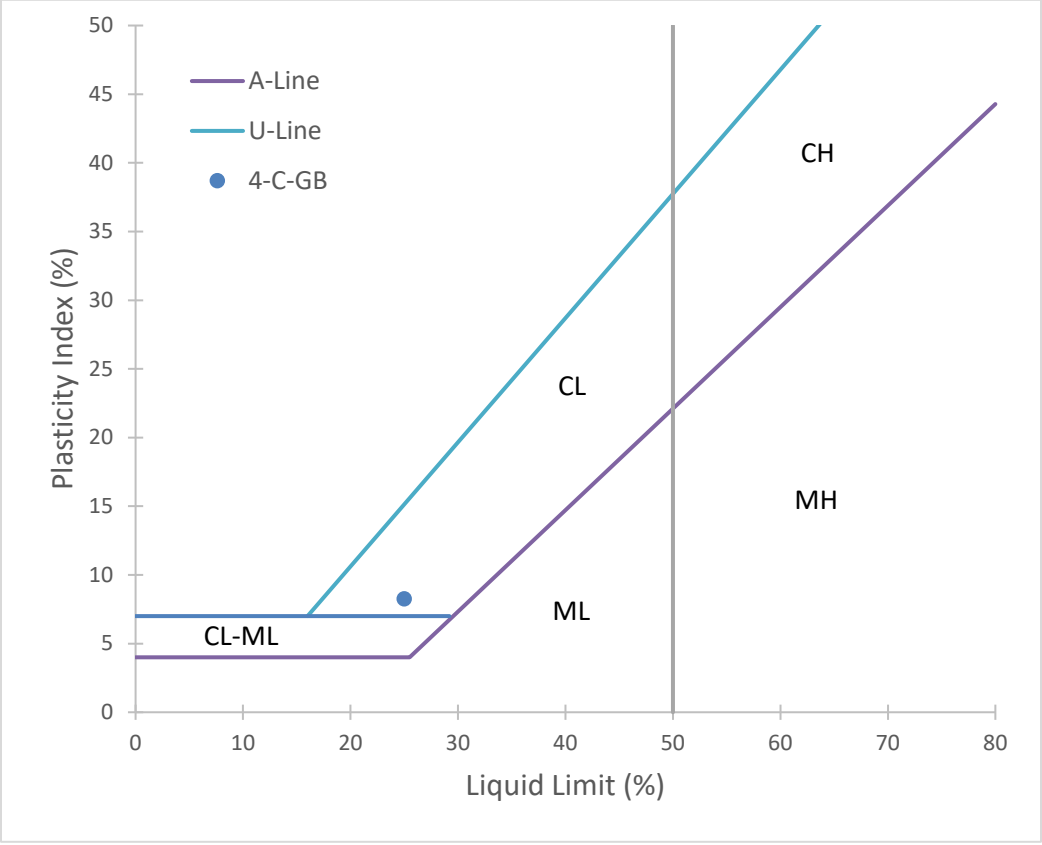

ASTM D4318 Standard Test Methods for Liquid Limit, Plastic Limit, and Plasticity Index of Soils					
Project:	SR-10		Date:	3/15/2019	
Location:	5-C-UTBC		Personnel:	HB	
	Liquid Limit Determination			Plastic Limit Determination	
Tare No.:	6	2	16	3	4
Tare wt. (g):	25.98	26.92	22.79	26.78	22.40
Wet + tare wt. (g):	46.24	44.20	40.79	31.85	28.05
Dry + tare wt. (g):	42.60	41.28	37.56	31.17	27.31
Water content (%):	21.90	20.33	21.87	15.49	15.07
Blows:	21	47	19		
Log Blows:	1.32	1.67	1.28		
Slope:	-4.12				
Intercept:	27.24				
Liquid Limit:	21				
Plastic Limit:	15				
Plasticity Index:	6				

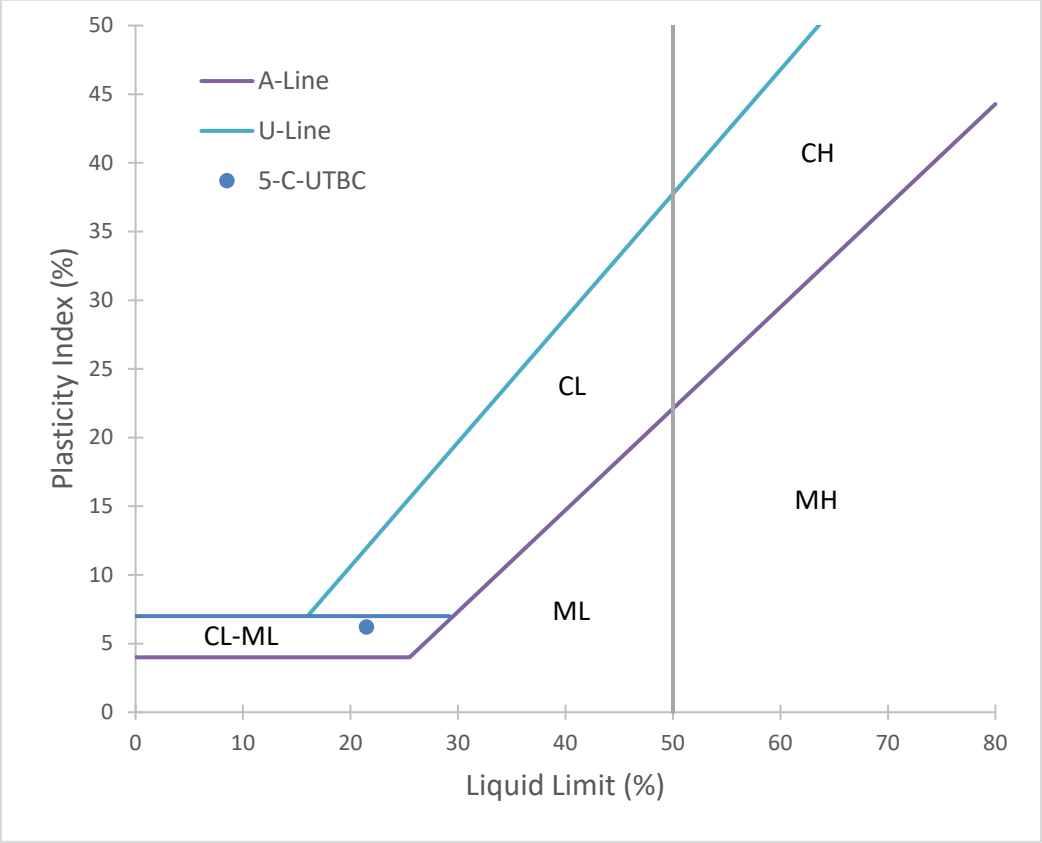

ASTM D4318 Standard Test Methods for Liquid Limit, Plastic Limit, and Plasticity Index of Soils					
Project:	SR-10		Date:	4/8/2019	
Location:	5-C-GB		Personnel:	HB	
	Liquid Limit Determination			Plastic Limit Determination	
Tare No.:	6	3	9	2	13
Tare wt. (g):	24.99	26.19	26.74	25.89	22.93
Wet + tare wt. (g):	38.99	42.57	38.14	33.28	28.40
Dry + tare wt. (g):	37.25	40.30	36.44	32.47	27.78
Water content (%):	14.19	16.09	17.53	12.31	12.78
Blows:	25	21	15		
Log Blows:	1.40	1.32	1.18		
Slope:	-14.33				
Intercept:	34.54				
Liquid Limit:	15				
Plastic Limit:	13				
Plasticity Index:	2				

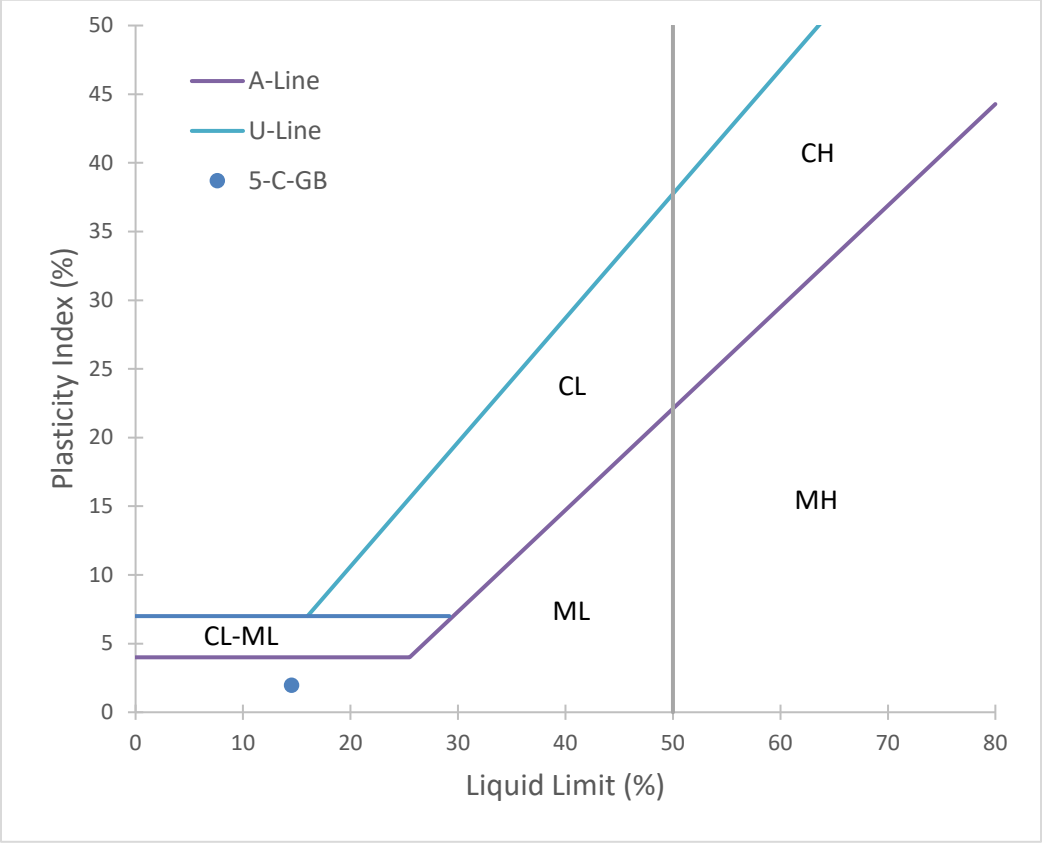

ASTM D4318 Standard Test Methods for Liquid Limit, Plastic Limit, and Plasticity Index of Soils					
Project:	SR-10		Date:	4/9/2019	
Location:	6-C-UTBC		Personnel:	HB	
	Liquid Limit Determination			Plastic Limit Determination	
Tare No.:	17	2	13	18	6
Tare wt. (g):	22.84	25.88	22.92	26.74	25.10
Wet + tare wt. (g):	36.34	38.72	39.42	32.94	31.67
Dry + tare wt. (g):	33.49	35.88	35.75	31.98	30.67
Water content (%):	26.76	28.40	28.60	18.32	17.95
Blows:	30	20	15		
Log Blows:	1.48	1.30	1.18		
Slope:	-6.34				
Intercept:	36.27				
Liquid Limit:	27				
Plastic Limit:	18				
Plasticity Index:	9				

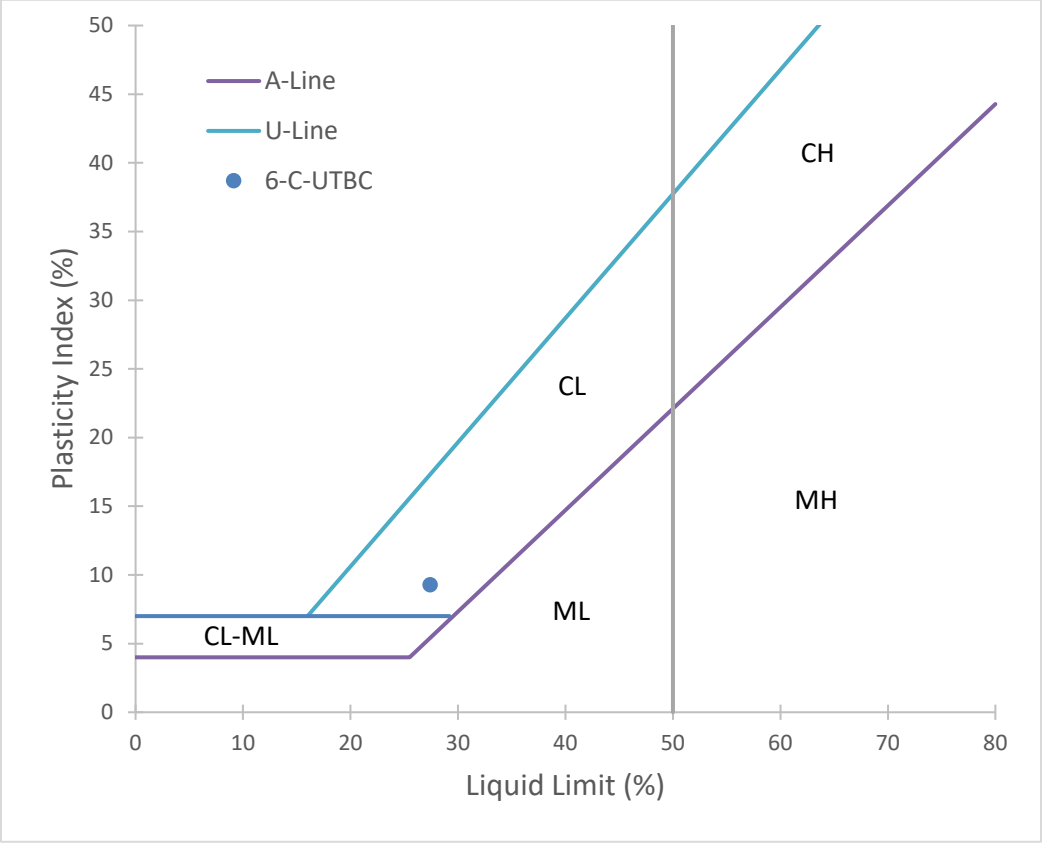

ASTM D4318 Standard Test Methods for Liquid Limit, Plastic Limit, and Plasticity Index of Soils					
Project:	SR-10		Date:	3/16/2019	
Location:	6-C-GB		Personnel:	HB	
	Liquid Limit Determination			Plastic Limit Determination	
Tare No.:	3	1	2	7	4
Tare wt. (g):	26.76	25.89	26.08	23.11	26.21
Wet + tare wt. (g):	44.45	41.52	45.08	28.01	30.98
Dry + tare wt. (g):	40.97	38.41	41.25	27.33	30.33
Water content (%):	24.49	24.84	25.25	16.11	15.78
Blows:	34	25	23		
Log Blows:	1.53	1.40	1.36		
Slope:	-3.96				
Intercept:	30.53				
Liquid Limit:	25				
Plastic Limit:	16				
Plasticity Index:	9				

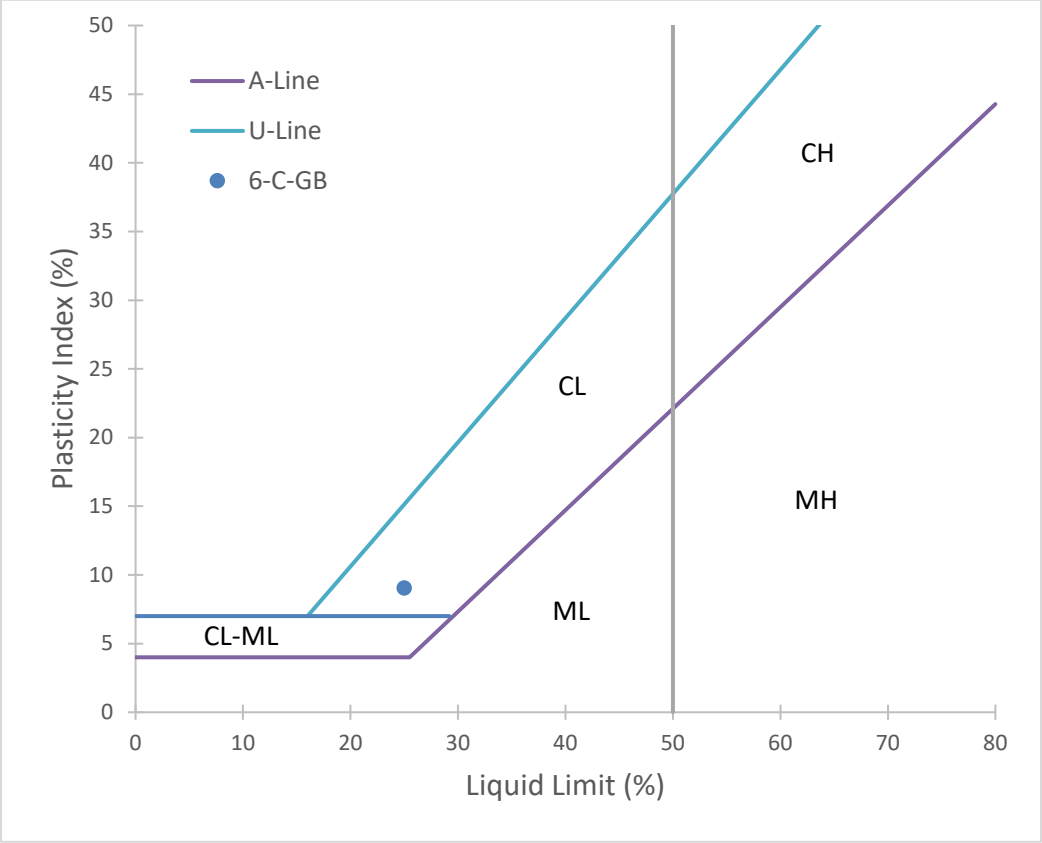

ASTM D4318 Standard Test Methods for Liquid Limit, Plastic Limit, and Plasticity Index of Soils						
Project:	SR-10		Date:		2/7/2019	
Location:	7-C-UTBC		Personnel:		HB	
	Liquid Limit Determination				Plastic Limit Determination	
Tare No.:	5	6	9	19	2	4
Tare wt. (g):	26.15	26.87	25.97	22.34	27.78	20.32
Wet + tare wt. (g):	38.45	41.52	39.53	47.86	32.13	27.70
Dry + tare wt. (g):	36.39	38.97	37.01	42.78	31.52	26.67
Water content (%):	20.12	21.07	22.83	24.85	16.31	16.22
Blows:	35	30	17	8		
Log Blows:	1.54	1.48	1.23	0.90		
Slope:	-7.13					
Intercept:	31.41					
Liquid Limit:	21					
Plastic Limit:	16					
Plasticity Index:	5					

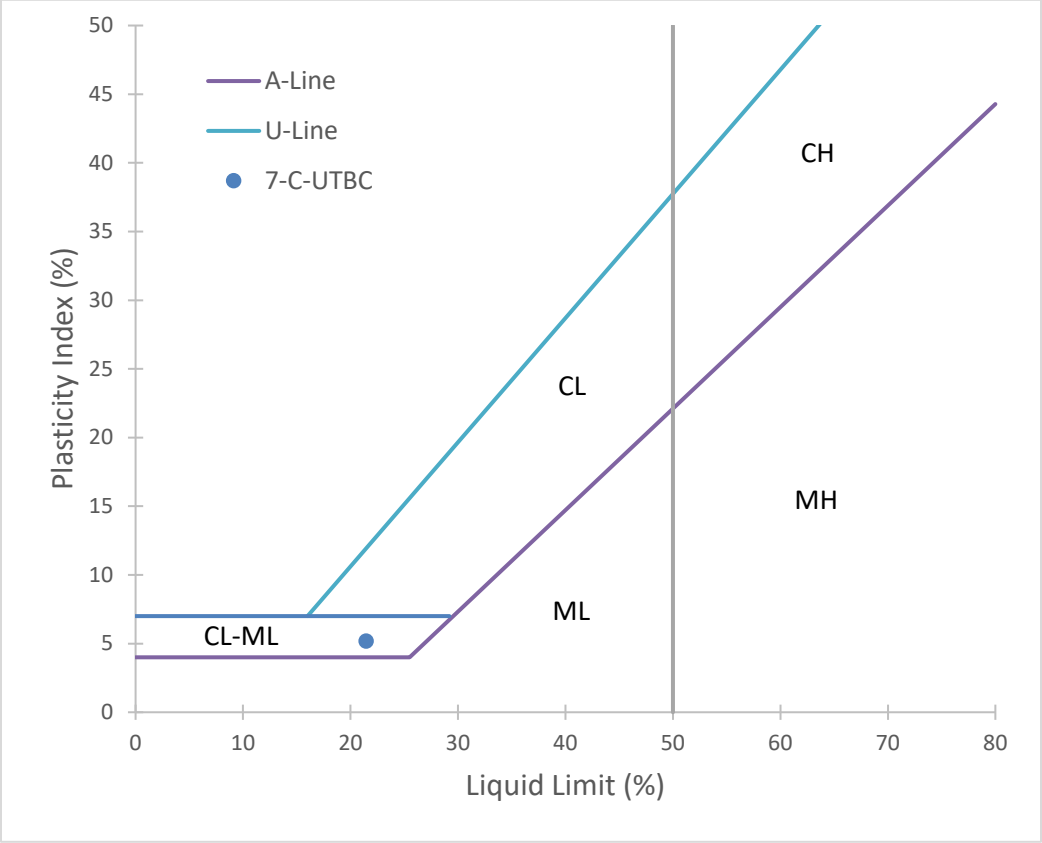

ASTM D4318 Standard Test Methods for Liquid Limit, Plastic Limit, and Plasticity Index of Soils					
Project:	SR-10		Date:	2/11/2019	
Location:	7-C-GB		Personnel:	HB	
	Liquid Limit Determination			Plastic Limit Determination	
Tare No.:	1	2	12	4	7
Tare wt. (g):	23.56	29.87	25.10	27.89	29.29
Wet + tare wt. (g):	47.65	52.57	54.74	37	39.41
Dry + tare wt. (g):	43.50	48.55	49.36	35.84	38.16
Water content (%):	20.81	21.52	22.18	14.59	14.09
Blows:	32	25	17		
Log Blows:	1.51	1.40	1.23		
Slope:	-4.87				
Intercept:	28.22				
Liquid Limit:	21				
Plastic Limit:	14				
Plasticity Index:	7				

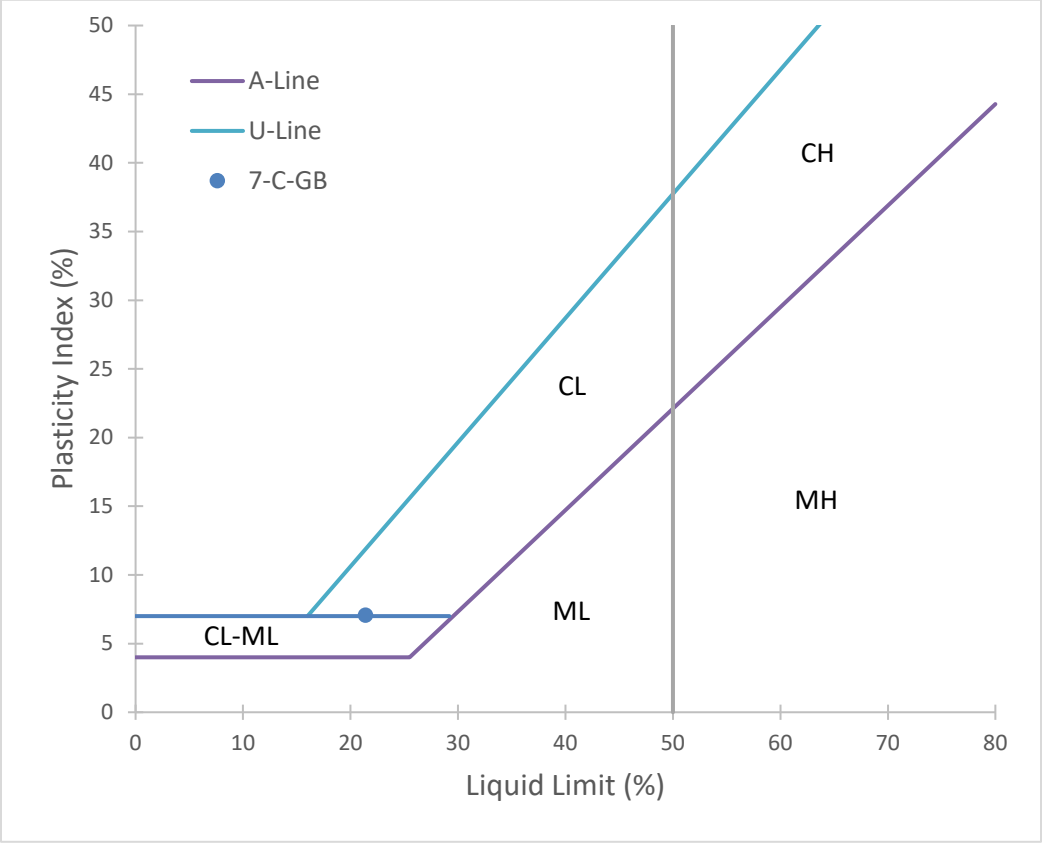

ASTM D4318 Standard Test Methods for Liquid Limit, Plastic Limit, and Plasticity Index of Soils					
Project:	SR-10		Date:	3/15/2019	
Location:	8-C-UTBC		Personnel:	HB	
	Liquid Limit Determination			Plastic Limit Determination	
Tare No.:	5	20	17	18	22
Tare wt. (g):	20.33	27.77	22.95	26.91	25.78
Wet + tare wt. (g):	36.04	43.81	46.78	36.42	33.73
Dry + tare wt. (g):	33.66	41.24	42.86	35.17	32.71
Water content (%):	17.85	19.08	19.69	15.13	14.72
Blows:	34	25	23		
Log Blows:	1.53	1.40	1.36		
Slope:	-10.36				
Intercept:	33.70				
Liquid Limit:	19				
Plastic Limit:	15				
Plasticity Index:	4				

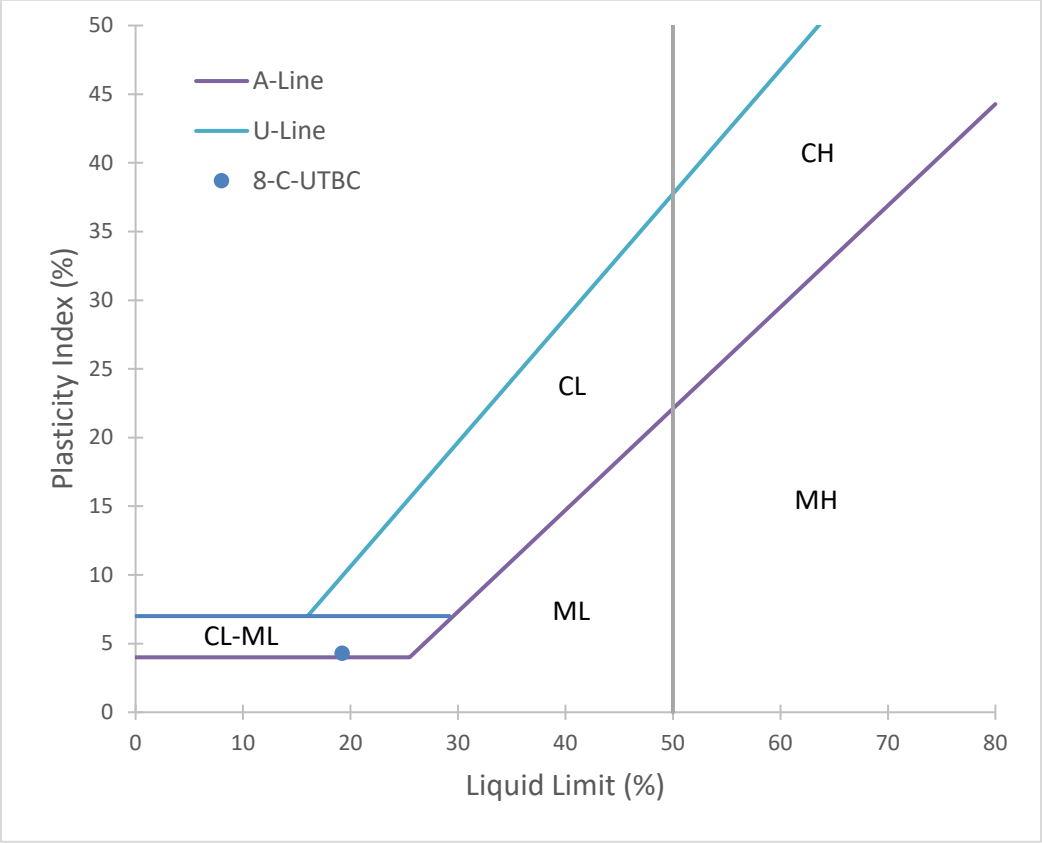

ASTM D4318 Standard Test Methods for Liquid Limit, Plastic Limit, and Plasticity Index of Soils					
Project:	SR-10		Date:	2/11/2019	
Location:	8-C-GB		Personnel:	HB	
	Liquid Limit Determination			Plastic Limit Determination	
Tare No.:	1	2	6	23	16
Tare wt. (g):	26.59	26.88	25.97	22.42	22.79
Wet + tare wt. (g):	43.19	48.59	46.48	29.07	27.23
Dry + tare wt. (g):	39.84	43.96	42.03	28.14	26.63
Water content (%):	25.28	27.11	27.71	16.26	15.63
Blows:	34	23	17		
Log Blows:	1.53	1.36	1.23		
Slope:	-8.19				
Intercept:	37.95				
Liquid Limit:	27				
Plastic Limit:	16				
Plasticity Index:	11				

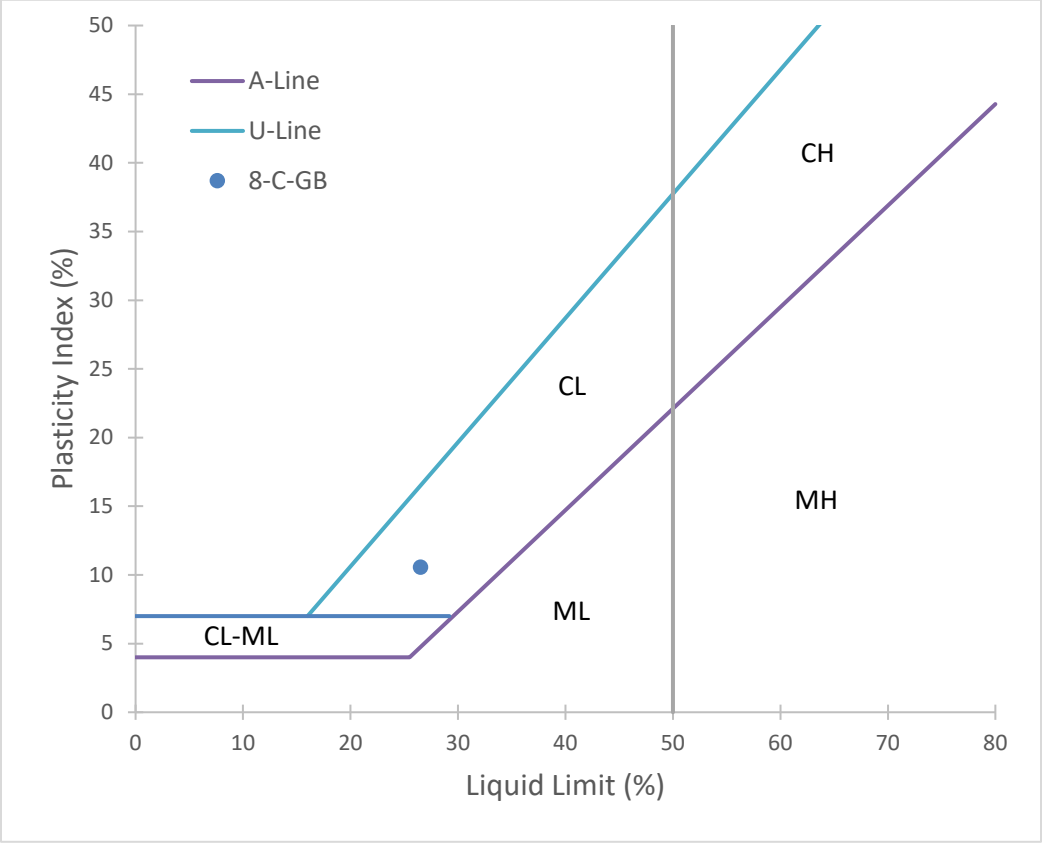

ASTM D4318 Standard Test Methods for Liquid Limit, Plastic Limit, and Plasticity Index of Soils					
Project:	SR-10		Date:	2/11/2019	
Location:	9-C-UTBC		Personnel:	HB	
	Liquid Limit Determination			Plastic Limit Determination	
Tare No.:	3	17	21	5	14
Tare wt. (g):	23.16	28.47	22.58	26.78	23.67
Wet + tare wt. (g):	49.79	52.67	53.94	34.05	31.24
Dry + tare wt. (g):	44.77	48.06	47.95	33.03	30.16
Water content (%):	23.23	23.53	23.61	16.32	16.64
Blows:	26	22	19		
Log Blows:	1.41	1.34	1.28		
Slope:	-2.83				
Intercept:	27.26				
Liquid Limit:	23				
Plastic Limit:	16				
Plasticity Index:	7				

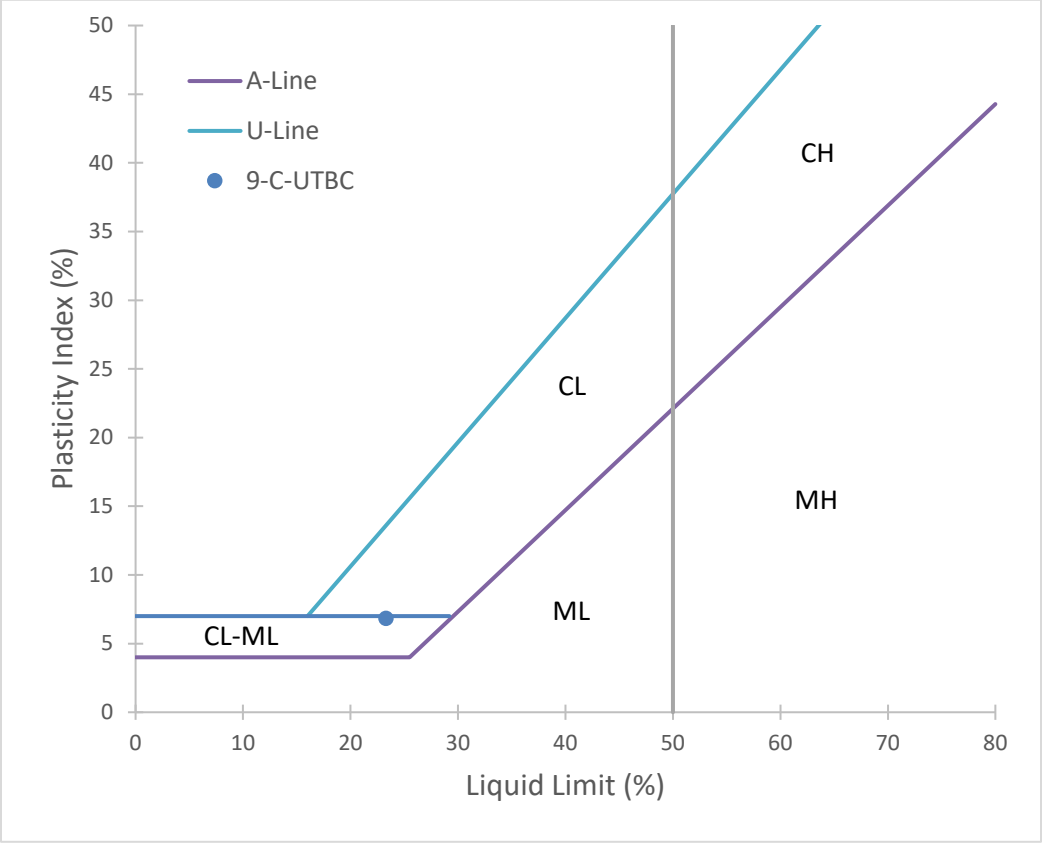

ASTM D4318 Standard Test Methods for Liquid Limit, Plastic Limit, and Plasticity Index of Soils					
Project:	SR-10		Date:	3/15/2019	
Location:	9-C-GB		Personnel:	HB	
	Liquid Limit Determination			Plastic Limit Determination	
Tare No.:	2	1	7	1	3
Tare wt. (g):	26.08	25.87	23.13	26.33	22.80
Wet + tare wt. (g):	44.93	51.32	50.52	34.39	27.45
Dry + tare wt. (g):	41.48	46.36	44.99	33.28	26.81
Water content (%):	22.40	24.21	25.30	15.97	15.96
Blows:	55	28	18		
Log Blows:	1.74	1.45	1.26		

Slope:	-5.98
Intercept:	32.83
Liquid Limit:	24
Plastic Limit:	16
Plasticity Index:	8

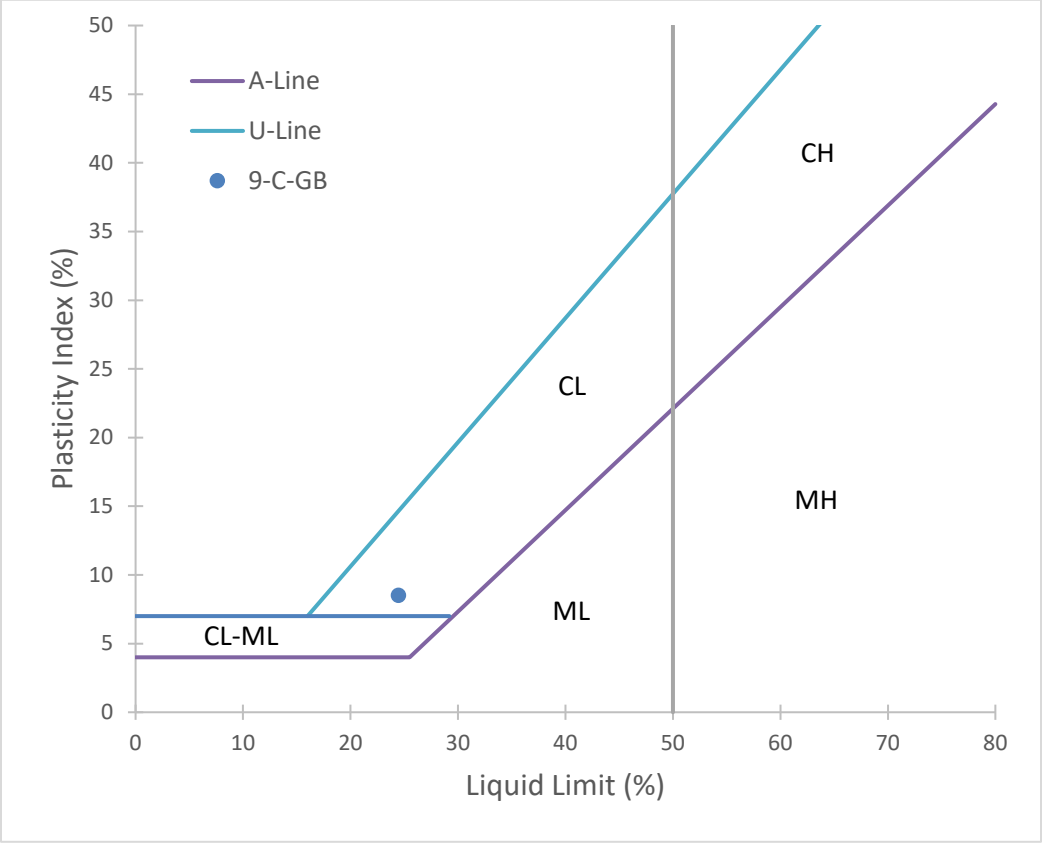

ASTM D4318 Standard Test Methods for Liquid Limit, Plastic Limit, and Plasticity Index of Soils					
Project:	SR-10		Date:	2/11/2019	
Location:	10-C-UTBC		Personnel:	HB	
	Liquid Limit Determination			Plastic Limit Determination	
Tare No.:	1	4	2	9	3
Tare wt. (g):	25.88	26.19	26.11	26.19	26.78
Wet + tare wt. (g):	46.77	49.76	49.64	32.15	33.63
Dry + tare wt. (g):	42.43	44.79	44.66	31.22	32.56
Water content (%):	26.22	26.72	26.85	18.49	18.51
Blows:	28	20	21		
Log Blows:	1.45	1.30	1.32		
Slope:	-3.95				
Intercept:	31.96				
Liquid Limit:	26				
Plastic Limit:	19				
Plasticity Index:	8				

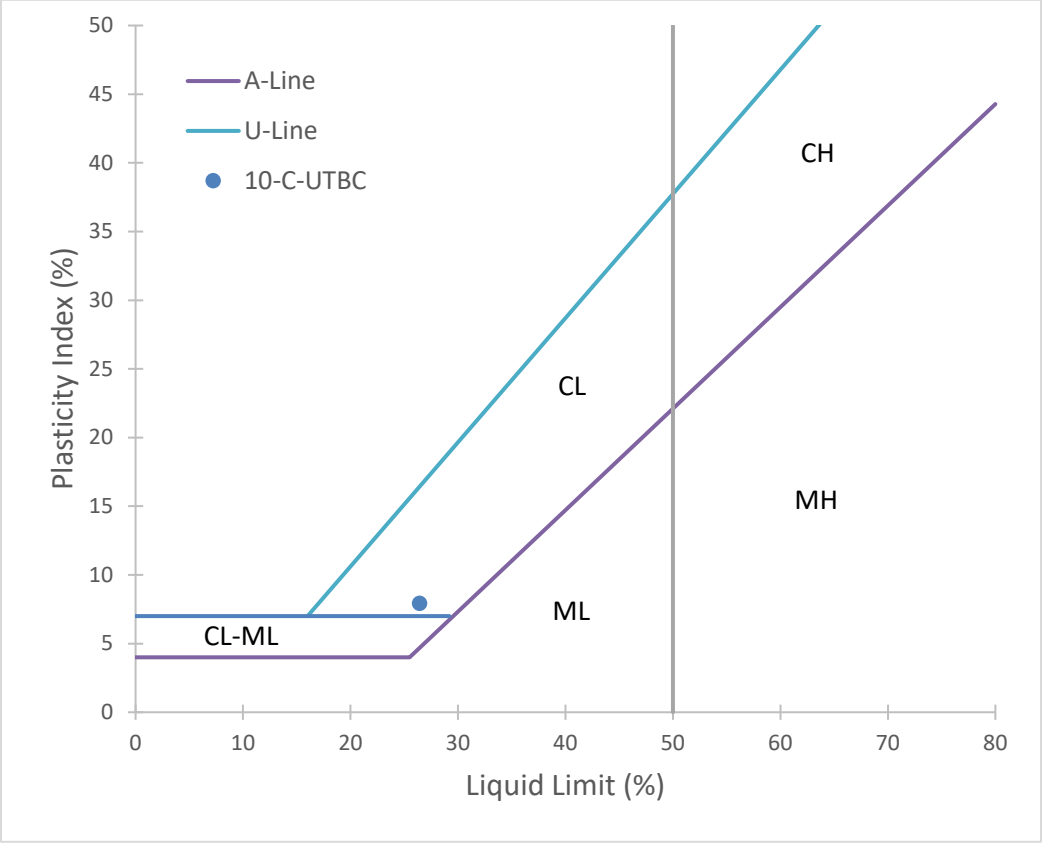

ASTM D4318 Standard Test Methods for Liquid Limit, Plastic Limit, and Plasticity Index of Soils					
Project:	SR-10		Date:	4/9/2019	
Location:	10-C-GB		Personnel:	HB	
	Liquid Limit Determination			Plastic Limit Determination	
Tare No.:	4	5	11	1	10
Tare wt. (g):	27.85	20.37	22.99	27.29	66.15
Wet + tare wt. (g):	41.58	35.36	40.35	33.88	72.28
Dry + tare wt. (g):	39.66	33.22	37.82	33.08	71.60
Water content (%):	16.26	16.65	17.06	13.82	12.48
Blows:	26	21	17		
Log Blows:	1.41	1.32	1.23		
Slope:	-4.35				
Intercept:	22.41				
Liquid Limit:	16				
Plastic Limit:	13				
Plasticity Index:	3				

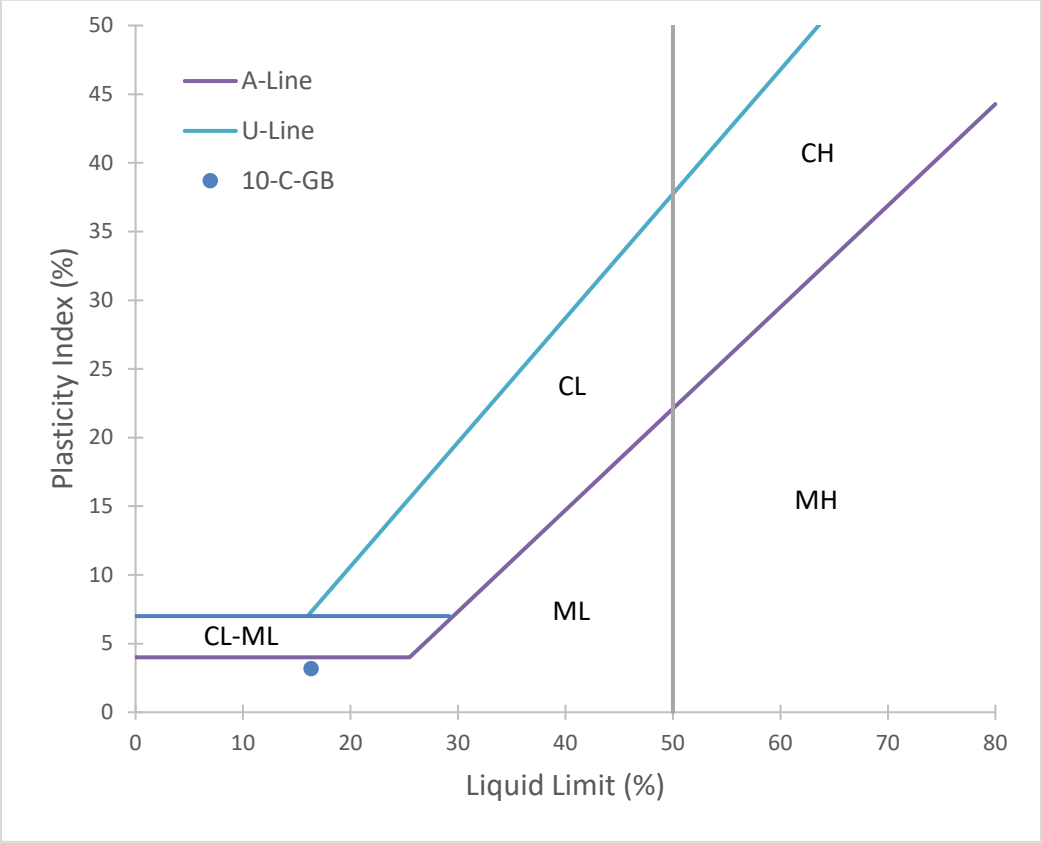

ASTM D4318 Standard Test Methods for Liquid Limit, Plastic Limit, and Plasticity Index of Soils					
Project:	SR-10		Date:	3/16/2019	
Location:	11-C-UTBC		Personnel:	HB	
	Liquid Limit Determination			Plastic Limit Determination	
Tare No.:	1	6	23	16	2
Tare wt. (g):	26.58	25.98	22.41	22.78	26.90
Wet + tare wt. (g):	43.89	43.05	45.08	29.25	32.99
Dry + tare wt. (g):	40.93	39.99	40.74	28.34	32.16
Water content (%):	20.63	21.84	23.68	16.37	15.78
Blows:	45	28	16		
Log Blows:	1.65	1.45	1.20		
Slope:	-6.81				
Intercept:	31.83				
Liquid Limit:	22				
Plastic Limit:	16				
Plasticity Index:	6				

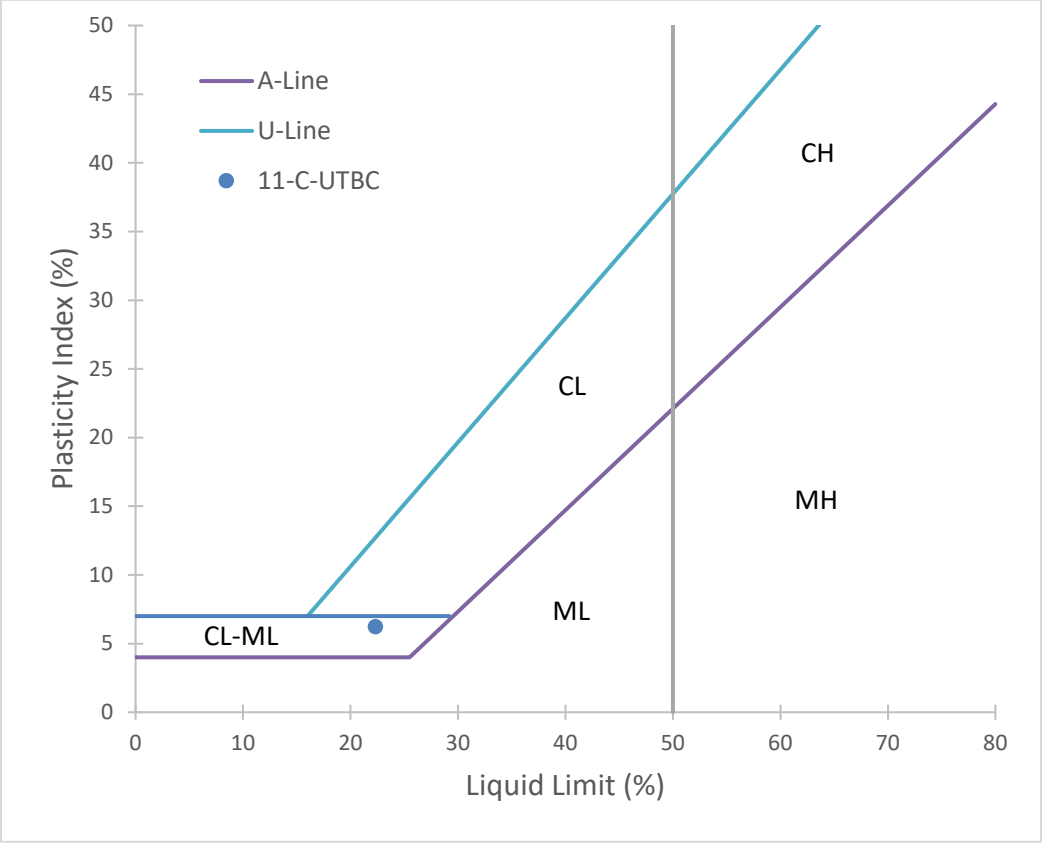

ASTM D4318 Standard Test Methods for Liquid Limit, Plastic Limit, and Plasticity Index of Soils					
Project:	SR-10		Date:	2/11/2019	
Location:	11-C-GB		Personnel:	HB	
	Liquid Limit Determination			Plastic Limit Determination	
Tare No.:	5	2	3	1	11
Tare wt. (g):	26.50	27.09	26.63	21.99	23.15
Wet + tare wt. (g):	51.44	54.47	52.66	29.85	30.48
Dry + tare wt. (g):	46.82	49.58	47.98	28.78	29.51
Water content (%):	22.74	21.74	21.92	15.76	15.25
Blows:	21	35	29		
Log Blows:	1.32	1.54	1.46		
Slope:	-4.62				
Intercept:	28.80				
Liquid Limit:	22				
Plastic Limit:	16				
Plasticity Index:	7				

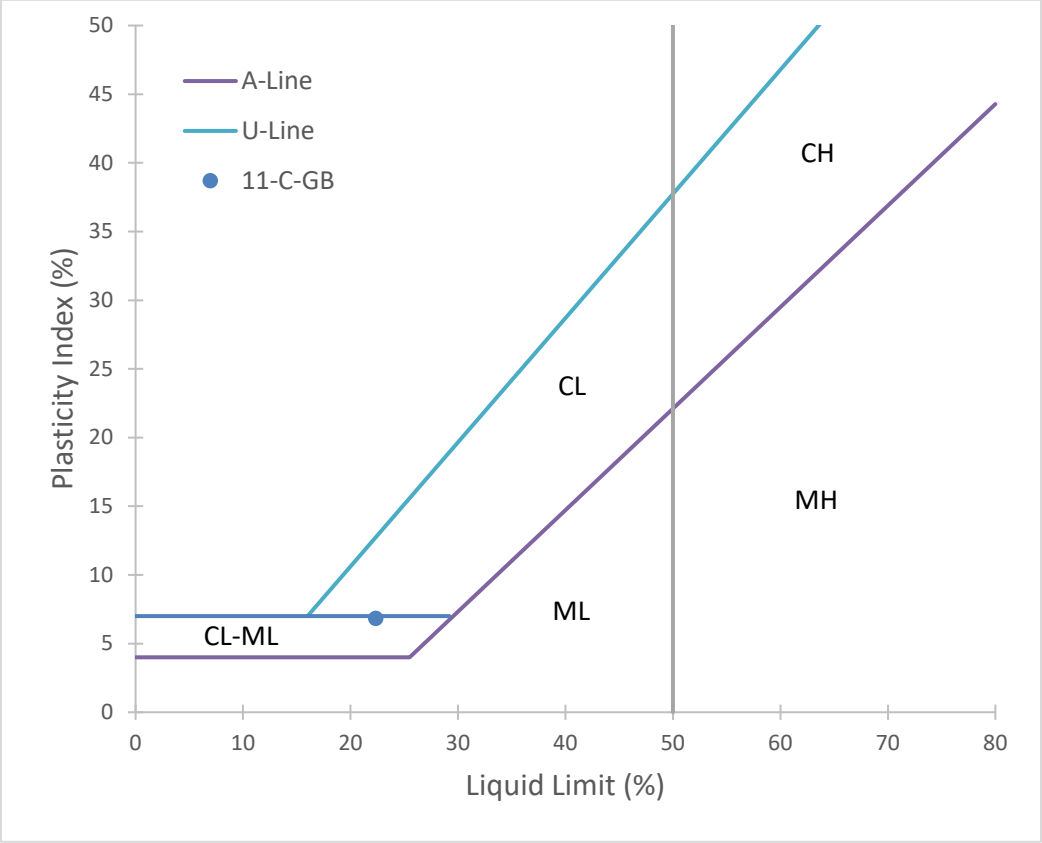

ASTM D4318 Standard Test Methods for Liquid Limit, Plastic Limit, and Plasticity Index of Soils					
Project:	SR-10		Date:	2/11/2019	
Location:	12-C-UTBC		Personnel:	HB	
	Liquid Limit Determination			Plastic Limit Determination	
Tare No.:	1	19	7	3	4
Tare wt. (g):	27.30	22.69	23.10	22.79	22.34
Wet + tare wt. (g):	50.05	47.96	47.79	29.87	28.94
Dry + tare wt. (g):	45.98	43.39	43.22	28.93	28.04
Water content (%):	21.79	22.08	22.71	15.31	15.79
Blows:	26	24	20		
Log Blows:	1.41	1.38	1.30		
Slope:	-8.11				
Intercept:	33.27				
Liquid Limit:	22				
Plastic Limit:	16				
Plasticity Index:	6				

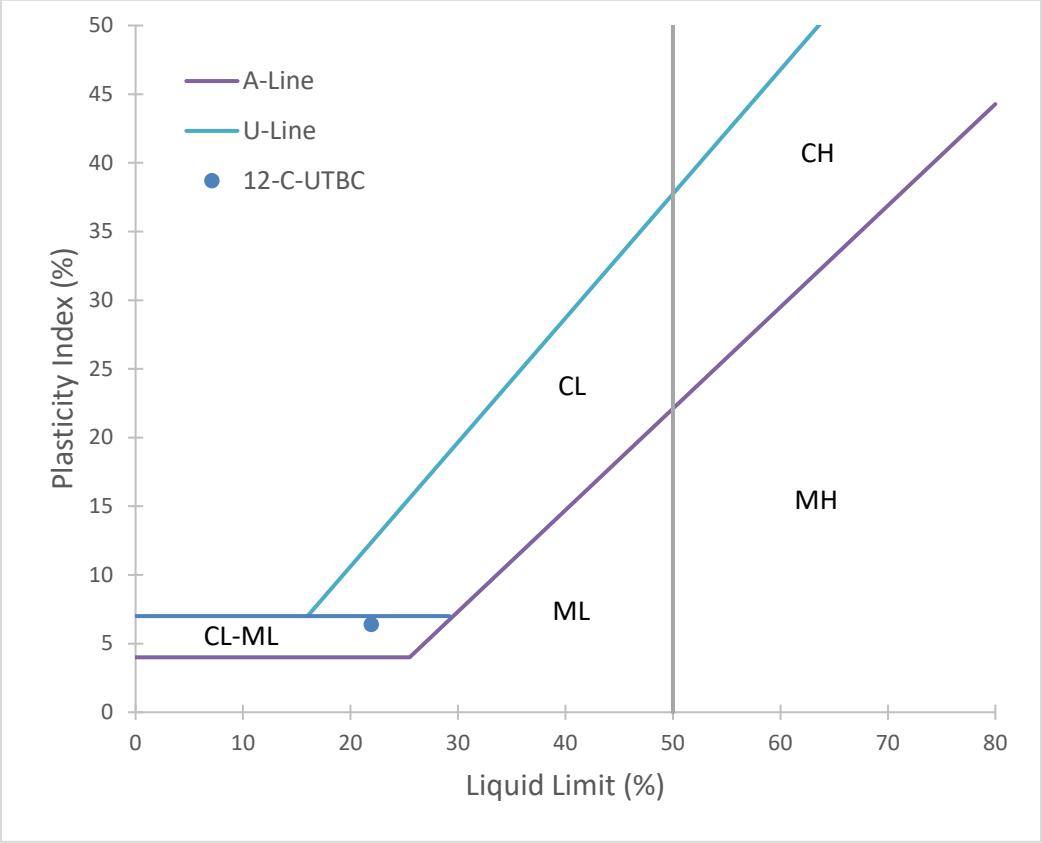

ASTM D4318 Standard Test Methods for Liquid Limit, Plastic Limit, and Plasticity Index of Soils					
Project:	SR-10		Date:	3/28/2019	
Location:	12-C-GB		Personnel:	HB	
	Liquid Limit Determination			Plastic Limit Determination	
Tare No.:	17	5	4	1	11
Tare wt. (g):	22.84	20.40	27.82	27.31	22.98
Wet + tare wt. (g):	32.54	31.23	38.48	33.61	29.84
Dry + tare wt. (g):	30.43	28.72	36.05	32.66	28.78
Water content (%):	27.80	30.17	29.53	17.76	18.28
Blows:	35	21	17		
Log Blows:	1.54	1.32	1.23		
Slope:	-6.46				
Intercept:	37.99				
Liquid Limit:	29				
Plastic Limit:	18				
Plasticity Index:	11				

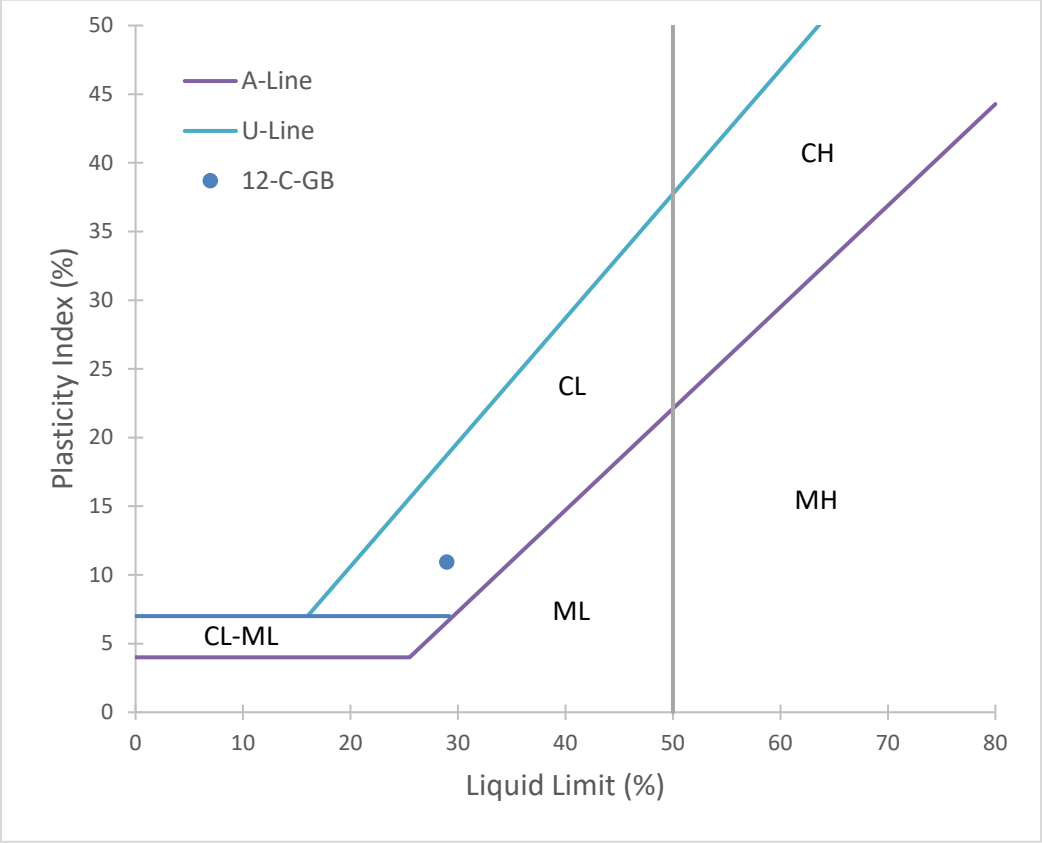

ASTM D4318 Standard Test Methods for Liquid Limit, Plastic Limit, and Plasticity Index of Soils					
Project:	SR-10		Date:	3/16/2019	
Location:	13-C-UTBC		Personnel:	HB	
	Liquid Limit Determination			Plastic Limit Determination	
Tare No.:	3	9	19	4	1
Tare wt. (g):	22.79	26.17	22.65	22.37	26.31
Wet + tare wt. (g):	39.85	43.03	42.23	28.16	33.49
Dry + tare wt. (g):	36.85	40.04	38.63	27.42	32.72
Water content (%):	21.34	21.56	22.53	14.65	12.01
Blows:	29	27	16		
Log Blows:	1.46	1.43	1.20		
Slope:	-4.48				
Intercept:	27.93				
Liquid Limit:	22				
Plastic Limit:	13				
Plasticity Index:	8				

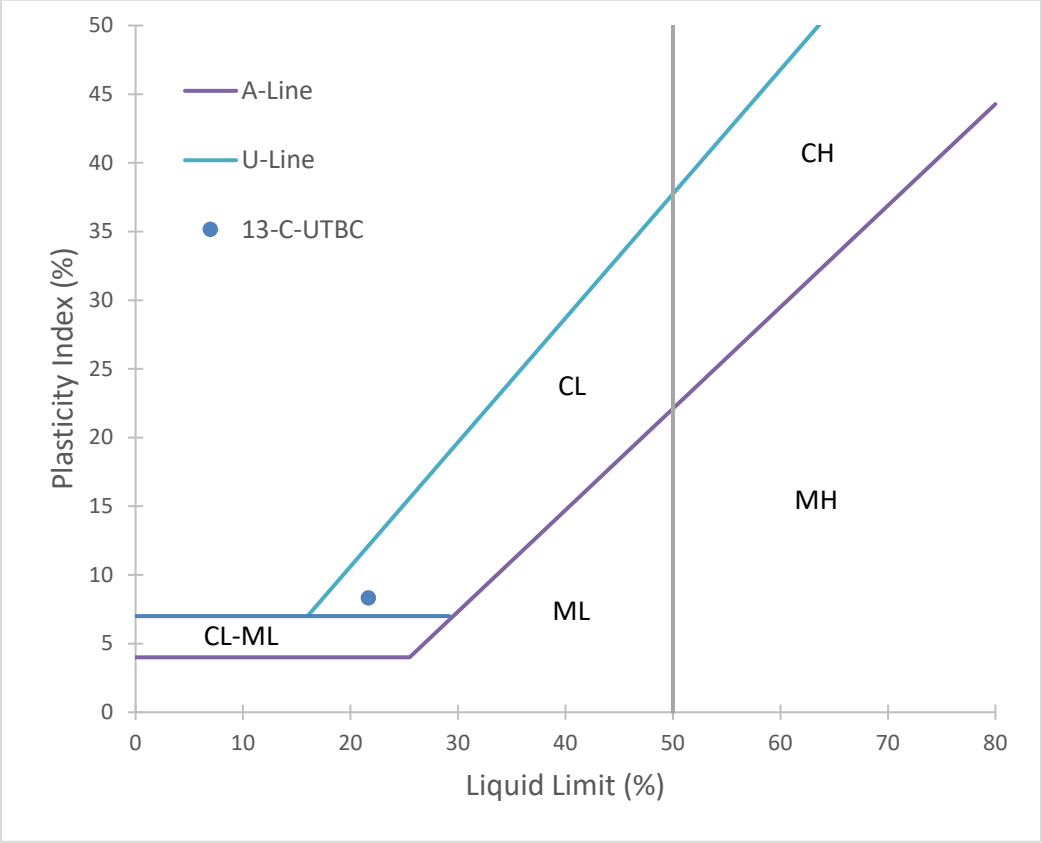

ASTM D4318 Standard Test Methods for Liquid Limit, Plastic Limit, and Plasticity Index of Soils					
Project:	SR-10		Date:	2/11/2019	
Location:	13-C-GB		Personnel:	HB	
	Liquid Limit Determination			Plastic Limit Determination	
Tare No.:	7	16	5	2	24
Tare wt. (g):	25.84	23.15	28.13	22.61	21.63
Wet + tare wt. (g):	48.58	43.71	51.71	31.5	29.59
Dry + tare wt. (g):	44.74	40.40	47.85	30.2	28.49
Water content (%):	20.32	19.19	19.57	17.13	16.03
Blows:	15	33	25		
Log Blows:	1.18	1.52	1.40		
Slope:	-3.30				
Intercept:	24.20				
Liquid Limit:	20				
Plastic Limit:	17				
Plasticity Index:	3				

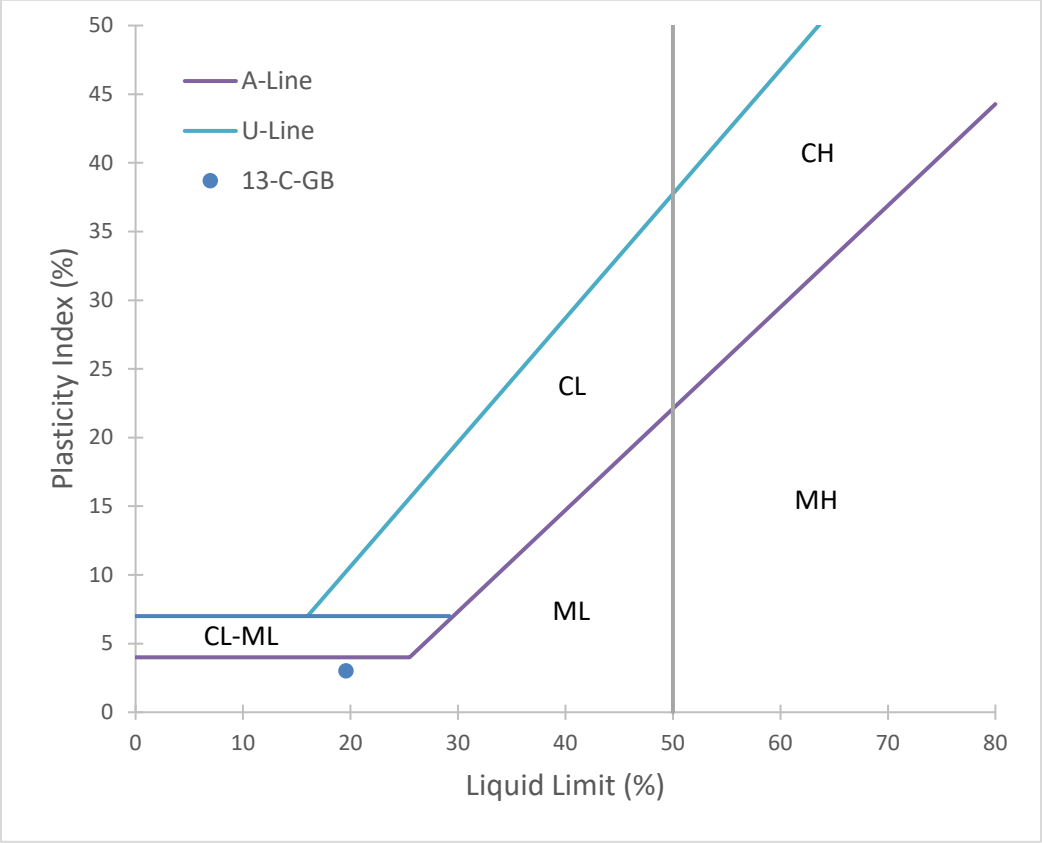

ASTM D4318 Standard Test Methods for Liquid Limit, Plastic Limit, and Plasticity Index of Soils					
Project:	SR-10		Date:	2/11/2019	
Location:	14-C-UTBC		Personnel:	HB	
	Liquid Limit Determination			Plastic Limit Determination	
Tare No.:	1	2	3	4	5
Tare wt. (g):	19.89	31.37	34.46	33.86	32.10
Wet + tare wt. (g):	40.62	56.53	64.71	41.72	39.88
Dry + tare wt. (g):	37.11	52.31	59.46	40.57	38.78
Water content (%):	20.38	20.15	21.00	17.14	16.47
Blows:	22	31	17		
Log Blows:	1.34	1.49	1.23		
Slope:	-3.16				
Intercept:	24.79				
Liquid Limit:	20				
Plastic Limit:	17				
Plasticity Index:	4				

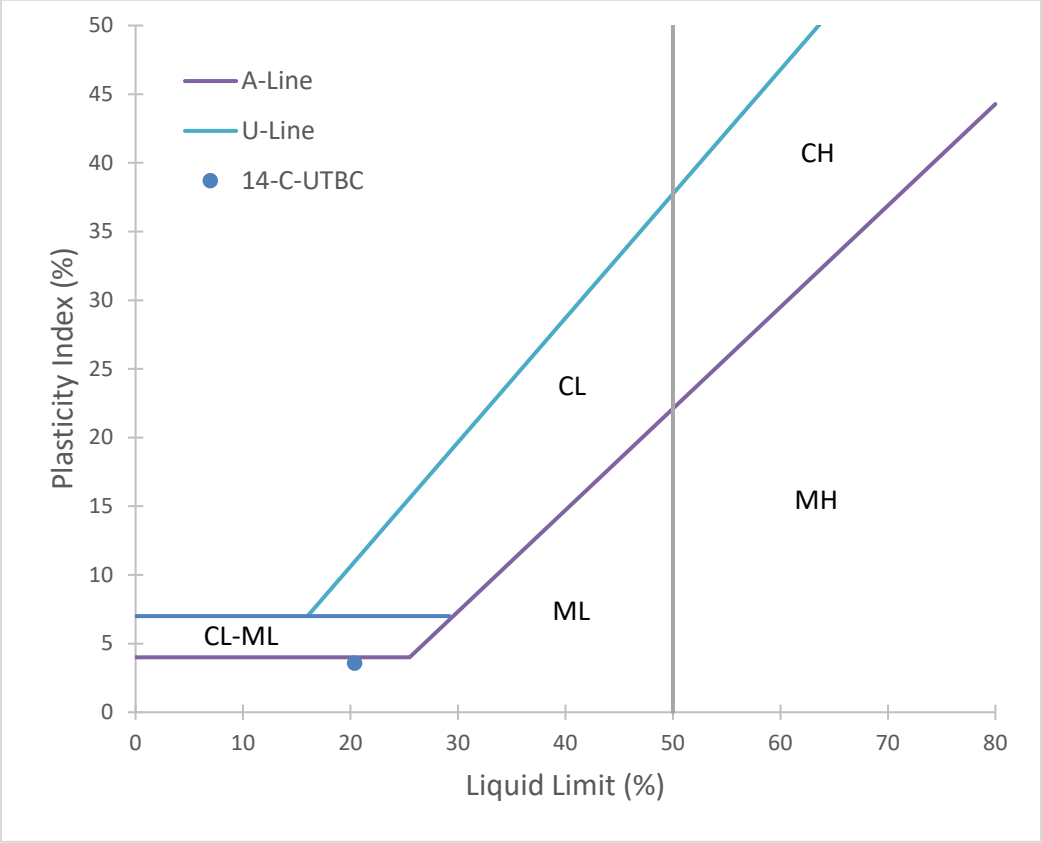

ASTM D4318 Standard Test Methods for Liquid Limit, Plastic Limit, and Plasticity Index of Soils					
Project:	SR-10		Date:	2/11/2019	
Location:	14-C-GB		Personnel:	HB	
	Liquid Limit Determination			Plastic Limit Determination	
Tare No.:	2	13	12	4	3
Tare wt. (g):	27.87	26.42	23.23	30.98	26.78
Wet + tare wt. (g):	54.74	53.15	53.06	38.21	34.47
Dry + tare wt. (g):	49.96	48.20	47.38	37.61	33.81
Water content (%):	21.64	22.73	23.52	9.05	9.39
Blows:	34	27	17		
Log Blows:	1.53	1.43	1.23		
Slope:	-5.92				
Intercept:	30.90				
Liquid Limit:	23				
Plastic Limit:	9				
Plasticity Index:	13				

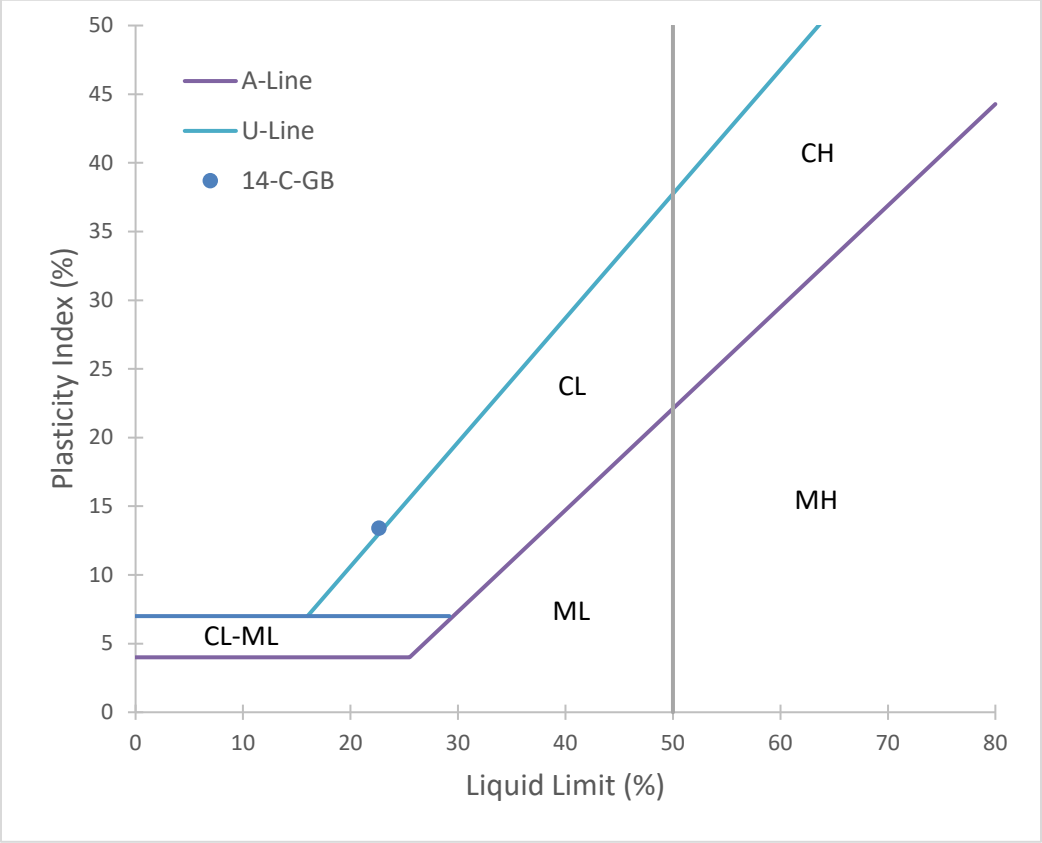

Fall Cone Test to Determine Liquid and Plastic Limits					
Sample Location:	1-A-UTBC				
Cup #:	1	2	3	4	
Penetration (mm):	16.87	19.64	22.41	25.37	
Cup weight (g):	26.40	23.29	24.99	22.96	
Wet weight (g):	37.43	42.78	44.93	37.84	
Dry weight (g):	35.76	39.80	41.77	35.41	
Water content (%):	17.84	18.05	18.83	19.52	
Liquid Limit:	18				
Plastic Limit:	11				
Plasticity Index:	7				

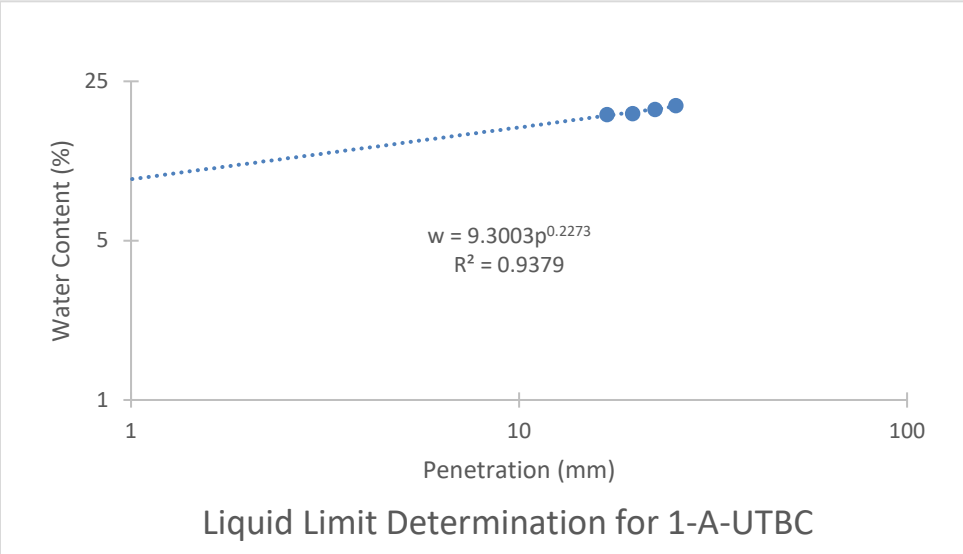

Liquid Limit Determination for 1-A-UTBC

Fall Cone Test to Determine Liquid and Plastic Limits					
Sample Location:	1-A-GB				
Cup #:		1	2	3	4
Penetration (mm):		11.99	17.09	24.83	30.13
Cup weight (g):		27.92	27.87	22.87	26.74
Wet weight (g):		39.14	44.95	43.59	44.53
Dry weight (g):		37.56	42.34	40.20	41.46
Water content (%):		16.39	18.04	19.56	20.86
Liquid Limit:	19				
Plastic Limit:	10				
Plasticity Index:	8				

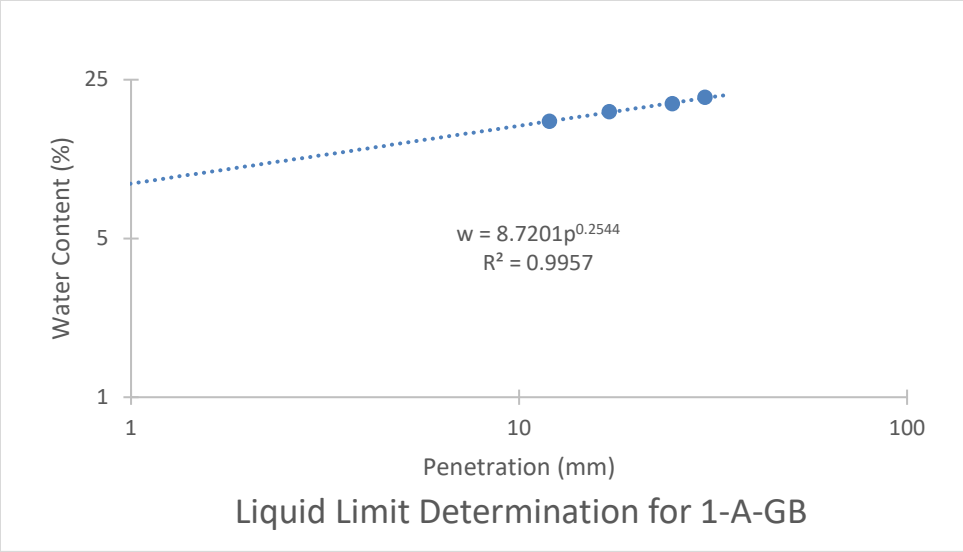

Fall Cone Test to Determine Liquid and Plastic Limits					
Date:	11/6/2018				
Sample Location:	2-C-UTBC				
Cup #:		1	2	3	4
Penetration (mm):		16.01	21.31	24.86	28.14
Cup weight (g):		27.91	27.86	22.85	26.73
Wet weight (g):		49.61	57.56	55.75	58.25
Dry weight (g):		46.42	52.94	50.48	52.99
Water content (%):		17.23	18.42	19.07	20.03

Liquid Limit:	18
Plastic Limit:	10
Plasticity Index:	8

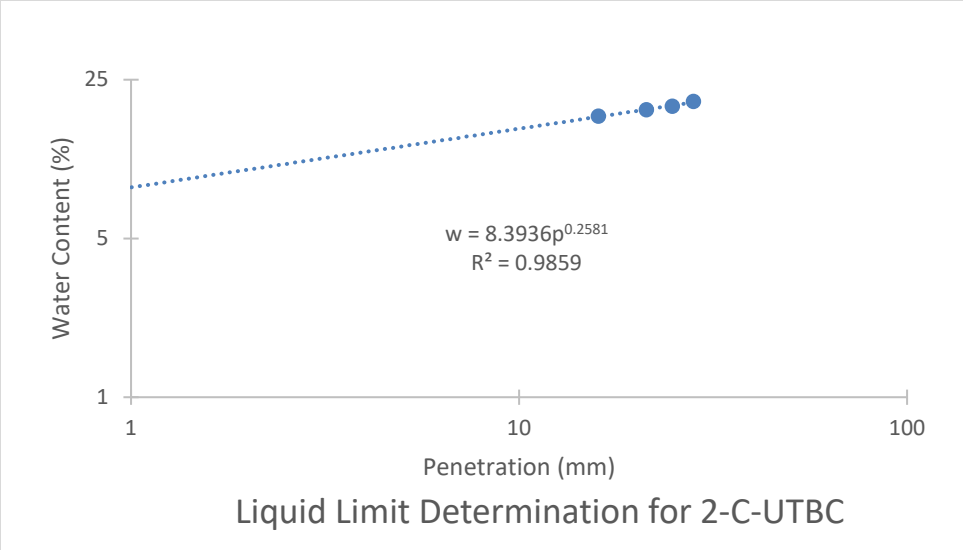

Fall Cone Test to Determine Liquid and Plastic Limits					
Date:	11/6/2018				
Sample Location:	2-C-GB				
Cup #:		1	2	3	4
Penetration (mm):		16.39	22.17	25.37	28.36
Cup weight (g):		26.41	23.30	25.02	22.96
Wet weight (g):		46.21	51.37	50.62	50.11
Dry weight (g):		43.15	46.77	46.28	45.34
Water content (%):		18.28	19.60	20.41	21.31
Liquid Limit:	19				
Plastic Limit:	10				
Plasticity Index:	9				

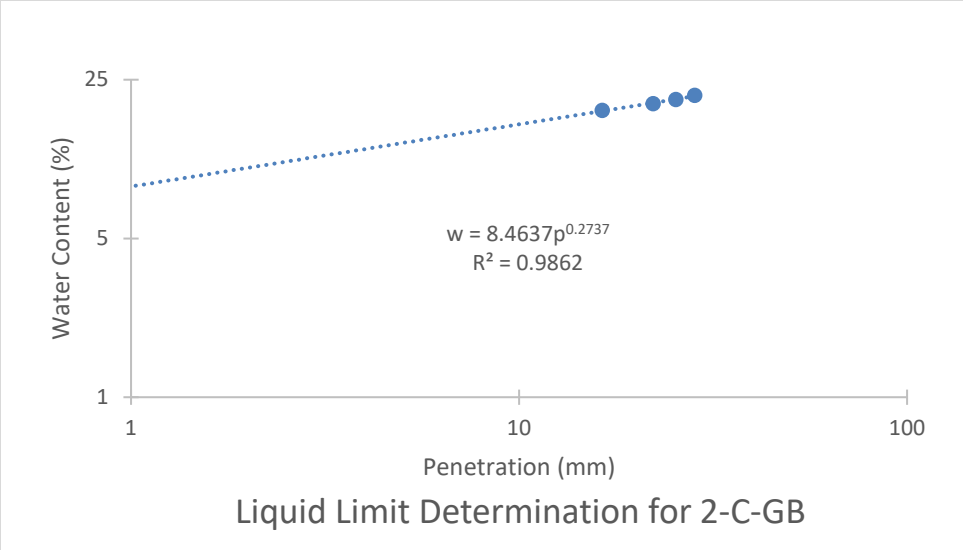

Fall Cone Test to Determine Liquid and Plastic Limits					
Sample Location:	3-C-UTBC				
Cup #:		1	2	3	4
Penetration (mm):		16.81	19.77	20.60	24.62
Cup weight (g):		28.53	26.85	22.55	27.70
Wet weight (g):		48.25	45.75	41.95	47.60
Dry weight (g):		45.40	42.88	38.96	44.46
Water content (%):		16.89	17.90	18.22	18.74
Liquid Limit:	18				
Plastic Limit:	10				
Plasticity Index:	8				

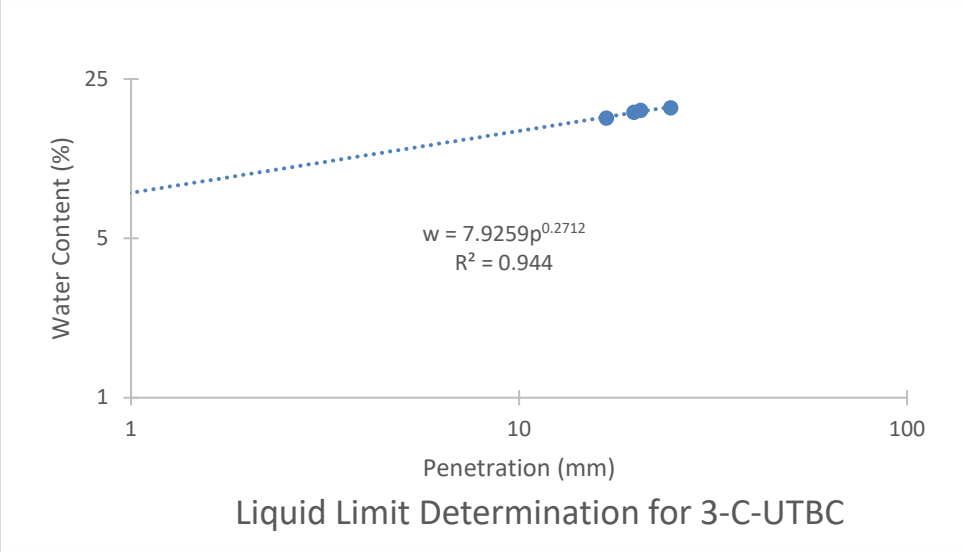

Fall Cone Test to Determine Liquid and Plastic Limits		
Sample Location:	3-C-GB	
Cup #:	1 2 3 4	
Penetration (mm):	Not enough sample to generate 4 specimens	
Cup weight (g):		
Wet weight (g):		
Dry weight (g):		
Water content (%):		
Liquid Limit:		
Plastic Limit:		
Plasticity Index:	0.00	

Fall Cone Test to Determine Liquid and Plastic Limits					
Date:	11/6/2018				
Sample Location:	4-C-UTBC				
Cup #:		1	2	3	4
Penetration (mm):		18.49	21.39	25.15	27.64
Cup weight (g):		28.54	26.87	22.59	27.84
Wet weight (g):		53.59	56.95	54.76	58.91
Dry weight (g):		49.75	52.23	49.56	53.73
Water content (%):		18.10	18.61	19.28	20.01
Liquid Limit:	18				
Plastic Limit:	11				
Plasticity Index:	8				

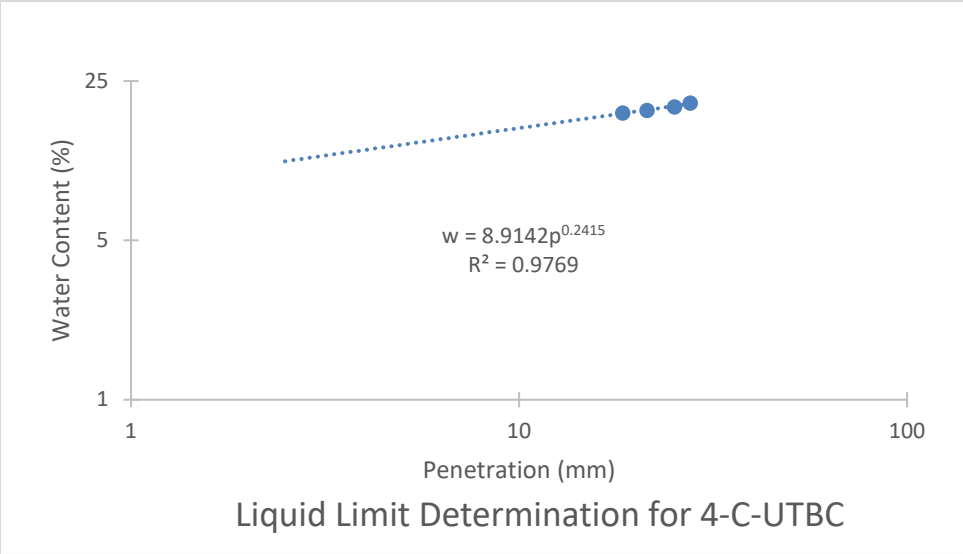

Fall Cone Test to Determine Liquid and Plastic Limits				
Date:	11/6/2018			
Sample Location:	4-C-GB			
Cup #:	1	2	3	Only enough soil for 3 specimens
Penetration (mm):	16.91	21.63	27.74	
Cup weight (g):	22.29	25.83	22.31	
Wet weight (g):	40.87	43.78	36.79	
Dry weight (g):	38.06	40.92	34.29	
Water content (%):	17.82	18.95	20.87	

Liquid Limit:	19
Plastic Limit:	9
Plasticity Index:	10

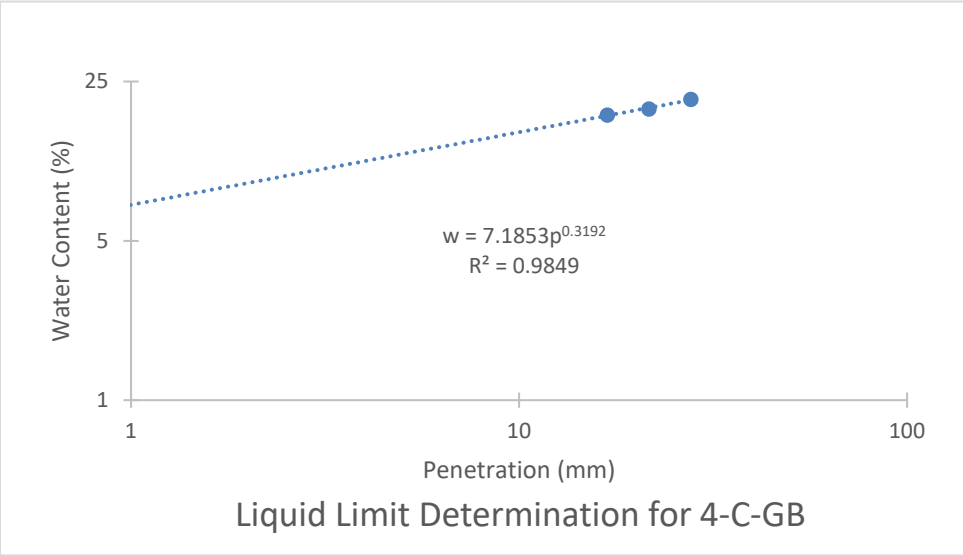

Fall Cone Test to Determine Liquid and Plastic Limits					
Sample Location:	5-C-UTBC				
Cup #:		1	2	3	4
Penetration (mm):		19.46	20.67	21.12	25.39
Cup weight (g):		27.87	27.84	22.85	26.71
Wet weight (g):		49.00	49.26	52.32	50.98
Dry weight (g):		45.78	45.97	47.77	47.06
Water content (%):		17.98	18.15	18.26	19.26
Liquid Limit:	18				
Plastic Limit:	10				
Plasticity Index:	8				

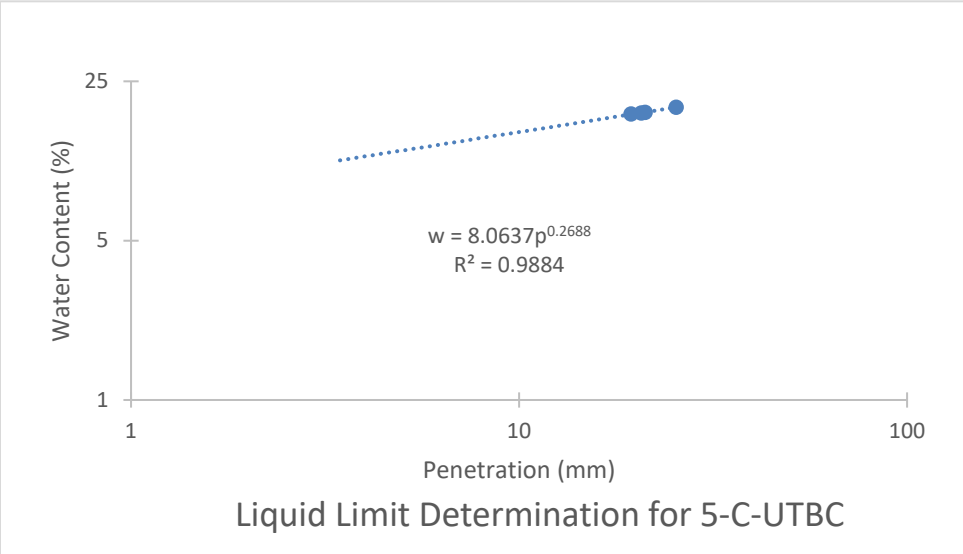

Fall Cone Test to Determine Liquid and Plastic Limits					
Date:	11/5/2018				
Sample Location:	5-C-GB				
Cup #:		1	2	3	4
Penetration (mm):		19.57	22.71	25.42	28.51
Cup weight (g):		27.90	27.84	22.83	26.72
Wet weight (g):		54.47	66.99	56.51	66.17
Dry weight (g):		50.30	60.67	50.89	59.39
Water content (%):		18.62	19.25	20.03	20.75
Liquid Limit:	19				
Plastic Limit:	10				
Plasticity Index:	9				

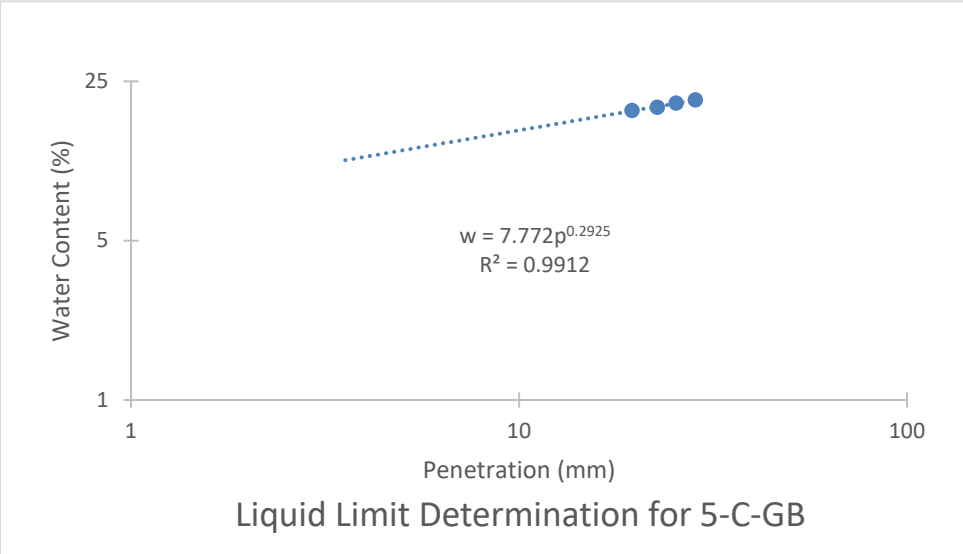

Fall Cone Test to Determine Liquid and Plastic Limits				
Sample Location:	6-C-UTBC			
Cup #:	1	2	3	4
Penetration (mm):	16.04	19.60	21.69	24.18
Cup weight (g):	28.56	26.83	22.52	27.71
Wet weight (g):	51.19	56.86	49.36	53.80
Dry weight (g):	47.71	51.94	44.92	49.39
Water content (%):	18.17	19.59	19.82	20.34

Liquid Limit:	19
Plastic Limit:	10
Plasticity Index:	9

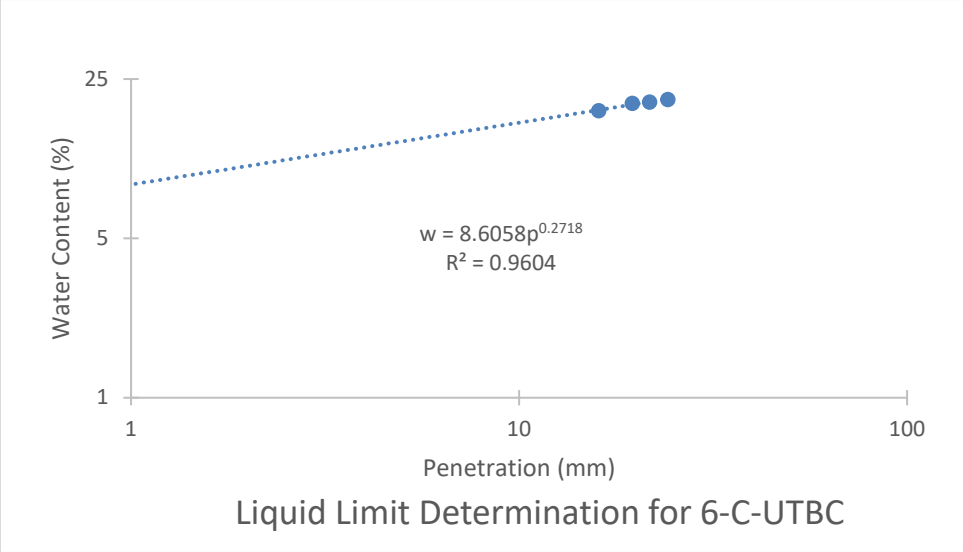

Fall Cone Test to Determine Liquid and Plastic Limits					
Sample Location:	6-C-GB				
Cup #:	1	2	3	4	
Penetration (mm):	22.53	20.39	19.66	18.98	
Cup weight (g):	26.31	26.01	23.01	22.16	
Wet weight (g):	46.94	61.73	46.03	50.42	
Dry weight (g):	43.24	55.43	41.98	45.52	
Water content (%):	21.85	21.41	21.35	20.98	

Liquid Limit:	21
Plastic Limit:	13
Plasticity Index:	8

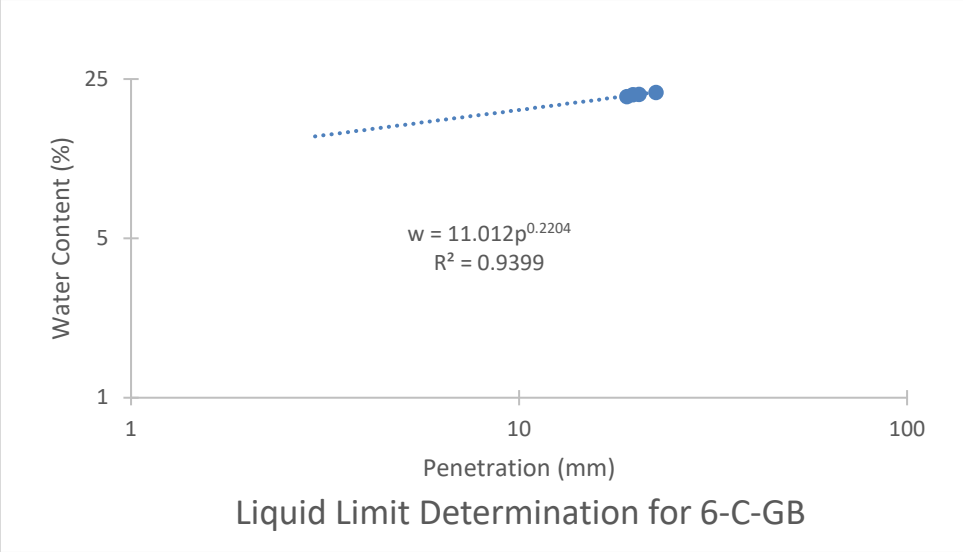

Fall Cone Test to Determine Liquid and Plastic Limits					
Sample Location:	7-C-UTBC				
Cup #:		1	2	3	4
Penetration (mm):		17.88	19.02	22.26	25.00
Cup weight (g):		26.07	24.48	23.04	23.10
Wet weight (g):		54.15	51.47	53.64	57.91
Dry weight (g):		50.03	47.35	48.88	52.32
Water content (%):		17.20	18.01	18.42	19.13
Liquid Limit:	18				
Plastic Limit:	9				
Plasticity Index:	9				

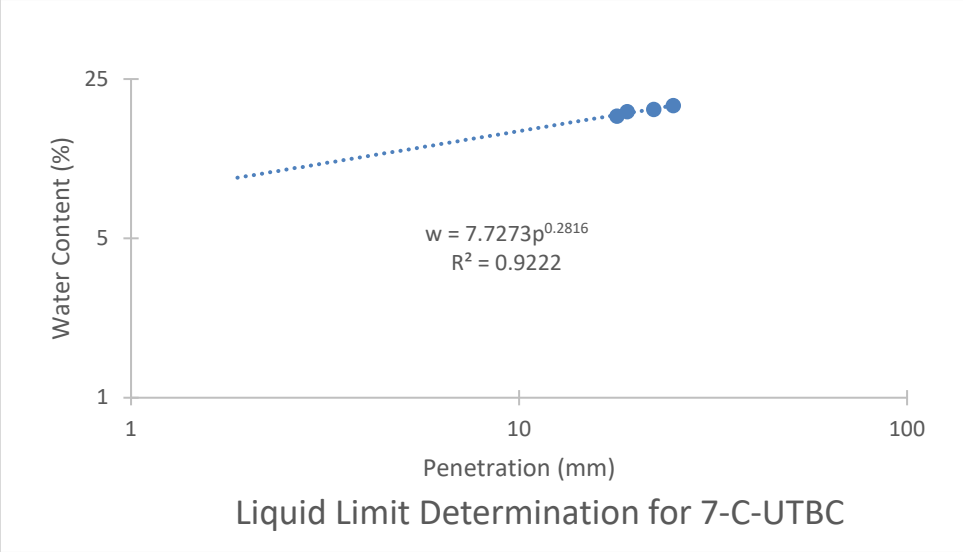

Fall Cone Test to Determine Liquid and Plastic Limits					
Sample Location:	7-C-GB				
Cup #:		1	2	3	4
Penetration (mm):		20.28	23.02	26.58	29.91
Cup weight (g):		28.56	26.89	22.61	27.86
Wet weight (g):		44.13	43.77	39.32	48.13
Dry weight (g):		41.68	41.02	36.50	44.63
Water content (%):		18.67	19.46	20.30	20.87
Liquid Limit:	19				
Plastic Limit:	10				
Plasticity Index:	9				

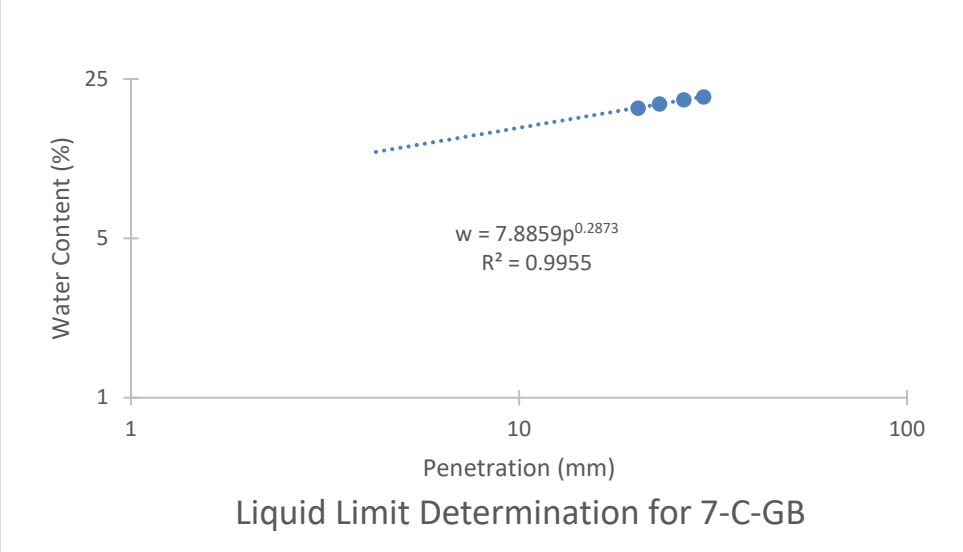

Fall Cone Test to Determine Liquid and Plastic Limits					
Sample Location:	8-C-UTBC				
Cup #:		1	2	3	4
Penetration (mm):		16.91	20.97	21.83	23.38
Cup weight (g):		26.42	23.30	25.03	22.84
Wet weight (g):		51.99	46.21	55.79	52.24
Dry weight (g):		48.05	42.57	50.85	47.45
Water content (%):		18.22	18.89	19.13	19.46
Liquid Limit:	19				
Plastic Limit:	12				
Plasticity Index:	7				

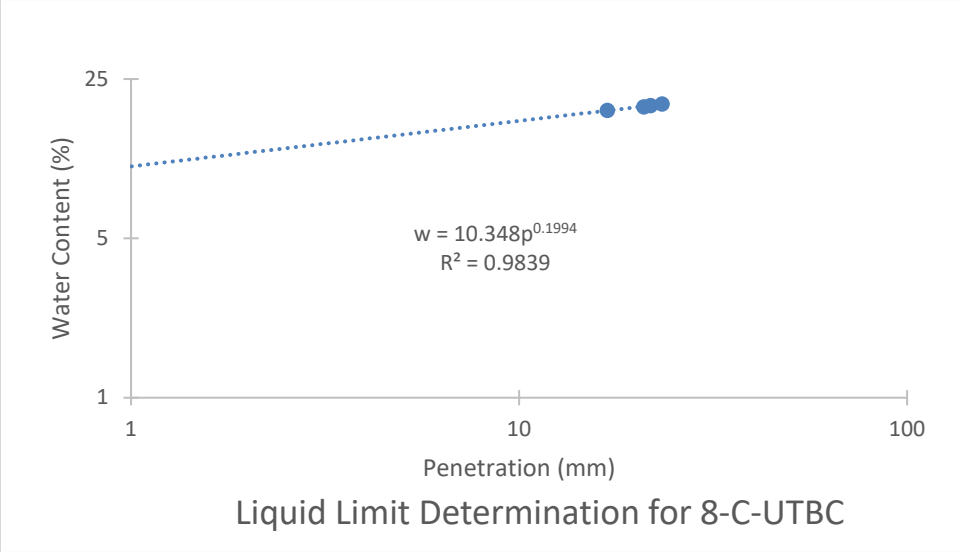

Fall Cone Test to Determine Liquid and Plastic Limits					
Sample Location:	8-C-GB				
Cup #:		1	2	3	4
Penetration (mm):		15.85	17.05	21.45	21.79
Cup weight (g):		26.08	24.52	23.05	23.12
Wet weight (g):		48.70	49.30	51.26	50.21
Dry weight (g):		45.36	45.52	46.85	45.94
Water content (%):		17.32	18.00	18.53	18.71
Liquid Limit:	18				
Plastic Limit:	11				
Plasticity Index:	7				

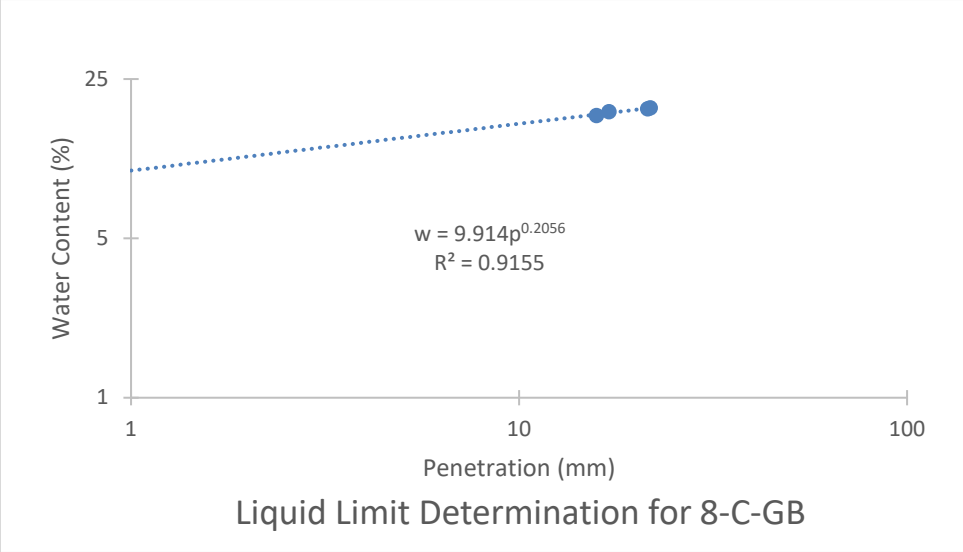

Fall Cone Test to Determine Liquid and Plastic Limits					
Date:	11/6/2018				
Sample Location:	9-C-UTBC				
Cup #:		1	2	3	4
Penetration (mm):		20.83	24.23	28.97	33.01
Cup weight (g):		26.09	24.49	23.07	23.17
Wet weight (g):		49.80	56.31	58.64	56.36
Dry weight (g):		46.21	51.18	52.73	50.59
Water content (%):		17.84	19.22	19.93	21.04
Liquid Limit:	18				
Plastic Limit:	8				
Plasticity Index:	10				

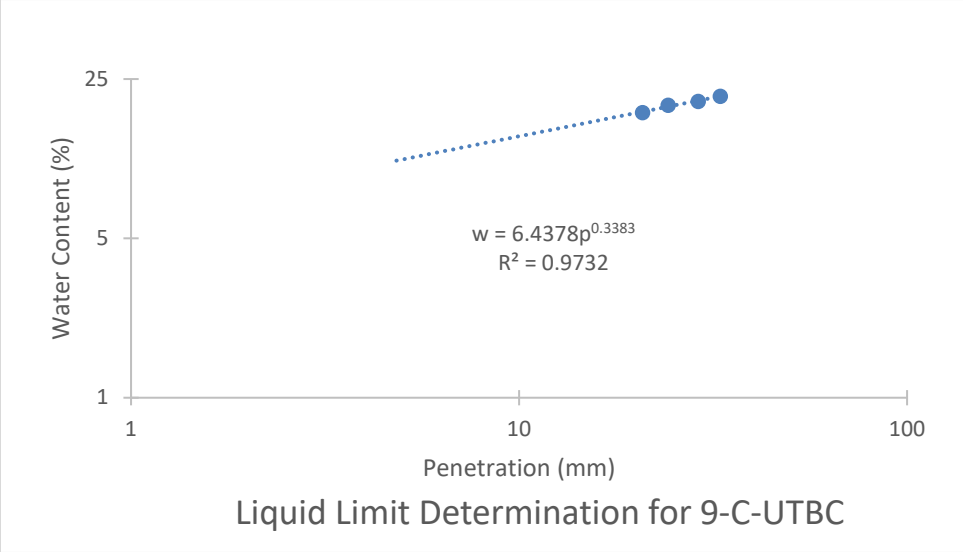

Fall Cone Test to Determine Liquid and Plastic Limits				
Date:	11/5/2018			
Sample Location:	9-C-GB			
Cup #:	1	2	3	4
Penetration (mm):	17.41	20.75	23.55	29.85
Cup weight (g):	26.41	23.30	25.00	22.96
Wet weight (g):	45.43	44.11	52.36	55.35
Dry weight (g):	42.68	40.94	48.04	50.03
Water content (%):	16.90	17.97	18.75	19.65

Liquid Limit:	18
Plastic Limit:	9
Plasticity Index:	8

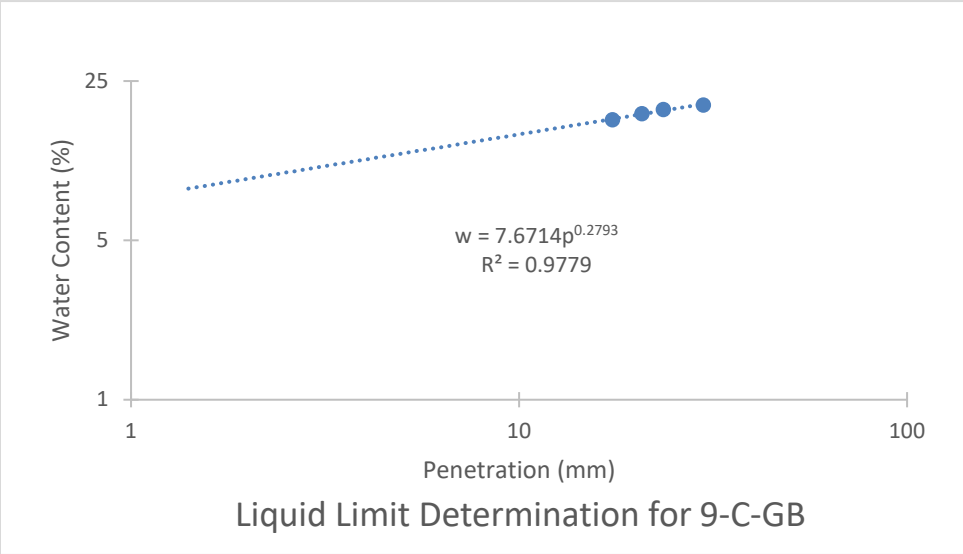

Fall Cone Test to Determine Liquid and Plastic Limits				
Date:	11/5/2018			
Sample Location:	10-C-UTBC			
Cup #:	1	2	3	4
Penetration (mm):	19.24	20.49	24.21	26.47
Cup weight (g):	28.56	26.86	22.55	27.70
Wet weight (g):	47.40	50.46	47.70	52.38
Dry weight (g):	44.42	46.65	43.53	48.16
Water content (%):	18.79	19.25	19.88	20.63

Liquid Limit:	19
Plastic Limit:	10
Plasticity Index:	9

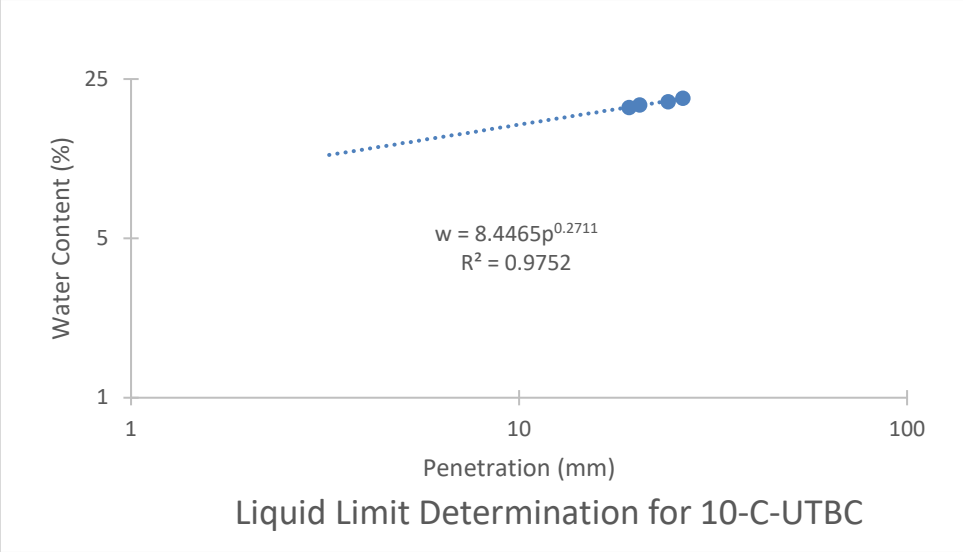

Fall Cone Test to Determine Liquid and Plastic Limits				
Date:	11/5/2018			
Sample Location:	10-C-GB			
Cup #:	1	2	3	4
Penetration (mm):	12.32	16.19	20.70	21.78
Cup weight (g):	26.37	26.01	23.01	22.19
Wet weight (g):	42.34	50.71	54.19	57.32
Dry weight (g):	40.15	47.06	49.36	51.64
Water content (%):	15.89	17.34	18.33	19.29

Liquid Limit:	18
Plastic Limit:	9
Plasticity Index:	9

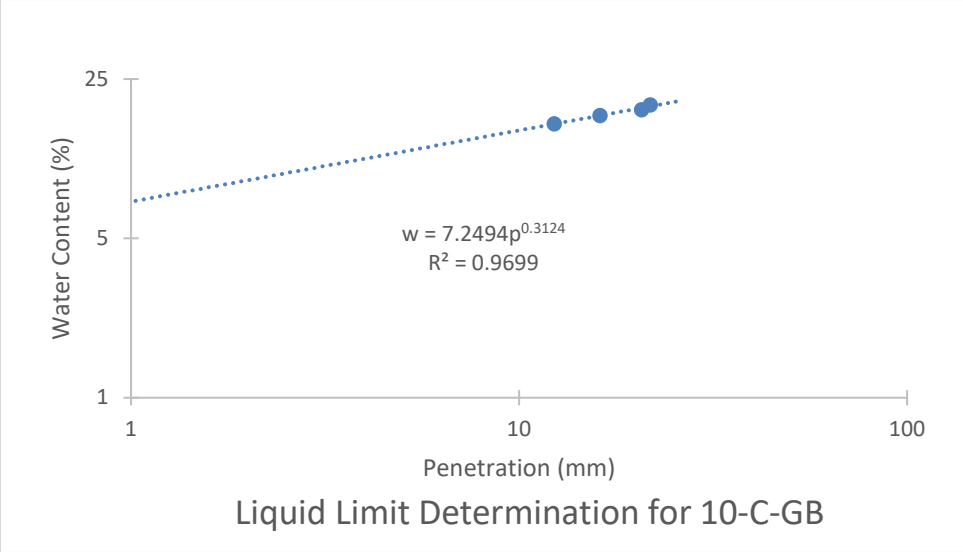

Fall Cone Test to Determine Liquid and Plastic Limits				
Date:	11/5/2018			
Sample Location:	11-C-UTBC			
Cup #:	1	2	3	4
Penetration (mm):	16.01	19.55	22.86	26.35
Cup weight (g):	22.30	25.83	22.28	21.39
Wet weight (g):	38.97	52.80	45.85	51.70
Dry weight (g):	36.49	48.56	42.05	46.67
Water content (%):	17.48	18.65	19.22	19.90

Liquid Limit:	19
Plastic Limit:	10
Plasticity Index:	8

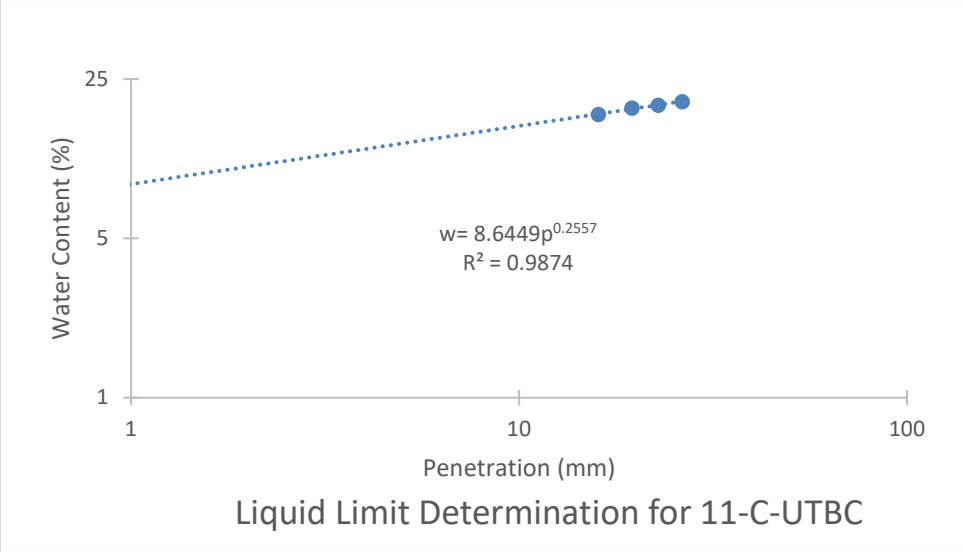

Fall Cone Test to Determine Liquid and Plastic Limits				
Date:	11/7/2018			
Sample Location:	11-C-GB			
Cup #:	1	2	3	4
Penetration (mm):	19.18	22.70	24.25	26.27
Cup weight (g):	26.12	24.50	23.09	23.17
Wet weight (g):	46.04	45.09	42.52	41.50
Dry weight (g):	43.00	41.82	39.36	38.44
Water content (%):	18.01	18.88	19.42	20.04

Liquid Limit:	18
Plastic Limit:	8
Plasticity Index:	10

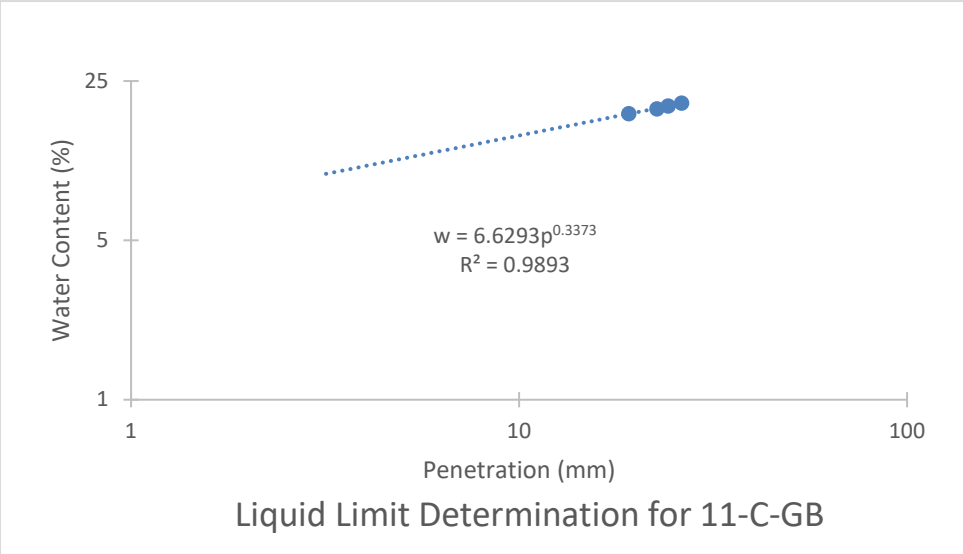

Fall Cone Test to Determine Liquid and Plastic Limits				
Sample Location:	12-C-UTBC			
Cup #:	1	2	3	4
Penetration (mm):	16.90	22.52	19.62	22.74
Cup weight (g):	22.32	25.83	22.28	21.37
Wet weight (g):	58.63	53.05	55.89	61.96
Dry weight (g):	53.31	48.87	50.75	55.63
Water content (%):	17.17	18.14	18.05	18.48

Liquid Limit:	18
Plastic Limit:	11
Plasticity Index:	7

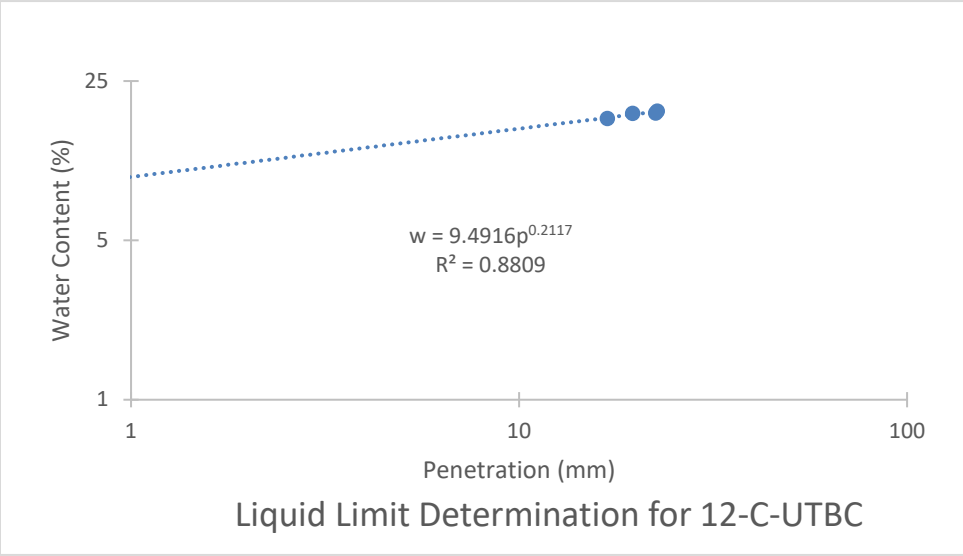

Fall Cone Test to Determine Liquid and Plastic Limits					
Sample Location:	12-C-GB				
Cup #:		1	2	3	4
Penetration (mm):		17.78	19.86	20.72	22.25
Cup weight (g):		26.33	26.01	23.00	22.18
Wet weight (g):		45.75	44.05	44.02	45.89
Dry weight (g):		42.89	41.31	40.80	42.21
Water content (%):		17.27	17.91	18.09	18.37
Liquid Limit:	18				
Plastic Limit:	9				
Plasticity Index:	8				

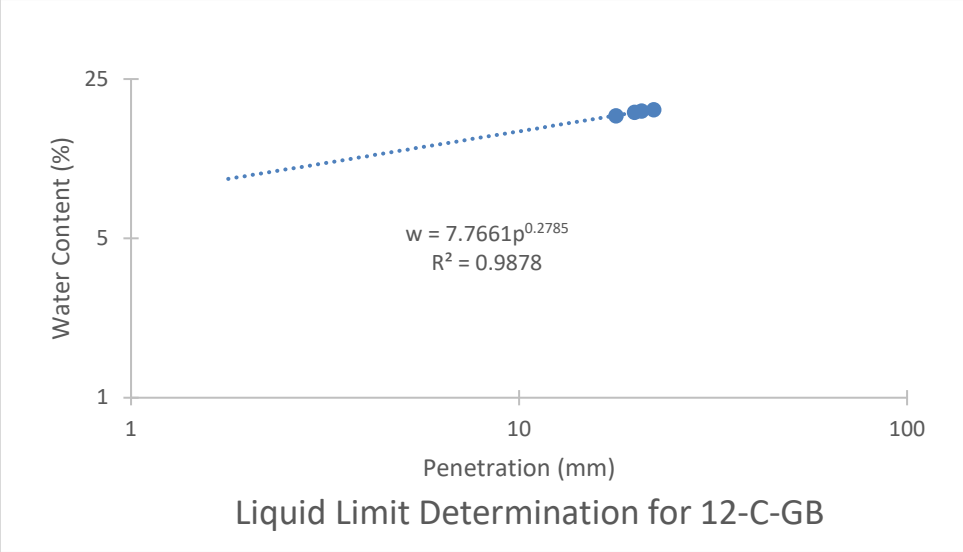

Fall Cone Test to Determine Liquid and Plastic Limits				
Sample Location:	13-C-UTBC			
Cup #:	1	2	3	4
Penetration (mm):	17.16	18.59	21.43	25.98
Cup weight (g):	27.87	27.85	22.85	26.71
Wet weight (g):	60.01	56.72	55.67	55.02
Dry weight (g):	55.06	52.19	50.38	50.32
Water content (%):	18.21	18.61	19.22	19.91

Liquid Limit:	19
Plastic Limit:	12
Plasticity Index:	7

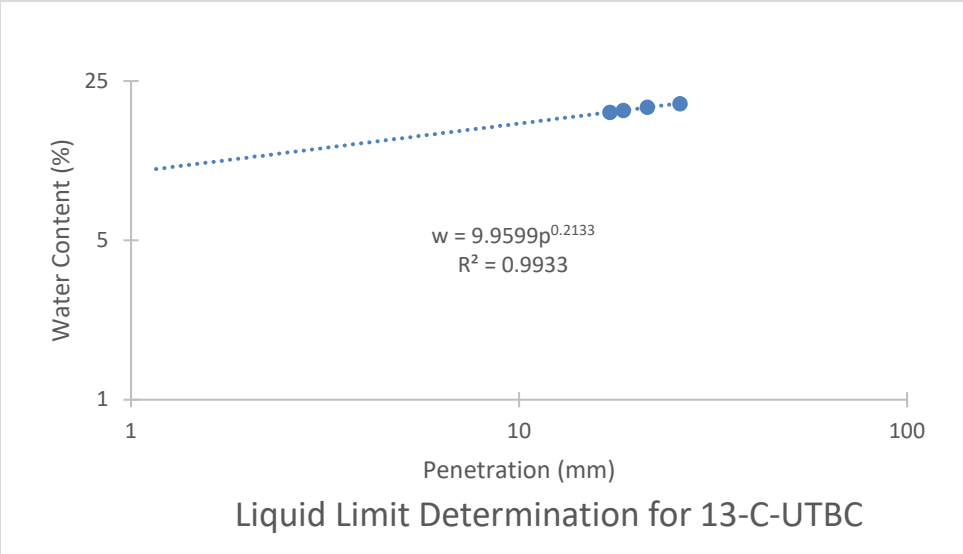

Fall Cone Test to Determine Liquid and Plastic Limits				
Date:	11/5/2018			
Sample Location:	13-C-GB			
Cup #:	1	2	3	4
Penetration (mm):	23.49	28.03	31.97	33.89
Cup weight (g):	26.08	24.47	23.05	23.13
Wet weight (g):	45.63	51.50	47.38	47.10
Dry weight (g):	42.59	47.16	43.35	43.04
Water content (%):	18.41	19.13	19.85	20.39

Liquid Limit:	18
Plastic Limit:	9
Plasticity Index:	8

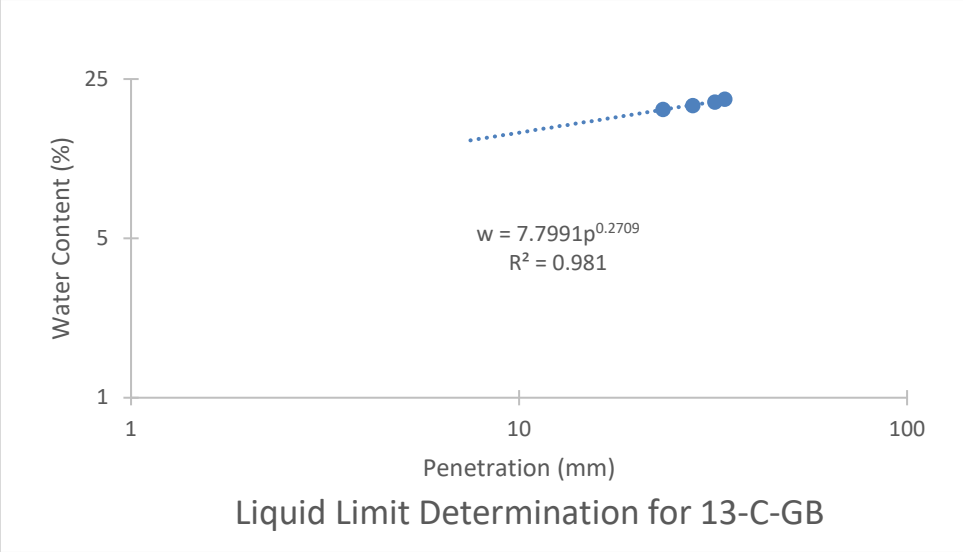

Fall Cone Test to Determine Liquid and Plastic Limits				
Date:	11/7/2018			
Sample Location:	14-C-UTBC			
Cup #:	1	2	3	4
Penetration (mm):	15.75	22.07	25.01	28.19
Cup weight (g):	26.41	23.31	25.04	22.98
Wet weight (g):	43.72	41.52	45.03	42.94
Dry weight (g):	41.19	38.71	41.83	39.63
Water content (%):	17.12	18.25	19.06	19.88

Liquid Limit:	18
Plastic Limit:	10
Plasticity Index:	8

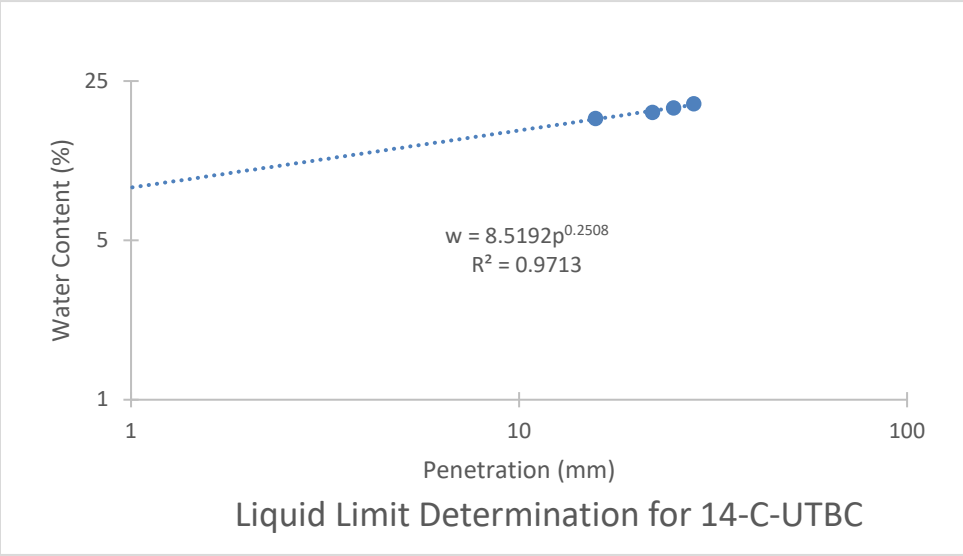

Fall Cone Test to Determine Liquid and Plastic Limits				
Date:	11/6/2018			
Sample Location:	14-C-GB			
Cup #:	1	2	3	4
Penetration (mm):	20.21	24.66	24.69	29.96
Cup weight (g):	26.37	26.02	23.04	22.27
Wet weight (g):	47.59	53.59	49.89	51.09
Dry weight (g):	44.23	49.06	45.39	45.96
Water content (%):	18.81	19.66	20.13	21.65

Liquid Limit:	19
Plastic Limit:	8
Plasticity Index:	10

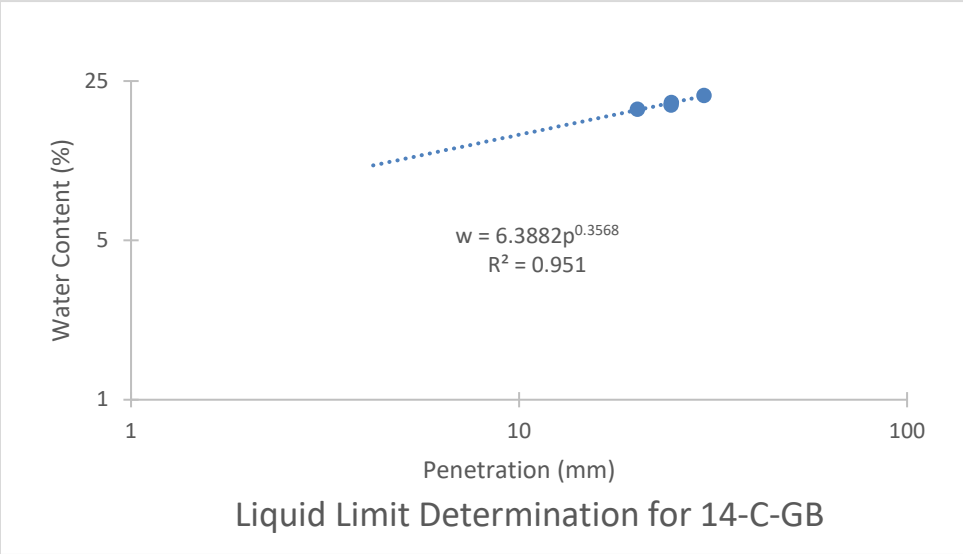

12. APPENDIX B: LABORATORY TESTING OF SUBGRADE SOIL

Particle size analysis, Atterberg limits, carbonate content, moisture-density relationship testing, and swell-collapse tests were carried out on the subgrade samples. The numbering methodology for the locations is as follows: The first number refers to the primary location, while the letter immediately after refers to the sub-location.

Rapid Determination of Carbonate Content - ASTM D4373

Project:	SR-10
No.:	July 2019 Subgrade Samples
Location:	Emery
Date:	8/19/2019
Personnel:	HB

Boring No.:	TP-1-A	TP-1-B	TP-2-A	TP-2-B	TP-2-C
Depth:	0.5'	1.0'	1.0'	1.0'	1.5'
Specimen Weight (g):	1.00	1.00	1.00	1.00	1.00
Pressure Reading (psi):	1.80	1.80	1.95	2.00	1.75
Carbonate Content, Calcite Equivalent (%):	20	20	22	22	20
Supplemental Pressure Readings (psi)					
10 min:	1.70	1.50	1.70	1.95	1.75
20 min:	1.75	1.65	1.80	2.00	1.75
30 min:	1.80	1.80	1.90	2.00	1.75
40 min:	1.80	1.80	1.95	2.00	-
50 min:	1.80	-	1.95	-	-

$CaCO_3$ Reactor Calibration Information

Personnel:	Jerry Flannery/Henrik Burns
Date:	8/14/2019

$CaCO_3$ Specimen Weight (g):	Pressure Gauge Reading (psi):
0.0	0.0
0.2	1.7
0.4	3.6
0.6	5.4
0.8	7.3
1.0	8.3

Slope:	0.1156077
Intercept:	-0.0062655

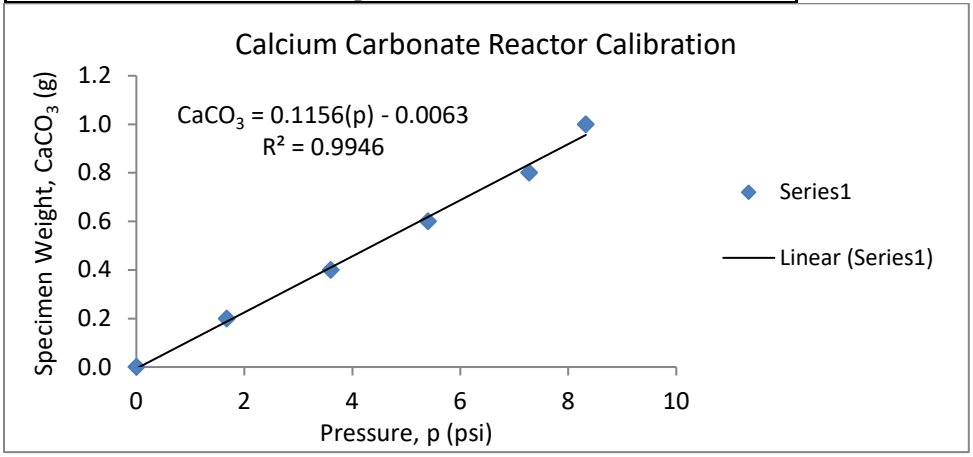

Standard Proctor AASHTO T99 Passing 3/8					
Project:	SR-10 Subgrade Samples				
Boring No.:	TP-1				
Depth:	0-1.0'				
Date:	8/26/2019				
Personnel:	HB				
Wet+Mold (g):	5948.9	6077	6171.3	6202.9	6165.5
Mold Weight (g):	4227.3	4227.3	4227.3	4227.3	4227.3
Wet Wt. (g):	1721.6	1849.7	1944	1975.6	1938.2
Wet Wt. (lb):	3.80	4.08	4.29	4.36	4.27
Dry Weight (lb):	3.45	3.59	3.65	3.63	3.42
Mold ID:	1	1	1	1	1
Mold Volume (ft^3):	0.03	0.03	0.03	0.03	0.03
Wet Density (pcf):	113.86	122.34	128.57	130.66	128.19
Dry Density (pcf):	103.49	107.81	109.45	108.89	102.67
Tare No.:	1	4	5	2	11
Wet+Tare (g):	152.02	163.92	144.57	171.93	175.73
Dry+Tare (g):	141.61	149.47	128.49	151.07	150.37
Tare Wt. (g):	27.30	27.82	20.40	25.87	22.97
Moisture Content (%):	9.11	11.88	14.88	16.66	19.91
$\gamma_{d,max}$ (pcf):	109.4				
w_{opt} (%):	15.8				
Gs (assumed):	2.70				
$S_{r,opt}$ (%):	79.1				

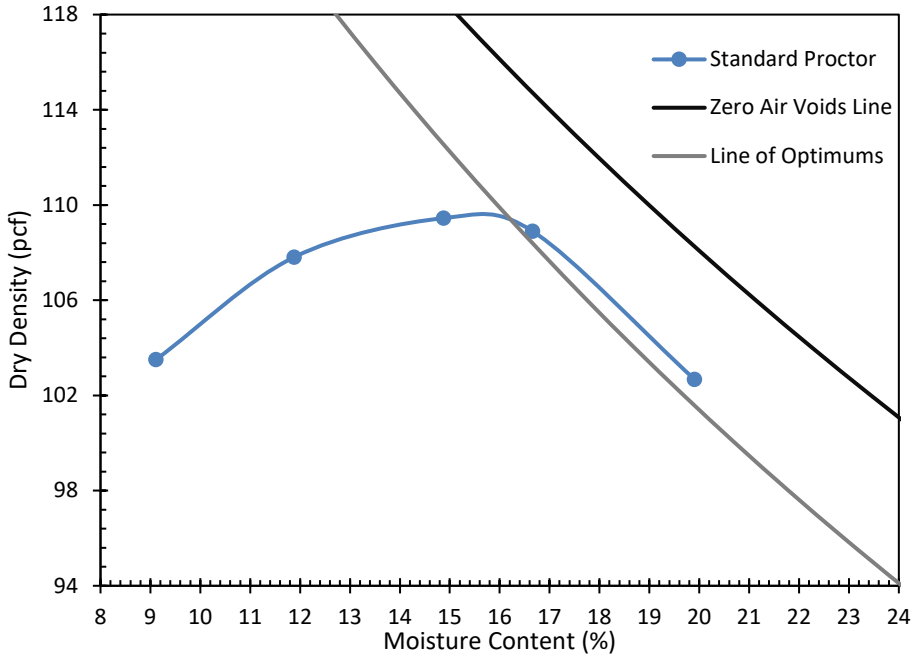

Harvard Miniature 5 Lifts, 25 Tamps, 13.3lb					
Project:	SR-10 Subgrade Samples				
Boring No.:	TP-1				
Depth:	0-1.0'				
Date:	9/20/2019				
Personnel:	HB				
Wet+Mold (g):	522.10	531.20	539.36	540.67	537.37
Mold Weight (g):	410.94	410.94	410.94	410.94	410.94
Wet Wt. (g):	111.16	120.26	128.42	129.73	126.43
Wet Wt. (lb):	0.25	0.27	0.28	0.29	0.28
Dry Weight (lb):	0.21	0.22	0.23	0.23	0.22
Mold ID:	1	1	1	1	1
Mold Volume (ft^3):	0.0022	0.0022	0.0022	0.0022	0.0022
Wet Density (pcf):	111.26	120.37	128.54	129.85	126.54
Dry Density (pcf):	95.32	100.67	104.35	104.02	98.45
Tare No.:	4	2	A80	3(1)	M#1
Wet+Tare (g):	138.50	145.05	155.11	149.62	149.05
Dry+Tare (g):	124.63	128.29	135.50	129.18	126.93
Tare Wt. (g):	27.81	25.87	31.28	26.42	27.28
Moisture Content (%):	14.33	16.36	18.82	19.89	22.20
$\gamma_{d,max}$ (pcf):	104.4				
w_{opt} (%):	19.4				
Gs (assumed):	2.70				
$S_{r,opt}$ (%):	85.2				

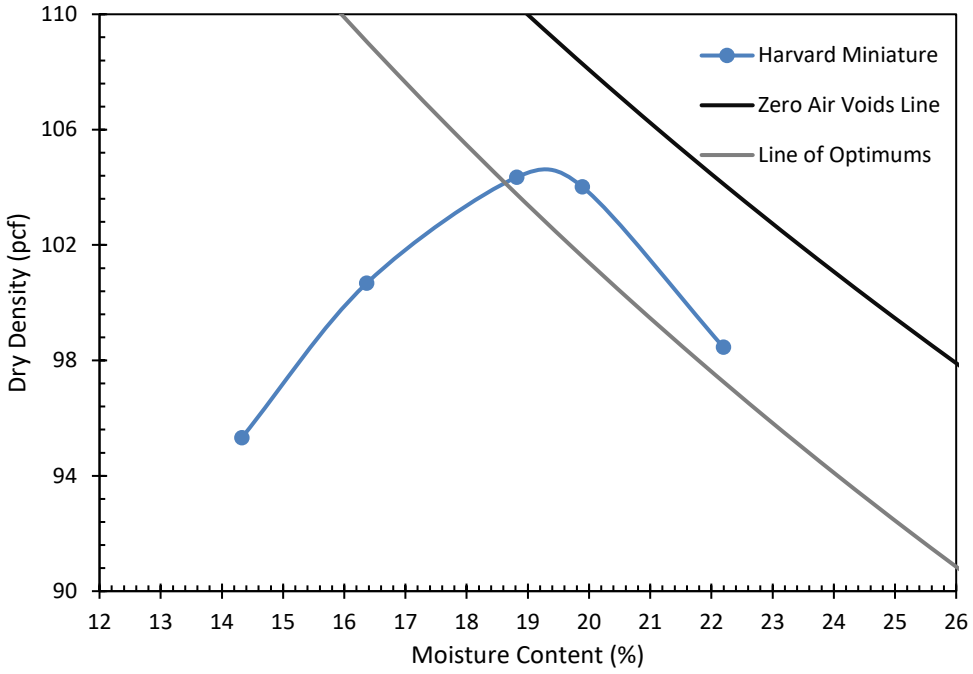

Standard Proctor AASHTO T99 Passing 3/8						
Project:	SR-10 Subgrade Samples					
Boring No.:	TP-2					
Depth:	1.0-1.5'					
Date:	9/11/2019					
Personnel:	HB					
Wet+Mold (g):	5934.8	6025.5	6150.7	6182.2	6167.5	6123.3
Mold Weight (g):	4227.1	4227.1	4227.1	4227.1	4227.1	4227.1
Wet Wt. (g):	1707.7	1798.4	1923.6	1955.1	1940.4	1896.2
Wet Wt. (lb):	3.76	3.96	4.24	4.31	4.28	4.18
Dry Weight (lb):	3.38	3.48	3.56	3.50	3.38	3.22
Mold ID:	1	1	1	1	1	1
Mold Volume (ft^3):	0.0332	0.0332	0.0332	0.0332	0.0332	0.0332
Wet Density (pcf):	113.38	119.40	127.71	129.80	128.83	125.89
Dry Density (pcf):	101.90	104.85	107.14	105.31	101.75	96.92
Tare No.:	11	5	M1	4	51	G3
Wet+Tare (g):	155.77	175.48	189.99	206.66	230.48	229.61
Dry+Tare (g):	143.56	158.63	167.42	178.27	195.05	191.52
Tare Wt. (g):	22.98	20.40	27.33	27.84	26.46	26.02
Moisture Content (%):	10.13	12.19	16.11	18.87	21.02	23.02
$\gamma_{d,max}$ (pcf):	107.7					
w_{opt} (%):	15.0					
Gs (assumed):	2.70					
$S_{r,opt}$ (%):	71.8					

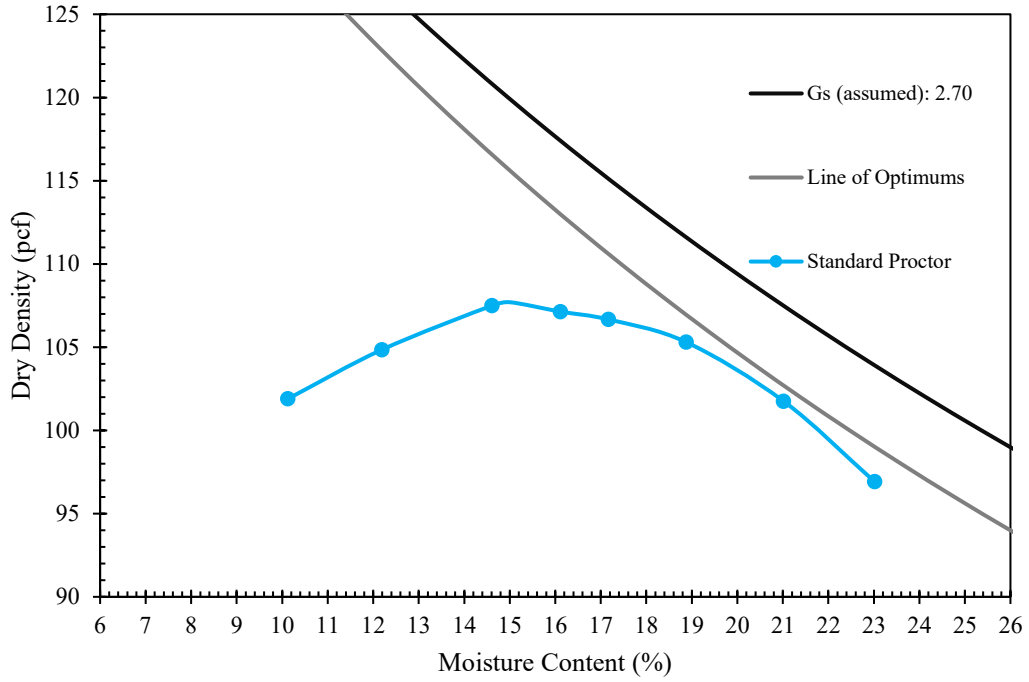

Harvard Miniature 5 Lifts 25 Tamps, 13.3 lb							
Project:	SR-10 Subgrade Samples						
Boring No.:	TP-1						
Depth:	1.0'-1.5'						
Date:	9/23/2019						
Personnel:	HB						
Wet+Mold (g):	519.26	525.04	534.62	539.98	538.73	536.47	534.20
Mold Weight (g):	410.93	410.93	410.93	410.93	410.93	410.93	410.93
Wet Wt. (g):	108.33	114.11	123.69	129.05	127.8	125.54	123.27
Wet Wt. (lb):	0.24	0.25	0.27	0.28	0.28	0.28	0.27
Dry Weight (lb):	0.20	0.21	0.22	0.23	0.22	0.21	0.20
Mold ID:	1	1	1	1	1	1	1
Mold Volume (ft^3):	0.0022	0.0022	0.0022	0.0022	0.0022	0.0022	0.0022
Wet Density (pcf):	108.61	114.41	124.01	129.39	128.13	125.87	123.59
Dry Density (pcf):	91.36	94.07	99.60	102.84	99.03	95.27	91.67
Tare No.:	11	4	M#1	2(2)	2	A80	3(1)
Wet+Tare (g):	130.18	141.40	148.96	95.05	148.81	151.68	145.56
Dry+Tare (g):	115.48	124.25	128.94	83.34	126.05	128.13	121.10
Tare Wt. (g):	22.95	27.76	27.25	26.27	25.84	31.25	26.40
Moisture Content (%):	15.89	17.77	19.69	20.52	22.71	24.31	25.83
$\gamma_{d,max}$ (pcf):	102.8						
w_{opt} (%):	20.5						
Gs (assumed):	2.70						
$S_{r,opt}$ (%):	86.8						

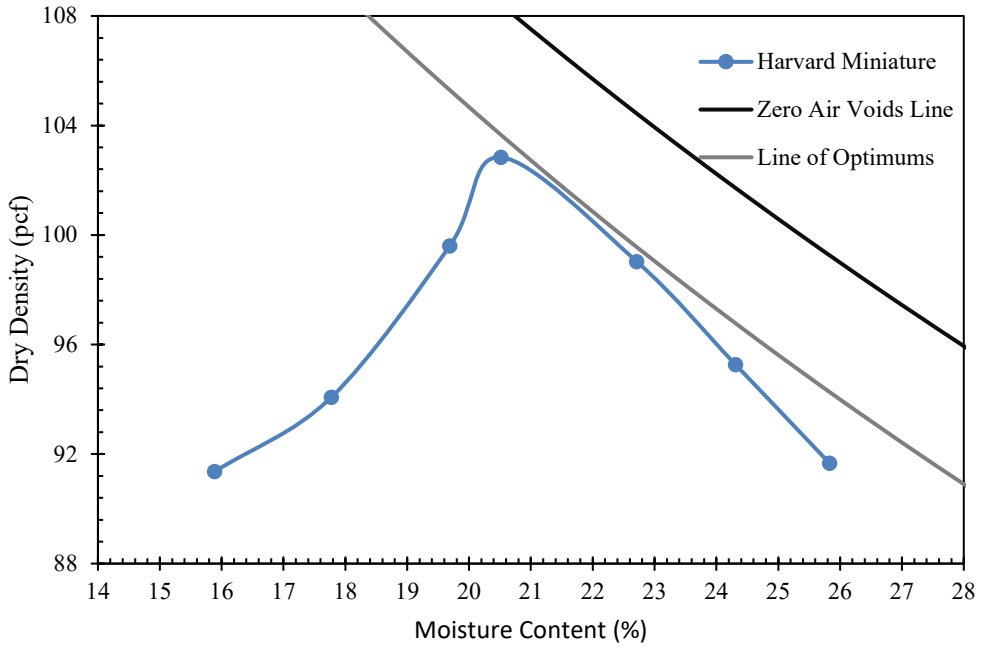

Harvard Miniature 5 Lifts 25 Tamps, 40 lb					
Project:	SR-10 Subgrade Samples				
Boring No.:	TP-2				
Depth:	1.0'-1.5'				
Date:	9/23/2019				
Personnel:	HB				
Wet+Mold (g):	530.09	538.12	542.20	543.61	542.27
Mold Weight (g):	410.93	410.93	410.93	410.93	410.93
Wet Wt. (g):	119.16	127.19	131.27	132.68	131.34
Wet Wt. (lb):	0.26	0.28	0.29	0.29	0.29
Dry Weight (lb):	0.23	0.24	0.24	0.24	0.23
Mold ID:	1	1	1	1	1
Mold Volume (ft^3):	0.0022	0.0022	0.0022	0.0022	0.0022
Wet Density (pcf):	119.47	127.52	131.61	133.02	131.68
Dry Density (pcf):	105.79	109.48	110.71	108.53	104.58
Tare No.:	1(1)	2	G5	A80	2(2)
Wet+Tare (g):	85.87	90.76	96.24	107.77	100.35
Dry+Tare (g):	79.70	82.85	86.81	95.86	87.71
Tare Wt. (g):	25.81	26.94	27.44	31.19	26.30
Moisture Content (%):	11.45	14.15	15.88	18.42	20.58
$\gamma_{d,max}$ (pcf):	111.2				
w_{opt} (%):	16.9				
Gs (assumed):	2.70				
$S_{r,opt}$ (%):	88.6				

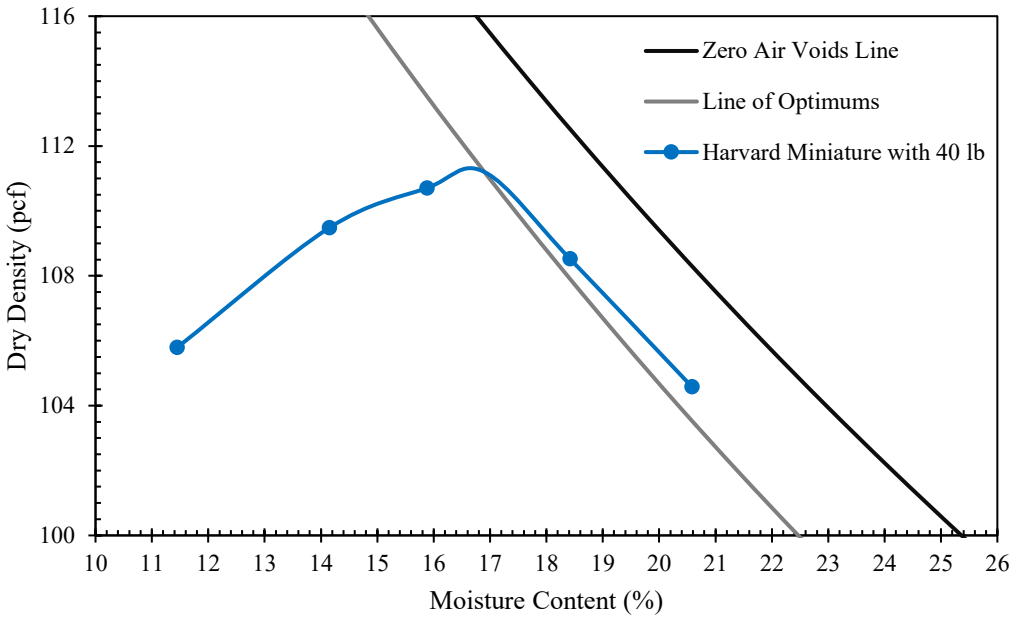

Modified Proctor				
Project:	SR-10 Subgrade Samples			
Boring No.:	TP-2			
Depth:	1.0'-1.5'			
Date:	10/29/2019			
Personnel:	HB			
Wet+Mold (g):	6099.90	6216.60	6278.90	6301.60
Mold Weight (g):	4226.1	4226.1	4226.1	4226.1
Wet Wt. (g):	1873.8	1990.5	2052.8	2075.5
Wet Wt. (lb):	4.13	4.39	4.53	4.58
Dry Weight (lb):	3.82	3.96	4.01	3.91
Mold ID:	1	1	1	1
Mold Volume (ft^3):	0.0332	0.0332	0.0332	0.0332
Wet Density (pcf):	124.41	132.15	136.29	137.80
Dry Density (pcf):	115.12	119.32	120.72	117.65
Tare No.:	#13	#1(1)	#2(2)	2
Wet+Tare (g):	82.41	108.87	142.33	128.50
Dry+Tare (g):	78.27	101.50	130.42	115.40
Tare Wt. (g):	22.82	25.61	26.18	25.82
Moisture Content (%):	7.47	9.71	11.43	14.62
$\gamma_{d,max}$ (pcf):	121.3			
w_{opt} (%):	10.7			
Gs (assumed):	2.70			
$S_{r,opt}$ (%):	74.3			

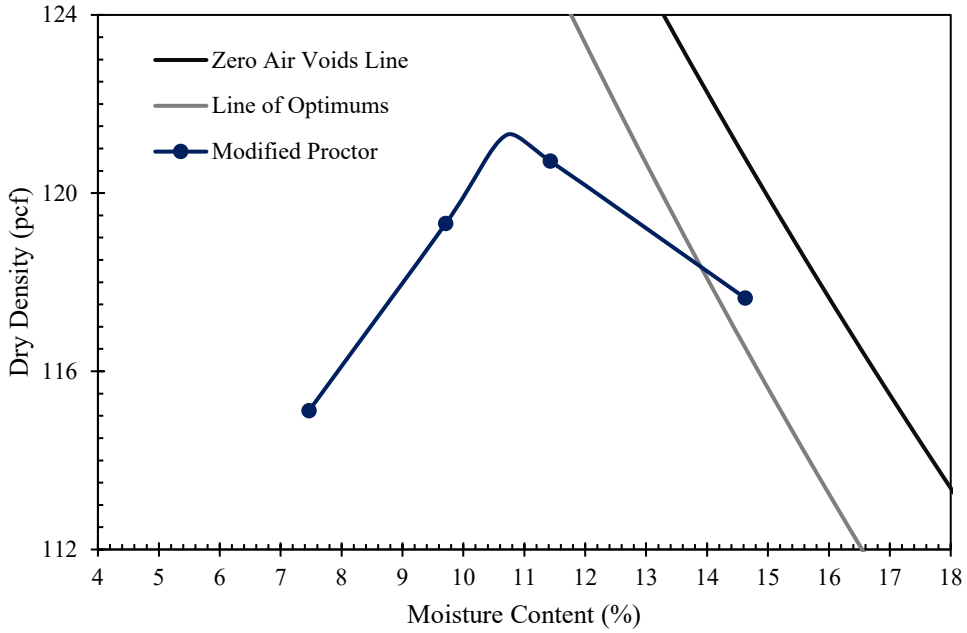

Project:	SR-10	Date:	7/16/2019	Shaker:	Mechanical
Location:	TP-1-A	Personnel:	HB/SS	Time:	10 min

Wt. of Dry Soil (g):	130.74
Wt. of Dry Soil (g):	2.88
-200 Wash (g):	127.86
Pan (g):	0.29

Sieve Number	Sieve Opening (mm)	Cumulative Retained (g)	Cumulative Passing (g)	Percent Passing (%)	Shape, Uniformity, and Classification	
3/4	19.000	0.00	130.74	100.00	Gravel (%)	0.02
3/8	9.500	0.01	130.73	99.99	Sand (%)	1.96
4	4.750	0.02	130.72	99.98	Fines (%)	98.02
10	2.000	0.04	130.70	99.97	D_{60}	<0.075
20	0.850	0.68	130.06	99.48	D_{30}	<0.075
40	0.425	0.97	129.77	99.26	D_{10}	<0.075
60	0.250	1.16	129.58	99.11	C_u	NA
100	0.150	1.39	129.35	98.94	C_c	NA
140	0.106	1.77	128.97	98.65	Gradation	NA
200	0.075	2.59	128.15	98.02	USCS	CL

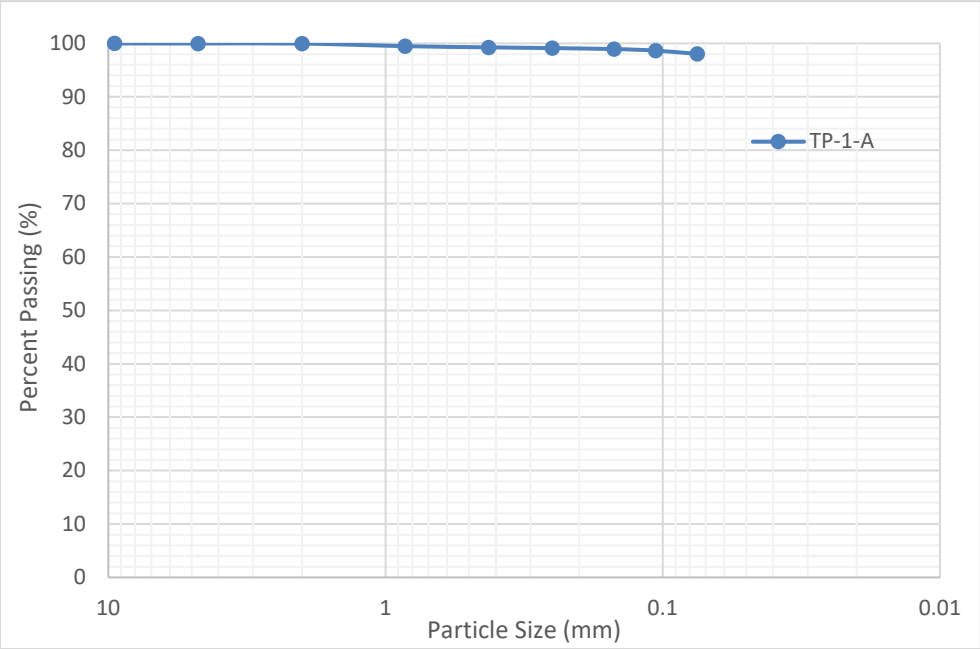

Project:	SR-10	Date:	7/16/2019	Shaker:	Mechanical
Location:	TP-1-B	Personnel:	HB/SS	Time:	10 min

Wt. of Dry Soil (g):	135.17
Wt. of Dry Soil (g):	4.46
-200 Wash (g):	130.71
Pan (g):	0.08

Sieve Number	Sieve Opening (mm)	Cumulative Retained (g)	Cumulative Passing (g)	Percent Passing (%)	Shape, Uniformity, and Classification	
3/4	19.000	0.00	135.17	100.00	Gravel (%)	0.01
3/8	9.500	0.01	135.16	99.99	Sand (%)	3.23
4	4.750	0.01	135.16	99.99	Fines (%)	96.76
10	2.000	0.01	135.16	99.99	D_{60}	<0.075
20	0.850	0.88	134.29	99.35	D_{30}	<0.075
40	0.425	1.54	133.63	98.86	D_{10}	<0.075
60	0.250	2.27	132.90	98.32	C_u	NA
100	0.150	2.94	132.23	97.82	C_c	NA
140	0.106	3.55	131.62	97.37	Gradation	NA
200	0.075	4.38	130.79	96.76	USCS	CL

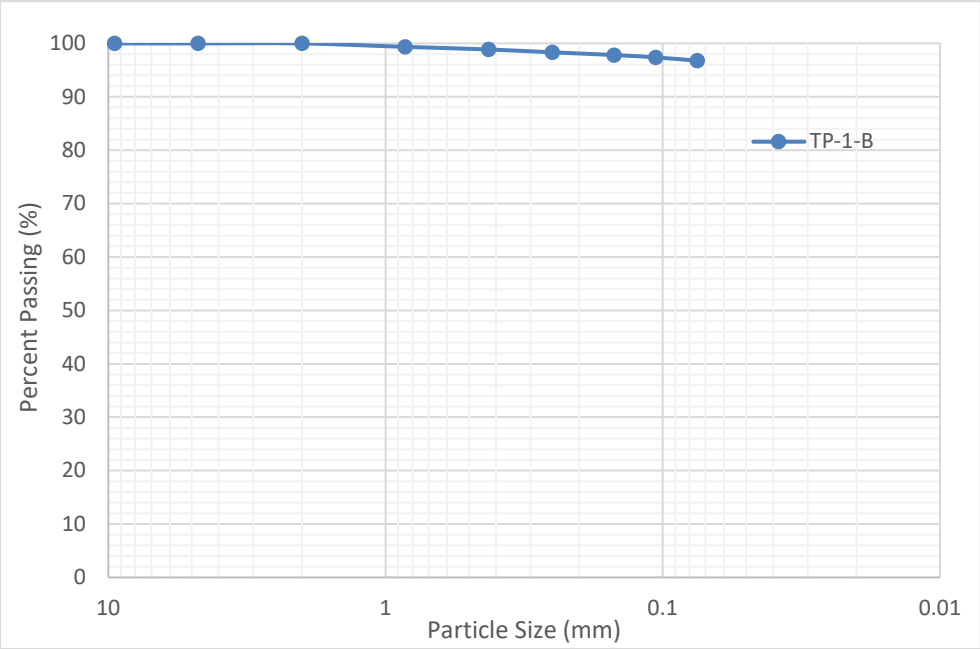

Project:	SR-10	Date:	7/15/2019	Shaker:	Mechanical
Location:	TP-2-A	Personnel:	HB/SS	Time:	10 min

Wt. of Dry Soil (g):	183.58
Wt. of Dry Soil (g):	72.36
-200 Wash (g):	111.22
Pan (g):	10.28

Sieve Number	Sieve Opening (mm)	Cumulative Retained (g)	Cumulative Passing (g)	Percent Passing (%)	Shape, Uniformity, and Classification	
3/4	19.000	0.00	183.58	100.00	Gravel (%)	0.02
3/8	9.500	0.00	183.58	100.00	Sand (%)	33.80
4	4.750	0.03	183.55	99.98	Fines (%)	66.18
10	2.000	1.60	181.98	99.13	D_{60}	<0.075
20	0.850	2.84	180.74	98.45	D_{30}	<0.075
40	0.425	6.88	176.70	96.25	D_{10}	<0.075
60	0.250	16.32	167.26	91.11	C_u	NA
100	0.150	31.30	152.28	82.95	C_c	NA
140	0.106	48.15	135.43	73.77	Gradation	NA
200	0.075	62.08	121.50	66.18	USCS	CL

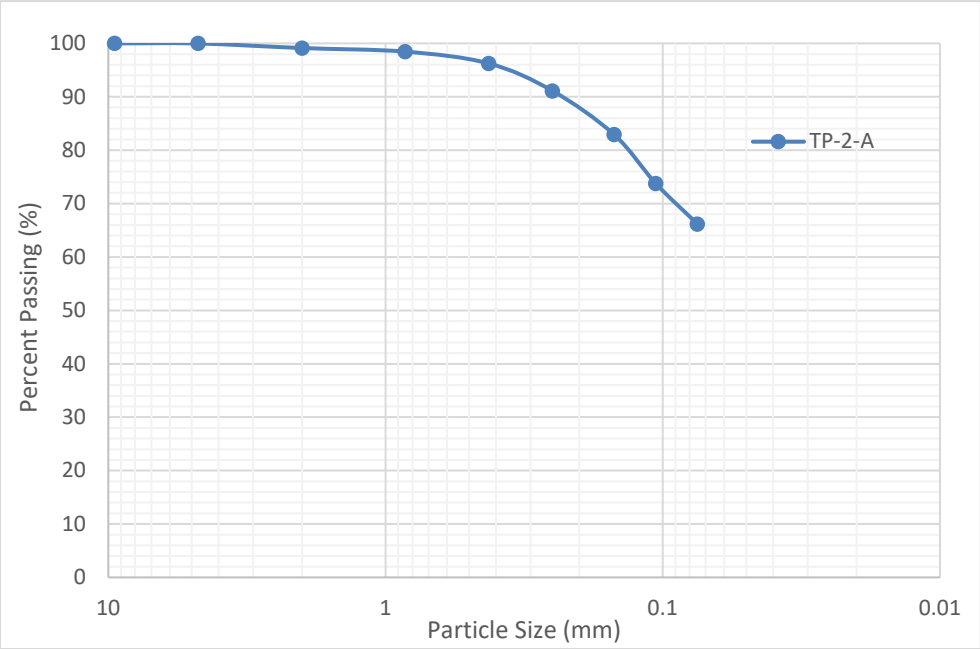

Project:	SR-10	Date:	7/16/2019	Shaker:	Mechanical
Location:	TP-2-B	Personnel:	HB/SS	Time:	10 min

Wt. of Dry Soil (g):	105.43
Wt. of Dry Soil (g):	6.46
-200 Wash (g):	98.97
Pan (g):	0.03

Sieve Number	Sieve Opening (mm)	Cumulative Retained (g)	Cumulative Passing (g)	Percent Passing (%)	Shape, Uniformity, and Classification	
3/4	19.000	0.00	105.43	100.00	Gravel (%)	0.03
3/8	9.500	0.00	105.43	100.00	Sand (%)	6.07
4	4.750	0.03	105.40	99.97	Fines (%)	93.90
10	2.000	0.11	105.32	99.90	D_{60}	<0.075
20	0.850	1.41	104.02	98.66	D_{30}	<0.075
40	0.425	2.84	102.59	97.31	D_{10}	<0.075
60	0.250	3.79	101.64	96.41	C_u	NA
100	0.150	4.63	100.80	95.61	C_c	NA
140	0.106	5.61	99.82	94.68	Gradation	NA
200	0.075	6.43	99.00	93.90	USCS	CL

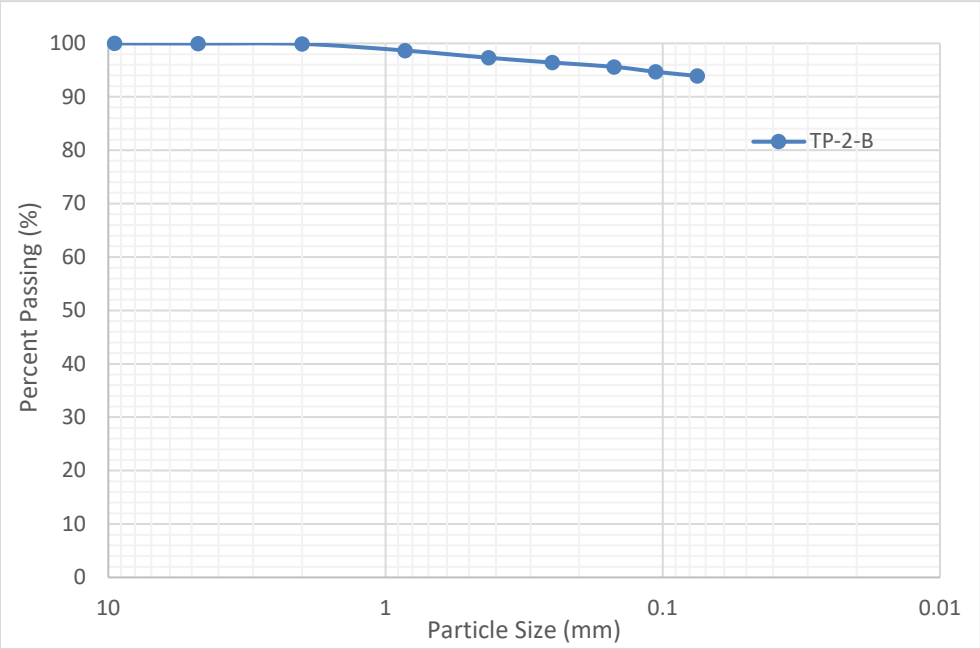

Project:	SR-10	Date:	7/15/2019	Shaker:	Mechanical
Location:	TP-2-C	Personnel:	HB/SS	Time:	10 min

Wt. of Dry Soil (g):	125.74
Wt. of Dry Soil (g):	8
-200 Wash (g):	117.74
Pan (g):	0.04

Sieve Number	Sieve Opening (mm)	Cumulative Retained (g)	Cumulative Passing (g)	Percent Passing (%)	Shape, Uniformity, and Classification	
3/4	19.000	0.00	125.74	100.00	Gravel (%)	0.03
3/8	9.500	0.00	125.74	100.00	Sand (%)	6.30
4	4.750	0.04	125.70	99.97	Fines (%)	93.67
10	2.000	0.15	125.59	99.88	D_{60}	<0.075
20	0.850	3.02	122.72	97.60	D_{30}	<0.075
40	0.425	4.71	121.03	96.25	D_{10}	<0.075
60	0.250	5.44	120.30	95.67	C_u	NA
100	0.150	6.19	119.55	95.08	C_c	NA
140	0.106	7.15	118.59	94.31	Gradation	NA
200	0.075	7.96	117.78	93.67	USCS	CL

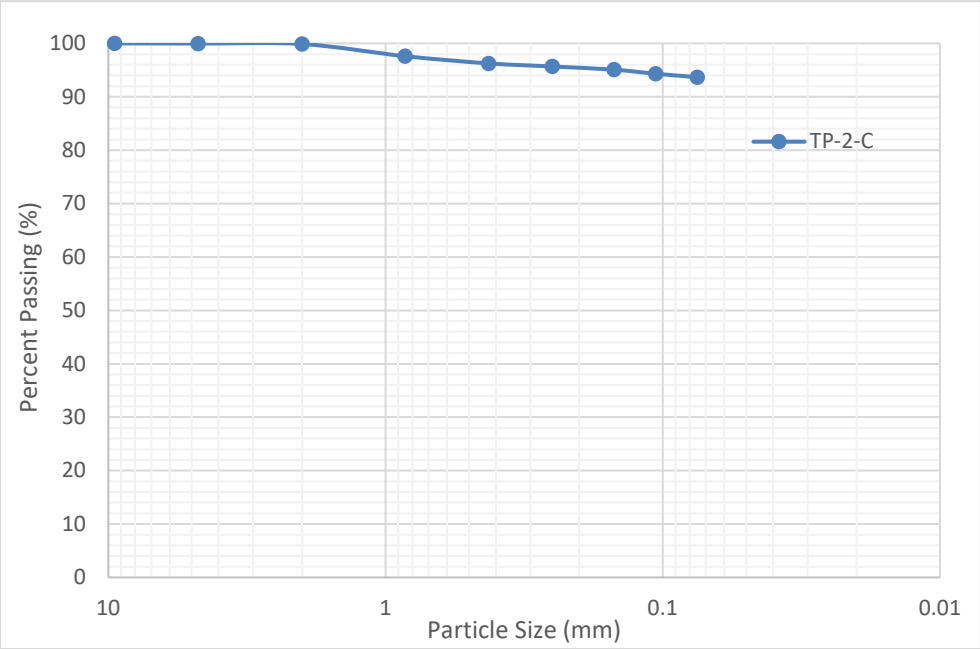

ASTM D4318 Standard Test Methods for Atterberg Limits Liquid Limit, Plastic Limit, and Plasticity Index of Soils					
Project:	SR-10		Date:		7/22/2019
Location:	TP-1-A		Personnel:		HB
	Liquid Limit Determination			Plastic Limit Determination	
Tare No.:	6	17	18	13	2
Tare wt. (g):	25.35	22.82	26.74	22.88	25.87
Wet + tare wt. (g):	42.14	46.58	43.49	27.46	32.57
Dry + tare wt. (g):	37.42	39.88	38.68	26.69	31.46
Water content (%):	39.11	39.27	40.28	20.21	19.86
Blows:	35	25	19		
Log Blows:	1.54	1.40	1.28		
Slope:	-4.32				
Intercept:	45.64				
Liquid Limit:	40				
Plastic Limit:	20				
Plasticity Index:	20				

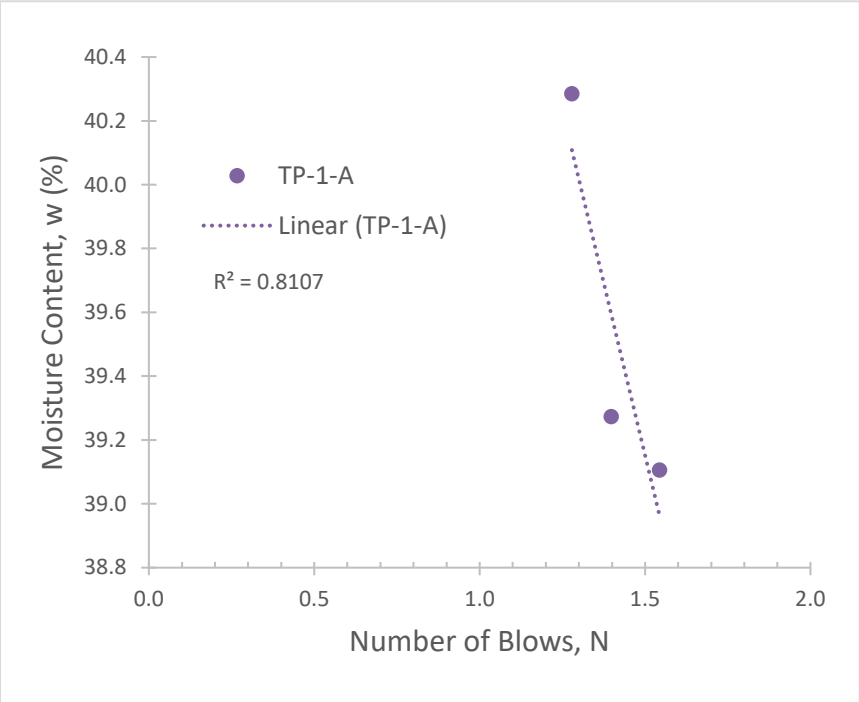

ASTM D4318 Standard Test Methods for Atterberg Limits Liquid Limit, Plastic Limit, and Plasticity Index of Soils					
Project:	SR-10		Date:	7/23/2019	
Location:	TP-1-B		Personnel:	HB	
	Liquid Limit Determination			Plastic Limit Determination	
Tare No.:	2	18	13	17	6
Tare wt. (g):	24.82	26.71	22.85	22.83	25.09
Wet + tare wt. (g):	46.04	47.43	49.86	32.68	34.61
Dry + tare wt. (g):	40.56	41.53	41.40	31.04	33.11
Water content (%):	34.82	39.81	45.61	19.98	18.70
Blows:	26	23	15		
Log Blows:	1.41	1.36	1.18		
Slope:	-41.54				
Intercept:	94.81				
Liquid Limit:	37				
Plastic Limit:	19				
Plasticity Index:	17				

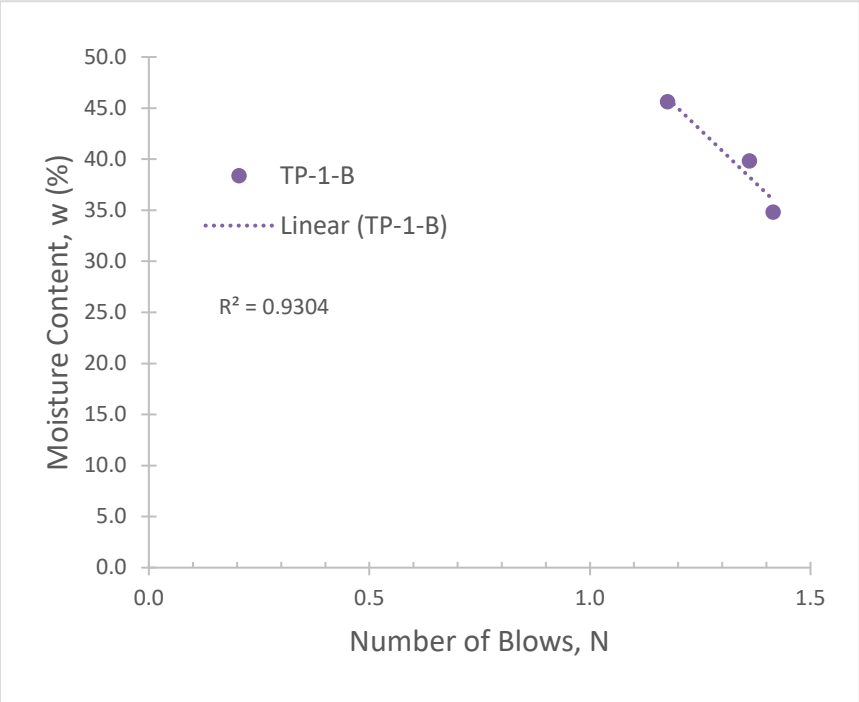

ASTM D4318 Standard Test Methods for Atterberg Limits Liquid Limit, Plastic Limit, and Plasticity Index of Soils					
Project:	SR-10		Date:	7/19/2019	
Location:	TP-2-A		Personnel:	HB	
	Liquid Limit Determination			Plastic Limit Determination	
Tare No.:	17	3	2	5	9
Tare wt. (g):	28.45	26.74	27.01	26.5	26.16
Wet + tare wt. (g):	47.67	39.85	40.29	28.29	28.57
Dry + tare wt. (g):	41.63	35.52	35.84	27.95	28.10
Water content (%):	45.83	49.32	50.40	23.45	24.23
Blows:	30	24	18		
Log Blows:	1.48	1.38	1.26		
Slope:	-20.03				
Intercept:	75.98				
Liquid Limit:	48				
Plastic Limit:	24				
Plasticity Index:	24				

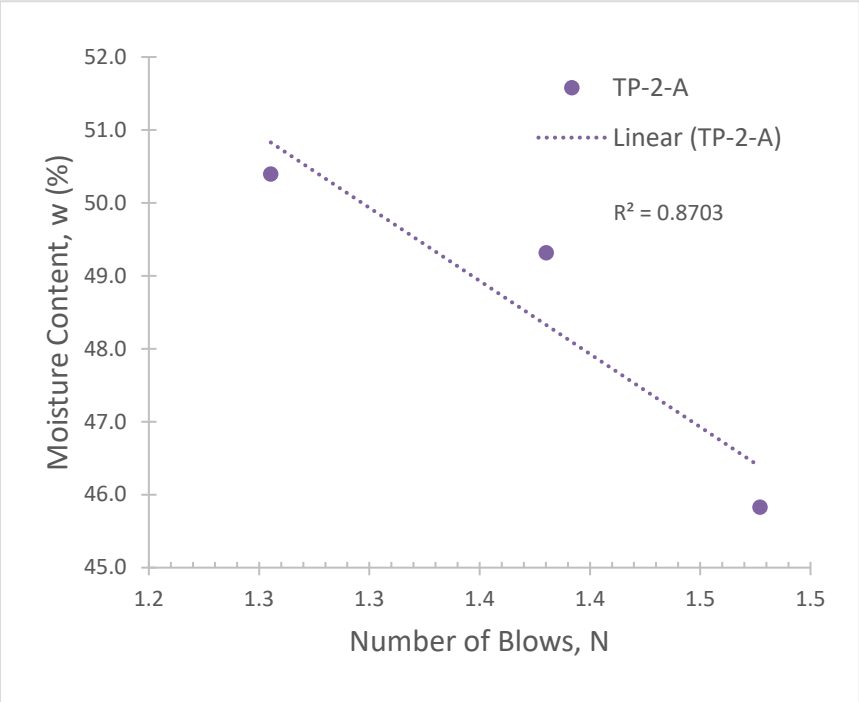

ASTM D4318 Standard Test Methods for Atterberg Limits Liquid Limit, Plastic Limit, and Plasticity Index of Soils					
Project:	SR-10		Date:	7/23/2019	
Location:	TP-2-B		Personnel:	HB	
	Liquid Limit Determination			Plastic Limit Determination	
Tare No.:	17	9	5	3	2
Tare wt. (g):	28.44	26.14	26.48	26.74	26.98
Wet + tare wt. (g):	51.13	44.61	47.06	32.63	34.63
Dry + tare wt. (g):	44.48	39.01	40.80	31.51	33.19
Water content (%):	41.46	43.51	43.72	23.48	23.19
Blows:	34	24	22		
Log Blows:	1.53	1.38	1.34		
Slope:	-12.40				
Intercept:	60.48				
Liquid Limit:	43				
Plastic Limit:	23				
Plasticity Index:	20				

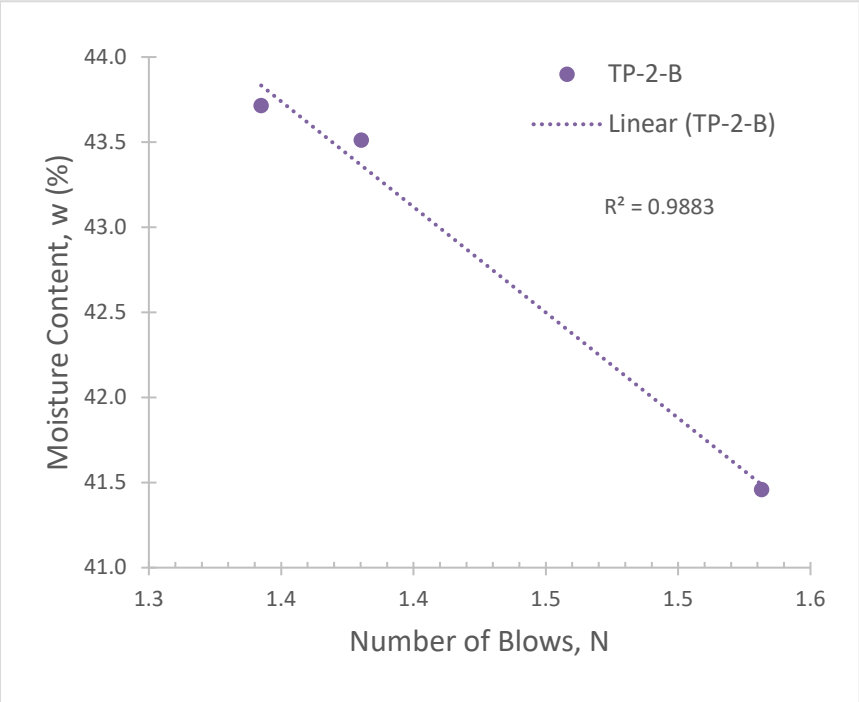

ASTM D4318 Standard Test Methods for Atterberg Limits Liquid Limit, Plastic Limit, and Plasticity Index of Soils					
Project:	SR-10		Date:	7/23/2019	
Location:	TP-2-C		Personnel:	HB	
	Liquid Limit Determination			Plastic Limit Determination	
Tare No.:	2	9	5	3	17
Tare wt. (g):	26.97	26.16	26.49	26.74	28.46
Wet + tare wt. (g):	48.55	44.89	47.68	34.49	35.64
Dry + tare wt. (g):	41.95	39.00	40.81	32.89	34.18
Water content (%):	44.06	45.87	47.97	26.02	25.52
Blows:	35	25	15		
Log Blows:	1.54	1.40	1.18		
Slope:	-10.55				
Intercept:	60.45				
Liquid Limit:	46				
Plastic Limit:	26				
Plasticity Index:	20				

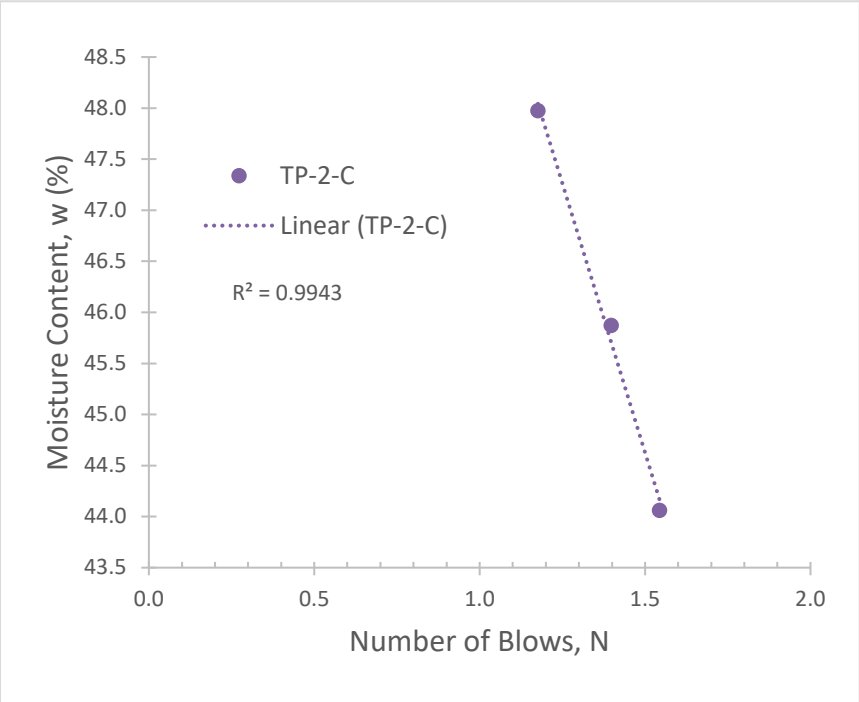

Hydrometer Analysis Data Sheet				
Personnel:	HB			
Date:	1/8/2020			
Location:	TP-1			
Hydrometer Sample			Moisture Sample	
Total Mass of Air-dried Soil (g):	36.83		Tare Wt. (g):	21.41
Assumed Specific Gravity, Gs	2.7		Wet + Tare (g):	34.25
Correction Factor, a	0.99		Oven Dry + Tare (g):	33.93
Mass of Solids (g):	35.91		Water Content (%):	2.56

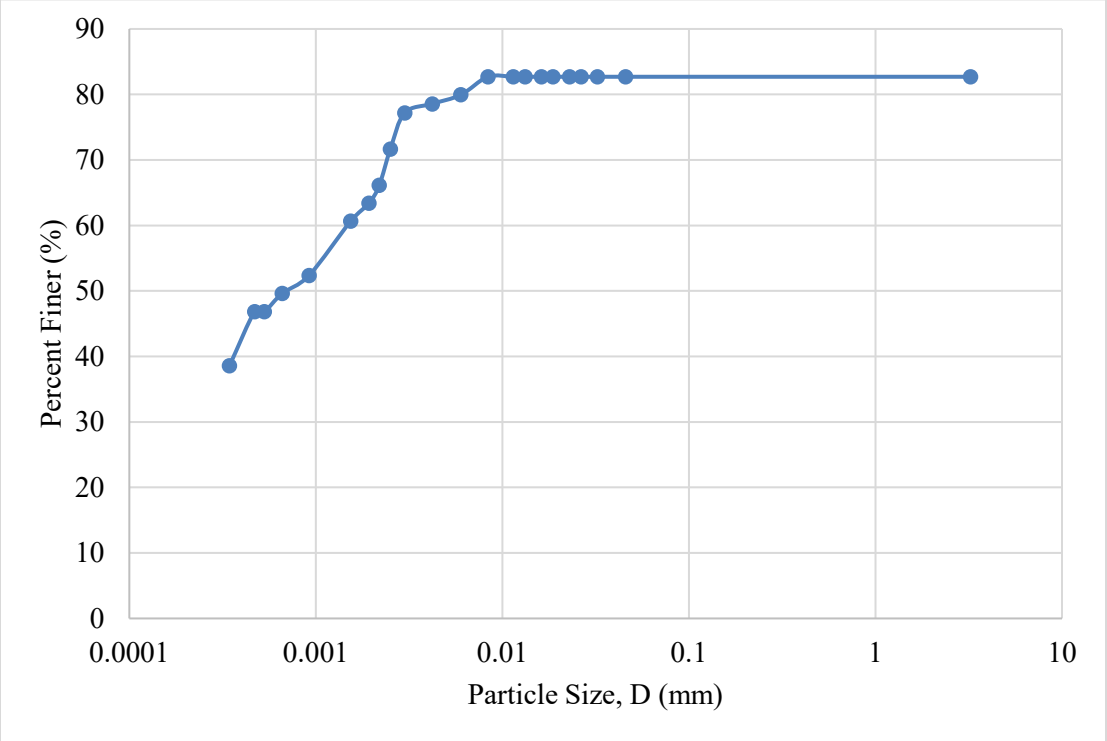

Control Jar				
Date:	Actual Elapsed Time:	Temp:	Hydrometer Reading, C_z:	Temperature Correction Factor, C_t:
1/8/2020	0.0001	19	35	-0.3
1/8/2020	0.5	19	35	-0.3
1/8/2020	1	19	35	-0.3
1/8/2020	1.5	19	35	-0.3
1/8/2020	2	19	35	-0.3
1/8/2020	3	19	35	-0.3
1/8/2020	4	19	35	-0.3
1/8/2020	6	19	35	-0.3
1/8/2020	8	19	35	-0.3
1/8/2020	15	19	35	-0.3
1/8/2020	30	19	35	-0.3
1/8/2020	60	20	35	0.0
1/8/2020	120	20	35	0.0
1/8/2020	180	20	35	0.0
1/8/2020	240	21	36	0.2
1/8/2020	300	22	37	0.4
1/8/2020	480	22	37	0.4
1/9/2020	1440	22	37	0.4
1/10/2020	2880	22	37	0.4
1/11/2020	4520	22	37	0.4
1/12/2020	5760	22	37	0.4
1/15/2020	10080	24	41	1.0

Soil Suspension							
Date:	Actual Elapsed Time:	Temp:	Hydrometer Reading, R_a:	Temperature Correction Factor, C_t:	Corrected Hydrometer Reading, R_{cP}:	Percent Finer (%):	Particle Diameter, D (mm):
1/8/2020	0.0001	19	65.0	-0.3	30.0	82.7	3.2361
1/8/2020	0.5	19	65.0	-0.3	30.0	82.7	0.0458
1/8/2020	1	19	65.0	-0.3	30.0	82.7	0.0324
1/8/2020	1.5	19	65.0	-0.3	30.0	82.7	0.0264
1/8/2020	2	19	65.0	-0.3	30.0	82.7	0.0229
1/8/2020	3	19	65.0	-0.3	30.0	82.7	0.0187
1/8/2020	4	19	65.0	-0.3	30.0	82.7	0.0162
1/8/2020	6	19	65.0	-0.3	30.0	82.7	0.0132
1/8/2020	8	19	65.0	-0.3	30.0	82.7	0.0114
1/8/2020	15	19	65.0	-0.3	30.0	82.7	0.0084
1/8/2020	30	19	64.0	-0.3	29.0	79.9	0.0060
1/8/2020	60	20	63.5	0.0	28.5	78.6	0.0042
1/8/2020	120	20	63.0	0.0	28.0	77.2	0.0030
1/8/2020	180	20	61.0	0.0	26.0	71.7	0.0025
1/8/2020	240	21	60.0	0.2	24.0	66.2	0.0022
1/8/2020	300	22	60.0	0.4	23.0	63.4	0.0019
1/8/2020	480	22	59.0	0.4	22.0	60.6	0.0015
1/9/2020	1440	22	56.0	0.4	19.0	52.4	0.0009
1/10/2020	2880	22	55.0	0.4	18.0	49.6	0.0007
1/11/2020	4520	22	54.0	0.4	17.0	46.9	0.0005
1/12/2020	5760	22	54.0	0.4	17.0	46.9	0.0005
1/15/2020	10080	24	55.0	1.0	14.0	38.6	0.0003

Hydrometer Analysis Data Sheet				
Personnel:	HB			
Date:	1/8/2020			
Location:	TP-2			
Hydrometer Sample			Moisture Sample	
Total Mass of Air-dried Soil (g):	36.83		Tare Wt. (g):	22.35
Assumed Specific Gravity, Gs	2.7		Wet + Tare (g):	30.74
Correction Factor, a	0.99		Oven Dry + Tare (g):	30.44
Mass of Solids (g):	35.51		Water Content (%):	3.71

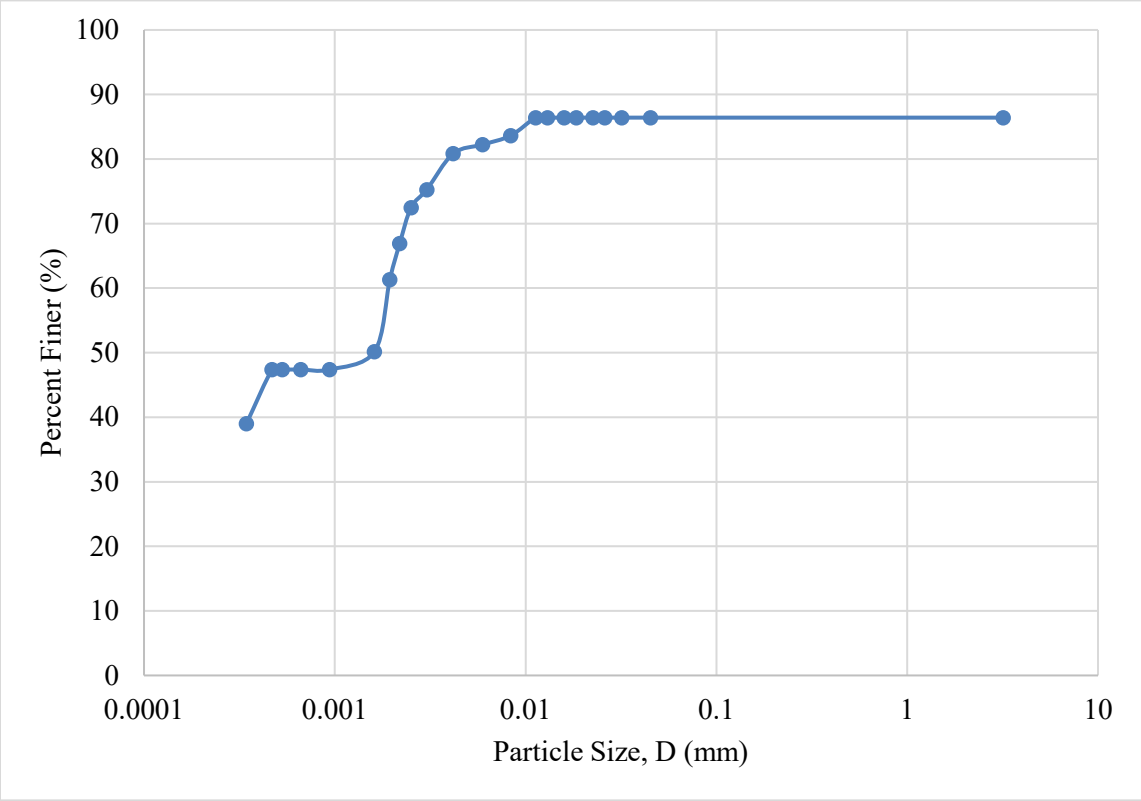

Control Jar				
Date:	Actual Elapsed Time:	Temp:	Hydrometer Reading, C_z:	Temperature Correction Factor, C_t:
1/8/2020	0.0001	19	35	-0.3
1/8/2020	0.5	19	35	-0.3
1/8/2020	1	19	35	-0.3
1/8/2020	1.5	19	35	-0.3
1/8/2020	2	19	35	-0.3
1/8/2020	3	19	35	-0.3
1/8/2020	4	19	35	-0.3
1/8/2020	6	19	35	-0.3
1/8/2020	8	19	35	-0.3
1/8/2020	15	19	35	-0.3
1/8/2020	30	19	35	-0.3
1/8/2020	60	20	35	0.0
1/8/2020	120	20	35	0.0
1/8/2020	180	20	35	0.0
1/8/2020	240	21	36	0.2
1/8/2020	300	22	37	0.4
1/8/2020	480	22	37	0.4
1/9/2020	1440	22	37	0.4
1/10/2020	2880	22	37	0.4
1/11/2020	4520	22	37	0.4
1/12/2020	5760	22	37	0.4
1/15/2020	10080	24	41	1.0

Soil Suspension							
Date:	Actual Elapsed Time:	Temp:	Hydrometer Reading, R_a:	Temperature Correction Factor, C_t:	Corrected Hydrometer Reading, R_{cP}:	Percent Finer (%):	Particle Diameter, D (mm):
1/8/2020	0.0001	19	66.0	-0.3	31.0	86.4	3.1892
1/8/2020	0.5	19	66.0	-0.3	31.0	86.4	0.0451
1/8/2020	1	19	66.0	-0.3	31.0	86.4	0.0319
1/8/2020	1.5	19	66.0	-0.3	31.0	86.4	0.0260
1/8/2020	2	19	66.0	-0.3	31.0	86.4	0.0226
1/8/2020	3	19	66.0	-0.3	31.0	86.4	0.0184
1/8/2020	4	19	66.0	-0.3	31.0	86.4	0.0159
1/8/2020	6	19	66.0	-0.3	31.0	86.4	0.0130
1/8/2020	8	19	66.0	-0.3	31.0	86.4	0.0113
1/8/2020	15	19	65.0	-0.3	30.0	83.6	0.0084
1/8/2020	30	19	64.5	-0.3	29.5	82.2	0.0060
1/8/2020	60	20	64.0	0.0	29.0	80.8	0.0042
1/8/2020	120	20	62.0	0.0	27.0	75.3	0.0030
1/8/2020	180	20	61.0	0.0	26.0	72.5	0.0025
1/8/2020	240	21	60.0	0.2	24.0	66.9	0.0022
1/8/2020	300	22	59.0	0.4	22.0	61.3	0.0019
1/8/2020	480	22	55.0	0.4	18.0	50.2	0.0016
1/9/2020	1440	22	54.0	0.4	17.0	47.4	0.0009
1/10/2020	2880	22	54.0	0.4	17.0	47.4	0.0007
1/11/2020	4520	22	54.0	0.4	17.0	47.4	0.0005
1/12/2020	5760	22	54.0	0.4	17.0	47.4	0.0005
1/15/2020	10080	24	55.0	1.0	14.0	39.0	0.0003

Standard Test Methods for One-Dimensional Swell or Collapse of Soils - ASTM D4546 - 14

Double Oedometer Method

Trial Type:	Wet		Pre	Post
Project:	SR-10 Subgrade samples	Weight (g):	147.55	158.39
Location:	TP-2	Height (mm):	25.345	21.589
Date:	10/14/2019 14:10:00	Volume (ft^3):	0.00282	0.00240
Personnel:	HB	Wet Wt. (g):	39.22	66.31
Compaction:	Harvard Miniature tamper	Dry Wt. (g):	37.54	59.25
Target (RC-WC):	96-12	Tare (g):	22.82	26.44
		Tare ID:	13	Larry 2
h (mm):	25.345	WC (%):	11.41	21.52
Δh1 (mm):	0.014	Dry Density (pcf):	103.64	119.75
h1 (mm):	25.331	RC (%):	96.23	111.19

Load (tsf):	0.01	Load (tsf):	0.25	Load (tsf):	0.5	Load (tsf):	1
WETTING							
Time (min):	Strain (%)	Time (min):	Strain (%)	Time (min):	Strain (%)	Time (min):	Strain (%)
0	0.055	0	-3.656	0	1.058	0	4.879
0.1	0.189	0.1	-0.529	0.1	2.621	0.1	6.853
0.25	0.229	0.25	-0.276	0.25	2.898	0.25	6.987
0.5	0.268	0.5	-0.016	0.5	3.166	0.5	7.209
1	0.308	1	0.166	1	3.442	1	7.453
2	0.324	2	0.379	2	3.703	2	7.738
4	0.340	4	0.537	4	3.940	4	8.038
8	0.300	8	0.671	8	4.145	8	8.338
15	0.126	15	0.782	15	4.295	15	8.551
30	-0.174	30	0.869	30	4.437	30	8.740
60	-0.695	60	0.940	60	4.571	60	8.898
120	-1.461	120	1.019	120	4.690	120	9.009
1440	-3.656	1440	1.058	1440	4.879	1440	9.182

Load (tsf):	2	Load (tsf):	4	Load (tsf):	8	Load (tsf):	0.01
Time (min):	Strain (%)	Time (min):	Strain (%)	Time (min):	Strain (%)	Time (min):	Strain (%)
0	9.182	0	13.225	0	17.109	0	21.105
0.1	10.927	0.1	15.009	0.1	19.075	0.1	19.747
0.25	11.054	0.25	15.159	0.25	19.154	0.25	19.660
0.5	11.204	0.5	15.278	0.5	19.241	0.5	19.589
1	11.441	1	15.428	1	19.336	1	19.462
2	11.630	2	15.594	2	19.470	2	19.320
4	11.851	4	15.775	4	19.636	4	19.131
8	12.112	8	15.996	8	19.881	8	18.854
15	12.349	15	16.217	15	20.070	15	18.523
30	12.577	30	16.470	30	20.339	30	18.025
60	12.767	60	16.691	60	20.584	60	17.402
120	12.909	120	16.833	120	20.741	120	16.604
1440	13.225	1440	17.109	1440	21.105	1440	14.772

Trial Type:	As-compacted		Pre	Post
Project:	SR-10 Subgrade samples	Weight (g):	147.93	143.55
Location:	TP-2	Height (mm):	25.332	23.996
Date:	10/14/2019 14:10:00	Volume (ft^3):	0.00282	0.00267
Personnel:	HB	Wet Wt. (g):	39.22	65.93
Compaction:	Harvard Miniature tamper	Dry Wt. (g):	37.54	62.92
Target (RC-WC):	96-12	Tare (g):	22.82	25.62
		Tare ID:	13	1(1)
h (mm):	25.332	WC (%):	11.41	8.07
Δh1 (mm):	0.000	Dry Density (pcf):	103.87	109.70
h1 (mm):	25.332	RC (%):	96.45	101.86

Load (tsf):	0.01	Load (tsf):	0.25	Load (tsf):	0.5	Load (tsf):	1
WETTING							
Time (min):	Strain (%)	Time (min):	Strain (%)	Time (min):	Strain (%)	Time (min):	Strain (%)
0	0.000	0	0.355	0	1.129	0	1.611
0.1	0.008	0.1	0.726	0.1	1.350	0.1	2.045
0.25	0.016	0.25	0.766	0.25	1.358	0.25	2.053
0.5	0.016	0.5	0.782	0.5	1.366	0.5	2.053
1	0.016	1	0.797	1	1.382	1	2.061
2	0.016	2	0.821	2	1.397	2	2.069
4	0.024	4	0.829	4	1.413	4	2.069
8	0.024	8	0.845	8	1.421	8	2.100
15	0.039	15	0.868	15	1.429	15	2.100
30	0.039	30	0.876	30	1.437	30	2.124
60	0.047	60	0.900	60	1.468	60	2.155
120	0.055	120	0.947	120	1.508	120	2.195
1440	0.355	1440	1.129	1440	1.611	1440	2.432

Load (tsf):	2	Load (tsf):	4	Load (tsf):	8	Load (tsf):	0.01
Time (min):	Strain (%)	Time (min):	Strain (%)	Time (min):	Strain (%)	Time (min):	Strain (%)
0	2.432	0	3.221	0	4.255	0	6.253
0.1	2.771	0.1	3.734	0.1	5.282	0.1	5.487
0.25	2.795	0.25	3.766	0.25	5.313	0.25	5.479
0.5	2.803	0.5	3.790	0.5	5.345	0.5	5.463
1	2.811	1	3.813	1	5.377	1	5.463
2	2.834	2	3.837	2	5.432	2	5.448
4	2.842	4	3.869	4	5.487	4	5.448
8	2.866	8	3.884	8	5.550	8	5.432
15	2.882	15	3.916	15	5.590	15	5.408
30	2.913	30	3.948	30	5.645	30	5.392
60	2.937	60	3.987	60	5.708	60	5.377
120	2.961	120	4.026	120	5.795	120	5.337
1440	3.221	1440	4.255	1440	6.253	1440	5.274

Standard Test Methods for One-Dimensional Swell or Collapse of Soils - ASTM D4546 - 14

Double Oedometer Method

Trial Type:	Wet		Pre	Post
Project:	SR-10 Subgrade samples	Weight (g):	150.4	159.93
Location:	TP-2	Height (mm):	25.345	23.201
Date:	11/4/2019 14:05	Volume (ft^3):	0.00282	0.00258
Personnel:	HB	Wet Wt. (g):	49.61	60.03
Compaction:	Harvard Miniature tamper	Dry Wt. (g):	46.97	53.94
Target (RC-WC):	96-14	Tare (g):	26.75	26.35
		Tare ID:	5	3(1)
h (mm):	25.345	WC (%):	13.06	22.07
Δh1 (mm):	0.004	Dry Density (pcf):	104.10	112.00
h1 (mm):	25.341	RC (%):	96.66	103.99

Load (tsf):	0.01	Load (tsf):	0.25	Load (tsf):	0.5	Load (tsf):	1
WETTING							
Time (min):	Strain (%)	Time (min):	Strain (%)	Time (min):	Strain (%)	Time (min):	Strain (%)
0	0.016	0	-4.704	0	-2.289	0	0.671
0.1	0.055	0.1	-3.417	0.1	-0.971	0.1	2.502
0.25	0.063	0.25	-3.236	0.25	-0.781	0.25	2.739
0.5	0.079	0.5	-3.086	0.5	-0.584	0.5	2.960
1	0.079	1	-2.920	1	-0.395	1	3.196
2	0.063	2	-2.762	2	-0.213	2	3.441
4	0.024	4	-2.644	4	-0.055	4	3.678
8	-0.055	8	-2.565	8	0.087	8	3.883
15	-0.213	15	-2.494	15	0.174	15	4.049
30	-0.560	30	-2.431	30	0.284	30	4.199
60	-1.010	60	-2.383	60	0.387	60	4.317
120	-1.736	120	-2.344	120	0.497	120	4.420
1440	-4.704	1440	-2.289	1440	0.671	1440	4.585

Load (tsf):	2	Load (tsf):	4	Load (tsf):	8	Load (tsf):	0.01
Time (min):	Strain (%)	Time (min):	Strain (%)	Time (min):	Strain (%)	Time (min):	Strain (%)
0	4.585	0	8.745	0	12.494	0	16.227
0.1	6.353	0.1	10.489	0.1	14.261	0.1	14.940
0.25	6.543	0.25	10.647	0.25	14.317	0.25	14.822
0.5	6.701	0.5	10.757	0.5	14.388	0.5	14.727
1	6.890	1	10.891	1	14.538	1	14.601
2	7.103	2	11.073	2	14.648	2	14.380
4	7.340	4	11.239	4	14.798	4	14.190
8	7.632	8	11.475	8	15.003	8	13.875
15	7.877	15	11.681	15	15.232	15	13.496
30	8.113	30	11.925	30	15.469	30	12.936
60	8.303	60	12.123	60	15.690	60	12.296
120	8.453	120	12.265	120	15.872	120	11.452
1440	8.745	1440	12.494	1440	16.227	1440	8.445

Trial Type:	As-compacted		Pre	Post
Project:	SR-10 Subgrade samples	Weight (g):	150.73	155.44
Location:	TP-2	Height (mm):	25.332	23.494
Date:	11/4/2019 14:05	Volume (ft^3):	0.00282	0.00261
Personnel:	HB	Wet Wt. (g):	49.61	58.08
Compaction:	Harvard Miniature tamper	Dry Wt. (g):	46.97	53.49
Target (RC-WC):	96-14	Tare (g):	26.75	26.75
		Tare ID:	5	#5
h (mm):	25.332	WC (%):	13.06	17.17
Δh1 (mm):	0.000	Dry Density (pcf):	104.30	111.91
h1 (mm):	25.332	RC (%):	96.84	103.91

Load (tsf):	0.01	Load (tsf):	0.25	Load (tsf):	0.5	Load (tsf):	1
WETTING							
Time (min):	Strain (%)	Time (min):	Strain (%)	Time (min):	Strain (%)	Time (min):	Strain (%)
0	0.000	0	0.158	0	0.632	0	1.105
0.1	0.000	0.1	0.308	0.1	0.695	0.1	1.216
0.25	0.000	0.25	0.316	0.25	0.711	0.25	1.232
0.5	0.000	0.5	0.316	0.5	0.711	0.5	1.232
1	0.000	1	0.324	1	0.718	1	1.240
2	0.000	2	0.324	2	0.718	2	1.240
4	0.000	4	0.324	4	0.718	4	1.247
8	0.000	8	0.339	8	0.726	8	1.247
15	0.000	15	0.363	15	0.734	15	1.271
30	0.000	30	0.379	30	0.750	30	1.287
60	0.000	60	0.395	60	0.766	60	1.311
120	0.000	120	0.418	120	0.797	120	1.358
1440	0.158	1440	0.632	1440	1.105	1440	1.634

Load (tsf):	2	Load (tsf):	4	Load (tsf):	8	Load (tsf):	8
						WET	
Time (min):	Strain (%)	Time (min):	Strain (%)	Time (min):	Strain (%)	Time (min):	Strain (%)
0	1.634	0	2.274	0	3.032	0.01	4.405
0.1	1.800	0.1	2.574	0.1	3.987	0.1	4.445
0.25	1.808	0.25	2.590	0.25	3.987	0.25	4.532
0.5	1.808	0.5	2.605	0.5	3.987	0.5	4.571
1	1.824	1	2.613	1	3.987	1	4.595
2	1.832	2	2.621	2	3.987	2	4.627
4	1.840	4	2.637	4	3.987	4	4.658
8	1.855	8	2.661	8	3.995	8	4.690
15	1.871	15	2.676	15	4.011	15	4.705
30	1.879	30	2.692	30	4.019	30	4.729
60	1.903	60	2.732	60	4.034	60	4.745
120	1.958	120	2.763	120	4.090	120	4.777
1440	2.274	1440	3.032	1440	4.405	1440	7.256

Standard Test Methods for One-Dimensional Swell or Collapse of Soils - ASTM D4546 - 14

Double Oedometer Method

			Pre	Post
Trial Type:	Wet			
Project:	SR-10 Subgrade samples	Weight (g):	167.53	170.27
Location:	TP-2	Height (mm):	25.392	26.824
Date:	10/5/2019	Volume (ft^3):	0.00284	0.00300
Personnel:	HB	Wet Wt. (g):	67.55	52.75
Compaction:	Harvard Miniature tamper	Dry Wt. (g):	62.12	48.82
Target (RC-WC):	106-12	Tare (g):	22.89	22.82
		Tare ID:	#13	13
h (mm):	25.392	WC (%):	13.84	15.12
Δh1 (mm):	-0.014	Dry Density (pcf):	114.40	108.85
h1 (mm):	25.406	RC (%):	106.22	101.06

Load (tsf):	0.01	Load (tsf):	0.25	Load (tsf):	0.5	Load (tsf):	1
WETTING							
Time (min):	Strain (%)	Time (min):	Strain (%)	Time (min):	Strain (%)	Time (min):	Strain (%)
0	-0.055	0	-9.470	0	-8.164	0	-6.998
0.1	-0.063	0.1	-9.085	0.1	-7.998	0.1	-6.558
0.25	-0.079	0.25	-9.006	0.25	-7.951	0.25	-6.495
0.5	-0.094	0.5	-8.935	0.5	-7.927	0.5	-6.432
1	-0.126	1	-8.856	1	-7.872	1	-6.353
2	-0.197	2	-8.762	2	-7.817	2	-6.274
4	-0.307	4	-8.652	4	-7.746	4	-6.164
8	-0.496	8	-8.534	8	-7.652	8	-6.046
15	-0.748	15	-8.423	15	-7.565	15	-5.904
30	-1.149	30	-8.305	30	-7.447	30	-5.715
60	-1.748	60	-8.211	60	-7.313	60	-5.526
120	-2.629	120	-8.156	120	-7.203	120	-5.322
1440	-9.470	1440	-8.164	1440	-6.998	1440	-5.078

Load (tsf):	2	Load (tsf):	4	Load (tsf):	8	Load (tsf):	0.01
Time (min):	Strain (%)	Time (min):	Strain (%)	Time (min):	Strain (%)	Time (min):	Strain (%)
0	-5.078	0	-2.582	0	0.567	0	3.913
0.1	-4.393	0.1	-1.637	0.1	1.472	0.1	3.047
0.25	-4.306	0.25	-1.567	0.25	1.567	0.25	2.944
0.5	-4.235	0.5	-1.456	0.5	1.645	0.5	2.850
1	-4.157	1	-1.362	1	1.732	1	2.755
2	-4.046	2	-1.244	2	1.858	2	2.598
4	-3.928	4	-1.102	4	2.015	4	2.409
8	-3.794	8	-0.937	8	2.204	8	2.126
15	-3.645	15	-0.756	15	2.448	15	1.787
30	-3.393	30	-0.488	30	2.779	30	1.275
60	-3.204	60	-0.165	60	3.157	60	0.575
120	-2.952	120	-0.134	120	3.558	120	-0.339
1440	-2.582	1440	0.567	1440	3.913	1440	-5.581

Trial Type:	As-compacted		Pre	Post
Project:	SR-10 Subgrade samples	Weight (g):	167.14	153.74
Location:	TP-2	Height (mm):	25.345	24.843
Date:	10/5/2019	Volume (ft^3):	0.00282	0.00276
Personnel:	HB	Wet Wt. (g):	67.55	88.52
Compaction:	Harvard Miniature tamper	Dry Wt. (g):	62.12	82.91
Target (RC-WC):	106-12	Tare (g):	22.89	26.22
		Tare ID:	#13	2(2)
h (mm):	25.345	WC (%):	13.84	9.90
Δh1 (mm):	0.000	Dry Density (pcf):	114.89	111.69
h1 (mm):	25.345	RC (%):	106.68	103.70

Load (tsf):	0.01	Load (tsf):	0.25	Load (tsf):	0.5	Load (tsf):	1
Time (min):	Strain (%)	Time (min):	Strain (%)	Time (min):	Strain (%)	Time (min):	Strain (%)
0	0.000	0	0.008	0	0.450	0	0.750
0.1	0.000	0.1	0.134	0.1	0.473	0.1	0.797
0.25	0.000	0.25	0.150	0.25	0.473	0.25	0.805
0.5	0.000	0.5	0.158	0.5	0.473	0.5	0.805
1	0.008	1	0.158	1	0.473	1	0.805
2	0.008	2	0.158	2	0.489	2	0.805
4	0.008	4	0.166	4	0.489	4	0.821
8	0.008	8	0.174	8	0.489	8	0.821
15	0.008	15	0.174	15	0.497	15	0.829
30	0.008	30	0.197	30	0.497	30	0.844
60	0.008	60	0.205	60	0.505	60	0.860
120	0.008	120	0.229	120	0.537	120	0.892
1440	0.008	1440	0.450	1440	0.750	1440	1.089

Load (tsf):	2	Load (tsf):	4	Load (tsf):	8	Load (tsf):	0.01
Time (min):	Strain (%)	Time (min):	Strain (%)	Time (min):	Strain (%)	Time (min):	Strain (%)
0	1.089	0	1.491	0	2.012	0	2.786
0.1	1.192	0.1	1.657	0.1	2.296	0.1	2.249
0.25	1.192	0.25	1.673	0.25	2.328	0.25	2.241
0.5	1.192	0.5	1.673	0.5	2.352	0.5	2.217
1	1.192	1	1.681	1	2.367	1	2.210
2	1.192	2	1.689	2	2.391	2	2.202
4	1.199	4	1.712	4	2.399	4	2.194
8	1.199	8	1.720	8	2.430	8	2.178
15	1.207	15	1.728	15	2.454	15	2.170
30	1.239	30	1.752	30	2.478	30	2.162
60	1.247	60	1.768	60	2.509	60	2.138
120	1.270	120	1.799	120	2.565	120	2.131
1440	1.491	1440	2.012	1440	2.786	1440	1.981

Standard Test Methods for One-Dimensional Swell or Collapse of Soils - ASTM D4546 - 14

Double Oedometer Method

Trial Type:	Wet		Pre	Post
Project:	SR-10 Subgrade samples	Weight (g):	153.28	153.12
Location:	TP-2	Height (mm):	25.34	22.30
Date:	11/15/2019 16:35	Volume (ft^3):	0.00	0.00
Personnel:	HB	Wet Wt. (g):	31.22	39.53
Compaction:	Harvard Miniature tamper	Dry Wt. (g):	30.59	37.14
Target (RC-WC):	96-16	Tare (g):	26.71	23.32
		Tare ID:	#5	G2
h (mm):	25.345	WC (%):	16.24	17.29
Δh1 (mm):	0.004	Dry Density (pcf):	103.19	116.10
h1 (mm):	25.341	RC (%):	95.82	107.80

Load (tsf):	0.01	Load (tsf):	0.25	Load (tsf):	0.5	Load (tsf):	1
WETTING							
Time (min):	Strain (%)	Time (min):	Strain (%)	Time (min):	Strain (%)	Time (min):	Strain (%)
0	0.016	0	-3.394	0	-1.602	0	-0.158
0.1	0.016	0.1	-2.470	0.1	-1.160	0.1	0.868
0.25	0.016	0.25	-2.289	0.25	-1.065	0.25	0.979
0.5	0.016	0.5	-2.170	0.5	-1.002	0.5	1.089
1	0.016	1	-2.060	1	-0.908	1	1.239
2	0.016	2	-1.949	2	-0.805	2	1.365
4	0.024	4	-1.855	4	-0.695	4	1.507
8	0.024	8	-1.768	8	-0.576	8	1.673
15	-0.016	15	-1.713	15	-0.497	15	1.792
30	-0.150	30	-1.673	30	-0.410	30	1.910
60	-0.387	60	-1.634	60	-0.339	60	2.005
120	-0.742	120	-1.610	120	-0.260	120	2.084
1440	-3.394	1440	-1.602	1440	-0.158	1440	2.249

Load (tsf):	2	Load (tsf):	4	Load (tsf):	8	Load (tsf):	0.01
Time (min):	Strain (%)	Time (min):	Strain (%)	Time (min):	Strain (%)	Time (min):	Strain (%)
0	2.249	0	5.580	0	8.784	0	0.000
0.1	4.025	0.1	7.135	0.1	10.221	0.1	0.000
0.25	4.199	0.25	7.245	0.25	10.331	0.25	0.000
0.5	4.333	0.5	7.324	0.5	10.434	0.5	0.000
1	4.499	1	7.435	1	10.568	1	0.000
2	4.593	2	7.561	2	10.678	2	0.000
4	4.728	4	7.711	4	10.820	4	0.000
8	4.885	8	7.861	8	10.994	8	0.000
15	5.035	15	8.034	15	11.160	15	0.000
30	5.185	30	8.208	30	11.365	30	0.000
60	5.288	60	8.366	60	11.554	60	0.000
120	5.398	120	8.484	120	11.704	120	0.000
1440	5.580	1440	8.713	1440	11.996	1440	0.000

Trial Type:	As-compacted		Pre	Post
Project:	SR-10 Subgrade samples	Weight (g):	153.52	144.15
Location:	TP-2	Height (mm):	25.33	23.77
Date:	11/15/2019 16:35	Volume (ft^3):	0.00282	0.00264
Personnel:	HB	Wet Wt. (g):	31.22	62.41
Compaction:	Harvard Miniature tamper	Dry Wt. (g):	30.59	58.65
Target (RC-WC):	96-16	Tare (g):	26.71	22.37
		Tare ID:	#5	21.00
h (mm):	25.332	WC (%):	16.24	10.36
Δh1 (mm):	0.000	Dry Density (pcf):	103.33	108.88
h1 (mm):	25.332	RC (%):	95.94	101.09

Load (tsf):	0.01	Load (tsf):	0.25	Load (tsf):	0.5	Load (tsf):	1
WETTING							
Time (min):	Strain (%)	Time (min):	Strain (%)	Time (min):	Strain (%)	Time (min):	Strain (%)
0	0.000	0	0.016	0	0.868	0	1.658
0.1	0.000	0.1	0.276	0.1	1.042	0.1	1.863
0.25	0.000	0.25	0.284	0.25	1.050	0.25	1.871
0.5	0.000	0.5	0.284	0.5	1.058	0.5	1.879
1	0.000	1	0.300	1	1.066	1	1.895
2	0.000	2	0.308	2	1.082	2	1.903
4	0.000	4	0.324	4	1.090	4	1.911
8	0.016	8	0.347	8	1.105	8	1.934
15	0.016	15	0.363	15	1.121	15	1.950
30	0.016	30	0.411	30	1.137	30	1.982
60	0.016	60	0.450	60	1.161	60	2.013
120	0.016	120	0.489	120	1.208	120	2.053
1440	0.016	1440	0.868	1440	1.658	1440	2.384

Load (tsf):	2	Load (tsf):	4	Load (tsf):	8	Load (tsf):	8
						WET	
Time (min):	Strain (%)	Time (min):	Strain (%)	Time (min):	Strain (%)	Time (min):	Strain (%)
0	2.140	0	3.111	0	4.698	0.01	0.000
0.1	2.534	0.1	3.608	0.1	5.416	0.1	0.000
0.25	2.550	0.25	3.640	0.25	5.432	0.25	0.000
0.5	2.574	0.5	3.655	0.5	5.448	0.5	0.000
1	2.590	1	3.679	1	5.471	1	0.000
2	2.613	2	3.703	2	5.487	2	0.000
4	2.637	4	3.742	4	5.519	4	0.000
8	2.653	8	3.766	8	5.558	8	0.000
15	2.676	15	3.798	15	5.582	15	0.000
30	2.700	30	3.837	30	5.613	30	0.000
60	2.740	60	3.876	60	5.653	60	0.000
120	2.787	120	3.924	120	5.692	120	0.000
1440	3.111	1440	4.374	1440	6.150	1440	0.000

13. APPENDIX C: LABORATORY TESTING OF ASPHALT-CONCRETE SAMPLES

The Illinois Flexibility Index Test was used to determine the fracture resistance of the asphalt-concrete field cores as explained in the main body of the report. All results and relevant parameters from the testing are included here. The following values are given: thickness, radius, ligament, notch depth, peak load, displacement at peak load, fracture energy, slope (post-peak), strength, flexibility (flexibility index), secant stiffness, 0%-10% slope (initial slope), and 10%-80% slope (initial).

Location:	1	1	1	1
Alignment:	A	A	A	A
Specimen:	T1	T2	B1	B2
Thickness (mm):	49.9	49.9	50.2	50.1
Ligament (mm):	58.3	59.2	57.4	59.1
Notch Depth (mm):	15.1	14.9	15.8	15.0
Peak Load (kN):	2.71	2.83	3.99	4.24
Disp. at Peak Load (mm):	0.78	0.93	0.68	0.71
Radius (mm):	73.4	74.1	73.2	74.1
Fracture Energy (kJ/m^2):	1149.7	1681.7	1314.9	1661.6
Slope (kN/mm):	-3.65	-2.08	-6.33	-5.74
Strength (kN):	371	383	544	571
Flexibility:	3.1	8	2	2.9
Secant Stiffness (kN/mm):	3.5	3.0	5.8	6.2
0-10% Slope:	6.4	4.5	3.5	2.7
10-80% Slope:	2.7	2.5	3.2	2.4

Location:	1	1	1	1
Alignment:	C	C	C	C
Specimen:	T1	T2	B1	B2
Thickness (mm):	50.2	50.2	50	49.9
Ligament (mm):	59.4	59.5	58.8	59.4
Notch Depth (mm):	14.3	14.9	14.5	14.7
Peak Load (kN):	3.01	2.74	2.65	3.19
Disp. at Peak Load (mm):	0.64	0.69	0.81	0.98
Radius (mm):	73.7	74.4	73.3	74.1
Fracture Energy (kJ/m^2):	839.2	1040.8	1306.2	1663
Slope (kN/mm):	-6.5	-3.43	-2.93	-3.22
Strength (kN):	407	367	361	432
Flexibility:	1.2	3	4.4	5.1
Secant Stiffness (kN/mm):	4.6	3.9	3.2	3.2
0-10% Slope:	6.4	6.2	4.1	9.7
10-80% Slope:	2.4	2.8	3.3	4

Location:	2	2	2	2
Alignment:	A	A	A	A
Specimen:	T1	T2	B1	B2
Thickness (mm):	50.4	50.4	52.4	52.2
Ligament (mm):	60.8	57.2	58.4	59.6
Notch Depth (mm):	14.6	15	15.4	15.4
Peak Load (kN):	5.45	3.79	4.61	6
Disp. at Peak Load (mm):	0.44	0.72	0.66	0.72
Radius (mm):	75.4	72.2	73.8	75
Fracture Energy (kJ/m^2):	1188.3	797.1	1619.6	2152.1
Slope (kN/mm):	-14.48	-18.4	-7.43	-8.05
Strength (kN):	718	521	596	766
Flexibility:	0.8	0.4	2.1	2.6
Secant Stiffness (kN/mm):	12	5.4	7	8.3
0-10% Slope:	6.4	4.5	3.5	2.7
10-80% Slope:	2.7	2.5	3.2	2.4

Location:	2	2	2	2
Alignment:	B	B	B	B
Specimen:	T1	T2	B1	B2
Thickness (mm):	49.9	49.8	50	50
Ligament (mm):	59.6	58.6	60.2	58.6
Notch Depth (mm):	14.4	14.8	14.2	14.5
Peak Load (kN):	2.79	2.49	3.56	3.97
Disp. at Peak Load (mm):	1.07	0.8	0.62	0.52
Radius (mm):	74	73.4	74.4	73.1
Fracture Energy (kJ/m^2):	1653.3	1467.1	1073.1	1085.1
Slope (kN/mm):	-2.4	-1.61	-7.88	-7.98
Strength (kN):	378	341	479	543
Flexibility:	6.8	9.1	1.3	1.3
Secant Stiffness (kN/mm):	2.6	3.1	5.7	7.6
0-10% Slope:	6.4	4.5	3.5	2.7
10-80% Slope:	2.7	2.5	3.2	2.4

Location:	3	3	3	3
Alignment:	A	A	A	A
Specimen:	T1	T2	B1	B2
Thickness (mm):	50.5	50.5	50.6	50.1
Ligament (mm):	59.2	60	59.6	58.5
Notch Depth (mm):	14.2	14.4	14.2	15.9
Peak Load (kN):	3.56	3.81	2.74	3.67
Disp. at Peak Load (mm):	0.6	0.66	0.7	0.56
Radius (mm):	73.4	74.4	73.8	74.4
Fracture Energy (kJ/m^2):	1538	797.1	1141.5	1353.4
Slope (kN/mm):	-3.72	-3.34	-3.36	-4.25
Strength (kN):	481	507	367	493
Flexibility:	4.1	5.3	3.4	3.1
Secant Stiffness (kN/mm):	5.9	5.8	3.9	6.5
0-10% Slope:	6.4	4.5	3.5	2.7
10-80% Slope:	2.7	2.5	3.2	2.4

Location:	3	3	3	3
Alignment:	B	B	B	B
Specimen:	T1	T2	B1	B2
Thickness (mm):	50.1	50.1	50.1	50.2
Ligament (mm):	59.7	59.1	60.1	58.9
Notch Depth (mm):	14.1	14.5	14.2	14.3
Peak Load (kN):	1.77	1.79	1.64	2.11
Disp. at Peak Load (mm):	0.84	1.03	0.41	0.55
Radius (mm):	73.8	73.6	74.3	73.2
Fracture Energy (kJ/m^2):	998.7	1297.8	405.8	669.8
Slope (kN/mm):	-1.41	-0.87	-4.08	-2.88
Strength (kN):	239	242	220	287
Flexibility:	7	14	0.9	2.3
Secant Stiffness (kN/mm):	2.1	1.7	4.0	3.8
0-10% Slope:	6.4	4.5	3.5	2.7
10-80% Slope:	2.7	2.5	3.2	2.4

Location:	3	3	3	3
Alignment:	C	C	C	C
Specimen:	T1	T2	B1	B2
Thickness (mm):	50.1	50.6	50	50.1
Ligament (mm):	58.9	59.3	59.1	59.9
Notch Depth (mm):	14.4	14.6	14.3	14.5
Peak Load (kN):	4.16	1.98	2.99	3.05
Disp. at Peak Load (mm):	0.82	0.53	0.49	0.52
Radius (mm):	73.3	73.9	73.4	74.4
Fracture Energy (kJ/m^2):	1519.6	797.1	671.3	639.9
Slope (kN/mm):	-7.83	-2.27	-6.51	-15.04
Strength (kN):	567	265	408	409
Flexibility:	1.9	2.9	1	0.4
Secant Stiffness (kN/mm):	5.1	3.7	6.1	5.9
0-10% Slope:	6.4	4.5	3.5	2.7
10-80% Slope:	2.7	2.5	3.2	2.4

Location:	4	4	4	4
Alignment:	A	A	A	A
Specimen:	T1	T2	B1	B2
Thickness (mm):	50.6	50.5	49.8	49.9
Ligament (mm):	59.1	60.2	59.9	58.4
Notch Depth (mm):	14.4	14.2	14.8	14.9
Peak Load (kN):	1.57	1.77	2.26	2.54
Disp. at Peak Load (mm):	0.4	0.33	0.74	0.7
Radius (mm):	73.5	74.4	74.7	73.3
Fracture Energy (kJ/m^2):	305.8	393.7	871.3	1047.7
Slope (kN/mm):	-3.8	-4.29	-3.83	-3.05
Strength (kN):	211	236	304	348
Flexibility:	0.8	0.9	2.2	3.4
Secant Stiffness (kN/mm):	3.9	5.3	3.0	3.6
0-10% Slope:	6.4	4.5	3.5	2.7
10-80% Slope:	2.7	2.5	3.2	2.4

Location:	4	4	4	4
Alignment:	B	B	B	B
Specimen:	T1	T2	B1	B2
Thickness (mm):	50.1	50.3	50.3	50.1
Ligament (mm):	59.4	59.3	59.3	59
Notch Depth (mm):	14.5	14.3	14.3	14.3
Peak Load (kN):	2.41	2.42	3.26	3.17
Disp. at Peak Load (mm):	0.68	0.92	0.58	0.69
Radius (mm):	73.9	73.6	73.6	73.3
Fracture Energy (kJ/m^2):	1351.5	1501.4	988.1	1019.4
Slope (kN/mm):	-1.57	-1.7	-4.96	-6.55
Strength (kN):	326	327	440	431
Flexibility:	8.6	8.8	1.9	1.5
Secant Stiffness (kN/mm):	3.5	2.6	5.6	4.6
0-10% Slope:	6.4	6.2	4.1	9.7
10-80% Slope:	2.4	2.8	3.3	4

Location:	4	4	4	4
Alignment:	C	C	C	C
Specimen:	T1	T2	B1	B2
Thickness (mm):	49.9	49.9	49.9	50
Ligament (mm):	58.8	59.1	58.8	59.4
Notch Depth (mm):	14.8	14.3	14.8	14.3
Peak Load (kN):	2.13	2.23	3.06	2.62
Disp. at Peak Load (mm):	0.59	0.86	0.66	0.79
Radius (mm):	73.6	73.4	73.7	73.7
Fracture Energy (kJ/m^2):	715.4	908.3	1061.5	1013.8
Slope (kN/mm):	-3.46	-3.46	-4.16	-2.69
Strength (kN):	291	305	416.4	355
Flexibility:	2	2.6	2.55	3.7
Secant Stiffness (kN/mm):	4	3	3	3
0-10% Slope:	0	0		0
10-80% Slope:	0	0		0

Location:	5	5	5	5
Alignment:	A	A	A	A
Specimen:	T1	T2	B1	B2
Thickness (mm):	50.6	50.5	50	49.9
Ligament (mm):	56.5	59.6	56.6	60.6
Notch Depth (mm):	16.6	15.4	16.6	14.0
Peak Load (kN):	3.53	3.59	2.1	3.16
Disp. at Peak Load (mm):	0.89	0.84	0.9	0.79
Radius (mm):	73.1	75	73.2	74.6
Fracture Energy (kJ/m^2):	2276.8	2526.6	1010.7	1167.6
Slope (kN/mm):	-2.46	-2.53	-2.62	-5.77
Strength (kN):	477	473	287	425
Flexibility:	9.2	9.9	3.8	2
Secant Stiffness (kN/mm):	4.0	4.2	2.3	4.0
0-10% Slope:	6.4	4.5	3.5	2.7
10-80% Slope:	2.7	2.5	3.2	2.4

Location:	5	5	5	5
Alignment:	B	B	B	B
Specimen:	T1	T2	B1	B2
Thickness (mm):	49.8	49.9	50.2	50
Ligament (mm):	59.9	58.5	60.3	58.4
Notch Depth (mm):	14.2	14.8	14.1	14.6
Peak Load (kN):	1.94	1.61	2.81	2.62
Disp. at Peak Load (mm):	0.83	0.71	0.66	0.72
Radius (mm):	74.1	73.3	74.4	73
Fracture Energy (kJ/m^2):	1001.7	1073.1	1358.1	1218.5
Slope (kN/mm):	-1.67	-1.34	-2.07	-1.89
Strength (kN):	263	220	376	360
Flexibility:	6	8	6.5	6.4
Secant Stiffness (kN/mm):	2.3	2.2	4.2	3.6
0-10% Slope:	6.4	4.5	3.5	2.7
10-80% Slope:	2.7	2.5	3.2	2.4

Location:	5	5	5	5
Alignment:	C	C	C	C
Specimen:	T1	T2	B1	B2
Thickness (mm):	50	50	49.8	49.8
Ligament (mm):	58.6	59.9	59.8	57.4
Notch Depth (mm):	15.0	14.1	14.2	16.0
Peak Load (kN):	4.55	4.25	4.58	4.07
Disp. at Peak Load (mm):	0.66	0.63	0.51	0.54
Radius (mm):	73.6	74	74	73.4
Fracture Energy (kJ/m^2):	1674.4	797.1	1051.8	1044.6
Slope (kN/mm):	-6.71	-4.75	-14.77	-9.77
Strength (kN):	618	574	622	557
Flexibility:	2.4	3.5	0.7	1
Secant Stiffness (kN/mm):	6.9	6.7	8.9	7.4
0-10% Slope:	6.4	4.5	3.5	2.7
10-80% Slope:	2.7	2.5	3.2	2.4

Location:	6	6	6	6
Alignment:	A	A	A	A
Specimen:	T1	T2	B1	B2
Thickness (mm):	50.4	50.1	50.2	50.1
Ligament (mm):	58.8	60.3	59.1	59.9
Notch Depth (mm):	14.1	14.4	14.4	14.0
Peak Load (kN):	3.54	3.92	4.57	3.52
Disp. at Peak Load (mm):	0.7	0.57	0.58	0.58
Radius (mm):	72.9	74.7	73.5	73.9
Fracture Energy (kJ/m^2):	1123.1	1156.1	965.6	891.6
Slope (kN/mm):	-6.45	-6.99	-12.94	-6.93
Strength (kN):	482	524	619	475
Flexibility:	1.7	1.6	0.7	1.2
Secant Stiffness (kN/mm):	5.0	6.9	7.8	6.0
0-10% Slope:	6.4	4.5	3.5	2.7
10-80% Slope:	2.7	2.5	3.2	2.4

Location:	6	6	6	6
Alignment:	B	B	B	B
Specimen:	T1	T2	B1	B2
Thickness (mm):	49.8	49.8	50.2	50.2
Ligament (mm):	58.9	59.1	59	58.9
Notch Depth (mm):	15.0	14.5	14.9	14.6
Peak Load (kN):	4.21	4.27	4.59	4.09
Disp. at Peak Load (mm):	0.81	0.92	0.74	0.64
Radius (mm):	73.9	73.6	73.9	73.5
Fracture Energy (kJ/m^2):	1549.7	1861.6	1505.1	1241.7
Slope (kN/mm):	-8.24	-5.5	-9.1	-8.4
Strength (kN):	572	583	618	555
Flexibility:	1.8	3.3	1.6	1.4
Secant Stiffness (kN/mm):	5.2	4.6	6.1	6.4
0-10% Slope:	6.4	6.2	4.1	9.7
10-80% Slope:	2.4	2.8	3.3	4

Location:	6	6	6	6
Alignment:	C	C	C	C
Specimen:	T1	T2	B1	B2
Thickness (mm):	50.5	50.5	49.3	49.4
Ligament (mm):	59.5	58.6	59.8	59.5
Notch Depth (mm):	14.6	14.9	14.4	14.1
Peak Load (kN):	3.89	3.58	3.39	3.65
Disp. at Peak Load (mm):	0.55	0.64	0.49	0.6
Radius (mm):	74.1	73.5	74.2	73.6
Fracture Energy (kJ/m^2):	1184	1200.4	784.9	895.8
Slope (kN/mm):	-6.32	-5.65	-7	-8.06
Strength (kN):	519	483	464.3	502
Flexibility:	1.8	2.1	1.12	1.1
Secant Stiffness (kN/mm):	7	6	7	6
0-10% Slope:	0	0		0
10-80% Slope:	0	0		0

Location:	7	7	7	7
Alignment:	B	B	B	B
Specimen:	T1	T2	B1	B2
Thickness (mm):	50.3	50.3	50.1	50.1
Ligament (mm):	60	59.1	60.4	58.8
Notch Depth (mm):	14.1	14.8	14.1	14.6
Peak Load (kN):	3.34	2.88	3.68	2.13
Disp. at Peak Load (mm):	0.58	0.68	0.47	0.41
Radius (mm):	74.1	73.9	74.5	73.4
Fracture Energy (kJ/m^2):	1102	1252.3	918.6	560
Slope (kN/mm):	-4.72	-2.29	-7.56	-3.92
Strength (kN):	449	387	493	290
Flexibility:	2.3	5.4	1.2	1.4
Secant Stiffness (kN/mm):	5.7	4.2	7.9	5.2
0-10% Slope:	6.4	4.5	3.5	2.7
10-80% Slope:	2.7	2.5	3.2	2.4

Location:	8	8	8	8
Alignment:	A	A	A	A
Specimen:	T1	T2	B1	B2
Thickness (mm):	50.2	50.1	50	49.9
Ligament (mm):	60	59.1	58.5	58.9
Notch Depth (mm):	14.2	14.6	14.9	14.6
Peak Load (kN):	2.55	4.08	2.97	3.78
Disp. at Peak Load (mm):	0.62	0.57	0.41	0.58
Radius (mm):	74.2	73.7	73.4	73.5
Fracture Energy (kJ/m^2):	622.5	1156.4	474.8	850.9
Slope (kN/mm):	-5.05	-7.17	NoneSt	-16.94
Strength (kN):	342	553	405	515
Flexibility:	1.2	1.6	Non	0.5
Secant Stiffness (kN/mm):	4.1	7.1	7.3	6.5
0-10% Slope:	6.4	4.5	3.5	2.7
10-80% Slope:	2.7	2.5	3.2	2.4

Location:	8	8	8	8
Alignment:	B	B	B	B
Specimen:	T1	T2	B1	B2
Thickness (mm):	50.1	50	49.9	49.8
Ligament (mm):	58.7	60.1	58.4	60
Notch Depth (mm):	14.6	14.2	14.5	14.6
Peak Load (kN):	4.53	4.92	2.88	2.94
Disp. at Peak Load (mm):	0.51	0.67	0.44	0.57
Radius (mm):	73.3	74.3	72.9	74.6
Fracture Energy (kJ/m^2):	1165.6	1336.4	810.4	896.1
Slope (kN/mm):	-8.02	-16.65	-4.59	-5.44
Strength (kN):	617	662	397	396
Flexibility:	1.4	0.8	1.7	1.6
Secant Stiffness (kN/mm):	8.9	7.3	6.6	5.1
0-10% Slope:	6.4	6.2	4.1	9.7
10-80% Slope:	2.4	2.8	3.3	4

Location:	8	8	8	8
Alignment:	C	C	C	C
Specimen:	T1	T2	B1	B2
Thickness (mm):	50	50.1	50	49.9
Ligament (mm):	59	59.3	59.8	58.7
Notch Depth (mm):	14.9	14.5	14.7	14.8
Peak Load (kN):	4.71	4.2	4.37	3.67
Disp. at Peak Load (mm):	0.61	0.7	0.56	0.55
Radius (mm):	73.9	73.8	74.5	73.5
Fracture Energy (kJ/m^2):	1372.9	1433.2	970	793.3
Slope (kN/mm):	-11.67	-8.05	-19.07	-13.88
Strength (kN):	638	568	587	501
Flexibility:	1.1	1.7	0.51	0.5
Secant Stiffness (kN/mm):	8	6	8	7
0-10% Slope:	0	0	0.88	0
10-80% Slope:	0	0		0

Location:	9	9	9	9
Alignment:	B	B	B	B
Specimen:	T1	T2	B1	B2
Thickness (mm):	50	50.2	49.8	49.8
Ligament (mm):	60.2	57.9	58.7	59.7
Notch Depth (mm):	14.1	15.0	14.4	14.9
Peak Load (kN):	2.4	2.21	1.87	1.72
Disp. at Peak Load (mm):	0.83	0.79	0.52	0.47
Radius (mm):	74.3	72.9	73.1	74.6
Fracture Energy (kJ/m^2):	1119.2	1058.6	715.8	437.1
Slope (kN/mm):	-2.56	-2.13	-2	-3.53
Strength (kN):	324	302	257	232
Flexibility:	4.3	4.9	3.5	1.2
Secant Stiffness (kN/mm):	2.9	2.7	3.5	3.6
0-10% Slope:	6.4	4.5	3.5	2.7
10-80% Slope:	2.7	2.5	3.2	2.4

Location:	9	9	9	9
Alignment:	C	C	C	C
Specimen:	T1	T2	B1	B2
Thickness (mm):	50.8	50.8	50.8	50.1
Ligament (mm):	59.9	59.3	59.3	58.6
Notch Depth (mm):	14.3	14.2	14.2	14.4
Peak Load (kN):	4.27	4.33	4.76	3.56
Disp. at Peak Load (mm):	0.82	0.78	0.53	0.43
Radius (mm):	74.2	73.5	73.5	73
Fracture Energy (kJ/m^2):	1873.8	797.1	1039.4	780.3
Slope (kN/mm):	-5.07	-4.28	-16.82	-8.39
Strength (kN):	566	580	638	487
Flexibility:	3.7	4.7	0.6	0.9
Secant Stiffness (kN/mm):	5.2	5.5	8.9	8.2
0-10% Slope:	6.4	4.5	3.5	2.7
10-80% Slope:	2.7	2.5	3.2	2.4

Location:	10	10	10	10
Alignment:	A	A	A	A
Specimen:	T1	T2	B1	B2
Thickness (mm):	50	49.9	50.3	49.9
Ligament (mm):	57.9	57.6	60	58.6
Notch Depth (mm):	15.2	16.7	14.7	14.4
Peak Load (kN):	3.25	2.69	2.74	2.29
Disp. at Peak Load (mm):	0.84	0.85	0.55	0.69
Radius (mm):	73.1	74.3	74.7	73
Fracture Energy (kJ/m^2):	1690.5	1507.1	889.7	945.5
Slope (kN/mm):	-3.32	-2.33	-4.67	-3.14
Strength (kN):	444	363	364	315
Flexibility:	5	6.4	1.9	3
Secant Stiffness (kN/mm):	3.8	3.1	5.0	3.3
0-10% Slope:	6.4	4.5	3.5	2.7
10-80% Slope:	2.7	2.5	3.2	2.4

Location:	10	10	10	10
Alignment:	B	B	B	B
Specimen:	T1	T2	B1	B2
Thickness (mm):	50	49.9	50.1	50.1
Ligament (mm):	59	59.4	59.9	58.8
Notch Depth (mm):	14.6	14.6	14.2	14.8
Peak Load (kN):	2.76	2.98	2.79	2.6
Disp. at Peak Load (mm):	0.48	0.67	0.55	0.75
Radius (mm):	73.6	74	74.1	73.6
Fracture Energy (kJ/m^2):	749.9	800.9	926.7	1118.6
Slope (kN/mm):	-3.88	-7.6	-2.75	-2.94
Strength (kN):	375	403	375	353
Flexibility:	1.9	1	3.3	3.8
Secant Stiffness (kN/mm):	5.6	4.4	5.0	3.4
0-10% Slope:	6.4	4.5	3.5	2.7
10-80% Slope:	2.7	2.5	3.2	2.4

Location:	11	11	11	11
Alignment:	A	A	A	A
Specimen:	T1	T2	B1	B2
Thickness (mm):	49.9	49.9	50	50.1
Ligament (mm):	59.6	58.3	58.9	59.6
Notch Depth (mm):	14.7	14.6	14.7	14.5
Peak Load (kN):	1.74	3.06	3.69	3.92
Disp. at Peak Load (mm):	0.54	0.59	0.6	0.76
Radius (mm):	74.3	72.9	73.6	74.1
Fracture Energy (kJ/m^2):	703.1	1065.7	1218.3	1295.8
Slope (kN/mm):	-1.75	-3.69	-6.33	-9.06
Strength (kN):	234	421	501	528
Flexibility:	4	2.8	1.9	1.4
Secant Stiffness (kN/mm):	3.2	5.5	6.1	5.1
0-10% Slope:	6.4	4.5	3.5	2.7
10-80% Slope:	2.7	2.5	3.2	2.4

Location:	11	11	11	11
Alignment:	B	B	B	B
Specimen:	T1	T2	B1	B2
Thickness (mm):	49.9	49.8	50.2	50.2
Ligament (mm):	60.1	59.5	59.9	59.8
Notch Depth (mm):	14.1	14.1	14.0	14.3
Peak Load (kN):	2.56	1.98	2.75	2.74
Disp. at Peak Load (mm):	0.77	0.63	0.56	0.56
Radius (mm):	74.2	73.6	73.9	74.1
Fracture Energy (kJ/m^2):	1028.6	902	797.5	869
Slope (kN/mm):	-2.64	-2.27	-5.57	-4.49
Strength (kN):	346	270	370	368
Flexibility:	3.9	3.9	1.4	1.9
Secant Stiffness (kN/mm):	3.3	3.1	4.9	4.8
0-10% Slope:	6.4	6.2	4.1	9.7
10-80% Slope:	2.4	2.8	3.3	4

Location:	11	11	11	11
Alignment:	C	C	C	C
Specimen:	T1	T2	B1	B2
Thickness (mm):	50	49.9	50.4	50.4
Ligament (mm):	59.8	59.5	58.7	60.3
Notch Depth (mm):	14.2	14.4	15.0	13.9
Peak Load (kN):	3.05	3.27	4.25	4.57
Disp. at Peak Load (mm):	0.66	0.76	0.66	0.93
Radius (mm):	74	73.9	73.7	74.2
Fracture Energy (kJ/m^2):	1061.1	1369.7	1666.3	1844
Slope (kN/mm):	-5.57	-3.29	-4.78	-5.31
Strength (kN):	413	444	572	611
Flexibility:	1.9	4.1	3.4	3.4
Secant Stiffness (kN/mm):	5	4	6.4	5
0-10% Slope:	0	0	0	0
10-80% Slope:	0	0	0	0

Location:	12	12	12	12
Alignment:	A	A	A	A
Specimen:	T1	T2	B1	B2
Thickness (mm):	49.8	49.9	50.7	50.7
Ligament (mm):	59.3	59.2	59.3	59.3
Notch Depth (mm):	14.7	14.6	14.9	14.9
Peak Load (kN):	2.45	2.75	4.53	4.75
Disp. at Peak Load (mm):	0.56	0.73	0.53	0.7
Radius (mm):	74	73.8	74.2	74.2
Fracture Energy (kJ/m^2):	805.2	956.4	1137.1	1256.6
Slope (kN/mm):	-3.95	-3.9	-10.4	-16.56
Strength (kN):	332	374	603	631
Flexibility:	2	2.4	1	0.7
Secant Stiffness (kN/mm):	4.3	3.7	8.6	6.8
0-10% Slope:	6.4	4.5	3.5	2.7
10-80% Slope:	2.7	2.5	3.2	2.4

Location:	12	12	12	12
Alignment:	B	B	B	B
Specimen:	T1	T2	B1	B2
Thickness (mm):	50.2	50.2	50	50
Ligament (mm):	59.6	59.7	59.6	59.6
Notch Depth (mm):	14.4	14.1	14.4	14.4
Peak Load (kN):	2.57	1.99	2.01	1.75
Disp. at Peak Load (mm):	0.77	0.53	0.62	0.52
Radius (mm):	74	73.8	74	74
Fracture Energy (kJ/m^2):	1305.8	889.1	715	532.3
Slope (kN/mm):	-1.95	-1.77	-2.11	-2.99
Strength (kN):	347	268	272	237
Flexibility:	6.6	5	3.3	1.7
Secant Stiffness (kN/mm):	3.3	3.7	3.2	3.3
0-10% Slope:	6.4	6.2	4.1	9.7
10-80% Slope:	2.4	2.8	3.3	4

Location:	12	12	12	12
Alignment:	C	C	C	C
Specimen:	T1	T2	B1	B2
Thickness (mm):	50	50.1	50.1	50
Ligament (mm):	59.1	59.7	58.3	61.1
Notch Depth (mm):	14.6	14.6	14.1	14.2
Peak Load (kN):	1.69	2.18	2.46	2.7
Disp. at Peak Load (mm):	0.39	0.44	0.87	0.97
Radius (mm):	73.7	74.3	72.4	75.3
Fracture Energy (kJ/m^2):	404.9	600.3	1317.3	1373.8
Slope (kN/mm):	-3.5	-4.09	-2.49	-3.19
Strength (kN):	230	293	340	359
Flexibility:	1.1	1.4	5.3	4.3
Secant Stiffness (kN/mm):	4	5	2.8	3
0-10% Slope:	0	0	0	0
10-80% Slope:	0	0	0	0

Location:	13	13	13	13
Alignment:	B	B	B	B
Specimen:	T1	T2	B1	B2
Thickness (mm):	49.9	49.9	50	49.7
Ligament (mm):	58.5	59.2	55.9	60.6
Notch Depth (mm):	15.1	15.3	16.9	14.8
Peak Load (kN):	3.33	2.89	2.5	2.64
Disp. at Peak Load (mm):	0.78	0.81	0.68	0.82
Radius (mm):	73.6	74.5	72.8	75.4
Fracture Energy (kJ/m^2):	1393.9	1267.3	1051.8	1059
Slope (kN/mm):	-4.67	-4.07	-2.86	-4.12
Strength (kN):	453	389	344	352
Flexibility:	2.9	3.1	3.6	2.5
Secant Stiffness (kN/mm):	4.2	3.5	3.6	3.2
0-10% Slope:	6.4	4.5	3.5	2.7
10-80% Slope:	2.7	2.5	3.2	2.4

Location:	14	14	14	14
Alignment:	A	A	A	A
Specimen:	T1	T2	B1	B2
Thickness (mm):	50.1	50.2	50	49.8
Ligament (mm):	59.8	57.6	58.9	59
Notch Depth (mm):	14.6	16.1	15.7	14.9
Peak Load (kN):	3.55	3.27	4.18	3.97
Disp. at Peak Load (mm):	0.97	0.93	0.93	0.84
Radius (mm):	74.4	73.7	74.6	73.9
Fracture Energy (kJ/m^2):	1784.4	1811.4	2033	2013.4
Slope (kN/mm):	-4.26	-2.73	-4.47	-3.41
Strength (kN):	477	442	561	539
Flexibility:	4.1	6.6	4.5	5.9
Secant Stiffness (kN/mm):	3.6	3.6	4.5	4.7
0-10% Slope:	6.4	4.5	3.5	2.7
10-80% Slope:	2.7	2.5	3.2	2.4

Location:	14	14	14	14
Alignment:	B	B	B	B
Specimen:	T1	T2	B1	B2
Thickness (mm):	49.5	49.4	49.9	49.6
Ligament (mm):	60.2	57.3	58.5	56.8
Notch Depth (mm):	14.7	16.2	16.3	16.7
Peak Load (kN):	4.38	3.76	1.88	2.2
Disp. at Peak Load (mm):	0.82	0.66	0.64	0.62
Radius (mm):	74.9	73.5	74.8	73.5
Fracture Energy (kJ/m^2):	1630.2	1452.2	927.5	868.6
Slope (kN/mm):	-6.28	-4.71	-1.43	-2.82
Strength (kN):	590	518	253	302
Flexibility:	2.6	3	6.4	3
Secant Stiffness (kN/mm):	5.3	5.8	2.9	3.5
0-10% Slope:	6.4	4.5	3.5	2.7
10-80% Slope:	2.7	2.5	3.2	2.4

14. APPENDIX D: CONE PENETRATION LOGS

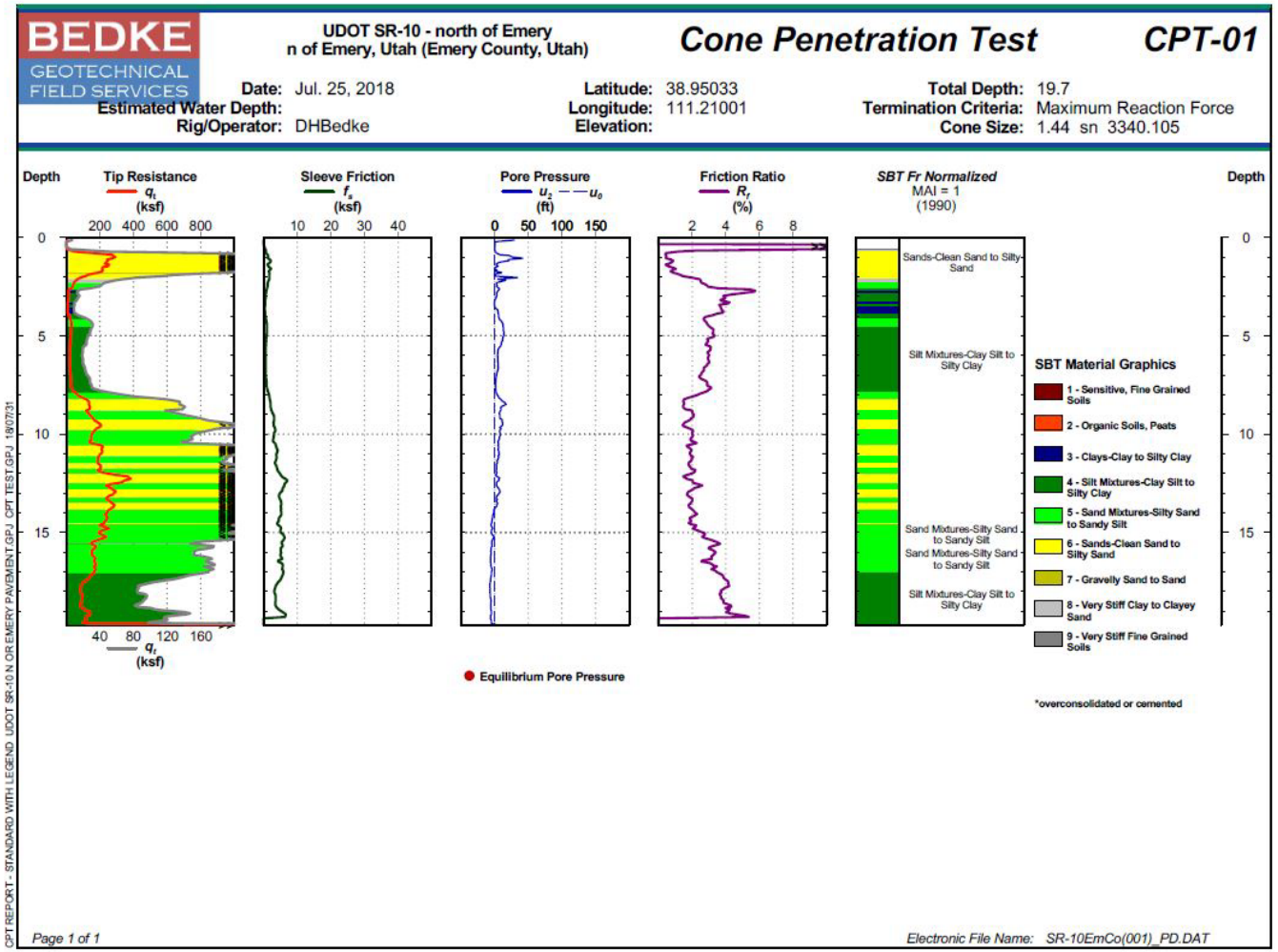

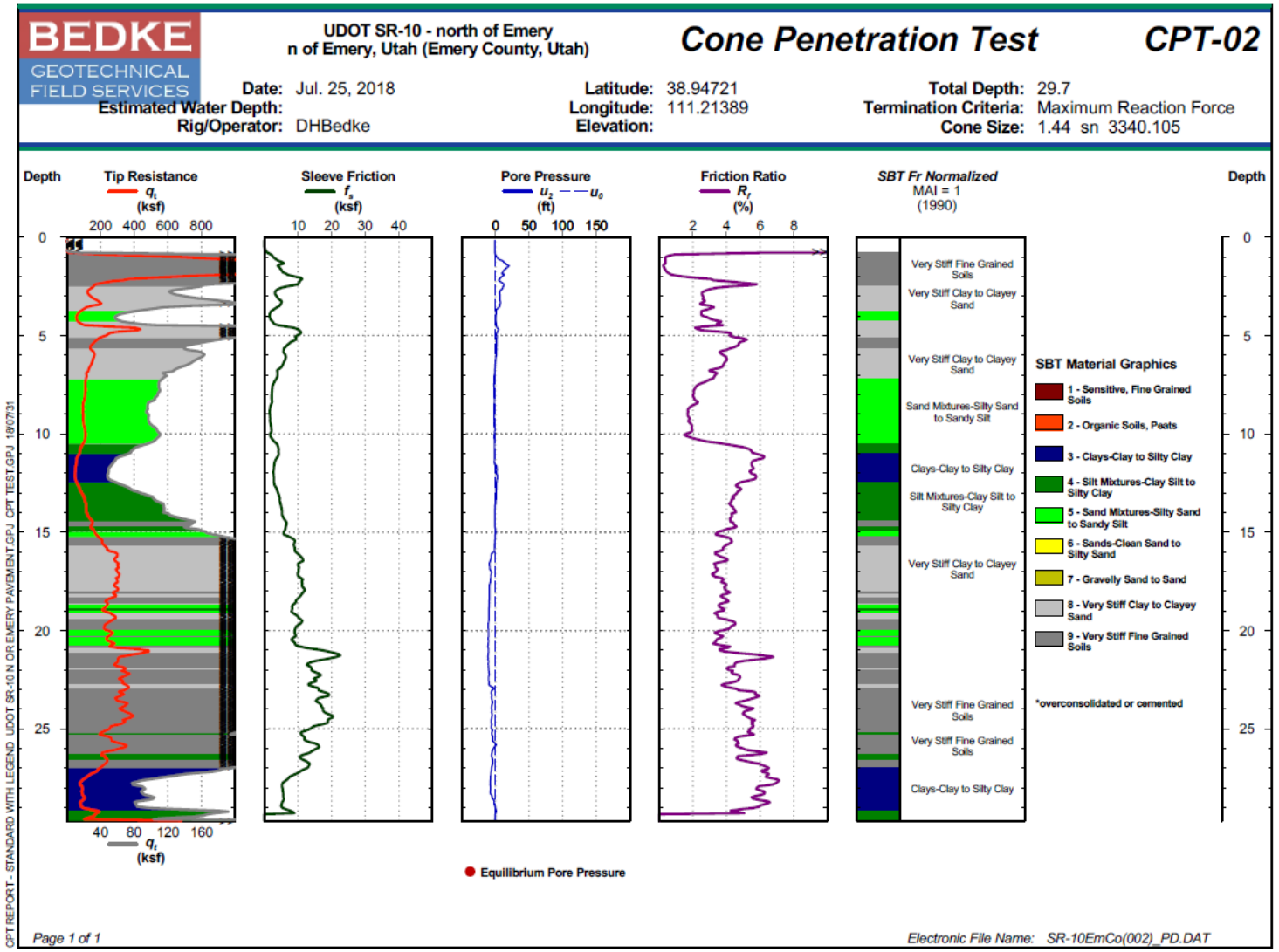
BEDKE
GEOTECHNICAL
FIELD SERVICES
UDOT SR-10 - north of Emery
n of Emery, Utah (Emery County, Utah)
Cone Penetration Test
CPT-02
Date: Jul. 25, 2018
Estimated Water Depth:
Rig/Operator: DHBedke
Latitude: 38.94721
Longitude: 111.21389
Elevation:
Total Depth: 29.7
Termination Criteria: Maximum Reaction Force
Cone Size: 1.44 sn 3340.105
Depth
Tip Resistance
q_t (ksf)
Sleeve Friction
f_s (ksf)
Pore Pressure
u_2 u_0 (ft)
Friction Ratio
R_f (%)
SBT Fr Normalized
MAI = 1
(1990)
Very Stiff Fine Grained Soils
Very Stiff Clay to Clayey Sand
Very Stiff Clay to Clayey Sand
Sand Mixtures-Silty Sand to Sandy Silt
Clays-Clay to Silty Clay
Silt Mixtures-Clay Silt to Silty Clay
Very Stiff Clay to Clayey Sand
Very Stiff Fine Grained Soils
Very Stiff Fine Grained Soils
Clays-Clay to Silty Clay
SBT Material Graphics
1 - Sensitive, Fine Grained Soils
2 - Organic Soils, Peats
3 - Clays-Clay to Silty Clay
4 - Silt Mixtures-Clay Silt to Silty Clay
5 - Sand Mixtures-Silty Sand to Sandy Silt
6 - Sands-Clean Sand to Silty Sand
7 - Gravelly Sand to Sand
8 - Very Stiff Clay to Clayey Sand
9 - Very Stiff Fine Grained Soils
*overconsolidated or cemented
Equilibrium Pore Pressure
CPT REPORT - STANDARD WITH LEGEND UDOT SR-10 N OR EMERY PAVEMENT.GPJ CPT TEST.GPJ 18/07/31
Page 1 of 1
Electronic File Name: SR-10EmCo(002)_PD.DAT

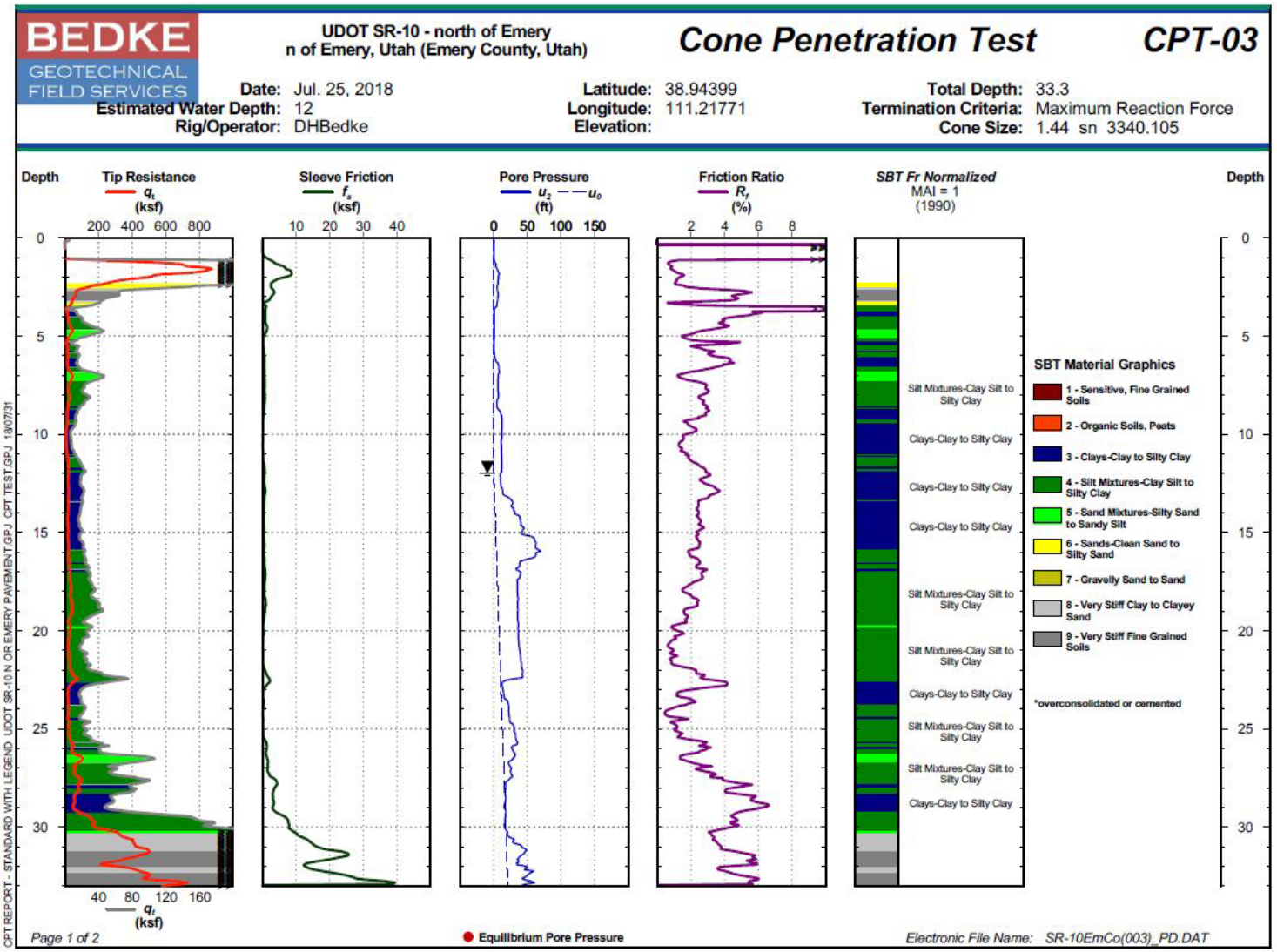
BEDKE
GEOTECHNICAL
FIELD SERVICES
UDOT SR-10 - north of Emery
n of Emery, Utah (Emery County, Utah)
Cone Penetration Test
CPT-03
Date: Jul. 25, 2018
Estimated Water Depth: 12
Rig/Operator: DHBedke
Latitude: 38.94399
Longitude: 111.21771
Elevation:
Total Depth: 33.3
Termination Criteria: Maximum Reaction Force
Cone Size: 1.44 sn 3340.105
Depth
Tip Resistance
q_t (ksf)
Sleeve Friction
f_s (ksf)
Pore Pressure
u_2 u_0 (ft)
Friction Ratio
R_f (%)
SBT Fr Normalized
MAI = 1
(1990)
Depth
Silt Mixtures-Clay Silt to Silty Clay
Clays-Clay to Silty Clay
Clays-Clay to Silty Clay
Clays-Clay to Silty Clay
Silt Mixtures-Clay Silt to Silty Clay
Silt Mixtures-Clay Silt to Silty Clay
Clays-Clay to Silty Clay
Silt Mixtures-Clay Silt to Silty Clay
Silt Mixtures-Clay Silt to Silty Clay
Clays-Clay to Silty Clay
SBT Material Graphics
1 - Sensitive, Fine Grained Soils
2 - Organic Soils, Peats
3 - Clays-Clay to Silty Clay
4 - Silt Mixtures-Clay Silt to Silty Clay
5 - Sand Mixtures-Silty Sand to Sandy Silt
6 - Sands-Clean Sand to Silty Sand
7 - Gravelly Sand to Sand
8 - Very Stiff Clay to Clayey Sand
9 - Very Stiff Fine Grained Soils
*overconsolidated or cemented
CPT REPORT - STANDARD WITH LEGEND UDOT SR-10 N OR EMERY PAVEMENT.GPJ CPT TEST.GPJ 19/07/31
Page 1 of 2
Equilibrium Pore Pressure
Electronic File Name: SR-10EmCo(003)_PD.DAT

BEDKE
GEOTECHNICAL
FIELD SERVICES

UDOT SR-10 - north of Emery
n of Emery, Utah (Emery County, Utah)

Cone Penetration Test

CPT-03

Date: Jul. 25, 2018
Estimated Water Depth: 12
Rig/Operator: DHBedke

Latitude: 38.94399
Longitude: 111.21771
Elevation:

Total Depth: 33.3
Termination Criteria: Maximum Reaction Force
Cone Size: 1.44 sn 3340.105

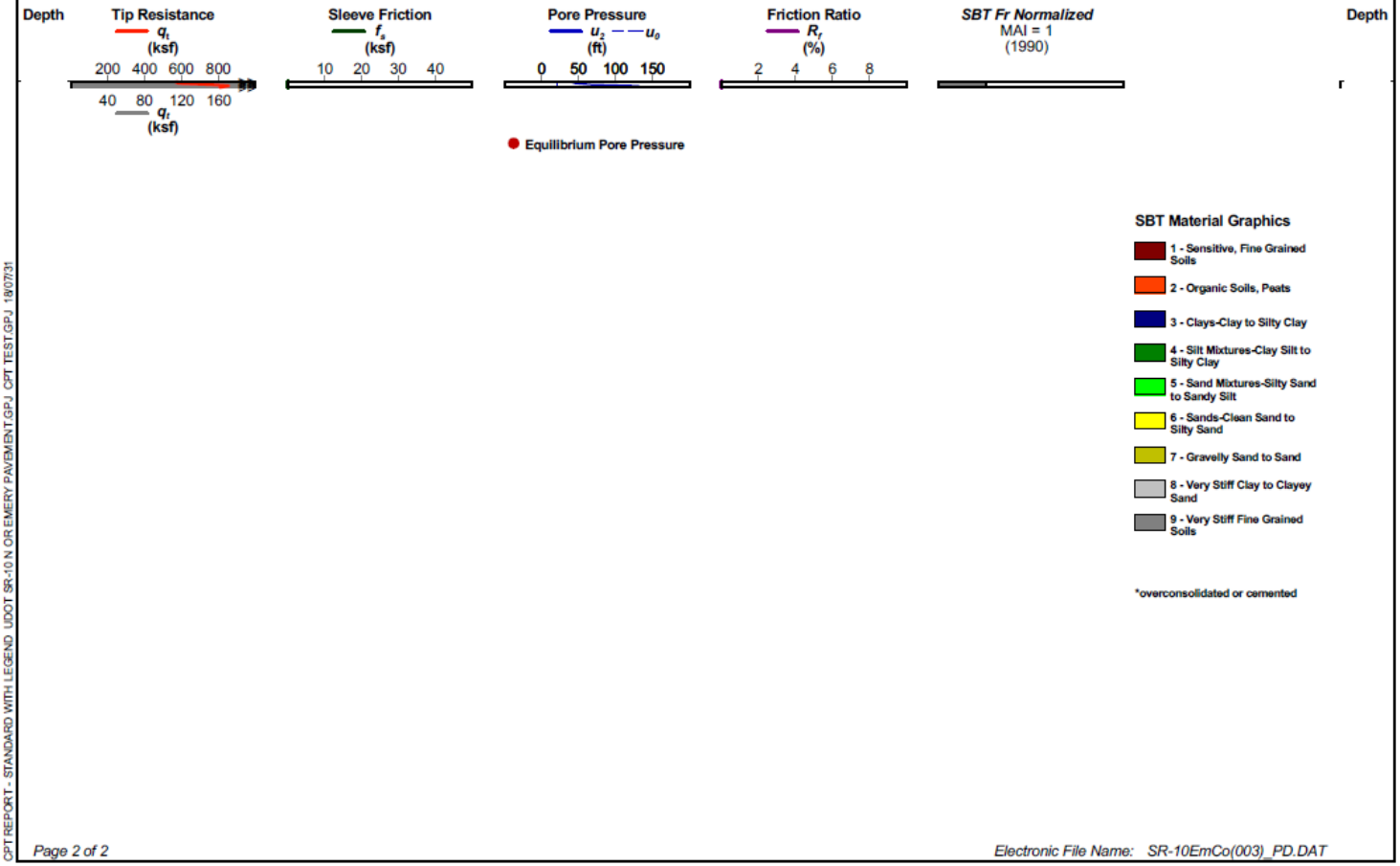

CPT REPORT - STANDARD WITH LEGEND_UDOT SR-10 N OR EMERY PAVEMENT.GPJ_CPT TEST.GPJ_19/07/31

Electronic File Name: SR-10EmCo(003)_PD.DAT

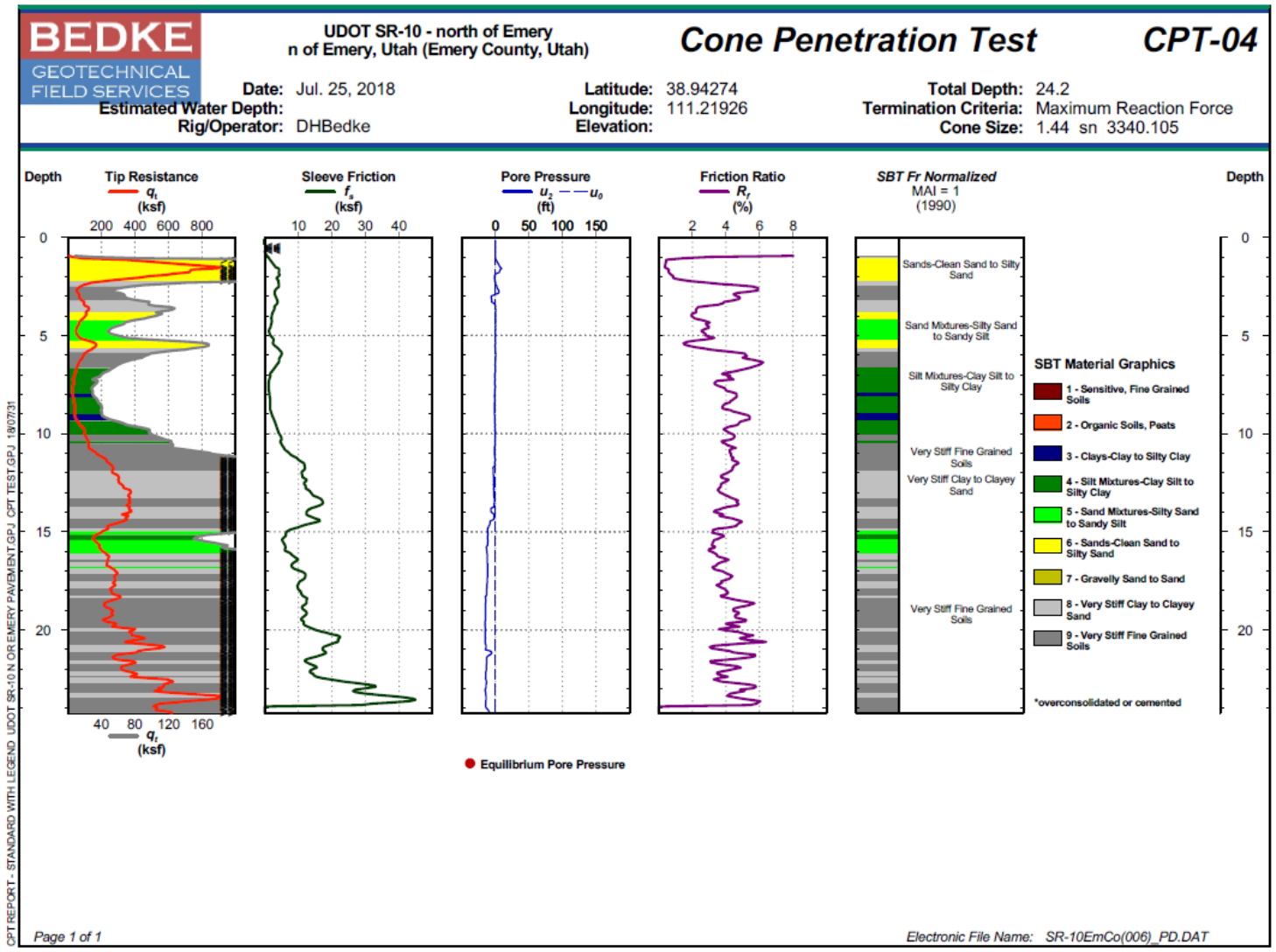
BEDKE
GEOTECHNICAL
FIELD SERVICES
UDOT SR-10 - north of Emery
n of Emery, Utah (Emery County, Utah)
Cone Penetration Test
CPT-04
Date: Jul. 25, 2018
Estimated Water Depth:
Rig/Operator: DHBedke
Latitude: 38.94274
Longitude: 111.21926
Elevation:
Total Depth: 24.2
Termination Criteria: Maximum Reaction Force
Cone Size: 1.44 sn 3340.105
Depth
Tip Resistance
q_t (ksf)
Sleeve Friction
f_s (ksf)
Pore Pressure
u_2 u_0 (ft)
Friction Ratio
R_f (%)
SBT Fr Normalized
MAI = 1
(1990)
Depth
q_t (ksf)
Equilibrium Pore Pressure
Sands-Clean Sand to Silty Sand
Sand Mixtures-Silty Sand to Sandy Silt
Silt Mixtures-Clay Silt to Silty Clay
Very Stiff Fine Grained Soils
Very Stiff Clay to Clayey Sand
Very Stiff Fine Grained Soils
SBT Material Graphics
1 - Sensitive, Fine Grained Soils
2 - Organic Soils, Peats
3 - Clays-Clay to Silty Clay
4 - Silt Mixtures-Clay Silt to Silty Clay
5 - Sand Mixtures-Silty Sand to Sandy Silt
6 - Sands-Clean Sand to Silty Sand
7 - Gravelly Sand to Sand
8 - Very Stiff Clay to Clayey Sand
9 - Very Stiff Fine Grained Soils
*overconsolidated or cemented
CPT REPORT - STANDARD WITH LEGEND UDOT SR-10 N OR EMERY PAVEMENT.GPJ CPT TEST.GPJ 18/07/31
Page 1 of 1
Electronic File Name: SR-10EmCo(006)_PD.DAT

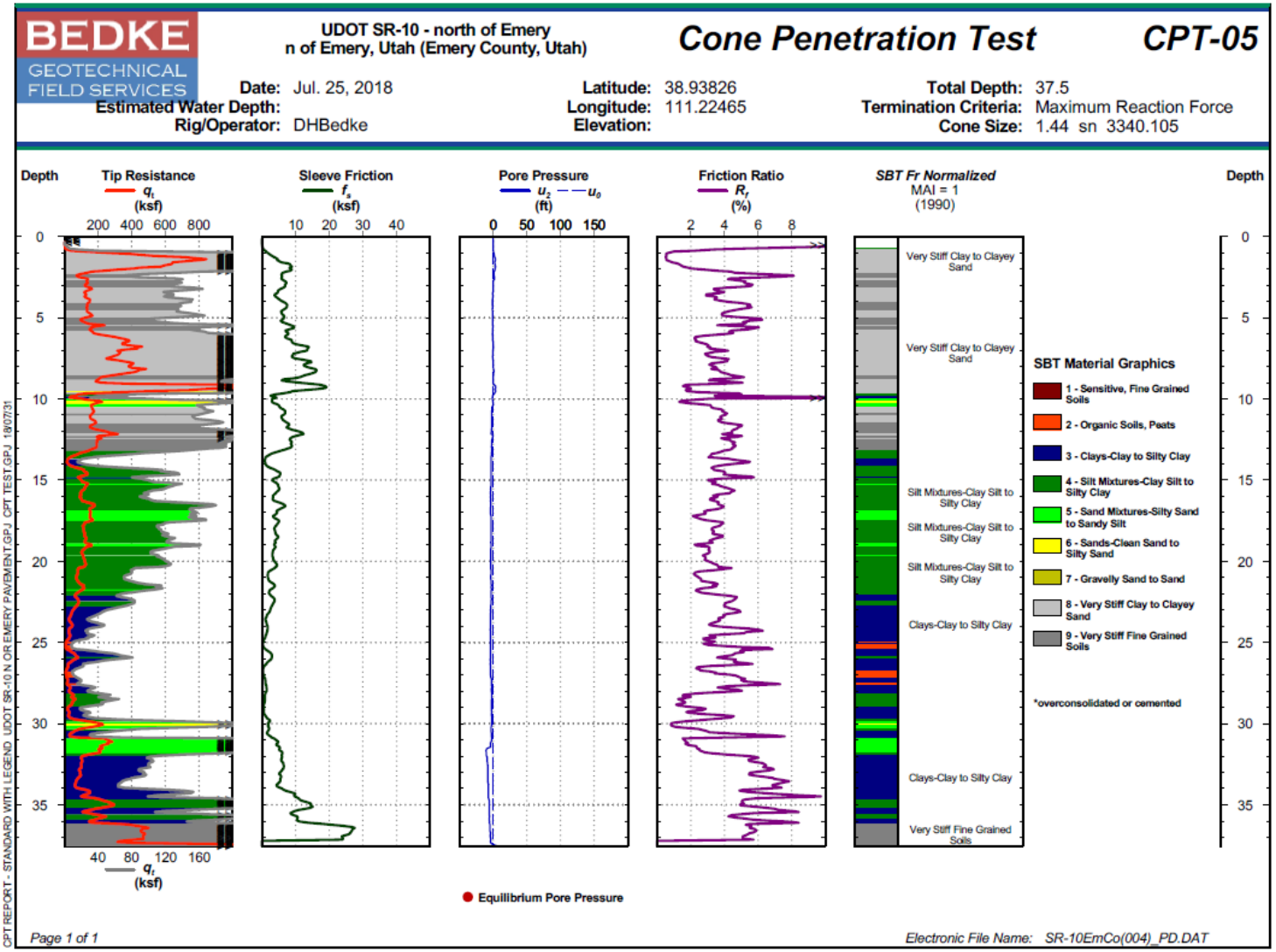
BEDKE
GEOTECHNICAL
FIELD SERVICES
UDOT SR-10 - north of Emery
n of Emery, Utah (Emery County, Utah)
Cone Penetration Test
CPT-05
Date: Jul. 25, 2018
Estimated Water Depth:
Rig/Operator: DHBedke
Latitude: 38.93826
Longitude: 111.22465
Elevation:
Total Depth: 37.5
Termination Criteria: Maximum Reaction Force
Cone Size: 1.44 sn 3340.105
Depth
Tip Resistance
q_t (ksf)
Sleeve Friction
f_s (ksf)
Pore Pressure
u_2 u_0 (ft)
Friction Ratio
R_f (%)
SBT Fr Normalized
MAI = 1
(1990)
Very Stiff Clay to Clayey Sand
Very Stiff Clay to Clayey Sand
Silt Mixtures-Clay Silt to Silty Clay
Silt Mixtures-Clay Silt to Silty Clay
Silt Mixtures-Clay Silt to Silty Clay
Clays-Clay to Silty Clay
Clays-Clay to Silty Clay
Very Stiff Fine Grained Soils
SBT Material Graphics
1 - Sensitive, Fine Grained Soils
2 - Organic Soils, Peats
3 - Clays-Clay to Silty Clay
4 - Silt Mixtures-Clay Silt to Silty Clay
5 - Sand Mixtures-Silty Sand to Sandy Silt
6 - Sands-Clean Sand to Silty Sand
7 - Gravelly Sand to Sand
8 - Very Stiff Clay to Clayey Sand
9 - Very Stiff Fine Grained Soils
*overconsolidated or cemented
Equilibrium Pore Pressure
CPT REPORT - STANDARD WITH LEGEND UDOT SR-10 N OR EMERY PAVEMENT.GPJ CPT TEST.GPJ 19/07/31
Page 1 of 1
Electronic File Name: SR-10EmCo(004)_PD.DAT

BEDKE GEOTECHNICAL FIELD SERVICES

UDOT SR-10 - north of Emery
n of Emery, Utah (Emery County, Utah)

Cone Penetration Test — CPT-06

Date: Jul. 25, 2018
Estimated Water Depth:
Rig/Operator: DHBedke

Latitude: 38.93435
Longitude: 111.22926
Elevation:

Total Depth: 3.2
Termination Criteria: Maximum Reaction Force
Cone Size: 1.44 sn 3340.105

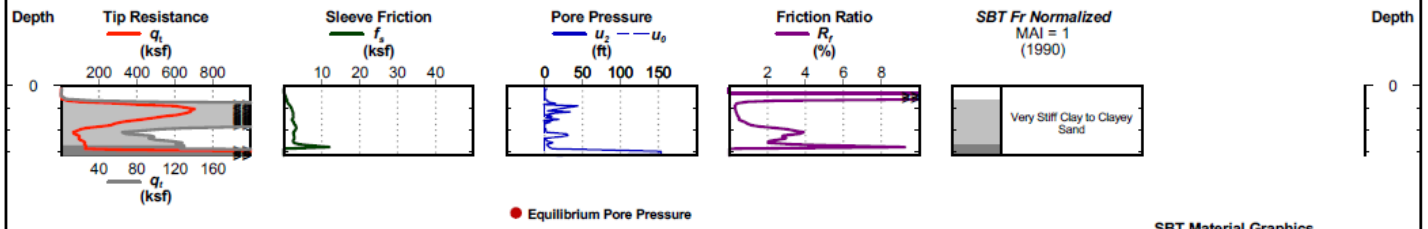

● Equilibrium Pore Pressure

SBT Material Graphics

- 1 - Sensitive, Fine Grained Soils
- 2 - Organic Soils, Peats
- 3 - Clays-Clay to Silty Clay
- 4 - Silt Mixtures-Clay Silt to Silty Clay
- 5 - Sand Mixtures-Silty Sand to Sandy Silt
- 6 - Sands-Clean Sand to Silty Sand
- 7 - Gravelly Sand to Sand
- 8 - Very Stiff Clay to Clayey Sand
- 9 - Very Stiff Fine Grained Soils

*overconsolidated or cemented

CPT REPORT - STANDARD WITH LEGEND UDOT SR-10 N OR EMERY PAVEMENT.GPJ CPT TEST.GPJ 18/07/31

Electronic File Name: SR-10EmCo(005)_PD.DAT

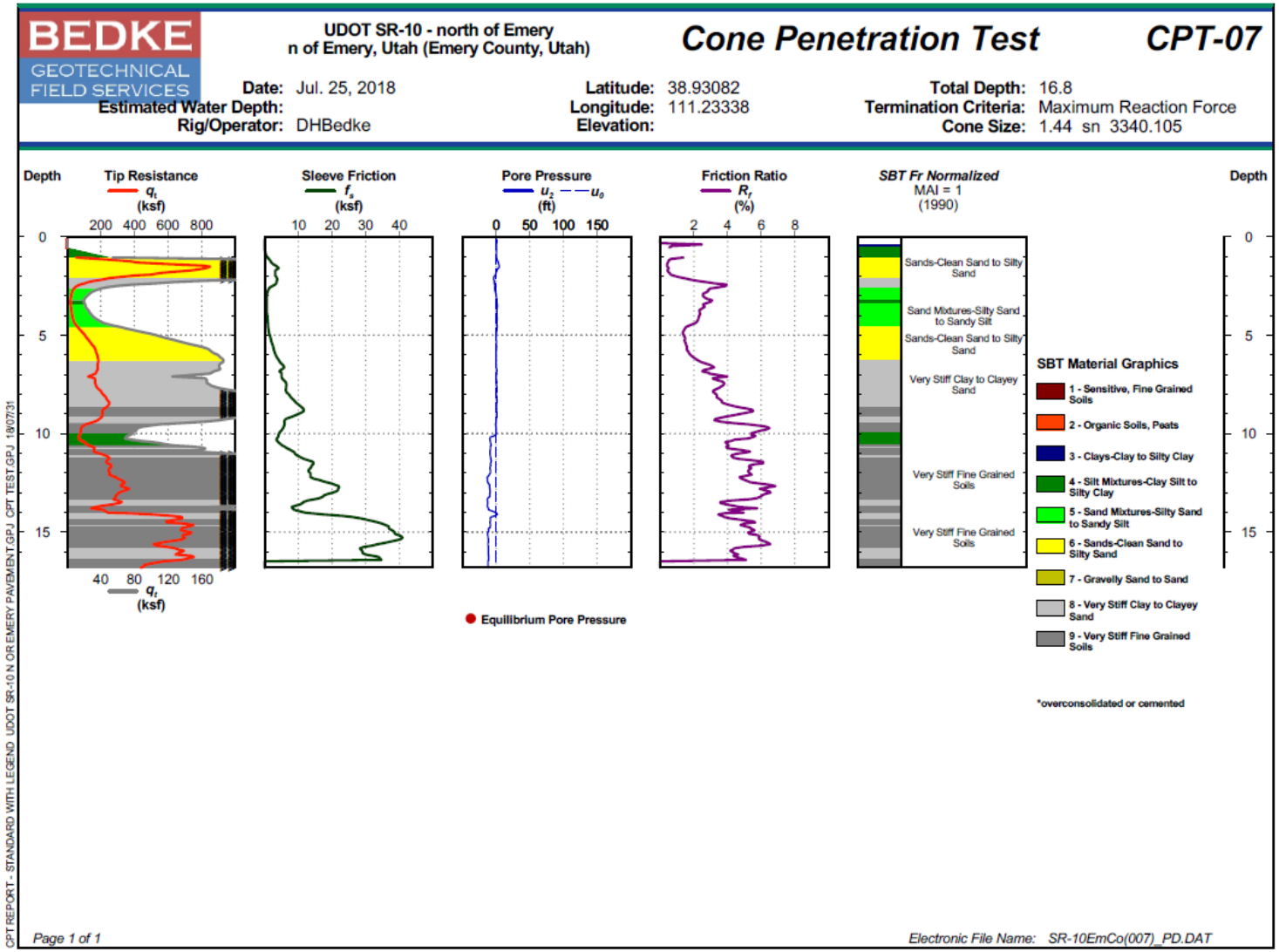
BEDKE
GEOTECHNICAL
FIELD SERVICES
UDOT SR-10 - north of Emery
n of Emery, Utah (Emery County, Utah)
Cone Penetration Test
CPT-07
Date: Jul. 25, 2018
Estimated Water Depth:
Rig/Operator: DHBedke
Latitude: 38.93082
Longitude: 111.23338
Elevation:
Total Depth: 16.8
Termination Criteria: Maximum Reaction Force
Cone Size: 1.44 sn 3340.105
Depth
Tip Resistance
q_t (ksf)
200 400 600 800
40 80 120 160
q_t (ksf)
Sleeve Friction
f_s (ksf)
10 20 30 40
Pore Pressure
u_2 u_0 (ft)
0 50 100 150
Equilibrium Pore Pressure
Friction Ratio
R_f (%)
2 4 6 8
SBT Fr Normalized
MAI = 1
(1990)
Sands-Clean Sand to Silty Sand
Sand Mixtures-Silty Sand to Sandy Silt
Sands-Clean Sand to Silty Sand
Very Stiff Clay to Clayey Sand
Very Stiff Fine Grained Soils
Very Stiff Fine Grained Soils
SBT Material Graphics
1 - Sensitive, Fine Grained Soils
2 - Organic Soils, Peats
3 - Clays-Clay to Silty Clay
4 - Silt Mixtures-Clay Silt to Silty Clay
5 - Sand Mixtures-Silty Sand to Sandy Silt
6 - Sands-Clean Sand to Silty Sand
7 - Gravelly Sand to Sand
8 - Very Stiff Clay to Clayey Sand
9 - Very Stiff Fine Grained Soils
*overconsolidated or cemented
0 5 10 15
CPT REPORT - STANDARD WITH LEGEND UDOT SR-10 N OR EMERY PAVEMENT.GPJ CPT TEST.GPJ 18/07/31
Page 1 of 1
Electronic File Name: SR-10EmCo(007)_PD.DAT

BEDKE
GEOTECHNICAL
FIELD SERVICES

UDOT SR-10 - north of Emery
n of Emery, Utah (Emery County, Utah)

Cone Penetration Test CPT-08

Date: Jul. 25, 2018
Estimated Water Depth:
Rig/Operator: DHBedke

Latitude: 38.92924
Longitude: 111.23546
Elevation:

Total Depth: 19.2
Termination Criteria: Maximum Reaction Force
Cone Size: 1.44 sn 3340.105

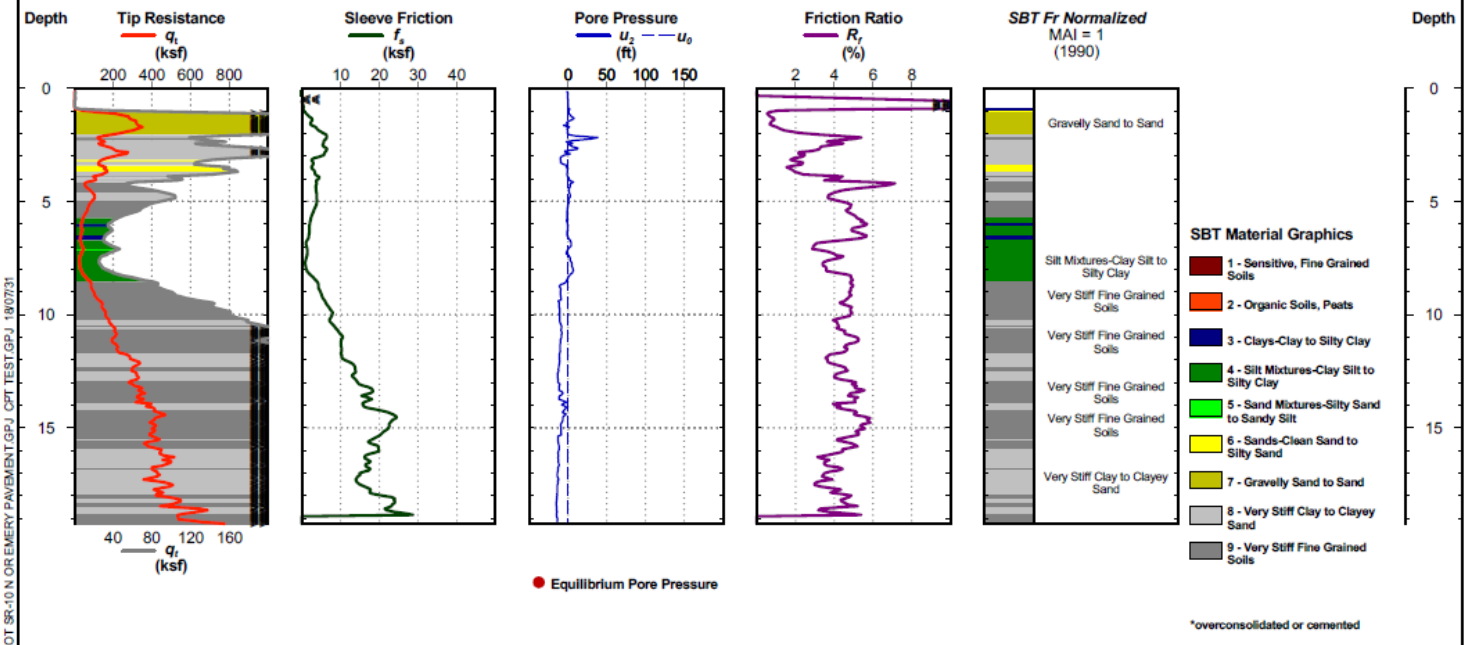

CPT REPORT - STANDARD WITH LEGEND UDOT SR-10 N OR EMERY PAVEMENT.GPJ CPT TEST.GPJ 19/07/31

Page 1 of 1

Electronic File Name: SR-10EmCo(008)_PD.DAT

BEDKE
GEOTECHNICAL
FIELD SERVICES

UDOT SR-10 - north of Emery
n of Emery, Utah (Emery County, Utah)

Cone Penetration Test CPT-09

Date: Jul. 25, 2018
Estimated Water Depth:
Rig/Operator: DHBedke

Latitude: 38.92809
Longitude: 111.23689
Elevation:

Total Depth: 11.6
Termination Criteria: Maximum Reaction Force
Cone Size: 1.44 sn 3340.105

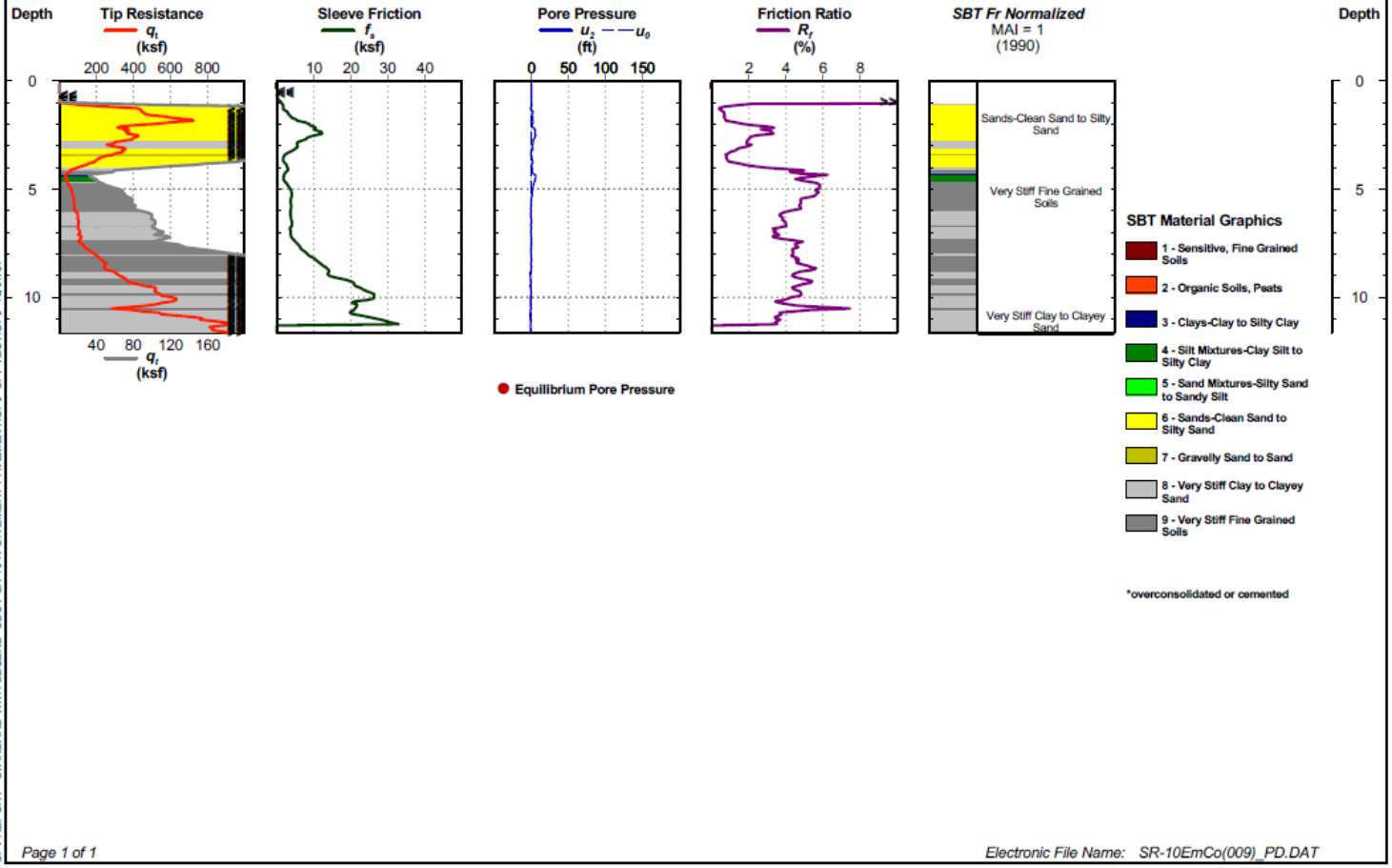

CPT REPORT - STANDARD WITH LEGEND UDOT SR-10 N OR EMERY PAVEMENT.GPJ CPT TEST.GPJ 18/07/31

Page 1 of 1

Electronic File Name: SR-10EmCo(009)_PD.DAT

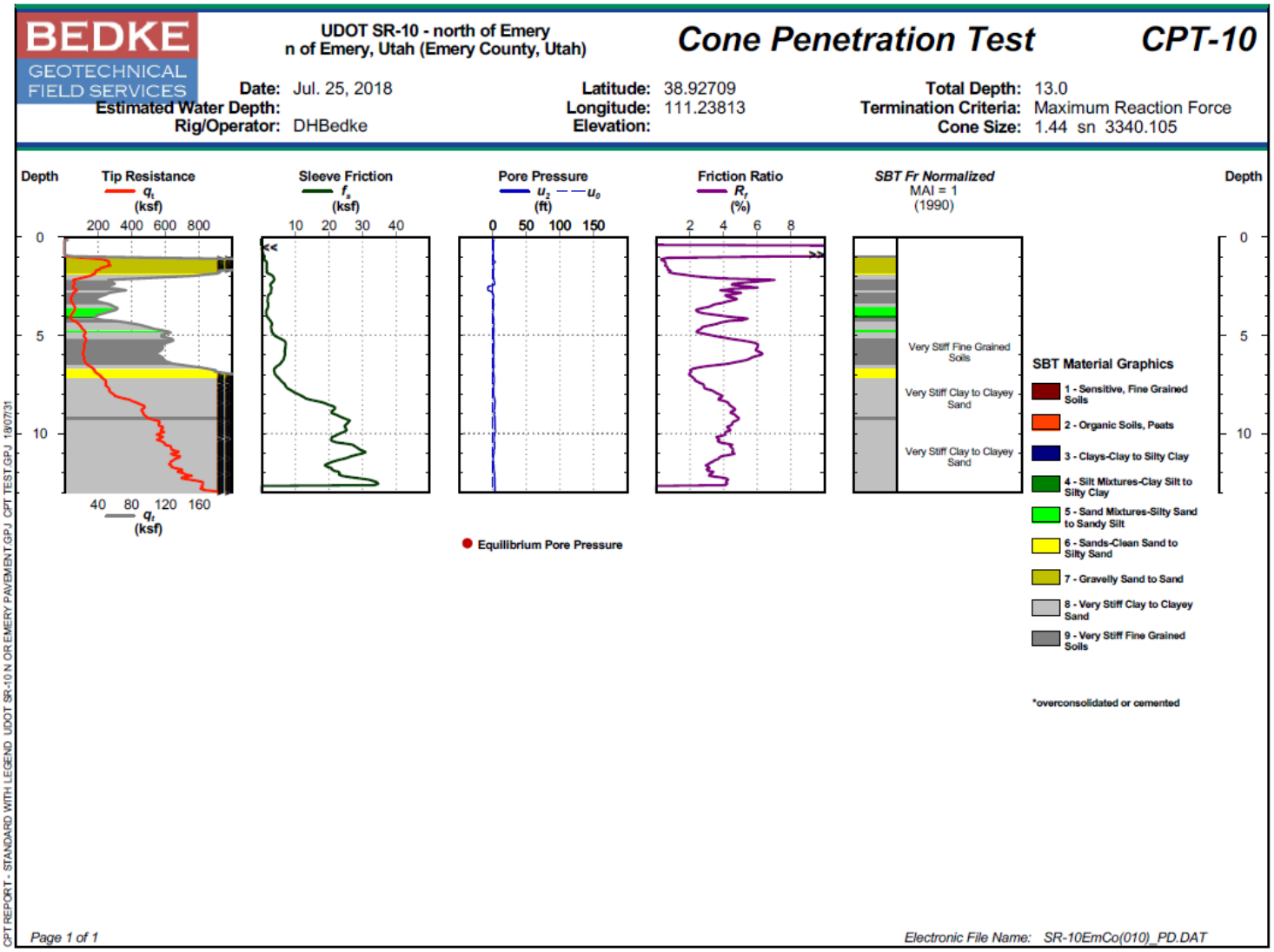
BEDKE
GEOTECHNICAL
FIELD SERVICES
UDOT SR-10 - north of Emery
n of Emery, Utah (Emery County, Utah)
Cone Penetration Test
CPT-10
Date: Jul. 25, 2018
Estimated Water Depth:
Rig/Operator: DHBedke
Latitude: 38.92709
Longitude: 111.23813
Elevation:
Total Depth: 13.0
Termination Criteria: Maximum Reaction Force
Cone Size: 1.44 sn 3340.105
Depth
Tip Resistance
q_t (ksf)
Sleeve Friction
f_s (ksf)
Pore Pressure
u_2 u_0 (ft)
Friction Ratio
R_f (%)
SBT Fr Normalized
MAI = 1
(1990)
Depth
Very Stiff Fine Grained Soils
Very Stiff Clay to Clayey Sand
Very Stiff Clay to Clayey Sand
Equilibrium Pore Pressure
SBT Material Graphics
1 - Sensitive, Fine Grained Soils
2 - Organic Soils, Peats
3 - Clays-Clay to Silty Clay
4 - Silt Mixtures-Clay Silt to Silty Clay
5 - Sand Mixtures-Silty Sand to Sandy Silt
6 - Sands-Clean Sand to Silty Sand
7 - Gravelly Sand to Sand
8 - Very Stiff Clay to Clayey Sand
9 - Very Stiff Fine Grained Soils
*overconsolidated or cemented
CPT REPORT - STANDARD WITH LEGEND UDOT SR-10 N OR EMERY PAVEMENT.GPJ CPT TEST.GPJ 19/07/31
Page 1 of 1
Electronic File Name: SR-10EmCo(010)_PD.DAT

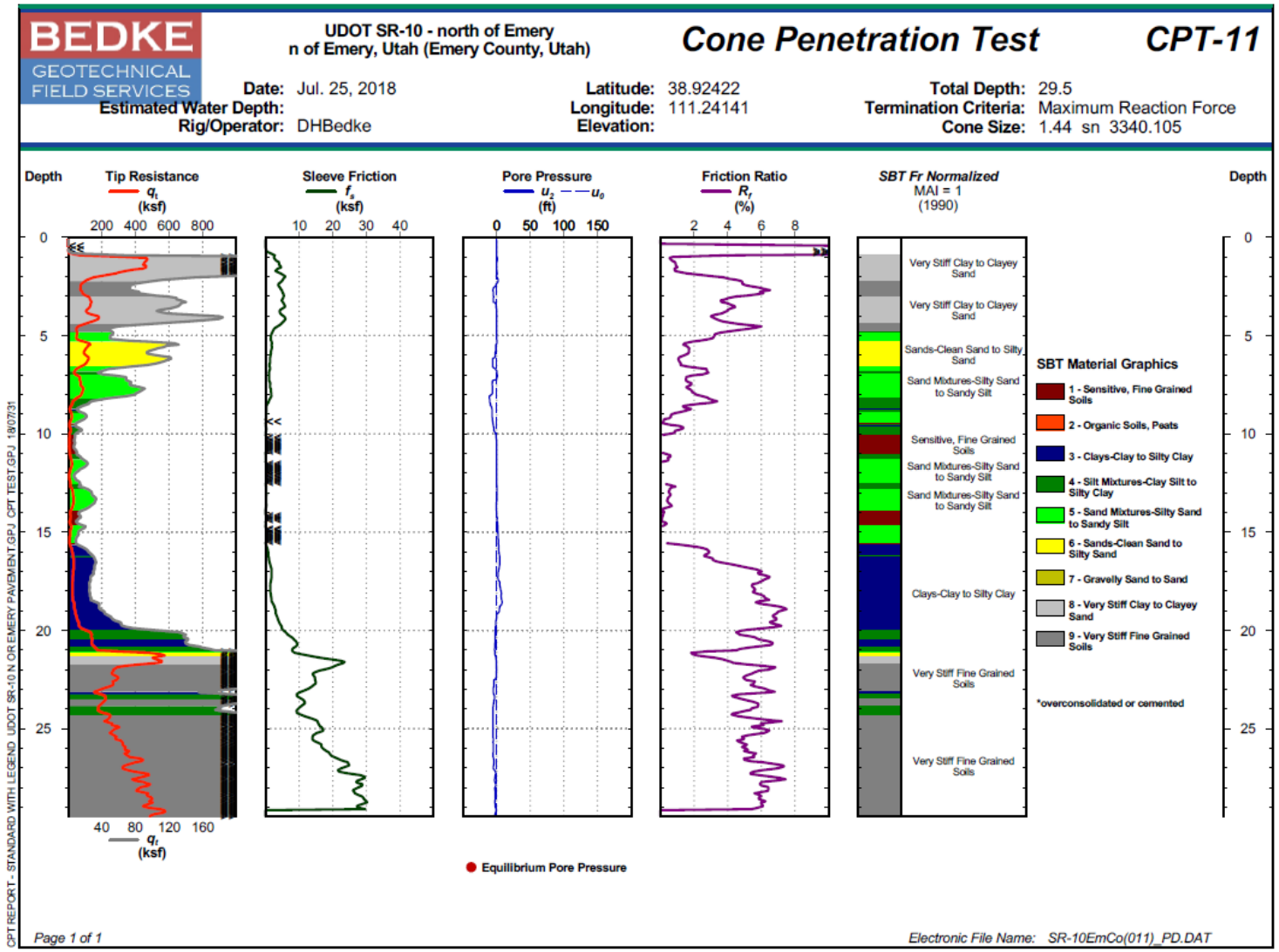
BEDKE
GEOTECHNICAL
FIELD SERVICES
UDOT SR-10 - north of Emery
n of Emery, Utah (Emery County, Utah)
Cone Penetration Test
CPT-11
Date: Jul. 25, 2018
Estimated Water Depth:
Rig/Operator: DHBedke
Latitude: 38.92422
Longitude: 111.24141
Elevation:
Total Depth: 29.5
Termination Criteria: Maximum Reaction Force
Cone Size: 1.44 sn 3340.105
Depth
Tip Resistance
q_t (ksf)
Sleeve Friction
f_s (ksf)
Pore Pressure
u_2 u_0 (ft)
Friction Ratio
R_f (%)
SBT Fr Normalized
MAI = 1
(1990)
Very Stiff Clay to Clayey Sand
Very Stiff Clay to Clayey Sand
Sands-Clean Sand to Silty Sand
Sand Mixtures-Silty Sand to Sandy Silt
Sensitive, Fine Grained Soils
Sand Mixtures-Silty Sand to Sandy Silt
Sand Mixtures-Silty Sand to Sandy Silt
Clays-Clay to Silty Clay
Very Stiff Fine Grained Soils
Very Stiff Fine Grained Soils
SBT Material Graphics
1 - Sensitive, Fine Grained Soils
2 - Organic Soils, Peats
3 - Clays-Clay to Silty Clay
4 - Silt Mixtures-Clay Silt to Silty Clay
5 - Sand Mixtures-Silty Sand to Sandy Silt
6 - Sands-Clean Sand to Silty Sand
7 - Gravelly Sand to Sand
8 - Very Stiff Clay to Clayey Sand
9 - Very Stiff Fine Grained Soils
*overconsolidated or cemented
Equilibrium Pore Pressure
CPT REPORT - STANDARD WITH LEGEND UDOT SR-10 N OR EMERY PAVEMENT.GPJ CPT TEST.GPJ 19/07/31
Page 1 of 1
Electronic File Name: SR-10EmCo(011)_PD.DAT

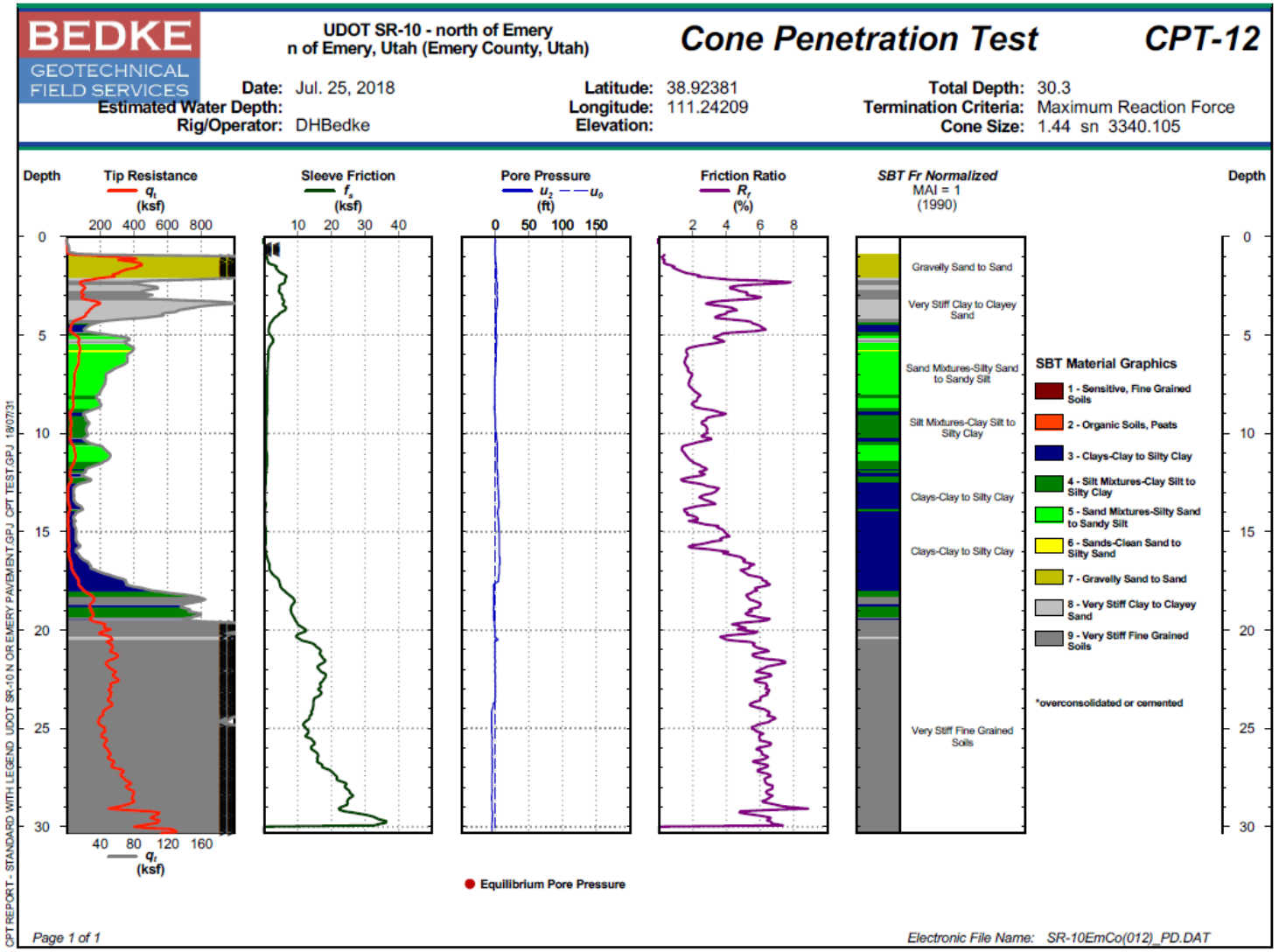
BEDKE
GEOTECHNICAL
FIELD SERVICES
UDOT SR-10 - north of Emery
n of Emery, Utah (Emery County, Utah)
Cone Penetration Test
CPT-12
Date: Jul. 25, 2018
Estimated Water Depth:
Rig/Operator: DHBedke
Latitude: 38.92381
Longitude: 111.24209
Elevation:
Total Depth: 30.3
Termination Criteria: Maximum Reaction Force
Cone Size: 1.44 sn 3340.105
Depth
Tip Resistance
q_t (ksf)
Sleeve Friction
f_s (ksf)
Pore Pressure
u_2 u_0 (ft)
Friction Ratio
R_f (%)
SBT Fr Normalized
MAI = 1
(1990)
Gravelly Sand to Sand
Very Stiff Clay to Clayey Sand
Sand Mixtures-Silty Sand to Sandy Silt
Silt Mixtures-Clay Silt to Silty Clay
Clays-Clay to Silty Clay
Clays-Clay to Silty Clay
Very Stiff Fine Grained Soils
SBT Material Graphics
1 - Sensitive, Fine Grained Soils
2 - Organic Soils, Peats
3 - Clays-Clay to Silty Clay
4 - Silt Mixtures-Clay Silt to Silty Clay
5 - Sand Mixtures-Silty Sand to Sandy Silt
6 - Sands-Clean Sand to Silty Sand
7 - Gravelly Sand to Sand
8 - Very Stiff Clay to Clayey Sand
9 - Very Stiff Fine Grained Soils
*overconsolidated or cemented
Equilibrium Pore Pressure
CPT REPORT - STANDARD WITH LEGEND UDOT SR-10 N OR EMERY PAVEMENT.GPJ CPT TEST.GPJ 19/07/31
Page 1 of 1
Electronic File Name: SR-10EmCo(012)_PD.DAT

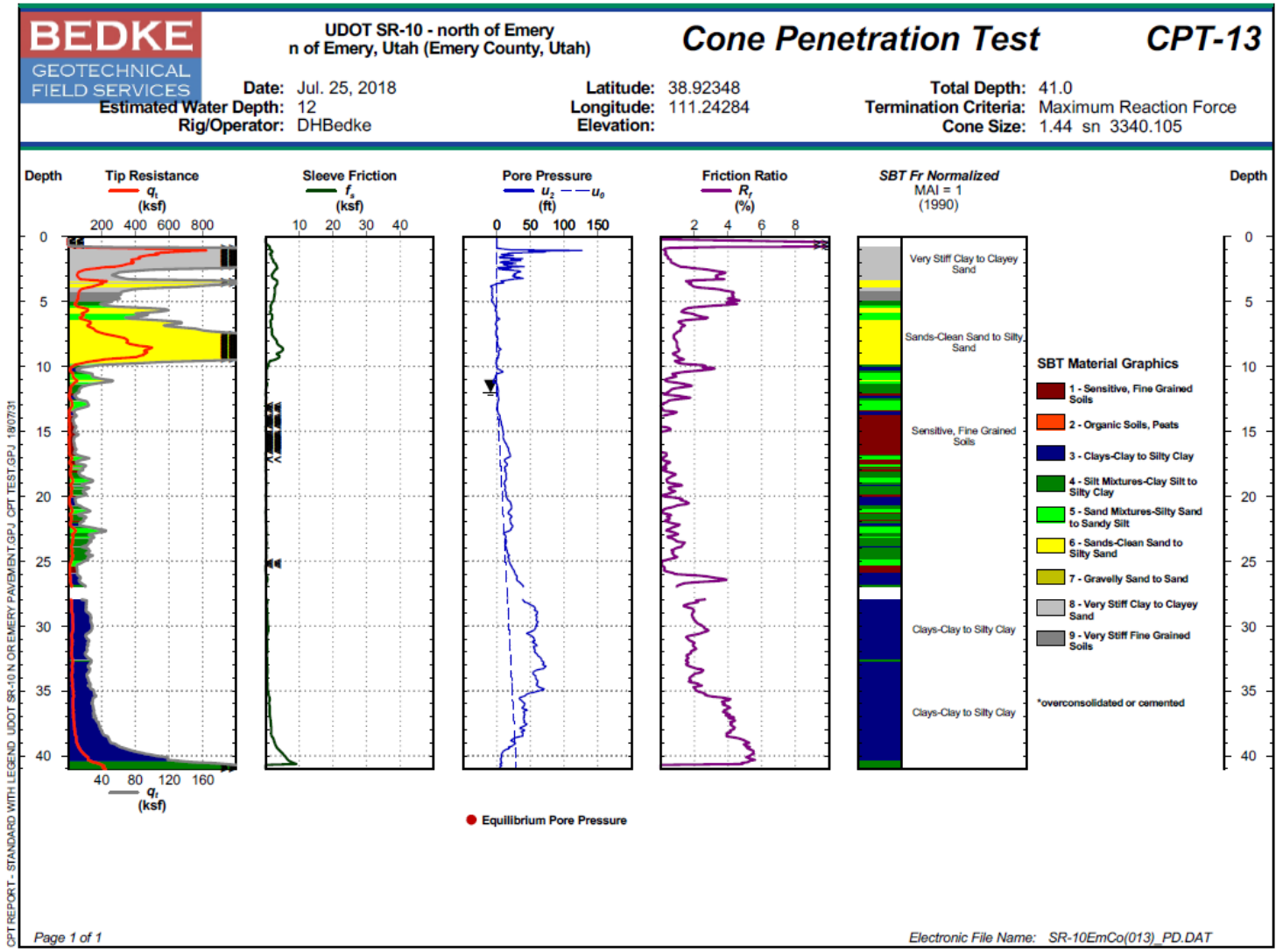
BEDKE
GEOTECHNICAL
FIELD SERVICES
UDOT SR-10 - north of Emery
n of Emery, Utah (Emery County, Utah)
Cone Penetration Test
CPT-13
Date: Jul. 25, 2018
Estimated Water Depth: 12
Rig/Operator: DHBedke
Latitude: 38.92348
Longitude: 111.24284
Elevation:
Total Depth: 41.0
Termination Criteria: Maximum Reaction Force
Cone Size: 1.44 sn 3340.105
Depth
Tip Resistance
q_t (ksf)
Sleeve Friction
f_s (ksf)
Pore Pressure
u_2 u_0 (ft)
Friction Ratio
R_f (%)
SBT Fr Normalized
MAI = 1
(1990)
Depth
Very Stiff Clay to Clayey Sand
Sands-Clean Sand to Silty Sand
Sensitive, Fine Grained Soils
Clays-Clay to Silty Clay
Clays-Clay to Silty Clay
SBT Material Graphics
1 - Sensitive, Fine Grained Soils
2 - Organic Soils, Peats
3 - Clays-Clay to Silty Clay
4 - Silt Mixtures-Clay Silt to Silty Clay
5 - Sand Mixtures-Silty Sand to Sandy Silt
6 - Sands-Clean Sand to Silty Sand
7 - Gravelly Sand to Sand
8 - Very Stiff Clay to Clayey Sand
9 - Very Stiff Fine Grained Soils
*overconsolidated or cemented
Equilibrium Pore Pressure
CPT REPORT - STANDARD WITH LEGEND UDOT SR-10 N OR EMERY PAVEMENT.GPJ CPT TEST.GPJ 19/07/31
Page 1 of 1
Electronic File Name: SR-10EmCo(013)_PD.DAT

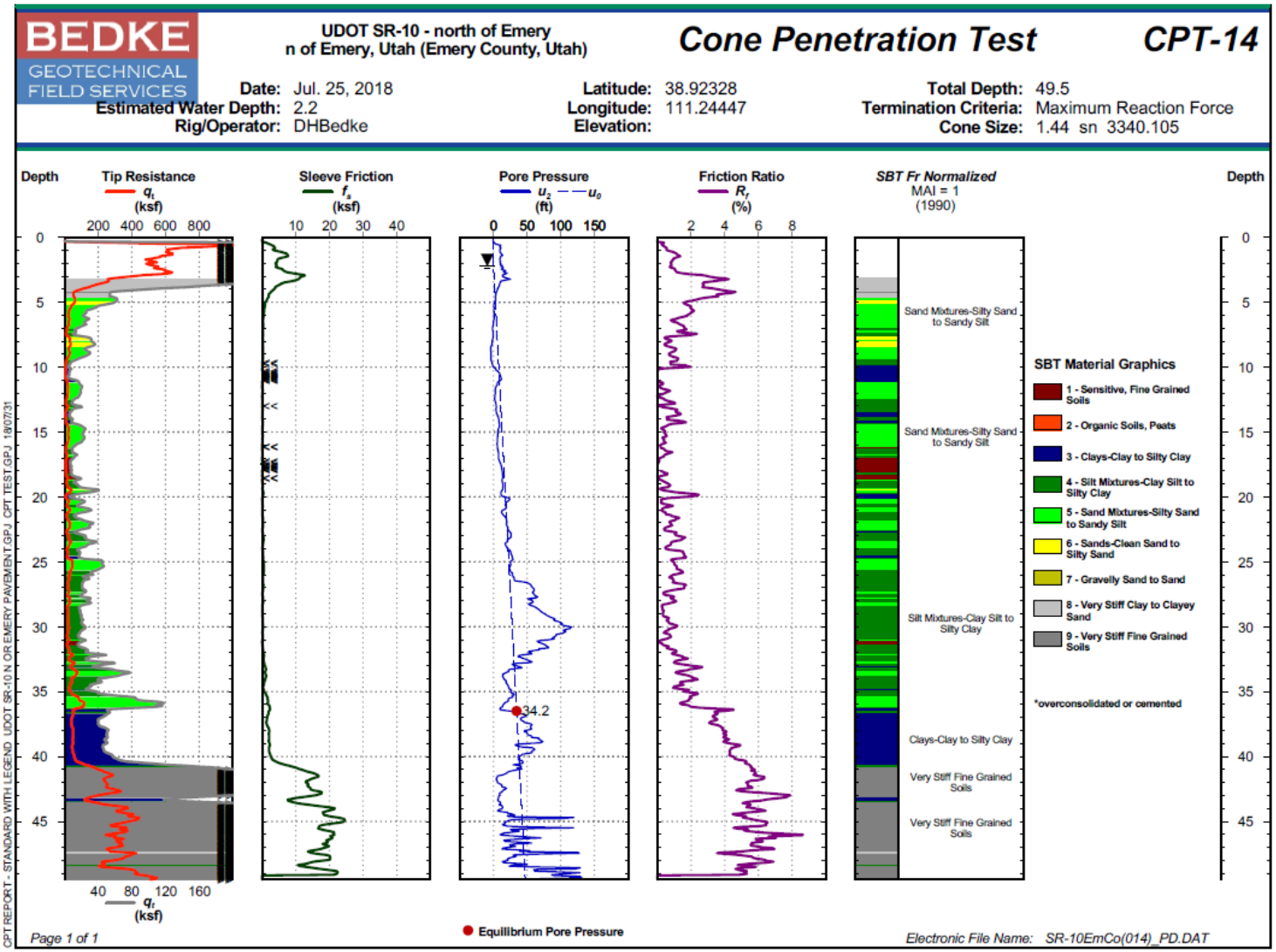
BEDKE
GEOTECHNICAL
FIELD SERVICES
UDOT SR-10 - north of Emery
n of Emery, Utah (Emery County, Utah)
Cone Penetration Test
CPT-14
Date: Jul. 25, 2018
Estimated Water Depth: 2.2
Rig/Operator: DHBedke
Latitude: 38.92328
Longitude: 111.24447
Elevation:
Total Depth: 49.5
Termination Criteria: Maximum Reaction Force
Cone Size: 1.44 sn 3340.105
Depth
Tip Resistance
q_t (ksf)
200 400 600 800
40 80 120 160
q_t (ksf)
Sleeve Friction
f_s (ksf)
10 20 30 40
Pore Pressure
u_2 u_0 (ft)
0 50 100 150
34.2
Friction Ratio
R_f (%)
2 4 6 8
SBT Fr Normalized
MAI = 1
(1990)
Sand Mixtures-Silty Sand to Sandy Silt
Sand Mixtures-Silty Sand to Sandy Silt
Silt Mixtures-Clay Silt to Silty Clay
Clays-Clay to Silty Clay
Very Stiff Fine Grained Soils
Very Stiff Fine Grained Soils
SBT Material Graphics
1 - Sensitive, Fine Grained Soils
2 - Organic Soils, Peats
3 - Clays-Clay to Silty Clay
4 - Silt Mixtures-Clay Silt to Silty Clay
5 - Sand Mixtures-Silty Sand to Sandy Silt
6 - Sands-Clean Sand to Silty Sand
7 - Gravelly Sand to Sand
8 - Very Stiff Clay to Clayey Sand
9 - Very Stiff Fine Grained Soils
*overconsolidated or cemented
Depth
0 5 10 15 20 25 30 35 40 45
CPT REPORT - STANDARD WITH LEGEND UDOT SR-10 N OR EMERY PAVEMENT.GPJ CPT TEST.GPJ 19/07/31
Page 1 of 1
Equilibrium Pore Pressure
Electronic File Name: SR-10EmCo(014)_PD.DAT

15. APPENDIX E: FALLING WEIGHT DEFLECTOMETER DATA SHEETS

M5									
Date-Time:	7/25/2018	5:43:50							
Sensors:	103-01F	103-02F	103-03F	103-04F	103-05F	103-06F	103-07F	103-08F	103-09F
Weight/spring:	3								
Location:	SR	10	SBL						
Temp:	73.61								
Operator:	Jeff								
Comments:	8/25/2018								

Location	Drop	Force	Sensor 1	Sensor 2	Sensor 3	Sensor 4	Sensor 5	Sensor 6	Sensor 7	Sensor 8	Sensor 9
1	1	9.83	31.96	28.23	25.17	21.21	17.63	11.83	8.47	6.13	25.15
1	1	10.1	32.09	28.38	25.31	21.43	17.81	11.95	8.4	6.13	25.41
1	1	10.05	31.86	28.29	25.22	21.4	17.81	11.97	8.43	6.21	25.3
1	1	12.15	37.76	33.35	29.98	25.21	21.06	14.16	9.96	7.26	29.91
1	1	12.23	38.09	33.63	30.11	25.48	21.22	14.3	10.14	7.38	30.11
1	1	12.23	38.09	33.66	30.14	25.56	21.27	14.35	10.15	7.45	30.17
1	1	14.34	43.58	38.62	34.69	29.09	24.14	16.27	11.48	8.35	34.33
1	1	14.41	44.34	39.32	35.09	29.52	24.52	16.46	11.62	8.47	34.89
1	1	14.32	44.43	39.29	35.07	29.58	24.54	16.55	11.62	8.49	34.88
Drop	Sequence	Time:	5:45	Air	Temp	(F):	73.6				
GPS:	Quality	Fi	Latitude	=	38	deg57.027581	N	Longitude	=	111	deg12.595522
Note:	SR	PDOP	=	0							

Location	Drop	Force	Sensor 1	Sensor 2	Sensor 3	Sensor 4	Sensor 5	Sensor 6	Sensor 7	Sensor 8	Sensor 9
2	1	10.32	7.78	6.64	5.92	5.19	4.49	3.45	2.84	2.25	5.94
2	1	10.54	7.95	6.77	6.02	5.32	4.61	3.55	2.88	2.29	6.07
2	1	10.55	7.92	6.75	6.03	5.3	4.61	3.54	2.89	2.29	6.07
2	1	12.62	9.43	8.09	7.22	6.38	5.53	4.24	3.46	2.78	7.27
2	1	12.69	9.48	8.11	7.25	6.4	5.53	4.31	3.43	2.79	7.31
2	1	12.61	9.42	8.07	7.22	6.38	5.52	4.29	3.45	2.78	7.27
2	1	14.96	11.22	9.59	8.56	7.56	6.55	5.05	4.09	3.27	8.64
2	1	14.61	11.01	9.42	8.42	7.46	6.41	4.98	4.09	3.23	8.49
2	1	14.54	10.92	9.37	8.37	7.4	6.41	4.94	4.05	3.21	8.44
Drop	Sequence	Time:	5:56	Air	Temp	(F):	77				
GPS:	Quality	Fi	Latitude	=	38	deg56.832920	N	Longitude	=	111	deg12.828372
Note:	SR	PDOP	=	1.4							

Location	Drop	Force	Sensor 1	Sensor 2	Sensor 3	Sensor 4	Sensor 5	Sensor 6	Sensor 7	Sensor 8	Sensor 9
3	1	9.87	9.82	8	7	6.08	5.26	3.93	3.11	2.55	7.05
3	1	10.12	9.92	8.12	7.12	6.2	5.32	4.03	3.18	2.61	7.17
3	1	10.26	10	8.19	7.19	6.27	5.39	4.05	3.19	2.6	7.23
3	1	11.72	11.46	9.39	8.25	7.14	6.16	4.67	3.66	2.98	8.29
3	1	12.01	11.68	9.6	8.44	7.32	6.37	4.75	3.74	3.05	8.48
3	1	12.18	11.84	9.73	8.56	7.41	6.4	4.83	3.78	3.05	8.61
3	1	14.13	13.66	11.23	9.9	8.56	7.43	5.57	4.35	3.48	9.95
3	1	14.3	13.92	11.45	10.09	8.75	7.55	5.65	4.43	3.57	10.15
3	1	14.23	13.86	11.43	10.06	8.72	7.56	5.65	4.43	3.56	10.12
Drop	Sequence	Time:	6:15	Air	Temp	(F):	74.7				
GPS:	Quality	Fi	Latitude	=	38	deg56.639239	N	Longitude	=	111	deg13.061472
Note:	SR	PDOP	=	1.6							

Location	Drop	Force	Sensor 1	Sensor 2	Sensor 3	Sensor 4	Sensor 5	Sensor 6	Sensor 7	Sensor 8	Sensor 9
4	1	9.03	9.82	8.23	7.18	6.31	5.32	4.01	3.09	2.51	7.19
4	1	9.63	10.35	8.72	7.63	6.71	5.71	4.25	3.32	2.7	7.63
4	1	9.76	10.49	8.82	7.72	6.82	5.73	4.35	3.39	2.69	7.74
4	1	10.99	11.75	9.92	8.71	7.7	6.54	4.91	3.82	3.12	8.72
4	1	11.36	12.15	10.29	9.02	7.98	6.76	5.09	3.96	3.23	9.03
4	1	11.49	12.25	10.42	9.12	8.05	6.84	5.1	3.99	3.22	9.15
4	1	13.15	13.81	11.8	10.49	9.17	7.76	5.82	4.54	3.67	10.37
4	1	13.57	14.36	12.24	10.96	9.53	8.07	5.97	4.7	3.8	10.77
4	1	13.68	14.47	12.38	10.99	9.62	8.15	6.06	4.82	3.84	10.9
Drop	Sequence	Time:	6:51	Air	Temp	(F):	74.2				
GPS:	Quality	Fi	Latitude	=	38	deg56.564630	N	Longitude	=	111	deg13.150618
Note:	SR	PDOP	=	1.7							

Location	Drop	Force	Sensor 1	Sensor 2	Sensor 3	Sensor 4	Sensor 5	Sensor 6	Sensor 7	Sensor 8	Sensor 9
5	1	9.6	12.55	9.42	7.6	6.16	4.7	2.86	1.88	1.37	7.82
5	1	10.23	13.12	9.87	7.98	6.53	4.98	3.04	2.05	1.47	8.23
5	1	10.09	12.81	9.69	7.83	6.28	4.89	3	1.99	1.45	8.1
5	1	11.68	14.82	11.19	9.1	7.5	5.7	3.51	2.34	1.67	9.36
5	1	11.91	15.15	11.45	9.34	7.7	5.79	3.6	2.44	1.72	9.58
5	1	12.02	15.29	11.58	9.39	7.56	5.85	3.66	2.38	1.74	9.67
5	1	13.72	17.39	13.15	10.79	8.58	6.7	4.18	2.77	1.99	11.02
5	1	13.82	17.73	13.42	11.03	8.83	6.8	4.32	2.79	2.03	11.25
5	1	13.91	17.69	13.4	10.99	8.78	6.83	4.25	2.82	2.02	11.21
Drop	Sequence	Time:	6:58	Air	Temp	(F):	74.3				
GPS:	Quality	Fi	Latitude	=	38	deg56.298239	N	Longitude	=	111	deg13.471095
Note:	SR	PDOP	=	1.7							

Location	Drop	Force	Sensor 1	Sensor 2	Sensor 3	Sensor 4	Sensor 5	Sensor 6	Sensor 7	Sensor 8	Sensor 9
6	1	10.02	9.63	7.09	5.78	4.46	3.32	1.8	1.05	0.58	5.81
6	1	10.5	9.85	7.26	5.9	4.59	3.43	1.88	1.08	0.62	5.95
6	1	10.34	9.55	7.08	5.78	4.49	3.36	1.84	1.08	0.59	5.8
6	1	12.1	11.19	8.31	6.75	5.21	3.86	2.14	1.22	0.68	6.8
6	1	12.31	11.32	8.42	6.84	5.3	3.92	2.18	1.25	0.7	6.9
6	1	12.19	11.26	8.41	6.84	5.28	3.92	2.18	1.25	0.72	6.89
6	1	14.02	12.94	9.66	7.85	6.03	4.45	2.47	1.4	0.79	7.92
6	1	14.13	13.07	9.77	7.93	6.08	4.52	2.49	1.43	0.8	8.01
6	1	14.08	13.07	9.78	7.95	6.11	4.5	2.5	1.43	0.8	8.03
Drop	Sequence	Time:	7:18	Air	Temp	(F):	77.8				
GPS:	Quality	Fi	Latitude	=	38	deg56.062859	N	Longitude	=	111	deg13.753877
Note:	SR	PDOP	=	1.4							

Location	Drop	Force	Sensor 1	Sensor 2	Sensor 3	Sensor 4	Sensor 5	Sensor 6	Sensor 7	Sensor 8	Sensor 9
7	1	9.56	14.33	11.84	10.44	9	7.78	5.8	3.84	3.46	10.41
7	1	10.13	14.98	12.49	11.01	9.53	8.29	6.2	6	3.69	11.02
7	1	10.09	14.83	12.39	10.93	9.5	8.22	6.15	5.75	3.65	10.95
7	1	11.6	17	14.23	12.57	11.07	9.42	7.05	6.99	4.14	12.58
7	1	11.89	17.56	14.72	12.98	11.38	9.7	7.31	5.71	4.28	13.03
7	1	11.98	17.62	14.81	13.09	11.33	9.72	7.31	5.79	4.29	13.11
7	1	13.79	20.35	17.1	15.14	13.18	11.34	8.46	6.25	4.99	15.16
7	1	13.98	20.67	17.38	15.39	13.33	11.47	8.63	6.47	5.07	15.39
7	1	13.99	20.85	17.54	15.54	13.58	11.59	8.74	6.61	5.1	15.57
Drop	Sequence	Time:	7:31	Air	Temp	(F):	78.9				
GPS:	Quality	Fi	Latitude	=	38	deg55.853838	N	Longitude	=	111	deg14.004830
Note:	SR	PDOP	=	1.5							

Location	Drop	Force	Sensor 1	Sensor 2	Sensor 3	Sensor 4	Sensor 5	Sensor 6	Sensor 7	Sensor 8	Sensor 9
8	1	9.93	11.82	9.39	7.83	6.3	5.09	3.53	2.69	2.16	7.83
8	1	10.49	12.3	9.81	8.2	6.62	5.37	3.75	2.84	2.24	8.2
8	1	10.33	11.97	9.56	7.99	6.49	5.24	3.64	2.73	2.16	8.04
8	1	11.95	13.79	11.04	9.23	7.5	6.04	4.19	3.16	2.48	9.25
8	1	12.13	13.97	11.22	9.36	7.6	6.14	4.27	3.2	2.54	9.41
8	1	12.04	13.94	11.22	9.37	7.59	6.14	4.27	3.24	2.55	9.42
8	1	13.99	16.16	12.97	10.85	8.79	7.13	4.95	3.68	2.9	10.9
8	1	14.17	16.47	13.16	11.05	8.95	7.2	5.02	3.77	2.96	11.08
8	1	14.22	16.46	13.22	11.07	8.98	7.24	5.02	3.76	2.95	11.1
Drop	Sequence	Time:	7:42	Air	Temp	(F):	78				
GPS:	Quality	Fi	Latitude	=	38	deg55.754735	N	Longitude	=	111	deg14.124394
Note:	SR	PDOP	=	1.5							

Location	Drop	Force	Sensor 1	Sensor 2	Sensor 3	Sensor 4	Sensor 5	Sensor 6	Sensor 7	Sensor 8	Sensor 9
9	1	10.04	8.26	6.65	5.68	4.71	3.8	2.5	1.85	1.46	5.84
9	1	10.19	8.26	6.67	5.7	4.76	3.8	2.54	1.9	1.5	5.87
9	1	10.14	8.15	6.61	5.66	4.73	3.82	2.54	1.9	1.48	5.83
9	1	11.94	9.55	7.74	6.64	5.57	4.44	2.98	2.28	1.72	6.8
9	1	12.13	9.68	7.86	6.74	5.61	4.47	3.04	2.33	1.79	6.91
9	1	12.15	9.72	7.89	6.78	5.66	4.58	3.05	2.35	1.77	6.95
9	1	14.02	11.11	9.04	7.77	6.46	5.2	3.51	2.66	2.01	7.96
9	1	14.08	11.19	9.11	7.82	6.53	5.27	3.55	2.72	2.08	8.04
9	1	14.17	11.29	9.17	7.91	6.59	5.32	3.56	2.72	2.08	8.1
Drop	Sequence	Time:	7:51	Air	Temp	(F):	76.4				
GPS:	Quality	Fi	Latitude	=	38	deg55.684144	N	Longitude	=	111	deg14.208793
Note:	SR	PDOP	=	1.5							

Location	Drop	Force	Sensor 1	Sensor 2	Sensor 3	Sensor 4	Sensor 5	Sensor 6	Sensor 7	Sensor 8	Sensor 9
10	1	9.67	16.85	14.34	12.6	10.76	9.11	6.34	4.6	3.45	13.16
10	1	10.15	17.52	14.95	13.16	11.27	9.56	6.67	4.83	3.55	13.72
10	1	9.99	17.11	14.65	12.89	11.06	9.42	6.57	4.76	3.47	13.46
10	1	11.72	19.98	17.13	15.11	13	10.99	7.68	5.58	4.08	15.73
10	1	11.89	20.22	17.35	15.3	13.16	11.18	7.79	5.65	4.12	15.93
10	1	12.11	20.69	17.75	15.69	13.49	11.45	8	5.77	4.24	16.32
10	1	13.78	23.3	19.98	17.66	15.14	12.82	8.99	6.47	4.72	18.37
10	1	13.83	23.65	20.28	17.93	15.37	12.99	9.1	6.56	4.8	18.65
10	1	13.93	23.79	20.41	18.05	15.46	13.08	9.15	6.61	4.83	18.76
Drop	Sequence	Time:	8:06	Air	Temp	(F):	79.4				
GPS:	Quality	Fi	Latitude	=	38	deg55.625307	N	Longitude	=	111	deg14.281857
Note:	SR	PDOP	=	1.5							

Location	Drop	Force	Sensor 1	Sensor 2	Sensor 3	Sensor 4	Sensor 5	Sensor 6	Sensor 7	Sensor 8	Sensor 9
11	1	9.74	11.15	8.77	7.46	6.17	5.03	3.34	2.48	1.97	7.78
11	1	10.26	11.57	9.17	7.82	6.49	5.33	3.54	2.64	2.14	8.16
11	1	9.91	11.13	8.85	7.56	6.27	5.11	3.43	2.57	2.05	7.87
11	1	11.77	13.19	10.46	8.96	7.44	6.06	4.04	2.96	2.36	9.31
11	1	11.93	13.31	10.61	9.08	7.54	6.15	4.09	3	2.38	9.44
11	1	12.04	13.4	10.7	9.15	7.61	6.19	4.14	3.04	2.41	9.52
11	1	13.76	15.36	12.29	10.52	8.74	7.1	4.76	3.51	2.77	10.94
11	1	14.06	15.69	12.55	10.74	8.92	7.25	4.85	3.55	2.8	11.17
11	1	14.11	15.77	12.63	10.81	9.01	7.29	4.9	3.61	2.82	11.28
Drop	Sequence	Time:	8:24	Air	Temp	(F):	79.7				
GPS:	Quality	Fi	Latitude	=	38	deg55.452101	N	Longitude	=	111	deg14.482383

Location	Drop	Force	Sensor 1	Sensor 2	Sensor 3	Sensor 4	Sensor 5	Sensor 6	Sensor 7	Sensor 8	Sensor 9
12	1	9.97	11.02	9.2	7.93	6.56	5.27	3.47	2.56	2.07	8
12	1	9.91	10.83	9.06	7.84	6.49	5.23	3.47	2.57	2.07	7.91
12	1	10.06	10.9	9.11	7.89	6.56	5.31	3.51	2.61	2.09	7.97
12	1	11.76	12.7	10.62	9.21	7.66	6.15	4.08	3.07	2.37	9.3
12	1	11.92	12.87	10.77	9.35	7.78	6.27	4.17	3.14	2.51	9.45
12	1	12.05	12.94	10.84	9.41	7.82	6.31	4.19	3.15	2.52	9.52
12	1	13.79	14.8	12.39	10.77	8.93	7.2	4.8	3.66	2.81	10.91
12	1	13.98	15.02	12.55	10.92	9.09	7.33	4.89	3.65	2.93	11.03
12	1	14.03	15.05	12.59	10.96	9.1	7.33	4.88	3.64	2.94	11.08
Drop	Sequence	Time:	8:29	Air	Temp	(F):	81				
GPS:	Quality	Fi	Latitude	=	38	deg55.430343	N	Longitude	=	111	deg14.519497
Note:	SR	PDOP	=	1.5							

Location	Drop	Force	Sensor 1	Sensor 2	Sensor 3	Sensor 4	Sensor 5	Sensor 6	Sensor 7	Sensor 8	Sensor 9
13	1	10.09	11.25	8.76	7.53	6.17	4.95	3.29	2.43	1.88	11.81
13	1	10.04	10.99	8.58	7.41	6.08	4.88	3.24	2.42	1.87	13.57
13	1	10.02	10.89	8.51	7.36	6.05	4.89	3.21	2.43	1.87	10.71
13	1	11.79	12.86	10.06	8.71	7.19	5.73	3.79	2.92	2.2	11.13
13	1	12.04	13.12	10.28	8.91	7.35	5.86	3.87	2.92	2.25	11.37
13	1	12.06	13.14	10.3	8.91	7.35	5.85	3.91	2.93	2.17	19.82
13	1	13.87	15.06	11.8	10.24	8.42	6.75	4.46	3.34	2.49	13.13
13	1	14.07	15.35	12.02	10.45	8.58	6.86	4.53	3.43	2.54	29.03
13	1	14.04	15.29	12	10.43	8.58	6.85	4.52	3.39	2.52	26.8
Drop	Sequence	Time:	8:31	Air	Temp	(F):	81.4				
GPS:	Quality	Fi	Latitude	=	38	deg55.411540	N	Longitude	=	111	deg14.566024
Note:	SR	PDOP	=	1.5							

Location	Drop	Force	Sensor 1	Sensor 2	Sensor 3	Sensor 4	Sensor 5	Sensor 6	Sensor 7	Sensor 8	Sensor 9
14	1	9.85	8.56	6.84	5.77	4.72	3.88	2.84	2.3	1.95	5.89
14	1	10.01	8.62	6.91	5.83	4.8	3.92	2.9	2.37	1.98	5.9
14	1	10.06	8.59	6.88	5.83	4.78	3.97	2.89	2.37	2.01	5.92
14	1	11.86	10.09	8.11	6.86	5.64	4.68	3.42	2.82	2.32	6.98
14	1	12.05	10.22	8.22	6.95	5.75	4.74	3.49	2.82	2.38	7.09
14	1	12.19	10.37	8.33	7.05	5.8	4.84	3.53	2.91	2.4	7.13
14	1	13.71	11.62	9.34	7.92	6.53	5.39	3.97	3.24	2.67	8.11
14	1	13.99	11.82	9.51	8.05	6.63	5.49	4.04	3.29	2.72	8.13
14	1	14.12	11.93	9.59	8.13	6.71	5.54	4.08	3.34	2.74	8.21
Drop	Sequence	Time:	8:47	Air	Temp	(F):	82.1				
GPS:	Quality	Fi	Latitude	=	38	deg55.393435	N	Longitude	=	111	deg14.666473
Note:	SR	PDOP	=	1.5							

16. APPENDIX F: REPETITIVE STATIC PLATE LOAD TEST DATA SHEETS

Repetitive Static Plate Load Test according to ASTM D1195-09(2015)					
Project:	SR-10		Date:	7/25/2018	
Location:	1		Personnel:	Dr. Lawton and Emad	
Material Classification:			Temperature:	24	
Pavement conditions:			Water Table Depth:		
				Dial 1	Dial 2
Load Reading	Load (lbs)	Time (min)		Dial reading (in)	Dial reading (in)
4064	27190.25			0.1020	0.0336
4186	28273.25			0.1010	0.0513
4183	28246.61			0.1007	0.0548
4188	28291.00			0.1006	0.0567
4236	28717.10	0		0.1002	0.0611
4234	28699.34	1		0.1000	0.0633
4236	28717.10	2		0.0996	0.0668
4234	28699.34	3		0.0994	0.0687
4235	28708.22	4		0.0993	0.0702
4218	28557.31	5		0.0992	0.0704
		6		0.0992	0.0704
4267	28992.28	0		0.0989	0.0738
4257	28903.51	2		0.0986	0.0774
4260	28930.14	3		0.0985	0.0784
4260	28930.14	4		0.0985	0.0784
4350	29729.07	0		0.0975	0.0889
4322	29480.52	1		0.0971	0.0925
4329	29542.66	2		0.0970	0.0932
4332	29569.29	4		0.0967	0.0967
4430	30439.23	0		0.0959	0.1057
4410	30261.69	1		0.0957	0.1079
4409	30252.82	2		0.0956	0.1094
4408	30243.94	3		0.0953	0.1170
4398	30155.17	7		0.0952	0.1123
4494	31007.36	0		0.0947	0.1194
4482	30900.84	1		0.0945	0.1207

4481	30891.96	2		0.0944	0.1217
4480	30883.08	3		0.0944	0.1217
4572	31699.77	0		#VALUE!	?
?	#VALUE!	1		0.0936	0.1303
4556	31557.74	2		0.0934	0.1313
4560	31593.24	3		0.0934	0.1317
4652	32409.93	0		0.0930	0.1410
4657	32454.31	1		0.0921	0.1442
4639	32294.53	2		0.0920	0.1458
4644	32338.91	3		0.0918	0.1470
4647	32365.54	4		0.0914	0.1508
4627	32188.00	6		0.0909	0.1577
4644	32338.91	8		0.0906	0.1599
4072	27261.27	0		0.0960	0.1000
4074	27279.02	1		0.0966	0.0944
4071	27252.39	2		0.0967	0.0924
4076	27296.78	3		0.0969	0.0906
4079	27323.41	4		0.0970	0.0897

Repetitive Static Plate Load Test according to ASTM D1195-09(2015)					
Project:	SR-10		Date:	7/25/2018	
Location:	4		Personnel:	Dr. Lawton and Emad	
Material Classification:			Temperature:	24	
Pavement conditions:			Water Table Depth:		
				Dial 1	Dial 2
Load Reading	Load (lbs)	Time (min)		Dial reading (in)	Dial reading (in)
710	-2583.21	0		0.1134	0.0013
768	-2068.34	0		0.1132	0.0033
762	-2121.60	1		0.1131	0.0043
763	-2112.73	2		0.1130	0.0064
763	-2112.73	3		0.1130	0.0064
808	-1713.26	0		0.1129	0.0070
802	-1766.52	1		.1128.5	0.0076
894	-949.84	0		0.1125	0.0110
885	-1029.73	1		0.1124	0.0119
882	-1056.36	2		0.1124	0.0119
881	-1065.24	3		0.1124	0.0119
971	-266.31	0		0.1120	0.0150
968	-292.94	1		0.1120	0.0154
967	-301.82	2		0.1121	0.0154
1065	568.13	0		.1122.5	0.0177
1052	452.73	1		0.1123	0.0183
1050	434.97	2		0.1125	0.0201
1047	408.34	3		0.1125	0.0206
1145	1278.29	0		0.1113	0.0221
1138	1216.15	1		0.1112	0.0228
1133	1171.76	2		0.1111.5	0.0234
1225	1988.45	0		0.1109	0.0256
1216	1908.56	1		0.1108	0.0265
1212	1873.05	2		0.1107	0.0273
1207	1828.66	3		0.1107	0.0275

1313	2769.62	0		0.1105	0.0292
1299	2645.35	1		0.1104	0.0297
1291	2574.33	2		0.1104	0.0303
1390	3453.15	0		0.1102	0.0325
1381	3373.26	1		0.1100	0.0329
1374	3311.12	2		0.1100	0.0330
1468	4145.56	0		0.1099	0.0393
1450	3985.77	2		0.1097	0.0369
1447	3959.14	3		0.1096	0.0369
1551	4882.35	0		0.1095	0.0375
1536	4749.20	2		0.1092	0.0402
1530	4695.93	3		0.1092	0.0402
1634	5619.14	0		0.1092	0.0409
1625	5539.25	1		0.1091	0.0413
1617	5468.23	2		0.1091	0.0417
1725	6426.95	0		0.1088	0.0448
1713	6320.42	1		0.1088	0.0449
1822	7288.02	0		0.1086	0.0465
1806	7145.99	1		0.1085	0.0467
1800	7092.72	2		0.1085	0.0473
1993	8805.98	0		0.1081	0.0505
1973	8628.44	1		0.1078	0.0537
1965	8557.43	2		0.1077	0.0538
2150	10199.67	0		0.1073	0.0581
2138	10093.15	1		0.1071	0.0602
2129	10013.26	2		0.1070	0.0603
2320	11708.76	0		0.1068	0.0622
2295	11486.84	1		0.1067	0.0633
2290	11442.45	2		0.1066	0.0641
2501	13315.50	0		0.1062	0.0679
2482	13146.84	1		0.1061	0.0693
2973	17505.44	2		0.1059	0.0702
2965	17434.43	3		0.1058	0.0713

2684	14939.99	0		0.1055	0.0754
2666	14780.21	1		0.1053	0.0768
2654	14673.68	2		0.1051	0.0788
2645	14593.79	3		0.1050	0.0793
2920	17034.96	0		0.1045	0.0833
2901	16866.30	1		0.1043	0.0866
2890	16768.65	2		0.1042	0.0870
2887	16742.02	3		0.1042	0.0878
3182	19360.74	0		0.1035	0.0948
3160	19165.44	1		0.1034	0.0958
3150	19076.67	2		0.1032	0.0972
3143	19014.53	3		0.1031	0.0985
3137	18961.27	4		0.1029	0.0993
715	-2538.82	0		0.1065	0.0589
715	-2538.82	1		0.1072	0.0529
714	-2547.70	2		0.1075	0.0503
714	-2547.70	3		0.1076	0.0494
714	-2547.70	4		0.1076	0.0485

Repetitive Static Plate Load Test according to ASTM D1195-09(2015)					
Project:	SR-10		Date:	7/25/2018	
Location:	6		Personnel:	Dr. Lawton and Emad	
Material Classification:			Temperature:	29	
Pavement conditions:			Water Table Depth:		
				Dial 1	Dial 2
Load Reading	Load (lbs)	Time (min)		Dial reading (in)	Dial reading (in)
696	-2707.49	0		0.0456	0.0251
824	-1571.23	0		0.0454	0.0252
816	-1642.25	1		0.0454	0.0252
1110	967.59	0		0.0445	0.0319
1070	612.51	1		0.0443	0.0333
1074	648.02	2		0.0441	0.0346
1087	763.42	3		0.0441	0.0346
1385	3408.77	0		0.0436	0.0386
1366	3240.11	1		0.0435	0.0392
1377	3337.75	2		0.0434	0.0392
1870	7714.11	0		0.0422	0.0484
1826	7323.53	1		0.0420	0.0499
1820	7270.26	2		0.0419	0.0508
1804	7128.23	3		0.0418	0.0513
2269	11256.04	0		0.0406	0.0611
2060	9400.74	1		0.0403	0.0628
2090	9667.05	3		0.0400	0.0649
1875	7758.50	4		0.0398	0.0664
790	-1873.05	0		0.0417	0.0515
517	-4296.47	1		0.0417	0.0503
528	-4198.82	2		0.0417	0.0485
558	-3932.51	3		0.0417	0.0485

Repetitive Static Plate Load Test according to ASTM D1195-09(2015)					
Project:	SR-10		Date:	7/25/2018	
Location:	8		Personnel:	Dr. Lawton and Emad	
Material Classification:			Temperature:	30	
Pavement conditions:			Water Table Depth:		
				Dial 1	Dial 2
Load Reading	Load (lbs)	Time (min)		Dial reading (in)	Dial reading (in)
1904	8015.93	0		0.2168	0.0262
2180	10465.98	0		0.2152	0.0474
2189	10545.88	1		0.2150	0.0507
2233	10936.46	2		0.2150	0.0523
2286	11406.95	3		0.2149	0.0538
2600	14194.32	0		0.2138	0.0702
2607	14256.46	1		0.2135	0.0740
2653	14664.80	2		0.2134	0.0757
2678	14886.73	3		0.2133	0.0773
2697	15055.39	4		0.2132	0.0778
2999	17736.25	0		0.2121	0.0903
3021	17931.54	1		0.2118	0.0940
3040	18100.20	2		0.2117	0.0958
3040	18100.20	3		0.2117	0.0967
3089	18535.18	4		0.2116	0.0981
3107	18694.96	5		0.2120	0.0990
3402	21313.68	0		0.2105	0.1079
3429	21553.36	1		0.2103	0.1099
3452	21757.53	2		0.2102	0.1116
3455	21784.16	3		0.2101	0.1125
3474	21952.82	4		0.2100	0.1135
2825	16191.65	0		0.2128	0.0863
2855	16457.96	1		0.2131	0.0813
2867	16564.48	2		0.2133	0.0793
2928	17105.98	3		0.2134	0.0778
2981	17576.46	4		0.2135	0.0770

Repetitive Static Plate Load Test according to ASTM D1195-09(2015)					
Project:	SR-10		Date:	7/25/2018	
Location:	11		Personnel:	Dr. Lawton and Emad	
Material Classification:			Temperature:	31	
Pavement conditions:			Water Table Depth:		
				Dial 1	Dial 2
Load Reading	Load (lbs)	Time		Dial reading (in)	Dial reading (in)
723	-2467.81	0		0.2197	-0.0020
826	-1553.48	0		0.2198	-0.0015
822	-1588.98	1		0.2198	-0.0015
822	-1588.98	2		0.2198	-0.0015
921	-710.16	0		0.2197	-0.0015
912	-790.05	1		0.2197	-0.0015
1104	914.33	0		0.2193	0.0011
1100	878.82	1		0.2192	0.0022
1095	834.44	2		0.2192	0.0023
1388	3435.40	0		0.2188	0.0079
1376	3328.88	1		0.2187	0.0091
1367	3248.98	2		0.2186	0.0100
1362	3204.60	3		0.2185	0.0101
1856	7589.84	0		0.2180	0.0166
1831	7367.91	1		0.2179	0.0185
1822	7288.02	2		0.2178	0.0193
1817	7243.63	3		0.2178	0.0203
				0.0000	0.0000
2302	11548.98	0		0.2172	0.0255
2279	11344.81	1		0.2171	0.0274
2268	11247.16	2		0.2170	0.0278
2263	11202.77	3		0.2170	0.0285
2740	15437.10	0		0.2166	0.0335
2715	15215.18	1		0.2165	0.0348
2706	15135.29	2		0.2163	0.0366
2691	15002.13	3		0.2163	0.0367
	-8885.88				

3183	19369.61	0		0.2159	0.0420
3155	19121.06	1		0.2157	0.0438
3192	19449.51	2		0.2156	0.0451
3130	18899.13	3		0.2156	0.0454
	-8885.88				
3611	23168.97	0		0.2151	0.0514
3543	22565.33	1		0.2150	0.0529
3578	22876.03	2		0.2149	0.0538
3571	22813.89	3		0.2148	0.0545
4041	26986.08	0		0.2144	0.0600
4016	26764.16	1		0.2143	0.0621
4001	26631.00	2		0.2142	0.0626
3992	26551.11	3		0.2141	0.0635
4481	30891.96	0		0.2138	0.0702
4462	30723.30	1		0.2136	0.0724
4452	30634.53	2		0.2135	0.0742
4446	30581.27	3		0.2134	0.0750
4440	30528.00	4		0.2133	0.0764
4435	30483.62	5		0.2133	0.0769
4872	34362.87	0		0.2128	0.0852
4865	34300.73	1		0.2127	0.0881
4859	34247.47	2		0.2126	0.0888
4858	34238.59	3		0.2125	0.0898
4857	34229.71	4		0.2125	0.0907
727	-2432.30	0		0.2162	0.0504
738	-2334.65	1		0.2167	0.0443
761	-2130.48	2		0.2167	0.0443
775	-2006.20	3		0.2167	0.0435

Repetitive Static Plate Load Test according to ASTM D1195-09(2015)					
Project:	SR-10		Date:	7/25/2018	
Location:	12		Personnel:	Dr. Lawton and Emad	
Material Classification:			Temperature:	29	
Pavement conditions:			Water Table Depth:		
				Dial 1	Dial 2
Load Reading	Load (lbs)	Time (min)		Dial reading (in)	Dial reading (in)
723	-2467.81	0		0.2136	0.1398
1009	71.02	0		0.2158	0.1443
999	-17.75	1		0.2157	0.1458
994	-62.14	2		0.2158	0.1458
992	-79.89	3		0.2157	0.1458
991	-88.77	4		0.2156	0.1474
990	-97.65	5		0.2156	0.1474
1501	4438.50	0		0.2158	0.1559
1478	4234.33	1		0.2146	0.1574
1472	4181.07	2		0.2146	0.1574
1966	8566.31	0		0.2140	0.1647
1942	8353.26	1		0.2137	0.1685
1931	8255.61	2		0.2137	0.1685
1927	8220.10	3		0.2137	0.1685
2404	12454.43	0		0.2132	0.1739
2382	12259.14	1		0.2130	0.1764
2371	12161.49	2		0.2130	0.1764
2369	12143.74	3		0.2130	0.1764
	-8885.88				
2844	16360.31	0		0.2123	0.1818
2817	16120.63	1		0.2123	0.1835
2806	16022.99	2		0.2123	0.1840
2798	15951.97	3		0.2123	0.1840
	-8885.88				
3275	20186.30	0		0.2115	0.1922
3247	19937.74	1		0.2115	0.1922
3235	19831.22	2		0.2115	0.1925
3694	23905.76	0		0.2110	

3681	23790.36	1		0.2107	0.2025
3668	23674.96	2		0.2107	0.2025
3660	23603.94	3		0.2106	0.2025
4136	27829.40	0		0.2100	0.2114
4129	27767.26	1		0.2098	0.2137
4121	27696.24	2		0.2097	0.2158
4116	27651.86	3		0.2097	0.2158
4110	27598.59	4		0.2096	0.2166
4348	29711.32	0		0.2093	0.2238
4340	29640.30	1		0.2084	0.2336
4332	29569.29	2		0.2084	0.2336
4326	29516.03	3		0.2084	0.2336
4512	31167.15	0		0.2085	0.2368
4504	31096.13	1		0.2085	0.2379
4499	31051.75	2		0.2085	0.2395
4495	31016.24	3		0.2085	0.2395
4491	30980.73	4		0.2085	0.2395
724	-2458.93	0		0.2094	0.2327
724	-2458.93	1		0.2095	0.2316
724	-2458.93	2		0.2095	0.2316
722	-2476.68	3		0.2095	0.2315

17. APPENDIX G: DYNAMIC CONE PENETROMETER TEST DATA SHEETS

Dynamic Cone Penetrometer Test According to ASTM D6951-18						
Project: SR-10				Date: 7-25-18		
Location: 1-C				Personnel: Henrik		
Depth of zero point below Surface:		419 mm		Hammer Weight: 8 kg		
Material Classification:				Temperature: 21 F		
Pavement conditions:				Water Table Depth:		
Number of Blows	Cumulative Penetration (mm)	Penetration Between Readings (mm)	Penetration per Blow (mm)	Hammer Factor	DCP Index (mm/blow)	CBR (%)
0	419					
3	455	36	12.00	1.00	12.00	18.06
3	477	22	7.33	1.00	7.33	31.35
3	494	17	5.67	1.00	5.67	41.85
5	512	18	3.60	1.00	3.60	69.55
5	533	21	4.20	1.00	4.20	58.53
5	549	16	3.20	1.00	3.20	79.36
5	586	37	7.40	1.00	7.40	31.03
5	621	35	7.00	1.00	7.00	33.03
5	675	54	10.80	1.00	10.80	20.32
5	731	56	11.20	1.00	11.20	19.51
5	897	166	33.20	1.00	33.20	5.78

Dynamic Cone Penetrometer Test According to ASTM D6951-18						
Project: SR-10				Date: 7-25-18		
Location: 2- C				Personnel: Henrik		
Depth of zero point below Surface: 348				Hammer Weight: 8 kg		
Material Classification:				Temperature: 24 C		
Pavement conditions:				Water Table Depth:		
Number of Blows	Cumulative Penetration (mm)	Penetration Between Readings (mm)	Penetration per Blow (mm)	Hammer Factor	DCP Index (mm/blow)	CBR (%)
0	348					
3	375	27	9.00	1.00	9.00	24.92
3	387	12	4.00	1.00	4.00	61.81
3	395	8	2.67	1.00	2.67	97.34
5	409	14	2.80	1.00	2.80	92.16
5	420	11	2.20	1.00	2.20	120.75
5	431	11	2.20	1.00	2.20	120.75
5	440	9	1.80	1.00	1.80	151.17
5	445	5	1.00	1.00	1.00	292.00
5	453	8	1.60	1.00	1.60	172.49
5	460	7	1.40	1.00	1.40	200.32
5	469	9	1.80	1.00	1.80	151.17
5	478	9	1.80	1.00	1.80	151.17
5	484	6	1.20	1.00	1.20	238.07
5	491	7	1.40	1.00	1.40	200.32
5	499	8	1.60	1.00	1.60	172.49
5	504	5	1.00	1.00	1.00	292.00
5	511	7	1.40	1.00	1.40	200.32
5	520	9	1.80	1.00	1.80	151.17
8	526	6	0.75	1.00	0.75	403.01
8	537	11	1.38	1.00	1.38	204.40
8	548	11	1.38	1.00	1.38	204.40
8	556	8	1.00	1.00	1.00	292.00
8	560	4	0.50	1.00	0.50	634.65
10	571	11	1.10	1.00	1.10	262.44
10	576	5	0.50	1.00	0.50	634.65
10	582	6	0.60	1.00	0.60	517.43
10	589	7	0.70	1.00	0.70	435.38
10	600	11	1.10	1.00	1.10	262.44
10	610	10	1.00	1.00	1.00	292.00
10	621	11	1.10	1.00	1.10	262.44
10	630	9	0.90	1.00	0.90	328.57
10	638	8	0.80	1.00	0.80	374.91

10	643	5	0.50	1.00	0.50	634.65
10	650	7	0.70	1.00	0.70	435.38
10	658	8	0.80	1.00	0.80	374.91
10	670	12	1.20	1.00	1.20	238.07
10	680	10	1.00	1.00	1.00	292.00
10	690	10	1.00	1.00	1.00	292.00
10	701	11	1.10	1.00	1.10	262.44
10	711	10	1.00	1.00	1.00	292.00
10	725	14	1.40	1.00	1.40	200.32
10	747	22	2.20	1.00	2.20	120.75
10	801	54	5.40	1.00	5.40	44.17

Dynamic Cone Penetrometer Test According to ASTM D6951-18						
Project: SR-10				Date: 7-25-18		
Location: 3- C				Personnel: Henrik		
Depth of zero point below Surface: 481				Hammer Weight: 8 kg		
Material Classification:				Temperature: 30.5 C		
Pavement conditions:				Water Table Depth:		
Number of Blows	Cumulative Penetration (mm)	Penetration Between Readings (mm)	Penetration per Blow (mm)	Hammer Factor	DCP Index (mm/blow)	CBR (%)
0	481					
3	505	24	8.00	1.00	8.00	28.44
3	524	19	6.33	1.00	6.33	36.94
3	543	19	6.33	1.00	6.33	36.94
5	571	28	5.60	1.00	5.60	42.40
5	586	15	3.00	1.00	3.00	85.31
5	595	9	1.80	1.00	1.80	151.17
5	602	7	1.40	1.00	1.40	200.32
5	610	8	1.60	1.00	1.60	172.49
5	620	10	2.00	1.00	2.00	134.35
5	628	8	1.60	1.00	1.60	172.49
5	635	7	1.40	1.00	1.40	200.32
5	643	8	1.60	1.00	1.60	172.49
5	650	7	1.40	1.00	1.40	200.32
5	662	12	2.40	1.00	2.40	109.53
5	667	5	1.00	1.00	1.00	292.00
5	670	3	0.60	1.00	0.60	517.43
5	676	6	1.20	1.00	1.20	238.07
5	682	6	1.20	1.00	1.20	238.07
8	692	10	1.25	1.00	1.25	227.43
8	702	10	1.25	1.00	1.25	227.43
8	715	13	1.63	1.00	1.63	169.52
8	736	21	2.63	1.00	2.63	99.07
8	755	19	2.38	1.00	2.38	110.83
10	789	34	3.40	1.00	3.40	74.15
10	852	63	6.30	1.00	6.30	37.16
3	907	55	18.33	1.00	18.33	11.23

Dynamic Cone Penetrometer Test According to ASTM D6951-18						
Project: SR-10				Date: 7-25-18		
Location: 4- C				Personnel: Henrik		
Depth of zero point below Surface: 411				Hammer Weight: 8 kg		
Material Classification:				Temperature: 34 C		
Pavement conditions:				Water Table Depth:		
Number of Blows	Cumulative Penetration (mm)	Penetration Between Readings (mm)	Penetration per Blow (mm)	Hammer Factor	DCP Index (mm/blow)	CBR %
0	411					
3	483	72	24.00	1.00	24.00	8.31
3	496	13	4.33	1.00	4.33	56.51
3	520	24	8.00	1.00	8.00	28.44
5	543	23	4.60	1.00	4.60	52.86
5	566	23	4.60	1.00	4.60	52.86
5	584	18	3.60	1.00	3.60	69.55
5	601	17	3.40	1.00	3.40	74.15
5	607	6	1.20	1.00	1.20	238.07
5	616	9	1.80	1.00	1.80	151.17
5	623	7	1.40	1.00	1.40	200.32
5	630	7	1.40	1.00	1.40	200.32
5	640	10	2.00	1.00	2.00	134.35
5	645	5	1.00	1.00	1.00	292.00
5	652	7	1.40	1.00	1.40	200.32
5	659	7	1.40	1.00	1.40	200.32
5	662	3	0.60	1.00	0.60	517.43
5	666	4	0.80	1.00	0.80	374.91
8	682	16	2.00	1.00	2.00	134.35
8	691	9	1.13	1.00	1.13	255.91
8	700	9	1.13	1.00	1.13	255.91
8	712	12	1.50	1.00	1.50	185.42
8	741	29	3.63	1.00	3.63	69.02
10	771	30	3.00	1.00	3.00	85.31
10	802	31	3.10	1.00	3.10	82.24
3	813	11	3.67	1.00	3.67	68.14

Dynamic Cone Penetrometer Test According to ASTM D6951-18						
Project: SR-10				Date: 7-25-18		
Location: 5- C				Personnel: Nadi		
Depth of zero point below Surface: 388				Hammer Weight: 8 kg		
Material Classification:				Temperature: 37 C		
Pavement conditions:				Water Table Depth:		
Number of Blows	Cumulative Penetration (mm)	Penetration Between Readings (mm)	Penetration per Blow (mm)	Hammer Factor	DCP Index (mm/blow)	CBR (%)
0	388					
3	443	55	18.33	1.00	18.33	11.23
3	468	25	8.33	1.00	8.33	27.17
3	485	17	5.67	1.00	5.67	41.85
5	529	44	8.80	1.00	8.80	25.56
5	540	11	2.20	1.00	2.20	120.75
5	565	25	5.00	1.00	5.00	48.14
5	573	8	1.60	1.00	1.60	172.49
5	582	9	1.80	1.00	1.80	151.17
5	592	10	2.00	1.00	2.00	134.35
5	600	8	1.60	1.00	1.60	172.49
5	629	29	5.80	1.00	5.80	40.77
5	638	9	1.80	1.00	1.80	151.17
5	640	2	0.40	1.00	0.40	814.85
5	644	4	0.80	1.00	0.80	374.91
5	669	25	5.00	1.00	5.00	48.14
5	688	19	3.80	1.00	3.80	65.47
5	699	11	2.20	1.00	2.20	120.75
5	707	8	1.60	1.00	1.60	172.49
8	743	36	4.50	1.00	4.50	54.17
8	804	61	7.63	1.00	7.63	30.01

Dynamic Cone Penetrometer Test According to ASTM D6951-18						
Project: SR-10				Date: 7-25-18		
Location: 6- C				Personnel: Nadi		
Depth of zero point below Surface: 380				Hammer Weight: 8 kg		
Material Classification:				Temperature: 36 C		
Pavement conditions:				Water Table Depth:		
Number of Blows	Cumulative Penetration (mm)	Penetration Between Readings (mm)	Penetration per Blow (mm)	Hammer Factor	DCP Index (mm/blow)	CBR (%)
0	380					
3	407	27	9.00	1.00	9.00	24.92
3	430	23	7.67	1.00	7.67	29.83
3	451	21	7.00	1.00	7.00	33.03
5	492	41	8.20	1.00	8.20	27.66
5	516	24	4.80	1.00	4.80	50.40
5	534	18	3.60	1.00	3.60	69.55
5	543	9	1.80	1.00	1.80	151.17
5	553	10	2.00	1.00	2.00	134.35
5	564	11	2.20	1.00	2.20	120.75
8	583	19	2.38	1.00	2.38	110.83
5	588	5	1.00	1.00	1.00	292.00
5	594	6	1.20	1.00	1.20	238.07
5	597	3	0.60	1.00	0.60	517.43
5	600	3	0.60	1.00	0.60	517.43
5	608	8	1.60	1.00	1.60	172.49
5	618	10	2.00	1.00	2.00	134.35
5	629	11	2.20	1.00	2.20	120.75
5	642	13	2.60	1.00	2.60	100.14
8	658	16	2.00	1.00	2.00	134.35
8	677	19	2.38	1.00	2.38	110.83
8	705	28	3.50	1.00	3.50	71.78
8	808	103	12.88	1.00	12.88	16.69

Dynamic Cone Penetrometer Test According to ASTM D6951-18						
Project: SR-10				Date: 7-25-18		
Location: 7- C				Personnel: Nadi		
Depth of zero point below Surface: 420				Hammer Weight: 8 kg		
Material Classification:				Temperature: 29 C		
Pavement conditions:				Water Table Depth:		
Number of Blows	Cumulative Penetration (mm)	Penetration Between Readings (mm)	Penetration per Blow (mm)	Hammer Factor	DCP Index (mm/blow)	CBR (%)
0	420					
3	460	40	13.33	1.00	13.33	16.05
3	481	21	7.00	1.00	7.00	33.03
3	499	18	6.00	1.00	6.00	39.25
5	525	26	5.20	1.00	5.20	46.07
5	547	22	4.40	1.00	4.40	55.55
5	573	26	5.20	1.00	5.20	46.07
5	586	13	2.60	1.00	2.60	100.14
5	593	7	1.40	1.00	1.40	200.32
5	597	4	0.80	1.00	0.80	374.91
5	604	7	1.40	1.00	1.40	200.32
5	607	3	0.60	1.00	0.60	517.43
5	612	5	1.00	1.00	1.00	292.00
5	621	9	1.80	1.00	1.80	151.17
5	625	4	0.80	1.00	0.80	374.91
5	633	8	1.60	1.00	1.60	172.49
5	642	9	1.80	1.00	1.80	151.17
5	647	5	1.00	1.00	1.00	292.00
5	655	8	1.60	1.00	1.60	172.49
8	666	11	1.38	1.00	1.38	204.40
8	677	11	1.38	1.00	1.38	204.40
8	688	11	1.38	1.00	1.38	204.40
8	697	9	1.13	1.00	1.13	255.91
8	704	7	0.88	1.00	0.88	339.10
8	722	18	2.25	1.00	2.25	117.74
8	739	17	2.13	1.00	2.13	125.53
8	762	23	2.88	1.00	2.88	89.48
8	805	43	5.38	1.00	5.38	44.40
3	820	15	5.00	1.00	5.00	48.14

Dynamic Cone Penetrometer Test According to ASTM D6951-18						
Project: SR-10				Date: 7-25-18		
Location: 8- C				Personnel: Nadi		
Depth of zero point below Surface: 391				Hammer Weight: 8 kg		
Material Classification:				Temperature: 30 C		
Pavement conditions:				Water Table Depth:		
Number of Blows	Cumulative Penetration (mm)	Penetration Between Readings (mm)	Penetration per Blow (mm)	Hammer Factor	DCP Index (mm/blow)	CBR (%)
0	391					
3	428	37	12.33	1.00	12.33	17.51
3	447	19	6.33	1.00	6.33	36.94
3	471	24	8.00	1.00	8.00	28.44
5	501	30	6.00	1.00	6.00	39.25
5	528	27	5.40	1.00	5.40	44.17
5	556	28	5.60	1.00	5.60	42.40
5	585	29	5.80	1.00	5.80	40.77
5	611	26	5.20	1.00	5.20	46.07
5	634	23	4.60	1.00	4.60	52.86
5	652	18	3.60	1.00	3.60	69.55
5	669	17	3.40	1.00	3.40	74.15
5	688	19	3.80	1.00	3.80	65.47
5	704	16	3.20	1.00	3.20	79.36
5	742	38	7.60	1.00	7.60	30.12
5	811	69	13.80	1.00	13.80	15.44

Dynamic Cone Penetrometer Test According to ASTM D6951-18						
Project: SR-10				Date: 7-25-18		
Location: 9- C				Personnel: Nadi		
Depth of zero point below Surface: 401				Hammer Weight: 8 kg		
Material Classification:				Temperature: 29 C		
Pavement conditions:				Water Table Depth:		
Number of Blows	Cumulative Penetration (mm)	Penetration Between Readings (mm)	Penetration per Blow (mm)	Hammer Factor	DCP Index (mm/blow)	CBR (%)
0	401					
3	425	24	8.00	1.00	8.00	28.44
3	448	23	7.67	1.00	7.67	29.83
3	461	13	4.33	1.00	4.33	56.51
5	482	21	4.20	1.00	4.20	58.53
5	501	19	3.80	1.00	3.80	65.47
5	526	25	5.00	1.00	5.00	48.14
5	559	33	6.60	1.00	6.60	35.28
5	586	27	5.40	1.00	5.40	44.17
5	612	26	5.20	1.00	5.20	46.07
5	633	21	4.20	1.00	4.20	58.53
5	655	22	4.40	1.00	4.40	55.55
5	671	16	3.20	1.00	3.20	79.36
5	689	18	3.60	1.00	3.60	69.55
5	705	16	3.20	1.00	3.20	79.36
5	724	19	3.80	1.00	3.80	65.47
5	740	16	3.20	1.00	3.20	79.36
5	765	25	5.00	1.00	5.00	48.14
5	790	25	5.00	1.00	5.00	48.14
8	861	71	8.88	1.00	8.88	25.32

Dynamic Cone Penetrometer Test According to ASTM D6951-18						
Project: SR-10				Date: 7-25-18		
Location: 10- C				Personnel: Nadi		
Depth of zero point below Surface: 478				Hammer Weight: 8 kg		
Material Classification:				Temperature: 28 C		
Pavement conditions:				Water Table Depth:		
Number of Blows	Cumulative Penetration (mm)	Penetration Between Readings (mm)	Penetration per Blow (mm)	Hammer Factor	DCP Index (mm/blow)	CBR (%)
0	478					
3	523	45	15.00	1.00	15.00	14.07
3	546	23	7.67	1.00	7.67	29.83
3	560	14	4.67	1.00	4.67	52.01
5	591	31	6.20	1.00	6.20	37.84
5	624	33	6.60	1.00	6.60	35.28
5	660	36	7.20	1.00	7.20	32.00
5	702	42	8.40	1.00	8.40	26.93
5	755	53	10.60	1.00	10.60	20.75
5	813	58	11.60	1.00	11.60	18.76
5	914	101	20.20	1.00	20.20	10.08

Dynamic Cone Penetrometer Test According to ASTM D6951-18						
Project: SR-10				Date: 7-25-18		
Location: 11- C				Personnel: Nadi		
Depth of zero point below Surface: 387				Hammer Weight: 8 kg		
Material Classification:				Temperature: 32 C		
Pavement conditions:				Water Table Depth:		
Number of Blows	Cumulative Penetration (mm)	Penetration Between Readings (mm)	Penetration per Blow (mm)	Hammer Factor	DCP Index (mm/blow)	CBR (%)
0	387					
3	422	35	11.67	1.00	11.67	18.64
3	436	14	4.67	1.00	4.67	52.01
3	450	14	4.67	1.00	4.67	52.01
5	470	20	4.00	1.00	4.00	61.81
5	491	21	4.20	1.00	4.20	58.53
5	507	16	3.20	1.00	3.20	79.36
5	528	21	4.20	1.00	4.20	58.53
5	545	17	3.40	1.00	3.40	74.15
5	565	20	4.00	1.00	4.00	61.81
5	581	16	3.20	1.00	3.20	79.36
5	600	19	3.80	1.00	3.80	65.47
5	619	19	3.80	1.00	3.80	65.47
5	637	18	3.60	1.00	3.60	69.55
5	663	26	5.20	1.00	5.20	46.07
5	694	31	6.20	1.00	6.20	37.84
5	724	30	6.00	1.00	6.00	39.25
5	759	35	7.00	1.00	7.00	33.03
5	803	44	8.80	1.00	8.80	25.56

Dynamic Cone Penetrometer Test According to ASTM D6951-18						
Project: SR-10				Date: 7-25-18		
Location: 12- C				Personnel: Nadi		
Depth of zero point below Surface: 322				Hammer Weight: 8 kg		
Material Classification:				Temperature: 30 C		
Pavement conditions:				Water Table Depth:		
Number of Blows	Cumulative Penetration (mm)	Penetration Between Readings (mm)	Penetration per Blow (mm)	Hammer Factor	DCP Index (mm/blow)	CBR (%)
0	322					
3	354	32	10.67	1.00	10.67	20.61
3	375	21	7.00	1.00	7.00	33.03
3	389	14	4.67	1.00	4.67	52.01
5	409	20	4.00	1.00	4.00	61.81
5	420	11	2.20	1.00	2.20	120.75
5	431	11	2.20	1.00	2.20	120.75
5	439	8	1.60	1.00	1.60	172.49
5	447	8	1.60	1.00	1.60	172.49
5	451	4	0.80	1.00	0.80	374.91
5	461	10	2.00	1.00	2.00	134.35
5	470	9	1.80	1.00	1.80	151.17
5	475	5	1.00	1.00	1.00	292.00
5	487	12	2.40	1.00	2.40	109.53
5	499	12	2.40	1.00	2.40	109.53
5	512	13	2.60	1.00	2.60	100.14
5	520	8	1.60	1.00	1.60	172.49
5	523	3	0.60	1.00	0.60	517.43
5	530	7	1.40	1.00	1.40	200.32
8	547	17	2.13	1.00	2.13	125.53
8	555	8	1.00	1.00	1.00	292.00
8	575	20	2.50	1.00	2.50	104.64
8	592	17	2.13	1.00	2.13	125.53
8	610	18	2.25	1.00	2.25	117.74
10	630	20	2.00	1.00	2.00	134.35
10	663	33	3.30	1.00	3.30	76.67
10	725	62	6.20	1.00	6.20	37.84

Dynamic Cone Penetrometer Test According to ASTM D6951-18						
Project: SR-10				Date: 7-25-18		
Location: 13- C				Personnel:		
Depth of zero point below Surface: 387				Hammer Weight: 8 kg		
Material Classification:				Temperature: 30 C		
Pavement conditions:				Water Table Depth:		
Number of Blows	Cumulative Penetration (mm)	Penetration Between Readings (mm)	Penetration per Blow (mm)	Hammer Factor	DCP Index (mm/blow)	CBR (%)
0	387					
3	410	23	7.67	1.00	7.67	29.83
3	418	8	2.67	1.00	2.67	97.34
3	424	6	2.00	1.00	2.00	134.35
5	435	11	2.20	1.00	2.20	120.75
5	441	6	1.20	1.00	1.20	238.07
5	458	17	3.40	1.00	3.40	74.15
5	472	14	2.80	1.00	2.80	92.16
5	490	18	3.60	1.00	3.60	69.55
5	506	16	3.20	1.00	3.20	79.36
5	525	19	3.80	1.00	3.80	65.47
5	542	17	3.40	1.00	3.40	74.15
5	561	19	3.80	1.00	3.80	65.47
5	579	18	3.60	1.00	3.60	69.55
5	600	21	4.20	1.00	4.20	58.53
5	615	15	3.00	1.00	3.00	85.31
5	644	29	5.80	1.00	5.80	40.77
5	654	10	2.00	1.00	2.00	134.35
5	672	18	3.60	1.00	3.60	69.55
8	719	47	5.88	1.00	5.88	40.19
8	749	30	3.75	1.00	3.75	66.45
8	782	33	4.13	1.00	4.13	59.72
3	790	8	2.67	1.00	2.67	97.34

Dynamic Cone Penetrometer Test According to ASTM D6951-18						
Project: SR-10				Date: 7-25-18		
Location: 14- C				Personnel: Nadi		
Depth of zero point below Surface: 356				Hammer Weight: 8 kg		
Material Classification:				Temperature: 33 C		
Pavement conditions:				Water Table Depth:		
Number of Blows	Cumulative Penetration (mm)	Penetration Between Readings (mm)	Penetration per Blow (mm)	Hammer Factor	DCP Index (mm/blow)	CBR (%)
0	356					
3	379	23	7.67	1.00	7.67	29.83
3	391	12	4.00	1.00	4.00	61.81
3	398	7	2.33	1.00	2.33	113.04
5	405	7	1.40	1.00	1.40	200.32
5	414	9	1.80	1.00	1.80	151.17
5	420	6	1.20	1.00	1.20	238.07
5	422	2	0.40	1.00	0.40	814.85
5	430	8	1.60	1.00	1.60	172.49
5	435	5	1.00	1.00	1.00	292.00
5	440	5	1.00	1.00	1.00	292.00
5	445	5	1.00	1.00	1.00	292.00
5	448	3	0.60	1.00	0.60	517.43
5	453	5	1.00	1.00	1.00	292.00
5	458	5	1.00	1.00	1.00	292.00
5	462	4	0.80	1.00	0.80	374.91
5	470	8	1.60	1.00	1.60	172.49
5	474	4	0.80	1.00	0.80	374.91
5	481	7	1.40	1.00	1.40	200.32
8	493	12	1.50	1.00	1.50	185.42
8	505	12	1.50	1.00	1.50	185.42
8	523	18	2.25	1.00	2.25	117.74
8	544	21	2.63	1.00	2.63	99.07
8	566	22	2.75	1.00	2.75	94.04
10	592	26	2.60	1.00	2.60	100.14
10	612	20	2.00	1.00	2.00	134.35
10	642	30	3.00	1.00	3.00	85.31
10	671	29	2.90	1.00	2.90	88.61
10	697	26	2.60	1.00	2.60	100.14
10	722	25	2.50	1.00	2.50	104.64
10	745	23	2.30	1.00	2.30	114.88
10	760	15	1.50	1.00	1.50	185.42

18. APPENDIX H: FIELD TEST LOCATION CROSS-SECTIONS

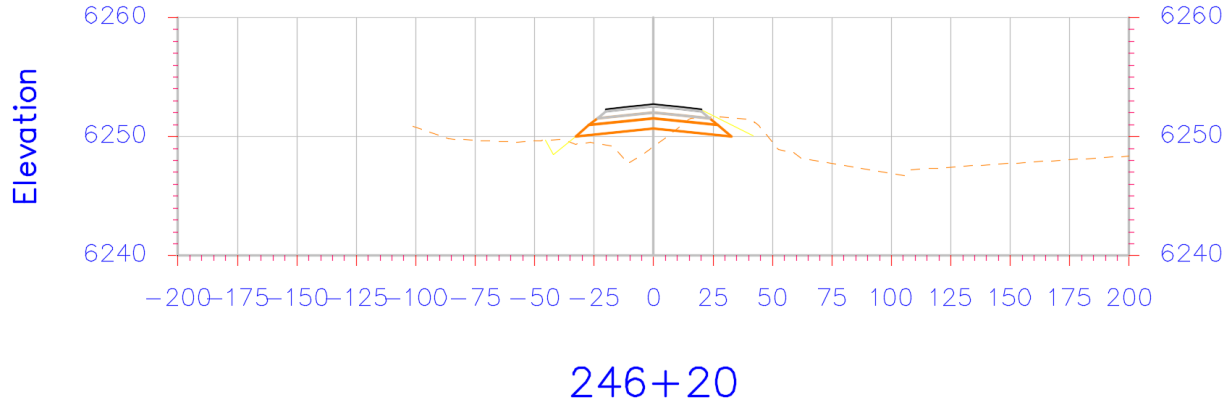

Location 1

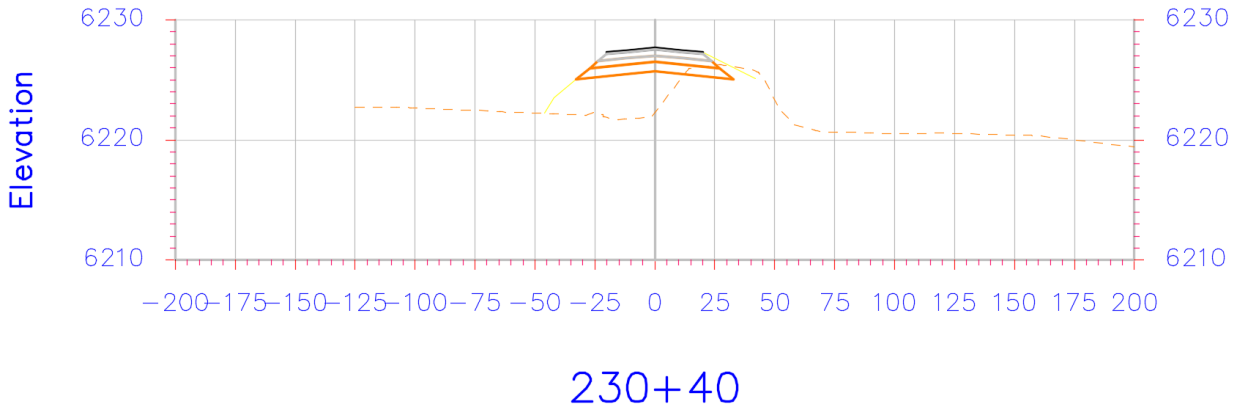

Location 2

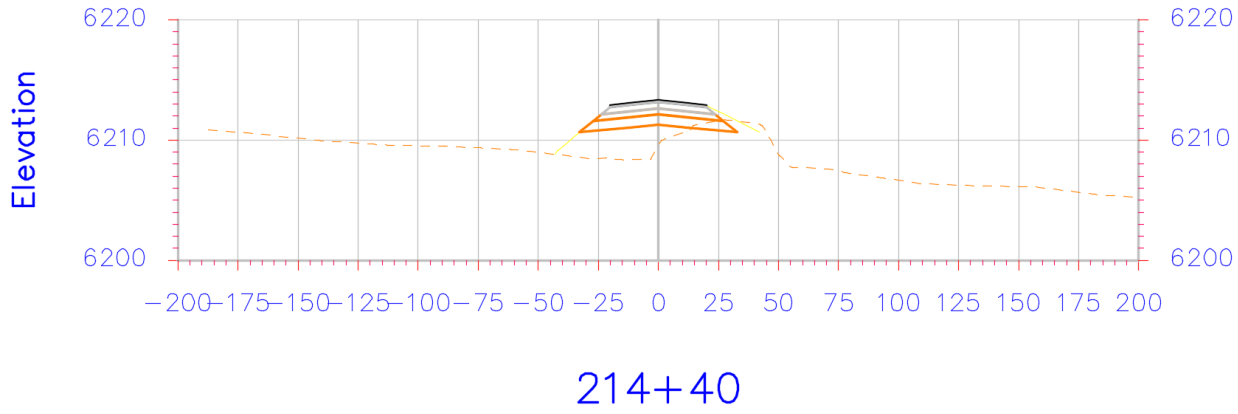

Location 3

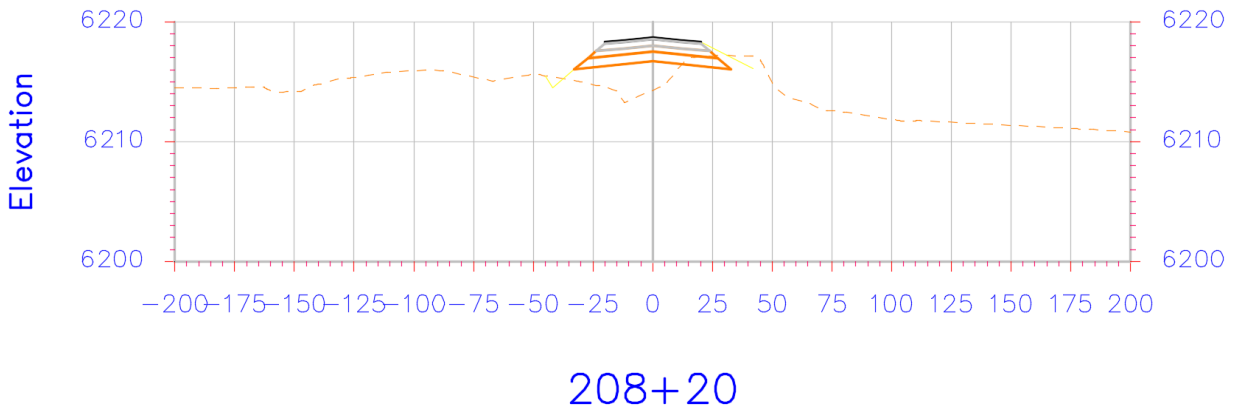

Location 4

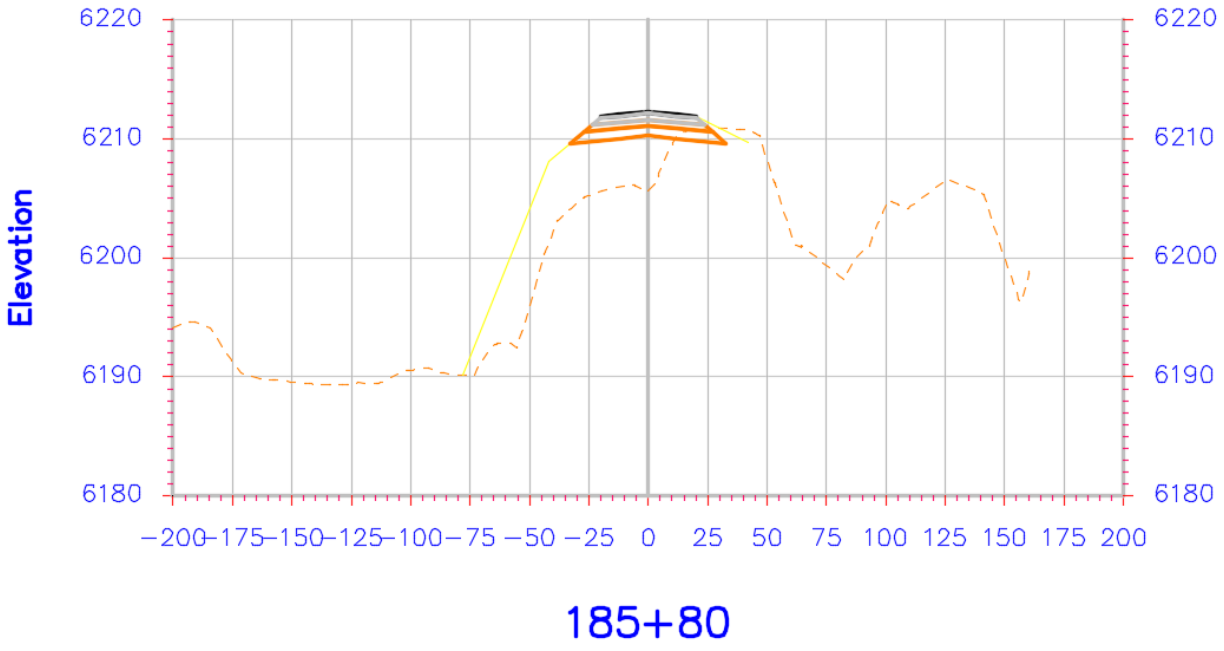

Location 5

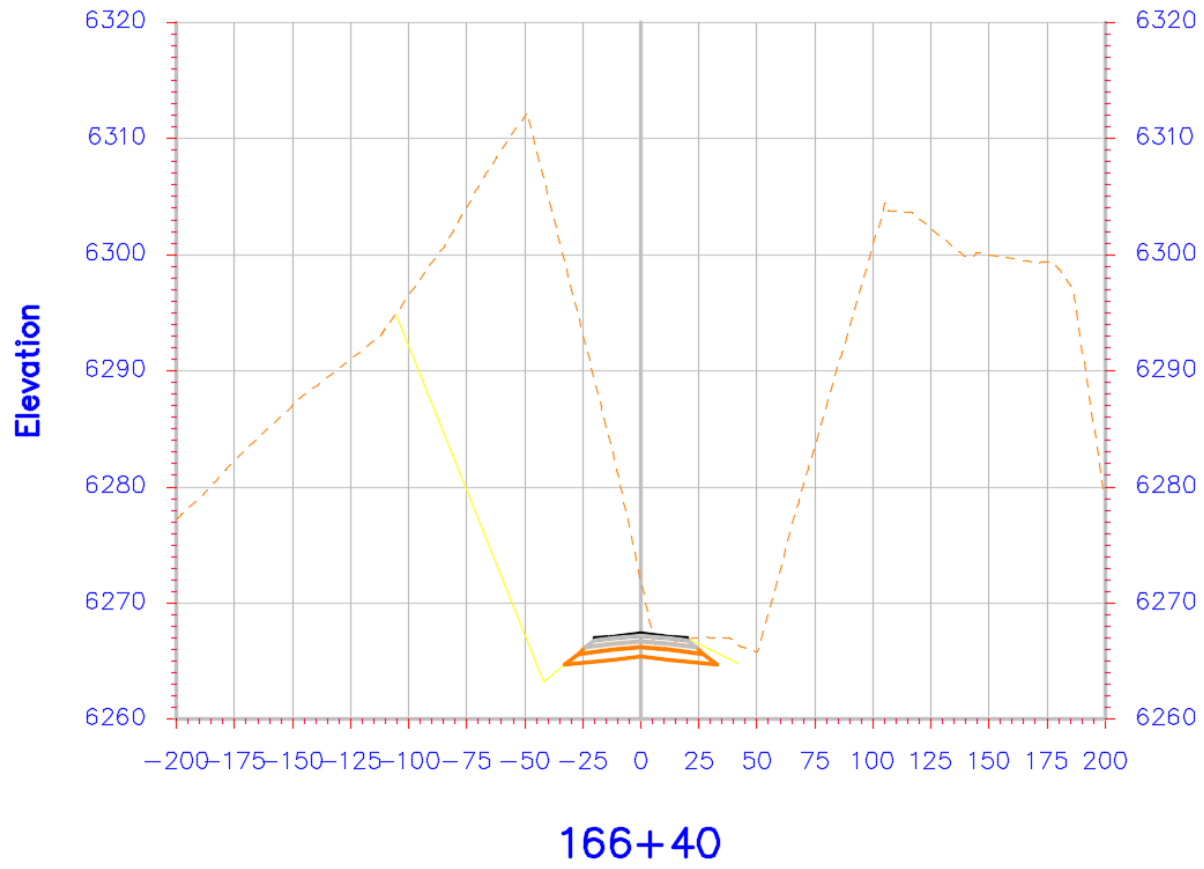

Location 6

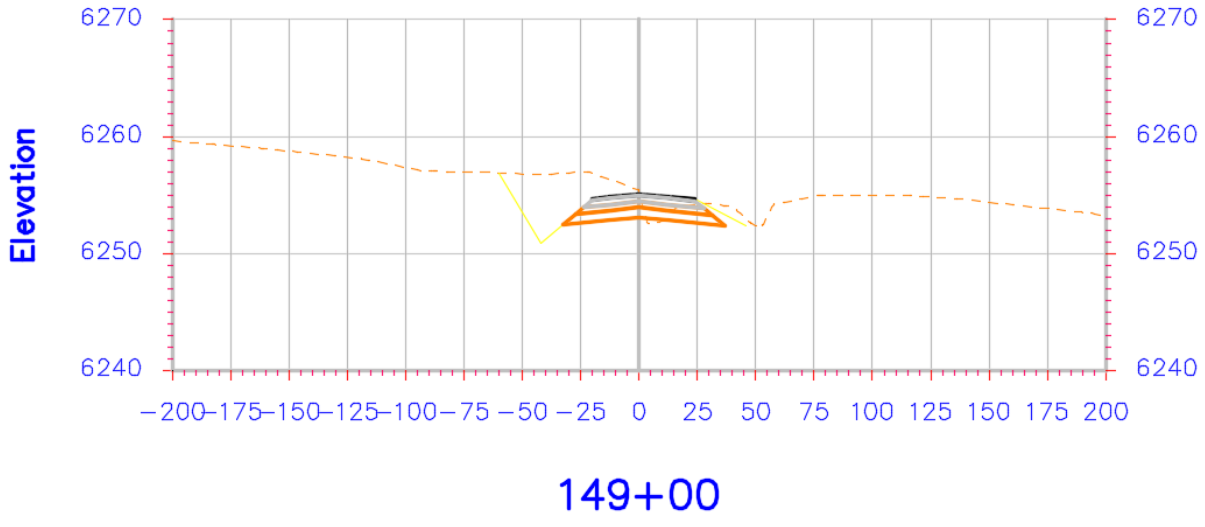

Location 7

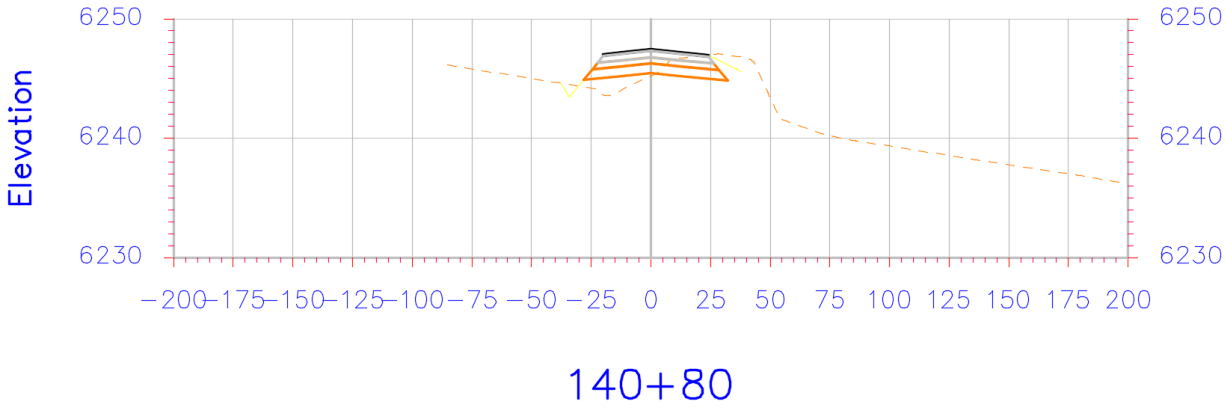

Location 8

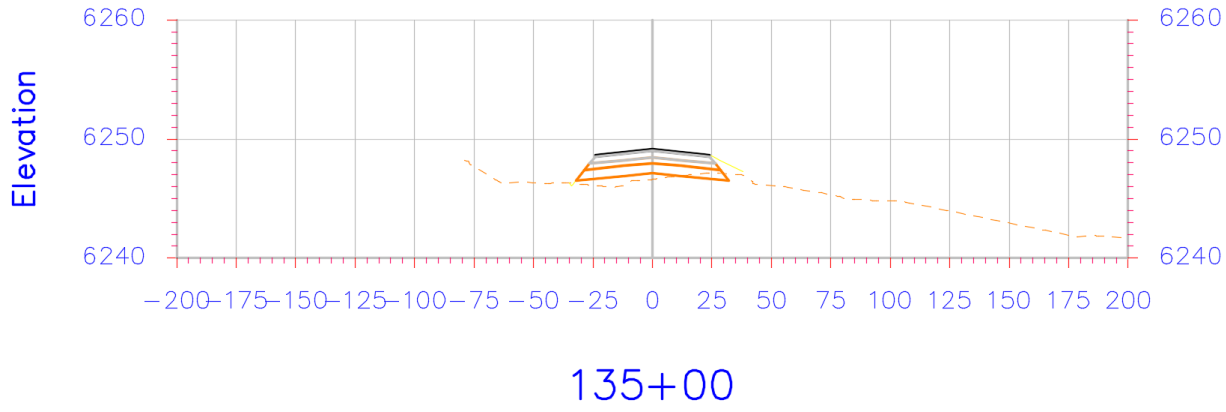

Location 9

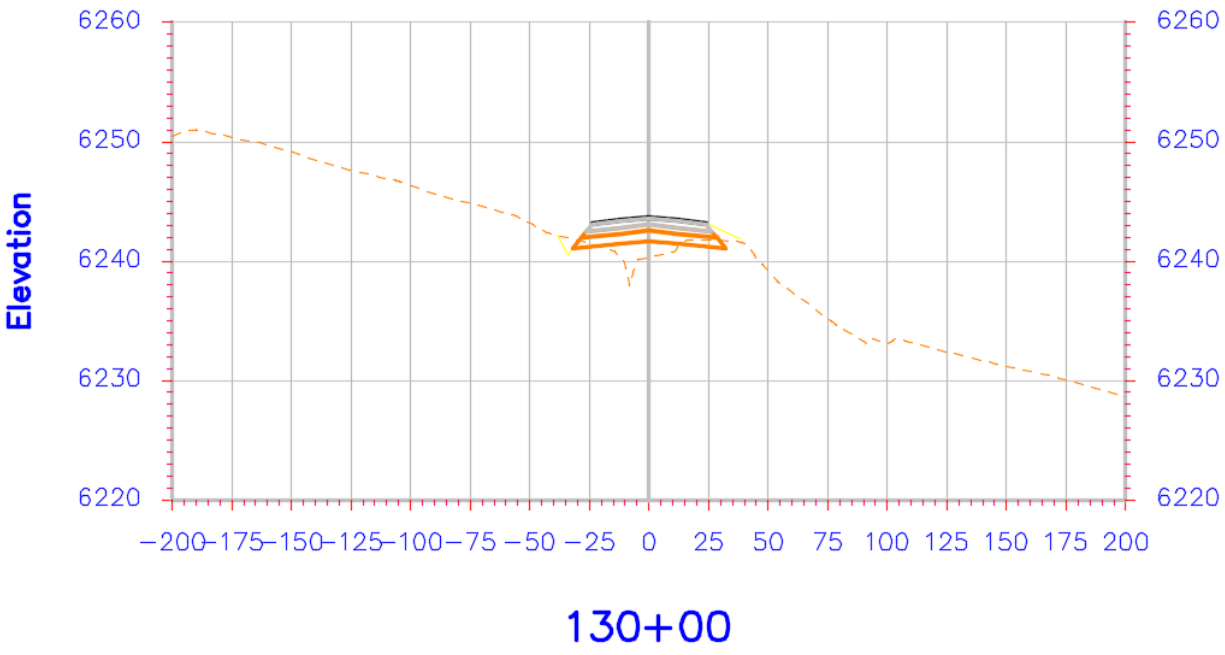

Location 10

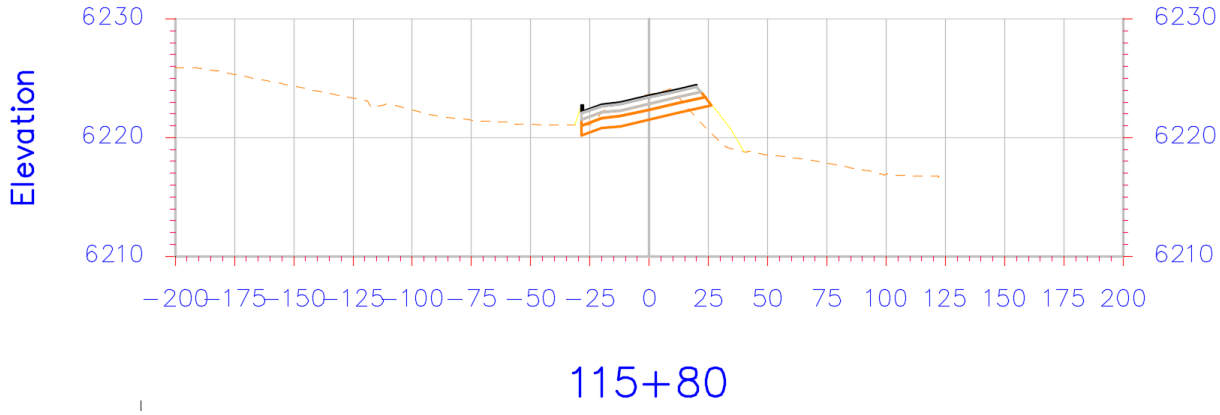

Location 11

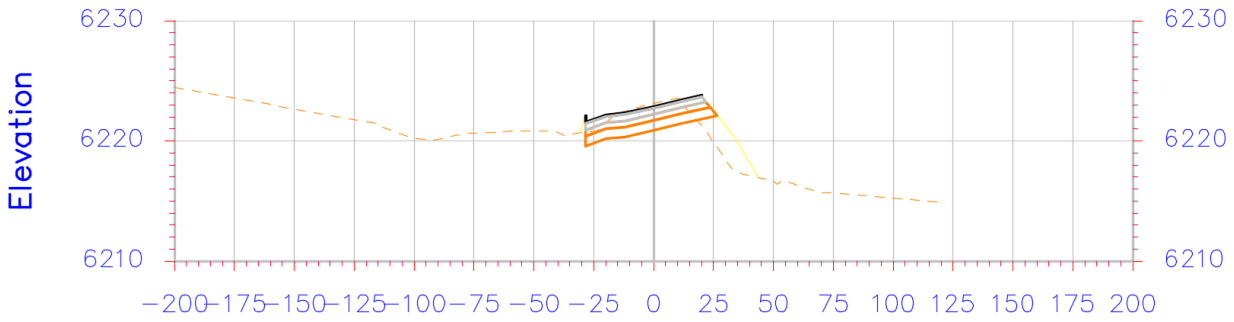

113+40

Location 12

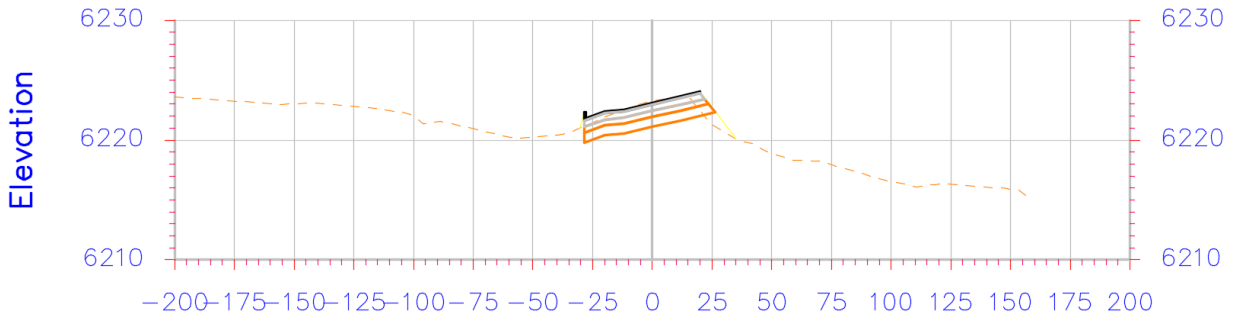

111+00

Location 13

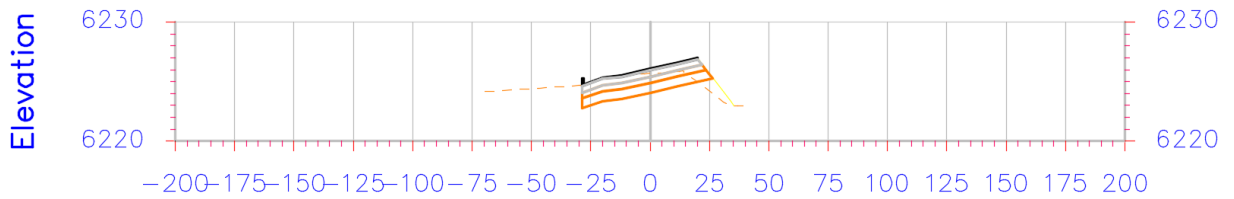

106+20

Location 14

19. APPENDIX I: GEOLOGICAL MAP

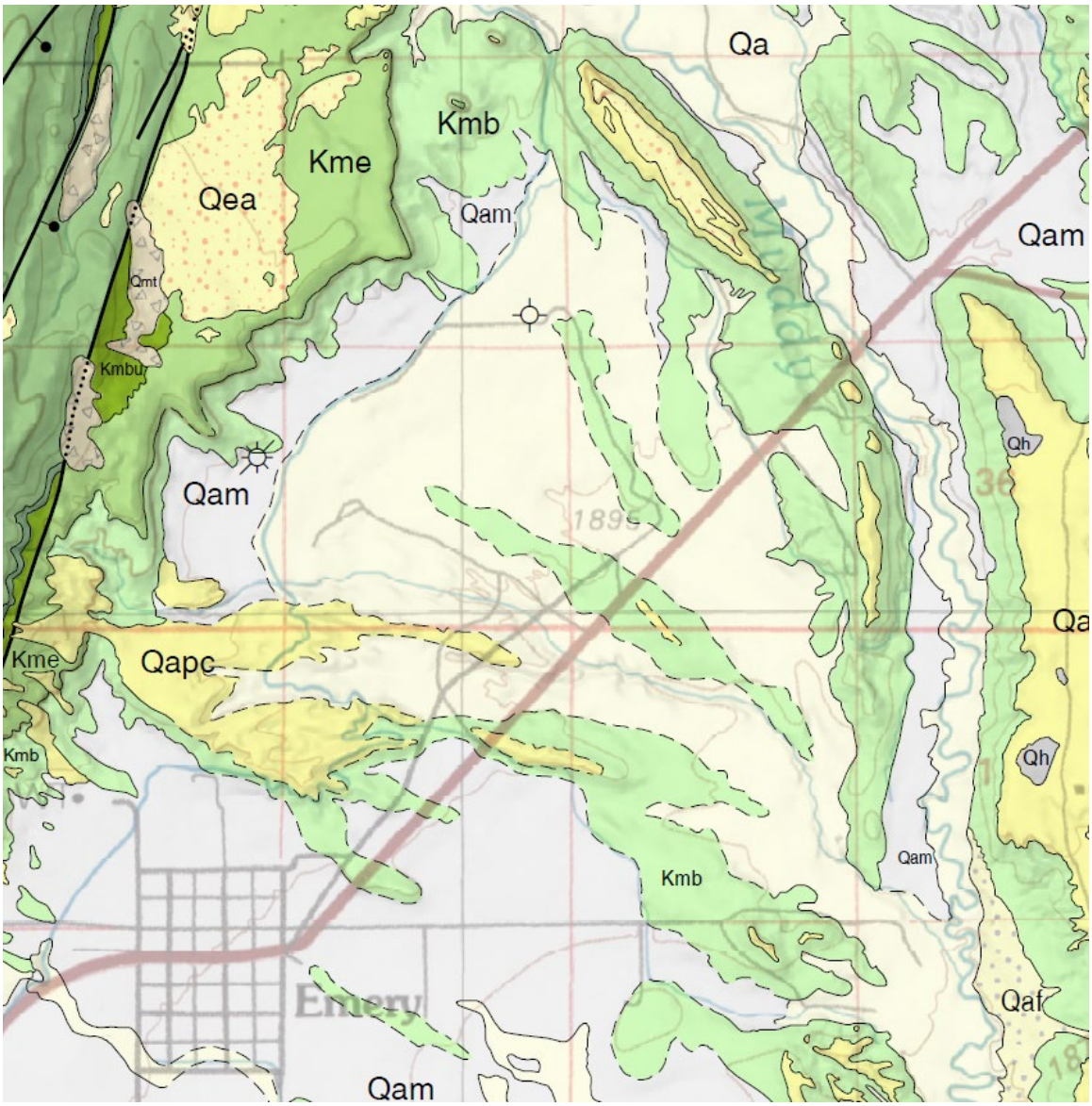

Source: Doelling, H., and Kuehne, P. (2016). "Interim Geologic Map of the East Half of the Salina 30' X 60' Quadrangle, Emery, Sevier and Wayne Counties, Utah." Utah Geological Survey, Salt Lake City, UT.

Primary Geological Units crossing SR-10 between Emery and Muddy Creek:

Kmb: Blue Gate Member of the Mancos Shale (Upper Cretaceous, Campanian Santonian):

Pale blue-gray, **marine shale**, nodular and irregularly bedded mudstone, and siltstone with several yellow-gray sandy beds; **weathers into low rolling hills and badlands**; the Blue Gate Member is Campanian to Santonian in age (Molenaar and Cobban, 1991); 300 to 490 meters (1000-1600 ft) thick.

Qam: Alluvial-mud deposits (Holocene to upper Pleistocene):

Mostly unconsolidated **clay, silt, and sand, deposited as fans** and mudflows; **eroded from Mancos Shale outcrops**; form valley fill and mud-dominated broad gently sloping alluvial fans; locally deeply incised by erosion; unstratified and nearly structureless; as much as 15 meters (50 ft) thick.

Qa: Alluvial river, stream, and wash deposits, undifferentiated (Holocene to upper Pleistocene):

Sand, silt, clay, granules, pebbles, and sparse cobbles in and adjacent to river, stream, and wash channels; commonly well sorted along rivers and larger streams and poorly to moderately sorted along smaller streams and washes; **commonly includes variable amounts of locally derived colluvium and slope wash, and windblown sand and silt; consists primarily of locally derived material along wash channels**; Qa includes deposits in active channels and on incised low-level benches and terraces generally up to about 10 meters (33 ft) above active channels (locally higher); deposits on larger benches are differentiated as Qa2, but smaller bench deposits are included in Qa where too thin to differentiate at this scale; locally includes other types of deposits too small to map separately; generally 0 to 10 meters (0-33 ft) thick.

All three geological units could have plastic or collapsible soils.